EMOSV
11/12/14

The Nottingham Trent University
Library & Information Services

SHORT LOAN COLLECTION

Date	Time	Date	Time

Please return this item to the Issuing Library.
Fines are payable for late return.

THIS ITEM MAY NOT BE RENEWED

Short Loan Coll May 1996

40 0681758 4

ProQuest Number: 10290061

All rights reserved

INFORMATION TO ALL USERS
The quality of this reproduction is dependent upon the quality of the copy submitted.

In the unlikely event that the author did not send a complete manuscript
and there are missing pages, these will be noted. Also, if material had to be removed,
a note will indicate the deletion.

ProQuest 10290061

Published by ProQuest LLC (2017). Copyright of the Dissertation is held by the Author.

All rights reserved.
This work is protected against unauthorized copying under Title 17, United States Code
Microform Edition © ProQuest LLC.

ProQuest LLC.
789 East Eisenhower Parkway
P.O. Box 1346
Ann Arbor, MI 48106 – 1346

MPHD15

Analysis of Dynamically Loaded Hydrodynamic Journal Bearings with particular reference to the Misaligned Marine Sterntube Bearing

By

R.W. Jakeman, M.Sc., C.Eng., F.I.Mar.E., M.I.Mech.E.

Submitted in partial fulfilment of the requirements for the Degree of Doctor of Philosophy

Sponsoring establishment:

Trent Polytechnic, Nottingham

Collaborating establishment:

Lloyds Register of Shipping, London

July 1988

This copy of the thesis has been sent on condition that anyone who reads it is understood to recognise that its copyright rests with the author and that no quotation from it or information derived from it may be published without the author's prior written consent.

Analysis of Dynamically Loaded Hydrodynamic Journal Bearings with particular reference to the Misaligned Marine Sterntube Bearing

by R.W. Jakeman

ABSTRACT

The objectives were to develop methods for predicting the steady load performance and dynamic characteristics of hydrodynamic journal bearings. Consideration is given to bearing interaction with shafting load distribution and lateral vibration, since it is often unrealistic to analyse bearings in isolation. Comparisons of results with other published theoretical and experimental data are included.

An original numerical hydrodynamic analysis method is described. The main assumptions are an isoviscous film of incompressible Newtonian lubricant with laminar flow, and rigid circular journal and bearing surfaces. A novel procedure for satisfying flow continuity within the cavitation zone is featured.

Predicted steady load results and linearised dynamic coefficients are presented, with particular consideration of misalignment. The application of steady load results to a computer program developed for practical application is outlined, and example results are given.

The results of studies on the influence of cavitation on oil film non-linearity in aligned crankshaft bearings, and misaligned sterntube bearings, are presented. Non-linear oil film response models based on the above results are described.

A new journal orbit analysis method has been developed for bearings with substantial dynamic loading. The associated results cover the influence of oil film history, journal mass and the interaction with lateral vibration of a marine propeller shafting system.

Contributions include the advancement of hydrodynamic bearing analysis methods. This includes the development of computer programs for practical application in the assessment of bearing operating conditions, and in modelling bearing support conditions for shaft alignment analysis. A further contribution is in the field of bearing influenced rotor dynamics with respect to marine propeller shafting. For the example shafting system considered, differences in lateral vibration amplitudes predicted with linear and non-linear bearing oil film models, were insignificant.

CONTENTS

NOTATION

The notation given below relates only to the main text of this thesis and Appendix 1. With regard to the notation for the papers by the author, which form Appendix 4., reference should be made to the notation given in each of these. Due to the fairly wide field covered, and the time span over which the papers were written, some duplication and alteration of the notation may be observed. In particular, it should be noted that the work on bearing interaction with shafting lateral vibration, reported in reference (92), incorporated a significant revision of the sign convention. It was considered that the complexity of this situation warranted a more unified approach to the sign convention for all the forces, moments, displacements and velocities. This may be illustrated by consideration of the vertical forces and displacements, where the downward direction was defined as positive. The applied load (external) W_y is normally positive, and the resultant oil film reaction F_y is therefore negative. Since a downward (i.e. positive) displacement results in an increase in the upward (i.e. negative) oil film reaction component, then the oil film stiffness coefficient A_{yy} will be negative in this convention. Full details of this sign convention are given in Fig. 1. This is contrary to the convention used in the papers prior to reference (92), where the oil film reaction force was considered to be positive despite the fact that it acted in the opposite direction to the positive applied load. Part of the notation, and the sign convention for the papers prior to reference (92) is shown in Fig. 2.

A_{xx}, etc.	Oil film stiffness coefficient.
B_{xx}, etc.	Oil film damping coefficient.
B_{ow}	Displacement of journal axis at bearing axial centre from straight line joining axis locations at bearing ends.
C_D	Diametral clearance.
C_R	Radial clearance.
D	Journal diameter.
F, F_x, F_y	Oil film force (total, horizontal and vertical components).
G_{RDFAC}	Grading factor for oil film element axial dimension.
I	Axial oil film element position reference.
J	Circumferential oil film element position reference.
L	Bearing length (refers to single "land" for full circumferential groove bearing).
M_c	No. of oil film element rows. (circumferential positions).
M, M_x, M_y	Oil film moment about bearing axial centre (total, horizontal and vertical components).
N	Journal speed (rev/s. except where otherwise indicated).
N_A	No. of oil film element columns (axial positions).
P_H	Oil head pressure acting on sterntube bearing.
P_{MAX}	Maximum oil film pressure.

P_s	Oil supply pressure (circumferential groove bearings).
Q	Oil flow rate through bearing (refers to flow from one side only in circumferential groove bearings).
R	Journal radius.
S	Sommerfeld No.
T_{OPFAC}	Ratio of M_c for top half of a sterntube bearing to M_c for bottom half.
U	Journal surface velocity (bearing assumed to be stationary in this work).
W, W_x, W_y	External force applied to journal (total, horizontal and vertical components). (refers to one "land" in circumferential groove bearings).
x, y	Horizontal, vertical journal displacement components from datum position.
$\dot{x}, \dot{y}$	Horizontal, vertical journal velocity components. (Datum velocities are generally zero).
$\alpha, \alpha_x, \alpha_y$	Total, horizontal and vertical journal axis misalignment angle components.
β	Angle of misalignment plane.
γ	Vertical angular displacement of journal axis from datum condition.
$\dot{\gamma}$	Angular velocity corresponding to γ
Δ	Used as a prefix to denote a change in a parameter value from the datum condition.

$\Delta a(I)$	Axial oil film element dimension at position reference I .
ϵ	Eccentricity ratio (at bearing axial centre unless otherwise specified).
η	Dynamic viscosity.
θ	Circumferential angular position co-ordinate.
θ_F	Angle of total oil film force vector.
θ_M	Angle of total oil film moment vector.
λ	Horizontal angular displacement of journal axis from datum condition.
$\dot{\lambda}$	Angular velocity corresponding to λ .
ψ	Attitude angle (at bearing axial centre unless otherwise specified).
ω	Journal rotational speed. rad/s.
Ω	Dynamic load cyclic frequency. rad/s.
—	Bar above parameter signifies a dimensionless group.

Dimensionless Parameters:

$\overline{A_{xx}} = \dfrac{A_{xx} C_D}{W}$, etc. $\quad \overline{A_{x\lambda}} = \dfrac{A_{x\lambda} C_D}{WL}$, etc. $\quad \overline{A_{\lambda x}} = \dfrac{A_{\lambda x} C_D}{WL}$, etc. $\quad \overline{A_{\lambda\lambda}} = \dfrac{A_{\lambda\lambda} C_D}{WL^2}$, etc.

$\overline{B_{xx}} = \dfrac{B_{xx} C_D}{W}$, etc. $\quad \overline{B_{x\lambda}} = \dfrac{B_{x\lambda} \omega C_D}{WL}$, etc. $\quad \overline{B_{\lambda x}} = \dfrac{B_{\lambda x} \omega C_D}{WL}$, etc. $\quad \overline{B_{\lambda\lambda}} = \dfrac{B_{\lambda\lambda} \omega C_D}{WL^2}$, etc.

$$\overline{P_{MAX}} = \frac{P_{MAX} LD}{W} \qquad \overline{P_H} = \frac{P_H LD}{W} \qquad \overline{P_S} = \frac{2 P_S C_R^2}{\eta U R} = \frac{2P_S}{\eta\omega}\left[\frac{C_D}{D}\right]^2$$

$$\overline{Q} = \frac{2Q}{C_R U L}$$

$$S = \frac{\eta U L}{2W}\left[\frac{R}{C_R}\right]^2 \qquad \overline{\alpha} = \frac{\alpha L}{C_D}$$

$$\overline{F_Y} = \frac{F_Y}{\eta N L D}\left[\frac{C_D}{D}\right]^2 \qquad \overline{M} = \frac{M}{\eta N L^2 D}\left[\frac{C_D}{D}\right]^2$$

1. INTRODUCTION

1.1. Computers and Numerical Methods

The author considers himself extremely fortunate in having lived in the age of the digital computer. It is the advent of this machine that has rendered the work reported in this thesis possible. One might argue that the computer is only a tool, which is strictly true, but it is a tool that has opened up a whole field which we refer to as numerical methods. At University the author recalls that numerical methods were regarded in some quarters with great disdain, as something to be resorted to if one was not clever enough to achieve a pure analytical solution. The value of the pure analytical solution, with respect to facilitating computational efficiency, is acknowledged. In achieving such a solution, however, it is often necessary to introduce approximations that would not be necessary when using numerical methods. The physical situation that we are endeavouring to model in our analysis is in fact extremely complex. This becomes only too apparent if we look closely enough at the details. Any analysis is therefore approximate, and the various methods therefore differ only in the degree of accuracy with which they correspond to reality. In practice the situation comes down to a trade off between relative accuracy and computational efficiency. Numerical methods tend to be biased towards the former feature, and analytical towards the latter. Analytical methods are therefore attractive for practical application provided the loss of accuracy is acceptable. For the marine sterntube bearing subject to dynamic misalignment, the sheer complexity of the operating condition is considered to defy the pure analytical approach. It is therefore the author's contention that without the use of numerical methods, and the availability of the digital computer with which to implement them, realistic analysis in this area would have been impossible. Simplifications and approximations have inevitably been made, but the adoption of numerical methods was considered essential in this area.

1.2. Direction and Strategy

The essential directing influence behind the work reported herein, was the need for performance and response prediction facilities for practical application with marine propulsion shafting systems. Fundamental research was not, therefore, a primary objective of the work. It is nevertheless felt that some light has been thrown on certain areas of hydrodynamic journal bearing performance which had hitherto received little attention. Such novel aspects of this work are partly a result of the unique nature of the marine sterntube bearing, and its complex operating and environmental conditions.

The research project, of which the journal bearing analysis work has formed a part, did not impose any rigidly defined objectives. This gave the author the opportunity to formulate his own ideas on the direction of the work. These were based on perceived needs in relation to the marine propulsion machinery consultancy activities which were undertaken alongside such research projects. The research was principally aimed at sterntube bearings, but the scope was wide, and work was also carried out on other types of bearings. This apparent side tracking, with respect to bearing type, was motivated by the availability of other published theoretical and experimental bearing performance data, which was used for comparison with the author's predictions. Apart from the obvious value of these comparisons, the work on other bearing types also contributed towards a better understanding of some fundamental aspects of bearing performance. It also proved to be of immense value with respect to the experience gained in developing computational techniques in relatively simple situations. This experience enabled these techniques to be extended to the substantially more complex conditions pertaining to the sterntube bearing, without undue difficulty.

The flexible nature of the research project enabled the direction of the work to be reviewed and modified from time to time in the light of experience. Unfortunately the constraints of the research project precluded the possibility of carrying out any experimental work. This made the above mentioned comparisons with published data imperative. Both theoretical and experimental published data were used, the latter being somewhat more limited in availability, particularly in relation to sterntube bearings.

1.3. Objectives

As indicated above, the main objective of this work was to develop computer programs suitable for practical application in design and performance analysis of sterntube bearings. A particular feature was the consideration of angular misalignment, both steady and dynamic, which is invariably present in sterntube bearings, and to which they are especially sensitive. The specific initial objectives were to develop programs for predicting the steady load performance of a sterntube bearing, and linearised oil film stiffness and damping coefficients to define the bearing response for lateral vibration analysis. With regard to the steady load performance, the main practical applications were to ensure satisfactory operating conditions from the reliability viewpoint, and to provide bearing response data for dynamic alignment calculations. The latter aspect was mainly concerned with determining the location of a single support point to represent the bearing. In a misaligned sterntube bearing this could be significantly displaced from the bearing axial centre.

In reviewing the "in service" measurements by Hyakutake et al (24), it was found that journal displacement amplitudes up to 30% or more of the clearance could occur in a sterntube bearing. This cast doubt on the adequacy of linearised oil film coefficients for modelling the sterntube bearing dynamic response, particularly with respect to lateral vibration amplitude prediction in propeller shafting. Accordingly a further objective was established to investigate the significance of non-linearity in the sterntube bearing oil film.

In view of the availability of measurements, the propeller shafting system used by Hyakutake et al (24) was adopted as a test case, for the final phase of this work, in which non-linearity effects were covered. A preliminary analysis of this system revealed a predicted fundamental mode lateral vibration resonance at about the service speed. This made it a particularly interesting test case, but clearly indicated that the sterntube bearing could not be analysed in isolation from the shafting system. The necessity of taking account of bearing and propeller shafting interaction, with respect to dynamic behaviour, was in accord with experience in applying the steady load bearing analysis to dynamic alignment calculations. In both cases separate analysis of the bearing and shafting problems appeared likely to lead to significant errors due to the degree of interaction between bearing and shafting behaviour. These factors resulted in a substantial extension of the work required to investigate the significance of oil film non-linearity. The final objective thus became the prediction of propeller shafting lateral vibration amplitudes using coupled bearing and shafting models. A similarly interactive solution of the dynamic alignment problem, for steady loads, was a subsidiary objective.

2. BACKGROUND

2.1. Sterntube Bearing Environmental Situation

The unusual environmental situation of the sterntube bearing, and the consequent influence on its design and operating conditions, has been dealt with in references (87) and (88). This section will therefore be confined to a list summarising the main features:

a) The cantilever action of the propeller weight at the shaft end results in a tendency to incur steady angular misalignment at the aft sterntube bearing.

b) The shaft diameter is mainly dictated by torque transmission considerations. This results in a relatively long aft sterntube bearing in order to meet the load imposed by the weight of the propeller and aft end of the shafting.

c) The propeller operates in a non-uniform stream of water, referred to as the wake field, due to the influence of the ships hull. This causes mean and dynamic components of transverse force and moment to be developed by the propeller, and thus applied to the shaft end. These are dependent on the propeller - hull geometry, speed, draught, rudder angle and sea state. Differences from steady state conditions will also occur during transient conditions arising from the ship accelerating or changing rudder angle. The dynamic components are of non-sinusoidal form, and repeat cyclically at propeller blade frequency. This propeller - wake field excitation results in the application of significant dynamic load to the aft sterntube bearing.

d) In order to prevent the ingress of sea water in the event of a defective aft seal, the sterntube is subjected to a head pressure of oil slightly in excess of the external sea water pressure at the shaft level. The oil head pressure acts on all boundaries of the sterntube bearing.

e) The generally low shaft speed, and resultant low power loss, in the sterntube bearing usually obviates the necessity for positive oil circulation through the sterntube for heat removal. This factor is enhanced by the ample heat sink provided by the surrounding sea water and ballast water in the aft peak tank.

2.2. Related Practical Problems

As in section 2.1., references (87) and (88) should be consulted for a more detailed account of the practical problems related to the operation of sterntube bearings. These references are mainly concerned with the steady load performance. A particularly comprehensive account of such problems combined with practical guidance on design aspects was given by Hill and Martin (46). References (4) and (33) by Hill are also recommended. Problems related to the dynamic loading arising from propeller - wake field interaction have been covered in reference (92). The paper by Velder (2) also gives a detailed discussion of the generation of dynamic forces and moments by the propeller. In view of the coverage by the above references, only a brief list of the related practical problems will be given as follows:

a) The maintenance of an acceptable safety margin with rspect to the bearing operating conditions. For the moderate specific bearing pressures and low shaft speeds associated with sterntube bearings, the factor upon which safe operation is assessed is minimum film thickness. Only full hydrodynamic operating conditions were covered in this work i.e. with a non-zero minimum film thickness. Such conditions should be maintained at the upper end of the operating speed range. Satisfactory operation under boundary lubrication conditions may occur at the lower end of the speed range. Under these conditions the minimum film thickness criterion is not applicable, and some guidance with regard to acceptability may be obtained from the paper by Nagata et al (34).

The achievement of a satisfactory minimum film thickness at the aft end of the bearing may be difficult due to misalignment. This problem is compounded by the greater sensitivity to misalignment associated with large L/D ratios.

b) The achievement of satisfactory lateral vibration characteristics for the propeller shafting. This is significantly dependent on the stiffness and damping properties of the sterntube bearing oil film.

2.3. Literature Review

Many of the references listed have been discussed in the papers previously published by the author. Table 1 lists the references concerned, and indicates the author's papers in which discussions may be found. The purpose of this review is to expand on the above discussions where appropriate, and to discuss the remaining references that are not included in Table 1 or covered elsewhere within this thesis. It should be noted that the list of references is given in chronological order. Since the range of topics covered is fairly wide, for the purposes of this review they have been grouped under suitable headings. This arrangement has resulted in some references being discussed more than once under separate headings. It must also be stressed that this review does not provide a comprehensive account of all aspects of the references given. Only those detailed aspects of the references which were considered relevant to the work covered by this thesis are discussed.

2.3.1. Oil Film Hydrodynamic Analysis

The review of lubrication theory developments by Lloyd et al (9) forms a good introduction to this area. In particular, it contains a comprehensive table of assumptions commonly made in lubrication theory, together with guidance on validity ranges and reference sources. The assumption that the contribution of viscous shear forces to the lateral oil film force components may be neglected, was indicated by Mitchell et al (3) in the context of transient orbit calculations for a rigid rotor.

Solution of the oil film pressure distribution has commonly been achieved by means of finite difference methods. More recently the finite element method has gained some popularity. Table 2 lists a sample of published papers showing the type of film pressure solution employed together with the mesh size and other relevant details. It may be noted that none of these analyses satisfied flow continuity within the cavitation zone. Of the cavitation models indicated, the technique of setting sub-cavitation pressures to the specified cavitation pressure (usually zero gauge) during the operation of an iterative relaxation solution, is the more accurate. The alternative technique of truncating the sub-cavitation pressures after completion of a "full film" solution for the complete bearing surface, has the advantage of permitting the use of matrix inversion.

Comparisons of the finite difference and finite element methods have been presented by Allaire et al (38) and Gero and Ettles (76). Allaire et al claimed a better accuracy for the finite element method, but their results indicated that for mesh sizes typical of those commonly used, the difference in accuracy was negligible. Gero and Ettles considered higher order formulations for both finite difference and finite element solutions. These were indicated to be justifiable only where prediction accuracies better than 0.1% were required. For first order solutions, Gero and Ettles concluded that the finite difference method was more accurate. The advantage of readily accommodating non-rectangular bearing surfaces, or parts of the surface, has been claimed for the finite element method. For practical purposes, however, the restriction of the finite difference method to a rectangular mesh is not considered to be a significant problem. Furthermore, the simplicity of the finite difference mesh makes the method more amenable to application on a "routine" rather than "special" basis.

Before the advent of the digital computer, which made the use of numerical film pressure solutions a practical proposition, approximate analytical solutions of Reynolds' equation were commonly used. These comprised the Ocvirk short bearing approximation, in which circumferential pressure gradients were assumed to be negligible relative to the axial pressure gradients, and the Sommerfeld long bearing approximation, in which the reverse assumption with respect to the relative pressure gradients, was made. Despite the limited accuracy, the approximate analytical solution is attractive with respect to computational efficiency. This is particularly advantageous for the time-stepping type of journal orbit analysis, since oil film pressure solutions are required at each time step. Holmes and Craven (19) employed this approach to study the influence of crankshaft and flywheel mass on the journal orbit within the adjacent bearing. The short bearing approximation was used, and this was considered to provide adequate accuracy for bearing L/D ratios up to 1.0. Later, Dede and Holmes (65) introduced correction factors for both the long and short bearing approximations in order to improve accuracy whilst retaining the advantage of computational efficiency. These techniques were referred to as semi-analytical methods.

In recent years cavitation models in which flow continuity is taken into account, have been introduced. One of the earlier examples of work in this area was that by Olsson (30), which also covered the dynamic loading situation. In handling the effect of squeeze action, Olsson's continuity equation for the cavitation zone was based on equating the nett rate of oil flow into an element to the rate of increase of oil volume within that element. The integration of this equation over a series of discrete time steps, in which a journal orbit is "marched out", in fact formed the basis of the author's oil film history model (77) (86). This type of analysis, however, has the problem of excessive computing time. In order to minimise computing time, the use of some form of pre-computed oil film response data is desirable. Unfortunately the nature of the oil film history model does not appear to lend itself to such treatment. It is, perhaps, for this reason, that Olsson's analysis was considered to be incapable of practical solution. The author's approach to the problem of squeeze interaction with cavitation is described in reference (90). This was based on satisfying flow continuity within the cavitation zone on a quasi-steady basis as far as practicable. Both the nett oil flow into an element and the rate of increase of oil volume within that element were therefore zero , and the situation may therefore be regarded as a special case of Olsson's continuity equation. The inevitable approximation arising from this quasi-steady treatment was considered justifiable since it facilitated the computation of oil film response data for use in journal orbit analysis. More recently Dowson et al (74) presented an analysis of a steadily loaded single axial oil groove bearing. This analysis used the algorithm originally developed by Elrod and Adams (29) and later refined by Elrod (53). The results of this work showed the influence of oil supply pressure on the extent of the cavitation zone, and consequently upon the load capacity. A detailed account of the analysis method used was given by Dowson et al in reference (63), and application to a circumferential oil groove bearing is presented in reference (73). Rowe and Chong (68) also presented an algorithm for cavitating bearings which considered flow continuity within the cavitation region. This work appeared to cover only steadily loaded bearings. Brewe (83) also used Elrod's algorithm, and claimed to be the first to apply it to the dynamically loaded bearing situation. Floberg (27) also devised an analysis method in which flow continuity was satisfied within the cavitation zone. In addition, Floberg considered the tensile strength of the oil, and this enabled the number of streamers into which oil within the cavitation zone divided, to be predicted. A further refinement related to the inclusion of tensile strength also permitted the prediction of sub-cavitation pressures within the oil streamers. Although valuable from the research viewpoint, the considerations related to oil tensile strength do not appear to be important with respect to practical applications.

The majority of hydrodynamic journal bearing analyses have assumed isoviscous conditions using an "effective" viscosity to represent the complete oil film. In addition to his cavitation studies, Olsson (4) also considered a variable viscosity oil film based on an energy balance in each of the rectangular elements into which the oil film was divided. The difference in predicted oil film pressure distribution from that obtained with an isoviscous model was found to be negligible. A similar conclusion was also reached by Glienicke et al (50) and Smith (58), the latter being in the context of a journal orbit analysis. Boncompain et al (79) carried out a combined thermal and hydrodynamic analysis. Their predicted results supported the commonly made assumption that about 90% of the heat generated by viscous oil shear is carried away by the oil. The results also indicated that distortion out of circularity, of the journal and bearing, was negligible, and that the axial temperature distribution was virtually constant. No comparative results for variable viscosity and isoviscous oil film models were given.

The different, but closely related problem, of oil mixing within an axial oil supply groove was studied by Heshmat and Pinkus (81). This indicated that significant carry over of hot oil from the upstream bearing surface can occur, if the oil supply pressure is insufficient to maintain fully flooded conditions in the oil groove. In general, however, it was indicated that hot oil carry over only became significant at extremely high loads. The associated analysis of groove flow mixing was fairly approximate, and did not appear to have been developed to a level suitable for practical application. It was evident that the above references substantiated the commonly used isoviscous oil film model for the range of conditions they covered. The neglect of hot oil carry over relative to supply grooves was also shown to be reasonable for most practical applications. This latter conclusion is based on the assumption of a reasonable oil supply pressure, and a bearing load that is not excessive.

Most of the analyses reviewed have taken the cavitation pressure to be atmospheric (i.e. zero gauge). This is based on the assumption that the cavitation is gaseous i.e. due to dissolved air coming out of solution, or to air drawn from the surroundings (ventilation). In their work on squeeze film bearings, Humes and Holmes (40) found that the assumption of substantially sub-atmospheric cavitation pressures was necessary in order to achieve reasonable agreement between predicted and measured journal orbits. The associated experimental measurements of film pressures in a squeeze film bearing confirmed the occurrence of the above sub-atmospheric cavitation pressures. This departure from atmospheric cavitation pressure is assumed to be due to the different operating conditions of squeeze film bearings relative to those for rotating journal bearings. Such differences may comprise a reduced possibility of ventilation due to the use of end seals, and reduced exposure of the oil to air, and hence a limited opportunity for air to become dissolved.

2.3.2. Bearing Steady Load Analysis

Discussion of this area overlaps that of the previous section, covering hydrodynamic analysis, to a substantial degree. The previous section was, however, concerned with the methods and assumptions related to hydrodynamic analysis. This section is concerned with theoretical results for steadily loaded bearings. A vast amount of literature has been published in this area, most of which has dealt with aligned bearings only. In view of the subject of this thesis, this part of the review will be restricted to literature in which misalignment was considered. As a result this section will be relatively short.

Hill and Martin (46) provided useful design guidance for misaligned sterntube bearings in graphical form. Results derived from these graphs were shown (72) to compare well with results produced by the author's analysis method. In addition, Hill and Martin provided a substantial amount of statistical data on both sterntube bearing and seal failures. A valuable discussion on service experience and problems was also given.

Vorus and Gray (45) produced steady load analysis results as part of an investigation into sterntube bearing failures during trials on a ro-ro carrier. Despite the limitation to steady load analysis and use of the simple truncated negative pressure cavitation model, the results confirmed the cause of the failure. This was shown to be due to the propeller - wake forces and moments causing the shaft to bear against an axial oil groove during a manoeuvering condition. As a result of this work, the oil grooves were moved to a position near the bearing top in a novel arrangement.

Pinkus and Bupara (47) also produced analysis results for a steadily loaded misaligned sterntube bearing. These were shown (72) to be generally in good agreement with comparative data obtained by use of the author's analysis method.

The analysis results of Reason and Siew (59) covered misalignment, but did not appear to consider any oil supply grooving. These results showed that both power loss and side leakage flow rate were insensitive to misalignment.

Mourelatos and Parsons (84) considered bearing elasticity in their analysis of a steadily loaded misaligned sterntube bearing. This was intended to investigate the reduced sensitivity to misalignment which has been claimed for reinforced resin sterntube bearings. The results showed reduced peak film pressures when the analysis took account of the bearing elasticity values corresponding to such materials. No indication of the effect of bearing elasticity on the minimum film thickness in misaligned bearings, was given. This is unfortunate in view of the generally accepted use of minimum film thickness as a criterion for satisfactory operation in such bearings. The predicted film pressures indicated that significant differences in the performance of reinforced resin and white metal sterntube bearings only occurred in heavily loaded cases.

2.3.3. Dynamically Loaded Bearing Analysis

This section is concerned with theoretical methods for the prediction of hydrodynamic oil film response to the dynamic load situation. Such methods form the basis of the analysis of dynamic interaction between bearings and shafting, which will be dealt with in the next section.

Where the level of dynamic loading is such that the journal displacement amplitudes are small relative to the bearing clearance, linearised stiffness and damping coefficients may be used. These define the oil film response to displacement and velocity changes from a datum condition. For aligned bearings, only force changes are involved, and these are covered by 4 stiffness and 4 damping coefficients. Several researchers have published data for these coefficients. An example is the paper by Woodcock and Holmes (12), which presented both theoretical and experimental coefficient data for a full circumferential groove bearing. Parkins (42) also gave theoretical and experimental data covering the above type of bearing. In addition, Parkins investigated the non-linearity of these coefficients at larger displacement and velocity amplitudes. This investigation was limited to the examination of coefficients with respect to the directly related displacement or velocity i.e. the $A_{YX} - x$, $B_{YY} - \dot{y}$, etc. relationships were considered but not, for example, $A_{YX} - y$, $A_{YX} - \dot{y}$ or $A_{YX} - \dot{x}$.

At larger displacement and velocity amplitudes, non-linearity naturally results in a loss of accuracy when using linearised coefficients. There appears to be little published data on amplitude limits with respect to acceptable accuracy when using such coefficients. The prediction of resonant frequencies of lateral vibration in the rotating system, seems to be less critical in this respect than amplitude prediction.

Bannister (35) addressed the problem of non-linearity by the addition of the second order terms of Taylor's series to the conventional oil film force equations in which eight stiffness and damping coefficients (first order terms) are used. This resulted in an additional 20 non-linear coefficients, and good correlation between predicted journal orbits and corresponding measurements made on an experimental test rig was reported. Bannister's work also examined the influence of bearing misalignment, but was confined to the steady variety, and did not include oil film moment coefficients.

The prediction of linearised oil film coefficients has been commonly achieved by means of numerical differentiation. Finite displacement and velocity perturbations are applied to the journal, and the corresponding oil film force component changes are computed. Klit and Lund (78) described an alternative approach referred to as the variational method. This is based on the mathematical differentiation of Reynolds' equation, and was claimed to be faster and more accurate than numerical differentiation. With respect to accuracy, this claim is undoubtedly valid where very small perturbations are used for numerical differentiation. The problem in this situation is that the oil film force change resulting from a small perturbation, may become comparable to the accuracy with which the force is determined by a numerical relaxation solution. When computing stiffness and damping coefficients for any specific application, it is considered appropriate to use perturbation magnitudes corresponding to the maximum anticipated journal displacement and velocity amplitudes that the real bearing will experience. In sterntube bearings, measurements by Hyakutake et al (24) have shown these amplitudes to be significant. The accuracy of numerical differentiation when using similar perturbation magnitudes, would be satisfactory. In addition, since the linearisation is averaged over realistic displacement and velocity ranges, some allowance is effectively made for non-linearity. The use of numerical differentiation to determine oil film coefficients in the above situation, is therefore likely to be more accurate than the method advocated by Klit and Lund (78).

In a bearing subject to dynamic misalignment conditions, angular displacements and velocities of the journal axis must be considered in addition to lateral motion. When the bearing L/D ratio is relatively large (> 1), oil film moment variation must also be accounted for. This is particularly relevant to sterntube bearings where L/D ratios are typically about 2. When using a linear oil film model, the author has shown (72) that 32 coefficients are required to cover dynamic misalignment. Pafelias (25) presented data for these coefficients at a range of conditions. The bearing concerned was a 150^{o} partial arc type with L/D = 0.5. Comparative coefficient data produced by the author's analysis method was given in reference (87).

Where the extent of dynamic loading is such that the journal orbit becomes comparable in size to the bearing clearance, non-linearity precludes the use of a single set of linearised coefficients. Such coefficients can be used on a local basis during the "marching out" of a journal orbit in a series of time steps, as shown by the author in reference (77). This process is heavy on computing time, since a new set of coefficients must be determined at each time step. These coefficients use the local conditions corresponding to the time step start point as the datum.

The use of approximate analytical solutions of Reynolds' equation, to overcome the computing time problem when predicting journal orbits, has been discussed in the previous section. Various methods based on the use of pre-computed data represent the main alternative. Some of these methods were reviewed in reference (91), including the method developed by the author, which was presented in reference (85). The subject of reference (91) was in fact a development of the author's method, to accommodate the more complex situation of the dynamically misaligned sterntube bearing.

2.3.4. Bearing - Shafting Dynamic Interaction

The review so far has looked at analysis methods for bearings in isolation. This approach effectively assumes that the behaviour of bearings, and the shafting systems they support, are entirely independent. In the real world this is not so, either for steadily or dynamically loaded bearings. The errors resulting from this assumption may be acceptable in many practical situations, but it is important to investigate this where any doubt exists. With regard to steadily loaded bearings, the author's reference (88) discussed this interaction in the context of marine propeller shafting. In particular, it showed how the load, misalignment angle and location of the effective support point in a sterntube bearing, should be determined by interactive bearing and shaft alignment analyses. The method described was designed for use with separate bearing and shafting analysis programs. It thus required an iterative form of solution. In reference (92), the author showed how a direct, fully coupled, shafting and bearing equilibrium solution could be obtained. This method used linearised oil film stiffness coefficients, and could therefore handle only limited journal displacements.

The remainder of this section will be devoted to literature involving interaction with respect to dynamically loaded bearings. This is the area referred to as rotor dynamics. A wide interpretation of the scope of rotor dynamics is taken in this thesis. An introductory sub-section is therefore given, before reviewing the literature of the various situations covered.

2.3.4.1. The Scope of Rotor Dynamics

The term rotor dynamics is commonly considered to refer only to relatively high speed purely rotating machinery. In this discussion a much wider, more general, view is taken; i.e. that rotor dynamics applies to any rotating machinery subject to exciting forces and/or moments, irrespective of speed, type of machinery or nature of the excitation.

At the extremities of this field are the turbine rotor, in which excitation is due mainly to out of balance forces and is relatively small, and the diesel engine crankshaft, in which the excitation due to combustion and inertia forces is dominant. For the turbine rotor, inertia forces arising from lateral motion are significant, but the amplitudes are generally at a sufficiently low level to enable linearised bearing oil film coefficients to be used without unduly compromising accuracy. In the diesel engine crankshaft, however, inertia forces due to lateral motion are usually neglected, although this may not be justifiable for bearings adjacent to the flywheel. These inertial forces should not be confused with those due to unbalanced reciprocating and rotational forces in pistons, connecting rods and cranks, which form part of the excitation. The diesel engine crankshaft also differs with regard to the large orbits of the journals in relation to the clearances of the main bearings. This results in the use of a single set of linearised oil film coefficients being totally unacceptable with respect to accuracy in this situation. Analysis of the diesel engine crankshaft thus requires a time stepping procedure, with bearing oil film responses estimated at each time step for the corresponding journal displacement and velocity components. The basic difference in the nature of the above rotor dynamics problems is that the turbine rotor is mainly a resonant response problem, whereas the diesel engine crankshaft is a forced-damped vibration problem with negligible dynamic magnification.

As a rotor dynamics problem, the marine propeller shaft falls somewhere between the above extremes with respect to excitation level and response. The propeller excitation resulting from operation in a non-uniform wake field substantially exceeds any excitation arising from out of balance forces. It is also complex in that vertical and horizontal components of both force and moment are involved, and their cyclic variation is non-sinusoidal. This situation was clearly confirmed by the measurements of Hyakutake et al (24) which showed journal orbits (major axis dimension) up to 35% of the bearing clearance at blade order frequency. At the outset of the work reported in reference (92), the marine propeller shaft was therefore considered to be in a "grey area" with respect to the applicability of linearised oil film coefficients. Accordingly, the non-linear model previously developed for aligned bearings (85), (86) was adapted to the misaligned sterntube bearing situation. In addition to the above factors relating to excitation, marine propeller shafting systems have some other distinguishing features with respect to the rotor dynamics problem:

1. The dominant mass/inertia, namely the propeller, is overhung at the end of the shafting. This cantilever loading situation leads to the possibility of significant steady and dynamic misalignment in the adjacent sterntube bearing.
2. The overhung location of the propeller also indicates the need to consider gyroscopic effects.
3. The propeller mass and inertia are increased by water entrainment which also introduces cross-coupling effects.
4. The propeller is subject to lateral and angular damping about all three axes, and this also involves cross coupling.

A review of the field of bearing - influenced rotor dynamics for the period 1973-78 was carried out by Dowson and Taylor (49). The above review concluded that further attention was required with respect to gyroscopic, transient and non-linear effects, thermal and elastic bearing distortion and the modelling of realistic bearing and rotor systems.

In the context of marine propeller shafting, the author (92) has addressed the gyroscopic and non-linear aspects. The system modelled was that for which measurements were taken by Hyakutake et al (24), i.e. the 210,000 d.w.t. tanker "Keiyo Maru".

2.3.4.2. Single Bearing - Journal Orbit Analysis

The simplest form of rotor is that in which a rigid journal, supported by a single bearing, is subjected to dynamic load. Practical realisations of this configuration are few, but it clearly represents a necessary stage in the development of bearing dynamics. In effect the single journal - bearing model eliminates consideration of elastic coupling, by means of shafting and/or support structure, with other bearings. Contrary to service applications, the above configuration may be achieved in experimental test rigs.

Workers in this area have tackled the bearing dynamics problem from several angles. Bannister (35), as shown in 2.3.3., developed a non-linear model based on the linearised coefficient approach. This model was designed to enable journal orbits to be predicted accurately at moderate displacement and velocity amplitudes. The journal orbit analysis method used by Bannister accounted for journal inertial forces, and excitation was simple harmonic due to out of balance forces. In test cases using only the eight first order oil film terms, direct solution of the journal orbit was achieved by matrix inversion. This form of direct solution was not possible with the non-linear oil film model, and time stepping procedures were therefore used. In view of the high computing time involved in time stepping solutions, Bannister also employed a modified Newton-Raphson method, based on the approximation of assuming the journal response to be simple harmonic.

Jones (57) examined the effect of oil film history using a finite difference solution of Reynolds' equation. The essential feature of the oil film history model is that it continuously monitors the extent of cavitation zones and the disposition of oil within them. This recognises that whilst the journal displacement and velocity conditions which generate a cavitation zone may disappear very rapidly, the cavitation zone itself will generally take rather longer to refill with oil. Jones showed that the significance of oil film history was dependent on the efficiency of the bearing oil feed arrangements. The time stepping journal orbit solution used by Jones was based on the determination of journal velocity vectors which resulted in equilibrium between the externally applied and oil film force components. Journal inertial forces were therefore neglected.

LaBouff and Booker (70) examined the influence of bearing elasticity using a finite element model. Elasticity was shown to be significant, but excessive computing time restricted this work to transient solutions not exceeding 200° of journal rotation. A similar journal orbit solution to that of Jones (57) was used.

Goenka and Oh (82) improved journal orbit computing time when taking account of bearing elasticity. This was achieved firstly by use of the Newton-Raphson method, and secondly by adopting an approximate solution of the oil film pressure distribution based on the assumption of a parabolic form in the axial direction. The latter technique was a refinement of the commonly used short bearing approximation, and was designed to improve accuracy.

The significance of journal inertial forces in conjunction with the application of an oil film history model was investigated by the author in reference (77). This work used the same test case as Jones (57). At low journal mass good agreement was found with the results by Jones for the half circumferential oil groove bearing. A comparison of theoretical and experimental orbits for the full circumferential oil groove bearing was carried out by the author and Parkins (86). This included a fast journal orbit solution based on the use of pre-computed oil film velocity coefficients as described in the authors reference (85). Journal orbits were also produced using the author's analysis method (77) both with and without the oil film history model. The experimental results were obtained from a test rig by Parkins (42).

2.3.4.3. Low Excitation Rotor Dynamics

The above heading represents the area most commonly associated with rotor dynamics, covering machinery such as turbines in which the main source of excitation is out of balance forces. Resonant response is therefore generally more important than forced-damped. The low level of excitation generally results in small journal orbits relative to the bearing clearances. This has justified the wide use of the well known eight linearised stiffness and damping coefficients to describe the dynamic response of bearing oil films. The adoption of linear bearing models combined with simple harmonic excitation has facilitated direct i.e. non-time stepping solutions of the dynamic response. Some of the earlier work in this area assumed the rotor to be rigid. Whilst this approach was reasonable for research into bearing dynamics only, it had little practical relevance.

More realistic analyses, such as that by Lund and Orcutt (11), took account of rotor flexibility. In particular, these authors indicated the significance of bearing damping, which in some machines reached a level at which the identification of critical speeds was difficult.

Despite the widespread acceptance of linearised oil film dynamic coefficients, doubts have remained concerning their adequacy with respect to amplitude prediction. The paper by Myrick and Rylander (37) is therefore noteworthy for its use of a realistic bearing model. In this work a time stepping solution was employed with a finite difference solution of Reynolds' equation at each time step. Cavitation was handled by setting negative pressures to zero during the relaxation procedure, but oil flow continuity within the cavitation zone was not considered. A symmetrical three mass rotor was used, with massless shafting elements in which the flexibility was based on bending only. Myrick and Rylander also included oil film moments due to steady and dynamic misalignment.

2.3.4.4. Crankshaft Analysis

The unique nature of the reciprocating engine crankshaft and its loading is reflected in the analysis methods employed. Various approximations have been used in order to cope with the complexity of the crankshaft situation. Since the relatively large non-sinusoidal excitation experienced by the crankshaft necessitates a time stepping type of solution, the estimation of bearing oil film response at each step is an area where there is a strong incentive for fast approximate solutions.

As noted in the previous section, inertial forces due to lateral motion of a crankshaft are usually neglected. The analysis of Craven and Holmes (21) is therefore interesting in that the above inertial forces were considered. A fast solution was obtained by use of the short bearing approximation to obtain the oil film forces. Elastic forces and moments due to relative displacements of the main bearing journals were assumed to be negligible. This enabled each main bearing to be analysed in isolation from its neighbours.

Analysis of a complete crankshaft - main bearing system, taking account of forces and moments transmitted through the crankshaft and crankcase, has been achieved more recently by Welsh and Booker (56). A finite element structural analysis was combined with a hydrodynamic analysis of each of the main bearings by the Mobility (vector) method.

Moes et al (64) presented a similar analysis to that by Welsh and Booker in which they introduced Mobility matricies as a development of the Mobility vector system.

2.3.4.5. Marine Propeller Shaft Analysis

A review of literature in this area is given in reference (92). Nothing of significance can be added to this.

2.3.5. Bearing Experimental and Service Measurements

Although the work reported in this thesis is purely theoretical, it is important to review any relevant measurements that are published. There are two aspects to the potential value of such a review:

a) Guidance with respect to the justification of assumptions made in the theoretical work.

b) Validation of theoretical methods by comparison of measured and predicted results.

The measurements related to thermal equilibrium in a steadily loaded bearing, by Dowson et al (7), supported some commonly used assumptions. Their results indicated that the oil outlet temperature is a reasonable basis for the effective viscosity when assuming an isoviscous film. The proportion of the heat generated by viscous shear, that was transferred to the oil, was also investigated. This was shown to be about 80% at the maximum speed of the 4 inch diameter test bearing (2,000 R.P.M.), but the proportion fell off rapidly at lower R.P.M.

Measurements on a misaligned 200 mm axial oil groove bearing, by Asanabe et al (17), indicated the power loss to be fairly insensitive to misalignment, provided that boundary lubrication did not occur. This was in agreement with the theoretical work by Reason and Siew (59), as discussed in 2.3.2.

The valuable "in service" measurements by Hyakutake et al (24) have been previously mentioned. These data were used for comparison with the author's predicted results in reference (92).

Parkins (51) obtained measurements from an experimental test rig to determine the 8 linearised dynamic coefficients. An aligned full circumferential groove bearing was used. The basis of the measurements was to provide suitably phased electromagnetic excitation, in the vertical and horizontal directions, such that vertical and horizontal line orbits were produced. Vertical and horizontal displacement and velocity perturbations were thereby applied individually. Correlation of theoretical and experimental dynamic coefficients was not good. It is considered that this may have been due to the following reasons:

a) Moderate orbit sizes were necessary in order to obtain measurable changes from the datum equilibrium condition. Non-linearity would therefore have been significant.

b) Substantial departures from the intended vertical and horizontal line orbits could not be avoided. The aim of applying perturbations individually, was consequently not achieved to a satisfactory level of accuracy.

A comparison (86) of some of the experimental orbits by Parkins with orbits predicted by the author were in reasonable agreement. This comparison did, however, indicate the presence of significant bearing elastic deformation. Differences in the experimental and predicted orbits, also suggested that the cavitation pressure may have been lower than the value used for the latter.

Morton (32) considered that many of the problems related to the measurement of oil film dynamic coefficients, were due to scale. In order to obtain accurate coefficient measurements for turbo-generator applications, Morton used a full scale bearing test rig. At the sizes involved ($>$ 400 mm diameter), continuous excitation of adequate magnitude was not considered to be feasible. The excitation system used involved the application of a gradually increasing load to the bearing until it was suddenly released by the breaking of a weak link. Determination of the dynamic coefficients was achieved by analysis of the resulting transient response.

2.3.6. Experimental Work and Discussions related to Cavitation

Cavitation is probably the most troublesome phenomenon with respect to the prediction of hydrodynamic bearing performance. The most sophisticated theoretical cavitation models appear to represent only crude approximations to reality. Fortunately for the majority of practical applications, this disparity between theory and reality does not have serious consequences. The overall bearing performance can still be predicted to an acceptable degree of accuracy despite the crude cavitation model. Some cavitation models are, however, better than others. It is also important that theoretical workers should be aware of experimental work related to cavitation, however alarming this may be!

Dowson and Taylor (26) presented a comprehensive discussion of the physical phenomena involved in bearing oil film cavitation. This paper also gave a resume of the development of cavitation models from Reynolds (who avoided the problem by considering only $\epsilon < 0.4$) onwards. The importance of accounting for flow continuity within the cavitation zone was indicated. An outline of the flow separation theory was also included. This explained the generation of a sub-cavity trough after film rupture.

Some apparent inconsistencies in the performance of dynamically loaded bearings were discussed by Marsh (28). These involved observed differences in situations that were equivalent according to hydrodynamic theory. The differences appeared to result from different cavitation behaviour. A detailed discussion of this area was given by the author in reference (90).

Evidence has been produced which shows that cavitation can also cause inconsistencies in the behaviour of steadily loaded bearings. Middleton et al (6) published experimental results in which the static journal locus was found to follow different paths for gradually increasing or decreasing load. This was indicated to be due to an apparent hysteresis effect with respect to the occurrence of film rupture.

The dynamically loaded bearing experiments by Olsson (4) showed good cyclic repeatability of the positive pressure regions. In the cavitation region, however, the cyclic behaviour was subject to a high degree of irregularity. Olsson's experimental work also indicated the cavitation pressure to be atmospheric. In some tests this was the result of ventilation. Nevertheless the cavitation pressure remained atmospheric even when the external air was blocked off.

In his experimental work on dynamically-loaded, aligned, axial-groove bearings, Patrick (10) observed periodic behaviour over about 50 to 100 load cycles. This appeared to be due to the accumulation of air generated by cavitation, which was periodically expelled from the bearing ends. The above accumulation was believed to result from the slow rate of re-absorption of air.

Etsion and Ludwig (55) conducted measurements on a steadily loaded submerged bearing. The results indicated the cavitation to be mainly gaseous, with a constant pressure slightly below atmospheric over most of the cavitation zone. A rise in pressure over about 45° of the circumference preceding film reformation was observed. This was also considered to be due to the finite time required for re-absorption of air. The bearing conditions used by Etsion and Ludwig ($\epsilon = 0.4$, $C_D/D = 0.004$ with no oil grooving), unfortunately were not representative of normal practical applications. This situation is not uncommon in experimental work in this area. Whilst such work is valuable in furthering our understanding of cavitation, the above conditions indicate the need for caution when endeavouring to apply it to practical situations.

Jacobson and Hamrock (62) carried out experiments on dynamically loaded bearings using high speed cine - photography to record the cavitation behaviour. This showed the co-existence of both gas and vapour cavitation bubbles, with the former surviving well into the high pressure region. The high speed film also showed both gas release and re-absorption to be relatively slow processes. In contrast, vapour bubbles were seen to form and collapse rapidly, and were not subject to any long term build up.

Experimental measurements on a squeeze film bearing by Dede and Holmes (69) gave peak film pressures substantially lower than predicted. This was similarly attributed to the persistence of cavitation bubbles into the high pressure part of the squeeze film cycle.

A test rig in which pure squeeze film conditions were invoked between circular pads, was used for the experimental work of Parkins and May-Miller (67). The fixed pad was transparent, thus permitting cine-photographic recording of the cavitation patterns using stroboscopic light. Different operating regimes resulted in the formation of cavitation bubbles from within the film, and bubbles drawn from the pad periphery (ventilation). Vaporous cavitation could not be positively identified, and the cavitation observed appeared to be predominantly gaseous.

Dowson et al (75) obtained measurements of the extent of cavitation in aligned bearings with three different lengths of axial oil groove. Correlation of the experimental and predicted (74) cavitation zones was good, except at low ϵ . At this condition, the predicted cavitation zone extended further downstream. The generally good correlation was considered to be due to the theoretical analysis satisfying flow continuity within the cavitation zone.

Transparent bearing cavitation studies by Heshmat and Pinkus (81) showed the axial cross sectional form of the cavitation zone. This appeared to lie between the commonly used striated cavitation model, and the less common adhered film model. An illustration of this observation is given in Fig. 3. of reference (88) by the author.

2.4. Outline of the Work Reported

Almost all the work reported in this thesis has been published or recently submitted for publication. The thesis itself therefore simply serves to link these papers into coherent whole, and to provide additional details where considered necessary. An outline of the areas of investigation covered was given in the statement of objectives (1.3). Reference to the above papers has also been made in the appropriate sections of the literature review. The purpose of this section is to present an outline of these papers in chronological sequence.

2.4.1. Reference (72)

The numerical analysis method for hydrodynamic journal bearings, developed by the author, is described in this paper. This method formed the basis of all the work subsequently reported. A comparison of results predicted by the above method, with other published and unpublished data for steadily loaded bearings, is included. The use of 32 linearised dynamic coefficients, to model the oil film response of a dynamically misaligned bearing, is discussed. An outline of a bearing performance computer program, developed for practical application, is given. This used the method described in reference (8), with numerical data bank matrices replacing the graphical data format.

2.4.2. Reference (77)

In this reference a time stepping form of journal orbit analysis method, developed by the author, is described. This is intended for use with bearings subject to high dynamic loading, such as crankshaft main bearings. The method included an optional oil film history modelling facility. An investigation of the influence of oil film history in a half circumferential oil groove bearing was carried out. The effect of variation of journal mass was also considered, and the results presented in the paper.

This work was inspired by that of Jones (57) on oil film history, and of Holmes and Craven (19) on crankshaft mass. Its novelty was in considering these factors simultaneously.

In relation to sterntube bearings, this and subsequent papers (85), (86), which dealt with aligned circumferential oil groove bearings, may appear to be a digression. However, measured journal amplitudes by Hyakutake et al (24) indicated that a time stepping journal orbit analysis would be necessary for sterntube bearings. In view of the complexities pertaining to the dynamically misaligned sterntube bearing, the experience gained in the above simpler situation proved to be an invaluable preliminary exercise.

2.4.3. Reference (87)

This paper presented some of the results of a steady load performance - parameter study for sterntube bearings. Data for the more significant linearised oil film stiffness and damping coefficients covering dynamic misalignment conditions were included. A comparison of dynamic co-efficient data with theoretical results by Pafelias (25) was given. The bearing concerned was a 150° partial arc type of L/D = 0.5, and the comparison extended to all 32 coefficients and 5 steady load performance parameters.

The practical bearing performance program, described in reference (72), was extended to include misalignment and oil head pressure as input variables. This program was used to conduct a realistic investigation into the optimum L/D ratio for sterntube bearings, as a function of mis-alignment angle and clearance. The results of this investigation are also presented.

2.4.4. Reference (85)

As part of the continuing work on journal orbit prediction, the oil film response to substantial journal lateral velocities was examined. This work was confined to the aligned full circumferential groove bearing, and highlighted the influence of cavitation on non-linear behaviour.

As a result of this study, a new method of predicting oil film force components was devised. This is called the Reaction Method, and is based on the use of pre-computed velocity coefficients. The predicted oil film response data were produced by means of an extended version of the numerical analysis method (72), which was published later (90).

2.4.5. Reference (86)

In this paper, the application of the Reaction Method (85) to journal orbit prediction is shown, together with orbits produced by the more rigorous method (77). The co-author, Dr. D.W. Parkins, produced comparative measured orbits using an experimental test rig. An aligned full circumferential oil groove bearing was used. Orbits were predicted both with and without the oil film history model, using the earlier (77) analysis method.

2.4.6. Reference (88)

This paper differs from the others in that it was an internal publication to Lloyds Register of Shipping. Consequently the basic aim of the paper differed from the others. It was intended to provide a broad account of the research carried out by the author, and was written for a readership which did not have a specialised knowledge of bearing hydrodynamics. Although it partly overlaps reference (87), this paper was considered to provide worthwhile additional information. The approval of the Committee of Lloyd's Register of Shipping was obtained for its inclusion in this thesis.

In relation to reference (87), considerably more detail is given with respect to sterntube bearing design and environmental factors. The interaction of bearings with shafting systems is discussed. In particular, the application of the practical bearing performance program to an interactive solution of the shaft alignment problem, is shown. Results are included to illustrate the use of the above program for bearing clearance and length optimisation, and in providing generalised guidance on maximum specific bearing pressure. Both of these examples included consideration of misalignment.

2.4.7. Reference (90)

The previously reported numerical analysis method (72) was extended to account for conditions involving significant journal lateral velocities. The principal factor concerned was the interaction of squeeze action with cavitation generated by wedge action. In addition to presenting details of the extended numerical analysis method, the paper discusses the complexities of observed cavitation behaviour. The associated problems of formulating adequate theoretical cavitations models are included in this discussion.

A quasi steady approach was necessary, since the objective was to facilitate the production of an oil film response data bank, for use in journal orbit analysis (85), (86). This was in contrast with the oil film history model (77), (86), and the advantages and limitations of the quasi steady approach are discussed.

2.4.8. Reference (91)

A study of the oil film response characteristics in a sterntube bearing was carried out, and the results reported in this paper. This work was similar to that reported in reference (85), but addressed the more complex situation of dynamic misalignment conditions. The extended numerical analysis method (90) was again used.

A non-linear oil film response model, using pre-computed coefficients, was developed. This was based on the Reaction Method (85), and adapted to the sterntube bearing conditions of operation. A full account of the development of this model is given.

2.4.9. Reference (92)

In the final stage of the work covered by this thesis, the performance of a sterntube bearing when subjected to dynamic load, was examined. The "in service" measurements by Hyakutake et al (24) were used for comparative purposes. Preliminary examination of the propeller shafting system concerned, indicated that any attempt to consider the sterntube bearing only, would be entirely inappropriate. Accordingly, the investigation reported in this paper encompassed the interaction of the bearings with lateral vibration of the propeller shafting.

Lateral vibration response predictions were made using both linearised coefficients, and the non-linear oil film model described in reference (91). The results presented indicate the significance of bearing damping. An investigation was also carried out of the effect on shafting lateral vibrations, of reducing the after sterntube bearing length.

2.4.10. Relationship with Previously Published Work

Some comments have already been made on the relationship between the work reported in this thesis and previous publications. In this section the main points will be summarised.

The numerical hydrodynamic analysis method (72) is essentially similar to the finite difference solution of Reynolds' equation. Many examples of the finite difference solution have been published, some of which are referred to in the literature review. The author's method differs in its direct approach to the finite solution format. In accounting for flow continuity within the cavitation zone, it is considered to be comparable to the work of Elrod (53). The precision with which the cavitation zone boundaries are located, is directly related to the oil film element mesh chosen. This is an approximate approach, but in terms of bearing performance prediction, the accuracy is acceptable for practical purposes. The form of this cavitation model makes it relatively simple to implement.

With respect to the extended version of the numerical analysis method (90), no comparable previously published literature is known to exist.

Both the steady load performance parameter data and practical bearing analysis program of reference (87) reflect the basic approach of ESDU 66023 (8). This work is novel, however, in applying this approach to the misaligned sterntube bearing with variable oil head pressure. As indicated in this paper, the use of 32 linearised oil film coefficients for dynamically misaligned bearings had been advanced by Pafelias (25). Again, it was the derivation of such coefficients for the sterntube bearing that rendered reference (87) unique. Reference (88) is essentially similar to (87), and simply presents additional material.

The preliminary excursion into journal orbit prediction (77) effectively combined the work of Holmes and Craven (19) on the influence of crankshaft mass, and that of Jones (57) on oil film history. An original method was developed for the solution of the time stepping procedure.

In examining the theoretical influence of cavitation on oil film non-linearity, reference (85) has no known counterpart in the published literature. The Reaction Method developed from this study is comparable to the other published oil film response prediction methods based on the use of pre-computed data e.g. Booker (16), Moes et al (64), Childs et al (39) and Moes et al (80). Of these, only the last is equivalent to the Reaction Method with respect to the capability of handling circumferentially asymmetric bearings. In relation to the previous methods, the Reaction Method is considered to be simple to apply, yet rigorous in its modelling of predicted oil film behaviour.

The validity of the Reaction Method was substantiated in reference (86).

Nothing comparable to the non-linear model for dynamically misaligned sterntube bearings (91) was found in the published literature. Earlier workers in this area Hylarides and Gent (44), and Hayama and Anoda (66), represented the sterntube bearing with linear stiffness terms only. No consideration was given to bearing damping, and a single mass (propeller) shafting model was used. The later work by Karni et al (89) employed a finite element analysis of the sterntube bearing oil film at each time step of an orbit "marching out" procedure. This was a realistic bearing model, apart from the crude treatment of cavitation (truncated negative pressures). The computing time required for the above solution would have been substantial, and the author's non-linear model represents a worthwhile advance in practical computing terms.

The work on marine propeller shafting lateral vibration prediction (92) represents an advance on that by Karni et al (89), in its application to a realistic shafting system. Other subsidiary advances were the indication of the significance of bearing damping, and of the acceptability of a linear oil film model for the test case used.

3. ANALYSIS TECHNIQUES

3.1. Assumptions and Approximations

Close examination of almost any physical phenomenon reveals a complexity that defies the imagination. It is invariably necessary to simplify observations in order to reduce them to a level at which the human observer can comprehend a behavioural pattern. To describe phenomena mathematically, in order that predictions of related behaviour may be made, usually requires an even greater degree of simplification. The making of assumptions and approximations is the implementation of the above simplification process.

Assumptions are made where it is necessary to cover gaps in our knowledge, in order that related analytical work may proceed. Such assumptions may be revised in the light of subsequent knowledge gained. Many assumptions are, however, made in the full knowledge that they are at variance with the physical realities. For example, in the bearing hydrodynamic analysis an isoviscous oil film was assumed by the author, in common with the majority of other workers in this field. No-one seriously believes that a real bearing oil film has a constant viscosity, but provided a suitable effective viscosity is chosen, the bearing performance predictions will be of acceptable accuracy. The assumption in this situation is made, not to cover any gaps in our knowledge, but to considerably simplify the analytical process. In this context, the term approximation would seem to be more appropriate than assumption. Since the usage of the word assumption in this manner is well established, this convention will be adhered to.

From the above comments it follows that the assumptions made in this field are frequently inconsistent with observed behaviour. This is justifiable in terms of the simplification and/or enhanced efficiency of the associated analysis method, provided the prediction accuracy is acceptable.

The assumptions made for the work reported in thesis are set out in the published papers where appropriate. A summary of the main features is given below:

The assumptions related to the numerical hydrodynamic analysis method are given in reference (72). These are generally fairly standard assumptions for work in this area. Despite the accounting for flow continuity within the cavitation zone, the related assumptions are not in accord with experimental observations. This comment is particularly applicable to the assumption that cavities may form or collapse instantaneously, where required, to satisfy flow continuity and the specified constant cavitation pressure. The cavitation model is nevertheless considered to be adequate, with respect to overall bearing performance predictions, in most realistic applications. Furthermore, in the present state of knowledge of bearing cavitation, the feasibility of a more rigorous, yet practical cavitation model, is questionable.

The extended hydrodynamic analysis method (90) retained the assumptions of reference (72). In addition, the assumption that the dynamic situation may be treated in a quasi-steady manner, was incorporated. The quasi-steady assumption contrasts with the oil film history model described in reference (77). It has been shown (57), (86), that the effects of oil film history are only significant where the journal orbit is large in relation to the bearing clearance, and the oil feed geometry is relatively inefficient. In situations other than the above, the quasi-steady assumption is considered to be consistent with an acceptable level of journal orbit prediction accuracy. This assumption facilitates a relatively fast journal orbit analysis by the use of pre-computed oil film response data.

The journal orbit predictions covered by references (77) and (86), assumed that a single bearing and journal mass could be analysed in isolation. This was valid for the experimental test rig from which the measurements presented in reference (86) were obtained. For diesel engine main bearings, however, it may not be justifiable to neglect the elastic coupling between main bearings due to the crankshaft. The analysis of all the bearings in a system, taking account of elastic coupling by the shafting, was carried out in the work covered by reference (92).

3.2. Numerical Hydrodynamic Analysis Method

The details of the numerical hydrodynamic analysis method are well documented in reference (72), and the extended version covering significant journal lateral velocities in reference (90). No additional explanation or comment is needed here. The influence of the element mesh upon the accuracy of this method is examined in Appendix 1.

3.3. Practical Bearing Analysis Program

The need for a practical analysis program is outlined and its implementation, following the method described in ESDU 66023 (8), is given in reference (72). A further development of this type of program, specifically designed for the sterntube bearing, is described in reference (87). In this later program, misalignment and oil head pressure are added to the input variables. Additional details of the sterntube bearing practical analysis program are given in reference (88). In particular, it is shown how this program simulates the interaction of parameters in a real bearing.

3.4. Linearised Dynamic Coefficients

Reference (72) indicates how the linearised dynamic coefficients may be derived by the use of numerical differentiation, in conjunction with finite displacement and velocity perturbations applied to the journal. The requirement of 32 such coefficients for the dynamically misaligned sterntube bearing is also indicated. Reference (87) illustrated the influence on calculated coefficients of displacement perturbation amplitude in both the positive and negative directions. The diminished effect of perturbation amplitude, on the average coefficients calculated with positive and negative perturbations, is also shown. This averaging process has been used by the author, except when calculating the "local" coefficients at each time step during a journal orbit "marching out" procedure : see references (77), (86), (92). Such "local" coefficients use the estimated time step displacement and velocity changes, positive or negative, as perturbations. In this way the coefficients are matched to the time step conditions, thereby enhancing accuracy. Reference (88) gives a more detailed discussion of linearised dynamic coefficients, with particular reference to the sterntube bearing.

3.5. Non-Linear Oil Film Models

Bearing oil films are highly non-linear with respect to both stiffness and damping. As discussed in reference (91), the former is due to the characteristics of viscous flow in relation to oil film geometry. Non-linear damping differs in that it is mainly due to cavitation, as shown in reference (85).

The extent of the non-linearity problem imposes a limit, with respect to journal displacement and velocity amplitudes, on the usage of linearised coefficients. This limit also depends on the acceptable level of prediction accuracy.

The crankshaft main bearing clearly falls into an area where the amplitudes are such that linearised coefficients cannot be used, except on a "local" basis as indicated in the previous section. In order to solve the non-linear response problem, the journal orbit is "marched out" in a series of finite time steps. Where this process relies upon the use of numerical hydrodynamic solutions for the oil film force components and dynamic coefficients at each time step, the computing time is excessive. This was the situation in reference (77) and in method A of reference (85).

The computing time for a journal orbit analysis can be substantially reduced by the use of a suitable form of pre-computed data. This was the motivation for the development of the non-linear oil film model for aligned bearings, which is fully described in reference (85).

The discussion in section 2.3.4.1. indicated that the sterntube bearing - marine propeller shaft system appeared to be in a "grey" area, with respect to the acceptability of linearised coefficients. Accordingly the above non-linear model for aligned bearings (85) was adapted for use with the dynamically misaligned sterntube bearing. This is a considerably more complex situation, and consequently necessitated a major revision of the way in which journal displacement was handled. The number of coefficients required was also substantially increased. A detailed account of this development is given in reference (91).

3.6. Journal Orbit Analysis

The preceding section indicated the need for the journal orbit type of analysis in situations where the non-linearity of the oil film response becomes significant. In this section the nature of the journal orbit analysis will be considered.

The basis of this method is the "marching out" of the journal orbit in a series of finite time steps. In order to carry out this process, it is necessary to predict the unknown journal displacement and velocity components at the end of any given time step, from corresponding known conditions at the start. The author's solution to the time step prediction problem is based on the equations of motion for the mean conditions during the time step. Linearised dynamic coefficients calculated for the "local" conditions at each time step, and matched to the estimated displacements and velocity changes during the time step, are used in this solution.

The journal orbit analysis is capable of dealing with transient response problems, but this is outside the scope of the work reported in this thesis. For cyclic (i.e. non-transient) dynamic load, the "marching out" process is continued until an acceptable convergence of successive orbits is obtained. The journal location at the start of the analysis is arbitrary. A suitable choice for the initial location may, however, minimise the number of orbits required to attain convergence.

This type of analysis is prone to numerical instability. Various techniques have been employed by the author to deal with such problems. Whilst these techniques could undoubtedly be improved by further development, satisfactory operation of the associated computer programs was attained.

Details of the journal orbit analysis theory and operation, for an aligned bearing with a single journal mass, are given in reference (77). This is repeated in reference (85), which differed only in the addition of the Reaction Method as an optional means of deriving the oil film force components and dynamic coefficients at each time step.

Reference (92) extended the above journal orbit analysis method to the dynamically misaligned sterntube bearing - propeller shaft system. For the test case used this involved the simultaneous prediction of the orbits for six elastically coupled mass elements each having four degrees of freedom. A total of three bearings were included in the model. The basis of the time step prediction method was identical to that used in references (77) and (85). In view of the considerable increase in complexity, matrix inversion was employed for the solution in reference (92). More elaborate measures for dealing with numerical instability were also incorporated.

3.7. Estimation of Propeller - Wake Excitation

The estimation of propeller excitation due to the operation in a ship's wake is peripheral to the main theme of this thesis. Nevertheless, it was necessary to employ some method of estimation for the work reported in reference (92). No wake field data were available for the test case used; i.e. the 210,000 d.w.t. tanker "Keiyo Maru". In view of the above factors, the use of a quasi-steady analysis method was considered to be justifiable. This is regarded as a fairly simple, approximate method. Details of this method are given in a Germanischer Lloyd publication (20), and the following is a brief outline:

The analysis comprised derivation of the mean advance coefficient taking account of the variation of water and blade velocity over the length of the blade. Computation of the mean advance coefficient was carried out for a range of blade rotation angles from 0° to 180°. The propeller torque and thrust coefficients were obtained from a computer program based on data given by Oosterveld and Oossanen (31). These coefficients were used in conjunction with the mean advance coefficient data to compute the axial and tangential forces acting on a single propeller blade. The above forces were computed for the range of rotation angles from 0° to 180°, the forces from 180° to 360° being a "mirror image" due to the assumed wake field symmetry. Finally the tangential force components and the moment components due to axial force were summated for all the propeller blades, taking account of the relative disposition of each blade to the wake field.

Since the propeller of the "Keiyo Maru" test case, had five blades, these forces and moments were periodic over 72° of shaft rotation.

4. RESULTS

4.1. Steadily Loaded Bearings

Reference (72) presents comparisons of performance results for steadily loaded aligned crankshaft bearings, and misaligned sterntube bearings, with other published theoretical results. An unpublished cavitation map, for an aligned circumferential oil groove bearing, was kindly provided by Mr. F.A. Martin of the Glacier Metal Co. This is included in reference (72) together with a comparative cavitation map derived by means of the author's analysis method.

A similar cavitation map comparison has been carried using theoretical results produced by Dowson et al (73) and Lundholm (13). This comparison is shown in Fig. 3.

Reference (87) gives load capacity, power loss, oil flow rate and oil film moment data for a steadily loaded misaligned sterntube bearing. The data was computed by means of the author's numerical analysis method (72). All the data are plotted in dimensionless terms as a function of eccentricity ratio. The data shown are examples of the type utilised in the practical bearing analysis program.

Reference (88) repeats the presentation of the above data and, in addition, the following results are given:

a) The effect upon axial load distribution of eccentricity ratio, misalignment angle,. L/D ratio and journal bow (axis curvature).

b) The effect of oil head pressure upon the extent of cavitation in the top and bottom halves of the bearing.

c) The effect of oil head pressure upon load capacity when aligned and misaligned.

d) The effect of load vector angle on load capacity and attitude angle.

All the above results are given in dimensionless terms.

Both references (87) and (88) include the results of an investigation into the optimum L/D ratio for a misaligned sterntube bearing. The practical bearing analysis program was used for this investigation. These results show the optimum L/D ratio as a function of misalignment for two diametral clearances. The results for the normal sterntube bearing clearance (C_D/D = 0.002), indicated the optimum L/D ratio to lie well above the usual value of about 2.0, except at misalignment angles that would be considered excessive in normal practise. At the reduced bearing, clearance (C_D/D = 0.001) the sensitivity to misalignment is significantly increased, and the optimum L/D ratio correspondingly reduced.

In reference (88) results illustrating two other applications of the practical bearing analysis program are presented. The first shows bearing clearance - length optimisation for a particular example case with a given misalignment angle. In the second application, generalised guidance on maximum specific bearing pressure as a function of misalignment angle and L/D ratio is given.

4.2. Linearised Dynamic Coefficients

No published data were found for linearised dynamic coefficient data applicable to either aligned or misaligned sterntube bearings. In order to verify the results of the author's analysis method, a comparison with theoretical and experimental data by Parkins (51), was originally made. This comparison related to an aligned full circumferential oil groove bearing, and the results are given in Figs 4 to 7. The dynamic coefficients are plotted against their corresponding displacement or velocity perturbation amplitudes (positive and negative). A good correlation between the two sets of theoretical results was obtained. The correlation with the experimental dynamic coefficients was poor. Possible reasons for this were discussed in section 2.3.5.

With regard to the 32 dynamic coefficients required for a dynamically misaligned bearing, the only published data found were for a 150° partial arc bearing of L/D = 0.5 by Pafelias (25). A comparison with these data is given in reference (87) The correlation of these results was considered to be reasonable, and possible reasons for the differences are discussed in reference (87). Reference is made to comparative results at $\epsilon = 0.4$ where the correlation is much better. These results are given in Table 3.

Reference (87) presents some examples of stiffness and damping coefficient data for a dynamically misaligned sterntube bearing. This is restricted to the force - lateral motion and moment - angular motion coefficients. The force - angular motion and moment - lateral motion coefficients are considered likely to be of less significance. This assessment is supported by examination of the data in Table 4, which corresponds to that used for propeller shaft lateral vibration prediction in reference (92). The ultimate test of their significance would be to delete these coefficients when carrying out the lateral vibration prediction, and observe the change in result. This test has not been carried out to date. In giving the oil film force and moment changes due to positive and negative perturbations, Table 4 also provides an indication of the degree of non-linearity.

The stiffness and damping coefficient data in reference (87) is given as a function of eccentricity ratio. This data is repeated in reference (88), and in addition, the significant influence of load vector angle is shown. In view of the number of variables involved (ϵ, L/D, θ_F , P_H , α, β, B_{ow}) a comprehensive investigation of their influence upon the steady load performance and dynamic coefficients is not practicable. A few general comments upon the influence of some of these parameters is given in reference (88).

Reference (92) tabulates the linearised dynamic coefficient data used for all three of the bearings incorporated in the "Keiyo Maru" propeller shafting model.

4.3. Oil Film Forces in Aligned Dynamically Loaded Bearings

Reference (85) presents oil film force component data as a function of journal lateral velocity. Although these results are for an aligned full circumferential oil groove bearing, they are valuable in providing an insight to the influence of cavitation upon non-linear behaviour. In particular, they show how cavitation affects the interaction of squeeze and wedge action in such a way that the principle of superposition is not applicable. These results are subject to the limitations of the quasi-steady approach, as discussed in section 3.1.

4.4. Journal Orbits for Single Mass Systems

This section relates to single bearing and journal mass systems with no elastic shafting forces or misalignment. As in section 4.3., the results covered by the above heading are not directly concerned with the misaligned sterntube bearing. These results nevertheless contribute towards a clearer understanding of the factors influencing journal orbits. This understanding is enhanced by the relatively simple configuration.

The journal orbit results in reference (77) show the significance of both oil film history and journal mass for a half circumferential oil groove bearing. In addition, they indicate the degree of interaction between these two factors. This is due to a response lag induced by the higher journal mass, which thus provides more time for the dissipation of cavitation, and thereby decreases the influence of oil film history.

Reference (86) verifies the author's theoretical methods by comparison of predicted journal orbits with examples obtained experimentally by Dr. D.W. Parkins. The bearing concerned was an aligned full circumferential oil groove type. This paper also includes a comparison of orbits derived by the rigorous method described in reference (77), and those obtained by use of the Reaction Method, which is described in reference (85). The influence of oil film history modelling was investigated by means of the rigorous method, and found to be negligible in this instance. This is attributed to a combination of a fairly small orbit in relation to the clearance circle, and the relatively efficient oil feed provided by a full circumferential oil groove.

The correlation between the journal orbits produced by the two theoretical methods is good. Whilst the correlation between the journal orbits produced by both theoretical methods, and those obtained experimentally is considered to be generally good, two notable differences did occur.

The first concerned part of the orbit where oil film forces would be small, and cavitation extensive. This involved a greater movement to the right, in the theoretical orbits relative to the experimental orbits. It was postulated that this may be due to the cavitation pressure during dynamic conditions being substantially less than that for steady conditions. Cavitation pressures derived by Dr. Parkins to obtain agreement between experimental and theoretical results at steady load, were used in the computation of the theoretical orbits.

The second difference, between the theoretical and experimental journal orbits, concerned the significantly greater eccentricity ratio of the latter in the maximum load region of the dynamic cycle. This difference was attributed to bearing elastic deflection, despite the substantial bearing housing used in the experimental test rig.

4.5. Oil Film Forces and Moments in a Dynamically Misaligned Bearing

Example results from a study of the relationship between oil film forces and moments, and both lateral and angular journal axis velocities, are presented in reference (91). These results relate specifically to the after sterntube bearing of the tanker "Keiyo Maru", which was used as the test case in reference (92). The results exhibit similarities to those for the aligned full circumferential oil groove bearing (see section 4.3. and reference (85)). Differences due to the additional complexity resulting from the inclusion of angular journal axis velocity are, however, evident. Further differences due to the lack of circumferential symmetry, resulting from the presence of two axial oil grooves, are also significant.

In this situation, the number of variables precludes an exhaustive investigation. The example results given in reference (91) are sufficient to illustrate the main features of the force and moment - journal velocity relationships. As in section 4.3. and reference (85), these results are subject to the limitations of the quasi - steady approach.

4.6. Lateral Vibration of a Marine Propeller Shafting System

Results covering the interaction of hydrodynamic bearings with the lateral vibration of a marine propeller shafting system are given in reference (92). The investigation described by this paper utilised the measurements by Hyakutake et al (24), for comparative purposes. The measurements were obtained on the tanker "Keiyo Maru". Both sterntube bearings and the aft plummer bearing were included in the theoretical model.

The theoretical journal orbits derived using both linear and non-linear (see reference (91)) oil film models for the after sterntube bearing, did not differ significantly. A comparison of the theoretical and measured journal orbits is shown in reference (92). The largest discrepancy is in the vertical direction of the aft end of the aft sterntube bearing. This discrepancy is most likely to be due to bearing elasticity, which was neglected in the theoretical work. The general correlation of the predicted and measured journal orbits is considered to be good, when allowances are made for the uncertainties relating to "in service" measurements.

Results are also presented which show the predicted vertical and horizontal lateral vibration amplitudes at the propeller, over a range of shaft speeds. A simple forced - damped response analysis was applied to this data. The results of this analysis indicate the system to be highly damped, to the extent that no peaking of the amplitude occurs at the predicted fundamental lateral vibration resonance. A significant contribution to this damping is considered to be due to the aft sterntube bearing. Further investigation would be required to determine positively the significance of the various sources of damping.

The vertical vibration amplitudes for the complete shafting model are shown in graphical form. This includes results showing the effect of reducing the aft sterntube bearing length. The effect of the corresponding reduction in moment - angular motion coefficients for the aft stern-tube bearing is clearly shown. This comprises an increase in the angular displacement amplitude in way of the aft sterntube bearing, which results in an increase in lateral displacement amplitude between the aft sterntube bearing and the aft plummer bearing. The results indicate that the lightly loaded forward sterntube bearing offers very little resistance to lateral vibration. Lateral vibration amplitude at the propeller was not significantly increased by the reduction in aft sterntube bearing length. This was due to the length being reduced from the forward end of the bearing only, thereby simulating a realistic modification to an existing system. The effect of increased amplitude of angular motion at the aft sterntube bearing was therefore offset by a shift of the effective support point in the aft direction.

5. DISCUSSION ON PREDICTION ACCURACY

5.1. Quantitative and Qualitative Accuracy Considerations

With regard to prediction accuracy, there are two basic viewpoints to be considered. These may be referred to as pure research and applied research. The former essentially seeks to advance our understanding of observed phenomena, and the development of theoretical models to simulate the behaviour contributes towards this aim. In applied research, however, theoretical models are similarly developed, but the main motivation is the application to practical problems such as design assessment or failure analysis. The work reported in this thesis is biased towards the latter. This distinction between pure and applied research is intended to reflect only a difference in emphasis, rather than a firm demarcation. The fact is that pure research frequently results in enhanced predictive techniques for practical application. Conversely, applied research usually makes some contribution towards an understanding of the related physical phenomena.

In both pure and applied research, prediction accuracy in quantitative terms is not considered to be of critical importance. This should not be taken to mean that the prediction of magnitudes is totally unimportant, since any large disparity with corresponding measurements may indicate unsatisfactorry assumptions or modelling details in the theory. The measured data, with which the theoretical predictions are compared, are also subject to some degree of inaccuracy. In certain areas of bearing experimental research, accurate measurements are particularly difficult to achieve e.g. bearing clearance in the operating condition.

The qualitative value of predicted results is considered to be more important than quantitative accuracy for both pure and applied research. In the former, if the theoretical model succeeds in simulating the main characteristics of the observed behaviour, then the understanding of the situation is likely to be good. If such qualitative agreement is attained we can then, for example, use the theoretical method to explore the significance of the various parameters individually. Such an exercise may be difficult or even impossible to carry out on an experimental basis.

In applied research, the theory should be properly regarded as the rational basis upon which measurements and service experience may be assessed. It provides a framework upon which all the relevant parameters may be taken into account. The theory alone, however, does not generally enable safe operating limits to be satisfactorily determined. For this, the theory must be related to service and/or test experience. In practical applications some degree of empiricism is therefore usually necessary.

The areas in which the work reported in this thesis are considered to require more experimental and service experience feedback are as follows:

1. Correlation of the predicted minimum film thickness for sterntube bearings under steady and dynamic misaligned conditions, with service experience i.e. excessive local wear or total failure by wiping.

2. Correlation of dynamic alignment predictions with measurements made under service conditions. The location of the effective support point in the aft sterntube bearing is of particular interest.

3. Correlation of predicted lateral vibration amplitudes in way of seals with excessive leakage and/or seal failure.

4. The measurement of cavitation extent and pressure, and bearing temperature distribution under service conditions for a sterntube bearing. Whilst these measurements would be useful, they are not considered to be as important as the above aspects.

5.2. Review of Assumptions

The majority of the assumptions made in this investigation are likely to be satisfactory for most practical purposes. It is important, however, that an open minded view on this area is retained. All assumptions should be subject to review and amendment, where appropriate, in the light of new experimental evidence. This does not mean that the theory should necessarily take account of all new findings, since this may lead to a prohibitive increase in computing time for an insignificant improvement in prediction accuracy.

With respect to sterntube bearings, the availability of reliable experimental data is, at present, very limited. The only assumption on which serious doubt has been cast by comparisons with measured data, is that bearing elasticity may be neglected. An indication of this shortcoming is given in reference (86) for the aligned full circumferential groove bearing, in relation to the relatively well defined conditions of an experimental test rig. More significant evidence of bearing elastic deformation is given in reference (92), for the sterntube bearing under service conditions. The details of this "in service" situation were not accurately defined, and the apparent bearing elasticity could only be considered as a rough indication.

Although sterntube bearing elasticity may be significant, there is a strong practical incentive to retain the rigid bearing assumption. The incentive concerned is that of computing time, as indicated in the literature review. In this situation the use of approximate hydrodynamic solutions, to overcome the computing time problem, are rendered more difficult by misalignment. A suggested compromise theoretical approach would be to compute the elastically deformed bearing shape for the steady load corresponding to the mean running condition, and then to "freeze" this shape for subsequent dynamic calculations. This would appear to be a reasonable proposition for the relatively modest dynamic loading generally associated with sterntube bearings.

The semi-empirical approach, as indicated in the previous section may, however, enable satisfactory correlation of service experience with theoretical predictions based on the rigid bearing assumption, to be attained. Further work in this area is clearly necessary, and more detailed "in service" measurements are desirable.

5.3. The Non-Linear Oil Film Model

In the development work leading to the Reaction Method, which is described in reference (85), the linearised stiffness and damping coefficients were found to be completely inadequate. This finding was in relation to the experimental test rig orbits measured by Parkins (86). It was therefore concluded that non-linearity of the oil film response was significant in this situation, hence the need to develop the Reaction Method non-linear model. The essential features of the above orbits, which are considered to have contributed to this conclusion, were as follows:

1. The orbits were of moderate size in relation to the clearance circle.

2. Relatively high eccentricity ratios (> 0.9) were attained.

3. No elastic shafting forces were involved.

For crankshaft bearings generally, the use of some form of non-linear oil film model is therefore considered to be necessary. The Reaction Method is an advanced example of such a model, and reference (86) demonstrated the results to be of generally good accuracy.

From the experience gained in the development of the Reaction Method, it was anticipated that a similar, but more complex, non-linear oil film model would be required for a realistic analysis of the dynamically loaded stern-tube bearing. The development of this model is described in reference (91). In reference (92), however, the results produced by the above non-linear model are shown to differ insignificantly from those produced by means of linearised oil film stiffness and damping coefficients. The reasons for the good correlation of linear and non-linear results are thought to be as follows:

1. The orbits were smaller in relation to the clearance circle than those measured by Parkins (86).

2. The maximum eccentricity ratios attained were relatively modest ($<$ 0.77 at the bearing aft end and substantially less at the axial centre).

3. The bearing oil film forces and moments would be rendered less significant by the inclusion of shafting elastic forces and moments.

These results were, however, for one particular test case. Whilst they are encouraging with respect to the potential saving in computing time, this level of agreement between linear and non-linear oil film model results may not be typical. Analysis of a whole range of real sterntube bearing - propeller shafting cases would be necessary before any general comment on the acceptability of linearised coefficients could be made. Until this exercise is carried out, the need for a non-linear oil film model in some sterntube bearing situations must be regarded as a possibility. This would be mainly dependent on the magnitude of the bearing load, both steady and dynamic.

6. DISCUSSION OF THE SIGNIFICANCE OF THE RESULTS

6.1. Steadily Loaded Bearing Results

The steadily loaded bearing results derived in this investigation have been shown to be of value with respect to the following practical applications:

1. The assessment of operating condition safety. For the relatively low speed sterntube bearing, this is mainly judged by reference to the minimum oil film thickness.

2. Bearing design parameter optimisation.

3. Investigation of operation under "off design" conditions, e.g. significant displacement of the load vector angle from the commonly assumed vertically downward location.

4. The provision of generalised guidance on acceptable specific bearing pressures and misalignment angles for sterntube bearings. Prior to this work, the general practice in this field was to treat these parameters as being independent of each other, with prescribed non-generalised maximum limits that were purported to be related to service experience. Clearly a lightly loaded bearing can safety accept a larger misalignment angle than a heavily loaded bearing. The guidance provided recognises this parameter interdependence.

5. The calculation of the axial location of the effective single support point in a misaligned sterntube bearing. This location is required for shaft alignment analysis

purposes.

Although sterntube bearings are subject to dynamic loading, the level is such that satisfactory assessments, as indicated above, can be made on the basis of the mean steady load.

6.2. Dynamically Loaded Bearing Results

The earlier part of this work, relating to dynamically loaded bearings, involved the computation of linearised oil film stiffness and damping coefficients. These coefficients have been commonly used to model hydrodynamic bearings in the analysis of rotor dynamics problems. It has generally been assumed that oil film moments, arising from angular motion of the journal axis, are negligible. The result of this assumption is that only 8 force related coefficients are required. For sterntube bearings with typical L/D ratios of 2 or more, the neglect of oil film moments was considered to be unjustifiable. In this investigation 32 force and moment coefficients were therefore calculated for the sterntube bearing. The moment coefficients effectively render the sterntube bearing support semi encastre, in contrast with the simply supported conditions usually assumed. A reduction in sterntube bearing length was examined, and the resulting predicted lateral vibration amplitudes given in reference (92) indicate the significance of the moment coefficients. Reference (92) also showed the significance of damping in the marine propeller shafting system. The sterntube bearing appears to make an important contribution to this damping. As a result of the high level of damping, the influence of the moment coefficients upon lateral vibration resonant speeds is somewhat academic. However, as noted previously, the results in reference (92) are for one particular test case, and other cases may differ significantly.

The results relating to non-linear behaviour in dynamically loaded bearings are significant in the following distinct ways:

1. Reference (77) clearly illustrates the importance of oil film history considerations in a half circumferential groove aligned crankshaft bearing. The dependence of the oil film history effect upon journal orbit size and the oil feed efficiency, is also indicated by references (77) and (86). Reference (86) covers the full circumferential groove bearing with smaller orbits. In reference (77), the results show the additional effect of journal mass.

2. Reference (85) results clarify the significance of cavitation in determining the non-linear behaviour of bearing oil films in relation to journal lateral velocity. In reference (91) similar work was reported for the dynamically misaligned sterntube bearing. These results illustrate the additional influence of angular velocity of the journal axis. This was shown to be similar to lateral velocity with respect to the influence of cavitation upon non-linear response, when

viewed on a local basis, i.e. at a given axial location in the bearing. The axial oil supply grooves were also found to introduce further non-linearity when considering angular velocity of the journal axis about the bearing axis.

3. For the propeller shafting lateral vibration predictions reported in reference (92), the effects of non-linearity in the after sterntube bearing oil film response were shown to be insignificant. Provided this result can be demonstrated to be valid for a range of marine propeller shafting applications, it represents a valuable finding with respect to the potential saving in computing time.

7. CONCLUSIONS

7.1. Objectives Achieved

All the objectives set out in section 1.3. have been met. These encompass the development of computer programs for the prediction of sterntube bearing steady load performance and linearised dynamic coefficients (see references (87)(88)). The influence of misalignment on bearings having large L/D ratios (e.g. sterntube bearings) is included in the above programs. A novel journal orbit analysis method was introduced for bearings subject to substantial dynamic loading (77)(86). A new form of numerical hydrodynamic analysis for journal bearings has been developed (72)(90). All the programs described herein are based upon this analysis.

Non-linearity in bearing oil films has been examined, with particular reference to the influence of cavitation. New non-linear bearing oil film models resulting from this study have been presented (85)(91).

A program was developed for marine propeller shafting lateral vibration amplitude prediction (92). This uses a multi-mass shaft element model, and the above journal orbit analysis method. Interaction between bearings and shafting is covered, and the results for the example case used indicated the influence of bearing oil film non-linearity to be negligible. As a result of this finding, the development of a computer program using a direct solution based on linearised bearing oil film coefficients and sinusoidal excitation, is proposed. Such a program would be suitable for regular practical application in marine propeller shafting lateral vibration investigations.

The practical performance program, developed for the analysis of steadily loaded misaligned sterntube bearings, has been in regular use for consultancy work for over three years. This work comprises operating condition safety assessment, and the determination of the axial location of the effective support point for shaft alignment analysis. Correlation with service experience has not yet reached a level at which safe operating limits can be predicted with a satisfactory level of confidence. The assessment of safe operating conditions is therefore likely to be over conservative at present. A conservative approach is, however, justifiable in many practical applications due to the levels of uncertainty with respect to the actual operating conditions. Data for the propeller forces and moments due to wake field interaction, are not commonly available, consequently the load and degree of misalignment, to which the sterntube bearing is subjected, cannot be accurately calculated.

From the above comments, it follows that there is a clear need for more service experience feedback (see section 5.1.), and more propeller - wake field force and moment data.

7.2. Sterntube Bearing Design Implications

The wide range of load and misalignment conditions, to which sterntube bearings may be subjected, makes it inappropriate to offer generalised comments on the design implications arising from the work reported herein. This thesis contributes to the sterntube bearing design problem, by presenting computational facilities whereby the performance may be predicted for any specified set of design parameters and operating conditions. The use of these facilities enables the design to be optimised for the given operating conditions. Examples of such optimisations have been described (87)(88).

One design feature worth particular mention is the oil supply groove geometry. For many installations, the minimum oil film thickness could probably be improved by re-locating the axial grooves above the conventional 3 o'clock and 9 o'clock positions. The hydrodynamic analysis method developed (72)(90), could readily accommodate such changes by specifying appropriate oil film boundary positions. This type of design change should only be made when the sterntube bearing operating conditions can be specified with a reasonable degree of confidence. Having regard to the work by Vorus and Gray (45), the specification should also include allowance for the influence of ship manoeuvering conditions. As noted in the previous section, this level of detailed knowledge is not common in the marine field.

7.3. Contributions Made

The particular contributions of this work are as detailed below:

a.) The development of a robust numerical hydrodynamic analysis method for journal bearings, which takes account of flow continuity in the complete oil film, including the cavitation zone (72). This method was later extended to cover significant lateral velocities of the journal, such as may occur in a dynamically loaded bearing (90). The main feature of the latter work was the consideration of squeeze action in relation to cavitation. The simplicity and ease of operation of the computer programs developed to implement the above method rendered them suitable for practical application.

b.) The development of a practical bearing analysis program using an iterative thermal balance procedure similar to that described in reference (8), but featuring the following advances: The first version, for aligned bearings, took account of oil head pressure (as experienced by sterntube bearings), and produced the commonly used 8 linearised oil film stiffness and damping coefficients. In a second version, angular misalignment in the vertical plane was introduced. Production of the associated 32 linearised coefficients was not included due to the considerably larger data store that would have been required. A version of the hydrodynamic analysis program was specially adapted for the production of the 32 linearised coefficients relevant to dynamic misalignment conditions. The practical bearing analysis programs utilised dimensionless performance data computed by the hydrodynamic analysis program.

c.) The development of an oil film history computational model, and the investigation of its influence in association with that of journal mass (77)(86). This work was restricted to aligned bearings with half and full circumferential oil grooves, but nevertheless gave some useful insights into oil film behaviour.

d.) An investigation into the nature of non-linearity in relation to journal lateral velocity (85) showed the theoretical influence of cavitation upon the interaction of squeeze and wedge action. In relation to non-linearity, the investigation also predicted a sudden change in oil film response to occur when squeeze action undergoes a reversal of sign. The smoothing influence of wedge action upon the above sudden change was also shown. This investigation was subsequently extended to cover the dynamically misaligned sterntube bearing (91). In this situation a sudden change in oil film response upon reversal of the wedge action was also found. This was due to the circumferential asymmetry of the axial oil grooves relative to the location of the minimum film thickness position.

e.) The development of new forms of non-linear oil film model based on the above investigation. These covered the aligned full circumferential groove bearing (85) and the dynamically misaligned sterntube bearing (91).

f.) The investigation of interaction between hydrodynamic sterntube bearings and the lateral vibration of marine propeller shafting (92). This included the development of a suitable computer program which had provision for non-sinusoidal propeller excitation due to the wake field, propeller damping and water entrainment effects and gyroscopic moments. The difference in predicted lateral vibration response, when using linear or non-linear bearing oil film models, was included in this investigation.

8. RECOMMENDATIONS

8.1. Service and Experimental Feedback

This thesis has indicated that, in the area of marine sterntube bearings, there is a need for more feedback of service experience and measured data (see section 5.1.). With respect to service experience, the need is for both quality and quantity of data. When problems occur in service, those personnel immediately involved are often concerned only with rectifying the problem in order to get the ship back into service as quickly as possible. The commercial pressures are such that this response is understandable, but it may result in a short term solution to the problem. It is only when repeated serious problems occur that a detailed investigation into the causes of the problem is instigated e.g. Vorus and Gray (45). For many of the problems that occur in practise, an investigation involving "in service" measurements cannot be justified in relation to cost. In such situations, it is recommended that comprehensive recording of the details of the problem should at least be undertaken. This should include all relevant background information such as any history of related problems and operating condition history, particularly that immediately preceding the occurrence of the problem. In many cases, important information, for example the estimated misalignment angle at the sterntube bearing and propeller wake field forces and moments, may not be readily available. These omissions would severely limit the value of service data collection, and this information should be sought wherever possible.

It is also recommended that more measurements relating to sterntube bearing operation should be obtained, particularly with respect to misalignment. These should include both "in service" measurements, and those made in experimental test rigs. The above alternative types of measurement are considered to be complementary. With the former, the results have the advantage of being directly relevant to practical situations, but the disadvantages of limited instrumentation and parameter control. In the experimental test rig the above advantages and disadvantages are broadly reversed. It is recommended that experimental test rigs should be designed to simulate sterntube bearing service conditions as closely as possible. With respect to scale, this may not be justifiable in view of the potential escalation in cost. For fundamental research, it is acknowledged that there is a case for relatively simple test rigs, in order that the physical phenomena may be more clearly observed. The simple test rig also confers the advantage of easing the analysis of results, by the elimination of unnecessary parameter interaction.

8.2. Direct Solution of the Propeller Shafting Lateral Vibration Problem

As noted in section 7.1., the development of a computer program for marine propeller shafting lateral vibration amplitude prediction, using a direct solution method, is proposed. It is recommended that an extensive programme of correlations between the predicted results, and service experience and measurements, be undertaken. This should cover a wide range of shafting designs and sizes. In addition to the normal validation of the computer program predictions, this work should also indicate the extent to which linearised oil film coefficients may be satisfactorily employed.

8.3. Sterntube Bearing Elasticity

The results reported in reference (92) indicated that elastic deformation may be significant in sterntube bearings. It is recommended that further work should be carried out to determine the adequacy of the rigid bearing assumption for practical analysis applications. If a need to consider sterntube bearing elasticity is established, then approximate solutions for achieving this should be investigated. The desirability of seeking an approximate solution to the bearing elasticity problem is indicated by the excessive computing time that is incurred by the rigorous approach e.g. La Bouff and Booker (70). At present a minority of sterntube bearings utilise reinforced resin materials rather than the more usual white metal on a cast iron backing. For reinforced resin materials, the need to consider sterntube bearing elasticity is more likely.

8.4. Cavitation in Sterntube Bearings

Sterntube bearings operate in unusual conditions with respect to their being totally submerged, and having a head pressure of oil applied to all boundaries. The commonly used assumption that cavitation occurs at atmospheric pressure, has been adopted. The theoretical results reported in this thesis indicated that the choice of cavitation pressure was not critical, due to the reduction of the extent of cavitation arising from the oil head pressure. This is particularly true for more lightly loaded sterntube bearings, such as the test case example used in reference (92).

Although consideration of cavitation is regarded as a less important item than the foregoing recommendations, it is nevertheless recommended that details of the cavitation behaviour in sterntube bearings should be investigated experimentally. The motivation for making this recommendation arises mainly from the novel nature of the sterntube bearing and its operating environment. Both steady and dynamic load experiments are considered to be worthwhile, and conditions representative of those encountered in service should be simulated as closely as possible. The use of realistic oil head pressures is regarded as particularly important.

ACKNOWLEDGEMENTS

The author is indebted to many of his friends and colleagues for their help, advice and encouragement throughout this work, and specifically to the following:

Professor B.L. Button of Trent Polytechnic for initiating the idea of working for a Ph.D.

Dr. J. Montgomery of Trent Polytechnic for his constructive criticism and helpful discussions, and for his style of supervision which combined careful monitoring of the work whilst leaving the initiative firmly with the author.

Mr. F.A. Martin of the Glacier Metal Co. for his encouragement and many helpful discussions.

Dr. D.W. Parkins of Cranfield Institute of Technology for his freely given advice and knowledge related to the problems involved in both theoretical and experimental work. This was particularly valuable in the formative stages of the author's ideas on analysis techniques. Dr. Parkins collaboration with respect to reference (86) is also gratefully acknowledged.

Dr. E.V.L. Hughes of Lanchester Polytechnic for his helpful supervision of the earlier part of this work.

Mr. T.F. Brock of Lloyd's Register of Shipping for his enthusiasm and interest during the initial period, and above all for giving the author the freedom to develop his own ideas.

Mrs. Margaret Jakeman, the author's wife, for her "weeding out" of vast quantities of spelling mistakes, split infinitives, etc.

Mr. H.D. Parsons of H.D. Parsons (Maritime) Ltd, for his helpful advice and assistance with respect to the details and characteristics of marine propellers, in relation to the work of reference (92).

Mr. D.W.K. Lam of Lloyd's Register of Shipping, for his assistance in carrying out the lateral vibration frequency analysis for the "Keiyo Maru" test case used in reference (92). Mr. Lam's enthusiastic support throughout this work was also appreciated.

Mr. A. Ogasawara of Mitsubishi Heavy Industries Ltd. for his kind provision of unpublished details relating to the propeller shafting of the tanker "Keiyo Maru" (92).

Finally the author wishes to express his gratitude to the Committee of Lloyd's Register of Shipping for the opportunity to carry out this work, and for their permission to submit this thesis for the degree of Doctor of Philosophy.

REFERENCES

1. COLE. S.A. and HUGHES. C.J. "Visual study of film extent in dynamically loaded complete journal bearing". Proc. Conf. on Lub. & Wear. Paper 87. 1957. I. Mech. E. London. pp. 147-150.

2. VEDELER. A. "Operational problems with sterntube bearings". Marine Technology. Oct. 1964 pp. 59-70.

3. MITCHELL. J.R., HOLMES. R. and BYRNE. J. "Oil whirl of a rigid rotor in 360° journal bearings : further characteristics". Proc. I. Mech. E. Vol. 180 Part 1. No. 25. 1965-66. pp. 593-610.

4. OLSSON. K. "Cavitation in dynamically loaded bearings". Trans. Chalmers. Inst. Tech. No. 308. Report No. 26. Gothenburg, Sweden. 1965.

5. LLOYD. T., HORSNELL. R. and McCALLION. H. "An investigation into the performance of dynamically loaded journal bearings : theory". Proc. I. Mech. E. Vol. 181. Part 3B. 1966-7. pp. 1-8.

6. MIDDLETON. V., DUDLEY. B.R. and McCALLION. H. "An investigation into the performance of dynamically loaded journal bearings : experiment". Proc. I. Mech. E. Vol. 181. Part 3B. 1966-67. pp. 9-27.

7. DOWSON. D., HUDSON. J.D., HUNTER. B. and MARCH. C.N. "An experimental investigation of the thermal equilibrium of steadily loaded journal bearings". Proc. I. Mech. E. Vol. 181. Part 3B. 1966-67. pp. 70-80.

8. Engineering Sciences Data Unit. Item No. 66023 : "Calculation methods for steadily loaded pressure fed hydrodynamic journal bearings". Sept. 1966.

9. LLOYD. T. and McCALLION. H. "Recent developments in fluid film lubrication theory". Proc. I. Mech. E. Vol. 182. Part 3A. 1967-68. pp. 36-49.

10. PATRICK. J.K. "An experimental investigation into the performance of sleeve bearings subjected to a range of alternating loads". Proc. I. Mech. E. Vol. 182. Part 3N. 1967-68. pp. 77-88.

11. LUND. J.W. and ORCUTT. F.K. "Calculations and experiments on the unbalance response of a flexible rotor". A.S.M.E. Journal of Engineering for Industry. Nov. 1967. pp. 785-796.

12. WOODCOCK. J.S. and HOLMES. R. "The determination and application of the dynamic properties of a turbo - rotor bearing oil film". Proc. I. Mech. E. Vol. 184. Part 3L. 1969-70. pp. 111-119.

13. LUNDHOLM. G. "The circumferential groove journal bearing considering cavitation and dynamic stability". Acta Polytechnica Scandinavica. 1969. ME. 42.

14. WHITE. D.C. "Squeeze film journal bearings". Ph.D. Dissertation. Cambridge University 1970.

15. MORTON. P.G. "Measurement of the dynamic characteristics of a large sleeve bearing". Journal of Lubrication Technology. Trans. A.S.M.E. Series F. Vol. 93. Jan. 1971. pp. 143-150.

16. BOOKER. J.F. "Dynamically loaded journal bearings : numerical application of the mobility method". Journal of Lubrication Technology. Trans. A.S.M.E. Series F. Vol. 93. Jan. 1971. pp. 168-176.

17. ASANABE. S., AKAHOSHI. M. and ASAI. R. "Theoretical and experimental investigation on misaligned journal bearing performance". Proc. I. Mech. E. Paper C36/71. pp. 1-8.

18. McCALLION. H., LLOYD. T. and YOUSIF. F.B. "The influence of oil supply conditions on the film extent and oil flow in journal bearings". Proc. I. Mech. E. Paper C55/71 pp. 31-37.

19. HOLMES. R. and CRAVEN. A.H. "The influence of crankshaft and flywheel mass on the performance of engine main bearings". Proc. I. Mech. E. Paper C63/71. pp. 80-85.

20. GERMANISCHER LLOYD. "Regulations for the determination of dynamic stresses on propellers". Dec. 1971.

21. CRAVEN. A.H. and HOLMES. R. "The vibration of engine crankshafts - a fast numerical solution". International Journal for Numerical Methods in Engineering. Vol. 5. 1972. pp. 17-24.

22. TOMS. A.E. and MARTYN. D.K. "Whirling of line shafting". Trans. I. Mar. E. Vol. 84. 1972. pp. 176-191.

23. BANNISTER. R.H. "Non-linear oil film force coefficients for a journal bearing operating under aligned and misaligned conditions". Ph.D. Thesis. University of Aston. Dec. 1972.

24. HYAKUTAKE. J., ASAI. R., INOUE. M., FUKAHORI. K., WATANABE. N. and NONAKE. M. "Measurement of relative displacement between sterntube bearing and shaft of 210,000 d.w.t. tanker". Japan Shipbuilding & Marine Engineering. Vol. 7. No. 1. 1973. pp. 32-40.

25. PAFELIAS. T.A. "Solution of certain problems of viscous laminar flow with application in engineering problems". Ph.D. Thesis. Rensselaer Polytechnic Institute. Troy. New York. Jan. 1974.

26. DOWSON. D. and TAYLOR. C.M. "Fundamental aspects of cavitation in bearings". Proc. 1st. Leeds - Lyon Symposium in Tribology. Leeds. Sept. 1974. pp. 15-28.

27. FLOBERG. L. "Cavitation boundary conditions with regard to the number of streamers and tensile strength of the liquid." Proc. 1st. Leeds - Lyon Symposium in Tribology. Leeds. Sept. 1974. pp. 31 - 35.

28. MARSH. H. "Cavitation in dynamically loaded journal bearings". Proc. 1st. Leeds - Lyon Symposium in Tribology. Leeds. Sept. 1974. pp. 91-95.

29. ELROD. H.G. and ADAMS. M.L. "A computer program for cavitation and starvation problems". Proc. 1st. Leeds - Lyon Symposium in Tribology. Leeds. Sept. 1974. pp. 37-41.

30. OLSSON. K. "Theoretical and experimental investigation of pressure build up and cavitation regions in a bearing with stationary whirl". Chalmers University of Technology. Gothenburg. 1974.

31. OOSTERVELD. M.W.C. and OOSSANEN. P. VAN. "Further computer analysed data of the Wageningen B - Screw Series". International Shipbuilding Progress. Vol. 22. Jul. 1975.

32. MORTON. P.G. "Dynamic characteristics of bearings - measurement under operating conditions". G.E.C. Journal of Science & Technology. Vol. 42. No. 1. 1975. pp. 37-47.

33. HILL. A. "Modern bearing design and practise". Trans. I. Mar. E. Vol. 88. 1976. pp. 204-233.

34. NAGATA. M., WAKABAYSHI. K., DOI. Y. and SWADA. H. "Characteristics at low speeds on partially loaded bearings". Bulletin of Marine Engineering Society in Japan. Vol. 4. No. 2. 1976. pp. 127-135.

35. BANNISTER. R.H. "A theoretical and experimental investigation illustrating the influence of non-linearity and misalignment on the eight oil film force coefficients". I. Mech. E. Conference on Vibrations in Rotating Machinery. Paper C219/76. Cambridge. 1976.

36. PARKINS. D.W. "Static and dynamic characteristics of an hydrodynamic journal bearing". Ph.D. Thesis. Cranfield Institute of Technology. May 1976.

37. MYRICK. S.T. and RYLANDER. H.G. "Analysis of flexible rotor whirl and whip using a realistic hydrodynamic journal bearing model". A.S.M.E. Journal of Engineering for Industry. Nov. 1976. pp. 1136-1144.

38. ALLAIRE. P.E., NICHOLOS. J.C. and GUNTER. E.J. "Systems of finite elements for finite bearings". A.S.M.E. Journal of Lubrication Technology. April 1977. pp. 187-197.

39. CHILDS. D., MOES. H. and VAN LEEUWEN. H. "Journal bearing impedance descriptions for rotor dynamic applications". A.S.M.E. Journal of Lubrication Technology. April 1977. pp. 198-214.

40. HUMES. B. and HOLMES. R. "The role of sub-atmospheric film pressures in the vibration performance of squeeze film bearings". I. Mech. E. Journal of Mechanical Engineering Science. Vol. 20. No. 5. 1978. pp. 283-289.

41. LUND. J.W. and THOMSEN. K.K. "A calculation method and data for the dynamic coefficients of oil lubricated journal bearings". Topics in Fluid Film Bearing and Rotor Bearing System Design and Optimisation. A.S.M.E. Publication. 1978.

42. PARKINS. D.W. "Theoretical and experimental determination of the dynamic characteristics of a hydrodynamic journal bearing". A.S.M.E. Journal of Lubrication Technology. Vol. 101. April 1979. pp. 129-139.

43. ARCHER. C. and MARTYN. D.K. "Static and dynamic alignment". Trans. I. Mar. E. (C). Vol. 91. Conference No. 4. Paper C.31. 1979. pp. 24-34.

44. HYLARIDES. S. and VAN GENT. W. "Hydrodynamic reactions to propeller vibrations". Trans. I. Mar. E. (C). Vol. 91. Conference No. 4. Paper C.36. 1979. pp. 78-91.

45. VORUS. W.S. and GRAY. R.L. "Calculation of sterntube bearing eccentricity distributions : Applications in States Lines Ro/Ro bearing failure analysis". Trans. I. Mar. E. (C). Vol. 91. Conference No. 4. Paper C37. 1979 pp. 92-105.

46. HILL. A. and MARTIN. F.A. "Some considerations in the design of sterntube bearings and seals". Trans. I. Mar. E. (C). Vol. 91. Conference No. 4. Paper C39. 1979. pp. 119-137.

47. PINKUS. O. and BUPARA. S.S. "Analysis of misaligned grooved journal bearings". A.S.M.E. Journal of Lubrication Technology. Vol. 101. Oct. 1979. pp. 503-509.

48. HILL. A. "Factors affecting sterntube bearings". Marine Engineering Review. March 1980. pp. 25-31.

49. DOWSON. D. and TAYLOR. C.M. "The state of knowledge in the field of bearing influenced rotor dynamics". Tribology International. Oct. 1980. pp. 196-198.

50. GLIENICKE. J., HAN. D.C., and LEONHARD. M. "Practical determination and use of bearing dynamic coefficients". Tribology International. Vol. 13. No. 6. Dec. 1980. pp. 297-309.

51. PARKINS. D.W. "Measured characteristics of a journal bearing oil film". A.S.M.E. Journal of Lubrication Technology. Vol. 103. Jan. 1981. pp. 120-125.

52. PARSONS. M.G. and VORUS. W.S. "Added mass and damping estimates for vibrating propellers". S.N.A.M.E. Propellers. '81. Symposium. May. 1981. pp. 273-302.

53. ELROD. H.G. "A cavitation algorithm". A.S.M.E. Journal of Lubrication Technology. Vol. 103. July 1981. pp. 350-354.

54. VASSILOPOULOS. L. "Methods of computing stiffness and damping properties of main propulsion thrust bearings". International Shipbuilding Progress. Vol. 29. No. 329. Jan. 1982. pp. 13-31.

55. ETSION. I. and LUDWIG. L.P. "Observation of pressure variation in the cavitation region of submerged journal bearings". A.S.M.E. Journal of Lubrication Technology. Vol. 104. No. 2. April 1982. pp. 157-163.

56. WELSH. W.A. and BOOKER. J.F. "Dynamic analysis of engine bearing systems". Proc. 9th. Leeds - Lyon Symposium on Tribology. Leeds. Sept. 1982. pp. 29-36.

57. JONES. G.J. "Crankshaft bearings : Oil film history". Proc. 9th. Leeds - Lyon Symposium on Tribology. Leeds. Sept. 1982. pp. 83-88.

58. SMITH. E.H. "Temperature variations in crankshaft bearings". Proc. 9th. Leeds - Lyon Symposium in Tribology. Leeds. Sept. 1982. pp. 97-102.

59. REASON. B.R. and SIEW. A.H. "A numerical solution for the design and performance evaluation of journal bearings with misalignment". Proc. I. Mech. E. Paper No. C9/82. 1982. pp. 77-85.

60. PAN. C.H.T. Dynamic analysis of rupture in thin fluid films. 1. A non-inertial theory". A.S.M.E. Journal of Lubrication Technology. Vol. 105. Jan. 1983. pp. 96-104.

61. FANTINO. B., FRENE. J., and GODET. M. "Dynamic behaviour of an elastic connecting rod bearing - Theoretical study". SAE/SP - 539 - Studies in Engine Bearings and Lubrication. Paper No. 83037. Feb. 1983. pp. 23-32.

62. JACOBSON. B.O. and HAMROCK. B.J. "High speed motion picture camera experiments of cavitation in dynamically loaded journal bearings". A.S.M.E. Journal of Lubrication Technology. Vol. 105. No. 3. July 1983. pp. 446-452.

63. DOWSON. D., MIRANDA, A.A.S. and TAYLOR. C.M. "Implementation of an algorithm enabling the determination of film rupture and reformation boundaries in a liquid film bearing". Proc. 10th. Leeds-Lyon Symposium in Tribology. Lyon. Sept. 1983. pp. 60-70.

64. MOES. H., SIKKES. E.G., and BOSMA. R. "Dynamic analysis of diesel engine main bearings". Proc. 10th Leeds-Lyon Symposium in Tribology. Lyon. Sept. 1983. pp. 239-246.

65. DEDE. M.M. and HOLMES. R. "On prediction and experimental assessment of engine bearing performance". Proc. 10th. Leeds-Lyon Symposium in Tribology. Lyon. Sept. 1983. pp. 271-278.

66. HAYAMA. S. and ANODA. Y. "Dynamic responses of lateral vibration of marine shafting due to propeller induced forces and moments". 3rd. International Symposium in Marine Engineering. The Marine Engineering Society in Japan. Tokyo. 1983. pp. 691-698.

67. PARKINS. D.W. and MAY-MILLER. R. "Cavitation in an oscillating oil squeeze film". A.S.M.E. Journal of Tribology. Vol. 106. July 1984. pp. 360-367.

68. ROWE. W.B. and CHONG. F.S. "A computation algorithm for cavitating bearings". Tribology International. Vol. 17. No. 5. Oct. 1984. pp. 243-250.

69. DEDE. M. and HOLMES. R. "On prediction and experimental assessment of engine - bearing performance". Tribology International. Vol. 17. No. 5. Oct. 1984. pp. 251-258.

70. LA BOUFF. G.A. and BOOKER. J.F. "Dynamically loaded journal bearings : A finite element treatment for rigid and elastic bearings". A.S.M.E. Paper No. 84 - TRIB - 11. A.S.M.E./A.S.L.E. Joint Lubrication Conference. Oct. 1984.

71. LEEMANS. M. and ROODE. F. "Vibration analysis of a rotating propeller shaft in a rubber sterntube bearing". Conference : I.C.M.E.S. '84.

72. JAKEMAN. R.W. "A numerical analysis method based on flow continuity for hydrodynamic journal bearings". Tribology International. Vol. 17. No. 6. Dec. 1984. pp. 325-333.

73. DOWSON. D., RUDDY. A.V., SHARP. R.S. and TAYLOR. C.M. "An analysis of the circumferentially grooved journal bearing with consideration of lubricant film reformation". Proc. I. Mech. E. Vol. 199. No. C1. 1985. pp. 27-34.

74. DOWSON. D., MIRANDA. A.A.S., and TAYLOR. C.M. "The prediction of liquid film journal bearing performance with a consideration of lubricant film reformation : Part. 1. - Theoretical results". Proc. I. Mech. E. Vol. 199. No. C2. 1985. pp. 95-102.

75. DOWSON. D., MIRANDA. A.A.S., and TAYLOR. C.M. "The prediction of liquid film journal bearing performance with a consideration of lubricant film reformation : Part. 2. - Experimental results". Proc. I. Mech. E. Vol. 199. No. C2. pp. 103-111.

76. GERO. L.R. and ETTLES. C.M. Mc C. "An evaluation of finite difference and finite element methods for the solution of Reynold's equation". A.S.L.E. Preprint No. 85 - AM - 2E - 4. Conference May 1985.

77. JAKEMAN. R.W. "Journal orbit analysis taking account of oil film history and journal mass". Part 1. of Proc. of 4th International Conference on Numerical Methods in Laminar and Turbulent Flow. Swansea. July 1985. pp. 199-210.

78. KLIT. P. and LUND. J.W. "Calculation of the dynamic coefficients of a journal bearing, using a variational approach". A.S.M.E. Preprint No. 85 - TRIB - 7. A.S.L.E./A.S.M.E. Tribology Conference Oct. 1985.

79. BONCOMPAIN. R., FILLON. M. and FRENE. J. "Analysis of thermal effects in hydrodynamic bearings". A.S.M.E. Preprint. No. 85 - TRIB - 21. A.S.L.E./ A.S.M.E. Tribology Conference Oct. 1985.

80. MOES. H., SIKKES. E.G. and BOSMA. R. "Mobility and impedance tensor methods for full and partial arc journal bearings". A.S.M.E. Preprint No. 85 - TRIB - 25. A.S.L.E./A.S.M.E. Tribology Conference Oct. 1985.

81. HESHMAT. H. and PINKUS. O. "Mixing inlet temperatures in hydrodynamic bearings". A.S.M.E. Preprint. No. 85 - TRIB - 26. A.S.L.E./A.S.M.E. Tribology Conference. Oct. 1985.

82. GOENKA. P.K. and OH. K.P. "An optimum connecting rod design study - A lubrication viewpoint". A.S.M.E. Preprint. No. 85 - TRIB - 50. A.S.L.E./A.S.M.E. Tribology Conference. Oct. 1985.

83. BREWE. D.E. "Theoretical modelling of the vapor cavitation in dynamically loaded journal bearings". A.S.M.E. Preprint No. 85 - TRIB - 51. A.S.L.E./ A.S.M.E. Tribology Conference. Oct. 1985.

84. MOURELATOS. Z.P. and PARSONS. M.G. "Finite element analysis of elastohydrodynamic stern bearings". Trans. S.N.A.M.E. Vol. 93. 1985. pp. 225-259.

85. JAKEMAN. R.W. "The influence of cavitation on the non-linearity of velocity coefficients in a hydrodynamic journal bearing". Proc. 13th. Leeds - Lyon Symposium in Tribology. Leeds. Sept. 1986. pp. 473-480.

86. JAKEMAN. R.W. and PARKINS. D.W. "Theoretical and experimental orbits of a dynamically loaded hydrodynamic journal bearing". Proc. 13th. Leeds - Lyon Symposium in Tribology. Leeds. Sept. 1986. pp. 355-362.

87. JAKEMAN. R.W. "Performance and oil film dynamic coefficients of a misaligned sterntube bearing". Trans. A.S.L.E. Vol. 29. No. 4. Oct. 1986. pp. 441-450.

88. JAKEMAN. R.W. "Sterntube bearings : Performance characteristics and influence upon shafting behaviour". Lloyd's Register Technical Association. Paper No. 2. Session 1986-87.

89. KARNI. Z.H., PARSONS. M.G., and MOURELATOS. Z.P. "Time-varying behaviour of a statically indeterminate shafting system in a hydrodynamic journal bearing". A.S.M.E. Preprint. No. 86 - TRIB - 33.

90. JAKEMAN. R.W. "Numerical analysis of hydrodynamic bearings with significant journal lateral velocities". Tribology International. Vol. 20. No. 4. Aug. 1987. pp. 170-178.

91. JAKEMAN. R.W. "A non-linear oil film response model for the dynamically misaligned sterntube bearing". Submitted for publication in Tribology International. April 1988.

92. JAKEMAN. R.W. "The influence of sterntube bearings on lateral vibration amplitudes in marine propeller shafting". Submitted for publication in Tribology International. April 1988.

Table 1

Correlation of Thesis Reference Numbers with Reference Numbers in Papers by Author.

THESIS REF. NO.	REFERENCE NO. IN PAPER								
	72	77	85	86	87	88	90	91	92
1							6		
5	5				6	10			
8	8				11	19			
14							8		
15				11					
16		4		5		14		4	
18	3								
19		3		6		13			
22									9
23					13				
24					12	D1		2	2
25					10				
28							7		
35			4			17		10	
36	7								
37									10
39								6	
40				12					
41						D3			
42	2		6	1	7				
43					1	1			
44									3
45					2	2			
46	10				4				
47	9				9				
50	4								
51					8				
52									7
54						D4			
55						7	9		
57	6	2		7		12	4		
58		5							
60						8	10		
61				9		4			
64								5	
66									4
70		6	1	8		5			
71					3	3			
72		1	2	2	5	6	1	8	
77			3	3		11	3		8
80								7	
81						9	11		
82				10					
85				4		15	2	1	
86			5			16	5		6
87						D2		3	1
89									5
90								9	

Table 2. Published Finite Difference and Finite Element Solutions

AUTHORS	REF NO	FD/ FE	MESH CIRC/AXIAL	MISALIGNED ? Y/N	BEARING TYPE	CAVITATION MODEL	OTHER FEATURES
LLOYD et al	5	FD	64 x 16 32 x 8	N	CIRC	T	
McCALLION et al	18	FD	200 x 56	N	AX		
BANNISTER	35	FD	32 x 32	Y	120°PA		
MYRICK, RYLANDER	37	FD	16 x 6	Y		S	
PARKINS	42	FD		N	CIRC	S	1
VORUS & GRAY	45	FD	36 x 18	Y	AX	T	
PINKUS & BUPARA	47	FD	30 x 10	Y	AX	S	
REASON & SIEW	59	FD	42 x 16	Y		S	
LABOUFF & BOOKER	70	FE	25 x 6	N	CIRC	T	2
BONCOMPAIN et al	79	FD					3
MOURELATOS & PARSONS	84	FE	12 x 8	Y	AX	T	2
KARNI et al	89	FE		Y	AX		

Other Features:

1. Circumferential viscosity variation considered.

2. Elastic bearing.

3. Thermal effects investigated.

Key:

Bearing Type:

CIRC = Circumferential oil groove

AX = Axial oil groove

120° P.A = 120° Partial arc

Cavitation Model:

T = Pressures below specified cavitation pressure truncated after completion of film pressure solution.

S = Pressures below specified cavitation pressure set to that pressure during relaxation film pressure solution.

Table 3. Comparison of Dimensionless Oil Film Parameters with Results Published by Pafelias (25)

Bearing : 150° Partial Arc . L/D = 0.5
Source : A - Author . P - Pafelias (25)

CASE	1		3		5		7	
SOURCE	A	P	A	P	A	P	A	P
INPUT. ϵ	0.4		0.4		0.4		0.4	
INPUT. $\bar{\alpha}$	0		0.25		0.25		0.3535	
INPUT. β°	0		0		90		45	
$\bar{F}_y$	1.215	1.211	1.261	1.253	1.261	1.255	1.433	1.417
ψ°	54.01	54.01	55.08	55.19	50.51	50.69	49.70	49.98
$\bar{M}$	0	0	0.06339	0.06361	0.06307	0.06350	0.1403	0.1391
Θ_M	0	0	- 12.73	- 12.77	32.14	32.15	10.01	9.93
$\bar{P}_{max}$	2.347	2.360	2.522	2.488	2.452	2.442	3.083	3.025
$\bar{A}_{xx}$	3.48	3.48	3.33	3.36	3.56	3.57	3.44	3.40
$\bar{A}_{xy}$	- 2.10	- 2.13	- 1.92	- 1.99	- 1.94	- 1.99	- 1.46	- 1.48
$\bar{A}_{yx}$	7.84	7.89	7.63	7.73	8.08	8.16	8.05	8.06
$\bar{A}_{yy}$	4.62	4.62	4.95	4.92	4.98	4.97	5.84	5.82
$\bar{A}_{\lambda x}$	0	0	0.0974	0.098	0.364	0.372	0.477	0.474
$\bar{A}_{\lambda y}$	0	0	- 0.0566	- 0.050	0.0478	0.040	0.0737	- 0.066
$\bar{A}_{\gamma x}$	0	0	0.378	0.388	0.377	0.386	0.856	0.854
$\bar{A}_{\gamma y}$	0	0	0.421	0.430	0.166	0.164	0.759	0.752
$\bar{A}_{x\lambda}$	0	0	0.0727	0.072	0.378	0.366	0.478	0.446
$\bar{A}_{x\gamma}$	0	0	- 0.125	- 0.132	0.0662	0.062	0.0256	0.008
$\bar{A}_{y\lambda}$	0	0	0.334	0.310	0.410	0.392	0.826	0.784
$\bar{A}_{y\gamma}$	0	0	0.311	0.250	0.340	0.314	0.778	0.712
$\bar{A}_{\lambda\lambda}$	0.105	0.104	0.110	0.110	0.138	0.138	0.165	0.160
$\bar{A}_{\lambda\gamma}$	- 0.0467	- 0.046	- 0.0452	- 0.044	- 0.0377	- 0.042	- 0.0108	- 0.016
$\bar{A}_{\gamma\lambda}$	0.166	0.166	0.186	0.186	0.203	0.204	0.282	0.274
$\bar{A}_{\gamma\gamma}$	0.193	0.192	0.228	0.226	0.215	0.214	0.318	0.308

Continued:

CASE	1		3		5		7	
SOURCE	A	P	A	P	A	P	A	P
$\overline{B}_{xx}$	5.51	5.48	5.04	5.13	5.45	5.46	4.73	4.76
$\overline{B}_{xy}$	4.00	3.98	3.66	3.75	3.81	3.82	3.76	3.76
$\overline{B}_{yx}$	3.95	3.97	3.61	3.75	3.77	3.84	3.69	3.77
$\overline{B}_{yy}$	15.2	15.2	14.9	15.0	15.5	15.5	15.1	15.1
$\overline{B}_{\lambda x}$	0	0	0.0853	0.0780	0.368	0.382	0.383	0.394
$\overline{B}_{\lambda y}$	0	0	0.118	0.116	0.465	0.478	0.566	0.572
$\overline{B}_{\gamma x}$	0	0	0.140	0.144	0.406	0.416	0.538	0.548
$\overline{B}_{\gamma y}$	0	0	0.832	0.846	0.351	0.358	1.27	1.28
$\overline{B}_{x\lambda}$	0	0	0.0870	0.118	0.374	0.354	0.401	0.398
$\overline{B}_{x\gamma}$	0	0	0.143	0.168	0.416	0.394	0.555	0.542
$\overline{B}_{y\lambda}$	0	0	0.122	0.148	0.473	0.450	0.582	0.568
$\overline{B}_{y\gamma}$	0	0	0.855	0.850	0.366	0.340	1.30	1.25
$\overline{B}_{\lambda\lambda}$	0.135	0.132	0.128	0.130	0.169	0.172	0.169	0.168
$\overline{B}_{\lambda\gamma}$	0.0881	0.088	0.0898	0.092	0.111	0.112	0.158	0.154
$\overline{B}_{\gamma\lambda}$	0.0890	0.088	0.0904	0.094	0.111	0.112	0.158	0.154
$\overline{B}_{\gamma\gamma}$	0.295	0.298	0.344	0.348	0.328	0.330	0.434	0.430

Table 4. Data used to compute Linearised Dynamic Coefficients for the "Keiyo Maru" Aft Sterntube Bearing. (N.m. rad. s. units) (See reference (92))

PERTURBATION	ΔF_x	ΔF_y	ΔM_x	ΔM_y
$x = +8.0.10^{-6}$	$9.067.10^3$	$2.161.10^4$	$2.088.10^2$	$6.543.10^2$
$x = -8.0.10^{-6}$	$-8.785.10^3$	$-2.063.10^4$	$-1.987.10^2$	$-6.185.10^2$
$y = +8.0.10^{-6}$	$-3.954.10^3$	$1.015.10^4$	$-3.137.10^2$	$4.779.10^2$
$y = -8.0.10^{-6}$	$3.663.10^3$	$-9.067.10^3$	$+2.849.10^2$	$-4.051.10^2$
$\lambda = +3.347.10^{-6}$	$6.875.10^1$	$6.939.10^2$	$1.142.10^3$	$2.739.10^3$
$\lambda = -3.347.10^{-6}$	$-1.299.10^2$	$7.020.10^1$	$-1.149.10^3$	$-2.676.10^3$
$\gamma = +3.347.10^{-6}$	$-1.875.10^2$	$5.910.10^2$	$-5.565.10^2$	$1.414.10^3$
$\gamma = -3.347.10^{-6}$	$9.458.10^1$	$1.465.10^2$	$5.443.10^2$	$-1.347.10^3$
$\dot{x} = +3.986.10^{-5}$	$6.132.10^3$	$6.252.10^3$	$2.630.10^2$	$3.396.10^2$
$\dot{x} = -3.986.10^{-5}$	$-6.221.10^3$	$-5.469.10^3$	$-2.730.10^2$	$-2.693.10^2$
$\dot{y} = +3.986.10^{-5}$	$6.652.10^3$	$2.480.10^4$	$3.305.10^2$	$1.034.10^3$
$\dot{y} = -3.986.10^{-5}$	$-6.752.10^3$	$-2.404.10^4$	$-3.427.10^2$	$-9.867.10^2$
$\dot{\lambda} = +1.668.10^{-4}$	$1.175.10^3$	$1.796.10^3$	$9.186.10^3$	$7.949.10^3$
$\dot{\lambda} = -1.668.10^{-4}$	$-1.189.10^3$	$-1.158.10^3$	$-9.167.10^3$	$-7.897.10^3$
$\dot{\gamma} = +1.668.10^{-4}$	$1.351.10^3$	$4.634.10^3$	$8.681.10^3$	$3.070.10^4$
$\dot{\gamma} = -1.668.10^{-4}$	$-1.448.10^3$	$-4.488.10^3$	$-8.636.10^3$	$-3.065.10^4$

Basic Data:

D = 875 mm　　L = 2390 mm　　C_D = 1.6 mm

ω = 9.1106 rad/s　　Oil Supply Head = 14.7 m　　η = 0.07123 Pa.s

ϵ = 0.5　　$\psi = 47.12^0$　　$\beta = 0^0$　　$\alpha = 3.287.10^{-5}$ rads.

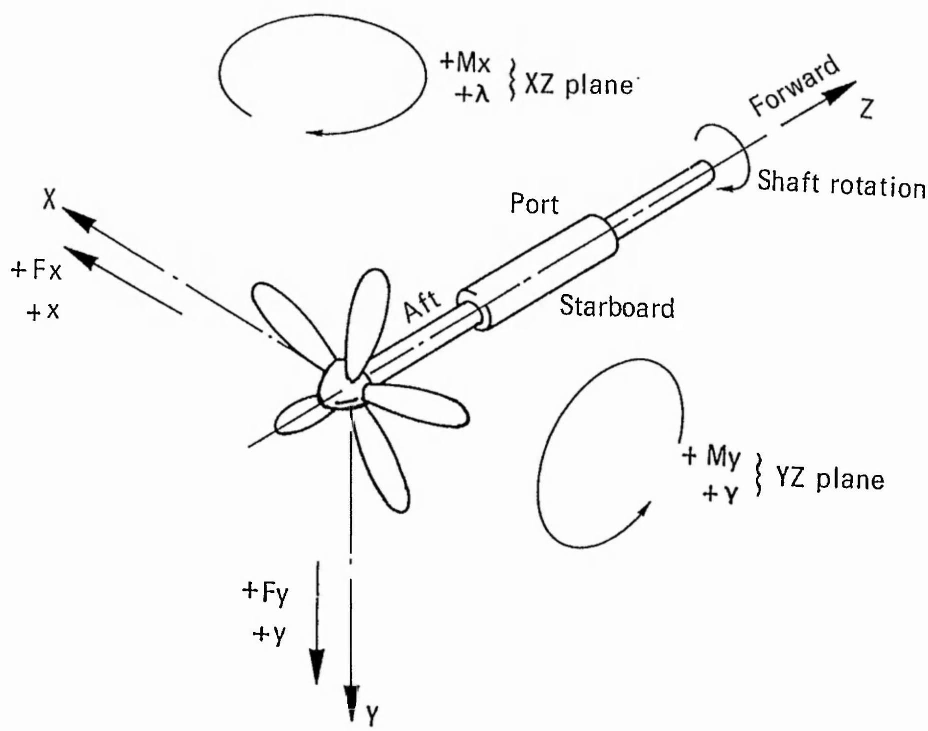

Fig 1 Sign Convention for Reference (92)

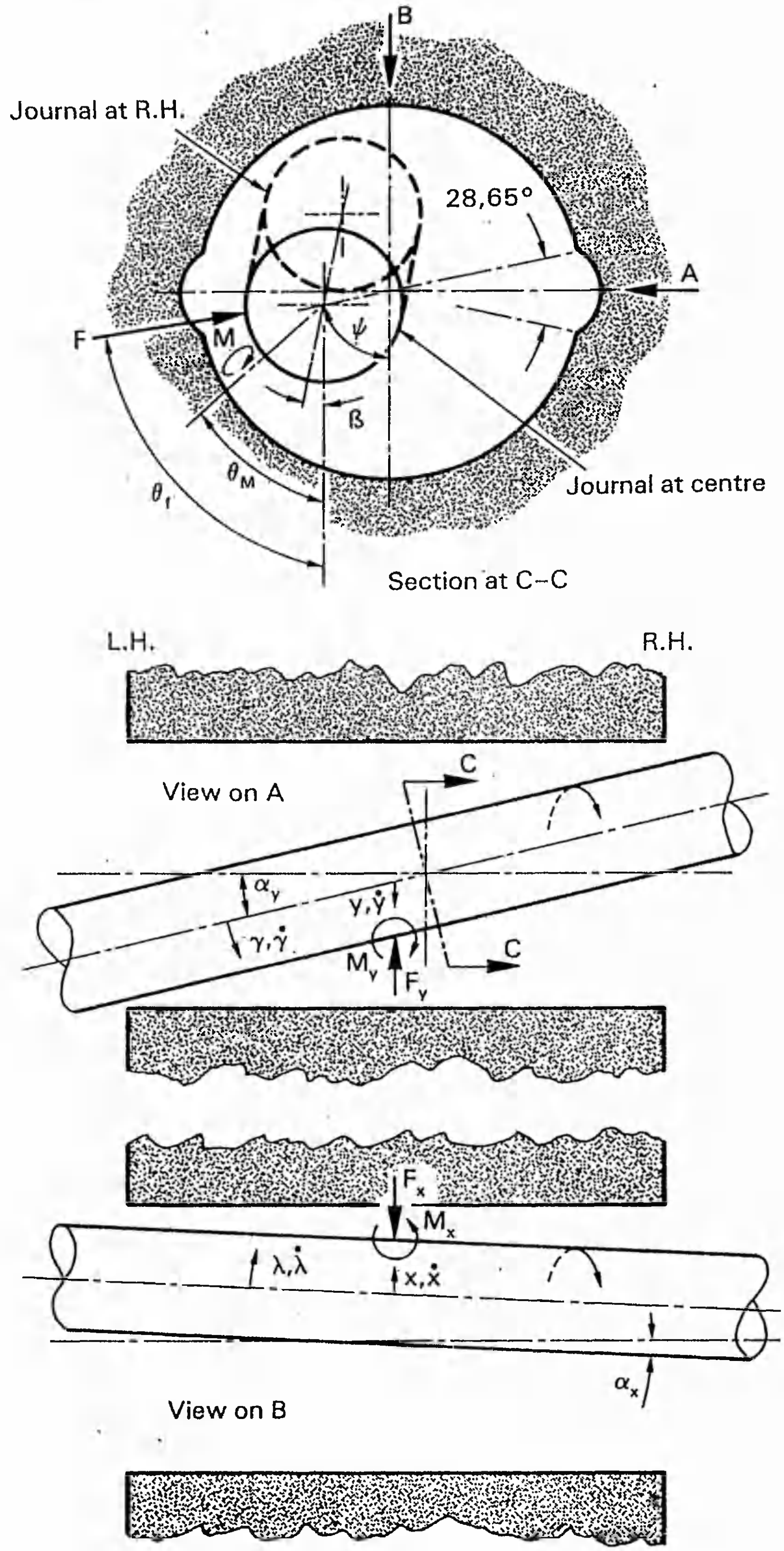

FIG. 2. NOTATION AND SIGN CONVENTION FOR PAPERS PRIOR TO REFERENCE (92)

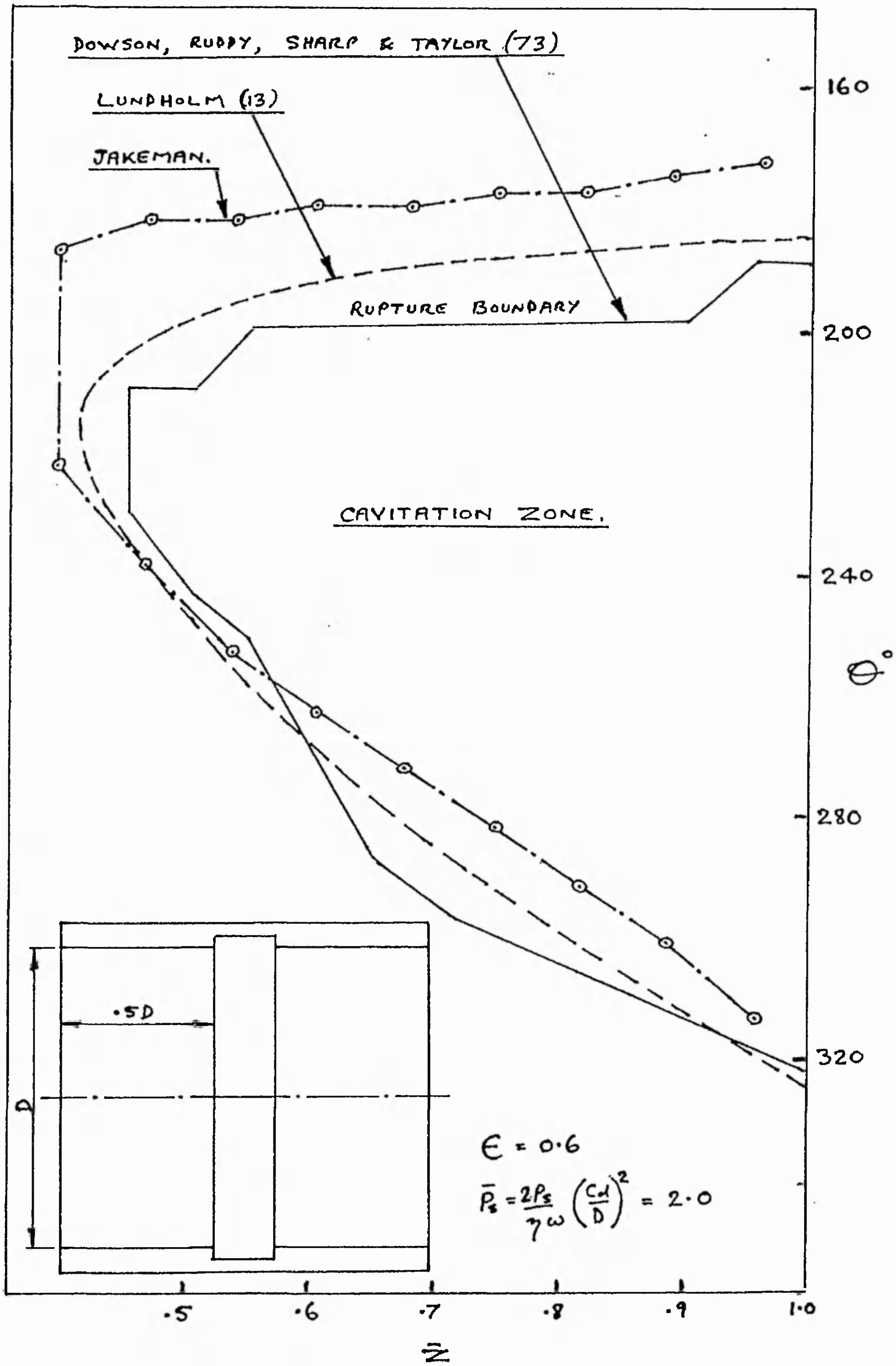

FIG. 3. PREDICTED CAVITATION MAP COMPARISONS.

	REF. (73)	JAKEMAN.
Ψ	72·1	71·67
S	·3965	·3879
$\bar{Q}$	1·665	1·610

Figs. 4 - 7. Comparison of Theoretical Oil Film Stiffness and Damping Coefficients by Author with Theoretical and Experimental Coefficients by Parkins (51).

Full Circumferential Groove Aligned Bearing.

See Reference (86) for details.

Fig. 4.	Stiffness Coefficients at ϵ = 0.790
5.	Stiffness Coefficients at ϵ = 0.857 to 0.869
6.	Damping Coefficients at ϵ = 0.788, 0.834
7.	Damping Coefficients at ϵ = 0.859

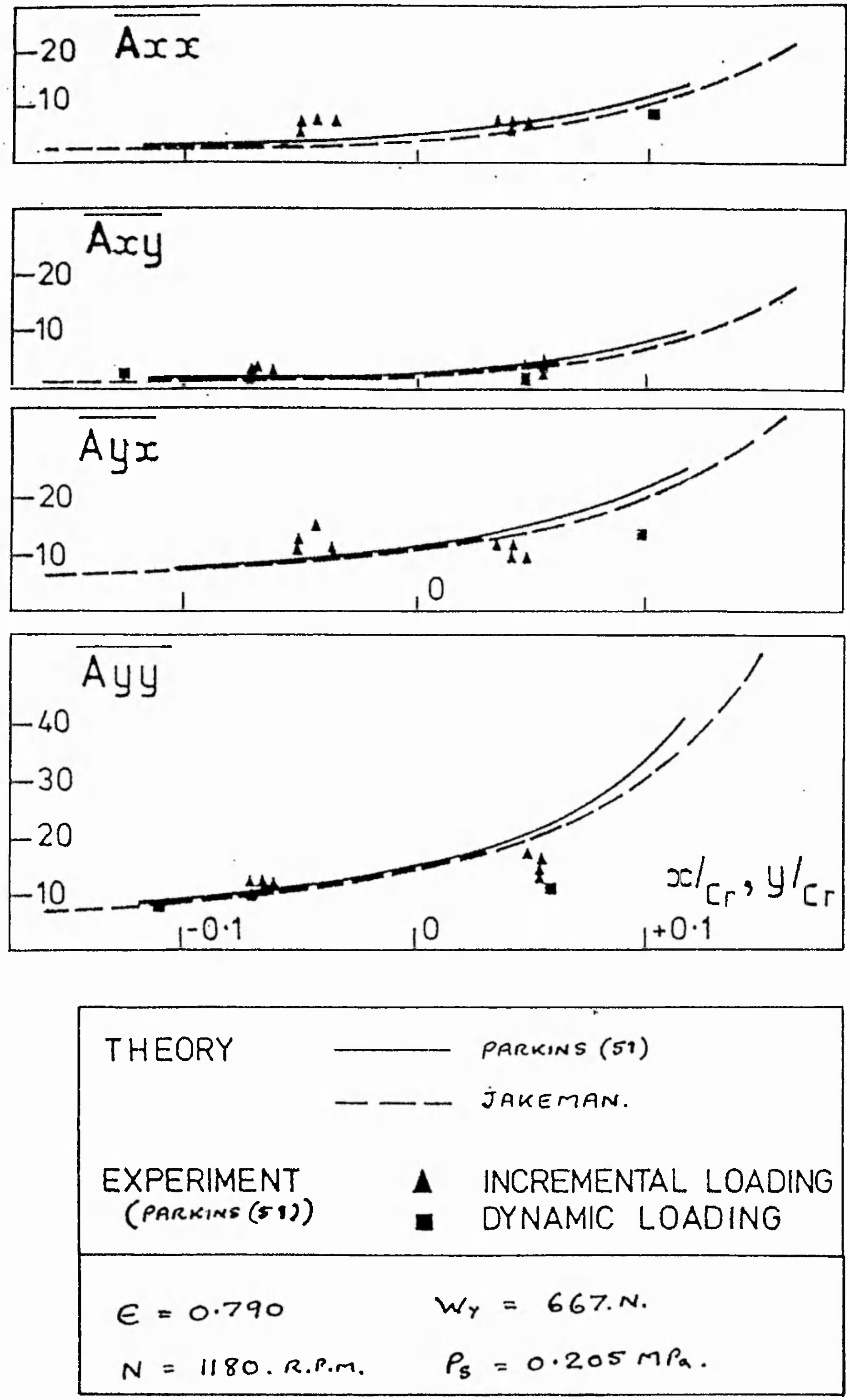

$\overline{Axx}$
20
10
$\overline{Axy}$
20
10
$\overline{Ayx}$
20
10
0
$\overline{Ayy}$
40
30
20
10
x/c_r, y/c_r
-0·1
0
+0·1
THEORY
PARKINS (51)
JAKEMAN.
EXPERIMENT
(PARKINS (51))
INCREMENTAL LOADING
DYNAMIC LOADING
ϵ = 0·790
W_Y = 667. N.
N = 1180. R.P.M.
P_S = 0·205 MPa.

FIG. 4

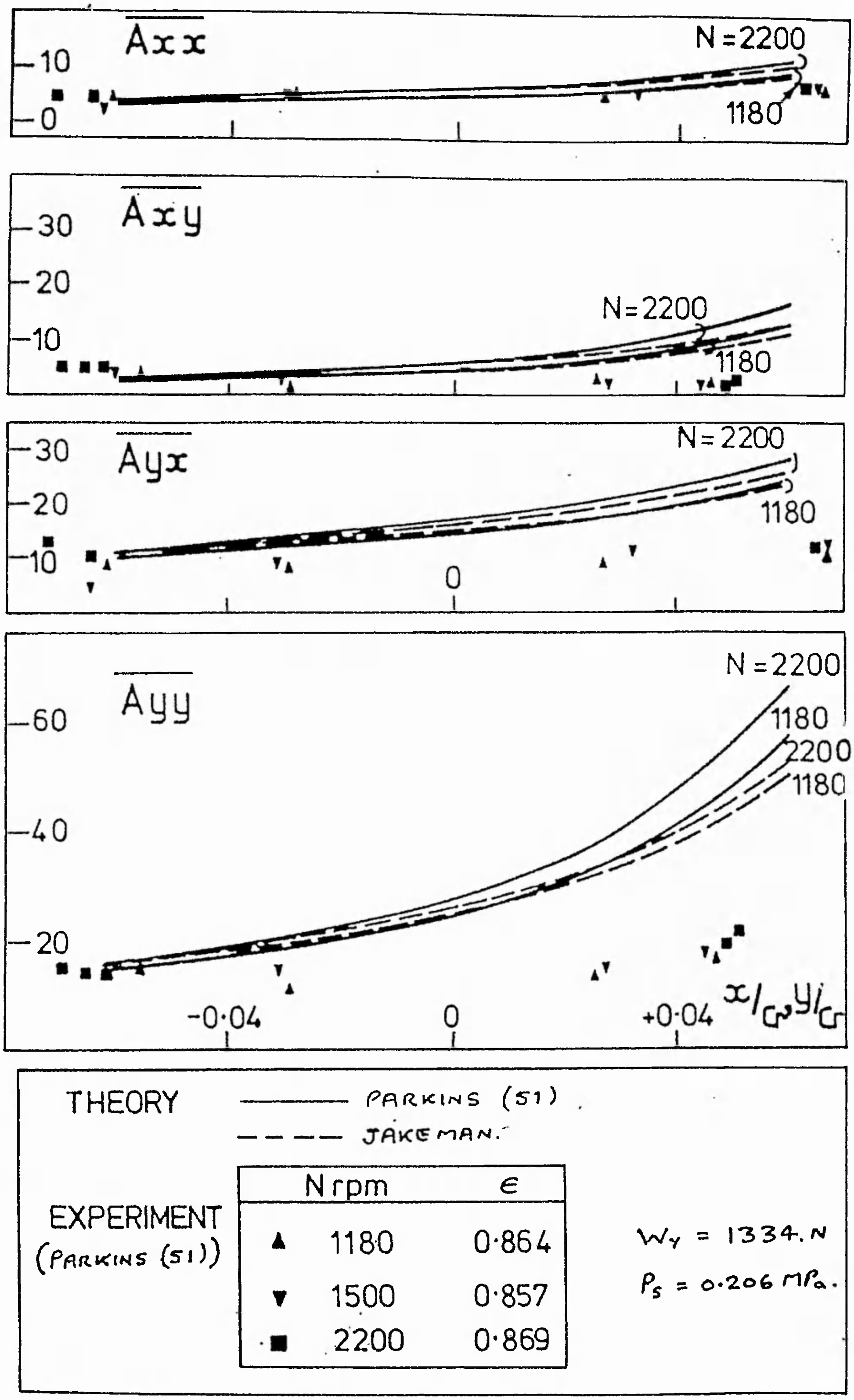

Axx
N = 2200
1180
10
0
Axy
N=2200
1180
30
20
10
Ayx
N = 2200
1180
30
20
10
0
Ayy
N = 2200
1180
2200
1180
60
40
20
-0·04
0
+0·04
x/Cr, y/Cr
THEORY
PARKINS (51)
JAKEMAN.
EXPERIMENT
(PARKINS (51))
N rpm
ε
1180
0·864
1500
0·857
2200
0·869
Wy = 1334. N
Ps = 0·206 MPa.

Fig. 5.

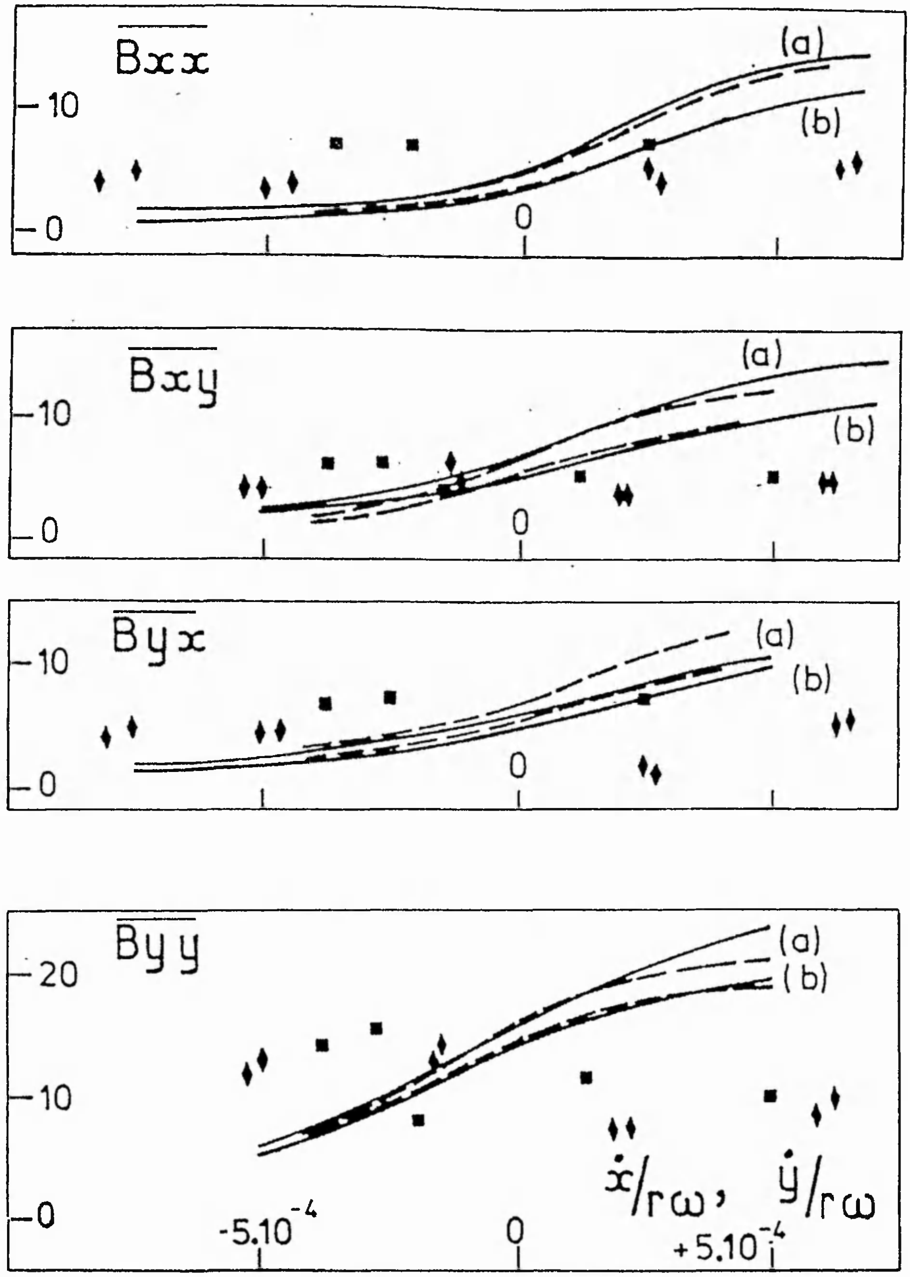

THEORY ——————— PARKINS. (51)
— — — — JAKEMAN.

$\epsilon = 0{\cdot}834$ (a) $W_Y = 667.$ N.

$\epsilon = 0{\cdot}788$ (b)

N = 1500. R.P.M. $P_S = 0{\cdot}103$. MPa.

EXPERIMENT ■ $\Omega/\omega = 1{\cdot}0$
♦ $\Omega/\omega = 2{\cdot}0$

FIG. 6.

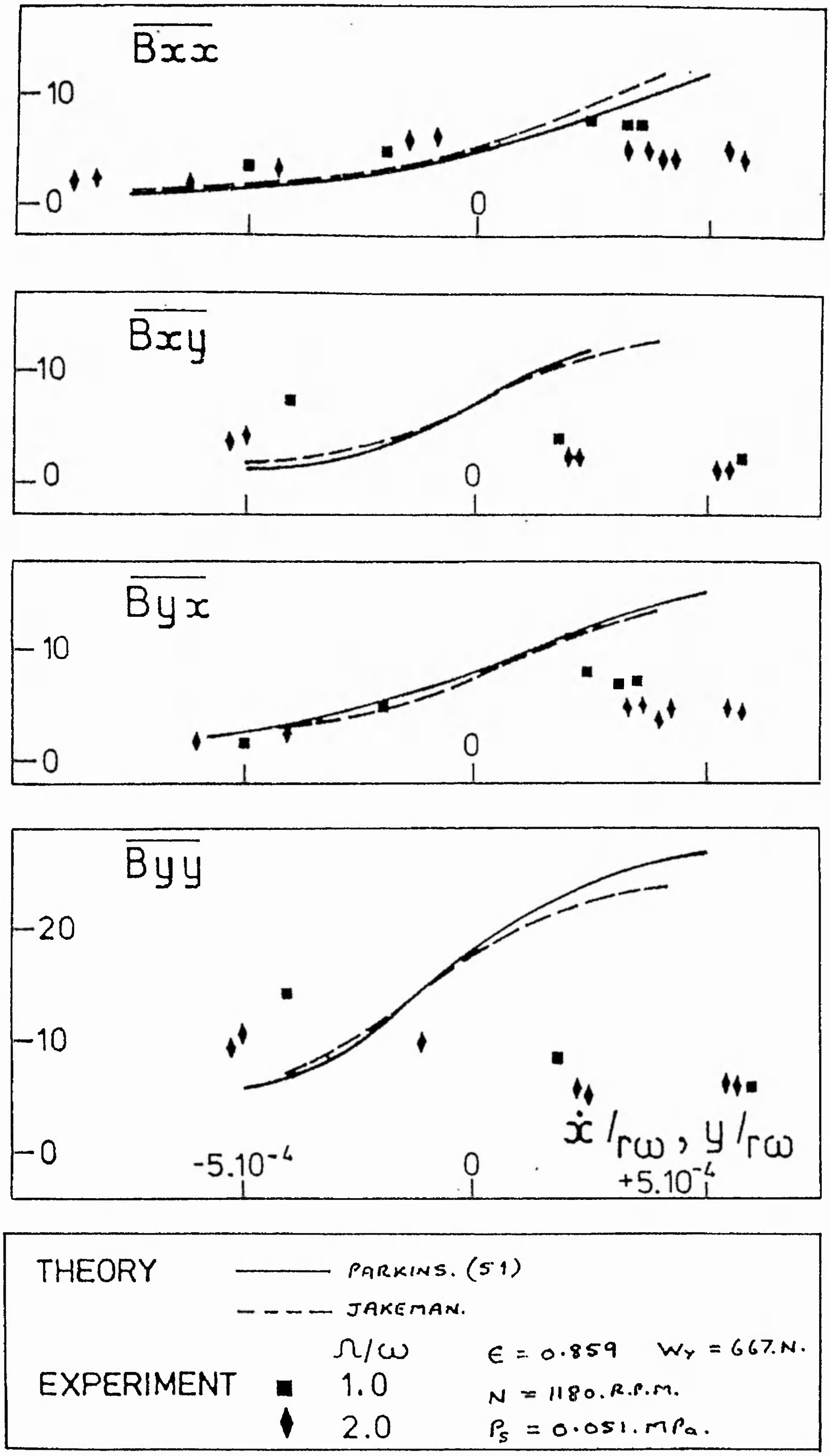

$\overline{Bxx}$
10
0
$\overline{Bxy}$
10
0
$\overline{Byx}$
10
0
$\overline{Byy}$
20
10
0
-5.10^-4
0
+5.10^-4
$\dot{x}/r\omega$, $y/r\omega$
THEORY
PARKINS. (5·1)
JAKEMAN.
EXPERIMENT
Ω/ω
1.0
2.0
ϵ = 0·859
W_y = 667.N.
N = 1180.R.P.M.
P_s = 0·051.MPa.

FIG. 7.

APPENDIX 1

Investigation of the Influence of Element Mesh upon the Accuracy of the Numerical Hydrodynamic Solution

This appendix reports the results of an investigation into the influence of the oil film element mesh details upon the hydrodynamic force and moment prediction accuracy. The variables considered were : Number of element rows (M_c) (circumferential positions), Number of element columns (N_A) (axial positions) and axial element grading factor (G_{RDFAC}) The last feature was introduced to improve the accuracy with a given number of elements. It recognises the relatively flat axial load distribution of the sterntube bearing due to high L/D ratio (generally 2), by using smaller axial element dimensions towards the bearing ends where there is a correspondingly sharp fall in load. The system for axial element grading adopted was based on the following equation:

$$\Delta a(I) = L \left[\frac{1}{G_{RDFAC} . N_A} + \frac{(I-1)(G_{RDFAC}-1)}{2 . G_{RDFAC} . K_\Sigma} \right]$$

where

$$K_\Sigma = \sum_{I=1}^{I=N_A/2} (I-1)$$

For the above system N_A must be an even number, and the equation is valid for $1 \leq I \leq N_A/2$. $\Delta a(I)$ in the range $N_A/2+1 \leq I \leq N_A$ is a "mirror image" of the above. Note that the axial dimension of the end element $\Delta a(1)$ is $1/G_{RDFAC}$ times the axial element dimension where no grading is used (G_{RDFAC} = 1). Fig. A.1.1. illustrates the result of this grading system for a range of G_{RDFAC} values.

A simple circumferential grading system was used. The number of circumferential element positions in the top half of the bearing was equated to T_{OPFAC} times the number of circumferential element positions in the bottom half. The results were found to be fairly insensitive to the value of T_{OPFAC}. For simplicity, the influence of T_{OPFAC} was not therefore considered in this investigation. A value of T_{OPFAC} = 0.5 was found to be generally satisfactory, and was used throughout this work with one exception. The exception concerned was the investigation of the influence of load vector angle, since significant hydrodynamic pressures were encountered in the top half of the bearing. Accordingly T_{OPFAC} = 1 was used for the load vector angle study.

It should be noted that mesh sizes specified in this investigation refer to the bottom half of the bearing. Thus a 70 x 14 mesh means 70 circumferential x 14 axial element positions in the bottom half of the bearing, and 35 circumferential x 14 axial element positions in the top half.

The degree of accuracy required for oil film force and moment prediction in steadily loaded situations depends upon the application. Consideration should be given to the influence of accuracy on related factors; e.g. the interaction with the prediction of shaft alignment conditions.

In the marine field it is not uncommon for the required prediction accuracy to be substantially better than the accuracy with which the predictions can be checked by measurement.! Practical situations also introduce a degree of uncertainty with respect to significant parameters. Such parameters include bearing clearance and lack of circularity in the operating condition, and for marine applications in particular : propeller - wake forces and moments, hull distortion at different draughts and sea states, etc. These uncertainties render a high level of bearing performance prediction accuracy unjustifiable. They are, however, difficult to quantify, consequently a degree of subjectivity is inevitable in the specification of prediction accuracy standards.

Journal orbit analysis for dynamically loaded bearings requires the computation of linearised dynamic coefficients. An acceptable standard of accuracy for these coefficients could be determined only by carrying out comparative orbit predictions at various accuracy levels. Due to the computing time involved in the journal orbit analysis methods emplpoyed to date, such comparative tests have not been carried out. The projected marine propeller shafting lateral vibration analysis program (see 7.1.), based on a direct orbit solution, will enable such comparative tests to be carried out more readily. At present the assessment of accuracy standards in this area is subjective.

For the assessment of the accuracy associated with any mesh, there are no absolute reference standards available. Tests indicated that the improvement in accuracy resulting from the use of meshes finer than 70 x 14, was insignificant. The 70 x 14 mesh was therefore adopted as the reference standard for this investigation.

The mesh size required to achieve a given accuracy is dependant on the journal position within the bearing clearance, and upon the bearing geometry. In view of the number of parameters involved, a comprehensive investigation is not practicable. The method employed in this investigation was, therefore, firstly to carry out a detailed mesh - accuracy study for a typical set of sterntube bearing parameters. A satisfactory element mesh was thus established for this typical case. The mesh thus determined was then checked for accuracy over a range of journal locations. Finally, a comprehensive set of accuracy checks, including the 32 linearised dynamic coefficients, were carried out for the aft sterntube bearing of the "Keiyo Maru" test case used in reference (92).

The range of test conditions used for this investigation is given in Table A.1.1. Note that Test. 1. applies to the detailed mesh - accuracy study, and Test. 9. to the "Keiyo Maru" test case of reference (92).

The initial part of the investigation (Test. 1) examined the influence of G_{RDFAC} . Fig A.1.2. shows the percentage error in F_y plotted against G_{RDFAC} for a range of mesh sizes. Fig. A.1.3. provides a similar plot for the percentage error in M_y for two mesh sizes. It is evident from these results that for values of 5 and above, G_{RDFAC} has little influence upon accuracy. G_{RDFAC} = 6 was adopted for the remainder of this investigation.

In Fig. A.1.4. the percentage error in F_y is plotted against the total number of elements (in the bottom half of the bearing) for each of the N_A values considered. There is clearly a threshold in the number of elements below which the accuracy starts to deteriorate quite rapidly. This threshold is reduced at lower values of N_A. The curves for different N_A values also tend to converge below the threshold.

Fig. A.1.5. presents the data for percentage error in M_y in a similar format to that for F_y in Fig. A.1.4. In relation to the results for percentage error in F_y, the rise in $\% M_y$ at a low number of elements is much less significant. Reference to the magnitude of the M_y errors in Fig. A.1.5., indicates that the accuracy of is substantially more sensitive to N_A, than the accuracy of F_y. In order to achieve an accuracy of about 1%, a 17 x 10 mesh would be satisfactory with respect to F_y. For M_y, however, a 20 x 12 mesh is required. A 20 x 12 mesh was therefore adopted for the accuracy tests over a range of conditions as specified in Table A.1.1. The percentage error results for F_y and M_y in the above tests are also given in Table A.1.1.

From the results in Table A.1.1. it is evident that some loss of accuracy occurs at high ϵ . This applies to both the mean value of ϵ , as indicated by the value at the bearing axial centre, and to the local ϵ at the bearing end. The loss of accuracy is due to the increased slopes in the film pressure profile at high ϵ , which require a finer mesh to achieve satisfactory modelling; i.e. to maintain the level of accuracy achieved at low ϵ .

Comprehensive details of the parameter accuracies found for the test 9 conditions, are given in Table A.1.2. These include the 32 linearised dynamic coefficients. It should be noted that the expression of accuracy in percentage error terms can be misleading in some circumstances. Where the magnitude of a parameter is small, a large percentage error may be insignificant. This comment applies to the data for M_x in Table A.1.2. With regard to the linearised dynamic coefficients, the largest errors are associated with some moment - lateral displacement, force - angular displacement and cross axis moment - angular displacement terms. The accuracy of the damping coefficients is generally better than that for the stiffness coefficients.

As noted earlier, the significance of the dynamic coefficient accuracies with respect to journal orbit/shafting lateral vibration analysis, cannot be determined until comparative analyses are carried out at different levels of coefficient accuracy. It should be noted, however, that at the time at which this mesh accuracy investigation was conducted, the computation of dynamic coefficients at each time step during a journal orbit analysis, was contemplated. The need to minimise the number of mesh elements for computing time considerations was therefore of paramount importance. It was subsequently decided that, for a dynamically misaligned sterntube bearing, the above approach to journal orbit analysis was not a practical proposition. The use of a single set of pre-computed dynamic coefficients for both the linear and non-linear oil film models was therefore adopted in reference (92). As a result of this change, the need to use the minimum tolerable number of mesh elements become less imperative. The mesh finally adopted for the computation of dynamic coefficients (linear and non-linear) in reference (92) was therefore 30 x 14 with $G_{RDFAC} = 6$. In the earlier work on sterntube bearings reported in references (87) and (88) a 50 x 14 mesh with $G_{RDFAC} = 5$ was used.

Table A.1.1. Accuracy Tests for a 20 x 12 * Mesh (GRDFAC = 6)

TEST	1	2	3	4	5	6	7	8	9
D mm	1000	1000	1000	1000	1000	1000	1000	1000	875
L mm	2000	2000	2000	2000	2000	2000	2000	2000	2390
C_D mm	2.0	2.0	2.0	2.0	2.0	2.0	2.0	2.0	1.6
N R.P.M.	100	100	100	100	100	100	100	100	87
HEAD, m	0	0	0	0	0	0	0	0	14.7
η Pa.s.	0.04116	0.04273	0.04147	0.03537	0.04277	0.03944	0.04277	0.04158	0.07201
ϵ (CENTRE)	0.7002	0.4978	0.7065	0.9085	0.4989	0.7678	0.4962	0.6021	0.5970
ϵ (END)	0.8721	0.4978	0.7065	0.9085	0.6585	0.9489	0.8280	0.9497	0.6388
ψ deg	34.67	43.25	35.03	22.52	43.55	28.08	45.26	38.02	37.70
α rad	2.10^{-4}	0	0	0	2.10^{-4}	2.10^{-4}	4.10^{-4}	4.10^{-4}	$1.5.10^{-4}$
β deg.	0	0	0	0	0	0	0	0	- 52
F_y ERROR %	- 0.40	+ 0.02	- 0.28	+ 0.09	- 0.16	- 0.73	- 0.61	- 0.77	- 0.41
M_y ERROR %	- 1.16	-	-	-	- 1.01	- 1.64	- 1.00	- 1.34	- 1.46

* Test 9 used a 20 x 14 mesh in view of the larger L/D ratio.

Table A.1.2. ACCURACY OF 20 X 14 MESH FOR TEST. 9 CONDITION

	VALUE	% ERROR		VALUE	% ERROR
F_y	$-9.477.10^5$	0.41	M_y	$6.664.10^4$	- 1.46
F_x	$6.973.10^4$	0.87	M_x	$8.018.10^4$	- 1.33
$\overline{A}_{xx}$	- 2.36	- 0.85	$\overline{B}_{xx}$	- 3.23	0
$\overline{A}_{xy}$	1.36	- 0.73	$\overline{B}_{xy}$	- 3.53	8.50
$\overline{A}_{yx}$	- 6.12	- 4.62	$\overline{B}_{yx}$	- 2.97	- 14.14
$\overline{A}_{yy}$	- 3.78	- 6.48	$\overline{B}_{yy}$	- 13.7	- 2.92
$\overline{A}_{\lambda x}$	0.210	- 1.41	$\overline{B}_{\lambda x}$	0.190	1.58
$\overline{A}_{\lambda y}$	0.124	- 3.86	$\overline{B}_{\lambda y}$	0.297	4.04
$\overline{A}_{\gamma x}$	0.0408	- 14.29	$\overline{B}_{\gamma x}$	0.278	4.32
$\overline{A}_{\gamma y}$	- 0.0971	2.02	$\overline{B}_{\gamma y}$	- 0.333	3.90
$\overline{A}_{x\lambda}$	0.213	- 1.41	$\overline{B}_{x\lambda}$	0.197	4.06
$\overline{A}_{x\gamma}$	0.133	11.28	$\overline{B}_{x\gamma}$	0.276	1.45
$\overline{A}_{y\lambda}$	0.0338	24.26	$\overline{B}_{y\lambda}$	0.304	9.54
$\overline{A}_{y\gamma}$	- 0.110	55.91	$\overline{B}_{y\gamma}$	- 0.364	3.30
$\overline{A}_{\lambda\lambda}$	- 0.135	1.48	$\overline{B}_{\lambda\lambda}$	- 0.187	1.07
$\overline{A}_{\lambda\gamma}$	0.0650	12.46	$\overline{B}_{\lambda\gamma}$	- 0.167	1.20
$\overline{A}_{\gamma\lambda}$	- 0.306	- 12.42	$\overline{B}_{\gamma\lambda}$	- 0.152	- 2.63
$\overline{A}_{\gamma\gamma}$	- 0.243	- 7.41	$\overline{B}_{\gamma\gamma}$	- 0.735	0.14

Forces and Moments are in N. m. units.

Coefficients are dimensionless.

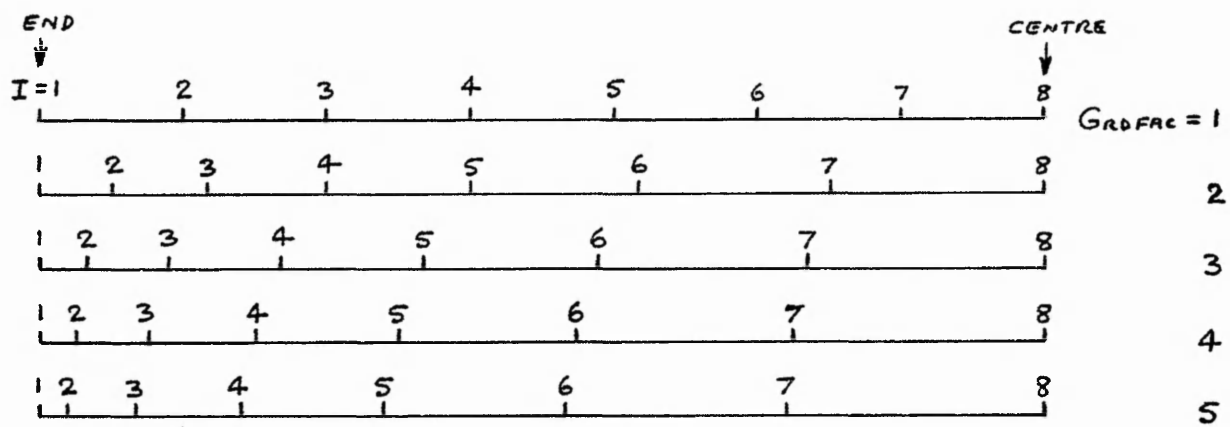

FIG. A.1.1. AXIAL ELEMENT GRADING.

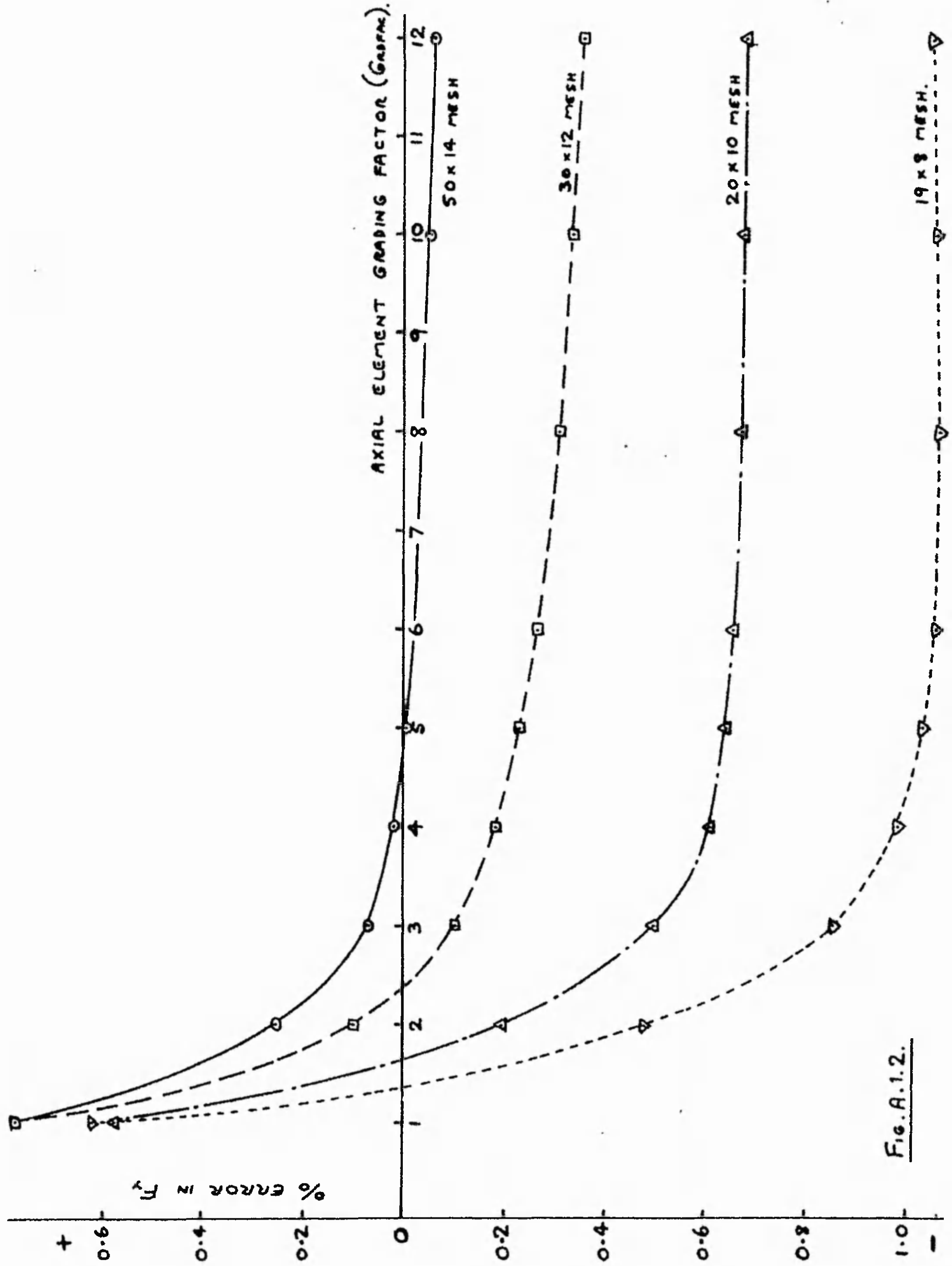
AXIAL ELEMENT GRADING FACTOR (GRDFAC).
% ERROR IN F_y
50 x 14 MESH
30 x 12 MESH
20 x 10 MESH
19 x 8 MESH.
+ 0·6
0·4
0·2
0
0·2
0·4
0·6
0·8
1·0
-
1
2
3
4
5
6
7
8
9
10
11
12

FIG. A.1.2.

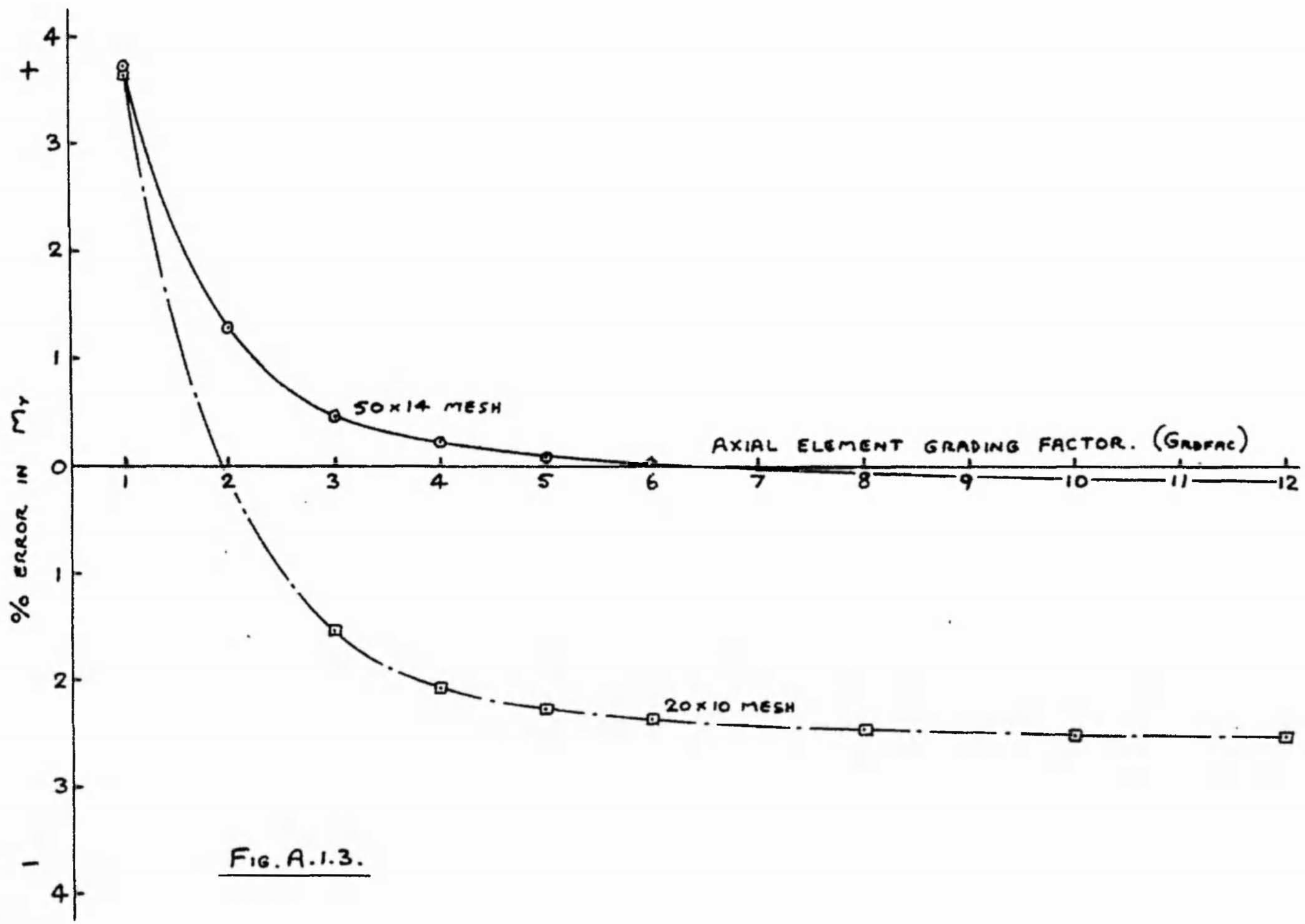

% ERROR IN M_Y
AXIAL ELEMENT GRADING FACTOR. (GRDFAC)
50×14 MESH
20×10 MESH

FIG. A.1.3.

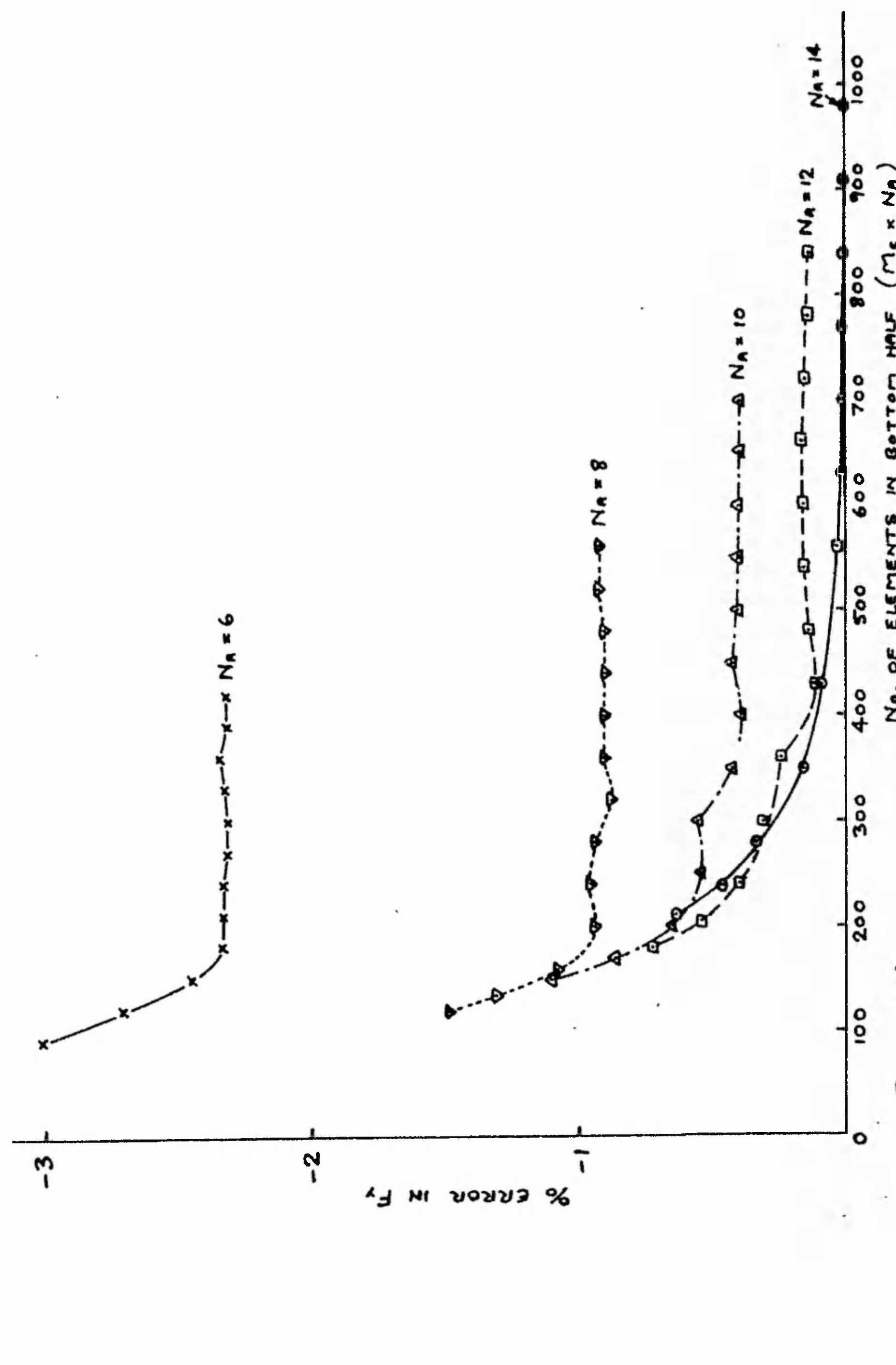

-3
-2
-1
% ERROR IN F_y
0
100
200
300
400
500
600
700
800
900
1000
No. OF ELEMENTS IN BOTTOM HALF ($M_c \times N_R$)
$N_R = 6$
$N_R = 8$
$N_R = 10$
$N_R = 12$
$N_R = 14$

FIG. A.1.4.

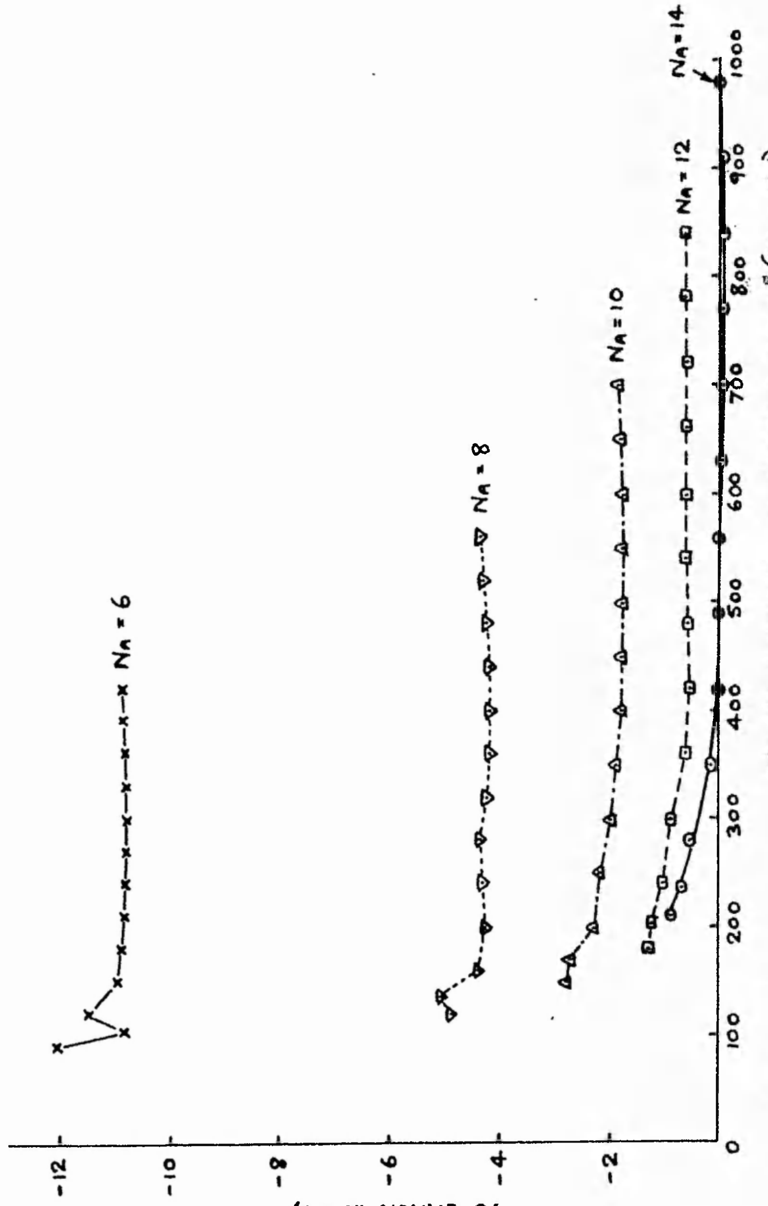

% ERROR IN My
-12
-10
-8
-6
-4
-2
0
100
200
300
400
500
600
700
800
900
1000
No. OF ELEMENTS IN BOTTOM HALF (Mc x NA)
NA = 6
NA = 8
NA = 10
NA = 12
NA = 14

FIG. A.1.5.

APPENDIX 2.

Glossary of Terms

A comprehensive glossary of terms used in the field of hydrodynamic journal bearings is given in Appendix 2 of reference (88). The following list covers a few additional terms:

Aft peak tank	:	A water ballast tank situated in the stern of a ship and used for trimming purposes. The sterntube generally passes through the lower part of this tank, and the water ballast thus provides a useful sink for heat generated in the sterntube bearings.
Dynamic alignment (of shafting)	:	Refers to the analysis of shafting systems in the running condition. For marine propeller shafting, only the mean values of cyclic forces and moments due to propeller - wake interaction are used.
Effective viscosity	:	The viscosity value used to represent a complete oil film when isoviscous conditions are assumed.

Flow rate	:	In the present context this refers to the nett oil flow rate through a hydrodynamic bearing. This is the oil expelled at the bearing ends, and does not include circumferentially recirculated oil.
Flow separation	:	The separation of oil from the bearing surface. This has been experimentally observed in cavitation studies.
Oil	:	The literal meaning of this term does not require clarification. It is used throughout this thesis in place of the term "lubricant" since it is more concise and generally relevant to practical situations. This work is equally applicable to bearings utilising other incompressible lubricants provided hydrodynamic operating conditions are attained.
Oil film force	:	Nett force due to hydrodynamic action acting on the journal.
Oil film moment	:	Nett moment due to hydrodynamic action acting on the journal at the bearing axial centre.

Outlet temperature	:	Mean temperature of oil expelled from the bearing ends.
Power loss	:	Loss due to viscous shear within a bearing oil film.

APPENDIX 3.

Computer Program Listings

Listings of all the computer programs written during the course of the work covered by this thesis would alone fill a fairly large volume. The selection of listings for this appendix has therefore been restricted to two. These relate to the work covered by references (90), (91) and (92), and include the most significant aspects of this work. The programs for which listings are given in this appendix are:

RWJ015D : STERNTUBE BEARING ANALYSIS

Issue : 19.05.87. (A.3. - 3 - 20)

This program includes the implementation of the numerical hydrodynamic analysis method in its latest form, as described in reference (90). It also covers the computation of the coefficients for the non-linear oil film model outlined in reference (92), together with the oil film forces and moments at the datum condition. The output is stored on disc for use as input to program RWJ043 which is referred to below.

RWJ043 : Tailshaft - Sterntube Bearing Lateral Vibration Model.

Issue : 03.11.87. (A.3. - 21 - 53)

Program RWJ043 carried out a lateral vibration analysis for marine propeller shafting. It represents the latest solution for the journal orbit time stepping process, as applied to a multi-mass system with shafting elastic forces and moments accounted for. Alternative linear and non-linear oil film models for the aft stern-tube bearing may be selected. This program formed the basis of the work reported in reference (92). In its present form it is a "research" program in that it has been "tailored" to the "Keiyo Maru" test case.

Both of the listings given in this appendix are written in BASIC for the Hewlett Packard 9836C desk top computer.

(1)

```
10    PRINTER IS 1 !     PROGRAMME-RWJO15D :STERNTUBE BEARING ANALYSIS.
20                 !     ( Thesis Version.)
30    DEG!               ------------------------------------------------
40    OPTION BASE 1 !     Issue : 19.05.87. Version for Computing Non-Linear
                          Stiffness & Damping Coefficients.
50    Orf=1.7 !  Over Relaxation Factor may be altered by manual EDIT.
60    Topfac=.5    !      Factor on No. of circ. elements in top half, may be
70    Tbi=104.325 !       altered by manual EDIT.
80    Tbo=255.675 !       Tbi....Tto are locations of inlet and outlet edges to
                  !       bearing bottom and top surfaces due to axial oil
90    Tti=284.325 !       grooves.
100   Tto=435.675
110   Datset=3        !        Manual Entry of DATSET No.
120   Eccent=.4800 !           Manual Entry of Journal Location Data.
130   Psi=59.00       !        ------------------"--------------------
140   Xseao=3.1344E-5 !        ------------------"--------------------
150   Phio=-1.9501E-5 !        ------------------"--------------------
160   Epert=.06       ! mm.    Manual Entry of Displacement Perturbations.
170   Psipert=7       ! deg.   ------------------"------------------------
180   Xseapert=1.2E-4!rad.     ------------------"------------------------
190   Phipert=9.E-5 ! rad.     ------------------"------------------------
200   Edpert=4        ! mm/s.  Manual Entry of Velocity Perturbations.
210   Psidpert=7      !rad/s.  ------------------"---------------------
220   Xseadpert=6.E-3! rad/s.  ------------------"---------------------
230   Phidpert=5.E-3 ! rad/s.  ------------------"---------------------
240   Pcav=0          !  Cavitation pressure set to zero gauge.
250   Gee=9.80665     !  m/s^2. Gravitational acceleration.
260   Zerco=0
270   PRINT FNLin$(10);"Programme RWJO15D : Sterntube Bearing Analysis."
280   PRINT "Issue : 19.05.87. Non-Linear Stiffness & Damping Coefficients."
290    PRINT FNLin$(10);"RWJO15: PROGRAMME RUNNING. (Initial Phase.)"
300    PRINTER IS 701
310    PRINT FNPage$;"##############################################################
##################"
320    PRINT "# RWJO15D: Sterntube Bearing Analysis. Issue : 19.05.87.
        #"
330    PRINT "# Version for Computing Non-Linear Stiffness & Damping Coefficients
        #"
340    PRINT "# (Fully Updated Cavitation Model.)
        #"
350    PRINT "##############################################################
#########"
360    DIM Frm(3,3,3,3),Ftm(3,3,3,3),Mrm(3,3,3,3),Mtm(3,3,3,3) !
           Values Computed by Hydrodynamic Analysis.
370    DIM Afr(3,3,3,3),Aft(3,3,3,3),Amr(3,3,3,3),Amt(3,3,3,3) !
           Non-Linear Stiffness Coefficients.
380    DIM Bfr(3,3,3,3),Bft(3,3,3,3),Bmr(3,3,3,3),Bmt(3,3,3,3) !
           Non-Linear Damping Coefficients.
390    DIM Kfr(3,3,3,3),Kft(3,3,3,3).Kmr(3,3,3,3),Kmt(3,3,3,3) !
           General Coefficient Storage Matricies for "Check" Subroutine.
400    DIM Kfm(3,3,3,3),Fm(3,3,3,3)                             !
       Coefficient & Force & Moment Storage Matricies for Non_lin_cof Subroutine.
410                    !        Section below is for entry of Bearing data which may
                       !        be changed by manual EDIT.
420    Head=14.7       !           Oil supply head. m.
430    D=875           !           Journal diameter. mm.
440    Le=2390         !           Bearing length. mm.
450    Cd=1.6          !           Diametral clearance. mm.
460    N=87            !           R.P.M.
470    Bow=0           !           Journal bow ( 0 signifies straight journal assumed
480    Et=7.201E-2     !           Effective oil viscosity. Pa.s.
```

```
490    Wvt=9.E+5       !        Approx. vertical bearing load. N. ( Used only as  ②
                       !        film pressure relaxation convergence criterion.)
500                    !     Section below is for entry of Mesh data which may be
                       !     changed by manual EDIT.
510    Mcirc=30        !        No. of circumferential element rows in bottom half
520    Nax=14          !        No. of axial element columns.
530    Grdfac=6        !        Axial element grading factor.
540    E=Eccent*Cd/2
550    Me=Mcirc+1
560    Ne=Nax+1
570    Mtcirc=INT(Mcirc*Topfac)!  Set Circumferential Divisions in Top Half=Topfa
c*Bottom.
580    Met=Mtcirc+1
590    PRINT "DATSET No. ";Datset
600    PRINT "__________________"
610    PRINT "E.Ratio        =";Eccent
620    PRINT "E              =";E;" mm."
630    PRINT "Psi            =";Psi;" deg."
640    PRINT "Xseao          =";Xseao;" rad."
650    PRINT "Phio           =";Phio;" rad."
660    PRINT "------------------------------------------------------------------"
670    PRINT "Epert          =";Epert;" mm."
680    PRINT "Psipert        =";Psipert;" deg."
690    PRINT "Xseapert       =";Xseapert;" rad."
700    PRINT "Phipert        =";Phipert;" rad."
710    PRINT "------------------------------------------------------------------"
720    PRINT "Edpert         =";Edpert;" mm/s."
730    PRINT "Psidpert       =";Psidpert;" rad/s."
740    PRINT "Xseadpert      =";Xseadpert;" rad/s."
750    PRINT "Phidpert       =";Phidpert;" rad/s."
760    PRINT "------------------------------------------------------------------"
770    PRINT "Head           =";Head;" m."
780    PRINT "D              =";D;" mm."
790    PRINT "Le             =";Le;" mm."
800    PRINT "Cd             =";Cd;" mm."
810    PRINT "N              =";N;" R.P.M."
820    PRINT "Bow            =";Bow
830    PRINT "Eta            =";Et;" Pa.s."
840    PRINT "__________________________________________________________________"
850    PRINT "No. of element rows in top half of bearing      =";Mtcirc
860    PRINT "ELEMENT DIVISION FOR BOTTOM HALF OF BEARING :-"
870    PRINT "No.of element rows (circumferential divisions) =";Mcirc
880    PRINT "No.of element columns (axial divisions)         =";INT(Nax/2)*2
890    PRINT "Axial element length grading factor             =";Grdfac
900    IF F>1 THEN 910
910    IF Bow=0 THEN 940
920    Rc=Le^2/Bow/8        !  Mean radius of curvature for bowed journal.
930    GOTO 950
940    Rc=0
950    DIM Kai(70,14),Kao(70,14),Psubcav(70,14),Kaib(70,14),Kait(70,14),Kaob(70,1
4),Kaot(70,14)
960    DIM H(71,15),Hb(71,15),Ht(71,15),Pb(70,14),Pt(70,14),Ex(15),Sx(15),Hxbot(7
1,14),Hxtop(71,14),Hyabot(70,14),Hyatop(70,14),Vnb(70,14),Vnt(70,14)
970    DIM Hx(71,14),Hyamat(70,14),Hybmat(70,14),P(70,14),Wvmat(14),Whmat(14),Wtv
(14),Wth(14),Wbv(14),Wbh(14),Qx(71,14),Qy(70,15),Void(70,14)
980    DIM Pbst(70,14),Ptst(70,14),Vn(70,14),Vt(71,14),Vv(14),Vh(14),Dymat(14),Hy
bbot(70,14),Hybtop(70,14),Lmid(14),Voidb(70,14),Voidt(70,14),Lcent(14)
990    DIM Esd(14),Psisd(14),Us(14),Vvr(14),Vhr(14),Vx(14),Vy(14)
1000 Avh=1
1010 Naxp=INT(Nax/2)*2 ! Full No. of axial elements required for misaligned
                       ! bearing - must be an even No.
1020 Nep=Naxp+1
1030 REDIM Wtv(Naxp),Wth(Naxp),Wbv(Naxp),Wbh(Naxp),Wvmat(Naxp),Whmat(Naxp),Dymat
(Naxp),Lmid(Naxp),Lcent(Naxp),Kaob(Mcirc,Naxp),Kaot(Mtcirc,Naxp)
1040 REDIM Hb(Me,Nep),Ht(Met,Nep),Kaib(Mcirc,Naxp),Kait(Mtcirc,Naxp),Pb(Mcirc,Na
xp),Pt(Mtcirc,Naxp),Ex(Nep),Sx(Nep),Hxbot(Me,Naxp),Hxtop(Met,Naxp)
```

```
1050 REDIM Hyabot(Mcirc,Naxp),Hyatop(Mtcirc,Naxp),Hybbot(Mcirc,Naxp),Hybtop(Mtci
rc,Naxp),Voidb(Mcirc,Naxp),Voidt(Mtcirc,Naxp),Pbst(Mcirc,Naxp),Ptst(Mtcirc,Naxp)
1060 REDIM Vnb(Mcirc,Naxp),Vnt(Mtcirc,Naxp)
1070 REDIM Esd(Naxp),Psisd(Naxp),Us(Naxp),Vvr(Naxp),Vhr(Naxp),Vx(Naxp),Vy(Naxp)
1080 Hcmin=(1-Eccent)*Cd/2
1090 Phd=.00833*Head         !  Oil supply head pressure. MPa.
1100 IF Avh=0 THEN 1140
1110 PRINT "Total No. of elements                                   =";Mcirc*Naxp
1120 PRINT "Element Axial/Circumferential Length Ratio              =";Le*Mcirc*360/Naxp/
PI/D/(Tbo-Tbi)
1130 GOTO 1160
1140 PRINT "Total No. of elements                                   =";Mcirc*Naxp*2
1150 PRINT "Element Axial/Circumferential Length Ratio              =";Le*Mcirc*180/Naxp/
PI/D/(Tbo-Tbi)
1160 PRINT "Over Relaxation Factor                                  =";Orf
1170 PRINT "----------------------------------------------------------------------
---------"
1180 Count=0
1190 Dyn=0
1200 R=D/2
1210 Ri=(D+Cd)/2
1220 Ec=Cd/2-Hcmin
1230 IF Avh=0 THEN 1260 !  Calculation of axial element dimensions Dymat(I) as a
1240 Naxq=Naxp/2        !  function of distance from bearing end using the Axial
1250 GOTO 1270          !  Grading Factor. ( Grdfac ).
1260 Naxq=Naxp
1270 FOR I=1 TO Naxq
1280 IF I>1 THEN 1310
1290 Ksig=0
1300 GOTO 1320
1310 Ksig=Ksig+(I-1)
1320 NEXT I
1330 Kinc=(Grdfac-1)/2/Grdfac/Ksig
1340 IF Avh=0 THEN 1400
1350 FOR I=1 TO Naxp/2
1360 Dymat(I)=Le*(1/Grdfac/Naxp+(I-1)*Kinc)
1370 Dymat(Nep-I)=Dymat(I)
1380 NEXT I
1390 GOTO 1430
1400 FOR I=1 TO Naxp
1410 Dymat(I)=Le*(.5/Grdfac/Naxp+(I-1)*Kinc)
1420 NEXT I
1430 Lcentb=0
1440 FOR I=1 TO Naxp
1450 IF I>1 THEN 1480
1460 Lcent(1)=Dymat(1)/2
1470 GOTO 1500
1480 Lcentb=Lcentb+Dymat(I-1)
1490 Lcent(I)=Lcentb+Dymat(I)/2
1500 NEXT I
1510 Dxb=PI*Ri/Mcirc*(Tbo-Tbi)/180   !  Ciccumferential element dimension for
                                     !  bottom half.
1520 Dxt=PI*Ri/Mtcirc*(Tto-Tti)/180  !  Circumferential element dimension for
                                     !  top half.
1530 MAT Wtv= (0)
1540 MAT Wbv= (0)
1550 MAT Wth= (0)
1560 MAT Wbh= (0)
1570 Xc=Le/2
1580 GOTO 6330
1590 Oil_force:   ! Main Subroutine to Compute Oil Film Forces & Moments.
1600 Wv=0 !   Requires specification of Ec, Sc, Xsea, Phi, Ed, Psid, Xsead, Phid
1610 Wh=0
1620 Mv=0 !   Initialize Oil Film Force and Moment variables.
1630 Mh=0
1640 Ecv=Ec*COS(Sc)          !  This section calculates journal location data in
```

③

```
1650 Ech=Ec*SIN(Sc)           !  Cartezian components as required for oil film    (4)
1660 Alpha=SQR(Xsea^2+Phi^2)! pressure distribution solution.
1670 IF Xsea=0 THEN 1700
1680 Beta=ATN(Phi/Xsea)+Sc
1690 GOTO 1710
1700 Beta=Sc+90
1710 Av=Alpha*COS(Beta)
1720 Ah=Alpha*SIN(Beta)
1730 Gam=0 !              Redundant terms as Cartezian angular displacement
1740 Lam=0 !              perturbations are no longer used.
1750 Vg=Xsead*COS(Sc)-Phid*SIN(Sc)
1760 Vl=Xsead*SIN(Sc)+Phid*COS(Sc)
1770 Avx=Av+Gam
1780 Ahx=Ah+Lam
1790 IF Rc=0 THEN 1820 ! Jump if journal is assumed to be straight.
1800 Lc=Rc*Avx+Le/2
1810 Yc=Rc/2*((Lc/Rc)^2-((Lc-Xc)/Rc)^2)-Xc*Avx
1820 FOR I=1 TO Nep
1830 IF I>1 THEN 1860
1840 Xs=0
1850 GOTO 1870
1860 Xs=Xs+Dymat(I-1)
1870 IF Rc=0 THEN 1910
1880  Ys=Rc/2*((Lc/Rc)^2-((Lc-Xs)/Rc)^2)-Xs*Avx
1890  Exv=Ecv+Yc-Ys+Avx*(Xc-Xs)
1900  GOTO 1920
1910  Exv=Ecv+Avx*(Xc-Xs)     !  This section calculates eccentricity Ex(I) and
1920  Exh=Ech+Ahx*(Xc-Xs)     !  attitude angle Sx(I) as a function of the axial
1930  Ex(I)=SQR(Exv^2+Exh^2) !  position locations corresponding to the element
1940  Sx(I)=ATN(Exh/Exv)      !  centres. These values are constant for an
1950  IF Exv<0 THEN 1970      !  aligned bearing.
1960  GOTO 2010
1970  IF Exh<0 THEN 2000
1980  Sx(I)=180+Sx(I)
1990  GOTO 2010
2000  Sx(I)=Sx(I)-180
2010  IF I>1 THEN 2080
2020  Eo=Ex(I)
2030  So=Sx(I)
2040  Homin=Cd/2-Eo
2050  IF Homin>0 THEN 2080    !  Test that specified journal position is possible
                              !  in relation to the bearing clearance at L H end.
2060  PRINT "Journal in contact with Bearing at L.H. end."
2070  GOTO 7950
2080  IF I<Nep THEN 2200
2090  IF Avh=0 THEN 2140
2100  Ei=Ex(I)
2110  Si=Sx(I)
2120  Himin=Cd/2-Ei
2130  GOTO 2170
2140  Ei=Eo
2150  Si=So
2160  Himin=Homin
2170  IF Himin>0 THEN 2200  !  Test as above at R H end.
2180  PRINT "Journal in contact with Bearing at R.H. end."
2190  GOTO 7950
2200  IF Ex(I)<Cd/2 THEN 2230
2210  PRINT "Journal in contact with Bearing at I =";I
2220  GOTO 7950
2230  NEXT I
2240  Ti=Tbi!        Set Bottom variables for H,Hx,Hy,Ka Subroutine.
2250  To=Tbo
2260  Dx=Dxb
2270  Mes=Me
2280  GOSUB 2500
2290  MAT Hb= H!      Store Bottom H,Hx,Hy,Ka Matricies.
```

5

```
2300  MAT Hxbot= Hx
2310  MAT Hyabot= Hyamat
2320  MAT Hybbot= Hybmat
2330  MAT Kaib= Kai
2340  MAT Kaob= Kao
2350  MAT Vnb= Vn
2360  Ti=Tti!        Set Top variables for H,Hx,Hy,Ka Subroutine.
2370  To=Tto
2380  Dx=Dxt
2390  Mes=Met
2400  GOSUB 2500
2410  MAT Ht= H!      Store Top H,Hx,Hy,Ka Matricies.
2420  MAT Hxtop= Hx
2430  MAT Hyatop= Hyamat
2440  MAT Hybtop= Hybmat
2450  MAT Kait= Kai
2460  MAT Kaot= Kao
2470  MAT Vnt= Vn
2480  GOTO 4860
2490  !               Start of H,Hx,Hy,Ka Subroutine.
2500  REDIM H(Mes,Nep),Hx(Mes,Naxp),Hyamat(Mes-1,Naxp),Hybmat(Mes-1,Naxp),Kai(Me
s-1,Naxp),Kao(Mes-1,Naxp),Vn(Mes-1,Naxp),Vt(Mes,Naxp),Vv(Naxp),Vh(Naxp)
2510  FOR J=1 TO Mes   !  This section calculates film thickness at all element
2520  FOR I=1 TO Nep   !  corner locations.
2530  H(J,I)=SQR(Ri^2+Ex(I)^2+2*Ri*Ex(I)*COS(Ti+(To-Ti)*(J-1)/(Mes-1)-Sx(I)))-R
2540  NEXT I
2550  NEXT J
2560  FOR J=1 TO Mes   !  This section calculates element axial pressure flow
2570  FOR I=1 TO Naxp  !  functions.
2580  Hx(J,I)=(H(J,I)+H(J,I+1))^3/9.6E-5/Et*Dymat(I)/Dx
2590  NEXT I
2600  NEXT J
2610  FOR J=1 TO Mes-1 ! This section calculates element circumferential
2620  FOR I=1 TO Naxp  ! pressure flow functions.
2630  IF I=1 THEN 2660
2640  Hyamat(J,I)=(H(J,I)+H(J+1,I))^3/4.8E-5/Et*Dx/(Dymat(I)+Dymat(I-1))
2650  GOTO 2670
2660  Hyamat(J,I)=(H(J,I)+H(J+1,I))^3/4.8E-5/Et*Dx/Dymat(I)
2670  IF I<Naxp THEN 2700
2680  Hybmat(J,I)=(H(J,I+1)+H(J+1,I+1))^3/4.8E-5/Et*Dx/Dymat(I)
2690  GOTO 2710
2700  Hybmat(J,I)=(H(J,I+1)+H(J+1,I+1))^3/4.8E-5/Et*Dx/(Dymat(I)+Dymat(I+1))
2710  NEXT I
2720  NEXT J
2730  FOR I=1 TO Naxp    !  This section calculates horizontal and vertical
                         !  velocitY components Vx(I),Vy(I) at element axial
2740  Vx(I)=Ed*SIN(Sc)+Ex(I)*Psid*COS(Sc)   ! centre locations due to Ed & Psid.
2750  Vy(I)=Ed*COS(Sc)-Ex(I)*Psid*SIN(Sc)
2760  Vv(I)=Vg*(Le/2-Lcent(I))+Vy(I)  !  As above but adding velocity components
2770  Vh(I)=Vl*(Le/2-Lcent(I))+Vx(I)  !  due to Vg,Vl (angular velocities) to
                                      !  give total components Vv(I),Vh(I).
2780  Esd(I)=Vv(I)*COS(Sc)+Vh(I)*SIN(Sc)! Calculates polar velocity components
                                        ! corresponding to the above axial
2790  Psisd(I)=(Vh(I)*COS(Sc)-Vv(I)*SIN(Sc))/Ex(I)  ! element centre locations.
2800  Us(I)=(PI*N/30-2*Psisd(I))*R     !  Journal surface velocity at element
                                      !  axial locations.
2810  Vvr(I)=Esd(I)*COS(Sc)        ! Local (axial) Cartezian journal velocity
2820  Vhr(I)=Esd(I)*SIN(Sc)        ! components expressed in terms of local polar
2830  NEXT I                       ! velocity components but with those parts due
2840  FOR J=1 TO Mes               ! to Psid deleted - see 1987 Trib. Int. paper.
2850  T=(To-Ti)*(J-.5)/(Mes-1)+Ti
2860  Tb=(To-Ti)*(J-1)/(Mes-1)+Ti
2870  FOR I=1 TO Naxp
2880  IF J=Mes THEN 2900
2890  Vn(J,I)=-(Vvr(I)*COS(T)+Vhr(I)*SIN(T))  ! Calculates element normal and
2900  Vt(J,I)=Vvr(I)*SIN(Tb)+Vhr(I)*COS(Tb)   ! tangential velocity components as
```

6

```
2910  NEXT I                                 ! a function of Esd(I) (radial
2920  NEXT J                                 ! velocity) only.
2930  FOR J=1 TO Mes-1   !  Calculates journal surface velocity induced flow at
2940  FOR I=1 TO Naxp    !  element centre axial locations.
2950  Kai(J,I)=(H(J,I+1)+H(J,I))*(Us(I)+Vt(J,I))*Dymat(I)/4
2960  Kao(J,I)=(H(J+1,I+1)+H(J+1,I))*(Us(I)+Vt(J+1,I))*Dymat(I)/4
2970  NEXT I
2980  NEXT J
2990  RETURN
3000 Relax: !   Start of Film Pressure Relaxation Subroutine.
3010  Noit=0 !  Resets iteration counter.
3020  MAT Void= (0) ! Resets Void (Gas/Vapour flow) matrix.
3030  Finit=0        ! Resets final iteration indicator.
3040  Pmax=0         ! Resets max. film pressure.
3050  Nocav=0
3060  Iter=0         ! Resets film pressure convergence indicator.
3070  FOR J=1 TO Mcircs ! Start of film pressure relaxation procedure.
3080  FOR I=1 TO Naxp
3090  Hxa=Hx(J,I)
3100  Hya=Hyamat(J,I)    ! Sets working values of element pressure flow functions
3110  Hxb=Hx(J+1,I)
3120  Hyb=Hybmat(J,I)
3130  IF J=1 THEN 3220      !  Oil film boundaries are identified here for
3140  IF J=Mcircs THEN 3250!  selection of program sections where appropriate
3150  IF I=1 THEN 3280      !  boundary conditions are set.
3160  IF I=Naxp THEN 3330
3170  Pxa=P(J-1,I)
3180  Pxb=P(J+1,I)          !  This sets working values for film pressures of
3190  Pya=P(J,I-1)          !  adjacent elements.
3200  Pyb=P(J,I+1)
3210  GOTO 3820
3220  IF I=1 THEN 3410
3230  IF I=Naxp THEN 3470
3240  GOTO 3710
3250  IF I=1 THEN 3560
3260  IF I=Naxp THEN 3620
3270  GOTO 3770
3280  Pya=Phd               !  Note all oil film boundaries of sterntube bearing
3290  Pxa=P(J-1,I)          !  are subject to oil head pressure Phd.
3300  Pxb=P(J+1,I)
3310  Pyb=P(J,I+1)
3320  GOTO 3820
3330  Pxa=P(J-1,I)
3340  Pxb=P(J+1,I)
3350  Pya=P(J,I-1)
3360  IF Avh=0 THEN 3390
3370  Pyb=Phd
3380  GOTO 3820
3390  Hyb=0                 !  No axial flow at elements adjacent to axial centre
3400  GOTO 3820             !  line for aligned bearing.
3410  Hxa=2*Hxa             !  Note that where factor 2 is applied to element
3420  Pxa=Phd               !  pressure flow function, this is to compensate for
3430  Pya=Phd               !  the distance over which the pressure drop occurs
3440  Pxb=P(J+1,I)          !  being halved. i.e. from element centre to boundary
3450  Pyb=P(J,I+1)          !  instead of element centre to adjacent element
3460  GOTO 3820             !  centre.
3470  Hxa=2*Hxa
3480  Pxa=Phd
3490  Pxb=P(J+1,I)
3500  Pya=P(J,I-1)
3510  IF Avh=0 THEN 3540
3520  Pyb=Phd
3530  GOTO 3820
3540  Hyb=0
3550  GOTO 3820
3560  Hxb=2*Hxb
```

⑦

```
3570  Pxb=Phd
3580  Pya=Phd
3590  Pxa=P(J-1,I)
3600  Pyb=P(J,I+1)
3610  GOTO 3820
3620  Hxb=2*Hxb
3630  Pxb=Phd
3640  Pxa=P(J-1,I)
3650  Pya=P(J,I-1)
3660  IF Avh=0 THEN 3690
3670  Pyb=Phd
3680  GOTO 3820
3690  Hyb=0
3700  GOTO 3820
3710  Hxa=2*Hxa
3720  Pxa=Phd
3730  Pxb=P(J+1,I)
3740  Pya=P(J,I-1)
3750  Pyb=P(J,I+1)
3760  GOTO 3820
3770  Hxb=2*Hxb
3780  Pxb=Phd
3790  Pxa=P(J-1,I)
3800  Pya=P(J,I-1)              !  Film pressure relaxation equation (below) is
3810  Pyb=P(J,I+1)              !  selected according to direction of effective (for
3820  IF Us(I)<0 THEN 3850 !  hydrodynamic action) journal surface velocity at
                                !  element centre.
3830  Prel=(Hxa*Pxa+Hya*Pya+Hxb*Pxb+Hyb*Pyb-Kao(J,I)+Kai(J,I)+Vn(J,I)*Dx*Dymat(I
)-Void(J,I))/(Hxa+Hya+Hxb+Hyb)
3840  GOTO 3890
3850  IF J=Mcircs THEN 3880
3860  Prel=(Hxa*Pxa+Hya*Pya+Hxb*Pxb+Hyb*Pyb-Kao(J,I)+Kai(J,I)+Vn(J,I)*Dx*Dymat(I
)+Void(J+1,I))/(Hxa+Hya+Hxb+Hyb)
3870  GOTO 3890
3880  Prel=(Hxa*Pxa+Hya*Pya+Hxb*Pxb+Hyb*Pyb-Kao(J,I)+Kai(J,I)+Vn(J,I)*Dx*Dymat(I
))/(Hxa+Hya+Hxb+Hyb)
3890  IF Prel>Pcav THEN 3920
3900  Psubcav(J,I)=Prel         !  Store subcavitation relaxation pressure.
3910  Prel=Pcav                 !  Reset subcavitation relaxation pressure to
3920  IF Pmax>Prel  THEN 3940 !  specified cavitation pressure Pcav.
3930  Pmax=Prel                 !  Pick out max. film pressure.
3940  Pdelt=ABS(Prel-P(J,I))
3950  IF Pdelt<Wvt/Le/D*.0001 THEN 3970 ! Test for film pressure convergence.
3960  Iter=1                    !  Set " Convergence not attained " indicator.
3970  IF Prel=Pcav THEN 4060
3980  P(J,I)=P(J,I)+Orf*(Prel-P(J,I)) ! Film pressure for non-cavitating
3990  IF Us(I)<0 THEN 4030             ! elements determined by relaxation
4000  IF J=Mcircs THEN 4740            ! pressure Prel and Over Relaxation Factor
                                       ! Orf.
4010  Void(J+1,I)=0             ! Gas/Vapour flow terms for element outlet boundary
4020  GOTO 4740                 ! (dependant on sense of Us(I)) are set to zero for
4030  IF Pxa=Pcav THEN 4740     ! non-cavitating elements.
4040  Void(J,I)=0
4050  GOTO 4740
4060  P(J,I)=Pcav          !  Film pressure for cavitating elements set to specified
                           !  cavitation pressure.
4070  Nocav=Nocav+1        !  Counts No. of elements subject to cavitation.
4080  IF Pxa>Pcav THEN 4120
4090  IF Pxb>Pcav THEN 4160
4100  Cavsqz=0             !  This section sets Cavsqz term which gives approx.
4110  GOTO 4200            !  ratio of circumferential length of element subject to
4120  IF Pxb>Pcav THEN 4190 ! full film to total circumferential length Dx for
                            ! elements containing rupture or reformation boundary
4130  Cavsqz=.5-(Pcav-Psubcav(J,I))/(Pxa-Psubcav(J,I))
4140  IF Cavsqz<0 THEN 4100
4150  GOTO 4200
```

```
4160  Cavsqz=.5-(Pcav-Psubcav(J,I))/(Pxb-Psubcav(J,I))
4170  IF Cavsqz<0 THEN 4100
4180  GOTO 4200
4190  Cavsqz=1
4200  Qxa=Kai(J,I)-Hxa*(Pcav-Pxa)
4210  Qxb=Kao(J,I)-Hxb*(Pxb-Pcav)
4220  IF Us(I)<0 THEN 4560 !  Jump to section covering cavitation when direction
4230  IF J=Mcircs THEN 4740!  of effective journal velocity is reversed.
4240  Void(J+1,I)=Qxb+Hya*(Pcav-Pya)-Hyb*(Pyb-Pcav)-Qxa+Void(J,I)-Vn(J,I)*Dx*Dym
at(I)*Cavsqz
4250  IF Qxb<0 THEN 4330              ! Above equation calculates Gas/Vapour flow
4260  IF Void(J+1,I)>Qxb THEN 4290 ! rates at downstream boundary for cavitating
4270  IF Void(J+1,I)<0 THEN 4310     ! elements. Note Cavsqz term allows a
4280  GOTO 4740                        ! proportion of the squeeze film term to be
4290  Void(J+1,I)=Qxb                  ! included where the element contains a
4300  GOTO 4740                        ! rupture or reformation boundary.
4310  Void(J+1,I)=0                    ! This section below equation ensures that
4320  GOTO 4740                        ! the downstream boundary gas/vapour flow is
4330  IF Void(J+1,I)<Qxb THEN 4360 ! in the same direction as the "total"
4340  IF Void(J+1,I)>0 THEN 4380     ! downstream boundary oil flow and does not
4350  GOTO 4740                        ! exceed it.
4360  Void(J+1,I)=Qxb
4370  GOTO 4740
4380  Void(J+1,I)=0
4390  GOTO 4740
4400  Void(1,I)=Qxb+Hya*(Pya-Pcav)-Hyb*(Pyb-Pcav)-Qxa+Void(J,I)-Vn(J,I)*Dx*Dymat
(I)*Cavsqz
4410  IF Qxb<0 THEN 4490
4420  IF Void(1,I)>Qxb THEN 4450
4430  IF Void(1,I)<0 THEN 4470
4440  GOTO 4740
4450  Void(1,I)=Qxb
4460  GOTO 4740
4470  Void(1,I)=0
4480  GOTO 4740
4490  IF Void(1,I)<Qxb THEN 4520
4500  IF Void(1,I)>0 THEN 4540
4510  GOTO 4740
4520  Void(1,I)=Qxb
4530  GOTO 4740
4540  Void(1,I)=0
4550  GOTO 4740               ! Section below covers cavitation when direction of
4560  IF J=Mcircs THEN 4590! effective journal surface velocity is reversed.
4570  Void(J,I)=Qxa-Hya*(Pcav-Pya)-Qxb+Hyb*(Pyb-Pcav)+Vn(J,I)*Dx*Dymat(I)*Cavsqz
+Void(J+1,I)
4580  GOTO 4600
4590  Void(J,I)=Qxa-Hya*(Pcav-Pya)-Qxb+Hyb*(Pyb-Pcav)+Vn(J,I)*Dx*Dymat(I)*Cavsqz
4600  IF Qxa<0 THEN 4680
4610  IF Void(J,I)>Qxa THEN 4640
4620  IF Void(J,I)<0 THEN 4660
4630  GOTO 4740
4640  Void(J,I)=Qxa
4650  GOTO 4740
4660  Void(J,I)=0
4670  GOTO 4740
4680  IF Void(J,I)<Qxa THEN 4710
4690  IF Void(J,I)>0 THEN 4730
4700  GOTO 4740
4710  Void(J,I)=Qxa
4720  GOTO 4740
4730  Void(J,I)=0
4740  GOTO 4750
4750  NEXT I   !  End of film pressure relaxation procedure.
4760  NEXT J
4770  Noit=Noit+1 ! Count No. of iterations for film pressure relaxation.
4780  Cvfac=Nocav/Mcircs/Naxp ! Proportion of No. elements subject to cavitation
```

9

```
4790   PRINTER IS 1              ! Print on VDU status of film pressure relaxation.
4800   PRINT FNLin$(5);"RWJ015:PROGRAMME RUNNING. Dyn=";Dyn;"Go=";Go;"It.No.";Noi
t
4810   PRINT USING "6A,S3D.4D,7A";"Pmax.=";Pmax;"N/mm^2."
4820   PRINTER IS 701
4830   IF Noit>100 THEN 4850 !          Limit on Max. No. of Iterations to cater
                             !          for convergence failure.
4840   IF Iter=1 THEN 3040   ! Repeat film pressure relaxation if convergence
                             ! failure is indicated. (Iter=1).
4850   RETURN  !  End of Film Pressure Relaxation Subroutine. ( Relax.)
##############################################################################
4860   Mcircs=Mcirc!      Set Bottom variables for Relaxation Subroutine.
4870   REDIM Hx(Me,Naxp),Hyamat(Mcirc,Naxp),Hybmat(Mcirc,Naxp),Kai(Mcirc,Naxp),Ka
o(Mcirc,Naxp),P(Mcirc,Naxp),Void(Mcirc,Naxp),Psubcav(Mcirc,Naxp),Vn(Mcirc,Naxp)
4880   MAT Hx= Hxbot
4890   MAT Hyamat= Hyabot
4900   MAT Hybmat= Hybbot
4910   MAT Kai= Kaib
4920   MAT Kao= Kaob
4930   MAT Vn= Vnb
4940   Dx=Dxb
4950   Go=1              !  Bottom half film pressure relaxation indicator.
4960   IF Count=0 THEN 4990
4970   MAT P= Pbst      !  Set relaxation procedure working film pressure matrix to
4980   GOTO 5000        !  matrix stored for previous computed condition (if any).
4990   MAT P= (Wvt/D/Le)!This provides a start condition for relaxation close to
5000   GOSUB Relax      !  solution, and thereby minimises the No. of iterations.
5010   Pmaxb=Pmax       !  A constant film pressure based on Wvt is used for film
5020   Noitb=Noit       !  pressure start if no previous film pressure solution in
5030   Cvfacb=Cvfac     !  current run exists.
5040   MAT Voidb= Void!  Store Bottom Void Flow Matrix.
5050   MAT Pb= P!         Store Bottom Film Pressure Matrix.
5060   Mcircs=Mtcirc!    Set Top variables for Relaxation Subroutine.
5070   REDIM Hx(Met,Naxp),Hyamat(Mtcirc,Naxp),Hybmat(Mtcirc,Naxp),Kai(Mtcirc,Naxp
),Kao(Mtcirc,Naxp),P(Mtcirc,Naxp),Void(Mtcirc,Naxp),Psubcav(Mtcirc,Naxp)
5080   REDIM Vn(Mtcirc,Naxp)
5090   MAT Hx= Hxtop
5100   MAT Hyamat= Hyatop
5110   MAT Hybmat= Hybtop
5120   MAT Kai= Kait
5130   MAT Kao= Kaot
5140   MAT Vn= Vnt
5150   Dx=Dxt
5160   Go=2          !  Top half film pressure relaxation indicator.
5170   IF Count=0 THEN 5200
5180   MAT P= Ptst
5190   GOTO 5210
5200   MAT P= ((Phd+Pcav)/2)  ! Top half constant film pressure for relaxation
5210   GOSUB Relax            ! start point where no film pressure solution in
                              ! current run exists.
5220   MAT Voidt= Void        ! Store Top Void Flow Matrix.
5230   MAT Pt= P              ! Store Top Film Pressure Matrix.
5240   Cvfact=Cvfac
5250   Pmaxt=Pmax
5260   IF Pmaxb>Pmaxt THEN 5290
5270   Pmaxab=Pmaxt
5280   GOTO 5300
5290   Pmaxab=Pmaxb
5300   Noitt=Noit
5310   Mcircs=Mcirc!  Set Bottom variables for Load & Moment Summation Subroutine
5320   REDIM P(Mcirc,Naxp)
5330   MAT P= Pb
5340   Ti=Tbi
5350   To=Tbo
5360   Dx=Dxb
5370   GOSUB Summate
```

10

```
5380   MAT Wbv= Wvmat
5390   MAT Wbh= Whmat
5400   Mcircs=Mtcirc! Set Top variables for Load & Moment Summation Subroutine
5410   REDIM P(Mtcirc,Naxp)
5420   MAT P= Pt
5430   Ti=Tti
5440   To=Tto
5450   Dx=Dxt
5460   GOSUB Summate
5470   MAT Wtv= Wvmat
5480   MAT Wth= Whmat
5490   IF Avh=1 THEN 6250
5500   Wv=2*Wv   !    Values doubled for aligned bearing since only half bearing
5510   Wh=2*Wh   !    area has been subject to film pressure relaxation solution,
5520   GOTO 6250!     other half being a mirror image.
5530 Summate:   MAT Wvmat= (0)!       Start of Load & Moment Summation Subroutine.
5540   MAT Whmat= (0)      !  Initialize Matricies for Axial Load Distribution Data
5550   FOR I=1 TO Naxp
5560   IF I>1 THEN 5590
5570   Lmid(I)=Dymat(I)/2 !  Computes axial distance from each element centre to
5580   GOTO 5600          !  bearing edge for oil film moment calculation. Note
                          !  axial element grading is used.
5590   Lmid(I)=Lmid(I-1)+(Dymat(I)+Dymat(I-1))/2
5600   NEXT I
5610   FOR I=1 TO Naxp    !  Dymcon and Dypcon are factors to allow for axial
                          !  element grading when computing film pressures
5620   FOR J=1 TO Mcircs  !  Pj,Pq, etc. at element boundary assuming linear
                          !  pressure change between element centres. Note these
5630   IF I=1 THEN 5650   !  factors are 0.5 where there is no axial element
                          !  grading.
5640   Dymcon=Dymat(I-1)/(Dymat(I-1)+Dymat(I))
5650   IF I=Naxp THEN 5670
5660   Dypcon=Dymat(I+1)/(Dymat(I+1)+Dymat(I))
5670   T=(To-Ti)*(J-.5)/Mcircs+Ti
5680   IF I=1 THEN 5790
5690   IF J=1 THEN 5720
5700   Pj=P(J-1,I-1)*(1-Dymcon)+P(J,I)*Dymcon   ! Calculation of element boundary
5710   GOTO 5730                                ! pressures.
5720   Pj=Phd
5730   Pq=P(J,I-1)*(1-Dymcon)+P(J,I)*Dymcon   !     Pk          Pr          Pl
5740   IF J=Mcircs THEN 5770                  !
5750   Pk=P(J+1,I-1)*(1-Dymcon)+P(J,I)*Dymcon!        |J+1,I        J+1,I+1|
5760   GOTO 5820                              !        |                    |
5770   Pk=Phd                                 !   Pq   |       P(J,I)       |Ps
5780   GOTO 5820                              !        |                    |
5790   Pj=Phd                                 !        |J,I            J,I+1|
5800   Pq=Phd                                 !        |____________________|
5810   Pk=Phd                                 !     Pj          Pn          Pm
5820   IF I=Naxp THEN 5930
5830   IF J=1 THEN 5860
5840   Pm=P(J-1,I+1)*(1-Dypcon)+P(J,I)*Dypcon
5850   GOTO 5870
5860   Pm=Phd
5870   Ps=P(J,I+1)*(1-Dypcon)+P(J,I)*Dypcon
5880   IF J=Mcircs THEN 5910
5890   Pl=P(J+1,I+1)*(1-Dypcon)+P(J,I)*Dypcon
5900   GOTO 6070
5910   Pl=Phd
5920   GOTO 6070
5930   IF Avh=0 THEN 5980
5940   Pm=Phd
```

11

```
5950  Ps=Phd
5960  Pl=Phd
5970  GOTO 6070
5980  IF J>1 THEN 6010
5990  Pm=Phd
6000  GOTO 6020
6010  Pm=(P(J,I)+P(J-1,I))/2 !   i.e. =Pn
6020  Ps=P(J,I)
6030  IF J<Mcircs THEN 6060
6040  Pl=Phd
6050  GOTO 6070
6060  Pl=(P(J,I)+P(J+1,I))/2 !   i.e. =Pr
6070  IF J=1 THEN 6100
6080  Pn=(P(J,I)+P(J-1,I))/2
6090  GOTO 6110
6100  Pn=Phd
6110  IF J=Mcircs THEN 6140
6120  Pr=(P(J,I)+P(J+1,I))/2
6130  GOTO 6150
6140  Pr=Phd
6150  We=Dx*Dymat(I)*(4*P(J,I)+Pj+Pq+Pk+Pr+Pl+Ps+Pm+Pn)/12 ! Element oil film
                                             ! force based on mean effective pressure.
6160  Wv=Wv-We*COS(T)                 ! Summation of vertical and horizontal
6170  Wh=Wh-We*SIN(T)                 ! components of element oil film force.
6180  Wvmat(I)=Wvmat(I)-We*COS(T)     ! Summation of element oil film force
6190  Whmat(I)=Whmat(I)-We*SIN(T)     ! components at axial location I for axial
                                      ! load distribution.(Not Printed Out here.)
6200  Mv=Mv-We*COS(T)*Lmid(I)         ! Summation of components of element oil film
6210  Mh=Mh-We*SIN(T)*Lmid(I)         ! moment about bearing aft end.
6220  NEXT J
6230  NEXT I
6240  RETURN                          ! End of Summate Subroutine.
6250  Mvc=Wv*Le/2-Mv ! Refers oil film moment components to bearing axial centre
6260  Mhc=Wh*Le/2-Mh
6270  Fr=Wv*COS(Psi)+Wh*SIN(Psi)       ! Computes radial and tangential components
6280  Ft=Wh*COS(Psi)-Wv*SIN(Psi)       ! of oil film force. Direction defined by
                                        ! Attitude Angle Sc. (Psi).
6290  Mrc=Mvc*COS(Psi)+Mhc*SIN(Psi)! Computes radial and tangential components
6300  Mtc=Mhc*COS(Psi)-Mvc*SIN(Psi)! of oil film moment.
6310  Omegao=PI*N/30-2*Psid             ! Effective angular velocity for hydrodynamic
                                        ! action. rads/s.
6320  RETURN !     End of Oil_force Subroutine.
6330  Ed=0          !  <-- Jumped from L.1640
6340  Psid=0        !  Set all velocity components to zero for stiffness
6350  Xsead=0       !  coefficient computation. (displacement perturbations only)
6360  Phid=0
6370  FOR Iscan=1 TO 3 ! Four nested loops to compute oil film forces and
6380  FOR Jscan=1 TO 3 ! moments for all combinations of negative, zero and
6390  FOR Kscan=1 TO 3 ! positive displacement component perturbations.
6400  FOR Lscan=1 TO 3 ! All in polar terms.
6410  Sc=E+Epert*(Iscan-2)
6420  Xsea=Xseao+Xseapert*(Jscan-2)    ! Note that the 4 dimentional matricies use
6430  Sc=Psi+Psipert*(Kscan-2)         ! the following system :
6440  Phi=Phio+Phipert*(Lscan-2)       ! Iscan : E perturbation reference.
6450  GOSUB Oil_force                  ! Jscan : Xsea perturbation reference. (Xi)
6460  Frm(Iscan,Jscan,Kscan,Lscan)=Fr! Kscan : Psi perturbation reference.
6470  Ftm(Iscan,Jscan,Kscan,Lscan)=Ft! Lscan : Phi perturbation reference.
6480  Mrm(Iscan,Jscan,Kscan,Lscan)=Mrc !   All perturbation references are :
6490  Mtm(Iscan,Jscan,Kscan,Lscan)=Mtc !   1 negative, 2 zero, 3 positive.
6500  NEXT Lscan
6510  NEXT Kscan
6520  NEXT Jscan
6530  NEXT Iscan
6540  Ip=Epert        ! Set perturbations for Non_lin_cof Subroutine to
6550  Im=-Epert       ! displacement perturbations.
6560  Jp=Xseapert     ! Following this the oil film force/moment parameter used in
```

```
6570 Jm=-Xseapert   ! the Non_lin_cof subroutine is set in turn to each of the
6580 Kp=Psipert     ! components of force and moment computed above.          (12)
6590 Km=-Psipert    ! The Non_lin_cof subroutine is then called to compute the
6600 Lp=Phipert     ! corresponding non-linear stiffness coefficients.
6610 Lm=-Phipert
6620 MAT Fm= Frm
6630 GOSUB Non_lin_cof
6640 MAT Afr= Kfm
6650 MAT Fm= Ftm
6660 GOSUB Non_lin_cof
6670 MAT Aft= Kfm
6680 MAT Fm= Mrm
6690 GOSUB Non_lin_cof
6700 MAT Amr= Kfm
6710 MAT Fm= Mtm
6720 GOSUB Non_lin_cof
6730 MAT Amt= Kfm        ! Set matricies used in Check Subroutine to computed
6740 MAT Kfr= Afr        ! non-linear stiffness coefficient matricies.
6750 MAT Kft= Aft
6760 MAT Kmr= Amr
6770 MAT Kmt= Amt
6780 GOSUB Check         ! Call Subroutine to check non-linear coefficients
6790 PRINT FNPage$;      ! ( stiffness in this instance ).
6800 PRINT "                 Afr Coefficients."
6810 PRINT "                 __________________" ! Print out computed non-linear
6820 MAT Kfm= Afr                                ! stiffness coefficients using
6830 GOSUB Print_coef                            ! Print_coef Subroutine. This
6840 PRINT "                 Aft Coefficients."  ! requires setting the Kfm matrix
6850 PRINT "                 __________________" ! used in the Print_coef
6860 MAT Kfm= Aft                                ! subroutine to the stiffness
6870 GOSUB Print_coef                            ! coefficient matrix to be printed
6880 PRINT "                 Amr Coefficients."  ! out.
6890 PRINT "                 __________________"
6900 MAT Kfm= Amr
6910 GOSUB Print_coef
6920 PRINT "                 Amt Coefficients."
6930 PRINT "                 __________________"
6940 MAT Kfm= Amt
6950 GOSUB Print_coef
6960 MASS STORAGE IS ":INTERNAL,4,0"            ! Store on disc computed non-linear
6970 CREATE ASCII "ACOEFS:INTERNAL,4,0",150 ! stiffness coefficients and data
6980 ASSIGN @File1 TO "ACOEFS:INTERNAL,4,0" ! set reference information.
6990 OUTPUT @File1;Datset,E,Psi,Xseao,Phio
7000 OUTPUT @File1;Afr(*)
7010 OUTPUT @File1;Aft(*)
7020 OUTPUT @File1;Amr(*)
7030 OUTPUT @File1;Amt(*)
7040 ASSIGN @File1 TO *
7050 CREATE ASCII "AFMDAT:INTERNAL,4,0",150 ! Store on disc oil film force and
7060 ASSIGN @File2 TO "AFMDAT:INTERNAL,4,0" ! moment data corresponding to the
7070 OUTPUT @File2;Frm(*)                   ! above non-linear stiffness
7080 OUTPUT @File2;Ftm(*)                   ! coefficients.
7090 OUTPUT @File2;Mrm(*)
7100 OUTPUT @File2;Mtm(*)
7110 ASSIGN @File2 TO *
7120 Ec=E                 ! Set all journal displacements to datum condition
7130 Xsea=Xseao           ! values (i.e. zero displacement perturbations) for
7140 Sc=Psi               ! damping coefficient determination.
7150 Phi=Phio
7160 FOR Iscan=1 TO 3     ! Four nested loops to compute oil film forces and
7170 FOR Jscan=1 TO 3     ! moments for all combinations of negative, zero and
7180 FOR Kscan=1 TO 3     ! positive velocity component perturbations. All in
7190 FOR Lscan=1 TO 3     ! polar terms. Note special treatment for Kscan=2
7200 Ed=Edpert*(Iscan-2)! which corresponds to Omegao=0=Psid/2 and not Psid=0.
7210 Xsead=Xseadpert*(Jscan-2)
7220 IF Kscan=2 THEN 7250
```

(13)

```
7230 Psid=Psidpert*(K[illegible]
7240 GOTO 7260
7250 Psid=PI*N/60
7260 Phid=Phidpert*(Lscan-2)
7270 GOSUB Oil_force
7280 Frm(Iscan,Jscan,Kscan,Lscan)=Fr  ! Four dimensional matrix system is
7290 Ftm(Iscan,Jscan,Kscan,Lscan)=Ft  ! similar to that used for displacement
7300 Mrm(Iscan,Jscan,Kscan,Lscan)=Mrc ! perturbations.
7310 Mtm(Iscan,Jscan,Kscan,Lscan)=Mtc
7320 NEXT Lscan
7330 NEXT Kscan
7340 NEXT Jscan
7350 NEXT Iscan
7360 Ip=Edpert               ! Set perturbations for Non_lin_cof subroutine to
7370 Im=-Edpert              ! velocity perturbations.
7380 Jp=Xseadpert            ! Following this the oilfilm force/moment parameter
7390 Jm=-Xseadpert           ! used in the Non_lin_cof subroutine is set in turn
7400 Kp=PI*N/30-2*Psidpert!  to each of the components of force and moment
7410 Km=PI*N/30+2*Psidpert!  computed above. The Non_lin_cof subroutine is then
7420 Lp=Phidpert             ! called to compute the corresponding non-linear
7430 Lm=-Phidpert            ! damping coefficients.
7440 MAT Fm= Frm
7450 GOSUB Non_lin_cof
7460 MAT Bfr= Kfm
7470 MAT Fm= Ftm
7480 GOSUB Non_lin_cof
7490 MAT Bft= Kfm
7500 MAT Fm= Mrm
7510 GOSUB Non_lin_cof
7520 MAT Bmr= Kfm
7530 MAT Fm= Mtm
7540 GOSUB Non_lin_cof
7550 MAT Bmt= Kfm
7560 MAT Kfr= Bfr        ! Set matricies used in Check Subroutine to computed
7570 MAT Kft= Bft        ! non-linear damping coefficient matricies.
7580 MAT Kmr= Bmr
7590 MAT Kmt= Bmt
7600 GOSUB Check         ! Call subroutine to check non-linear coefficients.
7610 PRINT FNPage$;      ! ( damping in this instance ).
7620 PRINT "                   Bfr Coefficients."
7630 PRINT "                   __________________" ! Print out computed
7640 MAT Kfm= Bfr                                  ! non-linear damping
7650 GOSUB Print_coef                              ! coefficients using
7660 PRINT "                   Bft Coefficients." ! Print_coef Subroutine.
7670 PRINT "                   __________________" ! This requires setting the
7680 MAT Kfm= Bft                                  ! Kfm matrix used in the
7690 GOSUB Print_coef                              ! Print_coef subroutine to
7700 PRINT "                   Bmr Coefficients." ! the damping coefficient
7710 PRINT "                   __________________" ! matrix to be printed out.
7720 MAT Kfm= Bmr
7730 GOSUB Print_coef
7740 PRINT "                   Bmt Coefficients."
7750 PRINT "                   __________________"
7760 MAT Kfm= Bmt
7770 GOSUB Print_coef
7780 MASS STORAGE IS ":INTERNAL,4,0"
7790 CREATE ASCII "BCOEFS:INTERNAL,4,0",150 ! Store on disc computed non-linear
7800 ASSIGN @File3 TO "BCOEFS:INTERNAL,4,0" ! damping coefficients.
7810 OUTPUT @File3;Bfr(*)
7820 OUTPUT @File3;Bft(*)
7830 OUTPUT @File3;Bmr(*)
7840 OUTPUT @File3;Bmt(*)
7850 ASSIGN @File3 TO *
7860 CREATE ASCII "BFMDAT:INTERNAL,4,0",150 ! Store on disc oil film force and
7870 ASSIGN @File4 TO "BFMDAT:INTERNAL,4,0" ! moment data corresponding to the
7880 OUTPUT @File4;Frm(*)                    ! above non-linear damping
```

```
7890  OUTPUT @File4;Ftm(*)                              ! coefficients.
7900  OUTPUT @File4;Mrm(*)
7910  OUTPUT @File4;Mtm(*)
7920  ASSIGN @File4 TO *
7930  GOTO 7950
7940  PRINT "-----------------------------------------------------------------------
---------"
7950  GOTO 9660
7960 Non_lin_cof:  !  General Subroutine for Computation of
7970               !  Non-Linear Coefficient Matrix.
7980               !  INPUT : Fm Matrix & Ip,Im,Jp,Jm,Kp,Km,Lp,Lm Perturbations.
7990               !  OUTPUT : Kfm Matrix.
8000   ! ZERO ORDER COEFFICIENT.
8010   Kfm(2,2.2.2)=Fm(2,2,2,2)
8020   ! FIRST ORDER COEFFICIENTS.
8030   Kfm(1,2,2,2)=(Fm(1,2,2,2)-Fm(2,2.2,2))/Im
8040   Kfm(3,2,2,2)=(Fm(3,2,2,2)-Fm(2,2,2,2))/Ip
8050   Kfm(2,1,2,2)=(Fm(2,1,2,2)-Fm(2,2,2,2))/Jm
8060   Kfm(2,3,2,2)=(Fm(2,3,2,2)-Fm(2,2,2,2))/Jp
8070   Kfm(2,2,1,2)=(Fm(2,2,1,2)-Fm(2,2.2,2))/Km
8080   Kfm(2,2,3,2)=(Fm(2,2,3,2)-Fm(2,2.2,2))/Kp
8090   Kfm(2,2,2,1)=(Fm(2,2,2,1)-Fm(2,2.2,2))/Lm
8100   Kfm(2,2,2,3)=(Fm(2,2,2,3)-Fm(2,2.2,2))/Lp
8110   ! SECOND ORDER COEFFICIENTS.
8120   Kfm(1,1,2,2)=(Fm(1,1,2,2)-Kfm(2,2,2,2)-Kfm(1,2,2,2)*Im-Kfm(2,1,2,2)*Jm)/I
m/Jm
8130   Kfm(1,3,2,2)=(Fm(1,3,2,2)-Kfm(2.2,2,2)-Kfm(1,2,2,2)*Im-Kfm(2,3,2,2)*Jp)/I
m/Jp
8140   Kfm(3,1,2,2)=(Fm(3,1,2,2)-Kfm(2,2,2,2)-Kfm(3,2,2,2)*Ip-Kfm(2,1,2,2)*Jm)/I
p/Jm
8150   Kfm(3,3,2,2)=(Fm(3,3,2,2)-Kfm(2,2,2,2)-Kfm(3,2,2,2)*Ip-Kfm(2,3,2,2)*Jp)/I
p/Jp
8160   Kfm(1,2,1,2)=(Fm(1,2,1,2)-Kfm(2,2,2,2)-Kfm(1,2,2,2)*Im-Kfm(2,2,1,2)*Km)/I
m/Km
8170   Kfm(1,2,3,2)=(Fm(1,2,3,2)-Kfm(2,2,2,2)-Kfm(1,2,2,2)*Im-Kfm(2,2,3,2)*Kp)/I
m/Kp
8180   Kfm(3,2,1,2)=(Fm(3,2,1,2)-Kfm(2,2,2,2)-Kfm(3,2,2,2)*Ip-Kfm(2,2,1,2)*Km)/I
p/Km
8190   Kfm(3,2,3,2)=(Fm(3,2,3,2)-Kfm(2,2,2,2)-Kfm(3,2,2,2)*Ip-Kfm(2,2,3,2)*Kp)/I
p/Kp
8200   Kfm(1,2,2,1)=(Fm(1,2,2,1)-Kfm(2,2,2,2)-Kfm(1,2,2,2)*Im-Kfm(2,2,2,1)*Lm)/I
m/Lm
8210   Kfm(1,2,2,3)=(Fm(1,2,2,3)-Kfm(2,2,2,2)-Kfm(1,2,2,2)*Im-Kfm(2,2,2,3)*Lp)/I
m/Lp
8220   Kfm(3,2,2,1)=(Fm(3,2,2,1)-Kfm(2,2,2,2)-Kfm(3,2,2,2)*Ip-Kfm(2,2,2,1)*Lm)/I
p/Lm
8230   Kfm(3,2,2,3)=(Fm(3,2,2,3)-Kfm(2,2,2,2)-Kfm(3,2,2,2)*Ip-Kfm(2,2,2,3)*Lp)/I
p/Lp
8240   Kfm(2,1,1,2)=(Fm(2,1,1,2)-Kfm(2,2,2,2)-Kfm(2,1,2,2)*Jm-Kfm(2,2,1,2)*Km)/J
m/Km
8250   Kfm(2,1,3,2)=(Fm(2,1,3,2)-Kfm(2,2,2,2)-Kfm(2,1,2,2)*Jm-Kfm(2,2,3,2)*Kp)/J
m/Kp
8260   Kfm(2,3,1,2)=(Fm(2,3,1,2)-Kfm(2,2,2,2)-Kfm(2,3,2,2)*Jp-Kfm(2,2,1,2)*Km)/J
p/Km
8270   Kfm(2,3,3,2)=(Fm(2,3,3,2)-Kfm(2,2,2,2)-Kfm(2,3,2,2)*Jp-Kfm(2,2,3,2)*Kp)/J
p/Kp
8280   Kfm(2,1,2,1)=(Fm(2,1,2,1)-Kfm(2,2,2,2)-Kfm(2,1,2,2)*Jm-Kfm(2,2,2,1)*Lm)/J
m/Lm
8290   Kfm(2,1,2,3)=(Fm(2,1,2,3)-Kfm(2,2,2,2)-Kfm(2,1,2,2)*Jm-Kfm(2,2,2,3)*Lp)/J
m/Lp
8300   Kfm(2,3,2,1)=(Fm(2,3,2,1)-Kfm(2,2,2,2)-Kfm(2,3,2,2)*Jp-Kfm(2,2,2,1)*Lm)/J
p/Lm
8310   Kfm(2,3,2,3)=(Fm(2,3,2,3)-Kfm(2,2,2,2)-Kfm(2,3,2,2)*Jp-Kfm(2,2,2,3)*Lp)/J
p/Lp
8320   Kfm(2,2,1,1)=(Fm(2,2,1,1)-Kfm(2.2,2,2)-Kfm(2.2,1,2)*Km-Kfm(2,2,2,1)*Lm)/K
m/Lm
```

14

```
8330    Kfm(2,2,1,3)=(Fm(2,2,1,3)-Kfm(2,2,2,2)-Kfm(2,2,1,2)*Km-Kfm(2,2,2,3)*Lp)/K
m/Lp
8340    Kfm(2,2,3,1)=(Fm(2,2,3,1)-Kfm(2,2,2,2)-Kfm(2,2,3,2)*Kp-Kfm(2,2,2,1)*Lm)/K
p/Lm
8350    Kfm(2,2,3,3)=(Fm(2,2,3,3)-Kfm(2,2,2,2)-Kfm(2,2,3,2)*Kp-Kfm(2,2,2,3)*Lp)/K
p/Lp
8360    ! THIRD ORDER COEFFICIENTS.
8370    Kfm(1,1,1,2)=(Fm(1,1,1,2)-Fm(1,1,2,2)-Kfm(2,2,1,2)*Km-Kfm(1,2,1,2)*Im*Km-
Kfm(2,1,1,2)*Jm*Km)/Im/Jm/Km
8380    Kfm(1,3,1,2)=(Fm(1,3,1,2)-Fm(1,3,2,2)-Kfm(2,2,1,2)*Km-Kfm(1,2,1,2)*Im*Km-
Kfm(2,3,1,2)*Jp*Km)/Im/Jp/Km
8390    Kfm(1,1,3,2)=(Fm(1,1,3,2)-Fm(1,1,2,2)-Kfm(2,2,3,2)*Kp-Kfm(1,2,3,2)*Im*Kp-
Kfm(2,1,3,2)*Jm*Kp)/Im/Jm/Kp
8400    Kfm(3,1,1,2)=(Fm(3,1,1,2)-Fm(3,1,2,2)-Kfm(2,2,1,2)*Km-Kfm(3,2,1,2)*Ip*Km-
Kfm(2,1,1,2)*Jm*Km)/Ip/Jm/Km
8410    Kfm(1,3,3,2)=(Fm(1,3,3,2)-Fm(1,3,2,2)-Kfm(2,2,3,2)*Kp-Kfm(1,2,3,2)*Im*Kp-
Kfm(2,3,3,2)*Jp*Kp)/Im/Jp/Kp
8420    Kfm(3,1,3,2)=(Fm(3,1,3,2)-Fm(3,1,2,2)-Kfm(2,2,3,2)*Kp-Kfm(3,2,3,2)*Ip*Kp-
Kfm(2,1,3,2)*Jm*Kp)/Ip/Jm/Kp
8430    Kfm(3,3,1,2)=(Fm(3,3,1,2)-Fm(3,3,2,2)-Kfm(2,2,1,2)*Km-Kfm(3,2,1,2)*Ip*Km-
Kfm(2,3,1,2)*Jp*Km)/Ip/Jp/Km
8440    Kfm(3,3,3,2)=(Fm(3,3,3,2)-Fm(3,3,2,2)-Kfm(2,2,3,2)*Kp-Kfm(3,2,3,2)*Ip*Kp-
Kfm(2,3,3,2)*Jp*Kp)/Ip/Jp/Kp
8450    Kfm(1,1,2,1)=(Fm(1,1,2,1)-Fm(1,1,2,2)-Kfm(2,2,2,1)*Lm-Kfm(1,2,2,1)*Im*Lm-
Kfm(2,1,2,1)*Jm*Lm)/Im/Jm/Lm
8460    Kfm(1,3,2,1)=(Fm(1,3,2,1)-Fm(1,3,2,2)-Kfm(2,2,2,1)*Lm-Kfm(1,2,2,1)*Im*Lm-
Kfm(2,3,2,1)*Jp*Lm)/Im/Jp/Lm
8470    Kfm(1,1,2,3)=(Fm(1,1,2,3)-Fm(1,1,2,2)-Kfm(2,2,2,3)*Lp-Kfm(1,2,2,3)*Im*Lp-
Kfm(2,1,2,3)*Jm*Lp)/Im/Jm/Lp
8480    Kfm(3,1,2,1)=(Fm(3,1,2,1)-Fm(3,1,2,2)-Kfm(2,2,2,1)*Lm-Kfm(3,2,2,1)*Ip*Lm-
Kfm(2,1,2,1)*Jm*Lm)/Ip/Jm/Lm
8490    Kfm(1,3,2,3)=(Fm(1,3,2,3)-Fm(1,3,2,2)-Kfm(2,2,2,3)*Lp-Kfm(1,2,2,3)*Im*Lp-
Kfm(2,3,2,3)*Jp*Lp)/Im/Jp/Lp
8500    Kfm(3,1,2,3)=(Fm(3,1,2,3)-Fm(3,1,2,2)-Kfm(2,2,2,3)*Lp-Kfm(3,2,2,3)*Ip*Lp-
Kfm(2,1,2,3)*Jm*Lp)/Ip/Jm/Lp
8510    Kfm(3,3,2,1)=(Fm(3,3,2,1)-Fm(3,3,2,2)-Kfm(2,2,2,1)*Lm-Kfm(3,2,2,1)*Ip*Lm-
Kfm(2,3,2,1)*Jp*Lm)/Ip/Jp/Lm
8520    Kfm(3,3,2,3)=(Fm(3,3,2,3)-Fm(3,3,2,2)-Kfm(2,2,2,3)*Lp-Kfm(3,2,2,3)*Ip*Lp-
Kfm(2,3,2,3)*Jp*Lp)/Ip/Jp/Lp
8530    Kfm(1,2,1,1)=(Fm(1,2,1,1)-Fm(1,2,1,2)-Kfm(2,2,2,1)*Lm-Kfm(1,2,2,1)*Im*Lm-
Kfm(2,2,1,1)*Km*Lm)/Im/Km/Lm
8540    Kfm(1,2,3,1)=(Fm(1,2,3,1)-Fm(1,2,3,2)-Kfm(2,2,2,1)*Lm-Kfm(1,2,2,1)*Im*Lm-
Kfm(2,2,3,1)*Kp*Lm)/Im/Kp/Lm
8550    Kfm(1,2,1,3)=(Fm(1,2,1,3)-Fm(1,2,1,2)-Kfm(2,2,2,3)*Lp-Kfm(1,2,2,3)*Im*Lp-
Kfm(2,2,1,3)*Km*Lp)/Im/Km/Lp
8560    Kfm(3,2,1,1)=(Fm(3,2,1,1)-Fm(3,2,1,2)-Kfm(2,2,2,1)*Lm-Kfm(3,2,2,1)*Ip*Lm-
Kfm(2,2,1,1)*Km*Lm)/Ip/Km/Lm
8570    Kfm(1,2,3,3)=(Fm(1,2,3,3)-Fm(1,2,3,2)-Kfm(2,2,2,3)*Lp-Kfm(1,2,2,3)*Im*Lp-
Kfm(2,2,3,3)*Kp*Lp)/Im/Kp/Lp
8580    Kfm(3,2,1,3)=(Fm(3,2,1,3)-Fm(3,2,1,2)-Kfm(2,2,2,3)*Lp-Kfm(3,2,2,3)*Ip*Lp-
Kfm(2,2,1,3)*Km*Lp)/Ip/Km/Lp
8590    Kfm(3,2,3,1)=(Fm(3,2,3,1)-Fm(3,2,3,2)-Kfm(2,2,2,1)*Lm-Kfm(3,2,2,1)*Ip*Lm-
Kfm(2,2,3,1)*Kp*Lm)/Ip/Kp/Lm
8600    Kfm(3,2,3,3)=(Fm(3,2,3,3)-Fm(3,2,3,2)-Kfm(2,2,2,3)*Lp-Kfm(3,2,2,3)*Ip*Lp-
Kfm(2,2,3,3)*Kp*Lp)/Ip/Kp/Lp
8610    Kfm(2,1,1,1)=(Fm(2,1,1,1)-Fm(2,1,1,2)-Kfm(2,2,2,1)*Lm-Kfm(2,1,2,1)*Jm*Lm-
Kfm(2,2,1,1)*Km*Lm)/Jm/Km/Lm
8620    Kfm(2,1,3,1)=(Fm(2,1,3,1)-Fm(2,1,3,2)-Kfm(2,2,2,1)*Lm-Kfm(2,1,2,1)*Jm*Lm-
Kfm(2,2,3,1)*Kp*Lm)/Jm/Kp/Lm
8630    Kfm(2,1,1,3)=(Fm(2,1,1,3)-Fm(2,1,1,2)-Kfm(2,2,2,3)*Lp-Kfm(2,1,2,3)*Jm*Lp-
Kfm(2,2,1,3)*Km*Lp)/Jm/Km/Lp
8640    Kfm(2,3,1,1)=(Fm(2,3,1,1)-Fm(2,3,1,2)-Kfm(2,2,2,1)*Lm-Kfm(2,3,2,1)*Jp*Lm-
Kfm(2,2,1,1)*Km*Lm)/Jp/Km/Lm
8650    Kfm(2,1,3,3)=(Fm(2,1,3,3)-Fm(2,1,3,2)-Kfm(2,2,2,3)*Lp-Kfm(2,1,2,3)*Jm*Lp-
Kfm(2,2,3,3)*Kp*Lp)/Jm/Kp/Lp
8660    Kfm(2,3,1,3)=(Fm(2,3,1,3)-Fm(2,3,1,2)-Kfm(2,2,2,3)*Lp-Kfm(2,3,2,3)*Jp*Lp-
```

15

```
Kfm(2,2,1,3)*Km*Lp)/Jp/Km/Lp
8670    Kfm(2,3,3,1)=(Fm(2,3,3,1)-Fm(2,3,3,2)-Kfm(2,2,2,1)*Lm-Kfm(2,3,2,1)*Jp*Lm-
Kfm(2,2,3,1)*Kp*Lm)/Jp/Kp/Lm
8680    Kfm(2,3,3,3)=(Fm(2,3,3,3)-Fm(2,3,3,2)-Kfm(2,2,2,3)*Lp-Kfm(2,3,2,3)*Jp*Lp-
Kfm(2,2,3,3)*Kp*Lp)/Jp/Kp/Lp
8690    ! FOURTH ORDER COEFFICIENTS.
8700    Fmsig=(Fm(1,3,1,3)-Fm(1,3,1,2)-Kfm(2,2,2,3)*Lp-Kfm(1,2,2,3)*Im*Lp-Kfm(2,3
,2,3)*Jp*Lp-Kfm(2,2,1,3)*Km*Lp-Kfm(1,3,2,3)*Im*Jp*Lp-Kfm(1,2,1,3)*Im*Km*Lp)
8710    Kfm(1,3,1,3)=(Fmsig-Kfm(2,3,1,3)*Jp*Km*Lp)/Im/Jp/Km/Lp
8720    Fmsig=(Fm(3,1,3,1)-Fm(3,1,3,2)-Kfm(2,2,2,1)*Lm-Kfm(3,2,2,1)*Ip*Lm-Kfm(2,1
,2,1)*Jm*Lm-Kfm(2,2,3,1)*Kp*Lm-Kfm(3,1,2,1)*Ip*Jm*Lm-Kfm(3,2,3,1)*Ip*Kp*Lm)
8730    Kfm(3,1,3,1)=(Fmsig-Kfm(2,1,3,1)*Jm*Kp*Lm)/Ip/Jm/Kp/Lm
8740    Fmsig=(Fm(3,1,1,1)-Fm(3,1,1,2)-Kfm(2,2,2,1)*Lm-Kfm(3,2,2,1)*Ip*Lm-Kfm(2,1
,2.1)*Jm*Lm-Kfm(2.2,1,1)*Km*Lm-Kfm(3,1,2,1)*Ip*Jm*Lm-Kfm(3,2,1,1)*Ip*Km*Lm)
8750    Kfm(3,1,1.1)=(Fmsig-Kfm(2,1,1,1)*Jm*Km*Lm)/Ip/Jm/Km/Lm
8760    Fmsig=(Fm(1,3,1,1)-Fm(1,3,1,2)-Kfm(2,2,2,1)*Lm-Kfm(1,2,2,1)*Im*Lm-Kfm(2,3
,2,1)*Jp*Lm-Kfm(2,2,1,1)*Km*Lm-Kfm(1,3,2,1)*Im*Jp*Lm-Kfm(1,2,1,1)*Im*Km*Lm)
8770    Kfm(1,3,1,1)=(Fmsig-Kfm(2,3,1,1)*Jp*Km*Lm)/Im/Jp/Km/Lm
8780    Fmsig=(Fm(1,1,3,1)-Fm(1,1,3,2)-Kfm(2,2,2,1)*Lm-Kfm(1,2,2,1)*Im*Lm-Kfm(2,1
,2.1)*Jm*Lm-Kfm(2,2,3,1)*Kp*Lm-Kfm(1,1,2,1)*Im*Jm*Lm-Kfm(1,2,3,1)*Im*Kp*Lm)
8790    Kfm(1,1,3,1)=(Fmsig-Kfm(2,1,3,1)*Jm*Kp*Lm)/Im/Jm/Kp/Lm
8800    Fmsig=(Fm(1,1,1,3)-Fm(1,1,1,2)-Kfm(2,2,2,3)*Lp-Kfm(1,2,2,3)*Im*Lp-Kfm(2.1
,2,3)*Jm*Lp-Kfm(2,2,1,3)*Km*Lp-Kfm(1,1,2,3)*Im*Jm*Lp-Kfm(1,2,1,3)*Im*Km*Lp)
8810    Kfm(1,1,1.3)=(Fmsig-Kfm(2,1,1,3)*Jm*Km*Lp)/Im/Jm/Km/Lp
8820    Fmsig=(Fm(1,1,1,1)-Fm(1,1,1,2)-Kfm(2,2,2,1)*Lm-Kfm(1,2,2,1)*Im*Lm-Kfm(2,1
,2,1)*Jm*Lm-Kfm(2,2,1,1)*Km*Lm-Kfm(1,1,2,1)*Im*Jm*Lm-Kfm(1,2,1,1)*Im*Km*Lm)
8830    Kfm(1,1,1,1)=(Fmsig-Kfm(2,1,1,1)*Jm*Km*Lm)/Im/Jm/Km/Lm
8840    Fmsig=(Fm(1,3,3,1)-Fm(1,3,3,2)-Kfm(2,2,2,1)*Lm-Kfm(1,2,2,1)*Im*Lm-Kfm(2,3
,2.1)*Jp*Lm-Kfm(2,2,3,1)*Kp*Lm-Kfm(1,3,2,1)*Im*Jp*Lm-Kfm(1,2,3,1)*Im*Kp*Lm)
8850    Kfm(1,3.3,1)=(Fmsig-Kfm(2,3,3,1)*Jp*Kp*Lm)/Im/Jp/Kp/Lm
8860    Fmsig=(Fm(1,1,3,3)-Fm(1,1,3,2)-Kfm(2,2,2,3)*Lp-Kfm(1,2,2,3)*Im*Lp-Kfm(2,1
,2,3)*Jm*Lp-Kfm(2,2,3,3)*Kp*Lp-Kfm(1,1,2,3)*Im*Jm*Lp-Kfm(1,2,3,3)*Im*Kp*Lp)
8870    Kfm(1,1,3,3)=(Fmsig-Kfm(2,1,3,3)*Jm*Kp*Lp)/Im/Jm/Kp/Lp
8880    Fmsig=(Fm(3,1,1,3)-Fm(3,1,1,2)-Kfm(2,2,2,3)*Lp-Kfm(3,2,2,3)*Ip*Lp-Kfm(2,1
,2,3)*Jm*Lp-Kfm(2,2,1,3)*Km*Lp-Kfm(3,1,2,3)*Ip*Jm*Lp-Kfm(3,2,1,3)*Ip*Km*Lp)
8890    Kfm(3,1,1,3)=(Fmsig-Kfm(2.1,1,3)*Jm*Km*Lp)/Ip/Jm/Km/Lp
8900    Fmsig=(Fm(3,3,1,1)-Fm(3,3,1,2)-Kfm(2,2,2,1)*Lm-Kfm(3,2.2,1)*Ip*Lm-Kfm(2,3
,2,1)*Jp*Lm-Kfm(2,2,1,1)*Km*Lm-Kfm(3,3,2,1)*Ip*Jp*Lm-Kfm(3,2,1,1)*Ip*Km*Lm)
8910    Kfm(3,3,1.1)=(Fmsig-Kfm(2,3,1,1)*Jp*Km*Lm)/Ip/Jp/Km/Lm
8920    Fmsig=(Fm(1,3,3,3)-Fm(1,3,3,2)-Kfm(2,2,2,3)*Lp-Kfm(1,2,2,3)*Im*Lp-Kfm(2,3
,2.3)*Jp*Lp-Kfm(2,2,3,3)*Kp*Lp-Kfm(1,3,2,3)*Im*Jp*Lp-Kfm(1,2,3,3)*Im*Kp*Lp)
8930    Kfm(1,3,3,3)=(Fmsig-Kfm(2,3,3,3)*Jp*Kp*Lp)/Im/Jp/Kp/Lp
8940    Fmsig=(Fm(3,1,3,3)-Fm(3,1,3,2)-Kfm(2,2,2,3)*Lp-Kfm(3,2,2,3)*Ip*Lp-Kfm(2,1
,2,3)*Jm*Lp-Kfm(2,2,3,3)*Kp*Lp-Kfm(3,1,2,3)*Ip*Jm*Lp-Kfm(3,2,3,3)*Ip*Kp*Lp)
8950    Kfm(3,1.3.3)=(Fmsig-Kfm(2,1,3,3)*Jm*Kp*Lp)/Ip/Jm/Kp/Lp
8960    Fmsig=(Fm(3,3,1,3)-Fm(3,3,1,2)-Kfm(2,2,2,3)*Lp-Kfm(3,2,2,3)*Ip*Lp-Kfm(2.3
,2,3)*Jp*Lp-Kfm(2,2,1,3)*Km*Lp-Kfm(3,3,2,3)*Ip*Jp*Lp-Kfm(3,2,1,3)*Ip*Km*Lp)
8970    Kfm(3,3,1,3)=(Fmsig-Kfm(2,3,1,3)*Jp*Km*Lp)/Ip/Jp/Km/Lp
8980    Fmsig=(Fm(3,3,3,1)-Fm(3,3,3,2)-Kfm(2,2,2,1)*Lm-Kfm(3,2,2,1)*Ip*Lm-Kfm(2.3
,2,1)*Jp*Lm-Kfm(2,2,3,1)*Kp*Lm-Kfm(3,3,2,1)*Ip*Jp*Lm-Kfm(3,2,3,1)*Ip*Kp*Lm)
8990    Kfm(3,3,3,1)=(Fmsig-Kfm(2,3,3,1)*Jp*Kp*Lm)/Ip/Jp/Kp/Lm
9000    Fmsig=(Fm(3,3,3,3)-Fm(3,3,3,2)-Kfm(2.2,2,3)*Lp-Kfm(3,2,2,3)*Ip*Lp-Kfm(2,3
,2,3)*Jp*Lp-Kfm(2,2,3,3)*Kp*Lp-Kfm(3,3,2,3)*Ip*Jp*Lp-Kfm(3,2,3,3)*Ip*Kp*Lp)
9010    Kfm(3,3,3,3)=(Fmsig-Kfm(2,3,3,3)*Jp*Kp*Lp)/Ip/Jp/Kp/Lp
9020                RETURN !          End of Non_lin_cof Subroutine.
9030 Check:     !  Subroutine to Check forces and moments calculated by Non-Linear
                   Coefficient Equation against force and moment data used to
9040            !  compute Non-Linear Coefficients.
9050            !  INPUT : Kfr,Kft,Kmr,Kmt representing either Afr,Aft,Amr,Amt or
                           Bfr,Bft,Bmr,Bmt.
9060            !          Ip,Jp,Kp,Km,Lp representing  displacement or
                           velocity perturbations according to wether A or B
9070            !          coefficients are being checked.
9080            !  OUTPUT :Any descrepancies in forces & moments by Hydrodynamic
                           Analysis and Non-Linear Coefficient Equation with
9090            !          corresponding I.J.K.L identified.
```

(16)

```
9100    FOR I=1 TO 3
9110    FOR J=1 TO 3
9120    FOR K=1 TO 3
9130    FOR L=1 TO 3
9140    Id=Ip*(I-2)
9150    Jd=Jp*(J-2)
9160    IF K=1 THEN 9200   ! This special treatment is due to Kd representing
9170    IF K=2 THEN 9220   ! Omegao. when damping coefficients are being dealt
9180    Kd=Kp              ! with, rather than Psid. Since equal magnitudes of
9190    GOTO 9230          ! positive and negative Psid perturbations were used,
9200    Kd=Km              ! corresponding negative and positive Omegao
9210    GOTO 9230          ! perturbations will be unequal in magnitude.
9220    Kd=0
9230    Ld=Lp*(L-2)
9240    MAT Kfm= Kfr
9250    GOSUB Equation
9260    Freqn=Feqn
9270    IF ABS(Frm(I,J,K,L)-Freqn)<1 THEN 9290
9280    PRINT USING "2(6A,X,SD.2DE),4(2X,2A,X,D)";"Frdat=",Frm(I,J,K,L),"Freqn="
,Freqn,"I=",I,"J=",J,"K=",K,"L=",L
9290    MAT Kfm= Kft
9300    GOSUB Equation
9310    Fteqn=Feqn
9320    IF ABS(Ftm(I,J,K,L)-Fteqn)<1 THEN 9340
9330    PRINT USING "2(6A,X,SD.2DE),4(2X,2A,X,D)";"Ftdat=",Ftm(I,J,K,L),"Fteqn="
,Fteqn,"I=",I,"J=",J,"K=",K,"L=",L
9340    MAT Kfm= Kmr
9350    GOSUB Equation
9360    Mreqn=Feqn
9370    IF ABS(Mrm(I,J,K,L)-Mreqn)<1 THEN 9390
9380    PRINT USING "2(6A,X,SD.2DE),4(2X,2A,X,D)";"Mrdat=",Mrm(I,J,K,L),"Mreqn="
,Mreqn,"I=",I,"J=",J,"K=",K,"L=",L
9390    MAT Kfm= Kmt
9400    GOSUB Equation
9410    Mteqn=Feqn
9420    IF ABS(Mtm(I,J,K,L)-Mteqn)<1 THEN 9440
9430    PRINT USING "2(6A,X,SD.2DE),4(2X,2A,X,D)";"Mtdat=",Mtm(I,J,K,L),"Mteqn="
,Mteqn,"I=",I,"J=",J,"K=",K,"L=",L
9440    NEXT L
9450    NEXT K
9460    NEXT J
9470    NEXT I
9480    RETURN !            End of Check Subroutine.
9490 Equation:    !        Subroutine to compute forces or moments using Non-Linear
                           Coefficient Equation for use in "Check" Subroutine.
9500              !        INPUT : Displacement or Velocity data : Id,Jd,Kd,Ld
9510              !                Data References : I,J,K,L
9520              !                Coefficient Matrix : Kfm
9530   Feqn1=Kfm(2,2,2,2)+Kfm(I,2,2,2)*Id+Kfm(2,J,2,2)*Jd+Kfm(2,2,K,2)*Kd+Kfm(2,
2,2,L)*Ld+Kfm(I,J,2,2)*Id*Jd+Kfm(I,2,K,2)*Id*Kd+Kfm(I,2,2,L)*Id*Ld
9540   Feqn2=Kfm(2,J,K,2)*Jd*Kd+Kfm(2,J,2,L)*Jd*Ld+Kfm(2,2,K,L)*Kd*Ld+Kfm(I,J,K,
2)*Id*Jd*Kd+Kfm(I,J,2,L)*Id*Jd*Ld+Kfm(I,2,K,L)*Id*Kd*Ld+Kfm(2,J,K,L)*Jd*Kd*Ld
9550   Feqn=Feqn1+Feqn2+Kfm(I,J,K,L)*Id*Jd*Kd*Ld
9560   RETURN
9570 Print_coef:    !      Subroutine to Print Out Non-Linear Coefficients.
                           INPUT : Kfm Matrix.
9580   PRINT " 11          12         13         21         22         23         31         32
       33"
9590   FOR I=1 TO 3
9600   FOR J=1 TO 3
9610   PRINT USING "8(SD.DE,X),SD.DE";Kfm(I,J,1,1),Kfm(I,J,1,2),Kfm(I,J,1,3),Kfm
(I,J,2,1),Kfm(I,J,2,2),Kfm(I,J,2,3),Kfm(I,J,3,1),Kfm(I,J,3,2),Kfm(I,J,3,3)
9620   NEXT J
9630   NEXT I
9640   PRINT "-----------------------------------------------------------------
-------------"
```

```
9650    RETURN
9660 DISP "RWJ015 : Programme Operation Completed."
9670 END
9680  ! LIBRARY SUB's ADDED BY THE TRANSLATOR
9690  !
9700  !
9710 DEF FNPage$    ! PAGE function of PRINT
9720    RETURN CHR$(13)&CHR$(12)
9730    FNEND
9740     !
9750     !
9760 DEF FNLin$(INTEGER X)  ! LIN function of PRINT
9770    INTEGER I
9780    IF X=0 THEN RETURN CHR$(13)
9790    ALLOCATE R$[ABS(X)+1]
9800    R$=CHR$(13)
9810    IF X<0 THEN R$=""
9820    FOR I=1 TO ABS(X)
9830      R$=R$&CHR$(10)
9840    NEXT I
9850    RETURN R$
9860    FNEND
9870     !
9880     !
```

(13)

(i)

```
10     PRINTER IS 1 !    PROGRAM : RWJ043 : Issue 03.11.87. Thesis Version.
20     DEG !             Tailshaft-Sterntube Bearing Lateral Vibration Model.
                         ( 6 ELEMENT VERSION.)
30     OPTION BASE 1 !   ________________________________________________________
40     N=82          !   Set R.P.M. by Manual EDIT.
50     Nonlin$="N"   !   Selects Non-Linear Model for Aft Sterntube Bearing.
60    !Time=.057471264!  Set orbit start time by Manual EDIT.(Overridden on
                         continuation runs.)
70     Time=0          ! Set orbit start time by Manual EDIT.
80     Continue$="Y"!    Y for Continuation of Run already started.( Requires
                         CONTIN and ORBITS files in place of STARTO file.)
90     Print$="N"    !   Select Data Input Print Out by Manual EDIT.
100    Cyclim=20     !   Set limit on max. No. of Cycles by Manual EDIT.
110    Ndlim=4000    !   Set limit on max. No. of Time Steps by Manual EDIT.
120    Cartflag=0    !   Flag to get Cart_oilfilm Subroutine to use fixed
                         perturbations at orbit start.
130    Stoprun=0     !   Resets Indicator to Stop Run.
140    Runend=0      !   Resets 2nd. Indicator to Stop Run after dumping CONTIN
                         and ORBITS data files onto disc.
150    Steady$="N"   !   Selects steady Propeller excitation of Mwy=-4.152E+5 N.m.
160    Kcrit=.02     !   Multiplying Factor on Critical Element Damping.
170    Dtmax=60/N/5/400! Max. Dt =1/400th of 5th (Blade) Order Excitation Cycle.
180    Dxymax=5.E-6      ! m.      Max. Dx,Dy for Aft Sterntube Bearing.
190    Dlgmax=1.25E-6     ! rad.    -"-  Dl,Dg -----------"--------------
200    Dxydmax=3.5E-5    ! m/s.    -"-  Dxd,Dyd ---------"--------------
210    Dlgdmax=2.5E-5     ! rad/s. -"-  Dld,Dgd ---------"--------------
220    DIM Afr(3,3,3,3),Aft(3,3,3,3),Amr(3,3,3,3),Amt(3,3,3,3),Ak(3,3,3,3)
230    DIM Bfr(3,3,3,3),Bft(3,3,3,3),Bmr(3,3,3,3),Bmt(3,3,3,3),Bk(3,3,3,3)
240    DIM Fwy(72),Fwx(72),Mwy(72),Mwx(72),Doe(6),Die(6),Le(6),Dos(6),Dis(6),Ls(6
)
250    DIM Ma(6),Jdia(6),Jpol(6),Kx(6),Ky(6),Kl(6),Kg(6),X(6),Y(6),Lam(6),Gam(6),
Xd(6),Yd(6),Lamd(6),Gamd(6),Xdd(6),Ydd(6),Lamdd(6),Gamdd(6)
260    DIM Kv(24),Km(24,24),Kinv(24,24),Xylgp(24),Xp(6),Yp(6),Lamp(6),Gamp(6),Xdp
(6),Ydp(6),Lamdp(6),Gamdp(6),Xddm(6),Yddm(6),Lamddm(6),Gamddm(6)
270    DIM Xddreg(6,5),Yddreg(6,5),Lddreg(6,5),Gddreg(6,5),Xcon(6),Xdiv(6),Ycon(6
),Ydiv(6),Lcon(6),Gcon(6),Xdcon(6),Xddiv(6),Ydcon(6),Yddiv(6)
280    DIM Ldcon(6),Lddiv(6),Gdcon(6),Gddiv(6),Xprt(6,21),Yprt(6,21),Lprt(6,21),G
prt(6,21)
290    DIM Axxelm(4),Axyelm(4),Axlelm(4),Axgelm(4),Ayxelm(4),Ayyelm(4),Aylelm(4),
Aygelm(4),Alxelm(4),Alyelm(4),Allelm(4),Algelm(4),Agxelm(4),Agyelm(4),Aglelm(4)
300    DIM Aggelm(4),Bxxelm(4),Bxyelm(4),Bxlelm(4),Bxgelm(4),Byxelm(4),Byyelm(4),
Bylelm(4),Bygelm(4),Blxelm(4),Blyelm(4),Bllelm(4),Blgelm(4),Bgxelm(4),Bgyelm(4)
310    DIM Bglelm(4),Bggelm(4),Fxelm(4),Fyelm(4),Mxelm(4),Myelm(4),Fxnlel(4),Fynl
el(4),Mxnlel(4),Mynlel(4),Xbelm(4),Ybelm(4),Lbelm(4),Gbelm(4),Xdbelm(4)
320    DIM Ydbelm(4),Ldbelm(4),Gdbelm(4),Bslat(6),Bsang(6),Xmean(6),Ymean(6),Eorb
(6,20),Porb(6,20),Eorbmax(6),Eorbmin(6)
330    DIM Lmn(6),Gmn(6),Lomax(6),Lomin(6),Gomax(6),Gomin(6),Zlorbmax(6),Zlorbmin
(6),Zgorbmax(6),Zgorbmin(6)
340    PRINTER IS 701
350    PRINT FNPage$;"###########################################################
#"
360    PRINT "#  RWJ043 : Issue : 03.11.87. (6 ELEMENT VERSION.)              #"
370    PRINT "#  Tailshaft-Sterntube Bearing Lateral Vibration Model.         #"
380    PRINT "#  (uses coefficients produced by RWJ015D Issue 19.05.87.)  #"
390    PRINT "############################################################"
400    PRINT "#  Subroutine Development Status :                              #"
410    PRINT "#  _____________________________________                        #"
420    PRINT "#  Nonlincomp              22.06.87.       Tested OK            #"
430    PRINT "#  Cartfm                  22.06.87.       Tested OK            #"
440    PRINT "#  Cart_oilfilm            30.06.87.       Tested OK            #"
450    PRINT "#  Predict                 17.07.87.       Tested OK            #"
```

```
460   PRINT "#  Timestep              19.10.87.      Checking          #"
470   PRINT "#  Printdisp             24.07.87.      Tested OK         #"
480   PRINT "#  Data_input            16.06.87.      Tested OK         #"
490   PRINT "#  Regression            21.07.87.      Tested OK         #"
500   PRINT "#  Wakefm_interp         22.07.87.      Tested OK         #"
510   PRINT "#  Full_print            31.07.87.      Tested OK         #"
520   PRINT "#  Set_dyncof            27.08.87.      Tested OK         #"
530   PRINT "##################################################################"
540   PRINT "Non-linear Aft Sterntube Bearing Model Selected : ";Nonlin$
550   PRINT "Data Input Print Out Selected : ";Print$
560   PRINT "Orbit Start Time : ";Time
570   PRINT "Limit on No. of Cycles : ";Cyclim
580   PRINT "Limit on No. of Time Steps : ";Ndlim
590   PRINT "Steady Propeller Excitation Selected : ";Steady$
600   PRINT "Kcrit = ";Kcrit;" ( Multiplying Factor on Critical Element Damping.
)".
610   PRINT "R.P.M.= ";N
620   PRINT "Continuation Run : ";Continue$
630   PRINT USING "10A,D.3DE,7A";"Dtmax = ",Dtmax," s."
640   PRINT USING "10A,D.3DE,7A";"Dxymax = ",Dxymax," m."
650   PRINT USING "10A,D.3DE,7A";"Dlgmax = ",Dlgmax," rad."
660   PRINT USING "10A,D.3DE,7A";"Dxydmax = ",Dxydmax," m/s."
670   PRINT USING "10A,D.3DE,7A";"Dlgdmax = ",Dlgdmax," rad/s."
680   PRINT "________________________________________________________________________
_____________"
690   GOSUB Data_input
700   MASS STORAGE IS ":INTERNAL,4,0"        ! Notes : STARTO file required to
                                               start a new run when
710   IF Continue$="Y" THEN 890              ! Continue$="N" has been selected.
                                               STARTO file may be produced by
720   ASSIGN @File5 TO "STARTO:INTERNAL,4,0"! RWJ051 Steady State Analysis
                                               Program for given propeller wake
730   ENTER @File5;X(*)           ! force and moment components. Corresponding time
                                    for these forces and moments should be manually
740   ENTER @File5;Y(*)           ! set as Orbit Start Time in this program.
                                    STARTO file may also be produced by
750   ENTER @File5;Lam(*)         ! transformation of CONTIN file produced in run
                                    with fairly similar conditions, using RWJ054
760   ENTER @File5;Gam(*)         ! for transformation. Latter system for producing
                                    STARTO file should give faster orbit convergence.
770   ENTER @File5;Xd(*)
780   ENTER @File5;Yd(*)
790   ENTER @File5;Lamd(*)
800   ENTER @File5;Gamd(*)
810   ENTER @File5;Xdd(*)
820   ENTER @File5;Ydd(*)
830   ENTER @File5;Lamdd(*)
840   ENTER @File5;Gamdd(*)
850   ASSIGN @File5 TO *
860   Cyc=1             !    Initialize Cycle counter.
870   Nd=0              !    Initialize Time Step counter.
880   GOTO 1200
890   ASSIGN @File8 TO "CONTIN:INTERNAL,4,0"
900   ENTER @File8;X(*)          ! CONTIN and ORBITS files are required for
                                   continuation of a run already started when
910   ENTER @File8;Y(*)          ! Continue$="Y" has been selected. These files are
                                   automatically purged and updated at the end of
920   ENTER @File8;Lam(*)        ! each orbit or on the manual command Stoprun=1 at
                                   any time. Continuation runs start from the Cycle,
930   ENTER @File8;Gam(*)        ! Time and Step No. at which the last CONTIN and
                                   ORBITS files were stored.
940   ENTER @File8;Xd(*)
950   ENTER @File8;Yd(*)
960   ENTER @File8;Lamd(*)
970   ENTER @File8;Gamd(*)
980   ENTER @File8;Xdd(*)
```

2

```
990    ENTER @File8;Ydd(*)
1000   ENTER @File8;Lamdd(*)
1010   ENTER @File8;Gamdd(*)
1020   ENTER @File8;Xddreg(*)
1030   ENTER @File8;Yddreg(*)
1040   ENTER @File8;Lddreg(*)
1050   ENTER @File8;Gddreg(*)
1060   ENTER @File8;Dt0,Dt1,Dt2,Dt3,Dt4,Time,Ayy,Ayx,Ayg,Ayl,Axy,Axx,Axg,Axl,Agy,
Agx,Agg,Agl,Aly,Alx,Alg,All
1070   ENTER @File8;Byy,Byx,Byg,Byl,Bxy,Bxx,Bxg,Bxl,Bgy,Bgx,Bgg,Bgl,Bly,Blx,Blg,B
ll,Fxa,Fya,Mxa,Mya,Fxnl,Fynl,Mxnl,Mynl
1080   ASSIGN @File8 TO *
1090   Cartflag=1
1100   ASSIGN @File9 TO "ORBITS:INTERNAL,4,0"
1110   ENTER @File9;Cyc
1120   ENTER @File9;Nd
1130   ENTER @File9;Xprt(*)
1140   ENTER @File9;Yprt(*)
1150   ENTER @File9;Lprt(*)
1160   ENTER @File9;Gprt(*)
1170   ENTER @File9;Tprt
1180   ASSIGN @File9 TO *
1190   Dtm1=Dt0
1200   GOSUB Full_print
1210   GOSUB Timestep
1220   PRINTER IS 1
1230   PRINT "RWJ043  Program Operation Completed."
1240   PAUSE
1250   GOTO 900 !################################################################"
1260 Cart_oilfilm:      !  Subroutine computes Cartezian Oil Film Stiffness &
1270                    !  Damping Coefficients using single direction displacement
1280                    !  and velocity perturbations corresponding to the change
                        !  from the current time step start conditions to the
1290                    !  predicted time step end conditions. This is only applic-
                        !  able to the Aft Sterntube Bearing, constant linearised
1300                    !  coefficients being used for all other bearings.
                        !  INPUT : X(2),Y(2),Lam(2),Gam(2),Xd(2),Yd(2),Lamd(2),
1310                    !          Gamd(2)....absolute values relative to Datum.
1320                    !          Xp(2),Yp(2),Lamp(2),Gamp(2),Xdp(2),Ydp(2),
                        !          Lamdp(2),Gamdp(2)....current estimates for end
1330                    !          of time step.
                        !  Polar Stiffness and Damping Coefficients for Aft
1340                    !  Sterntube Bearing Non-Linear Oil Film Model and polar
                        !  base conditions Eo,Psio,Xio,Phio. This data is read in
1350                    !  during Data_input subroutine operation, from ACOEFS and
                        !  BCOEFS data files which were produced by :
1360                    !  RWJ015D  Issue : 19.05.87.
1370                    !  OUTPUT : Axx......................Bgg (32 coefficients)
1380                    !           Fxa......Mya  Base condition forces & moments.
                           Fxnl.....Mynl Non-linear correction forces & moments.
1390                    !  Notes : 1. Non-linear factors Kfxnl, etc. are applied to
                        !  the coefficients to compensate for the non-applicability
1400                    !  of the principal of superposition.
                        !          2. Although Input is in m. units, this
1410                    !  subroutine (by tradition !) operates in mm. units and
                        !  converts Input at start.
1420                    !          3. Sign convention for oil film forces and
                        !  moments in this subroutine is reverse of that used in
1430                    !  the remainder of the program (i.e. in lateral vibration)
1440   Xa=X(2)*1000     !  ____________________________________________________________
1450   Ya=Y(2)*1000     !  Set working displacements and velocities to current time
                        !  step start conditions for element 2 i.e. in way of aft
1460   Axa=Lam(2)       !  sterntube bearing.
1470   Aya=Gam(2)
1480   Xda=Xd(2)*1000
1490   Yda=Yd(2)*1000
```
③

④

```
1500  Axda=Lamd(2)
1510  Ayda=Gamd(2)
1520  IF Cartflag=1 THEN 1620
1530  Dx=.008 !  mm.      For Start condition set fixed perturbations.
1540  Dy=.008 !  mm.
1550  Dl=3.E-6!  rad.
1560  Dg=3.E-6!  rad.
1570  Dxd=.04 !  mm/s.
1580  Dyd=.04 !  mm/s.
1590  Dld=2.E-4! rad/s.
1600  Dgd=2.E-4! rad/s.
1610  GOTO 1700
1620  Dx=(Xp(2)-X(2))*1000 ! Set perturbations according to current time step
                             change estimates. Note : Fixed values must be used
1630  Dy=(Yp(2)-Y(2))*1000 ! at Orbit start.
1640  Dl=Lamp(2)-Lam(2)
1650  Dg=Gamp(2)-Gam(2)
1660  Dxd=(Xdp(2)-Xd(2))*1000
1670  Dyd=(Ydp(2)-Yd(2))*1000
1680  Dld=Lamdp(2)-Lamd(2)
1690  Dgd=Gamdp(2)-Gamd(2)
1700  Xo=Eo*SIN(Psio)  !   Cartezian Equilibrium Lateral Displacements.
1710  Yo=Eo*COS(Psio)
1720  Ea=SQR(Xa^2+Ya^2)
1730  IF ABS(Ya)>1.E-12 THEN 1790
1740  IF Xa<0 THEN 1770
1750  Psia=90
1760  GOTO 1870
1770  Psia=270
1780  GOTO 1870
1790  Psia=ATN(Xa/Ya)
1800  IF Xa<0 THEN 1830
1810  IF Ya<0 THEN 1860
1820  GOTO 1870
1830  IF Ya<0 THEN 1860
1840  Psia=360+Psia
1850  GOTO 1870
1860  Psia=180+Psia
1870  Axo=Xio*SIN(Psio)+Phio*COS(Psio)   !   Cartezian Equilibrium Angular
                                             Displacements.
1880  Ayo=Xio*COS(Psio)-Phio*SIN(Psio)
1890  Xdo=0              !   Cartezian Equilibrium Velocities.
1900  Ydo=0
1910  Axdo=0
1920  Aydo=0
1930  Xia=Aya*COS(Psio)+Axa*SIN(Psio)
1940  Phia=Axa*COS(Psio)-Aya*SIN(Psio)
1950  Eda=Yda*COS(Psio)+Xda*SIN(Psio)
1960  Psida=(Xda*COS(Psio)-Yda*SIN(Psio))/Ea
1970  Xida=Ayda*COS(Psio)+Axda*SIN(Psio)
1980  Phida=Axda*COS(Psio)-Ayda*SIN(Psio)
1990  E=Ea-Eo
2000  Psi=Psia-Psio
2010  Xi=Xia-Xio
2020  Phi=Phia-Phio
2030  Ed=Eda
2040  Psid=Psida
2050  Xid=Xida
2060  Phid=Phida
2070  GOSUB Nonlincomp
2080  GOSUB Cartfm
2090  Fya=Fy          !  Oil Film Forces and Moments at Start of Current Time Step
2100  Fxa=Fx
2110  Mya=My/1.E+3  !  N.m.
2120  Mxa=Mx/1.E+3  !  N.m.
2130  E=SQR((Xa+Dx)^2+Ya^2)-Eo !       +Dx pert.
```

5

```
2140  IF ABS(Ya)>1.E-12 THEN 2200
2150  IF (Xa+Dx)<0 THEN 2180
2160  Psip=90
2170  GOTO 2280
2180  Psip=270
2190  GOTO 2280
2200  Psip=ATN((Xa+Dx)/Ya)
2210  IF (Xa+Dx)<0 THEN 2240
2220  IF Ya<0 THEN 2270
2230  GOTO 2280
2240  IF Ya<0 THEN 2270
2250  Psip=360+Psip
2260  GOTO 2280
2270  Psip=180+Psip
2280  Psi=Psip-Psio
2290  IF Dx=0 THEN 2410
2300  GOSUB Nonlincomp
2310  GOSUB Cartfm
2320  Fyp=Fy
2330  Fxp=Fx
2340  Myp=My/1.E+3
2350  Mxp=Mx/1.E+3
2360  Axx=(Fxp-Fxa)/Dx*1.E+3   !        N/m.
2370  Ayx=(Fyp-Fya)/Dx*1.E+3
2380  Alx=(Mxp-Mxa)/Dx*1.E+3   !        N.
2390  Agx=(Myp-Mya)/Dx*1.E+3
2400  GOTO 977
2410  Axx=0
2420  Ayx=0
2430  Alx=0
2440  Agx=0
2450  E=SQR(Xa^2+(Ya+Dy)^2)-Eo  !        +Dy pert.
2460  IF ABS(Ya+Dy)>1.E-12 THEN 2520
2470  IF Xa<0 THEN 2500
2480  Psip=90
2490  GOTO 2600
2500  Psip=270
2510  GOTO 2600
2520  Psip=ATN(Xa/(Ya+Dy))
2530  IF Xa<0 THEN 2560
2540  IF (Ya+Dy)<0 THEN 2590
2550  GOTO 2600
2560  IF (Ya+Dy)<0 THEN 2590
2570  Psip=360+Psip
2580  GOTO 2600
2590  Psip=180+Psip
2600  Psi=Psip-Psio
2610  IF Dy=0 THEN 2730
2620  GOSUB Nonlincomp
2630  GOSUB Cartfm
2640  Fyp=Fy
2650  Fxp=Fx
2660  Myp=My/1.E+3
2670  Mxp=Mx/1.E+3
2680  Axy=(Fxp-Fxa)/Dy*1.E+3   !        N/m.
2690  Ayy=(Fyp-Fya)/Dy*1.E+3
2700  Aly=(Mxp-Mxa)/Dy*1.E+3   !        N.
2710  Agy=(Myp-Mya)/Dy*1.E+3
2720  GOTO 2770
2730  Axy=0
2740  Ayy=0
2750  Aly=0
2760  Agy=0
2770  E=Ea-Eo !                         Reset E, Psi.
2780  Psi=Psia-Psio
2790  Xi=Aya*COS(Psio)+(Axa+Dl)*SIN(Psio)-Xio !       +Dl pert.
```

6

```
2800  Phi=(Axa+Dl)*COS(Psio)-Aya*SIN(Psio)-Phio
2810  IF Dl=0 THEN 2930
2820  GOSUB Nonlincomp
2830  GOSUB Cartfm
2840  Fyp=Fy
2850  Fxp=Fx
2860  Myp=My/1.E+3
2870  Mxp=Mx/1.E+3
2880  Ayl=(Fyp-Fya)/Dl     !         N/rad.
2890  Axl=(Fxp-Fxa)/Dl
2900  All=(Mxp-Mxa)/Dl     !         Nm/rad.
2910  Agl=(Myp-Mya)/Dl
2920  GOTO 2970
2930  Ayl=0
2940  Axl=0
2950  All=0
2960  Agl=0
2970  Xi=(Aya+Dg)*COS(Psio)+Axa*SIN(Psio)-Xio  !       +Dg pert.
2980  Phi=Axa*COS(Psio)-(Aya+Dg)*SIN(Psio)-Phio
2990  IF Dg=0 THEN 3110
3000  GOSUB Nonlincomp
3010  GOSUB Cartfm
3020  Fyp=Fy
3030  Fxp=Fx
3040  Myp=My/1.E+3
3050  Mxp=Mx/1.E+3
3060  Ayg=(Fyp-Fya)/Dg   !          N/rad.
3070  Axg=(Fxp-Fxa)/Dg
3080  Agg=(Myp-Mya)/Dg   !          Nm/rad.
3090  Alg=(Mxp-Mxa)/Dg
3100  GOTO 3150
3110  Ayg=0
3120  Axg=0
3130  Agg=0
3140  Alg=0
3150  Xi=Xia-Xio     !              Reset Xi, Phi
3160  Phi=Phia-Phio
3170  Ed=Yda*COS(Psio)+(Xda+Dxd)*SIN(Psio)   !       +Dxd pert.
3180  Psid=((Xda+Dxd)*COS(Psio)-Yda*SIN(Psio))/Ea
3190  IF Dxd=0 THEN 3310
3200  GOSUB Nonlincomp
3210  GOSUB Cartfm
3220  Fyp=Fy
3230  Fxp=Fx
3240  Myp=My/1.E+3
3250  Mxp=Mx/1.E+3
3260  Byx=(Fyp-Fya)/Dxd*1.E+3!         Ns/m.
3270  Bxx=(Fxp-Fxa)/Dxd*1.E+3
3280  Bgx=(Myp-Mya)/Dxd*1.E+3!         Ns.
3290  Blx=(Mxp-Mxa)/Dxd*1.E+3
3300  GOTO 3350
3310  Byx=0
3320  Bxx=0
3330  Bgx=0
3340  Blx=0
3350  Ed=(Yda+Dyd)*COS(Psio)+Xda*SIN(Psio)  !       +Dyd pert.
3360  Psid=(Xda*COS(Psio)-(Yda+Dyd)*SIN(Psio))/Ea
3370  IF Dyd=0 THEN 3490
3380  GOSUB Nonlincomp
3390  GOSUB Cartfm
3400  Fyp=Fy
3410  Fxp=Fx
3420  Myp=My/1.E+3
3430  Mxp=Mx/1.E+3
3440  Byy=(Fyp-Fya)/Dyd*1.E+3!        Ns/m.
3450  Bxy=(Fxp-Fxa)/Dyd*1.E+3
```

```
3460 Bgy=(Myp-Mya)/Dyd*1.E+3!        Ns.
3470 Bly=(Mxp-Mxa)/Dyd*1.E+3
3480 GOTO 3530
3490 Byy=0
3500 Bxy=0
3510 Bgy=0
3520 Bly=0
3530 Ed=Eda            !                    Reset Ed, Psid
3540 Psid=Psida
3550 Xid=Ayda*COS(Psio)+(Axda+Dld)*SIN(Psio)   !      +Dld pert.
3560 Phid=(Axda+Dld)*COS(Psio)-Ayda*SIN(Psio)
3570 IF Dld=0 THEN 3690
3580 GOSUB Nonlincomp
3590 GOSUB Cartfm
3600 Fyp=Fy
3610 Fxp=Fx
3620 Myp=My/1.E+3
3630 Mxp=Mx/1.E+3
3640 Byl=(Fyp-Fya)/Dld     !      Ns/rad.
3650 Bxl=(Fxp-Fxa)/Dld
3660 Bgl=(Myp-Mya)/Dld     !      Nms/rad.
3670 Bll=(Mxp-Mxa)/Dld
3680 GOTO 3730
3690 Byl=0
3700 Bxl=0
3710 Bgl=0
3720 Bll=0
3730 Xid=(Ayda+Dgd)*COS(Psio)+Axda*SIN(Psio)   !       +Dgd pert.
3740 Phid=Axda*COS(Psio)-(Ayda+Dgd)*SIN(Psio)
3750 IF Dgd=0 THEN 3870
3760 GOSUB Nonlincomp
3770 GOSUB Cartfm
3780 Fyp=Fy
3790 Fxp=Fx
3800 Myp=My/1.E+3
3810 Mxp=Mx/1.E+3
3820 Byg=(Fyp-Fya)/Dgd   !      Ns/rad.
3830 Bxg=(Fxp-Fxa)/Dgd
3840 Bgg=(Myp-Mya)/Dgd   !      Nms/rad.
3850 Blg=(Mxp-Mxa)/Dgd
3860 GOTO 3910
3870 Byg=0
3880 Bxg=0
3890 Bgg=0
3900 Blg=0
3910 E=SQR((Xa+Dx)^2+(Ya+Dy)^2)-Eo
3920 IF ABS(Ya+Dy)>1.E-12 THEN 3980
3930 IF (Xa+Dx)<0 THEN 3960
3940 Psip=90
3950 GOTO 4060
3960 Psip=270
3970 GOTO 4060
3980 Psip=ATN((Xa+Dx)/(Ya+Dy))
3990 IF (Xa+Dx)<0 THEN 4020
4000 IF (Ya+Dy)<0 THEN 4050
4010 GOTO 4060
4020 IF (Ya+Dy)<0 THEN 4050
4030 Psip=360+Psip
4040 GOTO 4060
4050 Psip=180+Psip
4060 Psi=Psip-Psio
4070 Xi=(Aya+Dg)*COS(Psio)+(Axa+Dl)*SIN(Psio)-Xio
4080 Phi=(Axa+Dl)*COS(Psio)-(Aya+Dg)*SIN(Psio)-Phio
4090 Ed=(Yda+Dyd)*COS(Psio)+(Xda+Dxd)*SIN(Psio)
4100 Psid=((Xda+Dxd)*COS(Psio)-(Yda+Dyd)*SIN(Psio))/(Eo+E)
4110 Xid=(Ayda+Dgd)*COS(Psio)+(Axda+Dld)*SIN(Psio)
```

7

```
4120  Phid=(Axda+Dld)*COS(Psio)-(Ayda+Dgd)*SIN(Psio)
4130  GOSUB Nonlincomp                                                            8
4140  GOSUB Cartfm
4150  Fxtot=Fx    !  Oil Film Forces and Moments at Predicted Time Step End
                     Conditions. i.e. when all displacement and velocity
4160  Fytot=Fy    !  perturbations are applied simultaneously.
4170  Mxtot=Mx/1.E+3!  Converted to N.m.
4180  Mytot=My/1.E+3!  ------"----------
4190  Fxnl=Fxtot-(Fxa+Axx*Dx/1.E+3+Axy*Dy/1.E+3+Axl*Dl+Axg*Dg+Bxx*Dxd/1.E+3+Bxy*
Dyd/1.E+3+Bxl*Dld+Bxg*Dgd)
4200  Fynl=Fytot-(Fya+Ayx*Dx/1.E+3+Ayy*Dy/1.E+3+Ayl*Dl+Ayg*Dg+Byx*Dxd/1.E+3+Byy*
Dyd/1.E+3+Byl*Dld+Byg*Dgd)
4210  Mxnl=Mxtot-(Mxa+Alx*Dx/1.E+3+Aly*Dy/1.E+3+All*Dl+Alg*Dg+Blx*Dxd/1.E+3+Bly*
Dyd/1.E+3+Bll*Dld+Blg*Dgd)   !  N.m.
4220  Mynl=Mytot-(Mya+Agx*Dx/1.E+3+Agy*Dy/1.E+3+Agl*Dl+Agg*Dg+Bgx*Dxd/1.E+3+Bgy*
Dyd/1.E+3+Bgl*Dld+Bgg*Dgd)   !  N.m.
4230   !  Non-Linear factors Fxnl, etc. above are calculated to cover the
          difference in oil film forces and moments when all perturbations are
4240   !  applied simultaneously, to those calculated with the stiffness and
          damping coefficients, which were based on the application of
4250   !  perturbations one at a time. The non-linear factors thus take account
          of the fact that the principle of superposition is not valid for an oil
4260   !  film due to the influence of cavitation.
4270  RETURN !#################################################################
4280 Nonlincomp:  !  Subroutine to select Non-Linear Coefficient Indicies
4290              !  according to the sense of E, Xi, Psi, Phi, Ed, Xid, Omo,Phid
4300              !  and then compute Fr, Ft, Mr, Mt.
                  !  Applicable to aft sterntube bearing only.
4310              IF E>0 THEN 4350
4320              IF E<0 THEN 4370
4330              I=2
4340              GOTO 4380
4350              I=3
4360              GOTO 4380
4370              I=1
4380              IF Xi>0 THEN 4420
4390              IF Xi<0 THEN 4440
4400              J=2
4410              GOTO 4450
4420              J=3
4430              GOTO 4450
4440              J=1
4450              IF Psi>0 THEN 4490
4460              IF Psi<0 THEN 4510
4470              K=2
4480              GOTO 4520
4490              K=3
4500              GOTO 4520
4510              K=1
4520              IF Phi>0 THEN 4560
4530              IF Phi<0 THEN 4580
4540              L=2
4550              GOTO 4590
4560              L=3
4570              GOTO 4590
4580              L=1
4590              IF Ed>0 THEN 4630
4600              IF Ed<0 THEN 4650
4610              Id=2
4620              GOTO 4660
4630              Id=3
4640              GOTO 4660
4650              Id=1
4660              IF Xid>0 THEN 4700
4670              IF Xid<0 THEN 4720
4680              Jd=2
```

⑨

```
4690            GOTO 4730
4700            Jd=3
4710            GOTO 4730
4720            Jd=1
4730            Omo=Om-2*Psid
4740            IF Omo<0 THEN 4780   !    Note the apparent reversal of the +/-
4750            IF Omo>0 THEN 4800   !    3/1 referencing is because it really
4760            Kd=2                 !    refers to the sense of Psid although
4770            GOTO 4810            !    the equation is based on Omo.
4780            Kd=3
4790            GOTO 4810
4800            Kd=1
4810            IF Phid>0 THEN 4850
4820            IF Phid<0 THEN 4870
4830            Ld=2
4840            GOTO 4880
4850            Ld=3
4860            GOTO 4880
4870            Ld=1
4880            MAT Ak= Afr
4890            MAT Bk= Bfr
4900            GOSUB Equation
4910            Fr=Feqn
4920            MAT Ak= Aft
4930            MAT Bk= Bft
4940            GOSUB Equation
4950            Ft=Feqn
4960            MAT Ak= Amr
4970            MAT Bk= Bmr
4980            GOSUB Equation
4990            Mr=Feqn
5000            MAT Ak= Amt
5010            MAT Bk= Bmt
5020            GOSUB Equation
5030            Mt=Feqn
5040            RETURN !###################################################################
5050 Equation:  !  Polar Force/Moment Non-Linear Coefficient Equation.
5060            !  INPUT : E, Xi, Psi, Phi, Ed, Xid, Psid, Om, Omo, Phid and
5070            !  Ak & Bk coefficient matricies for either Fr Ft Mr or Mt.
5080            !  Coefficient Indicies I, J, K, L, Id, Jd, Kd, Ld according
5090            ! to the sense of E, Xi, Psi, Phi, Xid, Psid, Phid respectivley
5100            ! ( 3 for Positive, 2 for Zero, 1 for Negitive.)
5110            !  OUTPUT : Feqn= Fr, Ft, Mr or Mt according to coefficient
5120            !  matricies input.
5130     Feqn0=Bk(2,2,Kd,2)*Omo
5140     Feqn1=Ak(I,2,2,2)*E+Ak(2,J,2,2)*Xi+Ak(2,2,K,2)*Psi+Ak(2,2,2,L)*Phi+Ak(I,
J,2,2)*E*Xi+Ak(I,2,K,2)*E*Psi+Ak(I,2,2,L)*E*Phi+Ak(2,J,K,2)*Xi*Psi
5150     Feqn2=Ak(2,J,2,L)*Xi*Phi+Ak(2,2,K,L)*Psi*Phi+Ak(I,J,K,2)*E*Xi*Psi+Ak(I,J
,2,L)*E*Xi*Phi+Ak(I,2,K,L)*E*Psi*Phi+Ak(2,J,K,L)*Xi*Psi*Phi
5160     Feqn3=Ak(I,J,K,L)*E*Xi*Psi*Phi+Bk(2,2,2,2)+Bk(Id,2,2,2)*Ed+Bk(2,Jd,2,2)*
Xid+Bk(2,2,2,Ld)*Phid+Bk(Id,Jd,2,2)*Ed*Xid+Bk(Id,2,Kd,2)*Ed*Omo
5170     Feqn4=Bk(Id,2,2,Ld)*Ed*Phid+Bk(2,Jd,Kd,2)*Xid*Omo+Bk(2,Jd,2,Ld)*Xid*Phid
+Bk(2,2,Kd,Ld)*Omo*Phid+Bk(Id,Jd,Kd,2)*Ed*Xid*Omo+Bk(Id,Jd,2,Ld)*Ed*Xid*Phid
5180     Feqn=Feqn0+Feqn1+Feqn2+Feqn3+Feqn4+Bk(Id,2,Kd,Ld)*Ed*Omo*Phid+Bk(2,Jd,Kd
,Ld)*Xid*Omo*Phid+Bk(Id,Jd,Kd,Ld)*Ed*Xid*Omo*Phid
5190     RETURN !##########################################################################
5200 Cartfm:   !   Subroutine to convert polar forces & moments to Cartezian.
5210           !   INPUT :  Fr, Ft, Mr, Mt      OUTPUT : Fx, Fy, Mx, My
5220           Fy=Fr*COS(Psio)-Ft*SIN(Psio)
5230           Fx=Fr*SIN(Psio)+Ft*COS(Psio)
5240           My=Mr*COS(Psio)-Mt*SIN(Psio)
5250           Mx=Mr*SIN(Psio)+Mt*COS(Psio)
5260           RETURN !###################################################################
5270 Data_input:      !    Subroutine to INPUT all required data either from disc
                           or by manual EDIT and reduce to useable form.
5280     MASS STORAGE IS ":INTERNAL,4,0"       ! N.B. Parameters which are
```

```
                                                     subject to variation for test
5290     ASSIGN @File1 TO "ACOEFS:INTERNAL,4,0"! purposes are set by manual EDIT  10
                                                     on first page of program for
5300     ENTER @File1;Datset,Eo,Psio,Xio,Phio    ! convenience. e.g. N. (R.P.M.)
5310     ENTER @File1;Afr(*)
5320     ENTER @File1;Aft(*)
5330     ENTER @File1;Amr(*)
5340     ENTER @File1;Amt(*)
5350     ASSIGN @File1 TO *
5360     ASSIGN @File2 TO "BCOEFS:INTERNAL,4,0"
5370     ENTER @File2;Bfr(*)
5380     ENTER @File2;Bft(*)
5390     ENTER @File2;Bmr(*)
5400     ENTER @File2;Bmt(*)
5410     ASSIGN @File2 TO *
5420     ASSIGN @File3 TO "WAKEFM:INTERNAL,4,0"
5430     ENTER @File3;Tint
5440     ENTER @File3;Fwy(*)  !  Cyclic forces and moments acting on propeller due
5450     ENTER @File3;Fwx(*)  !  to interaction with wake field.
5460     ENTER @File3;Mwy(*)
5470     ENTER @File3;Mwx(*)
5480     ASSIGN @File3 TO *
5490     ASSIGN @File4 TO "DYNCOF:INTERNAL,4,0"
5500     ENTER @File4;Axxelm(*)
5510     ENTER @File4;Axyelm(*)   ! Linearised Stiffness (bearings only) and
5520     ENTER @File4;Axlelm(*)   ! Damping (propeller and bearings) Coefficient
5530     ENTER @File4;Axgelm(*)   ! Data.
5540     ENTER @File4;Ayxelm(*)
5550     ENTER @File4;Ayyelm(*)
5560     ENTER @File4;Aylelm(*)
5570     ENTER @File4;Aygelm(*)
5580     ENTER @File4;Alxelm(*)
5590     ENTER @File4;Alyelm(*)
5600     ENTER @File4;Allelm(*)
5610     ENTER @File4;Algelm(*)
5620     ENTER @File4;Agxelm(*)
5630     ENTER @File4;Agyelm(*)
5640     ENTER @File4;Aglelm(*)
5650     ENTER @File4;Aggelm(*)
5660     ENTER @File4;Bxxelm(*)
5670     ENTER @File4;Bxyelm(*)
5680     ENTER @File4;Bxlelm(*)
5690     ENTER @File4;Bxgelm(*)
5700     ENTER @File4;Byxelm(*)
5710     ENTER @File4;Byyelm(*)
5720     ENTER @File4;Bylelm(*)
5730     ENTER @File4;Bygelm(*)
5740     ENTER @File4;Blxelm(*)
5750     ENTER @File4;Blyelm(*)
5760     ENTER @File4;Bllelm(*)
5770     ENTER @File4;Blgelm(*)
5780     ENTER @File4;Bgxelm(*)
5790     ENTER @File4;Bgyelm(*)
5800     ENTER @File4;Bglelm(*)
5810     ENTER @File4;Bggelm(*)
5820     ENTER @File4;Fxelm(*)    ! Oil film forces and moments at base condition
5830     ENTER @File4;Fyelm(*)    ! from which the dynamic coefficients were
5840     ENTER @File4;Mxelm(*)    ! calculated.
5850     ENTER @File4;Myelm(*)
5860     ENTER @File4;Fxnlel(*)   ! Non-linear correction terms. These are all zero
                                    for linearised coefficients, and are only non-
5870     ENTER @File4;Fynlel(*)   ! zero for the non-linear aft sterntube bearing
                                    oil film model which is covered by the
5880     ENTER @File4;Mxnlel(*)   ! Cart_oilfilm Subroutine.
5890     ENTER @File4;Mynlel(*)
5900     ENTER @File4;Xbelm(*)    ! Lateral and angular displacements from datum
```

```
                                  line to journal locations on which above
5910   ENTER @File4;Ybelm(*)    ! dynamic coefficients are based. This includes      11
                                  any offsets of bearing centres from the datum
5920   ENTER @File4;Lbelm(*)    ! line.
5930   ENTER @File4;Gbelm(*)
5940   ENTER @File4;Xdbelm(*)   ! Lateral and angular velocities on which above
                                  dynamic coefficients are based. In this work
5950   ENTER @File4;Ydbelm(*)   ! these are in fact all zero.
5960   ENTER @File4;Ldbelm(*)
5970   ENTER @File4;Gdbelm(*)
5980   ASSIGN @File4 TO *
5990   Doe(1)=.875              ! Units in m.  These diameters and lengths refer to
6000   Die(1)=.285              ! the shaft elements comprising each mass station;
6010   Le(1)=1.365              ! Propeller mass-inertia properties are added to
6020   Doe(2)=.875              ! mass station 1 later.
6030   Die(2)=.475
6040   Le(2)=2.390
6050   Doe(3)=.875
6060   Die(3)=.475
6070   Le(3)=1.780
6080   Doe(4)=.875
6090   Die(4)=.475
6100   Le(4)=1.770
6110   Doe(5)=.927
6120   Die(5)=0
6130   Le(5)=2.005
6140   Doe(6)=.688
6150   Die(6)=0
6160   Le(6)=2.200
6170   Dos(1)=.875             ! Units in m.  These diameters and lengths refer to
6180   Dis(1)=.475             ! the shaft elements between each mass station as
6190   Ls(1)=2.560             ! used to define the elastic properties connecting
6200   Dos(2)=.875             ! each mass.
6210   Dis(2)=.475
6220   Ls(2)=2.085
6230   Dos(3)=.875
6240   Dis(3)=.475
6250   Ls(3)=1.775
6260   Dos(4)=.875
6270   Dis(4)=.475
6280   Ls(4)=1.8875
6290   Dos(5)=.688
6300   Dis(5)=0
6310   Ls(5)=2.1025
6320   Dos(6)=.688
6330   Dis(6)=0
6340   Ls(6)=4.740 ! To built in end at next plummer bearing.
6350   Gee=9.80665 !  Gravitational Constant.  m/s^2.
6360   Rho=7920    !  Steel Density.  kg/m^3.
6370   Emod=2.069E+11 ! Youngs Modulus (Steel). Pa. (N/m^2.)
6380   Gmod=8.18E+10  ! Shear Modulus (Steel). Pa. (N/m^2.)
6390   Tcyc=60/N/5    ! Dynamic cycle time (Prop. blade (5th.) order excitation
6400   Om=PI*N/30     ! Omega. (rad/s.)
6410   Mprop=52130    ! Dry Propeller Mass. kg.
6420   Jprop=79485    ! Dry Propeller Diametral Inertia (W.K^2). Kg.m^2.
6430   Jpwprop=190249 ! Wet Propeller Polar Inertia. kg.m^2.
                      ( 158969 Dry + 31280 Entrained Water.)
6440   Myyprop=3.459E+3     !  Propeller Entrained Water Matrix.
6450   Myxprop=3.785E+2     !  kg. m. units.
6460   Mygprop=-1.543E+3
6470   Mylprop=1.735E+4
6480   Mxyprop=-3.785E+2
6490   Mxxprop=3.459E+3
6500   Mxgprop=-1.735E+4
6510   Mxlprop=-1.543E+3
6520   Mgyprop=1.543E+3
```

12

```
6530   Mgxprop=-1.735E+4
6540   Mggprop=1.348E+5
6550   Mglprop=-1.503E+4
6560   Mlyprop=1.735E+4
6570   Mlxprop=1.543E+3
6580   Mlgprop=-1.503E+4
6590   Mllprop=1.348E+5
6600  FOR Z=1 TO 6      !  Computes shaft elemement stiffness coefficients.
6610  Asect=PI*((Dos(Z))^2-(Dis(Z))^2)/4
6620  Isect=PI*((Dos(Z))^4-(Dis(Z))^4)/64
6630  Cla=(Ls(Z))^3/12/Emod/Isect+2*Ls(Z)/3/Gmod/Asect
6640  Clb=(Ls(Z))^2/6/Emod/Isect+4/3/Gmod/Asect
6650  Clc=Emod*Isect/Ls(Z)
6660  Cld=(Ls(Z))^2/2/Emod/Isect+4/3/Gmod/Asect
6670  Sfl(Z)=-1/Cla
6680  Sml(Z)=-Clc*Cld/Cla
6690  Sfa(Z)=-1/Clb
6700  Smao(Z)=-Clc*(1+Cld/Clb)
6710  Smae(Z)=-Clc*(1-Cld/Clb)
6720  NEXT Z
6730  FOR Z=1 TO 6     !  Computes element masses and inertias.
6740  IF Z>1 THEN 6770
6750  Diaconst=12       !  Recognises that shaft element is on forward side of
6760  GOTO 6780         !  Mass Station 1 ( Prop ) only.
6770  Diaconst=48
6780  Ma(Z)=PI*((Doe(Z))^2-(Die(Z))^2)*Le(Z)/4*Rho
6790  Jdia(Z)=PI*Le(Z)*Rho*(((Doe(Z))^4-(Die(Z))^4)/64+(Le(Z))^2*((Doe(Z))^2-(Di
e(Z))^2)/Diaconst)
6800  Jpol(Z)=PI*Le(Z)*Rho*((Doe(Z))^4-(Die(Z))^4)/32
6810  NEXT Z
6820  Ma(1)=Ma(1)+Mprop    !   Entrained Water Matrix for Propeller added
6830  Jdia(1)=Jdia(1)+Jprop    !   in Time Step Equations for Ma and Jd.
6840  Jpol(1)=Jpol(1)+Jpwprop !   Propeller Polar Entrained Water included.
6850  FOR Z=1 TO 6             !   Critical Shaft Element Damping set.
6860  IF Z=1 THEN 6900
6870  Bslat(Z)=-SQR(-(Sfl(Z-1)+Sfl(Z))*Ma(Z))*Kcrit      ! Calculation of min.
                                                          shaft element lateral
6880  Bsang(Z)=-SQR(-(Smao(Z-1)+Smao(Z))*Jdia(Z))*Kcrit! and angular damping.
                                                        ! Based on critical
6890  GOTO 6920                                         ! damping for element,
                                                        ! assuming it to be built
6900  Bslat(1)=-SQR(-Sfl(1)*Ma(1))*Kcrit                ! in at adjacent elements
                                                        ! and multiplied by
6910  Bsang(1)=-SQR(-Smao(1)*Jdia(1))*Kcrit             ! factor Kcrit.
6920  NEXT Z
6930  PRINT "DATSET No. = ";Datset ! Reference to computed data set for aft
                                   ! sterntube bearing non-linear coefficient
6940  PRINT "_________________"    ! model.
6950  PRINT USING "4(5A,X,SD.4DE,2X)";"Eo  =",Eo,"Psio=",Psio,"Xio =",Xio,"Phio=
",Phio
6960  PRINT "_________________________________________________________________
______________"
6970  PRINT "Critical Shaft Element Damping * Kcrit"
6980  PRINT "______________________________________"
6990  PRINT "No.     Bslat            Bsang"
7000  FOR Z=1 TO 6
7010  PRINT USING "2D,2(4X,SD.3DE)";Z,Bslat(Z),Bsang(Z)
7020  NEXT Z
7030  IF Print$="N" THEN 7860     ! Jump if full print out of input data is not
7040  MAT Kfm= Afr                ! required.
7050  PRINT FNPage$;
7060  PRINT "Afr Coefficients :"
7070  PRINT "__________________"
7080  GOSUB Print_nlcof
7090  MAT Kfm= Aft
7100  PRINT "Aft Coefficients :"
```

13

```
7110  PRINT "______________________"
7120  GOSUB Print_nlcof
7130  MAT Kfm= Amr
7140  PRINT "Amr Coefficients :"
7150  PRINT "______________________"
7160  GOSUB Print_nlcof
7170  MAT Kfm= Amt
7180  PRINT "Amt Coefficients :"
7190  PRINT "______________________"
7200  GOSUB Print_nlcof
7210  PRINT FNPage$;
7220  MAT Kfm= Bfr
7230  PRINT "Bfr Coefficients :"
7240  PRINT "______________________"
7250  GOSUB Print_nlcof
7260  MAT Kfm= Bft
7270  PRINT "Bft Coefficients :"
7280  PRINT "______________________"
7290  GOSUB Print_nlcof
7300  MAT Kfm= Bmr
7310  PRINT "Bmr Coefficients :"
7320  PRINT "______________________"
7330  GOSUB Print_nlcof
7340  MAT Kfm= Bmt
7350  PRINT "Bmt Coefficients :"
7360  PRINT "______________________"
7370  GOSUB Print_nlcof
7380  GOTO 7480
7390 Print_nlcof:  !  Subroutine to PRINT OUT ACOEFS and BCOEFS
7400  PRINT " 11          12          13          21          22          23          31          32
      33"
7410  FOR I=1 TO 3
7420  FOR J=1 TO 3
7430  PRINT USING "8(SD.DE,X),SD.DE";Kfm(I,J,1,1),Kfm(I,J,1,2),Kfm(I,J,1,3),Kfm(
I,J,2,1),Kfm(I,J,2,2),Kfm(I,J,2,3),Kfm(I,J,3,1),Kfm(I,J,3,2),Kfm(I,J,3,3)
7440  NEXT J
7450  NEXT I
7460  PRINT "________________________________________________________________________________
__________"
7470  RETURN
7480  PRINT FNPage$;
7490  PRINT "WAKEFM Data :"
7500  PRINT "________________"
7510  PRINT "Tint=";Tint
7520  PRINT "______________________________"
7530  PRINT "Angle (deg.)  Fwy (N.)       Fwx (N.)       Mwy (N.m.)     Mwx (N.m.)"
7540  FOR J=1 TO 72
7550  PRINT USING "2D,8X,4(3X,SD.3DE)";J-1,Fwy(J),Fwx(J),Mwy(J),Mwx(J)
7560  NEXT J
7570  PRINT "________________________________________________________________________________
__________"
7580  PRINT FNPage$;
7590  PRINT "Shaft Element Data for Mass Calculation :"
7600  PRINT "_________________________________________________"
7610  PRINT "Element No.      Doe          Die          Le     ( all in m. )"
7620  FOR Z=1 TO 6
7630  PRINT USING "2D,9X,3(5X,D.4D)";Z,Doe(Z),Die(Z),Le(Z)
7640  NEXT Z
7650  PRINT "________________________________________________________________________________
__________"
7660  PRINT "Shaft Element Data for Stiffness Coefficient Calculation :"
7670  PRINT "_______________________________________________________________________"
7680  PRINT "Element No.      Dos          Dis          Ls     ( all in m. )"
7690  FOR Z=1 TO 6
7700  PRINT USING "2D,9X,3(5X,D.4D)";Z,Dos(Z),Dis(Z),Ls(Z)
7710  NEXT Z
```

```
7720  PRINT "_____________________________________________________________________________
      "
7730  PRINT "Shaft Element Stiffness Coefficients :"
7740  PRINT "______________________________________"
7750  PRINT "No     Sfl              Sml              Sfa              Smao             Smae
(N. m. rad)"
7760  FOR Z=1 TO 6
7770  PRINT USING "2D,5(3X,SD.4DE)";Z,Sfl(Z),Sml(Z),Sfa(Z),Smao(Z),Smae(Z)
7780  NEXT Z
7790  PRINT "_____________________________________________________________________________
      "
7800  PRINT "Concentrated Mass Station Data :"
7810  PRINT "_______________________________"
7820  PRINT "No     Ma               Jdia             Jpol      ( kg. m. units.)"
7830  FOR Z=1 TO 6
7840  PRINT USING "2D,3(4X,D.4DE)";Z,Ma(Z),Jdia(Z),Jpol(Z)
7850  NEXT Z
7860  RETURN !###################################################################
7870 Predict:    ! Subroutine to predict the conditions at the end of the current
                   time step.
7880             ! INPUT : Time increment Dt; conditions at start point T :-
                   X, Y, Lam, Gam, Xd, Yd, Lamd, Gamd, Xdd, Ydd, Lamdd, Gamdd
7890             ! ( displacements from datum, velocities, accelerations.......
                   .....all functions of Mass Element No. : Nelem )
7900             ! Wake excitation at T : Fwxt, Fwyt, Mwxt, Mwyt
                   Wake excitation at T+Dt : Fwxtp, Fwytp, Mwxtp, Mwytp
7910             ! Aft Sterntube Bearing Oil Film Stiffness & Damping Coeffs.
                   valid for estimated T+Dt conditions and Fox, Foy, Mox, Moy if
7920             ! Non-Linear Model is selected. For Linear Model fixed
                   linearised coeffs. and equilibrium forces and moments are used
7930             ! OUTPUT : Conditions at end point T+Dt :-
                   Xp, Yp, Lamp, Gamp, Xdp, Ydp, Lamdp, Gamdp ( all functions of
7940             ! Nelem.) & Mean accelerations for time step :-
                   Xddm, Yddm, Lamddm, Gamddm ( all functions of Nelem.)
7950    Ko=3/Dt
7960    FOR Nelem=1 TO 6    ! Section to compute factors referred to as Kxn, Kyn,
                              Kln, Kgn in Theory.
7970    Kg(Nelem)=3*Gam(Nelem)/Dt+2*Gamd(Nelem)+Gamdd(Nelem)*Dt/2
7980    Kl(Nelem)=3*Lam(Nelem)/Dt+2*Lamd(Nelem)+Lamdd(Nelem)*Dt/2
7990    Ky(Nelem)=3*Y(Nelem)/Dt+2*Yd(Nelem)+Ydd(Nelem)*Dt/2
8000    Kx(Nelem)=3*X(Nelem)/Dt+2*Xd(Nelem)+Xdd(Nelem)*Dt/2
8010    NEXT Nelem
8020    FOR Zrow=1 TO 24
8030    Nelem=INT((Zrow-1)/4)+1 !     Mass Station No.
8040    IF Nelem=1 THEN 8080
8050    IF Nelem>4.5 THEN 8100
8060    Kbuoy=.881              !     Buoyancy correction for oil.
8070    GOTO 8110
8080    Kbuoy=.870              !     Buoyancy correction for sea water.
8090    GOTO 8110
8100    Kbuoy=1                 !     No buoyancy correction. i.e. element in air
8110    IF FRACT((Zrow-1)/4)>0 THEN 11130 ! Coeffs. only need to be set once for
8120    IF Nelem=1 THEN 9920              ! each Mass Station.
8130    IF Nelem=2 THEN 9390              ! i.e. at Zrow=1 for Nelem=1
8140    IF Nelem=4 THEN 9360              !      at Zrow=5 for Nelem=2
8150    IF Nelem=6 THEN 8650              !      at Zrow=9 for Nelem=3,etc.
8160    Byye=Bslat(Nelem)
8170    Byxe=0   !  Set Damping Coefficients for Mass Stations 3,5 ( Direct
8180    Byge=0   !  lateral and angular damping terms based on critical damping
8190    Byle=0   !  for element * factor Kcrit.)
8200    Bxye=0
8210    Bxxe=Bslat(Nelem)
8220    Bxge=0
8230    Bxle=0
8240    Bgye=0
8250    Bgxe=0
```

(14)

```
8260     Bgge=Bsang(Nelem)
8270     Bgle=0
8280     Blye=0
8290     Blxe=0
8300     Blge=0
8310     Blle=Bsang(Nelem)
8320     Ayye=0   !  Set Stiffness Coeffs. and Base Forces, Moments, Locations and
                     Velocities to zero for Mass Stations 3,5
8330     Ayxe=0
8340     Ayge=0
8350     Ayle=0
8360     Axye=0
8370     Axxe=0
8380     Axge=0
8390     Axle=0
8400     Agye=0
8410     Agxe=0
8420     Agge=0
8430     Agle=0
8440     Alye=0
8450     Alxe=0
8460     Alge=0
8470     Alle=0
8480     Fxbse=0
8490     Fybse=0
8500     Mxbse=0
8510     Mybse=0
8520     Fxnle=0
8530     Fynle=0
8540     Mxnle=0
8550     Mynle=0
8560     Xbse=0
8570     Ybse=0
8580     Lambse=0
8590     Gambse=0
8600     Xdbse=0
8610     Ydbse=0
8620     Lamdbse=0
8630     Gamdbse=0
8640     GOTO 9940
8650     Dyncof=4
8660     GOSUB Set_dyncof   !  Set Dynamic Coefs.,etc. for Aft Plummer Bearing.
8670     GOTO 9940 ! ##############################################################
8680 Set_dyncof:      !  Subroutine to set Dynamic Coefficients and associated
                         forces, moments, displacements and velocities for shaft
8690                  !  elements in way of Bearing or Prop.
8700                  !  Refs. :  Nelem   1     2    4     6
                                  Dyncof  1     2    3     4
8710     Axxe=Axxelm(Dyncof)
8720     Axye=Axyelm(Dyncof)
8730     Axle=Axlelm(Dyncof)
8740     Axge=Axgelm(Dyncof)
8750     Ayxe=Ayxelm(Dyncof)
8760     Ayye=Ayyelm(Dyncof)
8770     Ayle=Aylelm(Dyncof)
8780     Ayge=Aygelm(Dyncof)
8790     Alxe=Alxelm(Dyncof)
8800     Alye=Alyelm(Dyncof)
8810     Alle=Allelm(Dyncof)
8820     Alge=Algelm(Dyncof)
8830     Agxe=Agxelm(Dyncof)
8840     Agye=Agyelm(Dyncof)
8850     Agle=Aglelm(Dyncof)
8860     Agge=Aggelm(Dyncof)
8870     IF Nelem<3 THEN 8910   !  Elements 1 and 2 not subject to min. damping =
                                !  Critical * Kcrit.
```

16

```
8880    IF Bxxelm(Dyncof)<Bslat(Nelem) THEN 8910
8890    Bxxe=Bslat(Nelem)       !  Direct Damping to be not less than
8900    GOTO 8920               !  Critical * Kcrit.
8910    Bxxe=Bxxelm(Dyncof)
8920    Bxye=Bxyelm(Dyncof)
8930    Bxle=Bxlelm(Dyncof)
8940    Bxge=Bxgelm(Dyncof)
8950    Byxe=Byxelm(Dyncof)
8960    IF Nelem<3 THEN 9000
8970    IF Byyelm(Dyncof)<Bslat(Nelem) THEN 9000
8980    Byye=Bslat(Nelem)        !  Direct Damping to be not less than
8990    GOTO 9010                !  Critical * Kcrit.
9000    Byye=Byyelm(Dyncof)
9010    Byle=Bylelm(Dyncof)
9020    Byge=Bygelm(Dyncof)
9030    Blxe=Blxelm(Dyncof)
9040    Blye=Blyelm(Dyncof)
9050    IF Nelem<3 THEN 9090
9060    IF Bllelm(Dyncof)<Bsang(Nelem) THEN 9090
9070    Blle=Bsang(Nelem)        !  Direct Damping to be not less than
9080    GOTO 9100                !  Critical * Kcrit.
9090    Blle=Bllelm(Dyncof)
9100    Blge=Blgelm(Dyncof)
9110    Bgxe=Bgxelm(Dyncof)
9120    Bgye=Bgyelm(Dyncof)
9130    Bgle=Bglelm(Dyncof)
9140    IF Nelem<3 THEN 9180
9150    IF Bggelm(Dyncof)<Bsang(Nelem) THEN 9180
9160    Bgge=Bsang(Nelem)        !  Direct Damping to be not less than
9170    GOTO 9190                !  Critical * Kcrit.
9180    Bgge=Bggelm(Dyncof)
9190    Fxbse=Fxelm(Dyncof)
9200    Fybse=Fyelm(Dyncof)
9210    Mxbse=Mxelm(Dyncof)
9220    Mybse=Myelm(Dyncof)
9230    Fxnle=Fxnlel(Dyncof)
9240    Fynle=Fynlel(Dyncof)
9250    Mxnle=Mxnlel(Dyncof)
9260    Mynle=Mynlel(Dyncof)
9270    Xbse=Xbelm(Dyncof)
9280    Ybse=Ybelm(Dyncof)
9290    Lambse=Lbelm(Dyncof)
9300    Gambse=Gbelm(Dyncof)
9310    Xdbse=Xdbelm(Dyncof)
9320    Ydbse=Ydbelm(Dyncof)
9330    Lamdbse=Ldbelm(Dyncof)
9340    Gamdbse=Gdbelm(Dyncof)
9350    RETURN ! ################################################################
9360    Dyncof=3
9370    GOSUB Set_dyncof   !  Set Dynamic Coefs., for Fwd. Sterntube Bearing.
9380    GOTO 9940
9390    IF Nonlin$="N" THEN 9890 ! Select Linear Oil Film Model for Aft
                                   Sterntube Bearing.
9400    Ayye=-Ayy      !  Set Aft Sterntube Brg. Oil Film Coeffs. (Nelem=2)
9410    Ayxe=-Ayx      !  ( Non-Linear Model.)
9420    Ayge=-Ayg      !  Note : Coeff., Force & Moment sign convention reversed
9430    Ayle=-Ayl      !  from that used in Cart_oilfilm Subroutine.
9440    Axye=-Axy      !  Note : Ayy, etc. will be held from previous time step
9450    Axxe=-Axx      !  provided Cart_oilfilm Sub. has not been called since.
9460    Axge=-Axg      !  Predict Sub. working values Ayye, etc. need to be reset
9470    Axle=-Axl      !  every time this Sub. is used.
9480    Agye=-Agy
9490    Agxe=-Agx
9500    Agge=-Agg
9510    Agle=-Agl
9520    Alye=-Aly
```

17

```
9530    Alxe=-Alx
9540    Alge=-Alg
9550    Alle=-All
9560    Byye=-Byy
9570    Byxe=-Byx
9580    Byge=-Byg
9590    Byle=-Byl
9600    Bxye=-Bxy
9610    Bxxe=-Bxx
9620    Bxge=-Bxg
9630    Bxle=-Bxl
9640    Bgye=-Bgy
9650    Bgxe=-Bgx
9660    Bgge=-Bgg
9670    Bgle=-Bgl
9680    Blye=-Bly
9690    Blxe=-Blx
9700    Blge=-Blg
9710    Blle=-Bll
9720    Fxbse=-Fxa
9730    Fybse=-Fya
9740    Mxbse=-Mxa
9750    Mybse=-Mya
9760    Fxnle=-Fxnl
9770    Fynle=-Fynl
9780    Mxnle=-Mxnl
9790    Mynle=-Mynl
9800    Xbse=X(Nelem)
9810    Ybse=Y(Nelem)
9820    Lambse=Lam(Nelem)
9830    Gambse=Gam(Nelem)
9840    Xdbse=Xd(Nelem)
9850    Ydbse=Yd(Nelem)
9860    Lamdbse=Lamd(Nelem)
9870    Gamdbse=Gamd(Nelem)
9880    GOTO 9940
9890    Dyncof=2
9900    GOSUB Set_dyncof    !  Set Dynamic Coefs. etc. for Aft Sterntube Bearing.
9910    GOTO 9940           !  ( Linear Oil Film Model.)
9920    Dyncof=1
9930    GOSUB Set_dyncof    !  Set Dynamic Coefs. etc. for Propeller.
9940    IF Nelem=1 THEN 10510
9950    Myy=0 !                Entrained water masses are Zero for Nelem= 2 to 6
9960    Myx=0
9970    Myg=0
9980    Myl=0
9990    Mxy=0
10000   Mxx=0
10010   Mxg=0
10020   Mxl=0
10030   Mgy=0
10040   Mgx=0
10050   Mgg=0
10060   Mgl=0
10070   Mly=0
10080   Mlx=0
10090   Mlg=0
10100   Mll=0
10110   Sflnm=Sfl(Nelem-1) ! Set operating shaft stiffness coeffs. for aft side
10120   Sfanm=Sfa(Nelem-1) ! of all stations except Prop. i.e. for Nelem=2 to 6
10130   Smlnm=Sml(Nelem-1)
10140   Smaonm=Smao(Nelem-1)
10150   Smaenm=Smae(Nelem-1)
10160   Fwxte=0  !             Wake effects are Zero for Nelem= 2 to 6
10170   Fwyte=0
10180   Mwxte=0
```

18

```
10190   Mwyte=0
10200   Fwxtpe=0
10210   Fwytpe=0
10220   Mwxtpe=0
10230   Mwytpe=0
10240   Xme=X(Nelem-1)   !    Set operating condition values at Station N-1.
10250   Yme=Y(Nelem-1)
10260   Lamme=Lam(Nelem-1)
10270   Gamme=Gam(Nelem-1)
10280   Xdme=Xd(Nelem-1)
10290   Ydme=Yd(Nelem-1)
10300   Lamdme=Lamd(Nelem-1)
10310   Gamdme=Gamd(Nelem-1)
10320   IF Nelem=6 THEN 10420
10330   Xpe=X(Nelem+1)   !    Set operating condition values at Station N+1.
10340   Ype=Y(Nelem+1)
10350   Lampe=Lam(Nelem+1)
10360   Gampe=Gam(Nelem+1)
10370   Xdpe=Xd(Nelem+1)
10380   Ydpe=Yd(Nelem+1)
10390   Lamdpe=Lamd(Nelem+1)
10400   Gamdpe=Gamd(Nelem+1)
10410   GOTO 10960
10420   Xpe=0  !          Station 7 has no mass and is a "built in" forward end.
10430   Ype=4.330E-3 !m.  Corresponds to Hot Dynamic Alignment 11.06.87.
10440   Lampe=0
10450   Gampe=-3.065E-4! rad.-----------------"------------------------
10460   Xdpe=0
10470   Ydpe=0
10480   Lamdpe=0
10490   Gamdpe=0
10500   GOTO 10960
10510   Myy=Myyprop !     Set operating Prop. entrained mass matrix.
10520   Myx=Myxprop
10530   Myg=Mygprop
10540   Myl=Mylprop
10550   Mxy=Mxyprop
10560   Mxx=Mxxprop
10570   Mxg=Mxgprop
10580   Mxl=Mxlprop
10590   Mgy=Mgyprop
10600   Mgx=Mgxprop
10610   Mgg=Mggprop
10620   Mgl=Mglprop
10630   Mly=Mlyprop
10640   Mlx=Mlxprop
10650   Mlg=Mlgprop
10660   Mll=Mllprop
10670   Sflnm=0     !     No shaft element aft of Prop.
10680   Sfanm=0
10690   Smlnm=0
10700   Smaonm=0
10710   Smaenm=0
10720   Fwxte=Fwxt     !  Set working values of wake excitation at T (Nelem=1).
10730   Fwyte=Fwyt
10740   Mwxte=Mwxt
10750   Mwyte=Mwyt
10760   Fwxtpe=Fwxtp   !Set working values of wake excitation at T + Dt (Nelem=1)
10770   Fwytpe=Fwytp
10780   Mwxtpe=Mwxtp
10790   Mwytpe=Mwytp
10800   Xme=0          !  No mass station aft of Prop.
10810   Yme=0          !  This zero setting operation is designed to satisfy the
10820   Lamme=0        !  author's sense of tidyness, and does not fix the shaft
10830   Gamme=0        !  at the aft end since the relevant shaft stiffness
10840   Xdme=0         !  coefficients are zero.
```

(19)

```
10850    Ydme=0
10860    Lamdme=0
10870    Gamdme=0
10880    Xpe=X(Nelem+1)  ! Set operating condition values at Station N+1 for Prop.
10890    Ype=Y(Nelem+1)
10900    Lampe=Lam(Nelem+1)
10910    Gampe=Gam(Nelem+1)
10920    Xdpe=Xd(Nelem+1)
10930    Ydpe=Yd(Nelem+1)
10940    Lamdpe=Lamd(Nelem+1)
10950    Gamdpe=Gam(Nelem+1)
10960    Xe=X(Nelem)    !  Set operating condition values at Station N for all
                          elements.
10970    Ye=Y(Nelem)
10980    Lame=Lam(Nelem)
10990    Game=Gam(Nelem)
11000    Xde=Xd(Nelem)
11010    Yde=Yd(Nelem)
11020    Lamde=Lamd(Nelem)
11030    Gamde=Gamd(Nelem)
11040    Sflnp=Sfl(Nelem)  ! Set operating shaft stiffness coeffs. for forward
11050    Sfanp=Sfa(Nelem)  ! side of all Stations.
11060    Smlnp=Sml(Nelem)
11070    Smaonp=Smao(Nelem)
11080    Smaenp=Smae(Nelem)
11090    IF Nelem=6 THEN 11120
11100    Fwdend=1    !         Factor to allow for n+1 displacements being
11110    GOTO 11130 !          specified for element 6. i.e. boundary condition
                               at forward end of shaft.
11120    Fwdend=2
11130    IF 4*FRACT(Zrow/4)=1 THEN 11340 ! Select Kvxn equation.
11140    IF 4*FRACT(Zrow/4)=2 THEN 11280 ! Select Kvyn equation.
11150    IF 4*FRACT(Zrow/4)=3 THEN 11220 ! Select Kvln equation.
11160    !  Kvgn equation.   ( Selected by default.)
11170    Kvz1=(-(Jdia(Nelem)+Mgg)*(Kg(Nelem)+Gamde)-Mgl*(Kl(Nelem)+Lamde)-Mgy*(Ky
(Nelem)+Yde)-Mgx*(Kx(Nelem)+Xde))/Dt-Jpol(Nelem)*Om*(Kl(Nelem)-Lamde)/2
11180    Kvz2=-(Mwytpe+Bgxe*(Xde-Kx(Nelem)-2*Xdbse)+Bgye*(Yde-Ky(Nelem)-2*Ydbse)+
Bgle*(Lamde-Kl(Nelem)-2*Lamdbse)+Bgge*(Gamde-Kg(Nelem)-2*Gamdbse)+Mwyte)/2
11190    Kvz3=-(Smlnm*(Ye-Yme)+Smaonm*Game-Smaenm*Gamme-Smlnp*(Ye-Fwdend*Ype)+Sma
onp*Game-Smaenp*Fwdend*Gampe)/2
11200    Kv(Zrow)=Kvz1+Kvz2+Kvz3-(Agxe*(Xe-2*Xbse)+Agye*(Ye-2*Ybse)+Agle*(Lame-2*
Lambse)+Agge*(Game-2*Gambse))/2-Mybse-Mynle
11210    GOTO 11390
11220    !  Kvln equation.
11230    Kvz1=(-(Jdia(Nelem)+Mll)*(Kl(Nelem)+Lamde)-Mlg*(Kg(Nelem)+Gamde)-Mly*(Ky
(Nelem)+Yde)-Mlx*(Kx(Nelem)+Xde))/Dt+Jpol(Nelem)*Om*(Kg(Nelem)-Gamde)/2
11240    Kvz2=-(Mwxtpe+Blxe*(Xde-Kx(Nelem)-2*Xdbse)+Blye*(Yde-Ky(Nelem)-2*Ydbse)+
Blle*(Lamde-Kl(Nelem)-2*Lamdbse)+Blge*(Gamde-Kg(Nelem)-2*Gamdbse)+Mwxte)/2
11250    Kvz3=-(Smlnm*(Xe-Xme)+Smaonm*Lame-Smaenm*Lamme-Smlnp*(Xe-Fwdend*Xpe)+Sma
onp*Lame-Smaenp*Fwdend*Lampe)/2
11260    Kv(Zrow)=Kvz1+Kvz2+Kvz3-(Alxe*(Xe-2*Xbse)+Alye*(Ye-2*Ybse)+Alle*(Lame-2*
Lambse)+Alge*(Game-2*Gambse))/2-Mxbse-Mxnle
11270    GOTO 11390
11280    !  Kvyn equation.
11290    Kvz1=(-(Ma(Nelem)+Myy)*(Ky(Nelem)+Yde)-Myx*(Kx(Nelem)+Xde)-Myg*(Kg(Nelem
)+Gamde)-Myl*(Kl(Nelem)+Lamde))/Dt
11300    Kvz2=-(Fwytpe+Byxe*(Xde-Kx(Nelem)-2*Xdbse)+Byye*(Yde-Ky(Nelem)-2*Ydbse)+
Byle*(Lamde-Kl(Nelem)-2*Lamdbse)+Byge*(Gamde-Kg(Nelem)-2*Gamdbse)+Fwyte)/2
11310    Kvz3=-(Sflnm*(Ye-Yme)+Sfanm*(Game+Gamme)+Sflnp*(Ye-Fwdend*Ype)-Sfanp*(Ga
me+Fwdend*Gampe))/2
11320    Kv(Zrow)=Kvz1+Kvz2+Kvz3-(Ayxe*(Xe-2*Xbse)+Ayye*(Ye-2*Ybse)+Ayle*(Lame-2*
Lambse)+Ayge*(Game-2*Gambse))/2-Ma(Nelem)*Gee*Kbuoy-Fybse-Fynle
11330    GOTO 11390
11340    !  Kvxn equation.
11350    Kvz1=(-(Ma(Nelem)+Mxx)*(Kx(Nelem)+Xde)-Mxy*(Ky(Nelem)+Yde)-Mxg*(Kg(Nelem
)+Gamde)-Mxl*(Kl(Nelem)+Lamde))/Dt
```

```
11360    Kvz2=-(Fwxtpe+Bxxe*(Xde-Kx(Nelem)-2*Xdbse)+Bxye*(Yde-Ky(Nelem)-2*Ydbse)+
Bxle*(Lamde-Kl(Nelem)-2*Lamdbse)+Bxge*(Gamde-Kg(Nelem)-2*Gamdbse)+Fwxte)/2       20
11370    Kvz3=-(Sflnm*(Xe-Xme)+Sfanm*(Lame+Lamme)+Sflnp*(Xe-Fwdend*Xpe)-Sfanp*(La
me+Fwdend*Lampe))/2
11380    Kv(Zrow)=Kvz1+Kvz2+Kvz3-(Axxe*(Xe-2*Xbse)+Axye*(Ye-2*Ybse)+Axle*(Lame-2*
Lambse)+Axge*(Game-2*Gambse))/2-Fxbse-Fxnle
11390    FOR Zcol=1 TO 24
11400    IF 4*FRACT(Zrow/4)=1 THEN 12180 !      Select Kmx section.
11410    IF 4*FRACT(Zrow/4)=2 THEN 11930 !      Select Kmy section.
11420    IF 4*FRACT(Zrow/4)=3 THEN 11680 !      Select Kml section.
11430    IF Zcol=Zrow-6 THEN 11660       !  Kmgyn-1    Kmg section.  ( Selected by
11440    IF Zcol=Zrow-4 THEN 11640       !  Kmggn-1                    default.)
11450    IF Zcol=Zrow-3 THEN 11620       !  Kmgxn
11460    IF Zcol=Zrow-2 THEN 11600       !  Kmgyn
11470    IF Zcol=Zrow-1 THEN 11580       !  Kmgln
11480    IF Zcol=Zrow THEN 11560         !  Kmggn
11490    IF Zcol=Zrow+2 THEN 11540       !  Kmgyn+1
11500    IF Zcol=Zrow+4 THEN 11520       !  Kmggn+1
11510    GOTO 12420
11520    Km(Zrow,Zcol)=-Smaenp/2
11530    GOTO 12420
11540    Km(Zrow,Zcol)=Smlnp/2
11550    GOTO 12420
11560    Km(Zrow,Zcol)=-(Jdia(Nelem)+Mgg)*Ko/Dt+(Smaonm+Smaonp+Agge+Bgge*Ko)/2
11570    GOTO 12420
11580    Km(Zrow,Zcol)=-Mgl*Ko/Dt+(-Jpol(Nelem)*Om*Ko+Agle+Bgle*Ko)/2
11590    GOTO 12420
11600    Km(Zrow,Zcol)=-Mgy*Ko/Dt+(Smlnm-Smlnp+Agye+Bgye*Ko)/2
11610    GOTO 12420
11620    Km(Zrow,Zcol)=-Mgx*Ko/Dt+(Agxe+Bgxe*Ko)/2
11630    GOTO 12420
11640    Km(Zrow,Zcol)=-Smaenm/2
11650    GOTO 12420
11660    Km(Zrow,Zcol)=-Smlnm/2
11670    GOTO 12420
11680    IF Zcol=Zrow-6 THEN 11910              !  Kmlxn-1          Kml section.
11690    IF Zcol=Zrow-4 THEN 11890              !  Kmlln-1
11700    IF Zcol=Zrow-2 THEN 11870              !  Kmlxn
11710    IF Zcol=Zrow-1 THEN 11850              !  Kmlyn
11720    IF Zcol=Zrow THEN 11830                !  Kmlln
11730    IF Zcol=Zrow+1 THEN 11810              !  Kmlgn
11740    IF Zcol=Zrow+2 THEN 11790              !  Kmlxn+1
11750    IF Zcol=Zrow+4 THEN 11770              !  Kmlln+1
11760    GOTO 12420
11770    Km(Zrow,Zcol)=-Smaenp/2
11780    GOTO 12420
11790    Km(Zrow,Zcol)=Smlnp/2
11800    GOTO 12420
11810    Km(Zrow,Zcol)=-Mlg*Ko/Dt+(Jpol(Nelem)*Om*Ko+Alge+Blge*Ko)/2
11820    GOTO 12420
11830    Km(Zrow,Zcol)=-(Jdia(Nelem)+Mll)*Ko/Dt+(Smaonm+Smaonp+Alle+Blle*Ko)/2
11840    GOTO 12420
11850    Km(Zrow,Zcol)=-Mly*Ko/Dt+(Alye+Blye*Ko)/2
11860    GOTO 12420
11870    Km(Zrow,Zcol)=-Mlx*Ko/Dt+(Smlnm-Smlnp+Alxe+Blxe*Ko)/2
11880    GOTO 12420
11890    Km(Zrow,Zcol)=-Smaenm/2
11900    GOTO 12420
11910    Km(Zrow,Zcol)=-Smlnm/2
11920    GOTO 12420
11930    IF Zcol=Zrow-4 THEN 12160      !        Kmyyn-1              Kmy section.
11940    IF Zcol=Zrow-2 THEN 12140      !        Kmygn-1
11950    IF Zcol=Zrow-1 THEN 12120      !        Kmyxn
11960    IF Zcol=Zrow THEN 12100        !        Kmyyn
11970    IF Zcol=Zrow+1 THEN 12080      !        Kmyln
11980    IF Zcol=Zrow+2 THEN 12060      !        Kmygn
```

```
11990   IF Zcol=Zrow+4 THEN 12040    !       Kmyyn+1
12000   IF Zcol=Zrow+6 THEN 12020    !       Kmygn+1
12010   GOTO 12420
12020   Km(Zrow,Zcol)=-Sfanp/2
12030   GOTO 12420
12040   Km(Zrow,Zcol)=-Sflnp/2
12050   GOTO 12420
12060   Km(Zrow,Zcol)=-Myg*Ko/Dt+(Sfanm-Sfanp+Ayge+Byge*Ko)/2
12070   GOTO 12420
12080   Km(Zrow,Zcol)=-Myl*Ko/Dt+(Ayle+Byle*Ko)/2
12090   GOTO 12420
12100   Km(Zrow,Zcol)=-(Ma(Nelem)+Myy)*Ko/Dt+(Sflnm+Sflnp+Ayye+Byye*Ko)/2
12110   GOTO 12420
12120   Km(Zrow,Zcol)=-Myx*Ko/Dt+(Ayxe+Byxe*Ko)/2
12130   GOTO 12420
12140   Km(Zrow,Zcol)=Sfanm/2
12150   GOTO 12420
12160   Km(Zrow,Zcol)=-Sflnm/2
12170   GOTO 12420
12180   IF Zcol=Zrow-4 THEN 12410     !    Kmxxn-1              Kmx section.
12190   IF Zcol=Zrow-2 THEN 12390     !    Kmxln-1
12200   IF Zcol=Zrow THEN 12370       !    Kmxxn
12210   IF Zcol=Zrow+1 THEN 12350     !    Kmxyn
12220   IF Zcol=Zrow+2 THEN 12330     !    Kmxln
12230   IF Zcol=Zrow+3 THEN 12310     !    Kmxgn
12240   IF Zcol=Zrow+4 THEN 12290     !    Kmxxn+1
12250   IF Zcol=Zrow+6 THEN 12270     !    Kmxln+1
12260   GOTO 12420
12270   Km(Zrow,Zcol)=-Sfanp/2
12280   GOTO 12420
12290   Km(Zrow,Zcol)=-Sflnp/2
12300   GOTO 12420
12310   Km(Zrow,Zcol)=-Mxg*Ko/Dt+(Axge+Bxge*Ko)/2
12320   GOTO 12420
12330   Km(Zrow,Zcol)=-Mxl*Ko/Dt+(Sfanm-Sfanp+Axle+Bxle*Ko)/2
12340   GOTO 12420
12350   Km(Zrow,Zcol)=-Mxy*Ko/Dt+(Axye+Bxye*Ko)/2
12360   GOTO 12420
12370   Km(Zrow,Zcol)=-(Ma(Nelem)+Mxx)*Ko/Dt+(Sflnm+Sflnp+Axxe+Bxxe*Ko)/2
12380   GOTO 12420
12390   Km(Zrow,Zcol)=Sfanm/2
12400   GOTO 12420
12410   Km(Zrow,Zcol)=-Sflnm/2
12420   NEXT Zcol
12430   NEXT Zrow
12440   Kmdiag=0
12450   FOR Zrow=1 TO 24
12460   Kmdiag=Kmdiag+ABS(Km(Zrow,Zrow))
12470   NEXT Zrow
12480   Matscale=24/Kmdiag  !  Matrix Inversion Scale Factor = Inverse of average
                               of absolute value of main diagonal Km terms.
12490   PRINTER IS 1
12500   MAT Kv= Kv*(Matscale)
12510   MAT Km= Km*(Matscale)
12520   PRINT "Matrix Inversion Proceeding"
12530   PRINT USING "4A,X,2D,3X,3A,X,4D,2(3X,6A,X,3D),3X,9A,X,SD.2DE";"Cyc=",Cyc,
"Nd=",Nd,"Loop1=",Loop1,"Loop2=",Loop2,"Matscale=",Matscale
12540   MAT Kinv= INV(Km)
12550   PRINT "MATRIX INVERSION COMPLETE"
12560   PRINTER IS 701
12570   IF DET=0 THEN 12590 !  Test Determinant for validity of matrix inversion.
12580   GOTO 12610
12590   PRINT "DET=0 : Matrix Inversion is Invalid."
12600   PAUSE
12610   MAT Xylgp= Kinv*Kv
12620   FOR Zrow=1 TO 24
```

(21)

```
12630   Nelem=INT((Zrow-1)/4)+1
12640   IF 4*FRACT(Zrow/4)=1 THEN 12730   ! Select X.                        (22)
12650   IF 4*FRACT(Zrow/4)=2 THEN 12710   ! Select Y.
12660   IF 4*FRACT(Zrow/4)=3 THEN 12690   ! Select Lambda.
12670   Gamp(Nelem)=Xylgp(Zrow)           ! Gamma selected by default.
12680   GOTO 12740
12690   Lamp(Nelem)=Xylgp(Zrow)           ! This section unscrambles predicted
12700   GOTO 12740                        ! time step end lateral and angular
12710   Yp(Nelem)=Xylgp(Zrow)             ! displacements for each element from
12720   GOTO 12740                        ! matrix inversion solution : Xylgp(*)
12730   Xp(Nelem)=Xylgp(Zrow)
12740   NEXT Zrow
12750   FOR Nelem=1 TO 6
12760   Xdp(Nelem)=Ko*Xp(Nelem)-Kx(Nelem)      ! Calculate lateral and angular
12770   Ydp(Nelem)=Ko*Yp(Nelem)-Ky(Nelem)      ! velocity components for each
12780   Lamdp(Nelem)=Ko*Lamp(Nelem)-Kl(Nelem)  ! element at time step end.
12790   Gamdp(Nelem)=Ko*Gamp(Nelem)-Kg(Nelem)
12800   Xddm(Nelem)=(Xdp(Nelem)-Xd(Nelem))/Dt  ! Calculate mean acceleration
12810   Yddm(Nelem)=(Ydp(Nelem)-Yd(Nelem))/Dt  ! components for time step.
12820   Lamddm(Nelem)=(Lamdp(Nelem)-Lamd(Nelem))/Dt
12830   Gamddm(Nelem)=(Gamdp(Nelem)-Gamd(Nelem))/Dt
12840   NEXT Nelem
12850   RETURN    !     End of Predict Subroutine.
12860   !#######################################################################
12870  Regression:    ! Subroutine to estimate time step start point accelerations
                        using Linear Regression on either :
12880     Tim0=Dt0/2 !     (a) 4 previous time step mean accelerations.
                           (b) As (a) plus current estimate of mean accel. for
12890     Tim1=-Dt1/2 !         current time step.
                          Notation : Tim0 : Mean time for current time step.
12900     Tim2=-Dt1-Dt2/2!               Tim1 : Mean time for previous time step.
                                         Tim2,Tim3,Tim4 : Mean time for next previous
12910     Tim3=-Dt1-Dt2-Dt3/2!                          time steps.
                                        All times relate to time at start of current
12920     Tim4=-Dt1-Dt2-Dt3-Dt4/2 ! time step which is taken as Zero.
12930                      ! INPUT : Dt0,Dt1,Dt2,Dt3,Dt4 - Time step durations.
                                     A0,A1,A2,A3,A4 - Time step mean accelerations.
12940                      !         Nreg - Nunber of Data Sets for analysis
                                     Curtstep=1 to include current time step.
12950     IF Curtstep=1 THEN 12980 !          =0 to exclude current time step.
12960     Tim0=0
12970     A0=0
12980     IF Nreg=5 THEN 13170
12990     IF Curtstep=1 THEN 13130
13000     IF Nreg=4 THEN 13170
13010     IF Nreg=3 THEN 13040
13020     IF Nreg=2 THEN 13060
13030     IF Nreg=1 THEN 13090
13040     Tim4=0
13050     GOTO 13170
13060     Tim3=0
13070     Tim4=0
13080     GOTO 13170
13090     Tim2=0
13100     Tim3=0
13110     Tim4=0
13120     GOTO 13170
13130     IF Nreg=4 THEN 13040
13140     IF Nreg=3 THEN 13060
13150     IF Nreg=2 THEN 13090
13160     IF Nreg=1 THEN 13290
13170     Sigx=Tim0+Tim1+Tim2+Tim3+Tim4
13180     Sigy=A0+A1+A2+A3+A4
13190     Sigxy=Tim0*A0+Tim1*A1+Tim2*A2+Tim3*A3+Tim4*A4
13200     Sigx2=Tim0^2+Tim1^2+Tim2^2+Tim3^2+Tim4^2
13210     Sigy2=A0^2+A1^2+A2^2+A3^2+A4^2
```

23

```
13220     Dreg=Nreg*Sigx2-Sigx^2
13230     IF ABS(Dreg)>1.E-10 THEN 13260
13240     Breg=0
13250     GOTO 13270
13260     Breg=(Nreg*Sigxy-Sigx*Sigy)/Dreg
13270     Areg=(Sigy-Breg*Sigx)/Nreg
13280     GOTO 13300
13290     Areg=A0
13300     RETURN !######################################################################
13310 Wakefm_interp:       ! Subroutine to Interpolate Wake Forces & Moments at any
                             given Time from the start of the dynamic cycle.
13320                      ! INPUT : Time ( must not exceed Tcyc ).
                             OUTPUT : Fwxint,Fwyint,Mwxint,Mwyint.
13330                      ! N.B. Wake excitation data is specified at 72 equal
                             intervals over Tcyc therefore Fwx(1) refers to Time=0
13340                      ! and Fwx(72) refers to Time=Tcyc*71/72.
13350     IF Steady$="Y" THEN 13580
13360     Treset=0
13370     IF Time>Tcyc THEN 13390
13380     GOTO 13410
13390     Time=Time-Tcyc
13400     Treset=1   !   Flag to indicate Time in excess of Tcyc was reset.
13410     IF Time=Tcyc THEN 13440
13420     Nwfm=INT(Time/Tcyc*72+1) ! Selects Wake Force and Moment data index
                                   ! corresponding to time immediately preceeding
13430     GOTO 13450               ! time for which interpolation is required.
13440     Nwfm=1
13450     IF Nwfm=72 THEN 13510
13460     Fwxint=Fwx(Nwfm)+(Fwx(Nwfm+1)-Fwx(Nwfm))*(Time-(Nwfm-1)/72*Tcyc)/(Tcyc/
72)
13470     Fwyint=Fwy(Nwfm)+(Fwy(Nwfm+1)-Fwy(Nwfm))*(Time-(Nwfm-1)/72*Tcyc)/(Tcyc/
72)
13480     Mwxint=Mwx(Nwfm)+(Mwx(Nwfm+1)-Mwx(Nwfm))*(Time-(Nwfm-1)/72*Tcyc)/(Tcyc/
72)
13490     Mwyint=Mwy(Nwfm)+(Mwy(Nwfm+1)-Mwy(Nwfm))*(Time-(Nwfm-1)/72*Tcyc)/(Tcyc/
72)
13500     GOTO 13550
13510     Fwxint=Fwx(72)+(Fwx(1)-Fwx(72))*(Time-71/72*Tcyc)/(Tcyc/72)
13520     Fwyint=Fwy(72)+(Fwy(1)-Fwy(72))*(Time-71/72*Tcyc)/(Tcyc/72)
13530     Mwxint=Mwx(72)+(Mwx(1)-Mwx(72))*(Time-71/72*Tcyc)/(Tcyc/72)
13540     Mwyint=Mwy(72)+(Mwy(1)-Mwy(72))*(Time-71/72*Tcyc)/(Tcyc/72)
13550     IF Treset=0 THEN 13620
13560     Time=Time+Tcyc ! Re-convert Time in excess of Tcyc.
13570     GOTO 13620
13580     Fwxint=0         ! Fixed Wake Forces and Monents for tests with zero
13590     Fwyint=0         ! dynamic excitation.
13600     Mwxint=0
13610     Mwyint=-4.152E+5 ! N.m. ( Corresponds to hot running alignment analysis
                                   done on 11.06.87.)
13620     RETURN !######################################################################
13630 Timestep:      ! Subroutine to define sequence of Time Step calculations.
13640     IF Continue$="Y" THEN 13660
13650     Dtm1=Dtmax/600 ! Initial Dt will be equal to 1.1*Dtm1
13660     Curtstep=0     ! Return point for time step sequence.
13670     IF Cyc>1 THEN 13710
13680     IF Nd>3 THEN 13710  !   Note that very small time step duration is used
13690     Nreg=Nd             !   at start of new case to allow a smooth settling
13700     GOTO 13720          !   down process.
13710     Nreg=4
13720     FOR Nelem=1 TO 6
13730     IF Nreg>0 THEN 13790
13740     Xdd(Nelem)=0
13750     Ydd(Nelem)=0
13760     Lamdd(Nelem)=0
13770     Gamdd(Nelem)=0
13780     GOTO 14030
```

```
13790     A1=Xddreg(Nelem,2)    ! Determination of time step start acceleration
13800     A2=Xddreg(Nelem,3)    ! components by Regression Subroutine.
13810     A3=Xddreg(Nelem,4)    ! Curtstep=0 signal makes Regression Subroutine
13820     A4=Xddreg(Nelem,5)    ! take account of 4 previous time step mean
13830     GOSUB Regression      ! acceleration components only.
13840     Xdd(Nelem)=Areg
13850     A1=Yddreg(Nelem,2)
13860     A2=Yddreg(Nelem,3)
13870     A3=Yddreg(Nelem,4)
13880     A4=Yddreg(Nelem,5)
13890     GOSUB Regression
13900     Ydd(Nelem)=Areg
13910     A1=Lddreg(Nelem,2)
13920     A2=Lddreg(Nelem,3)
13930     A3=Lddreg(Nelem,4)
13940     A4=Lddreg(Nelem,5)
13950     GOSUB Regression
13960     Lamdd(Nelem)=Areg
13970     A1=Gddreg(Nelem,2)
13980     A2=Gddreg(Nelem,3)
13990     A3=Gddreg(Nelem,4)
14000     A4=Gddreg(Nelem,5)
14010     GOSUB Regression
14020     Gamdd(Nelem)=Areg
14030     NEXT Nelem
14040     IF Nonlin$="N" THEN 14070
14050     IF Cartflag=1 THEN 14070
14060     GOSUB Cart_oilfilm !Computes Dynamic Coefs. (Non-Lin.)for Aft Sterntube
                              Bearing using fixed perturbations at Orbit Start.
14070     GOSUB Wakefm_interp!In successive time steps GOSUB Cart_oilfilm is by-
                              passed in first loop and previous time step values
14080     Fwxt=Fwxint        !are used by default.
14090     Fwyt=Fwyint
14100     Mwxt=Mwxint          ! Determine propeller wake force and moment
14110     Mwyt=Mwyint          ! components at time step start time.
14120     Dt=1.1*Dtm1          ! Set time step duration initially to 10% more than
                               ! previous time step duration.
14130     IF Dt<Dtmax THEN 14150
14140     Dt=Dtmax      !     Prevents Dt exceeding Dtmax.
14150     Loop1=0       !     Initialize First Loop Counter.
14160     Loop2=0       !     Initialize Second Loop Counter.
14170     GOTO 14190
14180     Time=Time-Dtprov ! First Loop Start Point.
14190     Time=Time+Dt
14200     Loop1=Loop1+1 !     Index First Loop Counter.
14210     Dtprov=Dt     !     Stores current trial Dt as provisional value Dtprov.
14220     GOSUB Wakefm_interp
14230     Fwxtp=Fwxint
14240     Fwytp=Fwyint  !     Determine propeller wake force and moment components
14250     Mwxtp=Mwxint  !     at currently predicted time step end time.
14260     Mwytp=Mwyint
14270     GOSUB Predict !     Call Predict Subroutine.
14280     Xdel=Xp(2)-X(2)
14290     Ydel=Yp(2)-Y(2)       ! Set current predictions for element time step
14300     Ldel=Lamp(2)-Lam(2)   ! displacement and velocity component changes for
14310     Gdel=Gamp(2)-Gam(2)   ! checking against max. permitted changes.
14320     Xddel=Xdp(2)-Xd(2)
14330     Yddel=Ydp(2)-Yd(2)
14340     Lddel=Lamdp(2)-Lamd(2)
14350     Gddel=Gamdp(2)-Gamd(2)
14360     IF ABS(Xdel)<Dxymax THEN 14390 ! Check that current predictions for
14370     Dt=.9*Dt                       ! element 2 time step displacement and
14380     GOTO 14180                     ! velocity changes are less than max.
14390     IF ABS(Ydel)<Dxymax THEN 14420 ! specified allowable changes. If not
14400     Dt=.9*Dt                       ! reduce Dt by 10% and return to start
14410     GOTO 14180                     ! of first loop.
```

25

```
14420   IF ABS(Ldel)<Dlgmax THEN 14450
14430   Dt=.9*Dt
14440   GOTO 14180
14450   IF ABS(Gdel)<Dlgmax THEN 14480
14460   Dt=.9*Dt
14470   GOTO 14180
14480   IF ABS(Xddel)<Dxydmax THEN 14510
14490   Dt=.9*Dt
14500   GOTO 14180
14510   IF ABS(Yddel)<Dxydmax THEN 14540
14520   Dt=.9*Dt
14530   GOTO 14180
14540   IF ABS(Lddel)<Dlgdmax THEN 14570
14550   Dt=.9*Dt
14560   GOTO 14180
14570   IF ABS(Gddel)<Dlgdmax THEN 14600
14580   Dt=.9*Dt
14590   GOTO 14180                 !  First Loop End.
14600   IF Nonlin$="N" THEN 16230  !  Skips Second Loop completely if Linear Aft
                                   !  Sterntube Bearing Model is selected.
14610   Cartflag=1                 !  Sets flag to get Cart_oilfilm Subroutine
                                      to use current Xp(2),etc. to calc. perts.
14620   GOSUB Cart_oilfilm         !  Second Loop Start Point.
14630   FOR Nelem=1 TO 6
14640   Xdiv(Nelem)=Xcon(Nelem)    !  Indexing and Storage of previous time step
14650   Ydiv(Nelem)=Ycon(Nelem)    !  end point estimates for convergence and
14660   Ldiv(Nelem)=Lcon(Nelem)    !  divergence tests.
14670   Gdiv(Nelem)=Gcon(Nelem)
14680   Xddiv(Nelem)=Xdcon(Nelem)
14690   Yddiv(Nelem)=Ydcon(Nelem)
14700   Lddiv(Nelem)=Ldcon(Nelem)
14710   Gddiv(Nelem)=Gdcon(Nelem)
14720   Xcon(Nelem)=Xp(Nelem)
14730   Ycon(Nelem)=Yp(Nelem)
14740   Lcon(Nelem)=Lamp(Nelem)
14750   Gcon(Nelem)=Gamp(Nelem)
14760   Xdcon(Nelem)=Xdp(Nelem)
14770   Ydcon(Nelem)=Ydp(Nelem)
14780   Ldcon(Nelem)=Lamdp(Nelem)
14790   Gdcon(Nelem)=Gamdp(Nelem)
14800   NEXT Nelem
14810   IF Curtstep=0 THEN 15180   ! Updating of start accels. to include latest
                                     estimate of current time step mean accel.
14820   IF Cyc>1 THEN 14860        ! cannot be done until first pass through
                                     Loop2 is completed.
14830   IF Nd>4 THEN 14860
14840   Nreg=Nd+1
14850   GOTO 14870
14860   Nreg=5
14870   Dt0=Dt
14880   FOR Nelem=1 TO 6
14890   A0=Xddreg(Nelem,1)
14900   A1=Xddreg(Nelem,2)
14910   A2=Xddreg(Nelem,3)
14920   A3=Xddreg(Nelem,4)
14930   A4=Xddreg(Nelem,5)
14940   GOSUB Regression
14950   Xdd(Nelem)=Areg
14960   A0=Yddreg(Nelem,1)
14970   A1=Yddreg(Nelem,2)
14980   A2=Yddreg(Nelem,3)
14990   A3=Yddreg(Nelem,4)
15000   A4=Yddreg(Nelem,5)
15010   GOSUB Regression
15020   Ydd(Nelem)=Areg
15030   A0=Lddreg(Nelem,1)
```

26

```
15040     A1=Lddreg(Nelem,2)
15050     A2=Lddreg(Nelem,3)
15060     A3=Lddreg(Nelem,4)
15070     A4=Lddreg(Nelem,5)
15080     GOSUB Regression
15090     Lamdd(Nelem)=Areg
15100     A0=Gddreg(Nelem,1)
15110     A1=Gddreg(Nelem,2)
15120     A2=Gddreg(Nelem,3)
15130     A3=Gddreg(Nelem,4)
15140     A4=Gddreg(Nelem,5)
15150     GOSUB Regression
15160     Gamdd(Nelem)=Areg
15170     NEXT Nelem
15180     Loop2=Loop2+1        !   Index Second Loop Counter.
15190     GOSUB Predict
15200     Contest=0      !  Reset Convergence Indicator.
15210     Divtest=0      !  Reset Divergence Indicator.
15220     Kdivmax=1      !  Reset Max. Divergence Dt reduction factor.
15230     Curtstep=1     !  Set signal to get Regression Subroutine to use current
                         !  time step predicted mean acceleration components when
15240                    !  determining time step start acceleration components.
15250     FOR Nelem=1 TO 6
15260     Xddreg(Nelem,1)=Xddm(Nelem)   ! Set Regression Subroutine input
15270     Yddreg(Nelem,1)=Yddm(Nelem)   ! accelerations corresponding to current
15280     Lddreg(Nelem,1)=Lamddm(Nelem)! time step mean accelerations.
15290     Gddreg(Nelem,1)=Gamddm(Nelem)
15300     !  The following series of convergence and divergence tests for all
          !  displacement and velocity components are all of the format :
15310     !  Convergence test : Is change in current predicted parameter at time
          !  step end ( Xp, etc.) from previous prediction (Xcon,etc.) within
15320     !  specified limit.
          !  If not, set " NOT CONVERGED " indicator : Contest=1.
15330     !  Divergence test : Is parameter change from previous prediction at
          !  time step end (Xp-Xcon, etc.) diverging relative to previous such
15340     !  change (Xcon-Xdiv, etc.).
          !  If diverging set " DIVERGING " indicator : Divtest=1
15350     !  If diverging set divergence factor Kdiverg provided Xcon-Xdiv, etc.
          !  exceeds specified min. value.
15360     !  Test for max. divergence factor Kdivmax.
15370     IF ABS(Xp(Nelem)-Xcon(Nelem))<2.E-6 THEN 15450
15380     Contest=1
15390     IF ABS(Xp(Nelem)-Xcon(Nelem))<ABS(Xcon(Nelem)-Xdiv(Nelem)) THEN 15450
15400     Divtest=1
15410     IF ABS(Xcon(Nelem)-Xdiv(Nelem))<2.E-6 THEN 15450
15420     Kdiverg=ABS((Xp(Nelem)-Xcon(Nelem))/(Xcon(Nelem)-Xdiv(Nelem)))
15430     IF Kdivmax>Kdiverg THEN 15450
15440     Kdivmax=Kdiverg
15450     IF ABS(Yp(Nelem)-Ycon(Nelem))<2.E-6 THEN 15530
15460     Contest=1
15470     IF ABS(Yp(Nelem)-Ycon(Nelem))<ABS(Ycon(Nelem)-Ydiv(Nelem)) THEN 15530
15480     Divtest=1
15490     IF ABS(Ycon(Nelem)-Ydiv(Nelem))<2.E-6 THEN 15530
15500     Kdiverg=ABS((Yp(Nelem)-Ycon(Nelem))/(Ycon(Nelem)-Ydiv(Nelem)))
15510     IF Kdivmax>Kdiverg THEN 15530
15520     Kdivmax=Kdiverg
15530     IF ABS(Lamp(Nelem)-Lcon(Nelem))<1.E-6 THEN 15610
15540     Contest=1
15550     IF ABS(Lamp(Nelem)-Lcon(Nelem))<ABS(Lcon(Nelem)-Ldiv(Nelem)) THEN 15610
15560     Divtest=1
15570     IF ABS(Lcon(Nelem)-Ldiv(Nelem))<1.E-6 THEN 15610
15580     Kdiverg=ABS((Lamp(Nelem)-Lcon(Nelem))/(Lcon(Nelem)-Ldiv(Nelem)))
15590     IF Kdivmax>Kdiverg THEN 15610
15600     Kdivmax=Kdiverg
15610     IF ABS(Gamp(Nelem)-Gcon(Nelem))<1.E-6 THEN 15690
15620     Contest=1
```

```
15630   IF ABS(Gamp(Nelem)-Gcon(Nelem))<ABS(Gcon(Nelem)-Gdiv(Nelem)) THEN 15690
15640   Divtest=1
15650   IF ABS(Gcon(Nelem)-Gdiv(Nelem))<1.E-6 THEN 15690                          27
15660   Kdiverg=ABS((Gamp(Nelem)-Gcon(Nelem))/(Gcon(Nelem)-Gdiv(Nelem)))
15670   IF Kdivmax>Kdiverg THEN 15690
15680   Kdivmax=Kdiverg
15690   IF ABS(Xdp(Nelem)-Xdcon(Nelem))<1.E-5 THEN 15770
15700   Contest=1
15710   IF ABS(Xdp(Nelem)-Xdcon(Nelem))<ABS(Xdcon(Nelem)-Xddiv(Nelem)) THEN 157
70
15720   Divtest=1
15730   IF ABS(Xdcon(Nelem)-Xddiv(Nelem))<1.E-5 THEN 15770
15740   Kdiverg=ABS((Xdp(Nelem)-Xdcon(Nelem))/(Xdcon(Nelem)-Xddiv(Nelem)))
15750   IF Kdivmax>Kdiverg THEN 15770
15760   Kdivmax=Kdiverg
15770   IF ABS(Ydp(Nelem)-Ydcon(Nelem))<1.E-5 THEN 15850
15780   Contest=1
15790   IF ABS(Ydp(Nelem)-Ydcon(Nelem))<ABS(Ydcon(Nelem)-Yddiv(Nelem)) THEN 158
50
15800   Divtest=1
15810   IF ABS(Ydcon(Nelem)-Yddiv(Nelem))<1.E-5 THEN 15850
15820   Kdiverg=ABS((Ydp(Nelem)-Ydcon(Nelem))/(Ydcon(Nelem)-Yddiv(Nelem)))
15830   IF Kdivmax>Kdiverg THEN 15850
15840   Kdivmax=Kdiverg
15850   IF ABS(Lamdp(Nelem)-Ldcon(Nelem))<5.E-5 THEN 15930
15860   Contest=1
15870   IF ABS(Lamdp(Nelem)-Ldcon(Nelem))<ABS(Ldcon(Nelem)-Lddiv(Nelem)) THEN 1
5930
15880   Divtest=1
15890   IF ABS(Ldcon(Nelem)-Lddiv(Nelem))<5.E-5 THEN 15930
15900   Kdiverg=ABS((Lamdp(Nelem)-Ldcon(Nelem))/(Ldcon(Nelem)-Lddiv(Nelem)))
15910   IF Kdivmax>Kdiverg THEN 15930
15920   Kdivmax=Kdiverg
15930   IF ABS(Gamdp(Nelem)-Gdcon(Nelem))<5.E-5 THEN 16010
15940   Contest=1
15950   IF ABS(Gamdp(Nelem)-Gdcon(Nelem))<ABS(Gdcon(Nelem)-Gddiv(Nelem)) THEN 1
6010
15960   Divtest=1
15970   IF ABS(Gdcon(Nelem)-Gddiv(Nelem))<5.E-5 THEN 16010
15980   Kdiverg=ABS((Gamdp(Nelem)-Gdcon(Nelem))/(Gdcon(Nelem)-Gddiv(Nelem)))
15990   IF Kdivmax>Kdiverg THEN 16010
16000   Kdivmax=Kdiverg
16010   NEXT Nelem
16020   IF Contest=0 THEN 16230   !  To time step Print out, Data storage &
                                     Indexing.
16030   IF Divtest=0 THEN 14620   !  Return to second loop start if convergence
                                     criteria not satisfied, but not diverging.
16040   Dtdiv=Dt/Kdivmax           !  Set reduced Dt if diverging.
                                  !  Below : Correct time step end displalements
16050                             !  and velocities for reduced Dt.
16060   Xdp(2)=Xd(2)+Xdd(2)*Dtdiv+(Xddm(2)-Xdd(2))*Dtdiv^2/Dt
16070   Ydp(2)=Yd(2)+Ydd(2)*Dtdiv+(Yddm(2)-Ydd(2))*Dtdiv^2/Dt
16080   Lamdp(2)=Lamd(2)+Lamdd(2)*Dtdiv+(Lamddm(2)-Lamdd(2))*Dtdiv^2/Dt
16090   Gamdp(2)=Gamd(2)+Gamdd(2)*Dtdiv+(Gamddm(2)-Gamdd(2))*Dtdiv^2/Dt
16100   Xp(2)=X(2)+(Xdp(2)+2*Xd(2))*Dtdiv/3+Xdd(2)*Dtdiv^2/6
16110   Yp(2)=Y(2)+(Ydp(2)+2*Yd(2))*Dtdiv/3+Ydd(2)*Dtdiv^2/6
16120   Lamp(2)=Lam(2)+(Lamdp(2)+2*Lamd(2))*Dtdiv/3+Lamdd(2)*Dtdiv^2/6
16130   Gamp(2)=Gam(2)+(Gamdp(2)+2*Gamd(2))*Dtdiv/3+Gamdd(2)*Dtdiv^2/6
16140   Time=Time-Dt     !     Reset to Time Step Start Point.
16150   Dt=Dtdiv
16160   Time=Time+Dt     !     Revised Time Step End Point.
16170   GOSUB Wakefm_interp
16180   Fwxtp=Fwxint
16190   Fwytp=Fwyint     !   Determine propeller wake forces and moments at
16200   Mwxtp=Mwxint     !   revised time step end time.
16210   Mwytp=Mwyint
```

```
16220     GOTO 14620        !  End of Second Loop.
16230     Dt4=Dt3           !  Index stored time step durations for Regression     28
16240     Dt3=Dt2           !  Subroutine to get start point accelerations.
16250     Dt2=Dt1
16260     Dt1=Dt0
16270     Dt0=Dt
16280     FOR Nelem=1 TO 6 !  Index stored accels. for Regression Subroutine.
16290     FOR Nregsto=5 TO 2 STEP -1
16300     Xddreg(Nelem,Nregsto)=Xddreg(Nelem,Nregsto-1)
16310     Yddreg(Nelem,Nregsto)=Yddreg(Nelem,Nregsto-1)
16320     Lddreg(Nelem,Nregsto)=Lddreg(Nelem,Nregsto-1)
16330     Gddreg(Nelem,Nregsto)=Gddreg(Nelem,Nregsto-1)
16340     NEXT Nregsto
16350     Xddreg(Nelem,1)=Xddm(Nelem)
16360     Yddreg(Nelem,1)=Yddm(Nelem)
16370     Lddreg(Nelem,1)=Lamddm(Nelem)
16380     Gddreg(Nelem,1)=Gamddm(Nelem)
16390     NEXT Nelem
16400     IF Fulprt=0 THEN 16420 ! Full_print Subroutine can be called on demand
                                 ! at any time by PAUSE in program execution and
16410     GOSUB Full_print       ! then manually setting Fulprt=1.
16420     Nd=Nd+1                ! Index Time Step Counter.
16430     IF Cyc>1 THEN 16540    ! Following section interpolates and stores
                                 ! displacement components for all elements at
16440     IF Nd>1 THEN 16540     ! intervals of 1/20th cycle time. Stored data is
                                 ! overwritten by each new computed cycle.
16450     Tprt=INT(Time/Tcyc*20)+1 ! Set initial time index Tprt for stored
                                   ! displacement data to correspond to first
16460     FOR Nelem=1 TO 6         ! orbit start time. This time may have been
                                   ! manually set to any value in the range zero
16470                              ! to Tcyc ( dynamic cycle time.).
16480     Xprt(Nelem,Tprt)=X(Nelem)! Store Print Out data for Orbit Start
                                   Condition.
16490     Yprt(Nelem,Tprt)=Y(Nelem)
16500     Lprt(Nelem,Tprt)=Lam(Nelem)
16510     Gprt(Nelem,Tprt)=Gam(Nelem)
16520     NEXT Nelem
16530     GOTO 17260
16540     IF Time<Tcyc THEN 17110
16550     GOSUB Full_print
16560     Tprt=21
16570     FOR Nelem=1 TO 6   !  Store data for last point in cycle corresponding
                             !  to Time=Tcyc ( Index Tprt=21 ).
16580     Xprt(Nelem,Tprt)=(Tcyc-Time+Dt)*(Xp(Nelem)-X(Nelem))/Dt+X(Nelem)
16590     Yprt(Nelem,Tprt)=(Tcyc-Time+Dt)*(Yp(Nelem)-Y(Nelem))/Dt+Y(Nelem)
16600     Lprt(Nelem,Tprt)=(Tcyc-Time+Dt)*(Lamp(Nelem)-Lam(Nelem))/Dt+Lam(Nelem)
16610     Gprt(Nelem,Tprt)=(Tcyc-Time+Dt)*(Gamp(Nelem)-Gam(Nelem))/Dt+Gam(Nelem)
16620     NEXT Nelem   !  Note that ORBITS and CONTIN files are automatically
                       !  stored at end of each cycle or, when stopping run on
16630                  !  manual demand signal : Stoprun=1.
16640     IF Continue$="Y" THEN 16660 ! For continuation run,old ORBITS file must
                                      ! be purged before storing new ORBITS file.
16650     IF Cyc=1 THEN 16670         ! No ORBITS file to purge on first cycle of
                                      ! a start run.
16660     PURGE "ORBITS:INTERNAL,4,0"
16670     MASS STORAGE IS ":INTERNAL,4,0"
16680     CREATE ASCII "ORBITS:INTERNAL,4,0",70  !  Store Last ORBIT Data.
16690     ASSIGN @File6 TO "ORBITS:INTERNAL,4,0"
16700     OUTPUT @File6;Cyc
16710     OUTPUT @File6;Nd       !  ORBITS file stores displacement data for all
16720     OUTPUT @File6;Xprt(*)  !  elements at 1/20th cycle time intervals for
16730     OUTPUT @File6;Yprt(*)  !  one dynamic cycle.
16740     OUTPUT @File6;Lprt(*)
16750     OUTPUT @File6;Gprt(*)
16760     OUTPUT @File6;Tprt
16770     ASSIGN @File6 TO *
```

```
16780     IF Continue$="Y" THEN 16800 ! Old CONTIN file must be purged before
                                      ! storing new CONTIN file on a continuation 29
16790     IF Cyc=1 THEN 16810         ! run, or on a start run once the first
                                      ! cycle has been completed.
16800     PURGE "CONTIN:INTERNAL,4,0"
16810     CREATE ASCII "CONTIN:INTERNAL,4,0",40
16820     ASSIGN @File7 TO "CONTIN:INTERNAL,4,0"
16830     OUTPUT @File7;X(*)
16840     OUTPUT @File7;Y(*)     !  CONTIN file stores all data, additional to
16850     OUTPUT @File7;Lam(*)   !  that in the ORBITS file, which is required to
16860     OUTPUT @File7;Gam(*)   !  enable subsequent continuation run to be
16870     OUTPUT @File7;Xd(*)    !  started from point at which the current run
16880     OUTPUT @File7;Yd(*)    !  was manually stopped, or from end of last
16890     OUTPUT @File7;Lamd(*)  !  dynamic cycle if not manually stopped.
16900     OUTPUT @File7;Gamd(*)
16910     OUTPUT @File7;Xdd(*)
16920     OUTPUT @File7;Ydd(*)
16930     OUTPUT @File7;Lamdd(*)
16940     OUTPUT @File7;Gamdd(*)
16950     OUTPUT @File7;Xddreg(*)
16960     OUTPUT @File7;Yddreg(*)
16970     OUTPUT @File7;Lddreg(*)
16980     OUTPUT @File7;Gddreg(*)
16990     OUTPUT @File7;Dt0,Dt1,Dt2,Dt3,Dt4,Time,Ayy,Ayx,Ayg,Ayl,Axy,Axx,Axg,Axl,
Agy,Agx,Agg,Agl,Aly,Alx,Alg,All
17000     OUTPUT @File7;Byy,Byx,Byg,Byl,Bxy,Bxx,Bxg,Bxl,Bgy,Bgx,Bgg,Bgl,Bly,Blx,B
lg,Bll,Fxa,Fya,Mxa,Mya,Fxnl,Fynl,Mxnl,Mynl
17010     ASSIGN @File7 TO *
17020     IF Runend=1 THEN 17420 !  Jump to end of subroutine if run is being
                                 !  stopped by manual signal Stoprun=1 which also
17030                            !  sets additional signal Runend=1.
17040     Tprt=1          !  Reset Print Data Ref.
17050     GOSUB Printdisp ! Print out displacement data for complete cycle at
                          ! cycle end.
17060     Cyc=Cyc+1       !  Index Cycle Counter.
17070     Nd=0            !  Reset Time Step Counter.
17080     Time=Time-Tcyc! Reset Time for start of new cycle.
17090     IF Cyc=Cyclim+1 THEN 17420 ! Terminate run if No. of cycles exceeds
17100     GOTO 17270                 ! prescribed limit.
17110     IF Nd>1 THEN 17190
17120     FOR Nelem=1 TO 6
17130     Xprt(Nelem,1)=Xprt(Nelem,21) ! First Print Out data on new cycle = last
17140     Yprt(Nelem,1)=Yprt(Nelem,21) ! data on old cycle.
17150     Lprt(Nelem,1)=Lprt(Nelem,21)
17160     Gprt(Nelem,1)=Gprt(Nelem,21)
17170     NEXT Nelem
17180     GOTO 17260
17190     IF Time<(Tprt-1)/20*Tcyc THEN 17270 ! Jump if time is less than next
                                              ! prescribed 1/20th. Tcyc time at
17200     FOR Nelem=1 TO 6                    ! which displacement data is to be
                                              ! interpolated and stored.
17210     Xprt(Nelem,Tprt)=((Tprt-1)/20*Tcyc-Time+Dt)*(Xp(Nelem)-X(Nelem))/Dt+X(N
elem)
17220     Yprt(Nelem,Tprt)=((Tprt-1)/20*Tcyc-Time+Dt)*(Yp(Nelem)-Y(Nelem))/Dt+Y(N
elem)
17230     Lprt(Nelem,Tprt)=((Tprt-1)/20*Tcyc-Time+Dt)*(Lamp(Nelem)-Lam(Nelem))/Dt
+Lam(Nelem)
17240     Gprt(Nelem,Tprt)=((Tprt-1)/20*Tcyc-Time+Dt)*(Gamp(Nelem)-Gam(Nelem))/Dt
+Gam(Nelem)
17250     NEXT Nelem    !  Section above interpolates and stores displacement data
                        !  at 1/20th. Tcyc intervals.
17260     Tprt=Tprt+1   !  Index Print Data Ref.
17270     FOR Nelem=1 TO 6     !  Index disps. & vels. for next time step
17280     X(Nelem)=Xp(Nelem)
17290     Y(Nelem)=Yp(Nelem)
17300     Lam(Nelem)=Lamp(Nelem)
```

```
17310     Gam(Nelem)=Gamp(Nelem)
17320     Xd(Nelem)=Xdp(Nelem)
17330     Yd(Nelem)=Ydp(Nelem)
17340     Lamd(Nelem)=Lamdp(Nelem)
17350     Gamd(Nelem)=Gamdp(Nelem)
17360     NEXT Nelem
17370     Dtm1=Dt
17380     IF Nd>Ndlim THEN 17420     !  Terminate run if No. of time steps exceeds
                                     !  prescribed limit.
17390     IF Stoprun=0 THEN 13660    !  Return to start of time step sequence if
                                     !  manual signal to stop run has not been set.
17400     Runend=1                   !  Set additional signal required for manually
                                     !  stopping run
17410     GOTO 16640                 !  Go to section for storing ORBITS and CONTIN
                                     !  files.
17420     RETURN !################################################################
17430 Printdisp:        !  Subroutine to Print Out all Mass Station displacement
                           data at 1/20th. Cycle Time intervals at the end of
17440                   !  each completed dynamic cycle plus additional Orbit data
                           INPUT : Print out data Xprt(Nelem,1).....Xprt(Nelem,21)
17450    PRINTER IS 701!   etc. generated in the Timestep Subroutine.
17460    Z=0
17470    PRINT FNPage$;"                  Cycle No. ";Cyc;"           Heading row
s give Time/Tcyc"
17480    PRINT "                          ________________"
17490    PRINT "X Displacements (m.)"
17500    PRINT USING "4A,2X,7(D.2D,7X)";"Mass",(Z)/20,(Z+1)/20,(Z+2)/20,(Z+3)/20,
(Z+4)/20,(Z+5)/20,(Z+6)/20
17510    FOR Nelem=1 TO 6
17520    PRINT USING "2D,X,7(2X,SD.2DE)";Nelem,Xprt(Nelem,Z+1),Xprt(Nelem,Z+2),Xp
rt(Nelem,Z+3),Xprt(Nelem,Z+4),Xprt(Nelem,Z+5),Xprt(Nelem,Z+6),Xprt(Nelem,Z+7)
17530    NEXT Nelem
17540    PRINT "___________________________________________________________________
_______________"
17550    PRINT "Y Displacements (m.)"
17560    PRINT USING "4A,2X,7(D.2D,7X)";"Mass",(Z)/20,(Z+1)/20,(Z+2)/20,(Z+3)/20,
(Z+4)/20,(Z+5)/20,(Z+6)/20
17570    FOR Nelem=1 TO 6
17580    PRINT USING "2D,X,7(2X,SD.2DE)";Nelem,Yprt(Nelem,Z+1),Yprt(Nelem,Z+2),Yp
rt(Nelem,Z+3),Yprt(Nelem,Z+4),Yprt(Nelem,Z+5),Yprt(Nelem,Z+6),Yprt(Nelem,Z+7)
17590    NEXT Nelem
17600    PRINT "___________________________________________________________________
_______________"
17610    PRINT "Lambda Displacements (rad.)"
17620    PRINT USING "4A,2X,7(D.2D,7X)";"Mass",(Z)/20,(Z+1)/20,(Z+2)/20,(Z+3)/20,
(Z+4)/20,(Z+5)/20,(Z+6)/20
17630    FOR Nelem=1 TO 6
17640    PRINT USING "2D,X,7(2X,SD.2DE)";Nelem,Lprt(Nelem,Z+1),Lprt(Nelem,Z+2),Lp
rt(Nelem,Z+3),Lprt(Nelem,Z+4),Lprt(Nelem,Z+5),Lprt(Nelem,Z+6),Lprt(Nelem,Z+7)
17650    NEXT Nelem
17660    PRINT "___________________________________________________________________
_______________"
17670    PRINT "Gamma Displacements (rad.)"
17680    PRINT USING "4A,2X,7(D.2D,7X)";"Mass",(Z)/20,(Z+1)/20,(Z+2)/20,(Z+3)/20,
(Z+4)/20,(Z+5)/20,(Z+6)/20
17690    FOR Nelem=1 TO 6
17700    PRINT USING "2D,X,7(2X,SD.2DE)";Nelem,Gprt(Nelem,Z+1),Gprt(Nelem,Z+2),Gp
rt(Nelem,Z+3),Gprt(Nelem,Z+4),Gprt(Nelem,Z+5),Gprt(Nelem,Z+6),Gprt(Nelem,Z+7)
17710    NEXT Nelem
17720    PRINT "___________________________________________________________________
_______________"
17730    IF Z=7 THEN 17770
17740    IF Z=14 THEN 17790
17750    Z=7
17760    GOTO 17470
17770    Z=14
```

```
17780    GOTO 17470
17790    PRINT FNPage$;"                    Cycle No. ";Cyc;"    ORBIT DATA :"            (31)
17800    PRINT "________________________________________________"
17810    PRINT "Mass     Max. Eccent at :   Min. Eccent at :"
17820    PRINT "         Time/Tcyc          Time/Tcyc"
17830    FOR Nelem=1 TO 6   ! Section below computes mean displacement components
17840    Xsigma=0           ! for the complete orbit. i.e. one dynamic cycle Tcyc.
17850    Ysigma=0
17860    Lsigma=0
17870    Gsigma=0
17880    FOR Z=1 TO 20
17890    Xsigma=Xsigma+Xprt(Nelem,Z)
17900    Ysigma=Ysigma+Yprt(Nelem,Z)
17910    Lsigma=Lsigma+Lprt(Nelem,Z)
17920    Gsigma=Gsigma+Gprt(Nelem,Z)
17930    NEXT Z
17940    Xmean(Nelem)=Xsigma/20
17950    Ymean(Nelem)=Ysigma/20
17960    Lmn(Nelem)=Lsigma/20
17970    Gmn(Nelem)=Gsigma/20
17980    FOR Z=1 TO 20           !  Section below computes eccentricity and attidude
                                 !  angle of each set of lateral displacement
17990                            !  components relative to the mean lateral locations
                                 !  of the orbit.
18000    Eorb(Nelem,Z)=SQR((Xprt(Nelem,Z)-Xmean(Nelem))^2+(Yprt(Nelem,Z)-Ymean(Ne
lem))^2)
18010    Porb(Nelem,Z)=ATN((Xprt(Nelem,Z)-Xmean(Nelem))/(Yprt(Nelem,Z)-Ymean(Nele
m)))
18020    IF (Xprt(Nelem,Z)-Xmean(Nelem))<0 THEN 18050
18030    IF (Yprt(Nelem,Z)-Ymean(Nelem))<0 THEN 18080
18040    GOTO 18090
18050    IF (Yprt(Nelem,Z)-Ymean(Nelem))<0 THEN 18080
18060    Porb(Nelem,Z)=360+Porb(Nelem,Z)
18070    GOTO 18090
18080    Porb(Nelem,Z)=180+Porb(Nelem,Z)
18090    NEXT Z    ! Section below picks out max. and min. values of eccentricity
                   ! for orbit.
18100    Emax1=MAX(Eorb(Nelem,1),Eorb(Nelem,2),Eorb(Nelem,3),Eorb(Nelem,4),Eorb(N
elem,5),Eorb(Nelem,6),Eorb(Nelem,7))
18110    Emax2=MAX(Eorb(Nelem,8),Eorb(Nelem,9),Eorb(Nelem,10),Eorb(Nelem,11),Eorb
(Nelem,12),Eorb(Nelem,13),Eorb(Nelem,14))
18120    Emax3=MAX(Eorb(Nelem,15),Eorb(Nelem,16),Eorb(Nelem,17),Eorb(Nelem,18),Eo
rb(Nelem,19),Eorb(Nelem,20))
18130    Eorbmax(Nelem)=MAX(Emax1,Emax2,Emax3)
18140    Emin1=MIN(Eorb(Nelem,1),Eorb(Nelem,2),Eorb(Nelem,3),Eorb(Nelem,4),Eorb(N
elem,5),Eorb(Nelem,6),Eorb(Nelem,7))
18150    Emin2=MIN(Eorb(Nelem,8),Eorb(Nelem,9),Eorb(Nelem,10),Eorb(Nelem,11),Eorb
(Nelem,12),Eorb(Nelem,13),Eorb(Nelem,14))
18160    Emin3=MIN(Eorb(Nelem,15),Eorb(Nelem,16),Eorb(Nelem,17),Eorb(Nelem,18),Eo
rb(Nelem,19),Eorb(Nelem,20))
18170    Eorbmin(Nelem)=MIN(Emin1,Emin2,Emin3)
18180    FOR Z=1 TO 20  !  This section identifies time reference index
                        !  corresponding to max. and min. eccentricities.
18190    IF Eorb(Nelem,Z)=Eorbmax(Nelem) THEN 18220
18200    IF Eorb(Nelem,Z)=Eorbmin(Nelem) THEN 18240
18210    GOTO 18250
18220    Zorbmax=Z
18230    GOTO 18250
18240    Zorbmin=Z
18250    NEXT Z      !  Line below prints out proportion of cycle time
                     !  corresponding to max. and min. eccentricities.
18260    PRINT USING "2D,6X,D.2D,14X,D.2D";Nelem,(Zorbmax-1)/20,(Zorbmin-1)/20
18270    Lomax(Nelem)=Lmn(Nelem)
18280    Lomin(Nelem)=Lmn(Nelem)  ! This section locates max. and min. values of
18290    Gomax(Nelem)=Gmn(Nelem)  ! the components of angular displacement and the
18300    Gomin(Nelem)=Gmn(Nelem)  ! corresponding time references.
```

```
18310   FOR Z=1 TO 20
18320   IF Lomax(Nelem)>Lprt(Nelem,Z) THEN 18350
18330   Lomax(Nelem)=Lprt(Nelem,Z)
18340   Zlorbmax(Nelem)=Z
18350   IF Lomin(Nelem)<Lprt(Nelem,Z) THEN 18380
18360   Lomin(Nelem)=Lprt(Nelem,Z)
18370   Zlorbmin(Nelem)=Z
18380   IF Gomax(Nelem)>Gprt(Nelem,Z) THEN 18410
18390   Gomax(Nelem)=Gprt(Nelem,Z)
18400   Zgorbmax(Nelem)=Z
18410   IF Gomin(Nelem)<Gprt(Nelem,Z) THEN 18440
18420   Gomin(Nelem)=Gprt(Nelem,Z)
18430   Zgorbmin(Nelem)=Z
18440   NEXT Z
18450   NEXT Nelem
18460   PRINT "____________________________________________________________________________________
________________"
18470   PRINT   ! Print out of max. and min. orbit eccentricities and
                ! corresponding attitude angles.
18480   PRINT "Mass      Mean                    Maximum                    Minimum"
18490   PRINT "      X            Y          Eccent       Psi          Eccent
Psi"
18500   FOR Nelem=1 TO 6
18510   PRINT USING "2D,6(2X,SD.3DE)";Nelem,Xmean(Nelem),Ymean(Nelem),Eorbmax(Ne
lem),Porb(Nelem,Zorbmax),Eorbmin(Nelem),Porb(Nelem,Zorbmin)
18520   NEXT Nelem
18530   PRINT "____________________________________________________________________________________
________________"
18540   PRINT "Angular Orbit Data :"
18550   PRINT "______________________"
18560   PRINT "Mass              Lambda                          Gamma"
18570   PRINT "       Mean        Plus        Minus        Mean        Plus
Minus"
18580   FOR Nelem=1 TO 6
18590  PRINT USING "2D,6(2X,SD.3DE)";Nelem,Lmn(Nelem),Lomax(Nelem)-Lmn(Nelem),Lm
n(Nelem)-Lomin(Nelem),Gmn(Nelem),Gomax(Nelem)-Gmn(Nelem),Gmn(Nelem)-Gomin(Nelem)
18600   NEXT Nelem
18610   PRINT "____________________________________________________________________________________
________________"
18620   PRINT "Time/Tcyc Data for above Angles :"
18630   PRINT "___________________________________"
18640   PRINT "Mass            Lambda                  Gamma"
18650   PRINT "            Plus        Minus        Plus        Minus"
18660   FOR Nelem=1 TO 6
18670   PRINT USING "2D,4(8X,D.2D)";Nelem,(Zlorbmax(Nelem)-1)/20,(Zlorbmin(Nelem
)-1)/20,(Zgorbmax(Nelem)-1)/20,(Zgorbmin(Nelem)-1)/20
18680   NEXT Nelem
18690   PRINT FNPage$;
18700   PRINTER IS 1
18710   RETURN ! ###################################################################
18720 Full_print:    ! Subroutine to Print Out all Disp.,Vel.,and Accel. data on
18730   PRINTER IS 701! demand by the sequence PAUSE,Fulprt=1,EXECUTE,CONTINUE
18740   PRINT FNPage$;! or as required during time step operation. Also called
                ! by program at each run start and at end of each cycle.
18750   PRINT USING "4A,X,2D,2X,3A,X,4D,2X,5A,X,D.4DE";"Cyc=",Cyc,"Nd=",Nd,"Time
=",Time-Dt
18760   PRINT "(All Data refers to time step start.)"
18770   PRINT "____________________________________________________________________________________
________________"
18780   PRINT "Displacements :"
18790   PRINT "_________________"
18800   PRINT "Mass    X           Y            Lambda        Gamma"
18810   FOR Nelem=1 TO 6
18820   PRINT USING "2D,2X,4(2X,SD.4DE)";Nelem,X(Nelem),Y(Nelem),Lam(Nelem),Gam(
Nelem)
18830   NEXT Nelem
```

(32)

```
18840   PRINT "________________________________________________________________________
________________"
18850   PRINT "Velocities :"
18860   PRINT "______________"
18870   PRINT "Mass    X             Y              Lambda        Gamma"
18880   FOR Nelem=1 TO 6
18890   PRINT USING "2D,2X,4(2X,SD.4DE)";Nelem,Xd(Nelem),Yd(Nelem),Lamd(Nelem),G
amd(Nelem)
18900   NEXT Nelem
18910   PRINT "________________________________________________________________________
________________"
18920   PRINT "Accelerations :"
18930   PRINT "_________________"
18940   PRINT "Mass    X             Y              Lambda        Gamma"
18950   FOR Nelem=1 TO 6
18960   PRINT USING "2D,2X,4(2X,SD.4DE)";Nelem,Xdd(Nelem),Ydd(Nelem),Lamdd(Nelem
),Gamdd(Nelem)
18970   NEXT Nelem
18980   PRINT "________________________________________________________________________
________________"
18990   PRINTER IS 1
19000   Fulprt=0  !      Resets demand signal for this Subroutine.
19010   RETURN !##############################################################
19020   END
19030   DEF FNPage$    !  PAGE function of PRINT
19040   RETURN CHR$(13)&CHR$(12)
19050   FNEND
```

33

APPENDIX 4.

Related Papers by the Author

This appendix contains copies of all the papers published or submitted for publication by the author, to which reference has been made. These papers cover most of the work described in this thesis. The papers are as follows:

(72) "A numerical analysis method based on flow continuity for hydrodynamic journal bearings". (A.4. - 3 -11.)

(77) "Journal orbit analysis taking account of oil film history and journal mass". (A.4. - 12 - 23)

(85) "The influence of cavitation on the non-linearity of velocity coefficients in a hydrodynamic journal bearing". (A4. - 24 - 31.)

(86) "Theoretical and experimental orbits of a dynamically loaded hydrodynamic journal bearing". (Co-author : Dr. D.W. Parkins) (A.4. - 32 - 39.)

(87) "Performance and oil film dynamic coefficients of a misaligned sterntube bearing". (A.4 - 40 - 49.)

(88) "Sterntube bearings : Performance characteristics and influence upon shafting behaviour". (A.4. - 50 - 77)

(90) "Numerical analysis of hydrodynamic bearings with significant journal lateral velocities". (A.4. - 78 - 86.)

(91) "A non-linear oil film response model for the dynamically misaligned sterntube bearing".
(A.4. - 87 - 120)

(92) The influence of sterntube bearings on lateral vibration amplitudes in marine propeller shafting.
(A.4. - 121 - 171.)

Full details of the above are given in the list of references.

ERRATA

Reference (87)	Fig. 11. W = 466,000N and not 46,600N as stated.
References (87)(88)	D should be deleted from the denomenator of all the dimensionless damping coefficient expressions. (See discussion on reference (88)).

REFERENCE. 72.

A numerical analysis method based on flow continuity for hydrodynamic journal bearings

R.W. Jakeman*

A numerical method of hydrodynamic bearing analysis is presented which is simple in concept, yet capable of development to handle complex situations such as dynamic misalignment. It is similar to the finite difference solution of Reynolds equation, but incorporates a more realistic modelling of cavitation. The approach to a numerical solution is direct, and should facilitate a better 'feel' for the way in which the physical processes are modelled. Results produced with this analysis are compared with other published data for aligned crankshaft bearings and misaligned sterntube bearings.

Keywords: *journal bearings, numerical analysis, hydrodynamic bearings, cavitation*

Hydrodynamic journal bearing operation, when considered in detail, is complex when factors such as oil film viscosity variation with temperature, pressure and shear rate, bearing surface elasticity, differential thermal expansion, etc., are taken into account. The choice of which factors should be included and which neglected should reflect the operating conditions of the bearing under consideration. In a sterntube bearing, for example, the low rotational speeds, moderate loading and effective cooling of the surrounding structure by sea water make the assumption of an isoviscous oil film reasonable. This results in a considerable simplification of the analysis in relation to any variable viscosity model.

For crankshaft bearing analysis, the assumption of isoviscosity is more open to question. Since the effects of temperature and pressure on oil film viscosity act in partial opposition, the author considers an isoviscous oil film to be an acceptable model for moderately loaded crankshaft bearings.[1] In practice the complexity of any analysis is limited by computing power requirements.

For moderate speeds where laminar flow conditions may be assumed and lubricant inertia effects neglected, many authors have used the finite difference solution of Reynolds equation[2–4]. When a numerical solution is adopted, however, it is not necessary to start with Reynolds equation. In this paper a direct approach to the numerical solution is made which is considered simpler and physically more meaningful. Reynolds equation does not in fact take cavitation into account, and some authors,[2,4] have simply truncated the predicted sub-cavitation pressure region. Depending upon the oil groove geometry and journal location, this model may lead to substantial inaccuracy in the predicted position of the downstream cavitation boundary. This is due to the implicit assumption that a full oil film is available to generate hydrodynamic pressure as soon as film convergence commences. Such an assumption may be at considerable variance with continuity requirements.

Lloyd's Register of Shipping, 74 Fenchurch Street, London EC3M 4BS, UK

In the solution presented in this paper, the oil film is divided into rectangular components referred to as elements. A continuity equation is written for each element in terms of the pressure at its centre and that of the surrounding four elements or boundaries. Linear pressure gradients are assumed between the element centres, or between the centre and an adjacent film boundary. This is satisfactory, provided the element dimensions are sufficiently small in relation to the rate of change of pressure gradient.

Within the cavitation zone a constant cavitation pressure (usually assumed to be atmospheric) is specified, and a gas/vapour flow term is introduced to satisfy continuity in this area. Film pressure distribution derived by this method approximates to the Swift–Steiber condition of zero pressure gradient at the cavitation zone boundaries. The above condition is not satisfied exactly because the circumferential positions of the cavitation zone boundaries are located only to an accuracy of $\pm \Delta c$. Specification of the zero pressure gradient condition is, however, unnecessary with this method. The only boundary conditions which need be defined are bearing ambient pressure, supply groove pressure and location and cavitation pressure.

The film pressure matrix is determined by a Gauss–Seidel iterative solution of the above equations using successive over relaxation. Derivation of the film pressure matrix is the fundamental part of the analysis, and computationally the most time consuming. Calculation of the total oil film force and moment components, flow rate, power loss and displacement and velocity coefficients is relatively straight forward.

Description of the analysis

Assumptions

For the analysis presented here, the following assumptions have been made:

- Laminar flow.
- Newtonian lubricant with constant effective viscosity within the oil film.
- Rigid and perfectly circular journal and bearing surfaces.

 0301–679X/84/060325–09 $03.00 © 1984 Butterworth & Co (Publishers) Ltd

A.4.-3.

- Pressure gradients between adjacent oil film element centres, or between the element centre and a specified adjacent film boundary, are assumed to be linear. These linear pressure gradients are assumed to be the effective values for the element boundary they cross for the purpose of calculating pressure-induced flow rate.
- Oil film rupture occurs at a specified cavitation pressure which remains constant throughout the ruptured region.
- Gas and/or vapour cavities may form or collapse instantaneously in order to satisfy continuity requirements and the specified cavitation pressure.

Film geometry equations

For any axial position in a journal bearing, the film thickness at angle θ from the bearing top may be calculated from:

$$h = C_d/2 + e\cos(\theta - \psi) \tag{1}$$

Where the bearing is subject to misalignment, e and ψ are functions of axial position and may be determined via the components of eccentricity in the vertical and horizontal planes thus:

$$e_s = [e_{sy}^2 + e_{sx}^2]^{1/2} \tag{2}$$

Notation

A_{xx}, etc.	Displacement (stiffness) coefficient, N/m
B_{xx}, etc.	Velocity (damping) coefficient, N s/m
B_{ai}, B_{ao}	Effective width of oil stream at inlet to and outlet from an element, allowing for presence of gas/vapour, m
C_d	Diametral clearance, m
D	Journal diameter, m
e	Journal eccentricity (general), m
e_{cy}, e_{cx}	Vertical and horizontal components of journal eccentricity at bearing axial centre, m
e_{sy}, e_{sx}	As above but at distance s from the bearing axial centre (positive to the left), m
F_c	Circumferential viscous shear force acting on an element, N
F_y, F_x	Vertical and horizontal components of total oil film force acting on journal, N
h	Oil film thickness (general), m
h_a, h_b, h_c, h_d	Oil film thickness at each corner of the element. For element J, I these thicknesses correspond respectively to $(h(J,I), h(J,I+1), h(J+1,I), h(J+1,I+1)$, m
H	Total power absorbed by oil film, N m/s
H_{ci}, H_{co}	Element inlet and outlet circumferential pressure flow functions, m^5/N s
H_{ai}, H_{ao}	As above but for axial flow, m^5/N s
I	Axial element position reference
J	Circumferential element position reference
K	Nett velocity-induced flow out of the element, m^3/s
L	Bearing length, m
M_c	No of element rows (circumferential positions)
M_y, M_x	Vertical and horizontal components of total oil film moment acting about the bearing axial centre. The terms vertical and horizontal refer to the planes in which the moments act, N m
N	Journal rotational speed, r/s
N_a	No of element columns (axial positions)
P	Film pressure at the element centre, N/m^2
P_c	Cavitation pressure, N/m^2
P_p	Value of P for a given element during the previous iteration, N/m^2
P_s	Supply pressure, N/m^2
$P_{ci}, P_{ai}, P_{ao}, P_{ao}$	Film pressures at the centres of the elements adjacent to the element under consideration. For element J, I these correspond respectively to $P(J-1, I)$, $P(J, I-1)$, $P(J+1, I)$, $P(J, I+1)$, N/m^2
Q_{vi}, Q_{vo}	Inlet and outlet element gas/vapour flow rates, m^3/s
Q_{ci}, Q_{co}	Inlet and outlet element circumferential lubricant flow rates (assuming a full lubricant film), m^3/s
Q_{ai}, Q_{ao}	Inlet and outlet element axial lubricant flow rates, m^3/s
s	Axial distance from bearing axial centre, m
U	Journal surface velocity due to rotation, m/s
V_N, V_T	Components of journal axis velocity normal and tangential to the element, m/s
$V_y(I), V_x(I)$	Vertical and horizontal components of journal axis velocity at the axial position corresponding to centre of element column I, m/s
$\bar{W}, \bar{H}, \bar{Q}_s$	Dimensionless load, power loss and side leakage flow (Fig 4)
y, x	Vertical and horizontal components of journal lateral displacement, m
$\dot{y}, \dot{x}$	Vertical and horizontal components of journal lateral velocity, m/s
α_y, α_x	Vertical and horizontal components of journal angular misalignment, rad
γ, λ	Angular displacement of journal axis in vertical and horizontal planes, rad
$\dot{\gamma}, \dot{\lambda}$	Angular velocity of journal axis in vertical and horizontal planes, rad/s
$\Delta a, \Delta c$	Element lengths in the axial and circumferential directions, m
ϵ	Eccentricity ratio $2e/D$
η	Dynamic viscosity, N s/m^2
θ	Angular distance from bearing top to required circumferential position, degrees
τ	Mean circumferential viscous shear stress on element journal surface, N/m^2
ψ	Attitude angle, degrees
ω	Journal rotational speed, rad/s

The main geometrical parameters are illustrated in Figs 1(a), (b) and (c).

A.4. - 4.

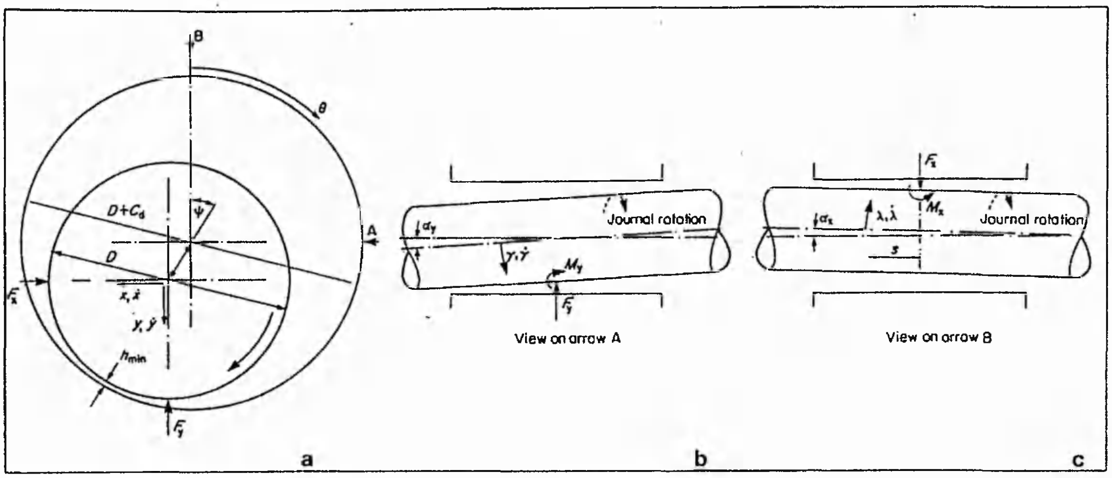

Fig 1 Sign convention for bearing: (a) end view; (b) view on vertical plane; (c) view on horizontal plane

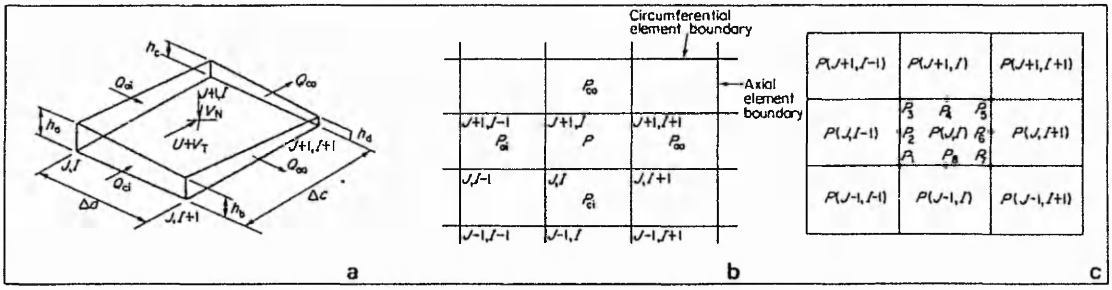

Fig 2 Oil film element details

$$\psi_s = \tan^{-1}(e_{sx}/e_{sy}) \tag{3}$$

where

$$e_{sy} = e_{cy} + s\alpha_y \tag{4}$$

$$e_{sx} = e_{cx} + s\alpha_x \tag{5}$$

For a specified journal eccentricity and misalignment, the film thickness h may thus be determined at any circumferential and axial position.

Element continuity equation

In Fig 2(a) an element of the oil film is shown, and in Fig 2(b) its circumferential and axial position reference system in relation to the neighbouring elements is specified. A continuity equation may be written for each element thus:

$$-H_{ci}(P-P_{ci}) - H_{ai}(P-P_{ai}) - Q_{vi} = K - H_{co}(P_{co}-P) - H_{ao}(P_{ao}-P) - Q_{vo} \tag{6}$$

Derivation of Eq (6) is given in Appendix 1. Outside the cavitation zone, $P > P_c$ and $Q_{vo} = 0$, therefore Eq (6) may be reduced to the following form:

$$P = \frac{H_{ai}P_{ai} + H_{ci}P_{ci} + H_{ao}P_{ao} + H_{co}P_{co} - K - Q_{vi}}{H_{ai} + H_{ci} + H_{ao} + H_{co}} \tag{7}$$

where

$$H_{ci} = \frac{(h_a + h_b)^3}{96\eta} \cdot \frac{\Delta a}{\Delta c} \tag{8}$$

$$H_{ai} = \frac{(h_a + h_c)^3}{96\eta} \cdot \frac{\Delta c}{\Delta a} \tag{9}$$

$$H_{co} = \frac{(h_c + h_d)^3}{96\eta} \cdot \frac{\Delta a}{\Delta c} \tag{10}$$

$$H_{ao} = \frac{(h_b + h_d)^3}{96\eta} \cdot \frac{\Delta c}{\Delta a} \tag{11}$$

$$K = (h_c + h_d - h_a - h_b) \cdot (U + V_T) \cdot \frac{\Delta a}{4} - V_N \cdot \Delta a \cdot \Delta c \tag{12}$$

In Eq (12) the terms V_T and V_N are the components of journal axis lateral velocity tangential and normal to the surface at the element centre. These may be calculated from:

$$V_N = -[V_y(I)\cos\theta + V_x(I)\sin\theta] \tag{13}$$

$$V_T = V_y(I)\sin\theta + V_x(I)\cos\theta \tag{14}$$

The journal axis lateral velocity is expressed as vertical and horizontal components which are a function of axial position for a journal subject to angular velocity of its axis:

$$V_y(I) = \dot{\gamma}\,\frac{L}{2}\left[1 - \frac{2}{N_a}(I - 0.5)\right] + \dot{y} \tag{15}$$

$$V_x(I) = \dot{\lambda}\,\frac{L}{2}\left[1 - \frac{2}{N_a}(I - 0.5)\right] + \dot{x} \tag{16}$$

Where an element is adjacent to a specified oil film boundary, (eg oil supply groove, bearing ends) the appropriate adjacent element pressure in Eq (7) is replaced by the specified boundary pressure. The corresponding pressure flow function value must then be multiplied by 2 since the pressure gradient is determined over half the relevant element dimension.

A clearer understanding of the above analysis may be gained by considering the following points:

- H_{ci} and H_{co} are functions which yield the upstream and downstream circumferential element pressure-induced flow rates respectively, when multiplied by the appropriate differential pressures. Strictly speaking the terms upstream and downstream in this context are arbitrary, and where reversal of the flow is encountered, the sign of the computed flow automatically changes.
- H_{ai} and H_{ao} are similarly related to the axial pressure-induced flow rates.
- K represents the nett circumferential flow out of the element induced by the velocity of the journal surface. As shown in Fig 2(a), the velocity of the journal surface comprises U due to the journal rotational speed and V_T due to the lateral velocity of the journal in direction tangential to the element centre, and V_N is the component of journal lateral velocity normal to the element centre.

Cavitation model

Where cavitation is present, the lubricant flow rates across the circumferential boundaries of an element may be reduced by the gas/vapour flow rate terms Q_{vi}, Q_{vo}. In these conditions the nett lubricant flow rates across the upstream and downstream boundaries are thus $Q_{ci} - Q_{vi}$ and $Q_{co} - Q_{vo}$, respectively. Derivation of Q_{vi} and Q_{vo} to satisfy continuity within the cavitation zone is as follows:

For any element, when Eq (7) predicts a pressure below the specified cavitation pressure (ie $P < P_c$), the predicted pressure is ignored and the element centre pressure is made equal to P_c. It should be noted that Eq (7) is based on the assumption that Q_{vo} is zero and that $P \geqslant P_c$, ie a full lubricant film at the element circumferential downstream boundary is assumed. Where substitution of P_c for P becomes necessary the above assumptions for Eq (7) are invalidated. Since this situation clearly indicates the presence of cavitation, it is postulated that continuity may be satisfied with $P = P_c$ by determining a finite value for Q_{vo}. For the circumferentially adjacent element in the downstream direction, the value of Q_{vi} will thus be equal to the above Q_{vo}, ie $Q_{vi}(J+1, I) = Q_{vo}(J, I)$. In general, when applying Eq (7), Q_{vi} is assumed to be zero unless a finite Q_{vo} has been calculated for the upstream circumferentially adjacent element. Where the $P = P_c$ substitution is made the value of Q_{vo} required to maintain continuity is calculated from:

$$Q_{vo} = K + Q_{vi} - (H_{ci}P_{ci} + H_{ai}P_{ai} + H_{co}P_{co} + H_{ao}P_{ao}) + P_c(H_{ci} + H_{ai} + H_{co} + H_{ao}) \qquad (17)$$

Solution technique

Solution of the film pressure matrix is achieved by application of Eq (7) to each element using the Gauss–Seidel relaxation process with successive over relaxation. The computation flow diagram for this solution is shown in Fig 3. Cavitation zone boundaries are automatically determined in this process. No detailed study of the optimum over relaxation factor (orf) has been carried out, but a value of 1.7 was found to give the minimum number of iterations in a limited range of tests.

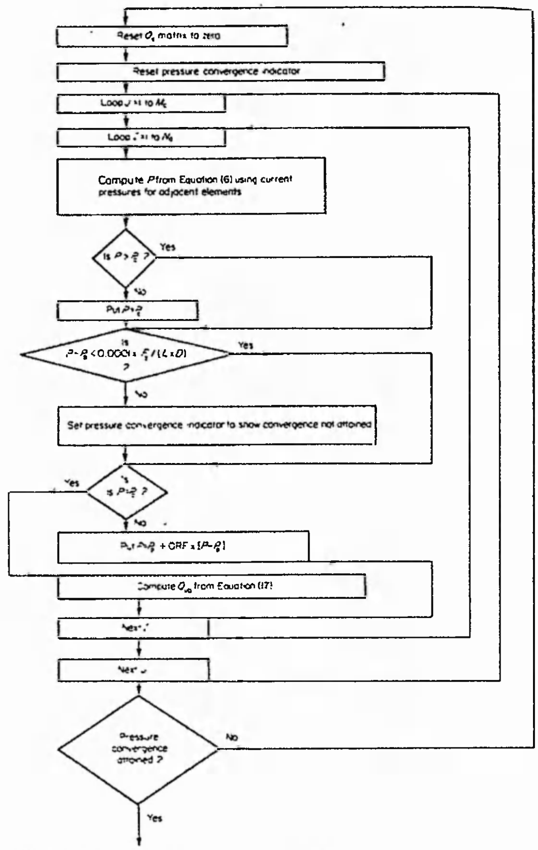

Fig 3 Film pressure solution procedure

Having determined the film pressure matrix, the total oil film force and moment vertical and horizontal components may be calculated by summation of the corresponding force and moment components for each element. To derive the oil film force on each element, the mean pressure is calculated from:

$$P_{mean} = \frac{4P + P_1 + P_2 + P_3 + P_4 + P_5 + P_6 + P_7 + P_8}{12} \qquad (18)$$

where P_1 to P_8 are the pressures at each corner of the element and at the centre of each boundary, as shown in Fig 2(c). These pressures are calculated from the linear pressure gradients to the adjacent elements or oil film boundaries, ie using the J, I element reference system:

$$P_1 = [P(J, I) + P(J-1, I-1)]/2$$

$$P_2 = [P(J, I) + P(J, I-1)]/2 \quad \text{etc.}$$

Flow rate

Once the film pressure matrix has been determined, the flow rate across any element boundary may be readily calculated from:

$$Q_{ci} = (h_a + h_b)\,U\,\frac{\Delta a}{4} - H_{ci}(P - P_{ci}) \qquad (19)$$

and

$$Q_{ai} = -H_{ai}(P - P_{ai}) \qquad (20)$$

A.4. – 6.

Similar equations for Q_{co} and Q_{ao} may be written, but with the exception of boundaries at $J = M_c$ and $I = N_a$, respectively, calculation of these values would simply duplicate the respective Q_{ci} and Q_{ai} values for the corresponding 'downstream' elements.

Power loss

Power loss is computed by summating the circumferential viscous shear force applied to the journal by each element. For this purpose, the circumferential shear stress on each element is calculated as the mean value of the shear stress at the circumferential boundaries. This results in:

$$F_c = U\,\Delta c\,\eta\left[\frac{B_{ai}}{h_a + h_b} + \frac{B_{ao}}{h_c + h_d}\right] + [(h_a + h_b)(P - P_{ci}) + (h_c + h_d)(P_{co} - P)]\,\Delta a/8 \qquad (21)$$

$$H = U\sum_{J=1,\,I=1}^{J=M_c,\,I=N_a} F_c \qquad (22)$$

where

$$B_{ai} = \Delta a - \frac{4Q_{vi}}{U(h_a + h_b)} \qquad (23)$$

and

$$B_{ao} = \Delta a - \frac{4Q_{vo}}{U(h_c + h_d)} \qquad (24)$$

B_{ai} and B_{ao} are the effective widths of the oil stream entering and leaving the element respectively, and will clearly be equal to the full width of the element Δa where no cavitation is present. For elements adjacent to a specified bearing oil film boundary, the appropriate pressures in Eq (21) are equated to the boundary pressure, and a factor of 2 is introduced to produce the correct pressure gradient. This process is similar to the corresponding modification of the film pressure Eq (7). It may be noted that in the right hand side of Eq (21), the expression:

$$U\,\Delta c\,\eta\left[\frac{B_{ai}}{h_a + h_b} + \frac{B_{ao}}{h_c + h_d}\right]$$

represents the shear force due to surface velocity-induced flow. The expression $[(h_a + h_b)(P - P_{ci}) + (h_c + h_d) \times (P_{co} + P)]\ \Delta a/8$ is the shear force due to pressure-induced flow, and clearly falls to zero in the cavitation zone.

Element grading

The above equations are for a constant element size. Smaller elements are desirable in areas where large changes in film pressure gradient occur. Straight forward modification of the equations may be introduced to vary the element dimensions in either the circumferential or axial directions. Grading of the element dimensions enables better modelling in areas of rapid change of film pressure gradient, without incurring a large increase in computing time. Lloyd *et al*[5] introduced circumferential grading in their finite difference solution of Reynolds equation by making the circumferential mesh length a function of film thickness. Where misalignment is present, circumferential grading becomes difficult due to variation in the circumferential position of minimum film thickness along the bearing axis. For heavy misalignment, axial grading is preferred, and the author has recently introduced this in his work on sterntube bearings. This has been achieved by making the element axial dimension increase as a linear function of the element column number (I) from the bearing left hand end to the centre, and in a similar symmetrical manner from the centre to the right hand end. A grading factor is defined as the ratio of axial element length for uniform size, to that of elements adjacent to the bearing ends, with grading and the same number of element columns.

Dynamic coefficients

To calculate oil film displacement and velocity coefficients, incremental displacements and velocities are applied to the journal. The film pressure relaxation and element force component summation subroutines are then repeated to determine the corresponding change in the oil film force and moment components. This is a quasi-static process and neglects the 'oil film history' effects outlined by Jones[6]. Since the displacement and velocity increments used are small, errors arising from the above procedure should be insignificant.

The terms displacement and velocity coefficient are alternatives to the commonly used 'stiffness' and 'damping coefficients'. Oil films exhibit a high degree of nonlinearity, use of 'stiffness' and 'damping coefficient' can therefore be misleading. In view of the nonlinearity, some workers[2,7] have adopted the terms displacement and velocity coefficient and have defined them with respect to zero amplitude. For computational purposes, finite amplitudes (incremental) must clearly be used, and must be large enough to produce a significant force or moment change in relation to the force and moment resolution accuracy of the numerical solution. To meet this requirement, and still obtain the best approximation to a 'zero' amplitude coefficient, the author uses equal positive and negative increments, and takes the mean value of the coefficients thus derived. This technique also facilitates computation of the coefficient gradients with respect to amplitude. These gradients are even more sensitive to force and moment resolution accuracy, and their practical usefulness is questionable.

Where dynamic misalignment conditions exist, 32 displacement and velocity coefficients are required:

$$\begin{bmatrix} F_y \\ F_x \\ M_y \\ M_x \end{bmatrix} = \begin{bmatrix} A_{yy} & A_{yx} & B_{yy} & B_{yx} & A_{y\gamma} & A_{y\lambda} & B_{y\gamma} & B_{y\lambda} \\ A_{xy} & A_{xx} & B_{xy} & B_{xx} & A_{x\gamma} & A_{x\lambda} & B_{x\gamma} & B_{x\lambda} \\ A_{\gamma y} & A_{\gamma x} & B_{\gamma y} & B_{\gamma x} & A_{\gamma\gamma} & A_{\gamma\lambda} & B_{\gamma\gamma} & B_{\gamma\lambda} \\ A_{\lambda y} & A_{\lambda x} & B_{\lambda y} & B_{\lambda x} & A_{\lambda\gamma} & A_{\lambda\lambda} & B_{\lambda\gamma} & B_{\lambda\lambda} \end{bmatrix} \times \begin{bmatrix} y \\ x \\ \dot{y} \\ \dot{x} \\ \gamma \\ \lambda \\ \dot{\gamma} \\ \dot{\lambda} \end{bmatrix} \qquad (25)$$

Practical analysis program

In the above analysis technique it is necessary to specify journal eccentricity as input and to derive journal load as output data. The author's analysis iterates film viscosity to meet a specified load, and where a specified load direction is required (usually vertical), the attitude angle is iterated accordingly. This was found to be necessary since the performance is dependent upon the specified film boundary pressure, due to the influence of this parameter

A.4. -7.

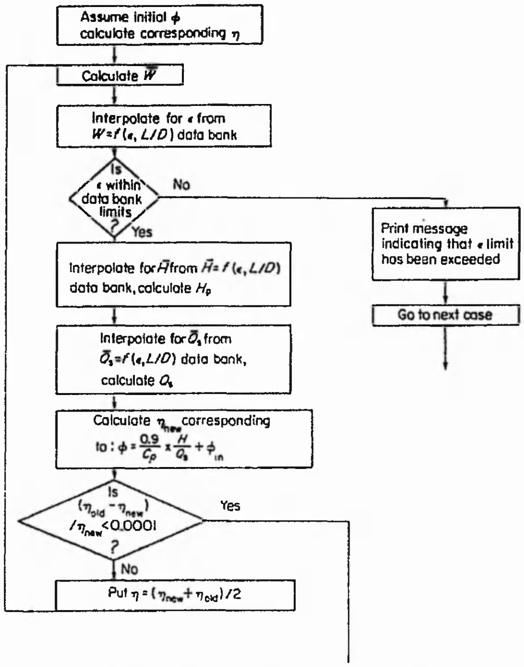

Fig 4 Practical analysis program. ϕ *= lubricant temperature,* $\overline{W} = (F_y/LD\eta N)(C_d/D)^2$, $\overline{H} = HC_d/\eta N^2 LD^3$, $\overline{Q}_s = Q_s L^2 \eta/C_d^3 F_y$, $\epsilon = 2e/C_d$, $C \cdot p$ *= lubricant specific heat* x *density*

on the extent of the cavitation zone. To generalize the data relating to this aspect of bearing performance, the boundary pressure was rendered dimensionless by division by the specific bearing pressure. The facility for specifying the journal load was therefore necessary to produce data for specified dimensionless boundary pressures.

Despite such refinements, the fact that journal eccentricity has to be specified as input data renders such a program unsuitable for practical analysis purposes. The main use of the above program is therefore to generate dimensionless performance data for building a data bank upon which a practical analysis program can be based. Such a program has been developed by the author for sterntube bearings and involves an iterative process in which the effective film viscosity is determined by the assumption that a fixed proportion of the heat generated is carried away by the oil. Operation of the program is thus essentially similar to the analysis method given in Ref 8 and is shown by the flow diagram in Fig 4.

Comparison with other data

The author has carried out several analyses of aligned 360° circumferential groove crankshaft bearings, for comparison with experimental and theoretical displacement and velocity coefficients derived by Parkins[2]. This has involved computing the usual eight displacement and velocity coefficients (relevant to bearings not subject to steady or dynamic misalignment) for both 'zero' amplitude and a range of finite amplitudes. Parkins' theoretical work incorporated a finite difference solution of Reynolds equation with the oil film viscosity varying as a function of temperature and pressure. Good agreement with the author's results was obtained[1].

Parkins[7] has also presented both experimental and theoretical data for the steady load performance of 360° circumferential groove bearings, covering both variable viscosity and isoviscous assumptions. Eight cases have been run for comparison with Parkins' isoviscous theoretical data, and the results presented in Table 1. It should be noted that Parkins adjusted his values of viscosity and cavitation pressure to obtain agreement between measured and theoretical load and attitude angle. In this paper the same values of viscosity and cavitation pressure have been used as input data.

The predicted extent of the cavitation zone for a 360° circumferential groove bearing is shown in Fig 5. This illustrates the effects of supply pressure variation, and includes comparitive theoretical data obtained by private communication with Mr F.A. Martin of the Glacier Metal Co Ltd. The Glacier results were obtained using a 72 circumferential x 15 finite difference mesh for each half of the bearing, while the present author used 72 x 14 elements.

For steadily loaded misaligned sterntube bearings, four

Table 1 Comparison of crankshaft bearing results with data in Ref 7

Case	Common input data					Parkins*		Jakeman	
	ϵ	C_d, mm	r/min	η, N s/m²	P_c, N/mm² (gauge)	W, N	ψ°	W, N	ψ°
1	0.790	0.0909	1180	0.04470	−0.0069	670.2	38.70	683.2	39.28
2	0.864	0.0941	1180	0.04139	−0.0965	1341.2	30.60	1352.0	31.59
3	0.869	0.0900	2200	0.01883	−0.1719	1285.2	31.84	1323.9	33.16
4	0.902	0.0952	1500	0.02897	−0.0896	2219.2	24.00	2212.0	24.84
5	0.917	0.0936	2900	0.01069	−0.2136	2230.3	23.30	2182.2	24.49
6	0.926	0.0968	1500	0.02414	−0.0413	3120.3	19.60	3044.6	20.29
7	0.930	0.0983	2200	0.01552	0	3125.0	18.70	3091.5	19.15
8	0.942	0.1003	2900	0.008794	−0.1171	3113.2	18.00	3089.6	18.63

Bearing data: Diameter · 63.5 mm; overall length = 23.68 mm; groove width = 5.08 mm (360° circumferential in bearing axial centre); supply pressure = 0.2067 N/mm²

**Table 10 of Ref 7 calculated data*

A.4. - 8.

cases have been computed for comparison with theoretical data presented by Pinkus and Bupara[9]. These results are given in Table 2 together with results given by Martin in the discussion of the above paper. It should be noted that all moments are positive for consistency with the author's sign convention. A further misaligned sterntube bearing case has been produced for comparison with the theoretical example given by Hill and Martin[10]. These data are shown in Table 3.

The above details show the theoretical results presented here to be in good agreement with published and other data derived by finite difference solutions of Reynolds equation.

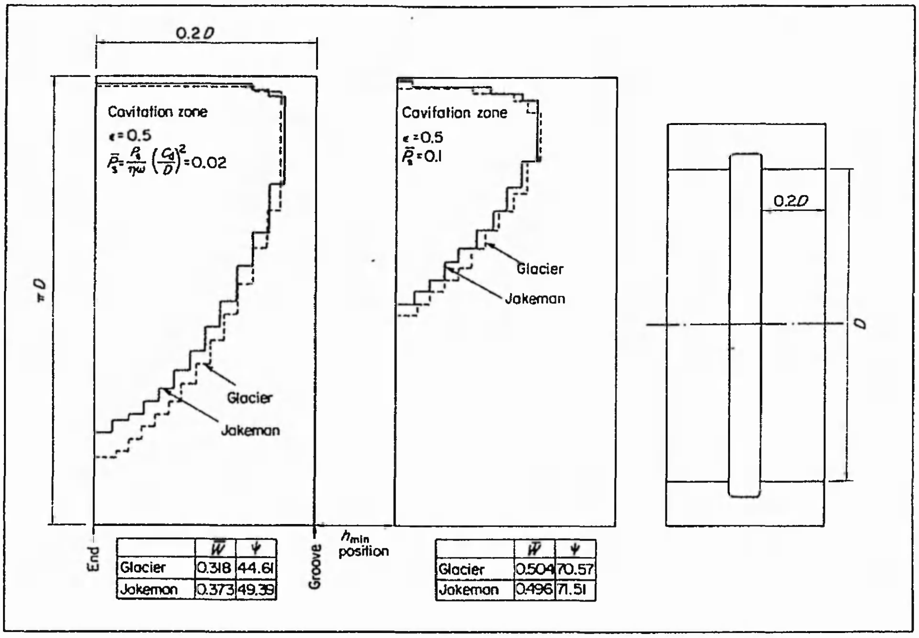

Fig 5 Comparison of predicted cavitation zones

Table 2 Comparison of sterntube bearing results with examples in Ref 9

		Case 1	Case 2	Case 3	Case 4
Load vector angle	Pinkus & Bupara	3°	1°	0°	2°
	Jakeman	3.4°	0.9°	0.3°	1.8°
Dimensionless parameters					
Eccentricity ratio	All	0.4	0.4	0.8	0.8
Load	Pinkus & Bupara	3.56	4.13	22.3	26.5
	Martin	3.56	4.13	22.3	26.5
	Jakeman	3.60	4.29	22.5	27.35
Vertical moment	Pinkus & Bupara	0.26	0.55	1.67	3.56
	Martin	0.27	0.58	1.5	3.2
	Jakeman	0.261	0.589	1.698	3.826
Minimum film thickness	Pinkus & Bupara	0.33	0.14	0.10	0.04
	Martin	0.34	0.15	0.105	0.05
	Jakeman	0.334	0.137	0.10	0.041
Vertical journal slope	Pinkus & Bupara	0.37	0.59	0.10	0.04
	Martin	0.37	0.59	0.10	0.16
	Jakeman	0.369	0.591	0.112	0.179

Bearing with 2 axial grooves subtending 30° are each at 90° and 270° from top; $L/D = 1$

A.4.-9.

Table 3 Comparison of sterntube bearing results with example in Ref 10

	Hill and Martin	Jakeman
Misalignment (vertical), rad	0.0002	0.0002
Min. film thickness, mm	0.123	0.123
Load, N	768 000	770 150
Moment, N mm	6.451×10^7	6.591×10^7

Bearing data: 800 mm diameter x 1200 mm long; 1.4 mm diametral clearance; 80 r/min. Axial grooves at ± 90° from top; film viscosity 0.125 N s/m^2

Further development

Where substantial journal amplitudes are involved, the adequacy of displacement and velocity coefficients is doubtful in view of their nonlinearity. For such conditions a journal orbit analysis is more appropriate. The numerical analysis method described in this paper can be readily adapted for use in this type of analysis. It is considered important, however, that the oil film history concept[6] should be incorporated. Since the author's approach is based directly upon continuity considerations, application of oil film history should be quite straight forward.

Considering oil flow through the cavitation zone, the oil flow will be purely circumferential since it is entirely due to journal surface velocity (with the exception of axial element boundaries at pressures differing from the cavitation pressure). It follows then, that in a steady state condition, the circumferential oilflow rate through a column of elements is constant throughout the cavitation zone. The flow rate through the cavitation zone is therefore mainly dictated by the film thickness at the upstream boundary. In a dynamic situation the film thickness at the upstream cavitation zone boundary will vary, thus the flow rate through the cavitation zone will be subject to a corresponding variation. Consider a small quantity of oil which passes the upstream cavitation zone boundary at axial position I and time $t1$ and subsequently passes element J, I at time $t2$. The flow rate through element J, I at time $t2$ is thus determined by the film thickness at the upstream cavitation zone boundary at axial position I and time $t1$.

No work involving variable viscosity oil films or elastohydrodynamic situations has been carried out and no special problems are envisaged in applying the analysis technique described in this paper to such areas. For any particular application, the justification for the substantial additional complexity of variable viscosity and elastohydrodynamics should be carefully weighed.

Conclusions

This paper presents a numerical analysis method which is essentially simple yet has demonstrated a perfectly acceptable standard of accuracy for practical purposes. More sophisticated analytical techniques undoubtedly exist, but the simplicity of this method should enable a much clearer understanding to be attained of the way in which the physical processes are being modelled.

It is the author's view that the most difficult part of any analytical work is in conceiving the nature of the physical processes involved. Developing a mathematical model for these processes is, or should be, the simpler part of the problem. The method advocated in this paper should enhance the 'feel' for the physical processes by avoiding undue mathematical complexity.

Appendix

Derivation of equations

Film pressures: For laminar flow conditions and assuming that the rectangular film elements are sufficiently small to consider the bearing and journal surfaces as parallel flat plates, the flow rates across the element boundaries may be expressed as:

Circumferential direction

$$h\,\Delta a\,\frac{U}{2} - h\,\Delta a\,\frac{h^2}{12\eta}\,\frac{\partial P}{\partial c}$$

Axial direction

$$-h\,\Delta c\,\frac{h^2}{12\eta}\,\frac{\partial P}{\partial a}$$

Assuming linear pressure gradients between the centre of the element under consideration and the centres of the axially and circumferentially adjacent elements, the flow rates across the four element boundaries may be written thus:

$$Q_{ci} = (h_a + h_b)(U + V_T)\,\Delta a/4 - H_{ci}(P - P_{ci})$$

$$Q_{ai} = -H_{ai}(P - P_{ai})$$

$$Q_{co} = (h_c + h_d)(U + V_T)\,\Delta a/4 - H_{co}(P_{co} - P)$$

$$Q_{ao} = -H_{ao}(P_{ao} - P)$$

Note that the tangential component of the journal axis velocity V_T has been added to the journal surface velocity due to rotation U. In addition, the viscous flow functions H_{ci}, etc., have been incorporated, these being based upon the mean film thickness for the boundaries concerned.

The continuity equation assuming the lubricant to be incompressible is:

$$Q_{ci} + Q_{ai} + V_N\,\Delta c\,\Delta a - Q_{vi} = Q_{co} + Q_{ao} - Q_{vo}$$

The component of the journal axis velocity normal to the surface at the element centre V_N is assumed to be the effective mean value for the element. The terms Q_{vi} and Q_{vo} represent the circumferential flow rates of gas or vapour across the upstream and downstream element boundaries respectively, the density of which is assumed to be negligible relative to the liquid phase of the lubricant.

Substituting the expressions for Q_{ci} etc., into the continuity equation we have:

$$(h_a + h_b)(U + V_T)\,\Delta a/4 - H_{ci}(P - P_{ci}) - H_{ai}(P - P_{ai})$$
$$+ V_N\,\Delta c\,\Delta a - Q_{vi} = (h_c + h_d)(U + V_T)\,\Delta a/4$$
$$- H_{co}(P_{co} - P) - H_{ao}(P_{ao} - P) - Q_{vo}$$

Substituting for the nett velocity-induced flow rate K, this reduces to:

$$-H_{ci}(P - P_{ci}) - H_{ai}(P - P_{ai}) - Q_{vi}$$
$$= K - H_{co}(P_{co} - P) - H_{ao}(P_{ao} - P) - Q_{vo}$$

During the film pressure relaxation process it is initially assumed that for each element $P > P_c$, and consequently that $Q_{vo} = 0$.

One may therefore solve for P by re-arranging this equation to:

$$P = \frac{H_{ci}P_{ci} + H_{ai}P_{ai} + H_{co}P_{co} + H_{ao}P_{ao} - K - Q_{vi}}{H_{ci} + H_{ai} + H_{co} + H_{ao}}$$

If the above equation results in $P < P_c$ then P is made equal to P_c and the continuity equation now becomes:

$$- H_{ci}(P_c - P_{ci}) - H_{ai}(P_c - P_{ai}) - Q_{vi}$$
$$= K - H_{co}(P_{co} - P_c) - H_{ao}(P_{ao} - P_c) - Q_{vo}$$

Thus a finite Q_{vo} may be determined to satisfy continuity with $P = P_c$ from:

$$Q_{vo} = K + Q_{vi} - (H_{ci}P_{ci} + H_{ai}P_{ai} + H_{co}P_{co} + H_{ao}P_{ao}) + (H_{ci} + H_{ai} + H_{co} + H_{ao})P_c$$

Power loss: To calculate power loss it is necessary to determine the tangential force exerted by each element on the journal surface in the circumferential direction. The viscous shear stresses from which the above force may be derived are: $\eta U/h$ due to surface velocity and $(h/2)\,\partial P/\partial c$ due to the pressure gradient. With the element configuration adopted, these viscous shear stresses may only be calculated at the element boundaries. The viscous shear stress for the complete element is therefore taken as the mean value for the two circumferential boundaries:

$$\tau = \frac{1}{2}\left[\frac{2\eta U}{h_a + h_b} + \frac{2\eta U}{h_c + h_d}\right] + \frac{1}{2}\left[\frac{1}{2}\left(\frac{h_a + h_b}{2}\right)\left(\frac{P - P_{ci}}{\Delta c}\right) + \frac{1}{2}\left(\frac{h_c + h_d}{2}\right)\left(\frac{P_{co} - P}{\Delta c}\right)\right]$$

$$\therefore\ \tau = \eta U\left[\frac{1}{h_a + h_b} + \frac{1}{h_c + h_d}\right] + \left[\frac{(h_a + h_b)(P - P_{ci}) + (h_c + h_d)(P_{co} - P)}{8\,\Delta c}\right]$$

Where a full film exists:

$$F_c = \tau\,\Delta a\,\Delta c$$

Where cavitation exists, however, it is assumed that the lubricant and gas/vapour form discrete streams of rectangular cross section. Δa is thus effectively reduced to B_{ai} and B_{ao} at the upstream and downstream circumferential boundaries respectively, where:

$$B_{ai} = \Delta a - \frac{4Q_{vi}}{U(h_a + h_b)}$$

$$B_{ao} = \Delta a - \frac{4Q_{vo}}{U(h_c + h_d)}$$

Since the pressure gradient terms in the equation for τ automatically became zero in the cavitation zone, no modification of Δa with respect to these terms is necessary, therefore we may write:

$$F_c = \eta U \Delta c\left[\frac{B_{ai}}{h_a + h_b} + \frac{B_{ao}}{h_c + h_d}\right] + [(h_a + h_b)(P - P_{ci}) + (h_c + h_d)(P_{co} - P)]\,\Delta a/8$$

Power loss may then be calculated by summating the above tangential forces and multiplying by the journal surface velocity:

$$H = U \sum_{J=1,\,I=1}^{J=M_c,\,I=N_a} F_c$$

Acknowledgements

The author wishes to express his gratitude to the Committee of Lloyd's Register of Shipping for permission to publish this paper. In addition the author is indebted to Dr. C. Y. Choi (Coventry (Lanchester) Polytechnic), Mr F. A. Martin (The Glacier Metal Co. Ltd.), Dr. D. W. Parkins (Cranfield Institute of Technology) and Mr D. Rennie O.B.E. (Lloyd's Register of Shipping) for their helpful discussions and comments on this paper.

References

1. Parkins D.W. and Jakeman R.W. A comparison of oil film coefficients from experimental and two theoretical methods *(to be published)*
2. Parkins D.W. Theoretical and experimental determination of the dynamic characteristics of a hydrodynamic journal bearing. *ASME: J. Lubr. Technol., April 1979,* **101**, *129*
3. McCallion H., Lloyd T. and Yousif F.B. The influence of oil supply conditions on the film extent and oil flow in journal bearings. *Proc. Inst. Mech. Eng., 1971*
4. Vorus W.S. and Gray R.L. Calculations of sterntube bearing eccentricity distributions: Applications in States Lines Ro/Ro bearing failure analysis. *Conf. on Oper. Aspects of Propulsion Shafting Systems. Inst. Mar. Eng., May 1979, Paper C37, 92*
5. Lloyd T., Horsnell R. and McCallion H. An investigation into the performance of dynamically loaded journal bearings: Theory. *Proc. Inst. Mech. Eng., 1966–67,* **181**, *Pt. 3B, 1*
6. Jones G.J. Crankshaft bearings: Oil film history. *9th Leeds-Lyon Tribology Symp., September 1982 (Butterworths, Borough Green, UK)*
7. Parkins D.W. Static and dynamic characteristics of an hydrodynamic journal bearing. *Cranfield Inst. Technol. PhD Thesis, May 1976*
8. Engineering Science Data Unit, *Item No 66023* Steadily loaded hydrodynamic journal bearings. *September 1966*
9. Pinkus O. and Bupara S.S. Analysis of misaligned grooved journal bearings. *ASME: J. Lubr. Technol., October 1979,* **101**, *503–509. Discussion: April 1980,* **102**, *257–260*
10. Hill A. and Martin F.A. Some considerations in the design of sterntube bearings and seals. *Trans. Inst. Mar. Eng. (C), May 1979,* **91**, *Conference No 4, Paper C39*

A.4.- 11.

4th International Conference on
Numerical Methods in Laminar and Turbulent Flow.
University College of Swansea. July 9th-12th 1985.

REFERENCE. 77.

JOURNAL ORBIT ANALYSIS TAKING ACCOUNT OF OIL FILM HISTORY AND JOURNAL MASS.

R.W. Jakeman.

Senior Surveyor,
Lloyd's Register of Shipping,
London.

SUMMARY.

This paper describes a journal orbit analysis for dynamically loaded hydrodynamic journal bearings operating with laminar flow. A time stepping procedure is used, with oil film forces and displacement and velocity coefficients computed at each step by means of a numerical analysis method [1]. The journal orbit analysis is based on the solution of equations of motion, representing the mean conditions during each time step. Computational strategies are described, whereby the effects of oil film non-linearity are minimised. At low journal mass, predicted journal orbits for a half circumferential groove crankshaft bearing of a 4-stroke cycle petrol engine are in reasonable agreement with those by Jones [2] for zero journal mass. The indicated significance of journal mass is consistent with the work by Holmes and Craven [3]. A degree of interaction between the effects of journal mass and oil film history is shown.

NOMENCLATURE.

a	Axial length of oil film elements.
A_{xx}, etc	Oil film displacement coefficients.
B_{xx}, etc	Oil film velocity coefficients.
C_r	Radial clearance.
$C_{av}(j,i)$	Cavitation indicator for element j,i.
F_x, F_y	Horizontal, vertical oil film forces at t *
F_{ex}, F_{ey}	Horizontal, vertical external forces at t *
$h\ (j,i)$	Film thickness at upstream boundary of element j,i.
j,i	Circumferential, axial element position reference
m	Journal mass.
$p\ (j,i)$	Film pressure at element j, i centre.

$q_v(j,i)$	Upstream boundary gas/vapour volume flow rate.
$q_n(j,i)$	Nett oil volume flow rate into element j,i.
t	Time at start of time step.
u	Journal surface velocity due to rotation *
$V_e(j,i)$	Total volume of element j,i.
$V_o(j,i)$	Volume of oil in element j,i.
x,y	Horizontal, vertical journal displacement at t *
$\dot{x},\dot{y}$	Horizontal, vertical journal velocity at t *
$\ddot{x},\ddot{y}$	Horizontal, vertical journal acceleration at t
$\Delta c,\Delta r$	Circumferential, radial displacement increment limits.
$\Delta\dot{c},\Delta\dot{r}$	Circumferenital, radial velocity increment limits
Δt	Time step increment.
ε	Eccentricity ratio (Journal eccentricity/C_r)

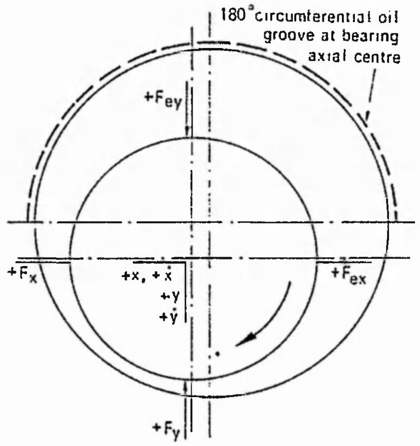

Fig 1 Force, Displacement and Velocity Sign Convention

Suffix Δ denotes conditions at $t + \Delta t$,
* Sign convention is indicated in Fig.1.
Consistent SI units are used throughout.

1. INTRODUCTION.

1.1 Significance of Journal Amplitude.

Dynamically loaded hydrodynamic journal bearings may be divided into two categories:
(a) Bearings in which a relatively small dynamic load component is superimposed upon a steady load; e.g. turbo-generator bearings with out-of-balance forces.
(b) Bearings having a dominant dynamic load such that any mean component is insignificant; e.g. crankshaft bearings.

Provided the journal displacement amplitudes are small in relation to the bearing clearance, the response of type (a) may be predicted by linearized oil film displacement and velocity coefficients (collectively referred to as dynamic coefficients). Amplitude limitations to the application of this approach due to the non-linearity of the dynamic coefficients, are not clearly defined, and depend upon the kind of information required, i.e. journal amplitude prediction is more critical than resonant lateral vibration frequency prediction.

In the second type of dynamically loaded bearing, large journal amplitudes combined with the high degree of non-linearity of the dynamic coefficients has led to use of the time stepping journal orbit analysis. This type of analysis generally requires a substantial amount of computation, and various approximations and assumptions have been adopted in order to minimise the computing time.

1.2 Journal Mass.

In a dynamically loaded bearing, the externally applied load is opposed by the force required to accelerate the effective mass of the journal, and the oil film forces arising from hydrodynamic and squeeze film action. At present, the more rigorous bearing analyses consider such bearings in isolation from the adjacent shaft - bearing system. In this approach, the extent of the adjacent shafting, crankwebs, flywheel, etc., which contribute to the effective journal mass, cannot be clearly defined. Ideally, all the bearings in a given shafting system should be analysed interactively with analysis of the shafting lateral motion, taking account of the shaft mass-elastic distribution. For a rigorous bearing analysis, such a comprehensive treatment is beyond the current state of the art.

1.3 Oil Film History.

The oil film history concept takes account of the fact that at any point in a dynamic load cycle, the extent of cavitation is dependent upon the history of the oil film. Where a quasi-steady film pressure solution is carried out at each step point, the extent of cavitation predicted may be substantially less than that derived by an oil film history solution. Modelling oil film history essentially comprises the continuous monitoring of the extent of cavitation and the volumetric distribution of oil within cavitation zones.

1.4 Brief Review of Previous Work.

The following is a very limited review of a few of the more significant papers on journal orbit analysis: Booker [4] presented a fast solution referred to as the Mobility method. The Mobility number is essentially the inverse of velocity coefficient. Computational speed is attained by utilising mobility data previously derived by theory or experiment. This method is theoretically, only applicable to circumferentially uniform bearings.

Holmes and Craven [3] investigated the influence of journal mass using the short bearing approximation to achieve a fast solution of Reynold's equation. A dimensionless parameter β was presented which indicated the significance of journal mass.

Jones [2] examined the effect of oil film history using a finite difference solutions of Reynold's equation, thereby taking account of oil feed features. The effect of oil film history was illustrated for bearings having a single oil hole, a half circumferential groove, and a full circumferential groove. This showed the significance of oil film history to be inversely related to the efficiency of the oil feed arrangement. Journal mass was neglected in this work.

Smith [5] investigated the effect of a variable viscosity oil film model. This allowed viscosity variation in the circumferential direction only, and assumed adiabatic conditions. The short bearing approximation for the solution of Reynold's equation was used to obtain fast computation. Results obtained did not indicate any significant difference from those given by a constant effective viscosity model. Journal mass was taken into account in this work, but its effect was not specifically investigated.

LaBouff and Booker [6] examined the effect of bearing elasticity using a finite element model. Elasticity was shown to be significant, but excessive computing time restricted this work to transient solutions not exceeding 200° of crank rotation.

In general, the fast solutions may produce results with substantial inaccuracies, in absolute terms, when compared with the more rigorous methods. They are nevertheless useful in predicting trends arising from changes in parameters such as journal mass. In addition, their low computing time makes some fast solutions attractive for practical application as design comparators, provided they are backed up by adequate test and service experience.

1.5 Objectives of this Work.

The foregoing review indicates the definitive journal orbit analysis to lie in the future, with progress dependent upon computer development. In this investigation, the writer has examined the effects of both journal mass and oil film history, using a finite bearing film pressure solution. This paper therefore brings together the previous work by Holmes and Craven [3] and Jones [2]. A rigorous analysis of the type described in this paper is considered to be unsuitable for routine practical application due to the computing time required, but it represents a standard against which the adequacy of faster, more approximate, analyses may be judged. Furthermore it can give a clearer insight into the causal factors related to bearing behaviour, and thereby provide a rational basis for design improvement.

2. THEORETICAL ANALYSIS.

2.1 Film Pressure Solution.

A numerical analysis method based on flow continuity [1] was used to derive the oil film pressure distribution and the resultant force components. The assumptions used are as given in the above reference the more noteworthy ones being: laminar flow; rigid circular bearing and journal surfaces; isoviscous oil film and a specified constant cavitation pressure (usually atmospheric). In addition, for this investigation, the journal and bearing axes were assumed to remain parallel at all times.

2.2 Time Step Equations.

Horizontal and vertical components of external force F_{ex}, F_{ey} were specified at intervals throughout the load cycle. The magnitude of the above intervals must be consistent with accurate determination of forces within them by linear interpolation (e.g. 10° crank angle intervals in the four stroke cycle test case used). Details of journal and bearing dimensions, rotational speed and oil viscosity complete the input data.

In the time stepping procedure, journal displacement and velocity components at the current time t $(x, y, \dot{x}, \dot{y})$ will be known, and the corresponding oil film force components F_x, F_y may be computed. The corresponding values after time step Δt must then be predicted. External force components F_{ex}, F_{ey} at t and $F_{ex\Delta}$, $F_{ey\Delta}$ at $t + \Delta t$ may be interpolated from the specified external load cycle data, thus the unknowns at $t + \Delta t$ are: x_Δ, y_Δ, $\dot{x}_\Delta$, $\dot{y}_\Delta$, $F_{x\Delta}$, $F_{y\Delta}$. These may be solved from the following 6 equations:

$$(F_{ex} - F_x + F_{ex\Delta} - F_{x\Delta})/2 = m\,(\dot{x}_\Delta - \dot{x})/\Delta t \qquad \ldots\ldots\ldots\ldots..(1)$$

$$(F_{ey} - F_y + F_{ey_\Delta} - F_{y\Delta})/2 = m\,(\dot{y}_\Delta - \dot{y})/\Delta t \qquad \ldots\ldots\ldots\ldots..(2)$$

$$F_{x\Delta} = F_x + A_{xx}(x_\Delta - x) + A_{xy}(y_\Delta - y) + B_{xx}(\dot{x}_\Delta - \dot{x}) + B_{xy}(\dot{y}_\Delta - \dot{y}) \qquad \ldots\ldots..(3)$$

$$F_{y\Delta} = F_y + A_{yy}(y_\Delta - y) + A_{yx}(x_\Delta - x) + B_{yy}(\dot{y}_\Delta - \dot{y}) + B_{yx}(\dot{x}_\Delta - \dot{x}) \qquad \ldots\ldots..(4)$$

$$x_\Delta - x = (2\dot{x} + \dot{x}_\Delta)\,\Delta t/3 + \ddot{x}\,.\,(\Delta t)^2/6 \qquad \ldots\ldots\ldots\ldots..(5)$$

$$y_\Delta - y = (2\dot{y} + \dot{y}_\Delta)\,\Delta t/3 + \ddot{y}\,.\,(\Delta t)^2/6 \qquad \ldots\ldots\ldots\ldots..(6)$$

Equations (1) and (2) are the equations of motion for the mean conditions during time step Δt. Equations (3) and (4) express the oil film force components $F_{x\Delta}, F_{y\Delta}$ at $t + \Delta t$ in terms of the displacement and velocity changes during Δt and the computed dynamic coefficients. Equations (5) and (6) relate the displacement to the velocity changes during Δt assuming that acceleration varies linearly with time during this interval. This assumption is consistent with equations (1) and (2).

2.3 Non-linearity Effects.

Hydrodynamic oil films exhibit a high degree of non-linearity, which could result in significant errors in the dynamic coefficients used in equations (3) and (4). Excessive error may be avoided by limiting the magnitude of displacement and velocity changes at each time step. Investigations indicated that such limits were best expressed in polar terms since radial sensitivity was much higher than circumferential. In addition, for an approximately constant oil film force prediction accuracy, the required limits were found to be inverse linear functions of eccentricity ratio ε. For the test case used, the following expressions for the maximum changes in displacement and velocity at any time step were found to yield a load prediction accuracy of $\pm$ 50.N ($\pm$ 1.1% of the steady load corresponding to $\varepsilon = 0.9$).

$$\Delta r/C_r = 0.0248 - 0.0242\,\varepsilon \quad \ldots\ldots\ldots\ldots (7)$$

$$\Delta c/C_r = 0.1242 - 0.1210\,\varepsilon \quad \ldots\ldots\ldots\ldots (8)$$

$$\Delta \dot{r}/u = 4.968.10^{-5} - 4.841.10^{-5}\varepsilon \quad \ldots\ldots\ldots\ldots (9)$$

$$\Delta \dot{c}/u = 2.484.10^{-4} - 2.420.10^{-4}\varepsilon \quad \ldots\ldots\ldots\ldots (10)$$

The above expressions may differ with other bearing geometries. In the computer programme developed, the above limits were converted to Cartesian terms to be consistent with equations (1) to (6).

Programme development indicated that in addition to the above limits, oil force prediction accuracy was also dependent upon closely matching the four perturbations used to compute the dynamic coefficients at each step, with the corresponding displacement and velocity changes. This was also achieved in the programme by iteratively reducing Δt until all the predicted step changes were within the limits derived from equations (7) to (10), and using dynamic coefficients computed during the previous time step. New dynamic coefficients for the current time step were then computed using the above step changes as perturbations. Final predictions of the displacement and velocity changes for the current time step were then made using the new dynamic coefficients. This process is shown by the flow diagram in Fig.2.

The other refinement introduced during programme development concerned the values of $\ddot{x}$ and $\ddot{y}$ required in equations (5) and (6). Originally these were respectively calculated from $(F_{ex} - F_x)/m$ and $(F_{ey} - F_y)/m$. This was found to be unduly sensitive to displacement and velocity prediction errors in the previous time step which resulted in a degree of numerical instability during some parts of the orbit. Accordingly the $\ddot{x}$ and $\ddot{y}$ values are now derived by extrapolating the mean accelerations from the four previous time steps using linear regression analysis. The choice of four previous time steps was considered to be a reasonable compromise between the need for adequate damping of any instability, whilst avoiding excessive error due to non-linearity of acceleration with time.

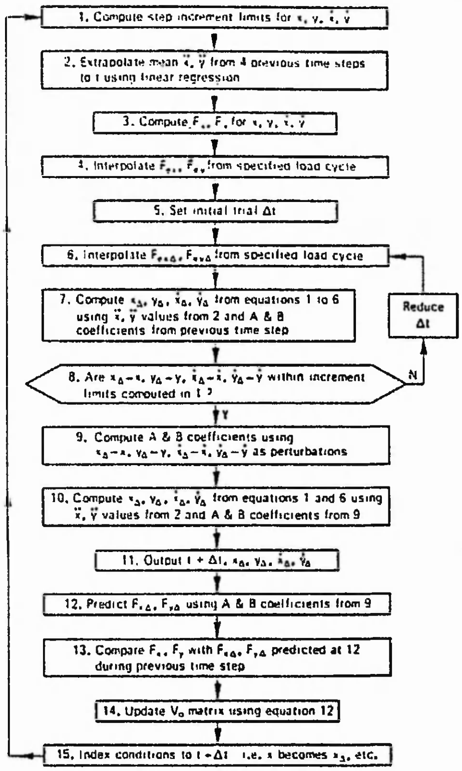

Fig 2 Flow Diagram for Time Step Process

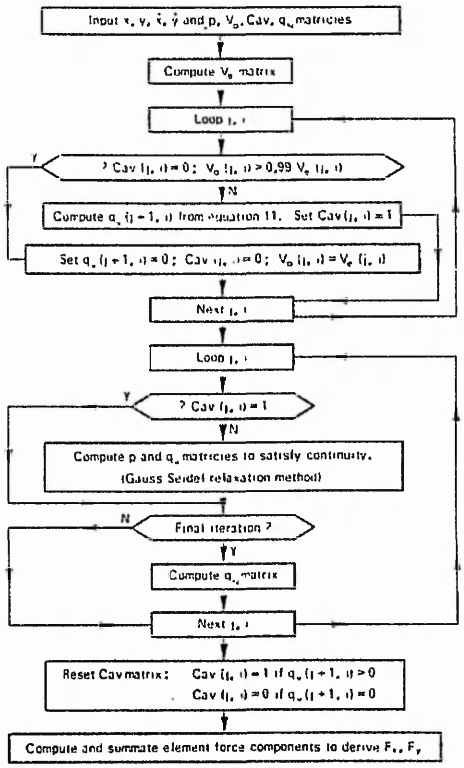

Fig 3 Flow Diagram for Oil Film Force Subroutine

2.4 Oil Film History Model.

Oil film elements outside cavitation zones must satisfy flow continuity under all conditions. Elements within a cavitation zone must also satisfy flow continuity for steady load situations, but during a dynamic load cycle they may be filling or emptying. An element is defined as being within a cavitation zone if a finite gas/vapour flow exists at its downstream boundary, i.e. $q_v(j + 1,i) > 0$. Where $q_v(j,i) > 0$ but

$q_v(j + 1, i) = 0$, the element concerned forms part of a cavitation zone reformation boundary, but is treated as being outside that cavitation zone.

For dynamically loaded bearings, elements outside cavitation zones are assumed to remain outside the time stepping procedure, except were a finite $q_v(j + 1, i)$ is required to maintain continuity during the film pressure solution. Elements within cavitation zones do not have to satisfy continuity and therefore by-pass the film pressure relaxtion process. During film pressure relaxation, the nett flow of oil to, or from such elements $q_n(j,i)$ is computed taking account of $q_v(j,i)$ and $q_v(j + 1,i)$. It is assumed that $q_v(j + 1, i)$ is dependent on the proportion of gas/vapour in the element thus:

$$q_v(j + 1, i) = \frac{h(j + 1).a.u}{2} \cdot \left[\frac{V_e(j,i) - V_o(j,i)}{V_e(j,i)}\right] \quad ....(11)$$

An element cavitation indicator matrix $C_{av}(j,i)$ facilitates the above process which is illustrated by the flow diagram in Fig.3.

The volume of oil in each element subject to cavitation $V_o(j,i)$ is updated at the end of each time step using the computed q_n matrix:

$$V_{o\Delta}(j,i) = V_o(j,i) + q_n(j,i).\Delta t \quad ....(12)$$

Where $V_o(j,i) > 0.99.\ V_e(j,i)$ the element, allowing for modelling approximations, is deemed to be full and consequently outside the cavitation zone, and thus subject to continuity requirements. This check is indicated towards the top of Fig.3.

The above model allows cavitation zone boundaries to expand or contract in any direction in accordance with the element flow monitoring procedure described.

3. DEVELOPMENT.

3.1 Test Case Used.

The test case used for this work was the intermain crankshaft bearing of a 1.8 litre 4-stroke cycle petrol engine, as used by Jones [2]. Details are as follows:

Diameter	= 54 mm.	Overall length	= 18.5 mm.
Diametral clearance	= 0.056 mm.	Journal speed	= 4000 RPM.
Effective viscosity	= 0.007 Pa.s	Oil Supply Pressure	= 0.275 MPa
Oil groove	= 180° x 3.2 mm. wide in top half.		

The external load cycle for this bearing is illustrated in Fig.4.

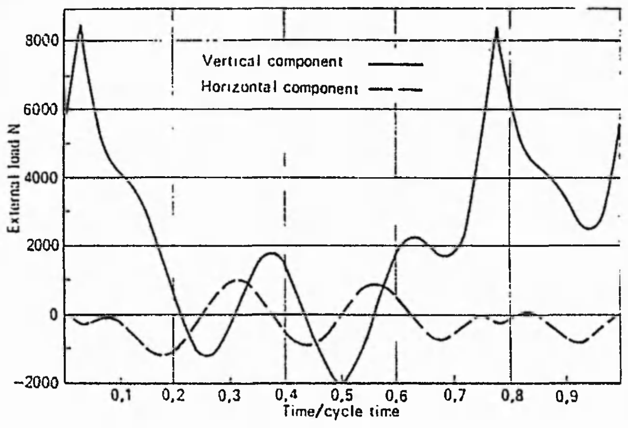

Fig 4 External Load Cycle

3.2 Oil Film Element Mesh.

In view of the amount of computation involved in this type of analysis, it is desirable to minimise the number of oil film elements. Trials carried out under steady load conditions indicated that a 24 circumferential by 6 axial element mesh would give satisfactory oil film force prediction. Six axial element divisions refers to half the bearing length due to the axial pressure distribution symmetry arising from aligned conditions. It was thus convenient to assume an oil groove width of one sixth of the length which is 3.6% less than that specified. This approximation is unlikely to have caused significant error.

LaBouff and Booker [6] examined the effect of mesh size on transient response under steady load. Results indicated that after 75^{o} rotation from a concentric start, a 25 x 6 mesh gave an ε only 1.5% greater than much finer meshes. For these tests, a rigid journal and bearing were assumed.

4. RESULTS.

Three journal masses were investigated with the given test case: 0.67kg., 6.7kg., and 67.0kg. The analysis programme incorporated facilities for by-passing the oil film history model. In this situation the extent of cavitation was determined entirely by the film pressure relaxation process of each step, which corresponds to the quasi-steady approach. Comparative orbits without and with the oil film history model at a journal mass of 6.7kg are presented in Fig.5. Corresponding orbits by Jones [2] , assuming zero journal mass, are given in Fig.6. Orbits with oil film history for journal masses of 0.67 and 67.0kg are shown in Fig.7.

Whilst polar plots of a journal orbit give a more meaningful representation of the results in relation to the clearance circle, they do not facilitate a clear indication of time.

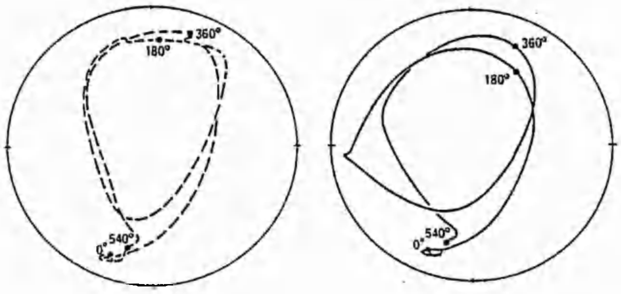

Without oil film history   With oil film history

Fig 5 Effect of Oil Film History on Journal Orbits (Journal mass = 6,7 kg)

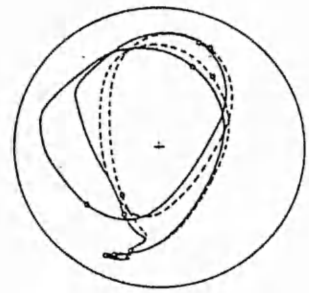

Fig 6 Journal Orbits by Jones [2]

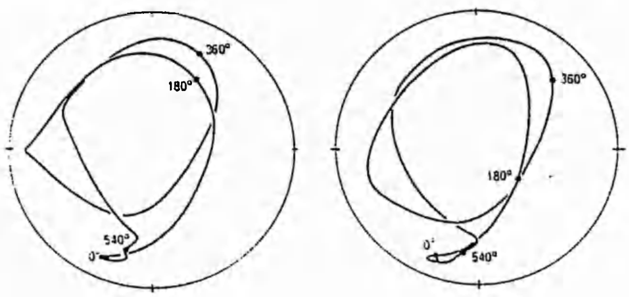

Mass = 0,67 kg   Mass = 67,0 kg

Fig 7 Effect of Journal Mass on Orbits with Oil Film History

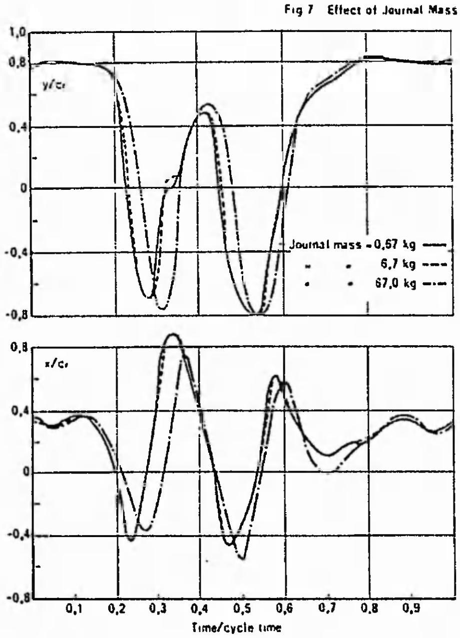

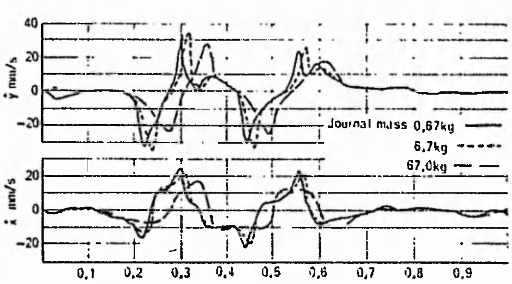

Fig 9 Effect of Journal Mass on Orbit Velocity Components

Fig 8 Effect of Journal Mass on Orbit Displacement Components

In order to overcome this problem, x and y are plotted against time for the three journal masses in Fig.8. The corresponding $\dot{x}$ and $\dot{y}$ are plotted against time in Fig.9. Results given in both Figs. 8 and 9 are with oil film history.

In general, several orbits were computed until plotted results showed no measurable difference between successive orbits. The minimum number of orbits computed with oil film history was four, but for the single case without oil film history only two orbits were necessary thus indicating faster convergence. The average number of steps per orbit was approximately 750.

5. DISCUSSION AND CONCLUSIONS.

5.1 Journal Mass.

Increase of journal mass resulted in a relative lag in the journal response which is clearly shown by both the displacement and velocity plots. With respect to the velocity results increase in journal mass also reduced the magnitude of the peaks. Differences between the results for 0.67 and 6.7kg journal mass were small, but significant changes were produced by the 67.0kg mass. This agrees with the findings of Holmes and Craven [3] , their corresponding β values being 97.12, 9.712 and 0.9712 for 0.67,6.7 and 67.0kg respectively. As a further criterion to indicate the significance of journal mass, the peak acceleration force corresponding to the peak computed vertical acceleration was divided by the peak vertical external force. The resulting ratios were 0.014, 0.072 and 0.522 for 0.67, 6.7 and 67.0kg respectively.

5.2 Oil Film History.

In the test case used, the most significant effect of oil film history occurred in the region of 250° crank angle. This was due to the continued existence of a substantial cavitation zone on the left hand side of the bearing generated during the period 530 to 140° crank angle throughout which there was relatively little journal movement and $\varepsilon \triangleq 0.85$. The presence of this cavitation zone permitted a much greater excursion of the journal towards the left of the clearance space when oil film history was taken into account. Predicted orbits at the lower journal masses, both with and without the oil film history model, were in reasonable agreement with the corresponding results published by Jones [2] for zero journal mass.

The significance of the above oil film history effect was diminished at the highest journal mass considered. This appeared to be due to the time lag introduced by the increase in mass, which thus provided more time for dissipation of the associated cavitation zone.

5.3 Future Work.

This paper has presented a journal orbit analysis method which takes account of oil film history and journal mass. For crankshaft bearings, particularly connecting rod big end bearings, probably the most important parameter towards which future work should, ideally, be directed, is bearing elasticity. At present the practicability of this questionable in view of the extent of computation required.

It is planned to apply the type of analysis described in this paper to sterntube bearings subject to dynamic misalignment conditions. The problem will be more complex since angular motion of the journal axis must be considered in addition to lateral motion. Sterntube bearings, however, fall into a "grey area" between the classifications of dynamically and steadily loaded bearings. Their journal displacement amplitudes are considerably less than those in crankshaft bearings, but nevertheless are such that direct application of dynamic coefficients is questionable. "Direct application" refers to the use of a single set of dynamic coefficients computed for the mean journal position. The use of a single set of dynamic coefficients with some form of compensation for non-linearity appears to be worth exploring.

6. REFERENCES.

1. JAKEMAN.R.W. "A Numerical Analysis Method based on Flow Continuity for Hydrodynamic Journal Bearings". Tribol.Int. Dec. 1984. 17, 6, pp 325 - 333.
2. JONES.G.J. "Crankshaft Bearings : Oil Film History". 9th Leeds-Lyon Tribol. Symp. Sept. 1982. pp 83 - 88.
3. HOLMES.R. and CRAVEN. A.H. "The Influence of Crankshaft and Flywheel Mass on the Performance of Engine Main Bearings". I.Mech.E. Tribol. Conv. 1971. Paper C63/71. pp 80 - 85.
4. BOOKER.J.F. "Dynamically Loaded Journal Bearings : Numerical Application of the Mobility Method". A.S.M.E. - J.Lub. Tech. Jan. 1971. pp 168 - 176.
5. SMITH.E.H. "Temperature Variations in Crankshaft Bearings". 9th Leeds-Lyon. Tribol. Symp. Sept. 1982. pp 97 - 102.
6. LABOUFF.G.A. and BOOKER.J.F. "Dynamically Loaded Journal Bearings : A Finite Element Treatment for Rigid and Elastic Surfaces". A.S.M.E. - A.S.L.E. Conf. Oct. 1984. A.S.M.E. Paper 84 - Trib. - 11.

ACKNOWLEDGEMENTS.

The author wishes to express his gratitude to the Committee of Lloyd's Register of Shipping for permission to publish this paper. In addition, the author is indebted to Mr G.J.Jones and Mr F.A. Martin (Glacier Metal Co.), Dr. I. Montgomery (Trent Polytechnic) and Mr. D. Rennie O.B.E. (Lloyd's Register of Shipping) for their helpful discussions and comments on this work.

REFERENCE 85.

Paper XV(ii)

The influence of cavitation on the non-linearity of velocity coefficients in a hydrodynamic journal bearing

R.W. Jakeman

This paper presents the results of a theoretical study of the oil film forces, arising from combined hydrodynamic squeeze and wedge actions, in a dynamically loaded bearing. In particular, it shows how the non-linearity of the force-journal velocity relationship is dependent upon cavitation. Simple equations for the total oil film force components, at any given eccentricity ratio, are fitted to the predicted force-velocity data. These equations introduce five velocity coefficients, which take account of the non-linear behaviour. Application of these equations to a fast journal orbit analysis, including comparison with experimental results, is described in reference (5).

1. INTRODUCTION

The work described in this paper was instigated primarily to produce a means of predicting the oil film force components, in a dynamically loaded journal bearing, for use in a fast journal orbit analysis method. This lead to a theoretical study of the relationship between oil film forces and journal lateral velocities.

As the work progressed the significance of cavitation, in relation to the non-linearity of the above relationship, became apparent. This aspect of the work was totally dependent on the cavitation model used, which took account of flow continuity throughout the cavitation zone. The literature contains much experimental evidence of the complexity of real cavitation phenomena, which indicates the substantial degree of approximation likely in any theoretical model. However, the cavitation model employed in this work is believed to represent the current state of the art, for practical analysis purposes. It undoubtedly offers a considerable improvement on the simpler cavitation models that have been widely used, particularly those in which the cavitation boundaries were fixed (e.g. the π film).

The most significant approximation in the theoretical analysis is the rigid bearing assumption. Recent work by La Bouff and Booker (1) has indicated that the computation time associated with modelling bearing elasticity in a journal orbit analysis is excessive. Since the initial objective was to develop a fast journal orbit analysis, consideration of bearing elasticity was incompatible with this aim.

1.1 Notation

b	Axial width of each bearing "land"
B_{rr}, etc	Velocity coefficients - see equations [5], [6]
C_d	Diametral clearance
D	Journal diameter
F_r, F_t	Radial, tangential components of oil film force *
h_{max}, h_{min}	Maximum, minimum film thickness
j,i	Circumferential, axial element position reference
N	Angular velocity of journal about its axis.rev/s
P_c	Cavitation pressure
P_s	Oil supply pressure
P_{spec}	Specific bearing pressure W/(LD)
q_v	Element gas/vapour volume flow rate
$\dot{R}$	Radial velocity of journal *
u	Journal surface velocity
V_n	Normal velocity of journal surface relative to element
W	Total bearing load
Δa, Δc	Axial, circumferential element dimensions
ε	Eccentricity ratio *
ψ	Attitude angle *
η	Effective dynamic viscosity of oil film
$\dot{\theta}$	Angular velocity of journal axis about bearing axis *
$\dot{\theta}_o$	Equivalent angular velocity $(= \dot{\theta} - \omega/2)$ *

ω Angular velocity of journal about its axis.rad/s *

* See figure 1.

Dimensionless parameters are indicated by a "bar" above them, and are defined in the text.

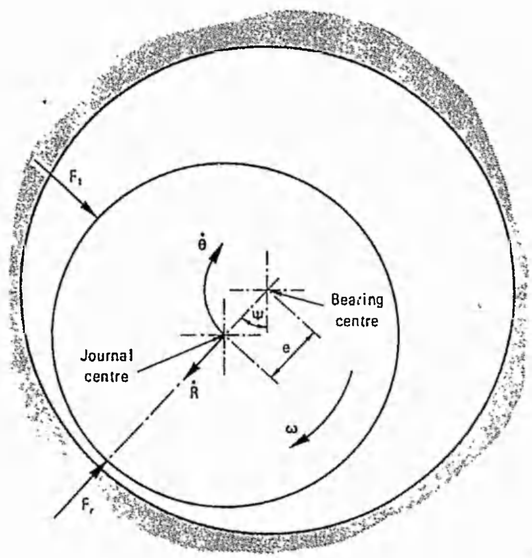

Effective angular velocity $\dot{\theta}_0 = \dot{\theta} - \frac{\omega}{2}$ (stationary bearing case)

Eccentricity ratio $\varepsilon = \frac{2e}{C_d}$

Fig. 1 Polar Oil Film Force - Journal Velocity System

2. BACKGROUND TO THE THEORETICAL ANALYSIS

2.1 Introduction

The numerical analysis method used for this work is based on that described in reference (2). Full details of the assumptions made are given in reference (2), these include: incompressible, isoviscous lubricant of negligible inertia, rigid circular journal and bearing, etc. This analysis method has been successfully applied to steadily loaded bearings, and to small journal displacement and velocity perturbations required for the computation of linearised stiffness and damping coefficients.

2.2 Previous Application to Journal Orbit Analysis

The above method has also been applied to journal orbit analysis taking account of oil film history and journal mass (3). A noteworthy feature of the oil film history model is that oil film elements subject to cavitation are not required to satisfy flow continuity. In these circumstances the downstream oil flow from a cavitating element is calculated in accordance with its degree of filling. This is determined by continuously monitoring the nett oil flow to the element over successive time steps, as the orbit is marched out.

2.3 Development of the Analysis for Large Lateral Velocities of the Journal

Initial application of the numerical analysis method (2) to journal lateral velocities, typical of those encountered in a dynamically loaded bearing, indicated some anomolies in the computed oil film force components. Whilst the apparent errors were small, the above anomolies were found to be entirely associated with cavitation. It was therefore considered important that they should be investigated, and eliminated. Full details of this development will be reported separately, and the following notes are a brief outline of the essential features:

(a) The squeeze film term $V_n.\Delta a.\Delta c$ was deleted from the continuity equation for cavitating elements. The hypothesis underlying this change was that in a cavitating element, the oil displaced by the normal velocity of the journal surface V_n, will result mainly in an axial velocity of the boundaries of the oil streams. The squeeze film term does not, therefore, result in any oil flow across the element boundary, and thus disappears from the continuity equation for such an element.

(b) The original cavitation model failed to satisfy continuity in cavitating elements when circumferential flow reversal relative to h_{min} occurred; i.e. $\dot{\theta} > \omega/2$. Elimination of this problem simply required recognition that, in the above circumstances, $q_v(j+1,i)$ referred to the upstream element boundary and $q_v(j,i)$ to the downstream boundry. For cavitating elements subject to flow reversal it was therefore necessary to compute $q_v(j,i)$ in order to satisfy continuity.

(c) The journal surface velocity u was calculated on the basis of the equivalent angular velocity, i.e. $u=(\omega-2\dot{\theta})D/2$ instead of the original $u = \omega D/2$. In addition, $\dot{\theta}_o$ was deleted from the computation of V_n, therefore V_n became a function of $\dot{R}$ only. The above measures effectively segregated the hydrodynamic squeeze and wedge actions in the analysis. This segregation is unnecessary in full film elements, but is advantageous with cavitating elements. The reason for this is that when eliminating the squeeze film term from the continuity equation for cavitating elements, as indicated in item (a), it was found that only that part of $V_n.\Delta a.\Delta c$ due to $\dot{R}$ should be eliminated.

2.4 Previous Related Work

No previous work is known to exist, which is really comparable to that described in this paper. The analysis by Bannister (4) took account of non-linearity effects in a 120^o partial arc bearing, subject to static misalignment, by including the second order terms of Taylor's series. This introduced 20 additional second derivative coefficients. Good correlation between predicted and measured orbits was reported, but the work covered only out of balance excitation and small orbits in relation to the clearance circle. During the course of the authors development work, the above non-linear coefficient approach was investigated. This included the use of both Cartezian and Polar co-ordinate systems and further expansion to include third derivative coefficients. Satisfactory oil film force prediction, throughout the range of journal displacement and velocity conditions encountered in reference (5), was not attained. It should be noted that the oil film force equations presented in this paper are virtually unrestricted with respect to journal displacement and velocity amplitudes.

3. OIL FILM RESPONSE TO LARGE JOURNAL LATERAL VELOCITIES

3.1 Introduction

In this section, the results of a theoretical study of the relationship between oil film forces and large lateral velocities will be presented and discussed. A polar system was used for velocity directions, which facilitated segregation of the hydrodynamic squeeze and wedge actions. In order to account for the total wedge action, an effective angular velocity ($\dot{\theta}_o$) was used, which combines the angular velocity of the journal about its own axis (ω) with the angular velocity of the journal axis about the bearing axis ($\dot{\theta}$). For the stationary bearing case we may therefore write: $\dot{\theta}_o = \dot{\theta} - \omega/2$. Reference to large lateral velocities means velocities of the order of those anticipated in a first order orbit traversing a large proportion of the clearance circle i.e. $\dot{\theta}_o \triangleq \omega$, $\dot{R} \triangleq \omega C_d/2$.

In order to enable comparisons to be made of the journal orbits predicted by this work with experimental data, the bearing details used in this study corresponded to test conditions used by Parkins (6):

Shaft Diameter = 63.5 mm.
Bearing Length = 2 x 9.3 mm. lands
Diametral Clearance = 0.0836 mm
Oil Groove = 5.08 mm x 360°
Journal Speed = 1180 rpm
Oil Supply Pressure = 0.0517 MPa (gauge)
Cavitation Pressure = -0.175 MPa (gauge)
Effective Viscosity = 0.0186 Pa.s.

3.2 Radial Oil Film Force (F_r)

The relationship between F_r and $\dot{R}$ at ε = 0.7 is shown in Figure 2a, from which the following characteristics may be noted:

(a) At $\dot{\theta}_o/\omega$ = 0 there is a marked change in slope as the sign of $\dot{R}$ changes, that for positive $\dot{R}$ being relatively steep and perfectly linear whilst that for negative $\dot{R}$ is fairly flat and clearly non-linear. The reason for this behaviour is that positive $\dot{R}$ generates high squeeze film pressures in the h_{min} region and no cavitation. Conversely negative $\dot{R}$ results in low squeeze film pressures in the h_{max} region, and readily generates cavitation in the h_{min} region.

(b) Where $\dot{\theta}_o/\omega \neq 0$ hydrodynamic wedge action occurs, which results in cavitation in the h_{min} region both at positive and negative $\dot{R}$. This results in a smoother transition of the $F_r - \dot{R}$ curve from negative to positive $\dot{R}$, with a degree of non-linearity at positive $\dot{R}$. Note that the curves are valid for both positive and negative values of $\dot{\theta}_o/\omega$.

(c) Cavitation due to wedge action is suppressed at higher positive $\dot{R}$, thus leading to convergence with the F_r-$\dot{R}$ curve for $\dot{\theta}_o/\omega = 0$, and linearity beyond the convergence point.

3.3 Tangential Oil Film Force (F_t)

The corresponding relationship between F_t and $\dot{\theta}_o$ at ε = 0.7 is shown in Figure 2b, and here the following observations may be made:

(a) The curves are given for positive $\dot{\theta}_o$ only. For negative $\dot{\theta}_o$ the data is identical except that the sign of F_t is reversed.

(b) As noted in 3.2 (c), positive $\dot{R}$ tends to suppress the cavitation induced by wedge action. This yields linearity of F_t with $\dot{\theta}_o$ to the point at which the positive $\dot{R}$ fails to suppress wedge cavitation. The magnitude of $\dot{\theta}_o$, above which the $F_t - \dot{\theta}_o$ response becomes non-linear, depends on the magnitude of the positive $\dot{R}$.

3.4 General Observations on the Oil Film Force - Journal Velocity Results

(a) F_r is primarily a function of $\dot{R}$, the secondary influence of $\dot{\theta}_o$ being a result of cavitation induced by hydrodynamic wedge action. The part of F_r due to $\dot{\theta}_o$ thus becomes zero when $\dot{R}$ is high enough to suppress the above cavitation. This explains the progressive convergence of the family of $F_r - \dot{R}$ curves for $\dot{\theta}_o \neq 0$, with the straight line for $\dot{\theta}_o = 0$ at positive $\dot{R}$ in Figure 2a.

(b). F_t is primarily a function of $\dot{\theta}_o$. Hydrodynamic squeeze action (i.e. $\dot{R}$) does not in itself, result is a finite F_t, therefore all curves pass through the origin in Figure 2b. The influence of $\dot{R}$ on F_t, indicated by the family of curves in Figure 2b, results purely from the interaction of squeeze action with wedge cavitation.

(c) The positive film pressure region and cavitation zone associated with squeeze action are circumferentially symmetrical with respect to the locations of h_{min} and h_{max}.

(d) The positive film pressure region and cavitation zone associated with wedge action are circumferentially assymmetrical with respect to the locations of h_{min} and h_{max}.

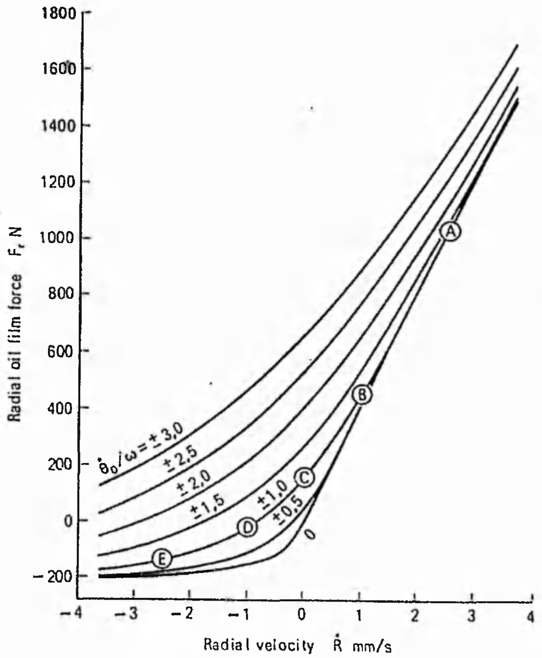

Fig. 2a Radial Force Data at $\varepsilon = 0,7$

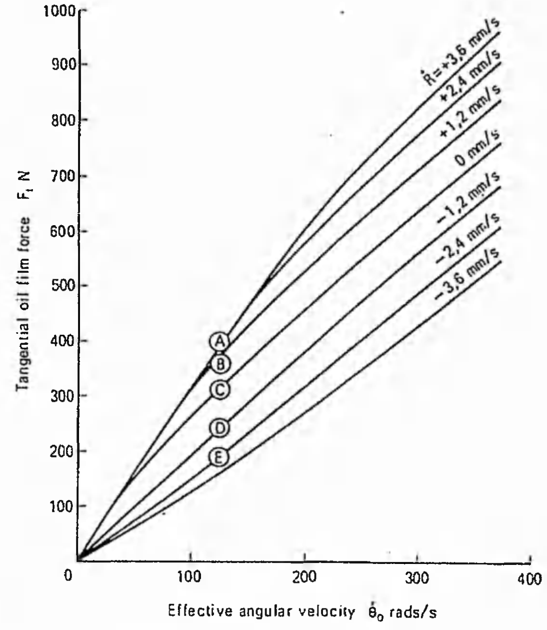

Fig. 2b Tangential Force Data at $\varepsilon = 0,7$

(e) As a result of (c) and (d), squeeze action is capable of virtually eliminating the positive film pressure region (by negative $\dot{R}$), or the cavitation zone (by positive $\dot{R}$), due to wedge action. This results in the trend towards convergence of the family of F_r - $\dot{R}$ curves in Figure 2a as the magnitude of $\dot{R}$ increases in both the positive and negative sense. Conversely, in no circumstances does wedge action have a dominant influence in relation to squeeze action. The family of F_t - $\dot{\theta}_o$ curves in Figure 2b does not therefore indicate and tendancy to converge associated with increasing $\dot{\theta}_o$.

(f) The interaction of squeeze and wedge action, associated with cavitation, invalidates the principle of superposition with respect to the oil film forces resulting from simultaneous application of $\dot{R}$ and $\dot{\theta}_o$. Where the conditions are such that all cavitation is supressed, the principle of superposition is redundant since F_r is a linear function of $\dot{R}$ only and F_t is a linear function of $\dot{\theta}_o$ only.

(g) The oil film behaviour underlying the interaction of squeeze and wedge actions is illustrated by Figure 3, which shows the family of circumferential film pressure profiles for $\dot{\theta}_o/\omega = 1.0$, at ε=0.7. In Figures 2a and 2b, the points corresponding to these profiles are identified. It may be noted that for point (A), $\dot{R}$ has attained a level where it has almost eliminated wedge induced cavitation. At point (A) in figure 2a, the F_r-$\dot{R}$ curve for $\dot{\theta}_o/\omega$ = 1.0 has therefore virtually converged with that for $\dot{\theta}_o/\omega$ =0. Conversely the profile for point (E) shows how the positive film pressure due to wedge action has been substantially reduced by the negative $\dot{R}$, and the cavitation zone extended.

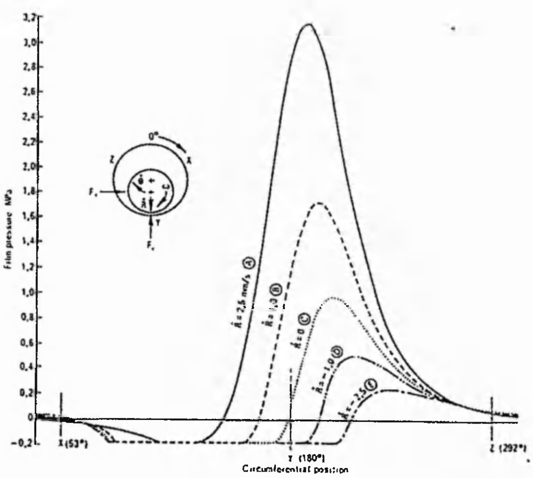

Fig. 3 Circumferential Pressure Profiles at Mid Land

3.5 Influence of Very Large Lateral Journal Velocities

Consideration was also given to the effect of lateral journal velocities approaching two orders of magnetude greater than those covered in the foregoing results. With regard to practical applications, this may appear somewhat academic. This additional analysis was nevertheless found to be of value in enhancing an understanding of the oil film response to large lateral journal velocities, particularly with regard of the significance of cavitation.

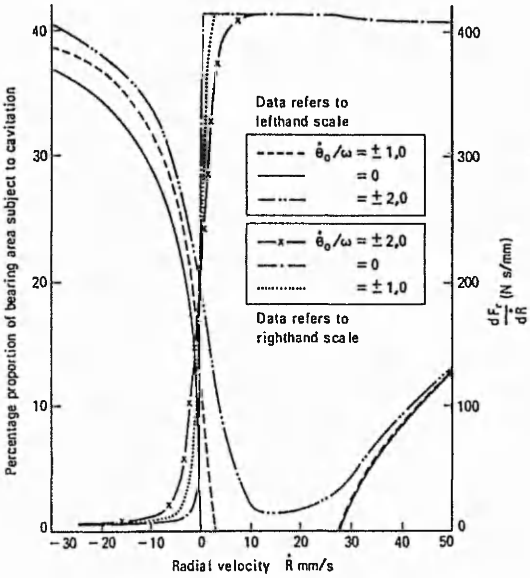

Fig.4 F_r - $\dot{R}$ Gradient and Cavitation at Very Large $\dot{R}$ Amplitude (ε=0.7)

Results computed for an $\dot{R}$ range of -25 to +50 mm/s are shown in Figure 4, this comprising the gradient $dF_r/d\dot{R}$ and the corresponding extent of cavitation. At negative $\dot{R}$ the $dF_r/d\dot{R}$ curves show the convergence referred to in section 3.4 (e). The corresponding portions of the cavitation curves confirm that the convergence is associated with a tendency towards "saturation" of the extent of cavitation. At positive $\dot{R}$, the initial linear response (constant $dF_r/d\dot{R}$) is seen to coincide with zero or virtually zero cavitation. Above $\dot{R}$ = 27.5 mm/s cavitation starts to occur in the h_{max} region, and results in a slight drop (1.2%) in $dF_r/d\dot{R}$. The reason for the above effect being very small is that the change in oil film force in the h_{max} region, arising from the onset of cavitation, is low in relation to the change in oil film force in the h_{min} region, due to the squeeze action associated with positive $\dot{R}$.

Figure 5 presents F_t results for the $\dot{\theta}_0/\omega$ range of 0 to 90, together with the corresponding extent of cavitation. It is evident that the F_t curves remain distinctly non-linear throughout this very large velocity range. The cavitation curves exhibit a similar behaviour, and the persistance of non-linearity in the F_t curves is clearly associated with the failure of the extent of cavitation to reach a "saturation" level.

It is important to note that the absolute maximum extent of cavitation associated with squeeze action is 50%. For wedge action, however, the extent of cavitation may approach 100% under oil starvation conditions. The application of very large $\dot{\theta}_0/\omega$, whilst maintaining a constant oil supply pressure P_s and cavitation pressure P_c, effectively results in a tendency towards oil starvation and thus an extent of cavitation exceeding 72% in Figure 5.

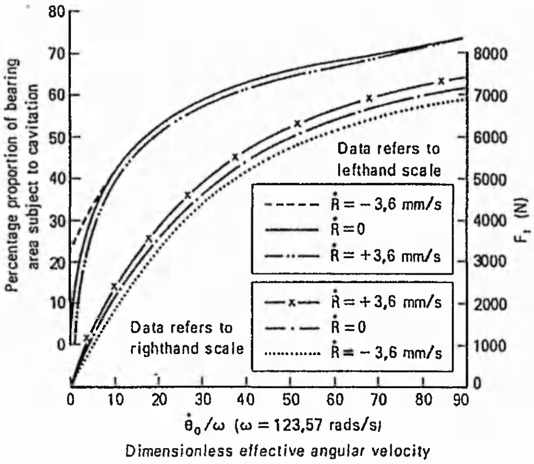

Fig. 5 F_t and Cavitation Data at Very Large $\dot{\theta}_0/\omega$ Amplitude (ε=0.7)

The above factors are best explained by consideration of the requirements for hydrodynamic similarity. The dimensionless load capacity parameter has been commonly used for steadily loaded hydrodynamic journal bearings:

$$\overline{W} = \frac{P_{spec}}{\eta N}\left(\frac{C_d}{D}\right)^2 \qquad [1]$$

This is constant for a given b/D ratio and eccentricity ratio ε, and is the inverse of the well known Sommerfeld No. At any instant in a dynamically loaded bearing, the appropriate dimensionless load capacity parameters associated with wedge and squeeze action may similarly be expressed respectively as:

$$\overline{W}_w = \frac{P_{spec}}{\eta|\dot{\theta}_o|}\left(\frac{C_d}{D}\right)^2 \; ; \; \overline{W}_s = \frac{P_{spec}\, C_d}{\eta|\dot{R}|}\left(\frac{C_d}{D}\right)^2 \qquad [2]$$

However, hydrodynamic similarity in both the steadily and dynamically loaded situations is also dependent upon the geometric similarity of the cavitation zone boundary relative to the bearing surface boundary. The cavitation zone boundary is dependent on the oil film boundary pressures P_s and P_c. In order to fulfil the above requirement for geometric similarity with respect to cavitation, the following dimensionless parameters must also be held constant:

For wedge action:

$$\overline{P}_{sw} = \frac{P_s}{\eta|\dot{\theta}_o|}\left(\frac{C_d}{D}\right)^2 \; ; \; \overline{P}_{cw} = \frac{P_c}{\eta|\dot{\theta}_o|}\left(\frac{C_d}{D}\right)^2 \qquad [3]$$

For squeeze action:

$$\bar{P}_{ss} = \frac{P_s\, C_d}{\eta|\dot{R}|}\left(\frac{C_d}{D}\right)^2 \; ; \; \bar{P}_{cs} = \frac{P_c\, C_d}{\eta|\dot{R}|}\left(\frac{C_d}{D}\right)^2 \qquad [4]$$

Since P_s, P_c and were held constant for the tests covered in Figure 5, the apparent oil starvation at high $\dot{\theta}_o/\omega$ is due to the corresponding reduction in $\bar{P}_{sw}$ and $\bar{P}_{cw}$. Had $\bar{P}_{sw}$ and $\bar{P}_{cw}$ been maintained constant, then the F_t curves in Figure 5 would have been linear.

4. DEVELOPMENT OF OIL FILM FORCE EQUATIONS

4.1 Introduction

In order to facilitate the operation of a fast journal orbit analysis programme, it was necessary to develop oil film force equations which would give a satisfactory approximation to computed data of the type given in Figures 2a and 2b. This data is for ε =0.7. At reduced eccentricity ratio the form of the force - velocity curves is essentially similar, but reduced cavitation due to wedge action results in the families of curves becomming more linear and closer together. The reverse trend occurs with increased eccentricity ratio.

The form of the force-velocity curves is clearly complex, and an extensive search was made for equation forms that would accurately fit this data. No solution was found which would yield satisfactory results over a wide range of eccentricity ratios. In attempting to find an accurate fit, there was an inevitable trend towards complex equations with excessive numbers of coefficients. The complex curve fit approach was therefore abandoned in favour of the much simpler partially linearised solution. This solution is described in the following section, and has resulted in satisfactory fast journal orbit predictions in tests carried out to date (5).

4.2 Partially Linearised Equations

Examination of Figure 2a indicates a need to use different F_r - $\dot{R}$ linearised slopes for the positive and negative ranges of $\dot{R}$. It is to the consequent use of two slopes that the term "partially linearised" refers. Figure 2a also shows a progressive increase in F_r - $\dot{R}$ slope for negative $\dot{R}$, and reduction in slope for positive $\dot{R}$, as the magnitude of $\dot{\theta}_o$ increases. In addition, the magnitude of F_r at $\dot{R}$ = 0 in seen to increase progressively with increase in the magnitude of $\dot{\theta}_o$. Assuming that the above influences of $\dot{\theta}_o$ are approximately linear, then the following equation may be written for F_r:

$$F_r = B_{rt}\,\dot{\theta}_o + B_{rr}\,\dot{R} + B_{rrt}\,\dot{R}\,\dot{\theta}_o \qquad [5]$$

As indicated above, different values of B_{rr} and B_{rrt} are used for $\dot{R}$ > 0 and $\dot{R}$ < 0. The B_{rrt} coefficient effectively represents the previously described interaction of squeeze and wedge actions. A single value of B_{rt} is used as this relates to the condition $\dot{R}$ = 0. The degree of approximation involved in linearising the coefficients B_{rt} and B_{rrt} is indicated by the curves for F_r and $dF_r/d\dot{R}$ at $\dot{R}$ = 0, which are plotted against $\dot{\theta}_o/\omega$ for ε = 0.7 in Figure 6. It may be noted that F_r is zero and $dF_r/d\dot{R}$ is constant up to $\dot{\theta}_o/\omega$ = 0.2, due to the absense of cavitation induced by wedge action at low $\dot{\theta}_o$. Since the family of curves for $\dot{\theta}_o/\omega \neq 0$ in Figure 2a are clearly asymptotic to that for $\dot{\theta}_o/\omega$ =0 for both positive and negative $\dot{R}$, the value of F_r predicted by equation [5] is subject to the condition $F_r \not\to B_{rr}\,\dot{R}$.

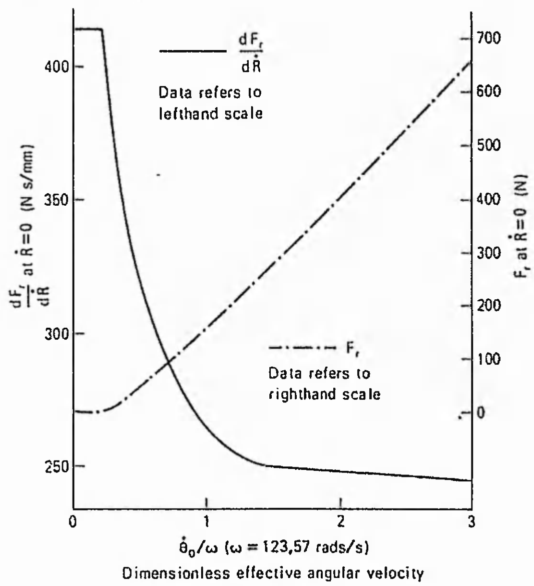

Fig.6 F_r and $dF_r/d\dot{R}$ at $\dot{R}=0$

A similar linearisation may be applied to the F_t data shown in Figure 2b. Since the straight line fitted to all the curves may clearly pass through F_t = 0 at $\dot{\theta}_o$ = 0, then no B_{tr} term is required, i.e. we may write:

$$F_t = B_{tt}\,\dot{\theta}_o + B_{trt}\,\dot{R}\,\dot{\theta}_o \qquad [6]$$

The curves for negative $\dot{\theta}_o$ are identical to those shown in Figure 2b, except that the sign of F_t is reversed, therefore only a single value of B_{tt} is required. B_{trt} also represents squeeze - wedge interaction in a similar manner to B_{rrt}, and the use of different values of this coefficient for $\dot{R}>0$ and $\dot{R}<0$ again gives a better fit to the computed data.

It is important to note that the linearised displacement and velocity coefficients, commonly used in lateral vibration analysis, only facilitate the estimation of change of oil film force components from an equilbrium condition. In contrast with this, the oil film force components given by equations [5] and [6] are the total values. The estimation of the oil film force components at any location of the journal within the bearing clearance space, requires the computation of the velocity coefficients B_{rt}, etc over the range of possible eccentricity ratios. Suitable interpolation is then used for the eccentricity ratio corresponding to the specified location.

The errors associated with the linearisation required to produce equations [5] and [6] will be minimised by computing the velocity coefficients with $\dot{R}$ and $\dot{\theta}_o$ pertubations corresponding to the maximum velocities anticipated for the case under consideration. Journal orbit tests using equations [5] and [6], have indicated that the predicted orbits are not unduly sensitive to this requirement.

4.3 Dimensionless Velocity Coefficients

For generalisation of velocity coefficient data, the following non-dimensional expressions may be used:

$$\bar{B}_{rr} = \frac{B_{rr}}{\eta b}\left(\frac{C_d}{D}\right)^3 \; ; \; \bar{B}_{rrt} = \frac{B_{rrt}}{\eta b}\left(\frac{\dot{R}\,\dot{\theta}_o}{C_d}\right)^{1/2}\left(\frac{C_d}{D}\right)^3$$

$$\bar{B}_{tt} = \frac{B_{tt}}{\eta b C_d}\left(\frac{C_d}{D}\right)^3 \; ; \; \bar{B}_{rt} = \frac{B_{rt}}{\eta b C_d}\left(\frac{C_d}{D}\right)^3 \; ;$$

$$\bar{B}_{trt} = \frac{B_{trt}}{\eta b}\left(\frac{\dot{R}\,\dot{\theta}_o}{C_d}\right)^{1/2}\left(\frac{C_d}{D}\right)^3$$

The above expressions are subject to the usual bearing geometric similarity requirement, i.e. they are valid for a given b/d ratio. In addition, as indicated in section 3.5, these expressions are also subject to the geometric similarity requirements with respect to the cavitation zone boundary.

The result of this is:

Coefficient:	Valid for given:
$\bar{B}_{rr}$	$\bar{P}_{ss}$, $\bar{P}_{cs}$,
$\bar{B}_{tt}$, $\bar{B}_{rt}$	$\bar{P}_{sw}$, $\bar{P}_{cw}$
$\bar{B}_{rrt}$, $\bar{B}_{trt}$	$\bar{P}_{ss}$, $\bar{P}_{cs}$, $\bar{P}_{sw}$, $\bar{P}_{cw}$

The above validity limitations appear to make the generalisation of these velocity coefficients totally impracticable. However, errors resulting from failure to satisfy the cavitation zone similarity requirements, are comparable to the errors arising from mismatching of the velocity pertubations used to derive the dimensional velocity coefficients, with the maximum velocity components occuring in the journal orbit under consideration.

The $\dot{R}$, $\dot{\theta}_o$ values used to derive $\bar{P}_{sw}$, $\bar{P}_{cw}$, $\bar{P}_{ss}$, $\bar{P}_{cs}$ and used in the dimensionless expressions for $\bar{B}_{rrt}$ and $\bar{B}_{trt}$, should correspond to the above maximum velocity components. Insensitivity of predicted orbits to the matching of $\dot{R}$, $\dot{\theta}_o$ pertubations, noted in section 4.2, should therefore similarly apply to the matching of $\bar{P}_{sw}$, $\bar{P}_{cw}$, $\bar{P}_{ss}$, $\bar{P}_{cs}$ with the corresponding values pertaining to any dimensionless velocity coefficient data used.

A noteable exception to the above approximation, arising from failure to satisfy the cavitation zone similarity requirements, is the $\bar{B}_{rr}$ coefficient for $\dot{R}>0$. This coefficient is a function of the b/D ratio only, due to the absence of cavitation associated with positive $\dot{R}$. Some cavitation in the h_{max} region has been shown to occur at very large positive $\dot{R}$, but the effect on $dF_r/d\dot{R}$, and hence on B_{rr}, was shown to be negligible.

Dimensionless coefficient-eccentricity ratio data, corresponding to the conditions given in 3.1, are presented in Figures 7 and 8. It may be noted that below about $\varepsilon = 0.4$, cavitation due to squeeze action disappears, hence the convergence of the $\bar{B}_{rr}$ curves for $\dot{R}>0$ and $\dot{R}<0$ seen in Figure 7. Cavitation arising from wedge action disappears a little below $\varepsilon = 0.6$, thus resulting in $\bar{B}_{rt}$ becoming zero. Figure 8 shows how the $\bar{B}_{rrt}$ and $\bar{B}_{trt}$ coefficients similarly disappear below about $\varepsilon = 0.6$ since they relate to the interaction of squeeze action upon wedge cavitation.

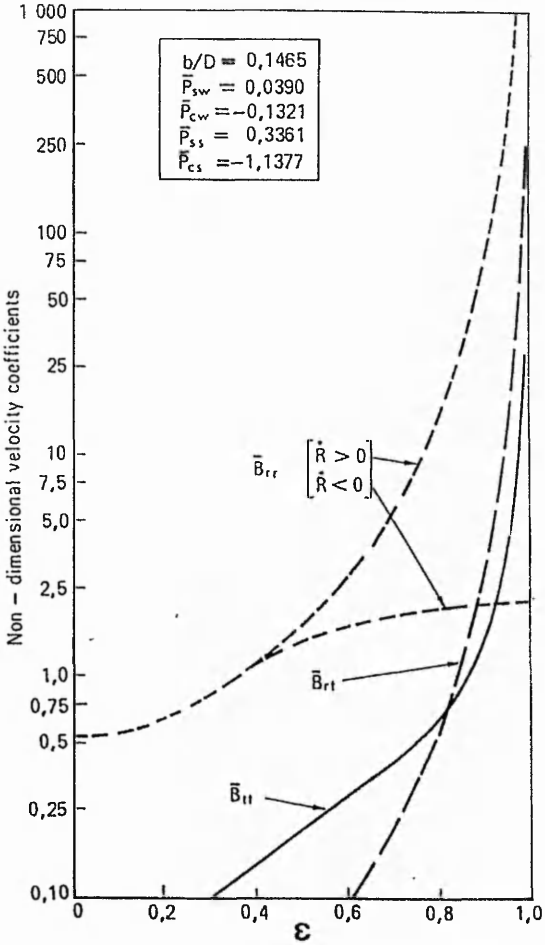

Fig. 7 Separate Squeeze and Wedge Action Velocity Coefficients

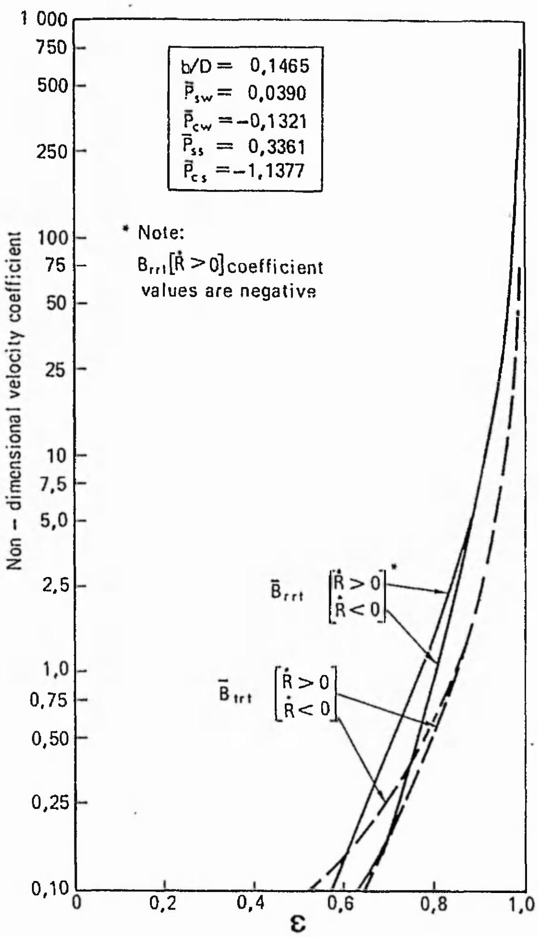

Fig. 8 Interactive Squeeze and Wedge Action Velocity Coefficients

6. CONCLUSIONS

This paper has presented data on the oil film forces associated with large lateral velocities of the journal in a hydrodynamic journal bearing. The theoretical cavitation model used has enabled the role of cavitation in relation to non-linearity, and in particular to the interaction of hydrodynamic squeeze and wedge actions, to be clearly shown.

Equations have been introduced for the oil film force components, based on partial linearisation of the computed force-velocity data. By using a Polar system, it was possible to segregate hydrodynamic wedge and squeeze action. The rotational velocity of the journal about its axis was combined with the angular velocity of the journal axis about the bearing axis, to give an equivalent angular velocity $\dot{\theta}_0$. The oil film force components given by the above equations are therefore total values, rather than changes from some equilibrium condition. These equations are suitable for fast journal orbit analysis, this application being covered by reference (5).

The results given in this paper are for an aligned 360° circumferential groove bearing. For this type of bearing, the velocity coefficients in the oil film force equations are functions of ε only. The equations are also applicable to non-circumferentially symmetrical bearings, by the derivation of velocity coefficients as functions of both ε and attitude angle ψ.

7. ACKNOWLEDGEMENT

The author wishes to express his gratitude to the Committee of Lloyd's Register of Shipping for permission to publish this paper.

References

(1) LA BOUFF, G.A. and BOOKER J.F. "Dynamically Loaded Journal Bearings: A Finite Element Treatment for Rigid and Elastic Surfaces". A.S.M.E./A.S.L.E. Conf. Oct. 1984. A.S.M.E. Paper 84 - TRIB - 11.

(2) JAKEMAN, R.W. "A Numerical Analysis Method based on Flow Continuity for Hydrodynamic Journal Bearings". Tribology International. Vol. 17. No. 6 Dec. 1984.

(3) JAKEMAN, R.W. "Journal Orbit Analysis taking account of Oil Film History and Journal Mass" Proc. of Conf.: Numerical Methods in Laminar and Turbulent Flow. Swansea July 1985 pp 199-210.

(4) BANNISTER, R.H. "A Theoretical and Experimental Investigation illustrating the influence of Non-Linearity and Misalignment on the Eight Oil Film Force Coefficients". Proc. I. Mech. E. Conf.: Vibration in Rotatinmg Machinery. Cambridge, 1976. Paper C219/76.

(5) JAKEMAN, R.W. and PARKINS D.W. "Theoretical and Experimental Orbits of a Dynamically Loaded Hydrodynamic Journal Bearing". To be published: 13th Leeds-Lyon Symposium on Tribology. Leeds. Sept. 1986.

(6) PARKINS, D.W. "Theoretical and Experimental Determination of the Dynamic Characteristics of a Hydrodynamic Journal Bearing". A.S.M.E. Journal of Lubrication Technology. Vol. 101. April 1979. pp. 129 - 139.

REFERENCE. 86

Paper XI(iii)

Theoretical and experimental orbits of a dynamically loaded hydrodynamic journal bearing

R.W. Jakeman and D.W. Parkins

This paper gives a comparison of theoretical and experimental orbits of a dynamically loaded journal bearing having a pressurised oil supply to a central 360° circumferential groove. The results of two theoretical analyses are presented: Methods A and B. Method B, referred to as the Reaction Method, features oil film force prediction by means of pre - computed velocity coefficients, thus facilitating quicker computation. Satisfactory correlation of the experimental results with the predictions of both theoretical methods is shown. Comparisions are made for three examples including different relative phase and amplitude of the excitation components at both once and twice rotational frequency.

1. INTRODUCTION

Linearised oil film displacement and velocity coefficients have been commonly used to model the influence of hydrodynamic journal bearings upon the lateral vibration characteristics of various shafting systems. These coefficients are subject to a high degree of non-linearity which may lead to substantial errors, particularly with respect to amplitude prediction, in situations where significant dynamic loading is encountered. In more extreme cases of dynamic loading, such as crankshaft bearings, non-linearity renders the use of a single set of displacement and velocity coefficients totally impractical. A time stepping journal orbit analysis is used in these situations. Journal orbit analysis is inherently heavy on computing time, particularly with the more rigorous types of analysis, where oil film characteristics must be computed at each time step. A considerable reduction in computing time can be gained by the use of either an approximate solution of the oil film pressure distribution or pre-computed oil film data.

The objective of the work reported in this paper was to compare the results of two journal orbit prediction methods with experimental data obtained from a test rig (1). Theoretical Method A is of the rigorous type thus using numerical film pressure solutions at each time step (2), whilst Method B, referred to as the Reaction Method, achieves a fast orbit solution by the use of pre-computed velocity coefficients. Method A has been previously described in reference (3), and the development of the oil film force equations upon which the Reaction Method is based is outlined in reference (4).

Alignment between the journal and bearing was maintained for all conditions covered in this paper, and the bearing featured a pressurised oil supply to a centrally positioned full circumferential groove. Both theoretical methods took account of journal inertial forces, and Method A had an optional facility for modelling oil film history.

1.1 Notation

A_{xx},etc. Linearised oil film coefficients for small displacement perturbations.

B_{xx},etc. Linearised oil film coefficients for small velocity perturbations.

B_{tt}, B_{rt}, B_{rr} Separate wedge and squeeze action velocity coefficents

B_{rrt}, B_{trt} Interactive wedge and squeeze action velocity coefficients.

C Radial clearance

F_r, F_t Radial, tangential oil film forces.

F_{ex}, F_{ey} Horizontal, vertical external forces.

F_x, F_y Horizontal, vertical oil film forces.

j, i Circumferential, axial element position reference

m Journal mass *

q_n (j,i) Nett oil volume flow rate into element j, i.

R Radial journal velocity

T Dynamic cycle time

t Time from start of dynamic cycle and at the start of time step Δt.

V_e(j,i) Total volume of element j, i.

V_o (j,i) Volume of oil in element j, i.

x, y Horiziontal, vertical journal displacement*

$\dot{x}$, $\dot{y}$ Horizontal, vertical journal velocity*

$\ddot{x}, \ddot{y}$	Horizontal, vertical journal acceleration*
Δt	Time step increment
$\dot{\theta}$	Angular velocity of journal axis about bearing axis. *
$\dot{\theta}_o$	Equivalent angular velocity of journal*
ε	Eccentricity ratio = $(x^2 + y^2)^{1/2}/C$
ω	Journal angular velocity about its own axis.
*	Referers to the normal situation of a "fixed" bearing. In the experimental test rig these parameters refer to the bearing housing since the journal is "fixed".

Suffixes:

h,j,o	bearing housing, journal, oil film.
p	perturbation used to compute A_{xx}, etc.
max	maximum permitted value.
s	initially estimated value.
Δ	denotes conditions at $t + \Delta t$, no suffix denotes conditions at t.

Prefix:

Δ	denotes the change in any parameter over Δt e.g. $\Delta x = x_\Delta - x$

2. BRIEF REVIEW OF PREVIOUS WORK

2.1 Factors relevant to Journal Orbit Analysis

There are three main factors pertaining to the journal orbit analysis methods published to date. The various options within these are outlined below:

(1) Oil film force derivation:

a. Solution of Reynolds equation by short bearing approximation.

b. Numerical film pressure solution for bearings of finite length.

c. Use of pre-computed or measured oil film properties to facilitate a fast orbit solution.

d. Oil film history modelling.

(2) Journal mass:

a. Inertial forces assumed to be negligible in relation to external and oil film forces, therefore journal velocity components are derived to produce oil film forces equal to the external forces at each step.

b. Inertial forces not neglected.

(3) Bearing elasticity:

a. Bearing assumed to be rigid.

b. Taken into account by interactive solution of film pressure distribution and corresponding bearing elastic deformation.

2.2 Previous Work

One of the best known fast solutions is the Mobility Method of Booker(5) which features option (1c). The Mobility data, upon which this method depends, was originally derived by the short bearing approximation (1a), and was consequently of lesser accuracy than more recent numerical solutions.

Finite bearing solutions or experimental measurements may also be used to produce Mobility data, thereby substantially improving accuracy. This method was designed for situations where journal inertial forces could be neglected (2a) and the rigid bearing assumption (3a), and is theoretically limited to bearings having circumferential symmetry.

The analysis by Holmes and Craven (6) is one of the few to have taken account of journal inertial forces (2b), their work being based on the short bearing approximation (1a), and applied to a rigid bearing (3a).

Oil film history modelling (1d) has also received very little attention, the paper by Jones (7) giving a good account of this, but with the limitations of neglecting inertial forces (2a) and the rigid bearing assumption (3a).

Little work has been carried out on the modelling of elasticity in a dynamically loaded bearing (3b) due to the excessive computing time involved. The paper by LaBouff and Booker (8) is an example of this, and used a finite bearing solution (1b) and neglected inertial forces (2a). Fantino et al (9) attained a more acceptable comouting time by using the short bearing approximation (1a), but with a consequent loss of accuracy. Goenka and Oh (10) used the basic methods of both (8) and (9), but with various refinements to improve both accuracy and computing time.

2.3 Relation of Methods A and B to Previous Work

In relation to the foregoing analysis option categories, it may be noted that theoretical Method A in this paper used a numerical finite bearing solution (1b), with an optional facility for oil film history modelling (1d). Journal inertial forces were taken into consideration (2b), but the bearing was assumed to be rigid (3a). Method A is therefore closely comparable to the theoretical work by Jones (7), and a comparison with results therefrom using the intermain crankshaft bearing of a 1.8 litre 4-stroke cycle petrol engine as a test case, was given in reference (3). The inclusion of inertial forces was the main difference between the above analyses, Method A herein and that by Jones (7). In this respect

Method A is comparable to the analysis by Holmes and Craven (6).

Method B differed from Method A, in that pre-computed velocity coefficients were used in order to obtain a fast orbit solution (1c). The coefficients were derived by a numerical finite bearing solution (1b), but this method negated the possibility of oil film history modelling (1d), for which no fast solution is known to exist. A particular feature of Method B is that the velocity coefficients used take account of the interaction of squeeze and wedge action resulting from the presence of cavitation, and the associated non-linear behaviour. In utilising pre-computed coefficients, Method B may be compared with Booker's Mobility Method (5), but differs in that it readily allows journal inertial forces to be taken into account. The Mobility Method may appear to be simpler than Method B in that only two parameters are required, namely the Mobility Number and the angle of the squeeze path relative to the load vector. However, these two parameters are functions of both eccentricity ratio and attitude angle, even for a circumferentially symmetrical bearing. Method B requires five velocity coefficients, but for the circumferentially symmetrical bearing these are functions of eccentricity ratio only. The total amount of pre-computed data required by Method B is therefore substantially less than for the Mobility Method. In addition, Method B may be extended to cover non-circumferentially symmetrical bearings by computing the five velocity coefficients as functions of eccentricity ratio and attitude angle.

3. EXPERIMENTAL METHOD

3.1 Design of Test Rig

Figure 1 shows the apparatus on which the experimental orbits were obtained. The rotating shaft is supported at either end in rolling element "slave" bearings, whilst the test bearing is mounted in a "floating" housing. In contrast to the normal practical situation, it was therefore the bearing housing orbits relative to the "fixed" journal, rather than journal orbits, that were measured experimentally. Steady forces were applied separately or together in both horizontal and vertical directions directly to the test bearing housing through tensioned wires.

Relative displacement between test bearing and journal was measured by four pairs of non-contacting inductive transducers located on each side of the bearing in the horizontal and vertical directions. This arrangement permitted calculations of displacement at either bearing end or the axial centre plane. The tensioned wires were attached to fixed points located at a distance many times (approximately 20,000:1) greater than the maximum possible housing motion. This prevented housing displacement from altering the direction of the steady forces. Stiffness of the spring elements in each loading system was made small compared to that of the oil film. This meant that test housing displacement did not alter the magnitude of

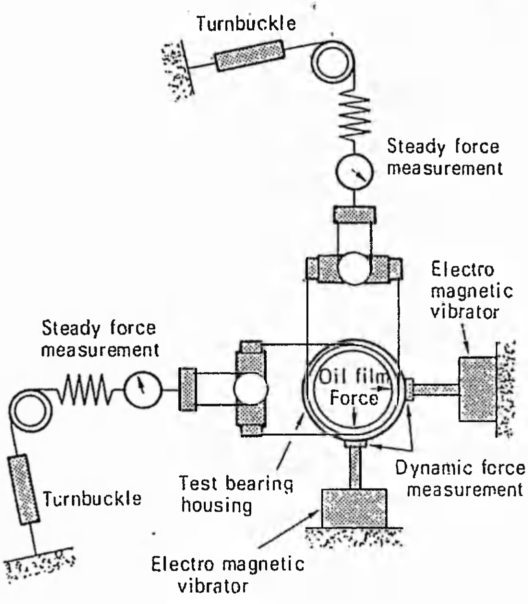

Fig.1 Schematic Arrangement of Test Rig Loading System

the steady forces. Figure 1 shows that the horizontal and vertical steady loading arrangements each have intermediate pulleys between the steady force gauge and the test bearing housing. These comprised wheels, supported by low friction rolling element bearings, which allowed the test bearing housing freedom to rotate around two mutually perpendicular transverse axes whilst under a large steady force. Freedom around these axes allows the bearing to align itself with the journal longitudinal axis. Moreover, this loading arrangement eliminated any constraint around the bearing centre line. Hence any torque exerted by the oil film was resisted by a separate torque restraining link.

A magnetic sensor indicated shaft orientation and provided a pulse for an accurate rotational speed indicator.

Dynamic bearing forces F_{ex}, F_{ey}, measured by piezo gauges, could be applied to the bearing housing either vertically or horizontally or together with any relative phase and magnitude by the two electro magnetic vibrators. Signals for these electro magnetic vibrators and their power amplifiers were created by a sinewave generator driven from the test shaft. The vibrator connectors were designed to impose negligible constraint on the test bearing housing, this condition being verified for each experiment.

With the steady force only applied to the test bearing, plus the torque restraint, the housing remains free to move a small axial distance along the shaft. This feature convieniently checked whether full hydrodynamic conditions had been established. However, when dynamic loads were applied it was found that only a microscopic misalignment thereof was sufficient to cause an unacceptably large longitudinal vibration and torsional oscillation about an axis perpendicular to journal centre line. To obviate this, locating wires parallel to the bearing centre line were introduced for the dynamic tests. They allowed the bearing to move transversely and remain parallel to the shaft whilst preventing any misalignment or axial motion. It was shown that these wires transmitted no static or dynamic forces to the test bearing housing in any direction perpendicular to the bearing centre line.

3.2 Test Rig Equations of Motion

Equations of motion for the housing and oil are:

$$F_{ex} - F_x = m_h \ddot{x}_h + m_o \ddot{x}_o$$
$$F_{ey} - F_y = m_h \ddot{y}_h + m_o \ddot{y}_o \quad [1]$$

where F_x, F_y are the oil film forces acting on the journal. These forces are functions of the relative housing to journal displacements x, y, (measured directly by transducers), and relative velocities $\dot{x}$, $\dot{y}$ obtained by numerical differentiation of the measured x, y time history.

Accelerometers attached to the housing measured $\ddot{x}_h$, $\ddot{y}_h$ with x_h, y_h obtained by double numerical integration. The journal displacements with respect to a fixed position in space were obtained from:

$$x_j = x_h - x \quad ; \quad y_j = y_h - y \quad [2]$$

It was shown that if $-3 < x_j/x_h < +3$ then $m_o\ddot{x}_o \leq 0.01 \; m_h\ddot{x}_h$, and similarly for the y direction.

All experimental data reported in this paper were found to meet this condition. Morton (11) also notes that the oil film transverse inertial forces may be neglected. The equations of motion may therefore be simplified to:

$$F_{ex}-F_x = m_h\ddot{x}_h; \; F_{ey}-F_y = m_h\ddot{y}_h \quad [3]$$

3.3 Test Bearing Data

The following data define the relevant test bearing dimensions and operating conditions used:

Journal diameter	=	63.5 mm.
Bearing Length	=	2x9.3 mm. lands
Diametral clearance	=	0.0836 mm
Oil groove	=	5.08 mm x 360°
Journal speed	=	1180.RPM.
Oil supply pressure	=	0.0517 MPa (gauge)
Cavitation pressure	=	-0.175 MPa (gauge)
Effective viscosity	=	0.0186 Pa.s

3.4 Test Procedure

At each steady load - speed combination, test rig temperatures were stabilised and the data obtained for the determination of attitude angle and eccentricity. Data reported in this paper were all obtained at a single value of steady eccentricity ratio and attitude angle. Time histories of the bearing housing horizontal and vertical displacements relative to the journal, external dynamic forces and housing acceleration were recorded. Immediately after each dynamic loading test forces F_{ex}, F_{ey} were smoothly reduced to zero and an "origin" displacement - time history recorded. This accounted for effects such as small out of balance forces and journal runout. Journal centre location was then checked. Displacements due to dynamic forces alone were subsequently obtained by subtracting the "origin" ordinates from those at corresponding cycle times in the immediately preceding dynamically loaded test.

4. THEORETICAL METHOD A: RIGOROUS JOURNAL ORBIT ANALYSIS

4.1 Introduction

This method is based on the prediction of journal displacement and velocity components at the end of each time step by means of displacement and velocity coefficients computed for the current conditions. A full description of this method is given in reference (3). In relation to Method A the, the description "rigorous", essentially refers to the use of a numerical solution of the film pressure distribution (2) at each orbit step. This type of solution can accommodate finite length to diameter ratios and pressurised oil feed features.

Inevitably the term "rigorous" is relative, and the most significant approximation of this method is considered to be the rigid bearing assumption. As indicated in the review of previous work, modelling bearing elasticity at present results in excessive computing time unless approximate film pressure solutions are used. Bearing elasticity may be quite appreciable in some practical applications, notably connecting rod bearings, but the test bearing used to obtain the experimental orbit presented in this paper, was contained in a substantial housing. Differences in the experimental and theoretical orbits due to bearing elasticity are therefore unlikely to be serious in this instance.

4.2 Cavitation Model

A cavitation model which took account of flow continuity, whilst assuming a constant cavitation pressure, was used in Method A. Details of this model are also given in reference (2). No account is taken of the negative pressure spike preceeding the rupture boundary which has been reported in several experimental studies, but no practical system for modelling this feature is known to exist at present. The method whereby continuity is satisfied within the cavitation zone is simple and easy to apply within a relaxation solution of the film pressure distribution. Only the cavitation pressure has to be specified, no assumptions or initial estimations for the location of the cavitation zone boundaries, or the pressure gradients at these boundaries, are necessary. Furthermore, this method is eminently suitable to oil film history modelling, which may be defined as the step by step monitoring and updating of the extent of cavitation zones and the volumetric distribution of oil within them throughout the journal orbit.

4.3 Oil Film History Model

A detailed description of the oil film history model is given in reference (3) and the following notes outline the main features:

The oil film is divided into rectangular elements, for the purpose of solving the film pressure distribution by consideration of flow continuity (2). Oil film history modelling is based on the premise that in a dynamically loaded bearing, elements subject to cavitation do not have to satisfy flow continuity, since they may be filling or emptying at any given time. During each orbit time step the nett flow rate of oil to each element is computed, this being used to update the volume of oil within each element at the time step end:

$$V_{0\Delta}(j,i) = V_0(j,i) + q_n(j,i).\ \Delta t \qquad [4]$$

Transfer of a cavitating element to a full film element occurs when equation [4] predicts an oil volume equal to or exceeding the element volume: $V_0(j,i) \geqslant V_e(j,i)$. The reverse transfer may occur during the film pressure relaxation process, when a sub-cavitation pressure is computed for a full film element. By means of the above processes, cavitation zones may expand or contract in any direction according to the prevailing conditions as the dynamic cycle proceeds.

4.4 Orbit Time Step Solution

Since journal mass inertial forces were included, the orbit time step procedure was based on the solution of the equations of motion for the mean conditions during each orbit step:

$$(F_{ex\Delta} - F_{x\Delta} + F_{ex} - F_x)/2 = m\,\Delta\dot{x}/\Delta t \qquad [5]$$

$$(F_{ey\Delta} - F_{y\Delta} + F_{ey} - F_y)/2 = m\,\Delta\dot{y}/\Delta t \qquad [6]$$

At the start of each time step the journal displacement and velocity components $(x,y,\dot{x},\dot{y})$ will be known, and the corresponding oil film forces F_x, F_y can thus be computed. External force components F_{ex}, F_{ey} at the start point and $F_{ex\Delta}$, $F_{ey\Delta}$ at the end point can be interpolated from the specified external load cycle data. There remains 6 unknowns x_Δ, y_Δ, $\dot{x}_\Delta$, $\dot{y}_\Delta$, $F_{x\Delta}$, $F_{y\Delta}$ corresponding to the end point. An additional four equations are therefore required in order to obtain a solution. Two further equations are provided by using oil film displacement and velocity coefficients to relate the oil film force changes with the corresponding displacement and velocity changes during the time step. The displacement and velocity coefficients are computed for the conditions corresponding to the start point, and it is assumed that these values do not vary significantly over the time step:

$$\Delta F_x = A_{xx}\Delta x + A_{xy}\Delta y + B_{xx}\Delta\dot{x} + B_{xy}\Delta\dot{y} \qquad [7]$$

$$\Delta F_y = A_{yx}\Delta x + A_{yy}\Delta y + B_{yx}\Delta\dot{x} + B_{yy}\Delta\dot{y} \qquad [8]$$

The remaining two equations required are obtained by relating the displacement changes during Δt with the corresponding velocity changes by assuming that acceleration varies linearly with time during this interval:

$$\Delta x = (2\dot{x} + \dot{x}_\Delta)\,\Delta t/3 + \ddot{x}(\Delta t)^2/6 \qquad [9]$$

$$\Delta y = (2\dot{y} + \dot{y}_\Delta)\,\Delta t/3 + \ddot{y}(\Delta t)^2/6 \qquad [10]$$

The displacement and velocity coefficients used in equations [5] and [6] were computed at each orbit step point by the application of displacement and velocity perturbations and film pressure solutions to determine the corresponding oil film forces. A critical feature of the time step solution was the minimising of errors arising from the non-linearity of these coefficients. This was achieved in two ways: Firstly, the duration of each time step (Δt) was computed to maintain the step displacement and velocity changes within certain maximum values. These maximum changes were computed from empirical functions of the form $\Delta(\ \ ) = K1 - K2.\varepsilon$ where K1 and K2 are constants. Secondly, the procedure made initial estimates of the step displacement and velocity changes, these values then being used as the perturbations to compute the coefficients. Full details of this method are given in reference (3).

5. THEORETICAL METHOD B: THE REACTION METHOD

5.1 Introduction

This method achieves a substantially faster orbit analysis by the use of pre-computed velocity coefficients. The name "Reaction Method" was chosen since the velocity coefficients enable the total oil film force reaction to be estimated for any combination of journal velocity and position within the bearing clearance. Both squeeze and wedge actions are included, together with the interaction between them due to cavitation.

5.2 Oil Film Force Equations

The oil film force equations, which form the basis of the Reaction Method, are expressed in polar co-ordinate terms:

$$F_t = B_{tt}\dot{\theta}_0 + B_{trt}\,\dot{R}\dot{\theta}_0 \qquad [11]$$

$$F_r = B_{rt}\dot{\theta}_0 + B_{rr}\,\dot{R} + B_{rrt}\,\dot{R}\dot{\theta}_0 \qquad [12]$$

The development of these equations is described in detail in reference (4), and the principal features are as follows:

a) The force components F_r, F_t are the total oil film forces and not changes in force from an equilibrium position. This is facilitated by $\dot{\theta}_0$ being the total effective wedge velocity since it incorporates both the angular velocity of the journal about its own axis (ω) and the angular velocity of the journal axis about the bearing axis ($\dot{\theta}$) i.e. $\dot{\theta}_0 = \dot{\theta} - \omega/2$ (assuming a stationary bearing).

b) The velocity coefficients are

computed for a range of particular values of eccentricity ratio and interpolation (linear or logarithmic) between the adjacent values is carried out for any given eccentricity ratio.

c) Consideration of the dimensionless forms for the velocity coefficients is fully detailed in reference (4). This indicated that the validity of dimensionless velocity coefficients is restricted to given values of dimensionless supply and cavitation pressures, which in turn are functions of $\dot{R}$, $\dot{\theta}_0$ and the product $\dot{R} \cdot \dot{\theta}_0$ according to the type of coefficient.

d) Predicted orbits using coefficients derived by $\dot{R}$ perturbation amplitudes of 0.6, 1.2 and 1.8 mm/s did not indicate significant differences. It is therefore evident that the predicted orbits are not unduly sensitive to the perturbation amplitude from which the velocity coefficients are obtained. This means that the prediction accuracy when using dimensionless velocity coefficient data is not critically dependant on satisfying the similarity requirements with respect to dimensionless supply and cavitation pressures.

e) Reference (4) indicated that the F_r - $\dot{R}$ curves for $\dot{\theta}_0 \neq 0$ are asymptotic to the curve for $\dot{\theta}_0 = 0$ as the magnitude of $\dot{R}$ increased in both positive and negative directions. Accordingly, when using the linearised equations [11] and [12], F_r is not allowed to fall below the value corresponding to $\dot{\theta}_0 = 0$; i.e. $F_r \not< B_{rr} \dot{R}$.

f) The determination of velocity coefficients by the application of velocity perturbations is a quasi dynamic solution in that it ignores the dependence on previous conditions in the oil film. In other words the Reaction Method does not take account of oil film history, and should therefore be used with caution in situations where this factor may be significant.

5.3 Fast Orbit Time Stepping Procedure

The orbit time stepping procedure was virtually identical to that used for Method A. A Cartezian co-ordinate system was retained with displacement and velocity coefficients in Cartezian terms computed by means of equations [11] and [12] with appropriate Polar - Cartezian transformation. The most important difference in the procedure concerned the determination of the time step duration Δt. As shown in reference (3), Δt for each time step was determined to ensure that the changes in the components of displacement and velocity during the step were within prescribed limits which were functions of eccentricity ratio. This was necessary in order to maintain an acceptable accuracy of the predicted of oil film force components at the time step end when using linearised displacement and velocity coefficients. Δt was found by progressive reduction of trial values until all the above limits were satisfied. In Method A the initial trial value of Δt was arbitrarily set equal to about 1.5% of the cycle time and reduced by 1% for each successive trial. This approach ensured that Δt was within 1% of the maximum Δt permitted by the increment limit constraints. The corresponding time required to compute Δt was a small part of the total computing time. With the Reaction Method, the computing time required to establish Δt became significant. It was clearly necessary to find a satisfactory compromise between the conflicting requirements to maximise Δt within the given constraints, and yet minimise the computing time required to determine this value. After several trials, the optimum solution for the test conditions covered in this paper was found to be as follows: The initial trial Δt was set at 30% greater than the value for the previous time step, and this value was then reduced by 10% for each successive trial.

6. DISCUSSION OF RESULTS

Journal orbits predicted by both theoretical methods and those measured with the experimental test rig are presented in Figures 2 to 4. The corresponding external force cycle data is also given in polar form. External force cycle frequencies are at once (Test conditions 1 and 3, Figures 2 and 4.) and twice (Test condition 2, Figure 3) the journal rotational frequency. The form of the external force cycle is similar for test conditions 1 and 2 and results in oblique orbits. However, the external force cycle for test condition 3 is different and results in a substantially horizontal orbit. All three test conditions show good agreement between the orbits predicted by both theoretical methods. The differences between the results of the two theoretical methods are mainly due to the approximations introduced when fitting the relatively simple equations [11] and [12], used in Method B, to predicted oil film force journal velocity data.

Agreement between the experimental orbits and those predicted by both theoretical methods is generally satisfactory. However, there are two regions in which significant differences between the experimental and theoretical orbits are apparent.

The largest apparent discrecancy was in test condition 3 where Figure 4. shows that both theoretical methods have substantially greater excursions in the direction against rotation. In approaching the orbit extremity at $t/T \simeq 0.15$ a stronger oil film wedge action will be generated by the anticlockwise movement of the journal centre (negative $\dot{\theta}$). This region also coincides with negative $\dot{R}$. These two effects combine to cause a much stronger tendency to cavitate in the area to the downstream side of the minimum film thickness position. It is therefore postulated that the difference in the experimental and theoretical orbits in this region, may be due to the cavitation pressure being significantly lower than that used for the prediction of this dynamic situation. The cavitation pressure used to compute the theoretical orbits, was based on the value derived by Parkins (1) to yield agreement between the experimental and predicted equilibruim positions. Sensitivity of the orbits to such differences in the cavitation pressure would be increased by the

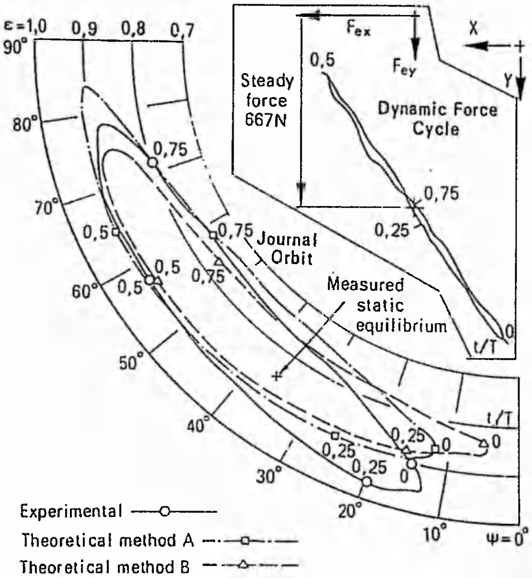

Test Condition 1 External Force Data and Journal Orbit
Fig 2

low forces in the corresponding part of the dynamic force cycle. Hume and Holmes (12) have also indicated that the correlation between experimental and theoretical orbits of a squeeze film bearing, is significantly dependent upon the provision for substantially sub-atmospheric cavitation pressures in the theoretical model.

In contrast with the above observations for test condition 3, the orbital movement against the direction of rotation in test condition 1 (Figure 2) corresponds to the build up to maximum load. This results in a mainly positive $\dot{R}$ and hence much less cavitation than that experienced in the corresponding part of the orbit for test condition 3. The reduced extent of cavitation, combined with the proximity to maximum load, would render oil film force prediction errors associated with cavitation insignificant in this situation. These conditions also apply to test condition 2 (Figure 3), and explains why the significant differences in the experimental and theoretical extent of movement against the direction of rotation in test condition 3 does not occur in the other test conditions.

The second important difference between the theoretical and experimental orbits, is the significantly greater eccentricity ratio of the experimental orbits in the vicinity of $\psi = 20^o$ in Figures 2 and 3, and similarly at $\psi = 40^o$ in Figure 4. In all three test conditions, the location of the above discrepancy corresponded to the region of maximum total load. Since the theoretical models assumed a rigid bearing and journal, elastic distortion is the most likely cause of the larger experimental eccentricity ratios at the more highly loaded parts of the dynamic cycle.

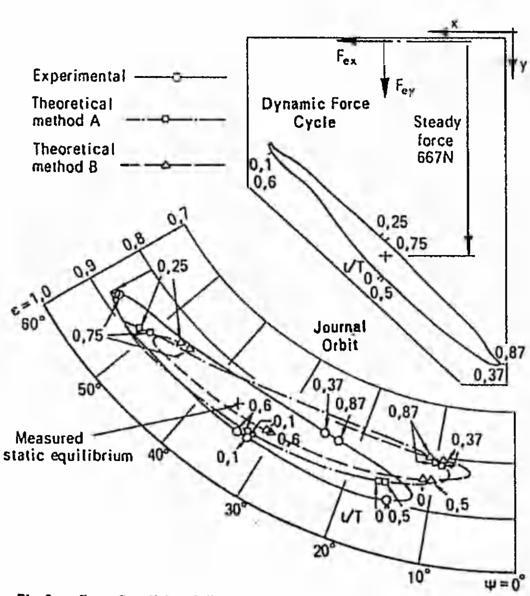

Fig 3 Test Condition 2 Force Data and Journal Orbit

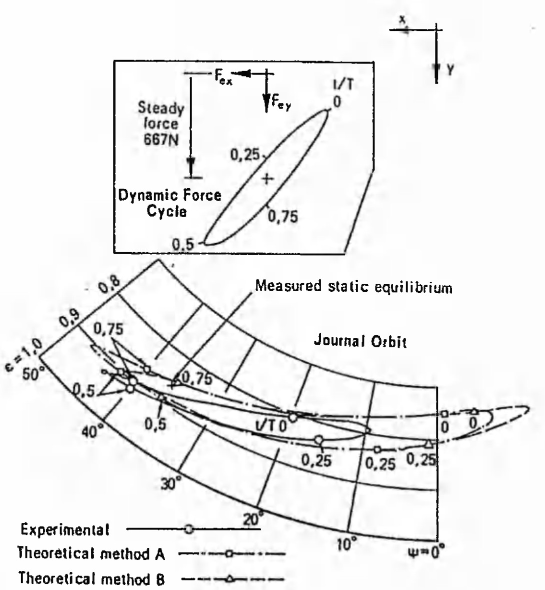

Test Condition 3 External Force Data and Journal Orbit
Fig 4

Theoretical journal orbits for test condition 1 (Figure 2) were computed both with and without the oil film history model using Method A. The differences were negligible. This result was considered to be due to the combination of a small orbit in relation to the clearance circle, and to the efficient supply of oil provided by the full circumferential groove.

7. CONCLUSIONS

This paper compares measured journal orbits with the predictions of two theoretical methods. The test conditions used covered different forms of excitation at both once and twice rotational frequency.

Good agreement was shown between the results of both theoretical methods, any difference being largely due to the approximations introduced in Method B in order to achieve faster computation. Method B, introduces simple equations for the total oil film force components, using a new type of velocity coefficient. An equivalent angular velocity is used which combines rotation of the journal about its axis with rotation of the journal axis about the bearing axis, thus facilitating application to both steady and dynamic situations. The computation time for this Method was reduced by a factor of over 300 relative to that for Method A.

The effect of oil film history was found to be negligible in the case analysed.

Generally good agreement between the experimental and theoretical orbits was attained. The main differences were considered to be related the influence of cavitation at low load and bearing elasticity at high load.

8. ACKNOLEDGEMENTS

The authors would like to thank the Head of the College of Manufacturing, Cranfield Institute of Technology and the Committee of Lloyd's Register of Shipping for permission to publish this paper. They would also like to thank their many colleagues at both Cranfield Institute of Technology and Lloyd's Register of Shipping for the help and cooperation throughout the work.

REFERENCES

(1) PARKINS D.W. "Theoretical and Experimental Determination of the Dynamic Characteristics of a Hydrodynamic Journal Bearing". A.S.M.E. Jnl. Lub. Tech. Vol. 101. April 1979 pp 129 - 139.

(2) JAKEMAN R.W. "A numerical analysis method based on flow continuity for hydrodynamic journal bearings". Tribol. Int. Vol. 17. No. 6. Dec. 1984 pp 325 - 333.

(3) JAKEMAN R.W. "Journal Orbit Analysis taking account of Oil Film History and Journal Mass". Proc. of Conf: Numerical Methods in Laminar and Turbulent Flow. Swansea. July 1985 pp 199 - 210.

(4) JAKEMAN R.W. "The Influence of Cavitation on the non-linearity of Velocity Coefficients in a Hydrodynamic Journal Bearing." To be published: Leeds - Lyon Tribol. Symp. Leeds Sept. 1986.

(5) BOOKER J.F. "Dynamically loaded Journal Bearings: Numerical Application of the Mobility Method". A.S.M.E. Jnl. Lub. Tech. Jan 1971. pp 168 - 176.

(6) HOLMES R. and CRAVEN A.H. "The Influence of Crankshaft and Flywheel mass on the Performance of Engine Main Bearings" I.Mech.E Tribol. Conv 1971 Paper C63/71 pp 80 - 85.

(7) JONES G.J. "Crankshaft Bearings: Oil Film History" 9th Leeds-Lyon Tribol Symp.Sept.1982 pp 83 - 88.

(8) LA BOUFF G.A. and BOOKER J.F. "Dynamically Loaded Journal Bearings: A Finite Element Treatment for Rigid and Elastic Surfaces". A.S.M.E./A.S.L.E. Conf. Oct. 1984 A.S.M.E. Paper 84 - TRIB - 11.

(9) FANTINO B., FRENE J. and GODET M. "Dynamic Behaviour of an Elastic Connecting Rod Bearing - Theoretical Study". SAE/SP-539 - Studies in Engine Bearings and Lubrication, Paper No. 83037, Feb. 1983 pp 23 - 32.

(10) GOENKA P.K. and OH K.P. "An Optimum Connecting Rod Design Study - A Lubrication Viewpoint". A.S.L.E./A.S.M.E Tribology Conference. Atlanta October 1985. A.S.M.E. Preprint No. 85 - Trib - 50.

(11) MORTON, P.G. "Measurement of the Dynamic Characteristics of a Large Sleeve Bearing". Trans. A.S.M.E. Jnl. Lub. Tech. Jan. 1971. pp. 143-150.

(12) HUMES, B and HOLMES, R. "The Role of Sub-Atmospheric Film Pressures in the Vibration Performance of Squeeze Film Bearings". I. Mech. E. Jnl of Mech. Eng. Science. Vol. 20. No. 5. 1978. p. 283.

REFERENCE. 87.

VOLUME 29, 4, 441–450
ASLE TRANSACTIONS

Performance and Oil Film Dynamic Coefficients of a Misaligned Sterntube Bearing©

R. W. JAKEMAN
Lloyd's Register of Shipping, London EC3M 4BS, United Kingdom

Sterntube bearings are commonly subjected to significant static and dynamic angular misalignment by the adjacent propeller. Results of a theoretical investigation into the performance of oil-lubricated sterntube bearings with static misalignment are reported. In addition, 32 oil film force and moment coefficients, which fully define the response to both lateral and angular motion of the journal axis, are presented. Limitations to the application of these coefficients arising from their nonlinearity are discussed. A practical sterntube bearing analysis program is described which utilizes computed dimensionless performance data. This program determines the effective oil film viscosity via an iterative heat balance procedure, and thus simulates the operating conditions of a real bearing. Results produced by this program are included, and give a realistic indication of the effect of L/D ratio variation for a range of misalignment angles.

**Presented as an American Society of Lubrication Engineers paper at the ASLE/ASME Tribology Conference in Atlanta, Georgia, October 8–10, 1985
Final manuscript approved June 19, 1985**

INTRODUCTION

Operating Environment

Location

Sterntube bearings support the aftermost end of marine propeller shafts. The sterntube forms an integral part of the hull structure, and frequently contains bearings at its forward and after ends, both being referred to as sterntube bearings. It is the after sterntube bearing, however, which is of principal concern, since it is closer to the propeller and is consequently subjected to the most arduous loading conditions.

Static Loading

The after end of a propeller shaft is subject to substantial cantilever loading due to the overhung weight of the propeller. This frequently leads to static angular misalignment between the shaft and sterntube bearing. Application of rational alignment analysis to the complete propeller shaft system (*1*) enables such misalignment to be reduced to ac-

NOMENCLATURE

$A_{xx}, A_{\lambda\lambda}$, etc.	= displacement coefficients
$B_{xx}, B_{\lambda\lambda}$, etc.	= velocity coefficients
Bow	= journal bow at bearing axial center
C_d	= diametral clearance
D	= journal diameter
e	= journal eccentricity at bearing axial center
h_{min}	= minimum film thickness
H	= power loss
L	= bearing length
M, M_x, M_y	= total oil film moment and components in horizontal and vertical planes
N	= journal rotational speed rev.s^{-1}
p_h	= oil head pressure
Q	= volume flow rate (side leakage)
u	= journal surface velocity due to rotation
W, W_x, W_y	= total oil film force and components acting in horizontal and vertical directions
x, y	= horizontal, vertical lateral displacement components
$\dot{x}, \dot{y}$	= horizontal, vertical lateral velocity components
α	= misalignment angle
β	= angle of misalignment plane
ε	= eccentricity ratio at bearing axial center ($2e/C_d$)
ϑ_m	= oil film moment plane TAN$^{-1}(M_x/M_y)$
ϑ_w	= oil film force direction TAN$^{-1}(W_x/W_y)$
ψ	= attitude angle at bearing axial center
λ, γ	= journal axis angular displacements in horizontal and vertical planes
$\dot{\lambda}, \dot{\gamma}$	= journal axis angular velocities in horizontal and vertical planes

A.4. - 40.

ω = journal rotational speed rad.s^{-1}
η = dynamic viscosity (constant effective value)

Several of the above parameters are clarified in Fig. 1. Consistent SI units are used throughout.

Suffixes

x = horizontal direction
y = vertical direction
λ = horizontal plane
γ = vertical plane

In the dynamic coefficients, the double suffixes are defined thus:

The first suffix indicates force direction (x,y) or moment plane (λ,γ). The second suffix indicates lateral displacement/velocity direction (x,y) or angular displacement/velocity plane (λ,γ).

Note that in this paper components of moments and angular displacement/velocity are defined with respect to the plane in which they act rather than about an axis.

Example coefficient definitions are:

$$A_{xy} = \frac{\partial W_x}{\partial y}, \; B_{\lambda x} = \frac{\partial M_x}{\partial \dot{x}}, \; A_{\gamma\lambda} = \frac{\partial M_y}{\partial \lambda}, \; B_{y\gamma} = \frac{\partial W_y}{\partial \dot{\gamma}}$$

Nondimensional Parameters

Nondimensional parameters are indicated by a "bar," and are defined as follows:

$$\overline{W} = \frac{W}{\eta NLD}\left(\frac{C_d}{D}\right)^2 \left[= \frac{1}{\text{Sommerfeld No.}}\right], \; \overline{M} = \frac{M}{\eta NL^2D}\left(\frac{C_d}{D}\right)^2$$

$$\overline{H} = \frac{H\,C_d}{\eta N^2LD^3}, \quad \overline{Q} = \frac{Q\eta L^2}{WC_d^3}$$

$$\overline{p}_h = \frac{p_hLD}{W}, \quad \overline{\alpha} = \frac{\alpha L}{C_d}$$

$$\overline{Bow} = \frac{2Bow}{C_d}$$

$$\overline{A}_{xx} = \frac{A_{xx}\,C_d}{W}, \text{ etc.}, \quad \overline{B}_{xx} = \frac{B_{xx}\,\omega\,C_d}{WD}, \text{ etc.}$$

$$\overline{A}_{x\lambda} = \frac{A_{x\lambda}\,C_d}{WL}, \text{ etc.}, \quad \overline{B}_{x\lambda} = \frac{B_{x\lambda}\,\omega\,C_d}{WLD}, \text{ etc.}$$

$$\overline{A}_{\lambda x} = \frac{A_{\lambda x}\,C_d}{WL}, \text{ etc.}, \quad \overline{B}_{\lambda x} = \frac{B_{\lambda x}\,\omega\,C_d}{WLD}, \text{ etc.}$$

$$\overline{A}_{\lambda\lambda} = \frac{A_{\lambda\lambda}\,C_d}{WL^2}, \text{ etc.}, \quad \overline{B}_{\lambda\lambda} = \frac{B_{\lambda\lambda}\,\omega\,C_d}{WL^2D}, \text{ etc.}$$

$$\overline{x} = \frac{2x}{C_d}, \text{ etc.}, \quad \overline{\dot{x}} = \frac{\dot{x}}{u}, \text{ etc.}$$

$$\overline{\lambda} = \frac{2L\lambda}{C_d}, \text{ etc.}, \quad \overline{\dot{\lambda}} = \frac{L\dot{\lambda}}{u}, \text{ etc.}$$

---

ceptable levels. Shafting design constraints lead to relatively long sterntube bearings ($L/D \approx 2$), which are, therefore, given larger clearance ratios ($Cd/D \approx 0.002$) in order to offset the sensitivity to misalignment.

Dynamic Loading

Marine propellers may produce significant dynamic loading due to their operation in a nonuniform flow of water. This results in the application of steady and dynamic components of moment and force to the propeller shaft end, thus causing steady and dynamic misalignment at the sterntube bearing. In general, the above effects are predominantly in the vertical plane, but, for a turning ship, the transverse flow relative to the stern may generate substantial components in the horizontal plane. Well-documented sterntube bearing failures arising from such conditions are described in Ref. (*2*).

Lubrication

Water-lubricated sterntube bearings are still used in smaller ships and in many naval ships where their overall simplicity is advantageous. The low viscosity of water and multiple axial grooves used in these bearings prevent effective hydrodynamic lubrication (*3*) thus resulting in relatively high wear-down rates. Consequently, oil-lubricated sterntube bearings have gained widespread acceptance in modern merchant ships, and the results reported are confined to this type. These bearings usually have two full, or nearly full-length axial oil grooves diametrically opposite on the horizontal center line. Since the low shaft speed results in a low level of heat generated by the bearing, and seawater provides an effective heat sink to the surrounding structure, the need for positive oil circulation to remove heat is eliminated in most cases.

The sterntube is fully flooded with oil which is maintained under pressure by a header tank. This pressure is set to slightly exceed that of the seawater at shaft level to prevent any ingress of seawater in the event of seal leakage. The sterntube bearing is thus subject to a constant oil head pressure along both axial grooves, and at its ends.

Reliability

Despite conservative loading, at present, the reliability of sterntube bearings cannot be regarded as entirely satisfactory (*4*). The indicated direct correlation between failure rate and shaft diameter conflicts with the current trend towards the use of larger propellers operating at lower speed. Safe operation is critically dependent on the sterntube bearing, and since it is extremely inaccessible, reliability is of paramount importance.

Objectives

The essential objective of this work is to improve the reliability of sterntube bearings by the provision of a comprehensive analysis facility. Steady-load performance data and dynamic coefficients for small amplitude shaft vibration

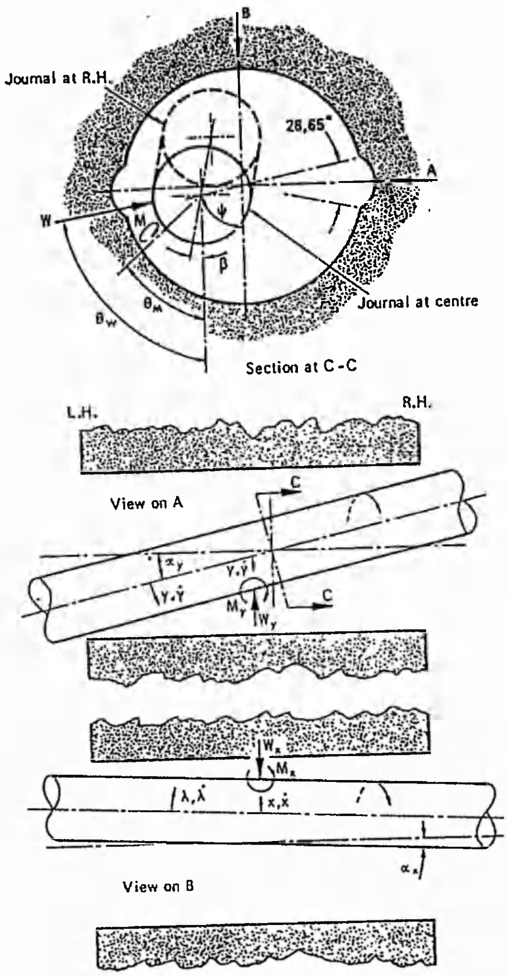

Fig. 1—Sterntube bearing load and geometrical parameters'

are included. For long bearings, no data on the oil film coefficients for dynamic misalignment are known to exist. As part of a continuing research program, large amplitude dynamic misalignment conditions will be investigated in the next stage.

THEORETICAL BASIS

Analysis Method

The theoretical results presented were produced by a finite bearing numerical analysis method based on flow continuity (5). In this method, the oil film is divided into rectangular elements. The pressure at the center of each element is solved by writing a flow continuity equation for each element, and then applying a Gauss-Seidel relaxation procedure. Continuity consideration includes the cavitation zone where gas/vapor flow terms are introduced to satisfy continuity when a constant cavitation pressure is specified.

Assumptions

The assumptions used for the analysis are as stated in (5). In relation to their application to sterntube bearings, the following comments are made:

Sterntube bearings operate at relatively low speed and moderate pressure (W/LD), therefore the oil temperature rise is small. In view of this, the commonly used assumption of a constant effective viscosity is reasonable.

The modest loading and the anticipated low level of thermal distortion justify the assumption of rigid circular journal and bearing surfaces. In recent years, small-scale use has been made of reinforced plastic, as the bearing material, in oil-lubricated sterntube bearings. The relatively high flexibility of such materials renders the assumption of rigidity unsatisfactory. This assumption is, therefore, considered to be applicable to the more commonly encountered white-metal-lined bearings only.

Element Division

The choice of oil film element division is a compromise between computing time and accuracy. Dynamic coefficients require a substantially finer element division than steady-load performance parameters, since they are computed from the change in oil film force or moment components resulting from small displacement or velocity perturbations. Tests indicated that an element division of 50 circumferential by 14 axial for the bottom half of the bearing and 25 circumferential by 14 axial for the top was satisfactory.

The use of 14 uniform axial element divisions would be inadequate for cases with large misalignment due to severe peaking of the axial film pressure profile. In order to overcome this problem without increasing the number of axial elements, axial element grading was introduced. The axial element dimension was reduced as a linear function of element number from the center to each end, and a grading factor of 5 adopted, i.e. the axial length of the elements adjacent to the bearing ends was one-fifth of that for a constant element length with the same number of axial divisions. Circumferential element grading as a function of film thickness, as used by Lloyd et al (6), was considered to be impractical in a misaligned bearing due to variation of the circumferential position of h_{min} along the bearing axis.

Dynamic Coefficients

"Dynamic coefficient" is used as a general term for oil film displacement and velocity coefficients. It covers both force and moment changes arising from lateral and angular displacement and velocity perturbations. Thirty-two such coefficients are required to define the oil film forces and moments produced by a dynamically misaligned sterntube bearing. These may be expressed as follows:

$$\begin{bmatrix} W_x \\ W_y \\ M_x \\ M_y \end{bmatrix} = \begin{bmatrix} A_{xx} & A_{xy} & A_{x\lambda} & A_{x\gamma} \\ A_{yx} & A_{yy} & A_{y\lambda} & A_{y\gamma} \\ A_{\lambda x} & A_{\lambda y} & A_{\lambda\lambda} & A_{\lambda\gamma} \\ A_{\gamma x} & A_{\gamma y} & A_{\gamma\lambda} & A_{\gamma\gamma} \end{bmatrix} \cdot \begin{bmatrix} x \\ y \\ \lambda \\ \gamma \end{bmatrix} + \begin{bmatrix} B_{xx} & B_{xy} & B_{x\lambda} & B_{x\gamma} \\ B_{yx} & B_{yy} & B_{y\lambda} & B_{y\gamma} \\ B_{\lambda x} & B_{\lambda y} & B_{\lambda\lambda} & B_{\lambda\gamma} \\ B_{\gamma x} & B_{\gamma y} & B_{\gamma\lambda} & B_{\gamma\gamma} \end{bmatrix} \begin{bmatrix} \dot{x} \\ \dot{y} \\ \dot{\lambda} \\ \dot{\gamma} \end{bmatrix} \quad (1)$$

The dynamic coefficients are determined by applying appropriate displacement and velocity perturbations to the steady-state solution, and computing the change in oil film force and moment components. These coefficients are subject to a high degree of nonlinearity and, for shaft whirling frequency prediction, so-called "zero amplitude" coefficients are used. In order to achieve a good approximation to zero amplitude, the smallest practicable perturbation amplitudes, in relation to the film pressure resolution accuracy (0.01 percent), are used. This is further enhanced by the use of positive and negative perturbation amplitudes, and computing the mean coefficients. The perturbation amplitudes used thoughout this work were:

$$\bar{x}, \bar{y} = 0.01 \quad ; \quad \bar{\dot{x}}, \quad \bar{\dot{y}} = 0.00001$$

$$\bar{\lambda}, \bar{\gamma} = 0.01 \quad ; \quad \bar{\dot{\lambda}}, \quad \bar{\dot{\gamma}} = 0.0001$$

Ideally, the amplitudes should be varied as a function of ε and $\bar{\alpha}$, but, for simplicity, tests indicated the above values to be adequate for all conditions covered. Nonlinearity of dynamic coefficients has been shown experimentally and theoretically by Parkins (*7*), (*8*).

COMPARISON OF RESULTS WITH PUBLISHED DATA

Static Load

Comparison of results produced by the author's program with those by Pinkus and Bupara (*9*) and Hill and Martin (*4*) are given in Ref. (*5*). These results indicated satisfactory agreement.

Dynamic Load

The only data found covering all 32 oil film coefficients for a dynamically misaligned bearing was that by Pafelias (*10*). These results were for a 150° partial arc bearing with $L/D = 0.5$. The pad boundary pressure and cavitation pressure were specified as zero gauge. Simple modifications to the author's program were carried out to facilitate the production of comparative results. Eight cases were examined covering high and low ε for a range of α and β. The comparative results of the four cases at higher ε are presented in Table 1. Differences in the dynamic coefficients may be partly due to the use of different perturbation amplitudes. Since the level of disagreement clearly correlated with the severity of peaking of the axial film pressure profile, the disparity is more likely to be due to differences in the oil film meshes. The author used 50 circumferential divisions by 14 axial with an axial grading factor of 5. Agreement in the four cases not shown, which had the same range of α, β but all at $\varepsilon = 0.4$, was very good.

The effect of perturbation amplitude on the A_{xx} and A_{yy} results for Case 8 is shown in Fig. 2. This also shows the benefit of using combined positive and negative perturbation amplitudes, and indicates the severity of the nonlinearity.

The author's system of accounting for continuity within the cavitation zone will not be significant in a 150° partial arc bearing, since there is no reformation boundary within the pad area.

RESULTS

A comprehensive investigation was undertaken in which the following parameters were treated as independent variables for computational purposes: L/D, ε, $\bar{\alpha}$, $\bar{p}_h$, β, ϑ_w, $\overline{Bow}$.

Comprehensive coverage of a large range of combinations of these parameters was not feasible due to the amount of computation involved. Variation of each parameter singly was, therefore, carried out while maintaining the remainder constant at the following datum conditions: $L/D = 2$, $\varepsilon = 0.7$, $\bar{\alpha} = 0$ and 0.2, $\bar{p}_h = 0$, $\beta = 0$, $\vartheta_w = 0$, $\overline{Bow} = 0$.

Computation of the steady-load solution only required about 10 percent of the time necessary for a full analysis including all 32 dynamic coefficients. Accordingly, a more comprehensive analysis program was conducted for the steady-load condition, the parameter range being: $L/D = 1$ to 3, $\bar{p}_h = 0$ to 0.2, $\varepsilon = 0.1$ to 0.95, $\bar{\alpha} = 0$ to 0.9 with β, ϑ_w and $\overline{Bow}$ held at zero.

It is only possible to present a small part of the results produced within the confines of this paper. The most significant independent variable is ε which has, therefore, been used as the selection basis for the results included. These are shown in Figs. 3 to 6 (steady-load parameters) and Figs. 7 to 10 dynamic coefficients.

PRACTICAL ANALYSIS PROGRAM

The fundamental solution to the hydrodynamic lubrication problem suffers from the disadvantage that the journal position within the bearing must be specified, and the load derived by the analysis. Thus ε, ψ, α, β are treated as independent variables and W, ϑ_w, M, ϑ_m are dependent.

In a practical sterntube bearing situation, it is possible to specify α, β, by means of a shaft alignment analysis, prior to analysis of the bearing. This feature results from the alignment conditions not generally being critically dependent on the bearing support conditions. Shaft alignment analysis using a rough estimate of the location of the effective point of support in the sterntube bearing will yield sufficiently accurate values of α and β. Sterntube bearing load (W, ϑ_w), however, determines ε and ψ which is a reversal of the fundamental hydrodynamic analysis.

The author's fundamental analysis program operates in dimensional terms, the required nondimensional parameters being derived at the output stage. For particular values of $\bar{p}_h$ to be realized, it is, therefore, necessary to specify W. This is achieved by an iterative procedure in which η is adjusted until the analysis produces the required W to a tolerance of $\pm$ 0.5 percent. A purely vertical load is generally specified ($\vartheta_w = 0$), and ψ is, therefore, also adjusted in the above procedure to yield $W_x = 0$ to a tolerance of $\pm$ 0.1 percent W_y. The above system enables useful dimensionless performance data to be produced. Since neither η or ψ are independent variables in a real bearing, this type of analysis is unsuitable for direct application to practical problems.

TABLE 1—COMPARISON OF DIMENSIONLESS OIL FILM PARAMETERS WITH RESULTS PUBLISHED IN REF. (*10*)

Bearing:	150° Partial Arc—L/D = 0.5
Source:	A—Author, 10—Pafelias—Ref. (*10*).
ε	Eccentricity ratio.
$\bar{\alpha}$	Misalignment angle (dimensionless).
β	Angle of misalignment plane (degrees).
$\bar{W}$	Load (dimensionless).
ψ	Attitude angle (degrees).
$\bar{M}$	Moment (dimensionless).
ϑ_m	Angle of moment plane (degrees).
$\bar{p}_{max}$	Maximum film pressure (dimensionless).
$\bar{A}$	Displacement coefficients (dimensionless).
$\bar{B}$	Velocity coefficients (dimensionless).

CASE	2		4		6		8	
SOURCE	A	(*10*)	A	(*10*)	A	(*10*)	A	(*10*)
INPUT ε	0.9		0.75		0.8		0.6	
INPUT $\bar{\alpha}$	0		0.25		0.25		0.3535	
INPUT $\beta°$	0		0		90		45	
$\bar{W}$	31.56	31.55	10.72	10.07	12.47	12.36	4.457	4.292
$\psi°$	22.10	22.10	30.33	31.20	25.29	25.59	32.83	33.93
$\bar{M}$	0	0	1.792	1.565	0.997	0.989	0.695	0.642
$\vartheta_m°$	0	0	4.67	4.28	23.63	23.60	11.70	11.33
$\bar{p}_{max}$	4.80	4.83	9.16	7.95	4.49	4.47	6.24	5.84
$\bar{A}_{xx}$	3.09	3.17	3.52	3.28	3.99	3.87	3.96	3.70
$\bar{A}_{xy}$	2.21	2.10	2.47	1.59	1.77	1.36	1.32	0.752
$\bar{A}_{yx}$	11.1	11.3	11.3	10.2	10.5	10.3	9.82	9.25
$\bar{A}_{yy}$	27.7	27.5	23.2	19.3	17.9	17.8	13.3	12.0
$\bar{A}_{\lambda x}$	0	0	0.830	0.672	0.787	0.734	1.04	0.888
$\bar{A}_{\lambda y}$	0	0	1.07	0.678	0.839	0.836	0.816	0.580
$\bar{A}_{\gamma x}$	0	0	2.81	2.22	1.67	1.58	2.26	1.95
$\bar{A}_{\gamma y}$	0	0	6.50	4.76	2.11	2.09	3.11	2.57
$\bar{A}_{x\lambda}$	0	0	0.795	0.614	0.801	0.708	1.02	0.824
$\bar{A}_{x\gamma}$	0	0	0.917	0.494	0.850	0.820	0.748	0.470
$\bar{A}_{y\lambda}$	0	0	2.75	2.07	1.74	1.57	2.25	1.82
$\bar{A}_{y\gamma}$	0	0	5.82	3.91	2.45	2.33	3.03	2.32
$\bar{A}_{\lambda\lambda}$	0.135	0.136	0.324	0.242	0.296	0.266	0.378	0.296
$\bar{A}_{\lambda\gamma}$	0.116	0.116	0.385	0.212	0.222	0.210	0.278	0.160
$\bar{A}_{\gamma\lambda}$	0.431	0.434	1.03	0.732	0.608	0.558	0.784	0.614
$\bar{A}_{\gamma\gamma}$	1.28	1.09	2.38	1.60	1.07	1.04	1.16	0.888
$\bar{B}_{xx}$	1.41	1.49	1.89	1.95	2.33	2.21	2.83	2.92
$\bar{B}_{xy}$	3.60	3.68	3.75	3.63	3.71	3.63	3.69	3.73
$\bar{B}_{yx}$	3.46	3.67	3.66	3.65	3.73	3.63	3.66	3.72
$\bar{B}_{yy}$	20.6	20.9	18.1	17.3	17.3	17.2	15.5	15.4
$\bar{B}_{\lambda x}$	0	0	0.318	0.290	0.386	0.338	0.543	0.534
$\bar{B}_{\lambda y}$	0	0	0.888	0.740	0.829	0.770	1.03	0.986
$\bar{B}_{\gamma x}$	0	0	0.858	0.746	0.774	0.706	0.987	0.942
$\bar{B}_{\gamma y}$	0	0	0.921	0.786	0.841	0.738	1.07	0.972
$\bar{B}_{x\lambda}$	0	0	0.346	0.306	0.384	0.326	0.567	0.530
$\bar{B}_{x\gamma}$	0	0	0.913	0.764	0.779	0.682	1.02	0.932
$\bar{B}_{y\lambda}$	0	0	0.921	0.786	0.841	0.738	1.07	0.972
$\bar{B}_{y\gamma}$	0	0	3.79	3.17	1.51	1.34	2.65	2.39
$\bar{B}_{\lambda\lambda}$	0.054	0.054	0.137	0.112	0.142	0.126	0.207	0.190
$\bar{B}_{\lambda\gamma}$	0.139	0.136	0.334	0.256	0.234	0.210	0.333	0.298
$\bar{B}_{\gamma\lambda}$	0.136	0.136	0.336	0.260	0.234	0.210	0.336	0.296
$\bar{B}_{\gamma\gamma}$	0.674	0.676	1.30	1.03	0.675	0.642	0.865	0.774

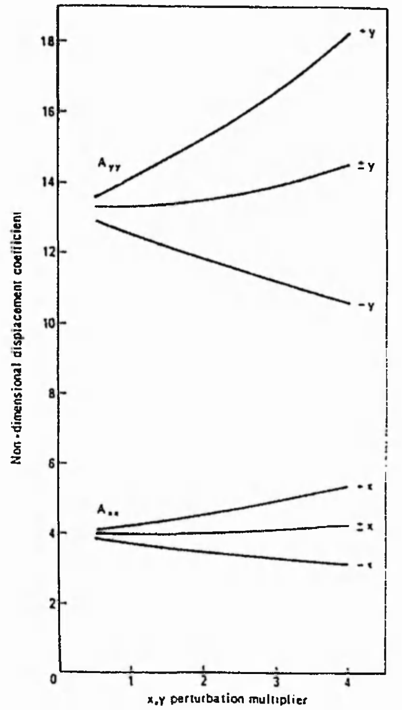

Fig. 2—Effect of perturbation amplitude on dynamic coefficients. Coefficients shown correspond to Case 8. in Table 1 for a 150° partial arc bearing with $L/D = 0.5$, $\varepsilon = 0.6$ $\bar{\alpha} = 0.3535$, $\beta = 45°$. Perturbation multiplier 1 corresponds to $\bar{x}, \bar{y} = 0.01$.

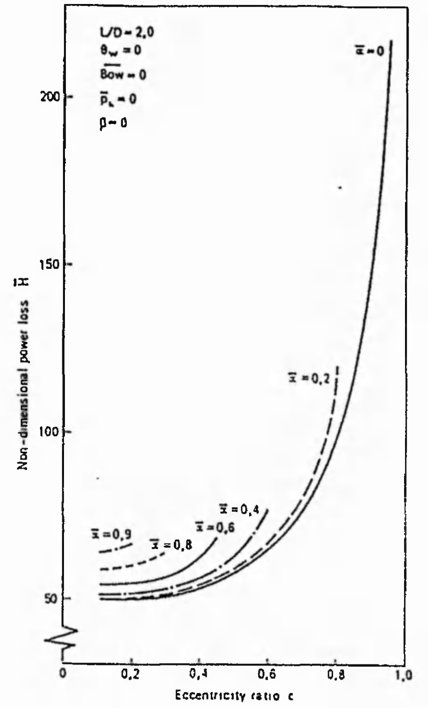

Fig. 4—Variation of nondimensional power loss with eccentricity ratio

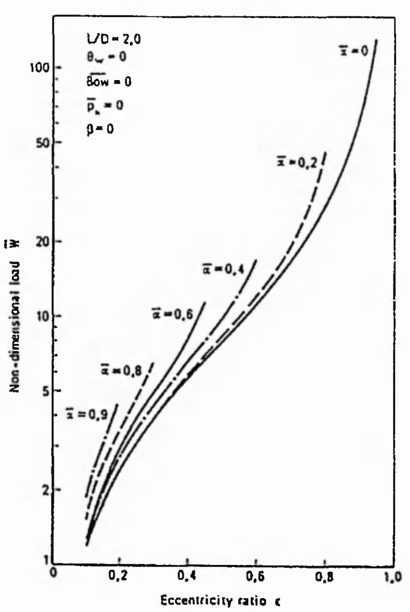

Fig. 3—Variation of nondimensional load with eccentricity ratio

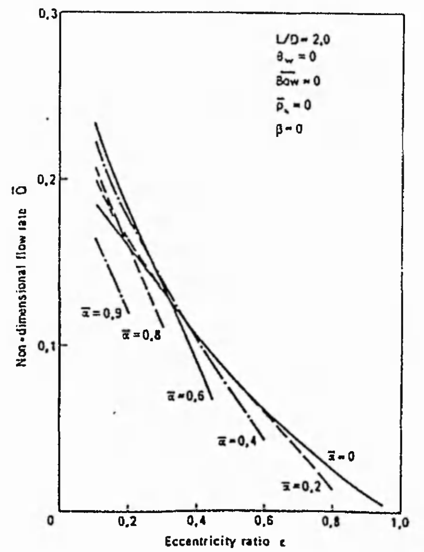

Fig. 5—Variation of nondimensional flow rate with eccentricity ratio

The other problem with the results given in the previous sections is that only one independent variable was changed at a time, while the remainder were held constant. This does not correspond to the behavior of a real bearing, but the dimensionless performance data produced can be utilized in a practical analysis program.

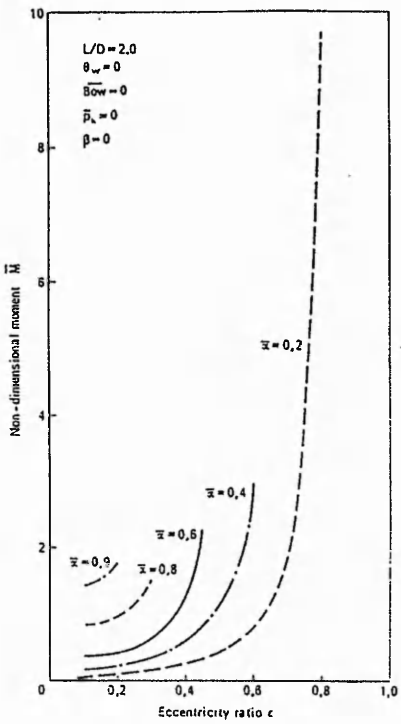

Fig. 6—Variation of nondimensional moment with eccentricity ratio

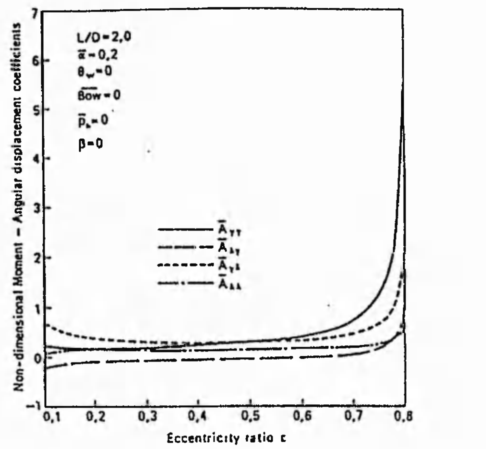

Fig. 8—Variation of nondimensional moment—angular displacement coefficients with eccentricity ratio.

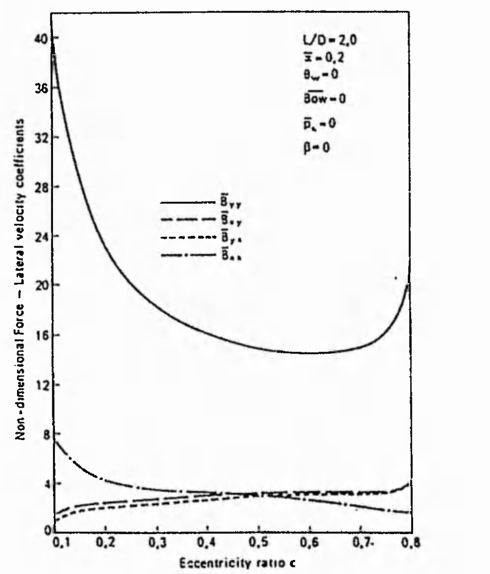

Fig. 9—Variation of nondimensional force—lateral velocity coefficients with eccentricity ratio.

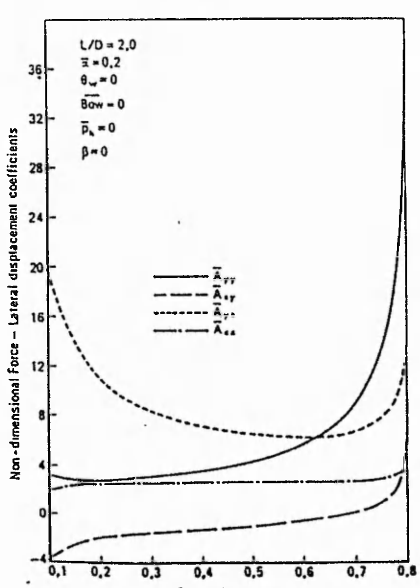

Fig. 7—Variation of nondimensional force-lateral displacement coefficients with eccentricity ratio.

Description

A practical analysis program is one in which W, ϑ_w, α, β may be specified, and ε, ψ computed. In addition, the effective film viscosity is derived in the program by an iterative heat balance procedure, the relevant input being simply oil supply temperature and temperature-viscosity characteristics. This type of analysis is described in detail in Ref. (*11*) for aligned bearings. A sterntube bearing performance program based on the above method has been developed. This program has provision for specifying W, α, and p_h as input

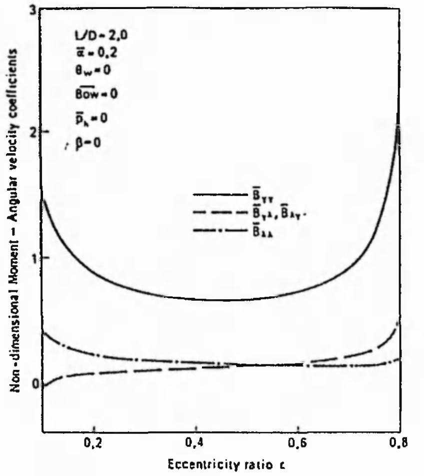

Fig. 10—Variation of nondimensional moment—angular velocity coefficients with eccentricity ratio.

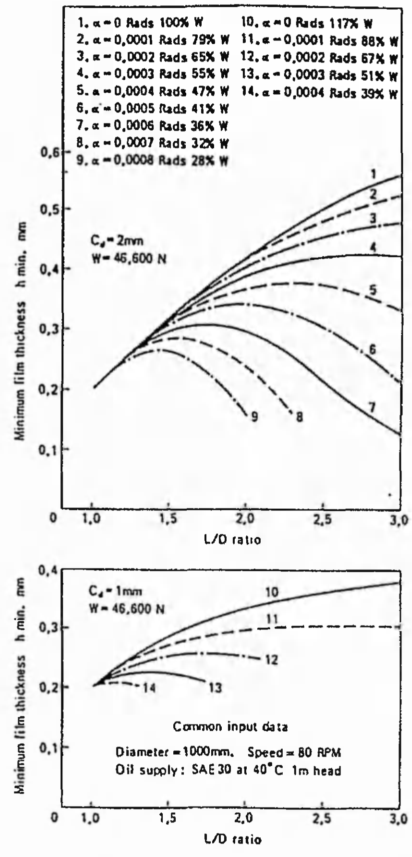

Fig. 11—Relationship between minimum film thickness and L/D ratio for a range of misalignment—load combinations and two clearances. These results are predicted by a practical analysis program in which the effective film viscosity is determined by a heat balance.

with β, ϑ_w and *Bow* being taken as zero. Dimensionless data of the type shown in Figs. 3 to 6 are utilized. The data banks are in the form of 4-dimensional matrices; for example, nondimensional load would be expressed as: $\overline{W}$ ($\bar{p}_h$, *L/D*, $\bar{\alpha}$, ε). In order to facilitate accurate interpolation of data from such matrices, various empirically derived linearizing functions are applied. The assumption that 90 percent of the heat generated goes to the oil is made. A more accurate result would be obtained by a rigorous heat-transfer analysis for a particular installation. Since the low shaft speeds associated with sterntube bearings yield low-temperature rises, and since the temperature of the oil supply and surrounding structure varies appreciably according to season and geographical location, such a refinement cannot be justified.

The essential feature of this program is that it simulates the behavior of a real bearing. It thus facilitates a realistic indication of the effect of changing any design parameter.

Optimum L/D Ratio

As noted earlier, the shaft diameter and loading constraints on a sterntube bearing lead to high *L/D* ratios, generally around 2 at present. Since long bearings are more sensitive to misalignment, there has been some pressure to reduce the *L/D* ratio, and values down to 1.5 have been adopted in some instances. The practical analysis program described above enables the effects of these conflicting factors to be quantified.

There are a number of alternative ways in which this problem could be studied. The essential feature of the one chosen is that it facilitates clear graphical presentation of the results. In all the cases analyzed, *W* was adjusted to give h_{min} = 0.2 mm at the bearing end with *L/D* = 1.0. The *L/D* ratio was then increased in steps, maintaining α and *W* constant. A family of curves for a range of α values was thus produced. The results are shown in Fig. 11 for C_d = 2 and 1 mm. At α = 0 and C_d = 2 mm, the above criterion (h_{min} = 0.2 mm at *L/D* = 1) was met by *W* = 46 600 N. This was taken as the datum load, and all other loads are expressed as a percentage of this value.

For C_d = 2 mm, it is evident that α must exceed 0.0005 rads before there is any incentive to reduce *L/D* below 2.0. Reducing C_d to 1 mm increases the load capacity at α = 0 due to the enhanced hydrodynamic effect. This effect is substantially offset by the higher operating temperature and hence reduced effective viscosity resulting from the tighter clearance. A more pronounced fall in *Q* as *L/D* increased was found for C_d = 1.0 mm, hence the much flatter family of curves. The direct effect of misalignment is more significant at reduced C_d; note that α = 0.0008 rads at C_d = 2 mm and α = 0.0004 rads at C_d = 1 mm yield the same $\bar{\alpha}$. At C_d = 1 mm, the misalignment threshold beyond which it is worthwhile to reduce *L/D* below 2.0 is about 0.00015 rads. These results clearly indicate the need for a reasonably generous clearance in sterntube bearings, particularly where higher levels of misalignment are predicted. Given an adequate clearance, levels of misalignment which result in an optimum *L/D* ratio of less than 2 are likely to be excessive. In such cases, the misalignment should be reduced by suitable alignment of the forward part of the shafting system, or by slope boring the sterntube bearing.

This problem is complex, and one which does not appear to be amenable to generalization. The results given are thus only intended to serve as an illustration of sterntube bearing characteristics. For any particular installation, the optimum bearing design for a specified W and α may be determined using a practical analysis program of the type described.

DISCUSSION

Accuracy of Results

Comparisons with other published theoretical data indicated that the accuracy of results presented in this paper should be adequate for practical purposes. Assumptions made to simplify the theory have been justified by the conservative loading conditions of sterntube bearings. However, with respect to circularity, substantial local distortion may be associated with the high local hydrodynamic pressure caused by severe misalignment. Such high local pressure peaks also directly affect prediction accuracy due to the approximations introduced by the rectangular element modeling. This problem is offset by the use of axial element grading. In general, some loss of accuracy is to be expected where high eccentricity ratios (local or overall) are experienced.

Steady-Load Results

The steady-load results given in Figs. 3 to 6 illustrate the well-known significance of eccentricity ratio ε. In addition, the families of curves of $\bar{\alpha}$ show the superimposed effect of misalignment. The effect of misalignment arises from the fact that for all performance parameters, the bearing end with increased ε, has a greater influence than the end where ε is reduced. The assumption that misalignment angle $\bar{\alpha}$ has purely geometric relationship with minimum film thickness, therefore, leads to a pessimistic result where $\bar{\alpha}$ is high. The constant $\bar{\alpha}$ curves are curtailed by $\varepsilon \rightarrow 1$ at the bearing end, the ε against which all figures are plotted being that at the axial center.

Dynamic Coefficients

For the single value of $\bar{\alpha} = 0.2$ used in Figs. 7 to 10, the form of the curves clearly indicate $\varepsilon \rightarrow 1$ at the bearing end when $\varepsilon = 0.8$ at the axial center. Over a wide range of ε, the coefficient curves are fairly flat with a generally rapid rise as the above condition is approached.

FUTURE WORK

Lateral Shaft Vibration

The significance of the various dynamic coefficients with respect to the prediction of shaft whirling frequencies will be studied in the next phase of the current research program. It is anticipated that the most interesting results will be those related to the moment coefficients, since their introduction will tend to raise the natural frequencies. In the absence of these coefficients, the shaft is assumed to be simply supported at the bearings. With the relatively long sterntube bearing, particularly when subject to misalignment, significant restraining moments may be developed. It would, therefore, be more appropriate to assume that the bearing supports were partially encastre. The adoption of moment coefficients effectively introduces this assumption.

Nonlinearity Limitations

Dynamic coefficients are, theoretically, only applicable to small amplitude vibrations due to their high degree of nonlinearity. There are indications that errors due to nonlinearity are more significant with respect to amplitude prediction than for whirling frequency prediction, but little data for quantifying this problem appears to exist. Measurements made on a 210 000 dwt tanker by Hyakutake et al (*12*) indicated shaft amplitudes at the sterntube bearing up to 30 percent of the clearance. This level appears to be substantial in relation to oil film nonlinearity.

Bannister (*13*) approached this problem on statically misaligned turbogenerator bearings by the introduction of 20 additional coefficients, which were in fact coefficient amplitude gradients, e.g. $\frac{\partial}{\partial x}(B_{xy}) = \frac{\partial^2 F_x}{\partial x \partial \dot{y}}$. Good prediction of resonant frequencies and amplitudes were reported with this method, but its complexity has inhibited practical application. Bannister dealt only with relatively short bearings, and did not, therefore, consider moment coefficients. For a dynamically misaligned sterntube bearing, the above method would require an additional 144 "amplitude gradient" coefficients. Despite apparent complexity, this approach is considered worthy of investigation.

Journal Orbit Analysis

Where journal amplitudes are large, e.g. crankshaft bearings, the appropriate approach is the time stepping journal orbit analysis. A rigorous analysis of this type is very heavy on computing time and is not, therefore, considered suitable for routine practical applications at the present stage of computer development. Development of a journal orbit program for dynamically misaligned sterntube bearings is planned. This will serve as a benchmark against which the adequacy of direct application of linearized dynamic coefficients may be judged. In addition, it should facilitate a clearer understanding of the behavior of sterntube bearings.

SUMMARY

Details of the sterntube bearing situation have been outlined, and problems related to its static and dynamic loading discussed.

Theoretical results for steady-load performance parameters and oil film dynamic coefficients have been presented. Application of the steady-load performance data in a practical analysis program, which simulates the behavior of a real sterntube bearing, has been described. The potential use of dynamic coefficients for shaft vibration analysis, and their limitations with respect to nonlinearity have been discussed.

Investigations to be carried out in the next stage of the present research program were indicated. These will be directed towards the nonlinearity problems at large journal amplitude.

ACKNOWLEDGMENTS

The author wishes to express his gratitude to the Committee of Lloyd's Register of Shipping for permission to publish this paper. In addition the author is indebted to I. Montgomery (Trent Polytechnic—Nottingham) and D. Rennie (Lloyd's Register of Shipping) for their helpful comments on this paper.

REFERENCES

(1) Archer, C. and Martyn, D. K., "Static and Dynamic Alignment." *Trans. I. Mar. E.*, *91*, Conf. No. 4., Paper C31, pp 24–34 (1979).

(2) Vorus, W. S. and Gray, R. L., "Calculation of Sterntube Bearing Eccentricity Distributions: Applications in States Lines *RoIRo* Bearing Failure Analysis," *Trans. I. Mar. E*, 91, Conf. No. 4, Paper C37, pp 92 (1979).

(3) Leemans, M. and Roode, F., "Vibration Analysis of a Rotating Propeller Shaft in a Rubber Stern Tube Bearing," Conf: Intl. Cooperation on Marine Eng. Systems, ICMES' 84. Trieste (1984).

(4) Hill, A. and Martin, F. A. "Some Considerations in the Design of Sterntube Bearings and Seals," *Trans. I. Mar. E.*, **91**, Conf. No. 4, Paper C39, pp 119–137 (1979).

(5) Jakeman, R. W., "A Numerical Analysis Method Based on Flow Continuity for Hydrodynamic Journal Bearings," *Tribol. Int.*, **17**, 6, pp 325–333, December (1984).

(6) Lloyd, T., Horsnell, R., and McCallion, H., "An Investigation into the Performance of Dynamically Loaded Journal Bearings: Theory," *Proc. I. Mech. E.*, **181**, 3B, pp 1.

(7) Parkins, D. W., "Theoretical and Experimental Determination of the Dynamic Characteristics of a Hydrodynamic Journal Bearing," *ASME J. Lubr. Technol.*, **101**, pp 129–139, April (1979).

(8) Parkins, D. W., "Measured Characteristics of a Journal Bearing Oil Film," *Trans. ASME.*, **103**, pp 120–125 January, (1981).

(9) Pinkus, O and Bupara, S. S., "Analysis of Misaligned Grooved Journal Bearings," *ASME J. Lubr. Technol.*, **101**, pp 503–509, October (1979).

(10) Pafelias, T. A., "Solution of Certain Problems of Viscous Laminar Flow with Applications in Engineering Problems," PhD Thesis, Rensselaer Polytechnic Inst., Troy, New York, (Jan. 1974).

(11) Engineering Sciences Data Unit. "Calculation Methods for Steadily Loaded Pressure Fed Hydrodynamic Journal Bearings." Item No. 66023. Pub: ESDU International Ltd., London, England. (Sept. 1966).

(12) Hyakutake, S., Asai, R., Inoue., M., Fukahori. K., Watanabe, N., and Nonake, M., "Measurement of Relative Displacement between Sterntube Bearing and Shaft on a 210,000 d.w.t. Tanker," *Japan Shipbuilding and Marine Eng.*, **7**, 1, pp 32–40 (1973).

(13) Bannister, R. H., "Non-Linear Oil Film Force Coefficients for a Journal Bearing Operating under Aligned and Misaligned Conditions," PhD Thesis, Univ. of Aston in Birmingham. (Dec. 1972).

REFERENCE. 88.

STERNTUBE BEARINGS: PERFORMANCE CHARACTERISTICS AND INFLUENCE UPON SHAFTING BEHAVIOUR

by

R. W. Jakeman

R. W. Jakeman served his apprenticeship at the College of Aeronautics, Cranfield, gained a B.Sc. degree from the University of Durham and an M.Sc. degree from the University of Newcastle upon Tyne. His design experience in marine steam turbines and gearing was obtained at Pametrada followed by research and development work on hydrodynamic bearings at Michell Bearings Ltd. and work on the ARG boiler at Clark Chapman & Co. Ltd.

He joined Lloyd's Register in 1971 and, after short initial periods with A.E.S. and MDAPAD. spent 7½ years with T.I.D. He returned to A.E.S. in 1981 and has since been involved in a substantial programme of research on analysis techniques for hydrodynamic journal bearings and in consultancy work concerning shafting alignment and vibration analysis.

SYNOPSIS

Sterntube bearings are introduced with a discussion of the key factors relating to their design and operating environment. The paper gives details of a theoretical study of the performance of oil lubricated sterntube bearings, with respect to both steady and dynamic loading. Particular attention has been given to the effects of angular misalignment. The practical applications of this work to bearing performance analysis and interaction with shaft alignment analysis are described. A comprehensive set of linearised oil film dynamic coefficients, which define the bearing response (forces and moments) to lateral vibration, are presented.

TABLE OF CONTENTS

1. INTRODUCTION

The sterntube bearing is the most critical bearing in relation to the safe operation of any ship. It is generally subject to particularly arduous operating conditions arising from the relatively low shaft speed and close proximity to the propeller. In addition to the consequent deleterious effect on reliability, the sterntube bearing is particularly inaccessible. The result of a total sterntube bearing failure is invariably immobilisation of the ship and the requirement of a drydock in order to carry out repairs. Whilst the effects of dynamic loading combined with angular misalignment are partially mitigated by conservative specific bearing pressures, the reliability of sterntube bearings cannot be regarded as entirely satisfactory.

The subject of this paper forms part of one of the Society's research projects. This project was instigated to improve and expand the facilities available for predicting the static and dynamic behaviour of marine propulsion shafting systems, with the ultimate objective of improved reliability. Particular emphasis was given to the hydrodynamic performance analysis

A.4.-50.

of bearings subject to angular misalignment; such conditions being usually applicable to sterntube bearings. The area of angular misalignment of bearings in general, has received relatively little attention in published literature.

This paper deals only with bearings in which the running surfaces are fully separated by a fluid film. In relation to current practice, this means that water lubricated bearings are not generally covered, as the low viscosity of water prevents complete hydrodynamic lubrication.

The scope of this paper includes a discussion of design and environmental factors together with consideration of reliability. Following this the theoretical basis of the analysis methods used is outlined, and bearing performance results related to the variation of several design and operating parameters are presented. Finally the practical applications of this work are indicated, with particular reference to the desk top computer bearing analysis programmes that have been developed.

2. DESIGN AND ENVIRONMENTAL FACTORS

2.1 Location

The sterntube, which is an integral part of a ship's aft end structure, forms the passage whereby the propeller shafting passes through the hull. The sterntube bearing (sometimes called a stern bush) is located within the after end of this component and thus supports the weight of the propeller and part of the tailshaft weight. In many cases a bearing is also located at the forward end of the sterntube, but this paper is only concerned with the after sterntube bearing.

In some multiple screw ships with fine hull lines the aftermost part of the propeller shaft may be supported outboard by bearings mounted in "A" brackets or similar structures. In general such bearings are water lubricated and consequently beyond the scope of this paper. Some oil lubricated "A" bracket bearings have been used, and, having regard to the nature of their design and loading, may be treated as sterntube bearings.

2.2 Static Loading

The after end of a propeller shaft is subject to substantial cantilever loading due to the overhung weight of the propeller. This frequently leads to static angular misalignment between the journal and sterntube bearing. Application of rational alignment analysis to the complete propeller shaft system enables such misalignment to be reduced to acceptable levels. The theoretical basis and related measurement techniques for alignment analysis have been described by Archer and Martyn[1].

Shafting design constraints lead to relatively long sterntube bearings, L/D ratios being typically in the region of 2 for oil lubrication. In order to offset their sensitivity to misalignment, sterntube bearing clearance to diameter ratios are relatively large ($C_d/D \simeq 0.002$).

2.3 Dynamic Loading

Marine propellers may produce significant dynamic loading due to their operation in a non-uniform flow of water. In relation to shaft alignment considerations, the propeller dynamic loading may be resolved into a moment applied to the shaft end due to thrust eccentricity and a lateral force due to torque eccentricity. Both the moment and the force vary in magnitude and direction cyclically at propeller blade frequency, the moment being more significant with respect to shaft excitation. In general the above excitation is larger in ships with a high block coefficient, such as tankers and bulk carriers. This is due to the correspondingly greater variation in the velocity of water entering the propeller, which is referred to as the wake field. Notwithstanding these comments, there have been a few notable examples of fine line ships, for example refrigerated cargo, in which substantial wake field effects have been recorded.

For single screw ships holding a straight course, the wake field is virtually symmetrical about the vertical axis passing through the propeller centre. The thrust eccentricty moment is therefore generally dominant in the vertical plane, and the torque eccentricty force is correspondingly dominant in the horizontal direction. The above observations may be invalidated by situations in which there is a significant angle between the mean direction of water flow and the propeller axis of rotation for instance due to rake of the propeller shaft. This is due to the consequent change in the blade angle of attack relative to the water on opposite sides of the vertical axis. In the more usual situation in which the water flow into the propeller is substantially axial, the thrust eccentricity moment acts in the sense that it tends to lift the shaft end. However, a few cases have been recorded in which operation in a ballast condition has resulted in the eccentric thrust moment becoming reversed, and thus acting in the same sense as the propeller weight. This is due to air entrained from the surface passing through the upper part of the propeller. In heavy sea conditions, the above phenomenon may be periodic as a result of the propeller breaking or coming close to the surface as a result of the ship's pitching motion.

When a ship is turning, the wake field becomes asymmetric, and this may result in a much greater horizontal component of eccentric thrust moment. In one notable case which was well documented by Vorus and Gray[2], the above moment when turning with the rudder at about 5° to starboard was sufficient to cause the shaft to be forced against the starboard oil groove of the sterntube bearing and thus precipitate failure.

The foregoing comments are intended to acquaint the reader with the significance and complexity of the dynamic load which may act on a sterntube bearing. It is clearly dangerous to generalise about the form of this loading. For example, it may seem a good idea to place the sterntube bearing oil grooves in the top half of the bearing rather than the conventional 3 o'clock and 9 o'clock positions. However, before proceeding with such an idea, it would be advisable to check that the sterntube bearing is not top loaded as a result of a high eccentric thrust moment. There is substantial evidence to indicate that this situation frequently exists in ships having a high block coefficient.

2.4 Water Lubrication

Water lubricated sterntube bearings are still used in smaller ships, and in many naval ships, where their overall simplicity is advantageous. The low viscosity of water and multiple axial grooves generally used in these bearings prevent effective hydrodynamic lubrication, thus resulting in relatively high wear-down rates. This failure to attain full hydrodynamic lubrication has been confirmed by Leemans and Roode[3]. The axial grooves originated from chamfering of the lignum vitae staves, which were almost exclusively used for such bearings prior to the introduction of modern synthetic materials. These grooves were intended to ensure adequate distribution of water for cooling purposes. More recently proposals have been made that the axial grooves should be omitted from the bottom half of water lubricated bearings made from certain synthetic materials, in order to promote hydrodynamic lubrication. The elimination of grooves from the bottom half would undoubtedly enhance the chances of attaining hydrodynamic lubrication. If, however, due to the low viscosity of water this mode of lubrication is not attained, then overheating is possible as a result of the diminished access of water for cooling. The crucial fact is that the load carrying capacity of a journal bearing is proportional to the effective lubricant viscosity, and the viscosity of water is of the order of one hundredth of that of SAE 30 lubricating oil.

A.4. - 51.

2.5 Oil Lubricaticn (Boundary and Hydrodynamic)

The problems of high wear down rate associated with water lubrication, and the consequent short bearing life, have been found to outweigh the advantage of simplicity in larger ships. Oil lubricated sterntube bearings have therefore come into widespread use in recent years. In these bearings full hydrodynamic lubrication is generally attained, and only very small amounts of wear down are normally experienced. Wear in such bearings should only occur during starting and stopping, and possibly during low speed operation.

The research which forms the basis of this paper was entirely confined to situations involving complete hydrodynamic lubrication. In practice this means that, apart from the introductory comments given in section 2.4, the paper only deals with oil lubricated sterntube bearings. As indicated above, even oil lubricated sterntube bearings may operate with boundary lubrication at low shaft speeds, particularly where misalignment is present. Boundary lubrication covers the transition region from stationary conditions to full hydrodynamic lubrication. In this region the bearing load is supported partly by direct contact between the journal and bearing surfaces, and partly by hydrodynamic action. Little is known about the acceptability of operation under these conditions, and there is a need for experimental work in this area, preferably at full scale. The following comments are intended as a qualitative guide to the main factors involved.

· Under boundary lubrication conditions there will be a substantial increase in the heat generated. This additional heat originates from the area in which journal to bearing contact is occurring. If the conditions are moderate, this may result only in local wear. In more severe conditions, mainly with respect to increased shaft speed, the surface temperature attained as a result of local heating may cause serious degradation of the bearing material and oil properties. This may lead to a catastrophic bearing failure, e.g. wiping of the white metal. The additional heat due to boundary lubrication further compounds the the problem by lowering the mean viscosity of the oil in the bearing, and consequently reducing the proportion of the load supported by hydrodynamic action.

When boundary lubrication occurs under misaligned conditions, the additional heating is confined to a relatively small area at one end of the bearing. For perfectly aligned conditions, however, if boundary lubrication is experienced, it would affect the full length of the bearing. At first sight, this might be construed to indicate that boundary lubrication is a less serious matter under misaligned conditions. Unfortunately the fact is that with misalignment, boundary lubrication may occur at a much higher shaft speed. Under these conditions, although the additional heating is confined to a small area, the higher speed produces a much greater heating intensity.

Present design philisophy is directed towards ensuring that complete hydrodynamic lubrication is attained under all continuous operating conditions. There is, however, much practical evidence to suggest that this is not always achieved. It may be difficult to distinguish between bearing wear originating from starting, stopping and operation on turning gear, and wear incurred during operation in the normal running speed range. Evidence of local overheating would be an indication of the latter, as would wear in the top half of the bearing. From the design viewpoint it may indeed be reasonable, in principle, to accept some degree of boundary lubrication at certain conditions within the running range. However, in the current absence of reliable guidelines for boundary lubrication acceptance criteria, it is considered prudent to aim for hydrodynamic lubrication as far as practicable.

2.6 Oil Feed Grooves

The commonly used oil feed groove arrangement for sterntube bearings is two axial grooves at the 3 o'clock and 9 o'clock positions covering the full, or nearly the full length of the bearing. For the optimum hydrodynamic performance, the location of an axial oil groove should be at the position of maximum film thickness, which is a function of load and misalignment angle. However, in the majority of sterntube bearings the conventional oil groove arrangement appears to be satisfactory. It would be feasible to determine a better oil groove arrangement for any given installation using the hydrodynamic analysis programme described in this paper. This would require the specification of the vertical and horizontal components of misalignment angle experienced by the sterntube bearing under all significant operating conditions. Unfortunately, at present such detailed information on the sterntube bearing operating conditions is rarely available. The previously cited failure described in reference 2 illustrates the hazards of this situation.

2.7 Oil Supply System

In general engineering practice, the lubricating oil supply to hydrodynamic bearings fulfils the secondary function of removal of most of the heat generated. This usually involves positive circulation of oil through the bearing, and the incorporation of an oil cooler in the closed circuit re-circulation system. Sterntube bearings, however, generally operate at fairly low shaft speeds and the heat they produce is consequently small in relation to their size. In addition to this, the close proximity of sea water to the adjacent structure and shaft end provides an effective heat sink. Experience has indicated that heat dissipation in this way is enhanced by maintaining sufficient water in the aft peak tank to cover the sterntube. For many installations, therefore, positive circulation of oil through the sterntube bearing is not necessary. Oil is supplied to the sterntube under pressure from a header tank, the pressure level being set to slightly exceed that of the sea water at shaft level. This arrangement is designed to prevent the ingress of sea water in the event of seal malfunction. The seal is required to have an adequate degree of flexibility in order to tolerate the lateral movement of the shaft arising from the propeller dynamic loading. This flexibility restricts the differential pressure that the seal can withstand, consequently for ships having a large draught range two or more header tanks may be used to maintain the seal differential pressure within acceptable limits. Fig. 1 shows a typical sterntube bearing lubricating oil system. The system shown features two header tanks to cater for a larger draught range, and some degree of oil circulation through the bearing with provision for oil cooling in the circuit.

2.8 Bearing Materials

The remarks in this section are confined to oil lubricated sterntube bearings. By far the most common sterntube bearing material is the tin based white metal with cast iron backing. Although, as noted earlier, the limits of safe operation in the boundary lubrication regime are not known, service experience indicates that white metal is capable of withstanding some degree of such conditions with only minor wear. The other well known virtue of white metal is that it is soft enough for solid particles contaminating the lubricating oil to become embedded in it, and thus rendered virtually harmless. Lastly, in the event of a catastrophic failure (wiping), consequential damage to the tailshaft is rarely serious.

In recent years reinforced resin materials have been used for oil lubricated sterntube bearings. The main advantages claimed for such materials is that their greater flexibility provides an enhanced tolerance to misalignment, and that they are able to operate on a "get you home" basis after a total seal failure.

A substantial amount of research has been carried out on the influence of bearing elasticity on aligned journal bearings. The main direct influence of bearing elasticity is that the shape of the

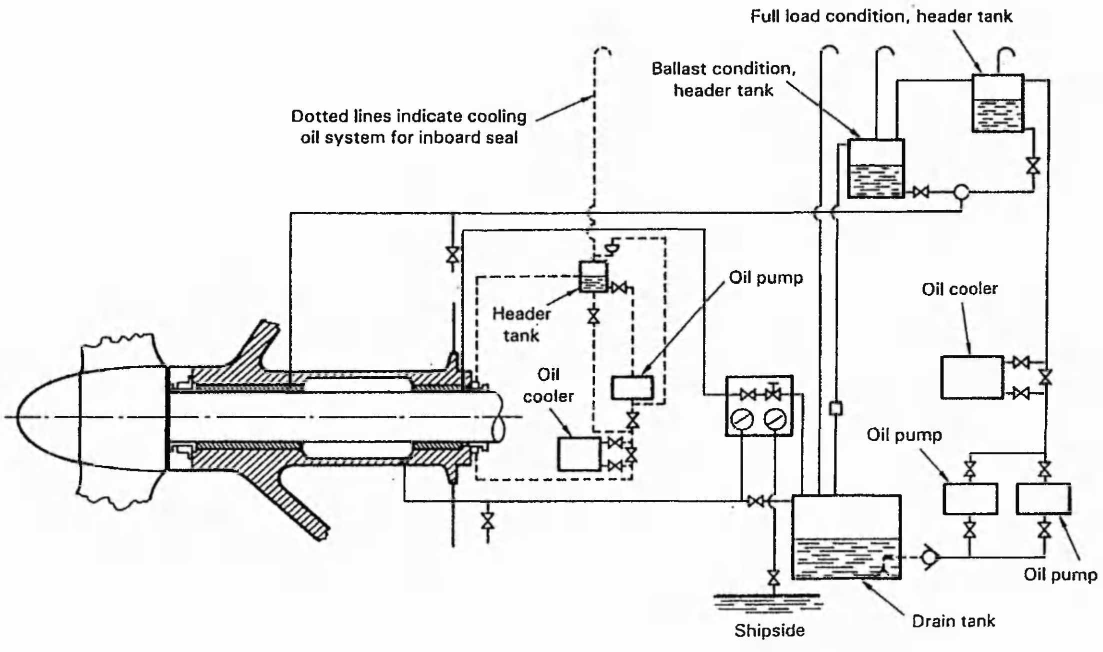

Fig. 1 Typical Arrangement showing Two Header Tanks for Vessels with Large Changes in Draught

bearing surface in the loaded half tends to conform to that of the journal. This is referred to as the "wrap around" effect. The resultant influence on bearing performance depends on the nature of the loading. Fantino et al[4] indicated that where normal hydrodynamic wedge action is dominant, the minimum film thickness is reduced by bearing elasticity. In a more recent paper by La Bouff and Booker[5], the results suggested that minimum film thickness is increased by bearing elasticity in a situation where squeeze film action is dominant. No research results covering the effect of bearing elasticity on misaligned journal bearings, are known to exist at present. The benefits, with respect to misalignment tolerance, of using reinforced resin bearing materials are therefore uncertain, and may well depend upon the severity of dynamic loading.

The main advantage of reinforced resin materials is their ability to operate in water for a limited period. This effectively provides a "get you home" capability in the event of an outboard seal failure. It must be stressed that this is strictly an emergency condition, and that a reduced operating speed is considered to be advisable.

Reinforced resin materials absorb a small amount of water and are consequently subject to slight swelling. The bearing clearance, as machined, must therefore be greater than that for a white metal bearing, in order to allow for swelling.

An important property of reinforced resin materials is thermal conductivity, which is very low relative to white metal. This means that, for monitoring purposes, thermocouples located within reinforced resin materials are virtually useless. The ability of reinforced resin bearings to dissipate heat is very poor. Asbestos is a commonly used reinforcing material, therefore under boundary lubrication conditions, the frictional heat generated may substantially exceed that for white metal. No reliable test data for such bearings is known to exist. Service experience, however, has indicated that under catastrophic failure conditions, severe overheating may occur resulting in serious damage to the tailshaft.

2.9 Reliability

A survey of sterntube bearing and aft seal defect rates has been carried out for the period January 1972 to June 1983. The results were compiled by the Technical Records Department from surveyors reports, and cover over 11,500 ship years of service. These results are summarised in Table 1.

It will be noted that most of the data given is for aft seal and bearing defects combined. This is due to the fact that aft seal defects invariably result in consequential damage to the bearing. It may also be noted that the defect rate for sterntube bearings only is substantially less than the combined seal and bearing defect rate. The apparent conclusion that the seal is a far more critical item than the bearing does not, however, take account of the interdependence of the seal and bearing performance. For the seal, the most exacting operating parameter is the amplitude of lateral shaft movement that it must be able to accommodate. This movement is partially dependent on the dynamic operating characteristics of the sterntube bearing, but the development of predictive techniques has not yet attained a level where the problem can be accurately quantified.

The most interesting result of this survey is the significant direct correlation between defect rate and shaft diameter. In view of the current trend towards the use of larger propellers operating at lower speed, in order to improve propulsive efficiency, there is a clear need to pay more attention to sterntube bearing design and performance. More recently, a limited number of vessels have been fitted with freely rotating vane wheels. The vane wheel is supported on an extension shaft aft of the propeller, with the object of recovering some of the kinetic energy from the propeller wake, which it converts into additional thrust. From the viewpoint of the sterntube bearing, the vane wheel represents a substantial additional mass (up to 50% of the propeller mass) acting at a much greater over-hang distance.

The number of oil lubricated reinforced resin sterntube bearings in service was about 8% of the total, the remainder

Table 1 Failure Statistics

After seal and sterntube bearing defects per 100 ship-years

Diameter (mm)	Defect rate
400–499	4,24
500–599	5,40
600–699	6,08
700–799	6,35
>800	7,03
Overall	5,42

Overall—Sterntube bearing only 1,12 defects per 100 ship-years

Bearing Material	Seal and bearing defect rate
White metal	5,98
Reinforced resin	8,35

No significant correlation of defect rate with:
Ship type Number of propeller blades Number of propellers Fixed or controllable pitch propellers

being almost exclusively white metal. Despite this small proportion, the relative defect rates for these materials were considered to be statistically significant. This data suggests that the previously outlined problems associated with reinforced resin sterntube bearings may in fact outweigh the advantages.

3. THEORETICAL ASPECTS

3.1 Assumptions

In common with theoretical work generally, it is necessary to make various simplifying assumptions in order to reduce the problem to a manageable level. A more complex analysis involving less assumptions is usually possible, but the type of application should be taken into consideration. A highly complex, computationally time consuming, type of analysis may be perfectly acceptable as a research tool but unjustifiable for regular practical application. In practical applications, more approximate but computationally efficient analysis methods are preferable, provided they are backed up by adequate service experience.

Full details of the assumptions made in this work are given in reference 6. In relation to their application to sterntube bearings, the following comments are relevant:

Since sterntube bearings operate at relatively low speed and moderate specific pressure (W/LD), the resultant oil temperature rise is small. In view of this, the commonly used assumption of a constant effective oil viscosity is reasonable. The low speed also ensures that sterntube bearings operate well within the laminar flow region, and that lubricant inertia effects may be neglected.

The modest loading, and the anticipated low level of thermal distortion, justify the assumption of rigid circular journal and bearing surfaces for white metal bearings. For reinforced resin sterntube bearings, the relatively high flexibility of such materials renders the assumption of rigidity unsatisfactory. The application of the Society's current analysis programmes to reinforced resin sterntube bearings inevitably involves some loss of accuracy, and further research is required on the effects of elasticity, particularly for misaligned bearings.

3.2 Hydrodynamic Analysis Method

For comprehensive details of the fundamental hydrodynamic analysis method used in this work, the reader should consult reference 6. The following is a brief outline of the essential features of this method:

In the last hundred years, papers on hydrodynamic analysis have invariably started with Reynold's equation. It is therefore appropriate to explain why reference 6 is an exception to this general rule. At the time it was written (1886), Reynold's equation was incapable of solution, except by means of approximations which yielded results of somewhat questionable accuracy. In addition, whilst this equation was based upon flow continuity within a complete lubricant film, it did not take account of cavitation, to which flow continuity is also generally applicable.

The advent of numerical analysis methods, made practicable by the development of the digital computer, have made it possible to solve Reynold's equation without the former approximations, which were mainly related to bearing length to diameter ratio. Where a numerical analysis method is to be used, there is little value in writing a general partial differential equation, particularly where this does not cover all the conditions encountered, i.e. cavitation. Such an equation must, in any event, be modified to a form suitable for the application of numerical analysis techniques before the solution can proceed. The analysis method used for this work eliminates the initial use of Reynold's equation by going directly to consideration of flow continuity in rectangular oil film elements. In addition to simplifying the analysis process, this approach readily facilitates taking account of continuity in the cavitation zone, which is beyond the scope of Reynolds's equation.

A Gauss-Seidel relaxation method, with successive over relaxation, is used in the above numerical analysis method [6]. The system by which flow continuity is taken into account both within the full film and cavitation regions is believed to be one of the simplest yet developed, and has been proved to function satisfactorily over a wide variety of static and dynamic conditions. In other comparable cavitation models it has been necessary to make initial estimates for the location of the cavitation zone boundary, and to specify the pressure gradient at the rupture boundary. There are no such requirements in the above analysis method. Only specification of the constant cavitation pressure is required, the location of the cavitation zone boundaries being automatically determined to the nearest rectangular oil film element boundary, during the film pressure relaxation process.

The analysis can handle any geometric condition such as angular misalignment between the journal and bearing axes. This simply requires specification of the geometric conditions such that the oil film thickness can calculated at any oil film element location by means of appropriate trigonometric relationships. Fig. 2 defines the appropriate geometric conditions for a misaligned sterntube bearing. In this figure curvature of the journal axis is neglected.

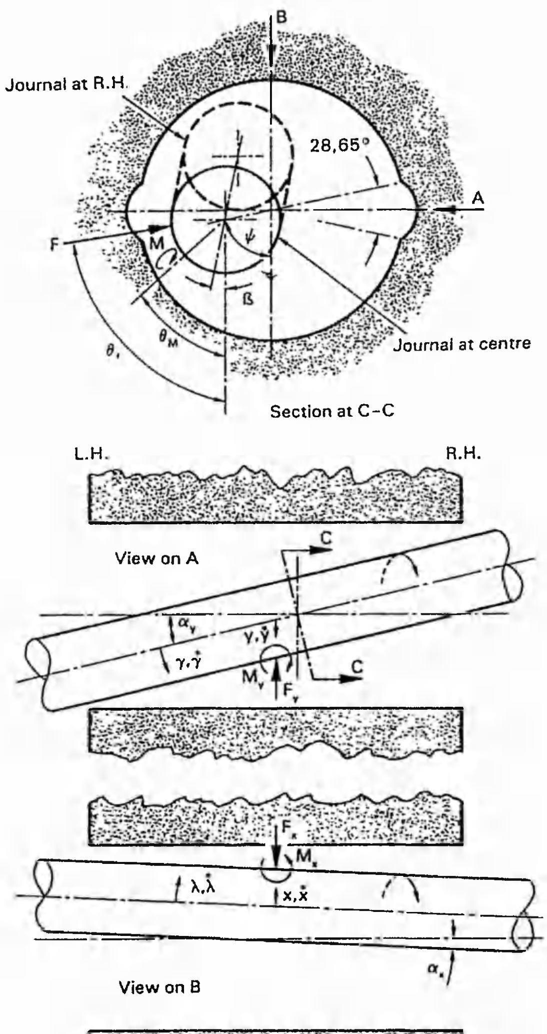

Fig. 2

3.3 Cavitation

In the previous section reference was made to the way in which cavitation has been modelled, by taking account of flow continuity within cavitating elements. This is a substantial improvement on earlier analysis methods in which continuity within the cavitation zone was ignored. The method can be readily incorporated into a film pressure solution where the relaxation technique is used, with little added complexity or computing time. Whilst this method is considered to be quite adequate for most practical applications, it is important to be aware of the approximations in relation to observed cavitation behaviour in real bearings.

The value of the assumed constant cavitation pressure is essentially dependent on the type of cavitation. There are two basic types of cavitation: vaporous and gaseous. For the vaporous type, the pressure within the oil film must drop to the local vapour pressure which, for practical purposes, is virtually zero absolute. Where the oil has absorbed air to saturation level, gaseous cavitation (i.e. air bubbles coming out of solution) may occur at approximately atmospheric pressure. The type of cavitation that is dominant in any particular bearing situation depends on the operating and environmental conditions. Guidance for this can only be very approximate at present, but in most practical bearing situations gaseous cavitation appears to be dominant, thus an atmospheric cavitation pressure is generally appropriate.

Experimental work, such as that by Etsion and Ludwig[7], has given useful insights into cavitation behaviour in bearings, but the bearing geometry and test parameters have not invariably been representative of normal service conditions. Application of such data to practical bearing analysis is therefore difficult. The general conclusion that can be drawn is that the occurrence of gaseous or vaporous cavitation is largely dependent on the time available for bubble release and re-absorption. Vapour release and reabsorption appear to be very rapid in relation to the corresponding times required for gas. Vaporous cavitation is therefore likely to be significant only in dynamic situations affording inadequate time for gas release and re-absorption. Where a bearing is surrounded by air, cavitation zones may be fed with air from the oil film boundaries. This is referred to as ventilation, and clearly cannot occur in fully submerged situations of the sterntube bearing type. The finite release time associated with gaseous cavitation, is believed to be responsible for the frequently observed negative pressure spike preceding the cavitation rupture boundary. Fortunately, this phenomenon appears to have little effect upon load capacity prediction accuracy, except for very lightly loaded bearings. The finite re-absorption time appears in some instances[7] to result in some cavitation bubbles being carried beyond the reformation boundary into the region of increasing film pressure. This clearly results in some variable degree of compressibility in the region of the film where such bubbles persist, with a consequent reduction in load capacity.

No practicable method of theoretically modelling the effects of finite gas release and re-absorption times are known to exist at present.

The flow of oil through the cavitation zone, in the model used for this work, was assumed to take the form of rectangular section streams of full film thickness. This is referred to as the striated model, and has been used in several other theoretical models. An alternative assumption is that the oil becomes fully detached from the bearing surface, and flows through the cavitation zone in a layer adhered to the journal surface. This model was used by Pan[8] and is referred to as the adhered film model. Provided continuity is taken into account within the cavitation zone, the striated and adhered film cavitation models yield the same bearing load capacity for a given effective oil viscosity. The adhered film model, however, results in a lower predicted power loss, since within the cavitation zone the shaft and bearing surfaces are fully separated by air. The power loss is therefore negligible in the cavitation zone. Experimental work such as that by Heshmat and Pinkus[9] has indicated that in reality the form of the oil flow through the cavitation zone may lie between the striated and adhered film models. This is illustrated in Fig. 3. No practical method of modelling the flow cross section through the cavitation zone more realistically, is known to exist at present. Errors arising from the use of the striated or adhered film models are unlikely to be significant in normal analysis applications.

The foregoing comments indicate that cavitation in journal bearings is a very complex phenomenon. Despite this complexity, the relatively simple theoretical model used appears to be adequate for normal practical applications. Indeed, having regard to the relevant uncertainties in any service bearing, such as the level of solid particle contamination and dissolved gas in the lubricating oil, it is doubtful if a more complex model is practicable.

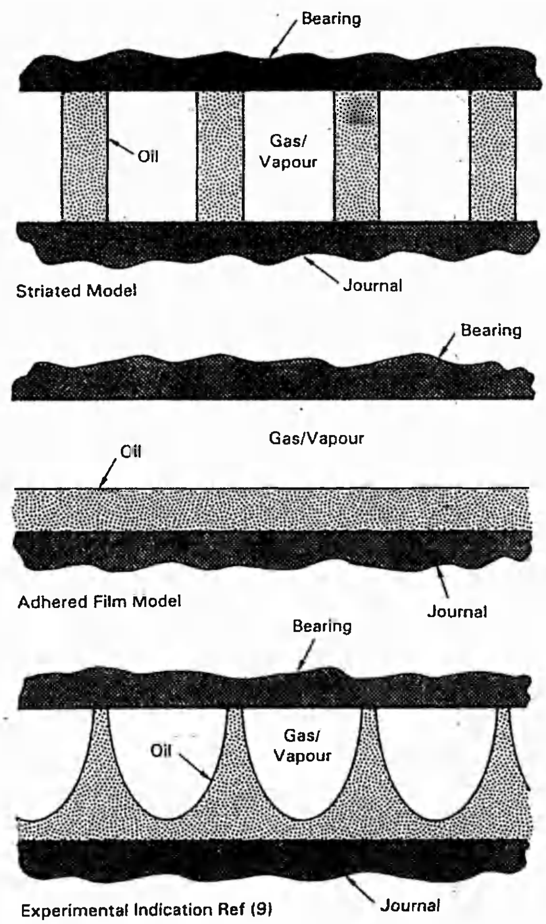

Fig. 3 Axial Cross Section of Flow Through Cavitation Zone

3.4 Element Division

As indicated in 3.2., for the numerical analysis method used, the oil film is divided into a number of rectangular elements. Naturally, a finer element grid will yield a more accurate result, but require more computing time. Clearly some compromise is required, but it is important to note that a finer grid is particularly required where higher rates of change of pressure gradient are encountered. The use of variable element dimensions, (referred to as element grading), therefore offers the possibility of improved accuracy whilst minimising the increase in computing time.

Lloyd et al[10] applied this approach in the circumferential direction, by making the circumferential element dimension a function of the local film thickness. It should be noted that the peak film pressure and maximum rate of change of pressure gradient in the circumferential direction, occur just before the position of minimum film thickness. This method is therefore a simple and effective means of improving accuracy by circumferential element grading.

The above system of circumferential element grading is unsuitable for misaligned sterntube bearings, due to the possibility of substantial variation of the circumferential location of the minimum film thickness position along the length of the bearing. For sterntube bearings the specific pressure (W/LD) is fairly conservative, but substantial angular misalignment is frequently encountered, which results in high local film pressures at one end. In addition, the high L/D ratios of sterntube bearings (typically $L/D \simeq 2.0$) yield a fairly flat axial film pressure profile, which leads to a greater rate of change of pressure gradient at both bearing ends. As a result of the above situations, the maximum rate of change of pressure gradient for a sterntube bearing will often be greater in the axial direction than in the circumferential direction. Consequently there is generally a greater incentive to adopt axial element grading for misaligned sterntube bearings. An axial element grading system was therefore adopted, and a typical element grid is shown in Fig. 4. Note that the circumferential element dimension in the bottom part of the bearing is one half of that for the top part. This effectively introduces a small degree of circumferential element grading within the limitations imposed by misalignment. Where large misalignment angles were encountered, such that significant positive film pressures were likely to be generated in the top half of the bearing at one end, the circumferential element dimension was made the same in both top and bottom halves.

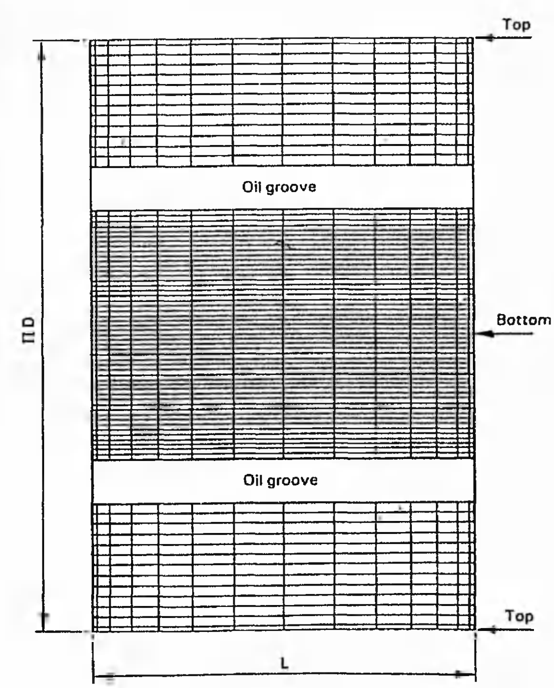

Fig. 4 Oil Film Element Grid

3.5 Oil film Dynamic Coefficients

For dynamic situations in which lateral displacements of the journal are small in relation to the bearing clearance, and the corresponding lateral velocities of the journal axis are also small, the resulting changes of oil film force and moment may be treated as approximately linear. The associated linearised oil film force and moment coefficients are sometimes referred to as displacement and velocity coefficients, but more frequently as stiffness and damping coefficients. The collective term "dynamic coefficient" is also used.

The dynamic coefficients may be computed by superimposing small lateral displacement or velocity changes (referred to as perturbations) on the equilibrium (steady load) solution, and thus deriving the corresponding changes in oil film forces and moments.

In cases where there is no angular misalignment of the shaft and bearing axes, the oil film moment components remain zero, and only eight stiffness and damping coefficients are required. These may be defined by the matrix equation:

$$\begin{bmatrix} F_x \\ F_y \end{bmatrix} = \begin{bmatrix} A_{xx} & A_{xy} \\ A_{yx} & A_{yy} \end{bmatrix} \cdot \begin{bmatrix} x \\ y \end{bmatrix} + \begin{bmatrix} B_{xx} & B_{xy} \\ B_{yx} & B_{yy} \end{bmatrix} \cdot \begin{bmatrix} \dot{x} \\ \dot{y} \end{bmatrix} \qquad [1]$$

(For nomenclature see Appendix I)

It should be noted that the behaviour of a bearing oil film results in cross axis terms. For example a displacement in the x direction results in a change in F_y as well as F_x, thus $A_{yx} = \frac{\partial F_y}{\partial x}$.

In general, sterntube bearings are subject to both steady and dynamic angular misalignment which thus involves both force and moment changes in the oil film response. This results in the need for thirty-two linearised stiffness and damping coefficients which are defined by the following matrix equation:

$$\begin{bmatrix} F_x \\ F_y \\ M_x \\ M_y \end{bmatrix} = \begin{bmatrix} A_{xx} & A_{xy} & A_{x\lambda} & A_{x\gamma} \\ A_{yx} & A_{yy} & A_{y\lambda} & A_{y\gamma} \\ A_{\lambda x} & A_{\lambda y} & A_{\lambda\lambda} & A_{\lambda\gamma} \\ A_{\gamma x} & A_{\gamma y} & A_{\gamma\lambda} & A_{\gamma\gamma} \end{bmatrix} \cdot \begin{bmatrix} x \\ y \\ \lambda \\ \gamma \end{bmatrix} + \begin{bmatrix} B_{xx} & B_{xy} & B_{x\lambda} & B_{x\gamma} \\ B_{yx} & B_{yy} & B_{y\lambda} & B_{y\gamma} \\ B_{\lambda x} & B_{\lambda y} & B_{\lambda\lambda} & B_{\lambda\gamma} \\ B_{\gamma x} & B_{\gamma y} & B_{\gamma\lambda} & B_{\gamma\gamma} \end{bmatrix} \cdot \begin{bmatrix} \dot{x} \\ \dot{y} \\ \dot{\lambda} \\ \dot{\gamma} \end{bmatrix} \qquad [2]$$

From the above equation it may be noted that the coefficients may be defined by:

$$A_{\lambda y} = \frac{\partial M_x}{\partial y} \; ; \; A_{\gamma\lambda} = \frac{\partial M_y}{\partial \lambda} \; ; \; B_{y\gamma} = \frac{\partial F_y}{\partial \dot{\gamma}} \; ; \; B_{\lambda\gamma} = \frac{\partial M_x}{\partial \dot{\gamma}} \; ; \text{ etc.}$$

Equation [2] defines the sterntube bearing oil film response to lateral vibration of the journal. The application of these coefficients to shafting lateral vibration analysis has yet to be explored, and the influence of some coefficients may prove to be negligible. In general the importance of bearing oil film stiffness and damping for lateral vibration analysis, will depend on the relative stiffness and damping of the shafting and bearing support structure, and upon the relative propeller damping. This is an area in which further research is required.

In current lateral vibration analyses, bearings are treated as single simple support points. It is therefore interesting to note that the coefficients relating oil film moment changes M_x, M_y to angular displacements λ, γ and velocities $\dot{\lambda}$, $\dot{\gamma}$ effectively apply some degree of restraint to angular motion of the journal axis. This effect may well be significant in sterntube bearings due to their relatively high L/D ratios. The application of these coefficients thus effectively renders the shaft semi "built in" at the sterntube bearing, rather than simply supported as usually assumed.

3.6 Non-linear Bearing Response: Journal Orbit Analysis

As noted in the preceding section, the application of linearised oil film stiffness and damping coefficients is only valid for small amplitude lateral vibrations. Fortunately, the errors arising from the use of these coefficients in cases where substantial vibration amplitudes are involved are less serious when only natural frequency prediction is required. Little information exists to quantify this situation, but acceptable frequency prediction accuracy has been claimed for cases involving journal amplitudes up to 30% of the bearing clearance. This figure can only be regarded as a very rough guide, since the prediction error will be strongly dependent on the relative stiffness of the shafting and bearing support structure.

Where the dynamic loading is such that large journal amplitudes will occur, and particularly where amplitude prediction is required, linearised coefficients are inadequate. In cases of this type, a journal orbit analysis is appropriate. This consists of the "marching out" of the journal orbit in a series of small time steps from some arbitary starting point, until successive orbits attain a satisfactory convergence. Equations of motion are applied at each time step taking account of the nett influence of external forces, mass accelerating forces and oil film forces.

A journal orbit analysis method for bearings operating without static or dynamic angular misalignment has been developed, and is fully described in reference 11. In particular, this work outlines a theoretical model for oil film history. This essentially comprises the continuous monitoring of the extent of cavitation zones and the disposition of oil within them. The principle effect of oil film history is that whilst the journal displacement and velocity conditions which produce a cavitation zone may disappear very rapidly, the cavitation zone itself will generally take rather longer to refill with oil. A cavitation zone which is still surviving after the conditions which induced it have been removed may exert a strong influence on the subsequent journal motion. This is due to the oil film offering very little resistance to motion of the journal in the direction of the cavitation zone, until that cavitation zone has been completely dissipated.

The significance of oil film history is dependent on the size of the orbit relative to the clearance circle (greater effect with larger orbits), and upon the efficiency of the oil feed arrangement. The latter influence has been well illustrated by Jones[12], who showed the progression from a fairly large effect with a single hole oil feed, to a small effect with a 360° central circumferential oil groove.

The journal orbit analysis methods described in references 11 and 12 are fairly rigorous, and consequently heavy on computing time to the extent that they are unsuitable for routine practical application. Their main shortcoming is the assumption of a rigid bearing, but modelling bearing elasticity is believed to add about another order of magnitude to the computing time (see reference 5). For practical purposes a much faster analysis time is required, absolute accuracy being less important provided the analysis is backed up by suitable service experience.

Many earlier analysis methods used the short bearing approximation of Reynolds equation in order to obtain a fast analytical solution of the oil film force components e.g. Holmes and Craven[13]. This approach can lead to substantial inaccuracy in the oil film force prediction. Cavitation in particular, is simply assumed to extend from the minimum to maximum film thickness positions, this being referred to as the π film model since hydrodynamic action is assumed to occur over an arc of π radians only. Various refinements of the short bearing approximation have been developed, with the aim of improving accuracy. Such methods still suffer from the disadvantages of failing to take account of the oil film boundary conditions arising from various oil feed groove geometries, and of using the very crude π film cavitation model.

The other basic approach to the problem of achieving a fast journal orbit analysis, is to interpolate from a pre-computed or measured data bank of suitable oil film paramenters, in order to obtain rapid force prediction. Probably the best known method of this type is the Mobility Method by Booker[14]. This method has the limitation of only being applicable to bearings having circumferential symmetry e.g. 360° circumferential groove bearings. A fast journal orbit method has been developed by the author, which is based on force prediction by means of five pre-computed velocity coefficients in polar terms:

$$F_t = B_{tt}\,\dot{\Theta} + B_{ttr}\,\dot{R}\dot{\Theta}_o \qquad [3]$$

$$F_r = B_{rt}\,\dot{\Theta}_o + B_{rr}\,\dot{R} + B_{rrt}\,\dot{R}\dot{\Theta}_o \qquad [4]$$

where $\dot{\Theta}_o = \dot{\Theta} - \omega/2$

The polar velocity and force direction system used is shown in Fig. 5. This analysis method is referred to as the Reaction Method, the development of equations [3] and [4] and application to a 360° circumferential groove bearing being described in references 15 and 16 respectively. The Reaction Method has the advantage of being readily applicable to aligned bearings with any oil groove geometry. As indicated above, this method has been applied to the 360° circumferential groove bearing. The circumferential symmetry of such bearings results in the velocity coefficients B_{tt} etc., of equations [3] and [4] being functions of eccentricity ratio ϵ only. In the more general case of a non-circumferentially symmetrical bearing, the velocity coefficients are functions of both ϵ and attitude angle ψ.

The dynamic excitation from marine propellers is such that the journal amplitude levels in many sterntube bearings may be well into the non-linear area. To explore the shafting behaviour under such conditions, it is proposed to apply journal orbit analysis to the misaligned sterntube bearing. An extensive survey of the literature has revealed no indication of this type of analysis having been attempted on a dynamically misaligned

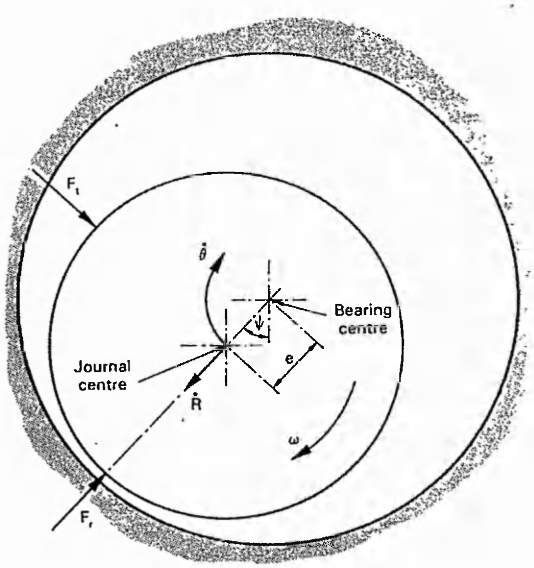

Effective angular velocity $\dot{\theta}_o = \dot{\theta} - \frac{\omega}{2}$ (stationary bearing case)

Eccentricity ratio $\epsilon = \frac{2e}{C_d}$

Fig. 5 Polar Oil Film—Journal Velocity System

bearing. The nearest relevant work appears to be that by Bannister[17], but this was restricted to a 120° partial arc bearing having an L/D ratio of only 1.0. Furthermore, Bannister only considered static misalignment, i.e. with no cyclic variation of the misalignment angle, and the excitation used was purely out of balance forces with relatively small journal displacement amplitudes. Extension of the journal orbit analysis method described in reference 11 to accommodate dynamic misalignment is not anticipated to pose any special problems. The sterntube bearing situation will clearly be more complex, but the basic analytical approach used for aligned bearings should be adaptable to meet this. It is intended to take account of accelerating forces and moments associated with the propeller and tailshaft mass and inertia, hydrodynamic forces and moments induced by the propeller, and elastic forces and moments from the shafting. The computing time associated with this type of journal orbit analysis will be at least twice that for the aligned condition consequently the work must be initially regarded as purely for research purposes. Application of the Reaction Method, for fast journal orbit analysis, to the dynamically misaligned sterntube bearing may be difficult. The main problem is that the velocity coefficients would become functions of four parameters, namely: eccentricity ratio and attitude angle at the bearing axial centre, misalignment angle and angle of the plane of misalignment. This indicates that a considerable increase in the size of the velocity coefficient data bank would be necessary. In addition, the development of the oil film force equations for an aligned bearing was based on the segregation of squeeze and wedge action, i.e. radial and effective angular velocities. Where misalignment is present, this segregation is impossible due to the variation of attitude angle along the length of the bearing. The above comments do not negate the possibility of applying the Reaction Method to dynamically misaligned bearings, but this will depend on the acceptability of substantial approximations.

3.7 Analysis Refinement for Large Lateral Journal Velocities

The hydrodynamic analysis method described in reference 6 has been found to be satisfactory for steadily loaded bearings and for the small journal displacement and velocity perturbations required to compute linearised stiffness and damping coefficients. In developing the oil film force equations [3] and [4] for the Reaction Method, it was necessary to carry out various hydrodynamic analyses with large lateral journal velocities. This was found to produce some anomalies in the results, and whilst the apparent errors were small, the analysis method was subject to further development to eliminate these problems. The following notes are an outline of the essential details:

(a) The squeeze film term (V_n. Δa. Δc.) was eliminated from the continuity equation for cavitating elements. The hypothesis underlying this change was that in a cavitating element, the oil displaced by the normal velocity of the journal surface V_n will mainly result in an axial velocity of the boundaries of the oil streams. The squeeze film term does not therefore result in any oil flow across the element boundary, and thus disappears from the continuity equation for such an element.

(b) The original cavitation model failed to satisfy continuity in cavitating elements when circumferential flow reversal relative to the h_{min} position occurred; i.e. $\dot{\Theta} < -\omega/2$. Elimination of this problem simply required recognition that, in the above circumstances, element upstream and downstream boundaries became reversed. The essential point is that the gas/vapour flow term computed to satisfy continuity in cavitating elements referred to the downstream element boundary.

(c) The journal surface velocity u was calculated on the basis of the equivalent angular velocity; i.e. $u=(\omega-2\dot{\Theta})D/2$ instead of the original $u=\omega D/2$. In addition, $\dot{\Theta}$ was deleted from the computation of V_n, therefore V_n became a function of $\dot{R}$ only. The above measures effectively segregated the hydrodynamic squeeze and wedge actions in the analysis. This segregation is unnecessary in full film elements, but is advantageous with cavitating elements. The reason for this is that when eliminating the squeeze film term from the continuity equation for cavitating elements, as indicated in item a., it was found that only that part of (V_n. Δa. Δc.) due to $\dot{R}$ should be eliminated. When applying this analysis modification to a misaligned bearing, it is necessary to apply it individually to each element column, since $\dot{R}$ and $\dot{\Theta}$ will vary with the axial position.

4. RESULTS

4.1 Parameter Study

A comprehensive investigation has been undertaken in which the influence of variation of the following parameters upon the steady load performance and dynamic coefficients was examined: L/D, ϵ, $\bar{\alpha}$, $\bar{p}_h$, β, Θ_r, $\bar{B}_{ow}$.

Exhaustive coverage of a large range of combinations of these parameters was not feasible due to the amount of computation involved. Variation of each parameter singly was, therefore, carried out while maintaining the remainder constant at the following datum conditions:

$L/D=2.0$, $\epsilon=0.7$, $\bar{\alpha}=0$ and 0.2, $\bar{p}_h=0$, $\beta=0$, $\Theta_r=0$, $\bar{B}_{ow}=0$.

It should be noted that the above treatment is necessary when generating analytical data in this field. This is not representative of the way in which a real bearing behaves, since it is generally impossible, particularly with a service bearing, to change one variable without affecting others. For example, in this type of analysis when $\bar{\alpha}$ was increased ϵ was held constant. Due to the non-linearity of the oil film, when increasing $\bar{\alpha}$ in a real bearing, the corresponding increase in oil film force at the bearing end where the journal eccentricity increases, exceeds the decrease in oil film force at the opposite end of the bearing. The result is that ϵ will decrease in order to maintain the same total oil film force. A practical bearing analysis technique, which utilizes precomputed data of the type presented in this section, is described in section 5.

Computation of the steady load solution only required about 10% of the computing time necessary for a full analysis including all 32 dynamic coefficients. Accordingly a more extensive analysis programme was conducted for steady load conditions, the parameter ranges being:

$L/D=1$ to 3, $\epsilon=0.1$ to 0.95, $\bar{\alpha}=0$ to 0.9, $\bar{p}_h=0$ to 0.2 with β, Θ_r and $\bar{B}_{ow}$ held at zero.

A few of the more interesting results of this parameter study are presented in 4.2 and 4.3. Complete details of this work are given in reference 18.

4.2 Steady Load Performance

The most significant "independent" variables are ϵ and $\bar{\alpha}$, and the performance parameters of greatest interest are $\bar{W}$, $\bar{H}$, $\bar{Q}$ and $\bar{M}$. The computed relationship between these parameters is illustrated in Figs. 6, 7, 8 and 9 respectively. A relationship clearly exists between $\bar{\alpha}$ and the maximum possible value of ϵ, which is due to the attainment of contact between the journal and bearing at one end. This is reflected in the corresponding limits to the extent of the curves in Fig. 6 to 9. All the performance parameters are highly dependent upon ϵ, but the above figures show that only $\bar{M}$ is substantially affected by $\bar{\alpha}$.

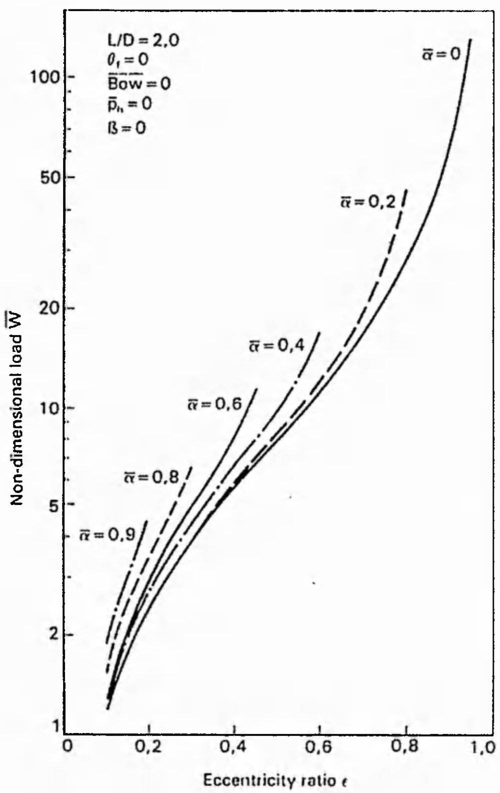

Fig. 6

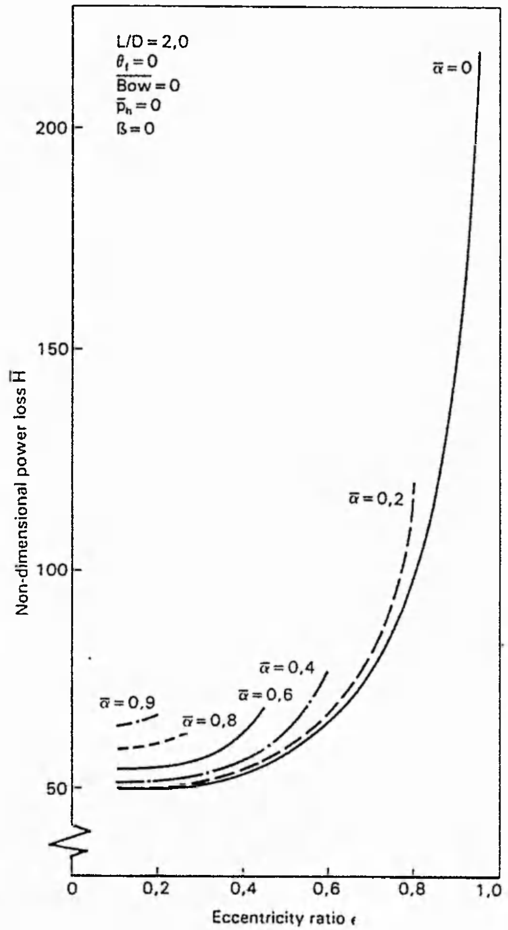

Fig. 7

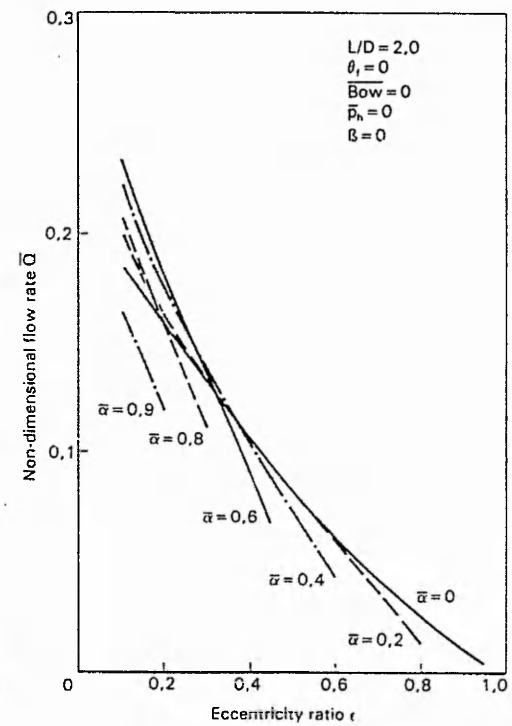

Fig. 8

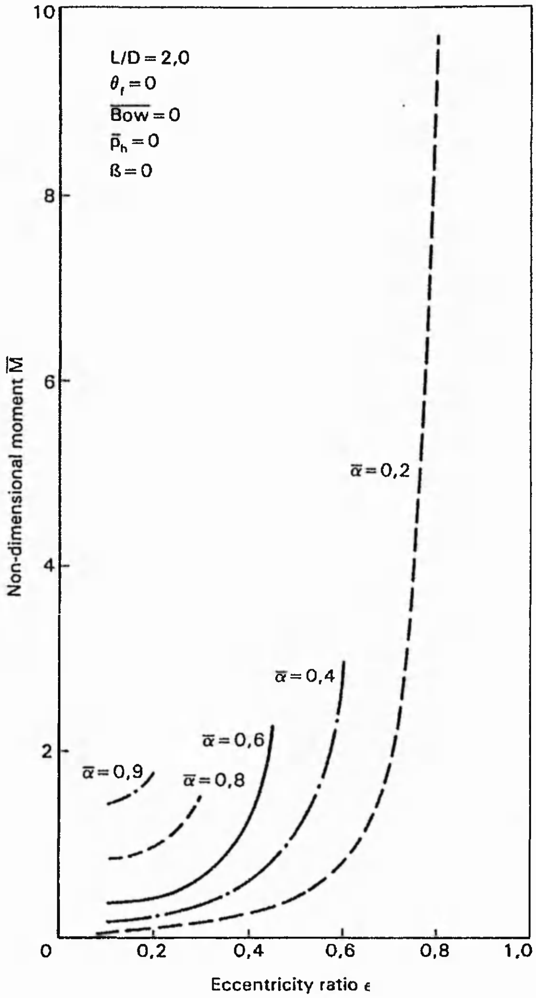

Fig. 9

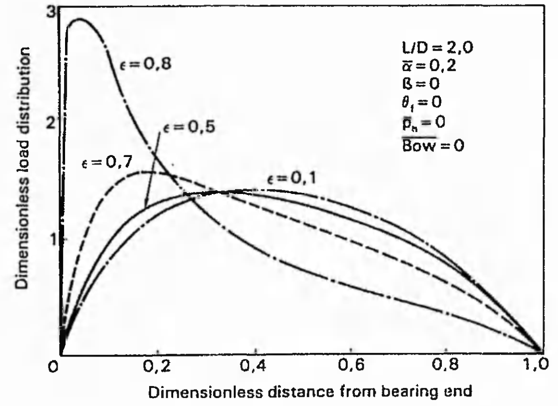

Fig. 10 Effect of ϵ on Load Distribution

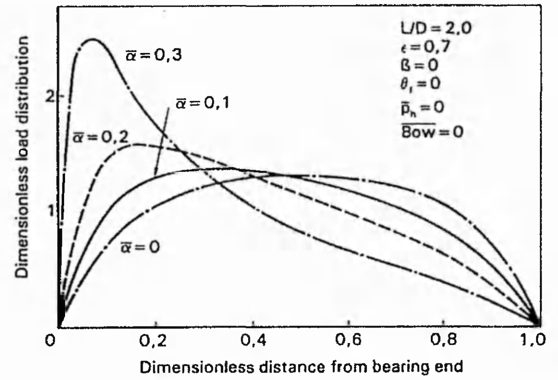

Fig. 11 Effect of Misalignment Angle $\bar{\alpha}$ on Load Distribution

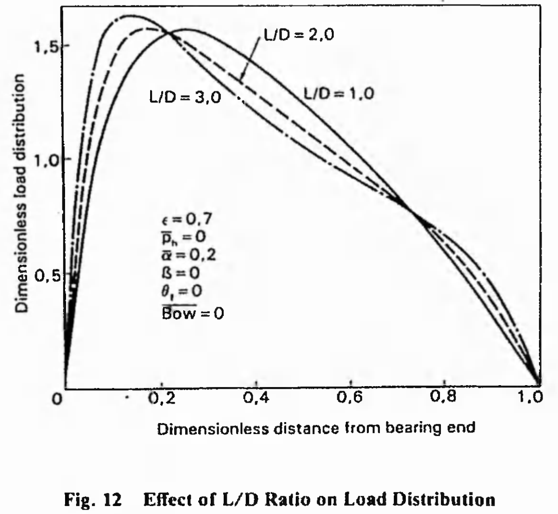

Fig. 12 Effect of L/D Ratio on Load Distribution

Figs. 10 and 11 indicate that both ϵ and $\bar{\alpha}$ have a similar effect on the axial load distribution. In Fig. 10, a finite value of $\bar{\alpha}$ must be present to produce the above similarity, particularly with respect to the assymmetry of the load distribution. The result of increasing ϵ is therefore to accentuate the effect of the misalignment.

An increase in L/D ratio leads to enhanced hydrodynamic efficiency due to the greater restriction to axial oil flow. This results in a flatter axial load distribution which is clearly shown by Fig. 12.

The main effect of increasing $\bar{p}_h$ is to suppress cavitation. This is illustrated by Fig. 13 which indicates that the head pressure at which complete elimination of cavitation is attained is much higher when misalignment is present. Fig. 14 shows the effect of increasing $\bar{p}_h$ on the dimensionless load $\bar{W}$. Increasing $\bar{p}_h$ effectively permits the existance of all or part of the negative pressure region in the top half of the bearing, which would

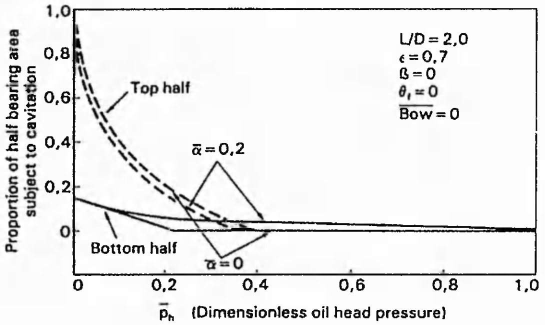

Fig. 13 Effect of $\bar{p}_h$ on the Extent of Cavitation

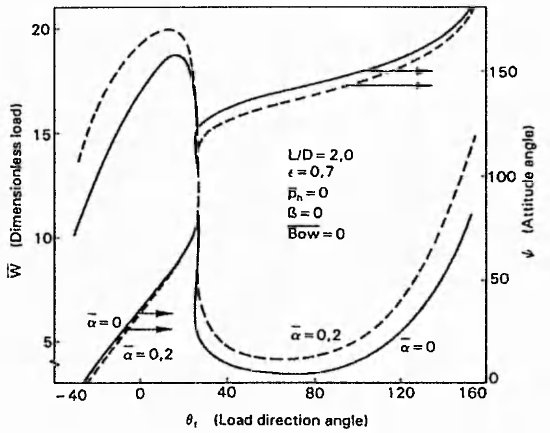

Fig. 15 Effect of θ_f on $\overline{W}$ and ψ

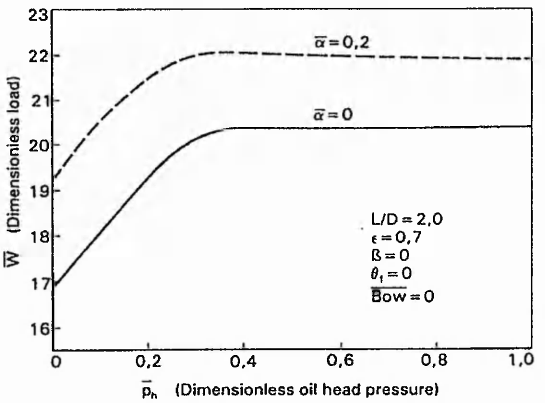

Fig. 14 Effect of $\bar{p}_h$ on $\overline{W}$

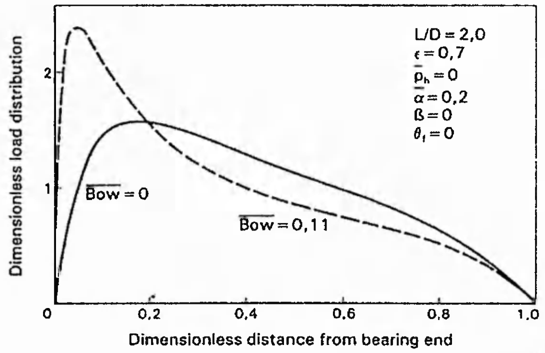

Fig. 16 Effect of $\overline{Bow}$ on Load Distribution

otherwise be eliminated by cavitation. It does this by raising the general pressure level of the oil film, thereby reducing the tendency for the cavitation pressure to be encountered. This results in a significant improvement in load capacity, as indicated by the left hand side of the curves in Fig. 14. In both the aligned ($\bar{\alpha}=0$) and misaligned $\bar{\alpha}=0.2$) cases analysed, complete elimination of cavitation in the top half of the bearing was attained at about $\bar{p}_h=0.4$ (Fig. 13) at which point $\overline{W}$ therefore attained its maximum value (Fig. 14). Beyond $\bar{p}_h=0.4$, $\overline{W}$ is constant for the aligned case since cavitation has been totally eliminated. In the misaligned case ($\bar{\alpha}=0.2$), the value of $\overline{W}$ falls slightly as $\bar{p}_h$ increases beyond 0.4. This is due to the more gradual elimination of cavitation in the bottom half of the bearing at the high journal eccentricity end, when misalignment is present. It should be noted that the extent of cavitation is particularly dependent on ϵ. For a lightly loaded bearing, the correspondingly low ϵ results in little or no cavitation, and the above influence of $\bar{p}_h$ therefore becomes negligible. Unfortunately improvement in load capacity by increasing $\bar{p}_h$ cannot be advocated due to the practical constraints outlined in section 2.7.

As outlined in section 2.3, propeller wake field effects may result in the mean load vector acting on the sterntube bearing being displaced from the vertical. Fig. 15 shows the effect of varying the load vector angle Θ_f upon $\overline{W}$ and ψ. This indicates a very dramatic fall in load capacity as ψ passes through 90°. The above behaviour is predictable since it corresponds to the h_{min} position passing over the left hand oil groove, thereby seriously interfering with the build up of film pressure due to hydrodynamic wedge action.

The effect of bowing of the journal due to the application of bending moment was investigated. This arises mainly from the overhung weight of the propeller, and for analytical purposes has been treated as a constant radius of curvature i.e. the journal bending moment was assumed to be approximately constant over the length of the bearing. The dominant effect of journal bow is to increase the eccentricity at the bearings ends. This tends to improve hydrodynamic efficiency by restricting axial oil flow in the high pressure region. The main results are a flattening of the axial load distribution, and an increased sensitivity to misalignment, both effects being clearly illustrated by Fig. 16. It is evident from the above results that the effects of increasing journal bow are analogous to those of increasing L/D ratio (see Fig. 12).

4.3 Dynamic Coefficients

The most important "independent" variable with respect to the dynamic coefficients is ϵ. This is illustrated for some of the coefficients in Figs. 17 to 20. The stiffness coefficient curves (Figs. 17 and 18) are generally seen to be fairly flat over a large part of the ϵ range, with significant increases only at fairly high ϵ. It should be noted that these curves are for $\bar{\alpha}=0.2$ and that ϵ refers to the bearing axial centre. The sharp increase in coefficient magnitude at $\epsilon=0.8$ corresponds to the local eccentricity ratio at one end of the bearing approaching unity. Figs. 19 and 20 show the damping coefficients to be similarly related to ϵ, but in some cases, notably B_{yy} and $B_{\gamma\gamma}$, a significant rise was also found at the lower end of the ϵ range.

The dynamic coefficients may be regarded as not being directly affected by $\bar{\alpha}$, but rather by the associated high local journal eccentricity at one end of the bearing. Bowing of the journal axis also influenced the dynamic coefficients in a similar indirect manner.

The effects of both L/D ratio and $\bar{p}_h$ upon the dynamic coefficients (not illustrated) were generally small.

A rather more interesting effect was that of Θ_f which is shown for the lateral stiffness coefficients (force—lateral displacement) in Fig. 21. The behaviour of the other dynamic coefficients was similar in that distinct kinks occurred at about $\Theta_f=37°$. Reference to Fig. 15 confirms that this corresponds to $\psi=90°$, and the kinks are therefore clearly due to the interference of the left hand oil groove with hydrodynamic wedge action which also resulted in the fall in $\overline{W}$ shown in Fig. 15.

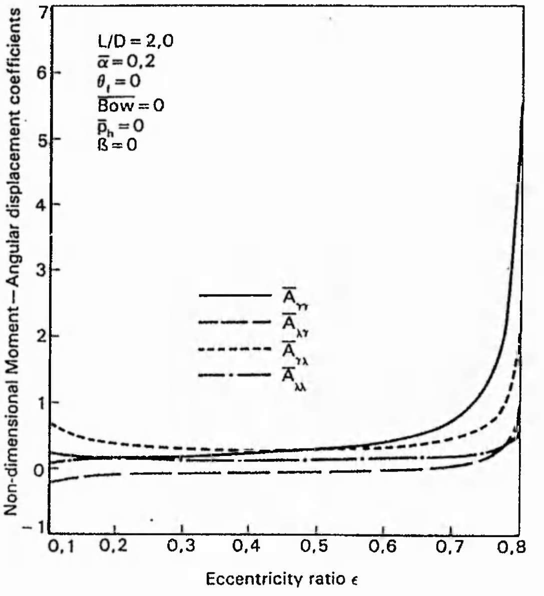

Fig. 18

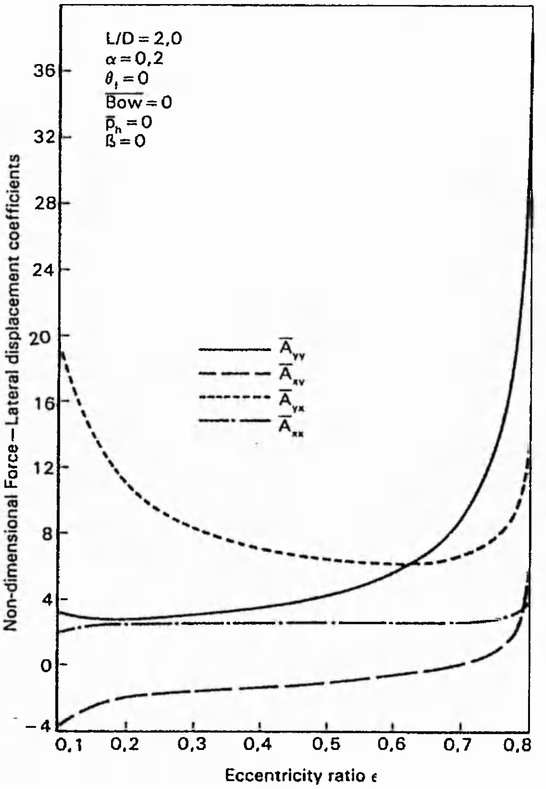

Fig. 17

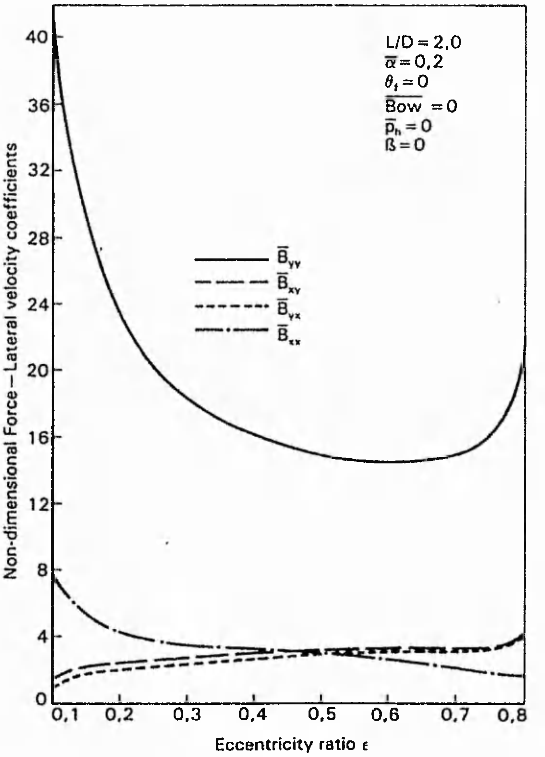

Fig. 19

A.4. -63.

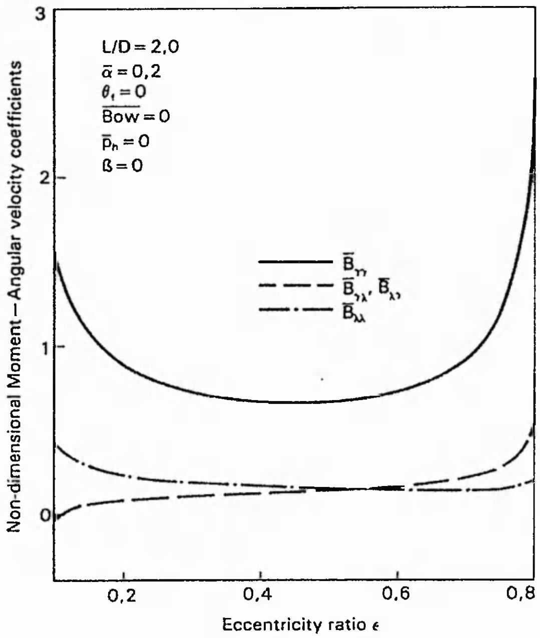

Fig. 20

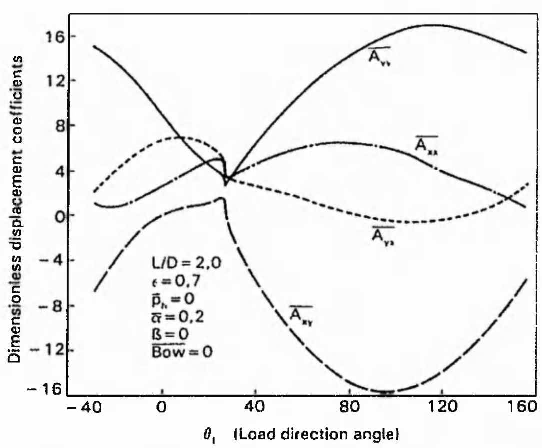

Fig. 21 Effect of θ_f on $\overline{A_{\gamma\gamma}}$, $\overline{A_{\gamma\lambda}}$, $\overline{A_{\lambda\gamma}}$, $\overline{A_{\lambda\lambda}}$ ($\bar{\alpha}=0,2$)

5. PRACTICAL BEARING ANALYSIS

5.1 Real Bearing Parameter Interaction

An inherent problem of the hydrodynamic analysis method described in section 3.2, is that the position of the journal within the bearing clearance must be specified and the corresponding oil film force computed, i.e. ϵ, ψ are independent variables and W, Θ_f are dependent variables. In the majority of practical applications it is necessary to treat the relationship between the above variables in the reverse sense. The only way in which this can be achieved with a hydrodynamic analysis, is to use an iterative solution for ϵ, ψ to meet a specified W, Θ_f. This would require substantial computing time, particularly in view of the non-linearity of the relationship between the above variables. In view of the above problem, practical bearing analysis programs utilize pre-computed data relating the various bearing performance parameters in dimensionless terms.

Fig. 22 shows the essential interaction between all the parameters in a practical bearing situation. A practical analysis program has been developed for misaligned sterntube bearings, which operates in a similar way to Fig. 22. This type of analysis has been described in detail, for aligned bearings, in reference 19. In the above program the bearing geometry data are combined with load, rotational speed and effective viscosity to give $\overline{W}$, thus enabling ϵ to be determined by interpolation from the data bank of pre-computed $\overline{W}-\epsilon$ data. It may be noted that the effective viscosity is the subject of an iterative solution, to satisfy thermal balance, in the loop at the right hand side of Fig. 22. Within this loop power loss and oil flow rate are derived by interpolation of pre-computed $\overline{H}-\epsilon$ and $\overline{Q}-\epsilon$ data. An initial effective viscosity corresponding to the oil supply temperature is assumed. The iterative thermal balance solution is thus analogous to a thermal transient condition. On completion of the thermal balance solution, ψ, $\overline{M}$ and Θ_m may be interpolated from the relevant data banks to complete the analysis.

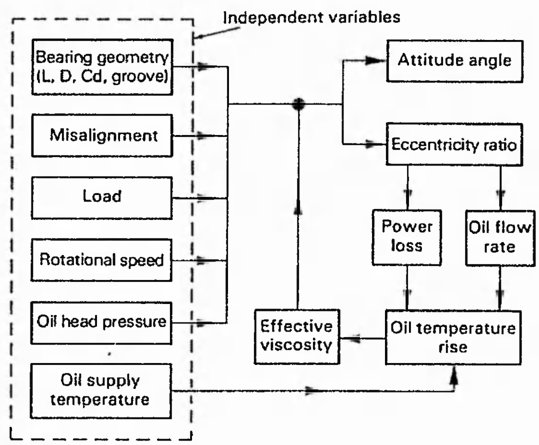

Fig. 22 Bearing Performance: Interaction of Parameters

In the misaligned sterntube bearing program data banks are required for $\overline{W}$, ψ, $\overline{H}$, $\overline{Q}$, $\overline{M}$ and Θ_m. Data for each of these parameters is stored as function of ϵ, $\bar{\alpha}$, L/D and $\bar{p}_h$, and four dimensional matrices are therefore used for this purpose. It follows from the above that the complete data bank comprises six four dimensional matrices, these comprising a total of 4,320 data items. In the present version of the program, variation of Θ_f, β and B_{ow} is not covered, these parameters being assumed to be zero. Expansion of the program to include variation of Θ_f, β and B_{ow} is theoretically possible, but would require an increase in the size of the data bank by about an order of magnitude for each variable.

At present, the misaligned sterntube bearing program is available on disc for use with the Hewlett Packard 9836c desk top computer, the program name being "STBPER". (Stern Tube Bearing Performance). Approximate operating times are as follows:

Load Program:	5 secs.
Initialize Program (reads data bank into operating matrices):	14 secs.
For one analysis case: Complete Data Input	40 secs.
Analysis	26 secs.
Print Out Results	15 secs.

The program has facilities for modifying the input data and re-running the analysis thus reducing the data input time for subsequent runs.

Program "STBPER" does not include computation of the thirty-two oil film stiffness and damping coefficients, since this would require an increase in the number of four dimensional data matrices from six to thirty-eight. The stiffness and damping coefficients may therefore be computed by program "STBSDC". (Stern Tube Bearing Stiffness and Damping Coefficients). This program uses a hydrodynamic analysis model to compute each coefficient, and consequently requires 5 to 6 hours running time on the Hewlett Packard 9836c.

Background notes and operating instructions for programs "STBPER" and "STBSDC" are given in reference 20.

5.2 Bearing—Shafting System Interaction

The misaligned sterntube bearing program (STBPER), decribed in the previous section, enables the lateral position of the journal within the bearing clearance space to be determined for a specified load and misalignment angle. In addition, the axial location of the effective support is computed, the displacement from the bearing axial centre being a function of the misalignment angle. Where any bearing forms part of a multi-bearing system, however, its load and misalignment angle are also dependent on the journal lateral position and the axial position of the support point for all the bearings in the system, due to the elastic coupling imposed by the shaft. This interaction of shafting and bearing response is shown diagramatically in Fig. 23. Note that the "journal position in bearing" box covers both the lateral position and the axial position of the effective support point. With respect to the latter, the oil film response of a misaligned bearing may be expressed as a force and moment applied at the axial centre, or a force only, displaced from the axial centre. For shaft alignment analysis, the displaced force is generally preferred.

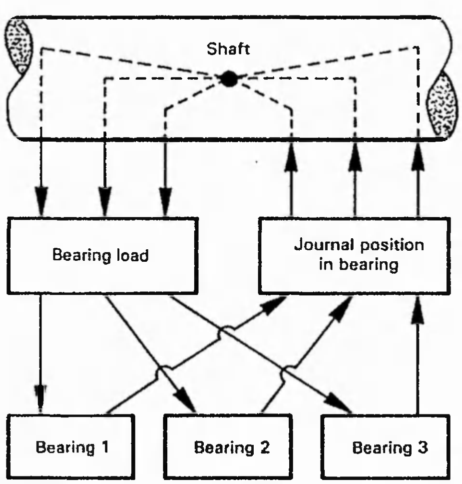

Fig. 23 Bearing Shaft Interaction

The shaft bearing interaction with respect to lateral position, is only significant in fairly stiff shafting systems. One exception to this is the situation in which the load direction in a bearing reverses, thus leading to a journal movement through a substantial proportion of the bearing clearance. This may occur in gear bearings between zero and full torque conditions, depending upon the gearbox design.

In a propeller shaft system, misalignment is generally insignificant in all bearings other than the sterntube bearing. This is due to their lower L/D ratios, which results in lower sensitivity to misalignment, and to their accessibility which facilitates the achievement of good alignment. With the sterntube bearing, however, misalignment is invariably significant. The effective support point in the sterntube bearing should therefore be determined by an interactive shaft alignment analysis and bearing analysis. An iterative process to achieve this type of interactive analysis is illustrated in Fig. 24. Tests have indicated rapid convergence (3 or 4 iterations) of the support position to a satisfactory degree of accuracy. At present, the iterations must be performed manually using separate shaft analysis and bearing analysis programs. The integration of these analyses into a single interactive analysis program is currently under consideration. Although Fig. 24 deals with the axial location of the effective support position, the iterative process is equally applicable to the solution of lateral position of the journal within the clearance space. It should be noted that the support point position in a misaligned sterntube bearing in the static condition is a Hertzian contact problem rather than hydrodynamic, and is not covered by the work reported in this paper.

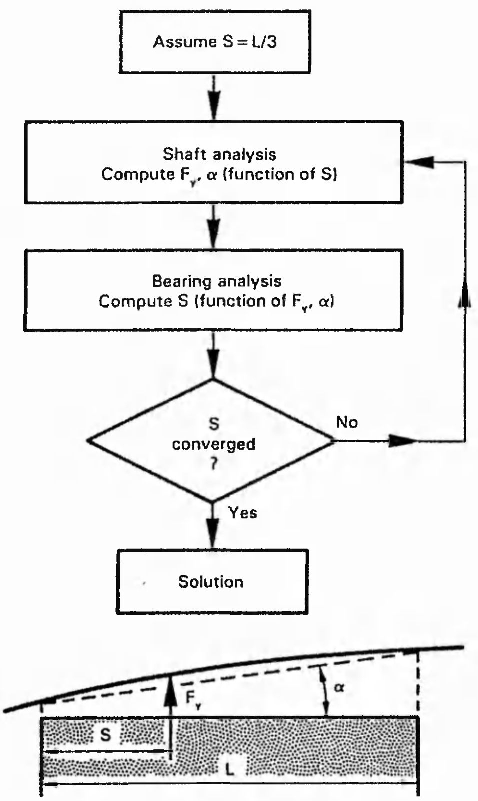

Fig. 24 Interactive Solution for Misaligned Bearing Support Point

A.4. - 65.

5.3 Practical Analysis Results

Controversy has existed for some time with respect to the optimum L/D ratio for sterntube bearings. Longer bearings have greater load carrying capacity, not only as a direct result of their increased area, but also due to their enhanced hydrodynamic efficiency (*see* section 4.2). Unfortunately longer bearings are also more sensitive to angular misalignment, which is usually present in sterntube bearings. This sensitivity is offset by the use of larger C_d/D ratios (*see* section 2.2).

Having regard to the above conflicting factors, it is evident that the optimum L/D ratio will depend on the amount of angular misalignment present in a given installation. It should be noted that the term optimum is used here purely with respect to operating reliability. A shorter bearing may, in practice, be dictated by available space or cost considerations.

The misaligned sterntube bearing program "STBPER" enables the optimum L/D ratio to be determined for any given operating conditions. There are various ways in which the correlation between optimum L/D ratio and misalignment angle may be illustrated. The essential feature of the method chosen in Fig. 25 is that it facilitates clear graphical presentation of the results. In all the cases analysed, the load (W) was adjusted to give $h_{min} = 0.2$ mm at the bearing end with L/D = 1.0. The L/D ratio was then increased in steps, maintaining α and W constant. A family of curves for a range of α values was thus produced. Results are given for $C_d = 2$ and 1. mm., the former being consistent with normal sterntube bearing practice ($C_d/D = 0.002$). At $\alpha = 0$ and $C_d = 2$ mm, the above criterion ($h_{min} = 0.2$ mm at L/D = 1.0) was met by W = 466 000 N. This was taken as the datum load, and all other loads are expressed as a percentage of this value.

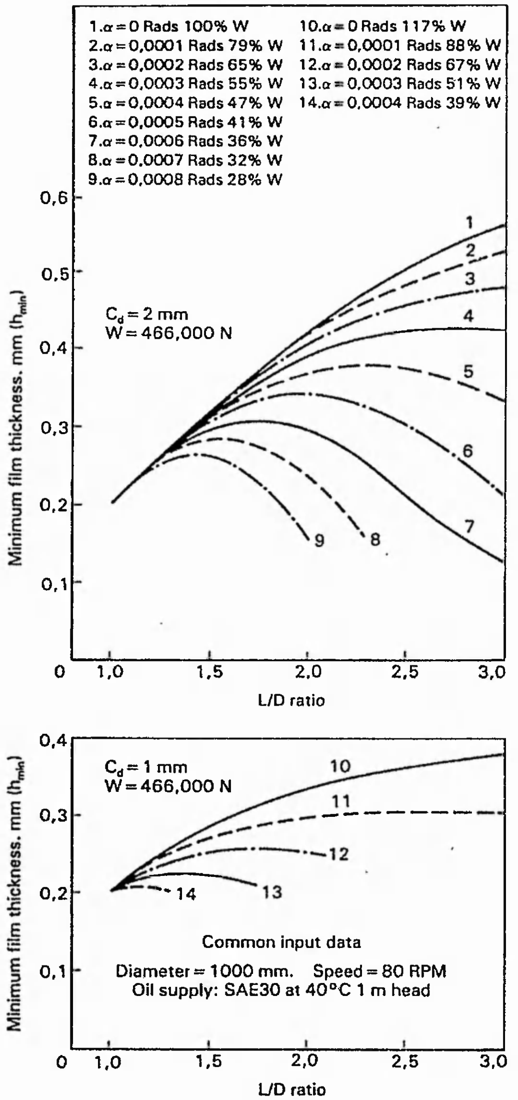

Fig. 25

A.4. - 66.

For $C_d = 2$ mm, it is evident that α must exceed 0.0005 rads before there is any incentive to reduce L/D below 2.0. Reducing C_d to 1 mm increases the load capacity at $\alpha = 0$ due to the enhanced hydrodynamic effect. This improvement is substantially offset by the higher operating temperature, and hence reduced effective viscosity resulting from the tighter clearance. A more pronounced fall in Q, as L/D increased, was found for $C_d = 1.0$ mm, hence the much flatter family of curves due to the above thermal effects becoming even more significant. The direct effect of misalignment is more pronounced at reduced C_d, since it is essentially dependent on dimensionless misalignment $\bar{\alpha}$ ($= \alpha$ L/C_d).

At $C_d = 1$ mm, the misalignment threshold beyond which it is worthwhile to reduce L/D below 2.0 is about 0.00015 rads. These results clearly indicate the need for a reasonably generous clearance in sterntube bearings, particularly where higher levels of misalignment are predicted. Given an adequate clearance, levels of misalignment which result in an optimum L/D ratio of less than 2 are likely to be excessive. In such cases, the misalignment should be reduced by suitable alignment of the shafting system, or by slope boring the sterntube bearing.

The results given in Fig. 25 clearly illustrate the influence of misalignment angle upon the optimum L/D ratio. In any given practical situation however, W and α would be virtually fixed by the shaft alignment conditions, and D would be mainly governed by the maximum torque transmitted. Only L and C_d would therefore be available as variables for design optimisation of the sterntube bearing. The results of an optimisation, subject to the above practical constraints, are shown in Fig. 26. As in Fig. 25, h_{min} is again used as the basis for assessing the operating safety margin of the bearing. It is evident from Fig. 26 that the absolute optimum (maximum h_{min}) in this instance lies beyond the L and C_d ranges considered. As previously indicated, the maximum L may be limited by available space or cost considerations. Where such constraints apply, Fig. 26 is useful for indicating the optimum C_d for a specified maximum L. It should be noted that for any constant C_d curve, h_{min} falls more rapidly if L is increased beyond the optimum value, compared with the fall below this point. If the misalignment angle is greater than predicted, the effect is to displace the operating point to the right of the optimum position on the appropriate constant C_d curve. It is therefore safer to select C_d a little above the optimum value in order to make some allowances for misalignment angle prediction error.

The results shown by Fig. 25 indicate an inverse correlation between the maximum acceptable specific bearing pressure and the maximum acceptable misalignment angle. In order to provide generalised guidance on this correlation, it is necessary to present the data in dimensionless terms. This has been done in Fig. 27 for a maximum eccentricity ratio at the bearing end of 0.9365. The choice of this eccentricity ratio is arbitrary, and should ultimately be related to service experience. A normal sterntube bearing C_d/D ratio of 0.002 was used to derive the curves in Fig. 27, but calculations indicated negligible differences for the range $0.0018 \leqslant C_d/D \leqslant 0.0022$. In the absence of specified information on oil type and operating temperature the assumption of an operating viscosity η of 0.033 Pa.s. is recommended. This is based on a SAE 30 oil at 60°C, and should generally err on the pessimistic side. It may be noted that a logarithmic scale has been used for dimensionless maximum specific bearing pressure. This form of presentation results in partial linearization of the curves, thereby enabling data to be extracted more accurately.

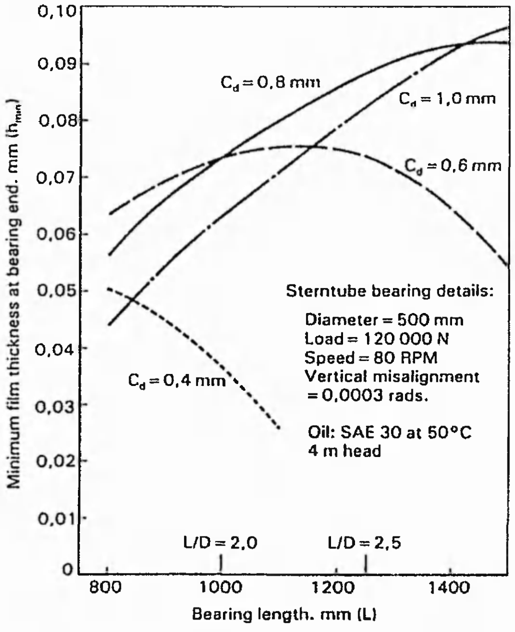

Fig. 26 Bearing Clearance and Length Optimisation

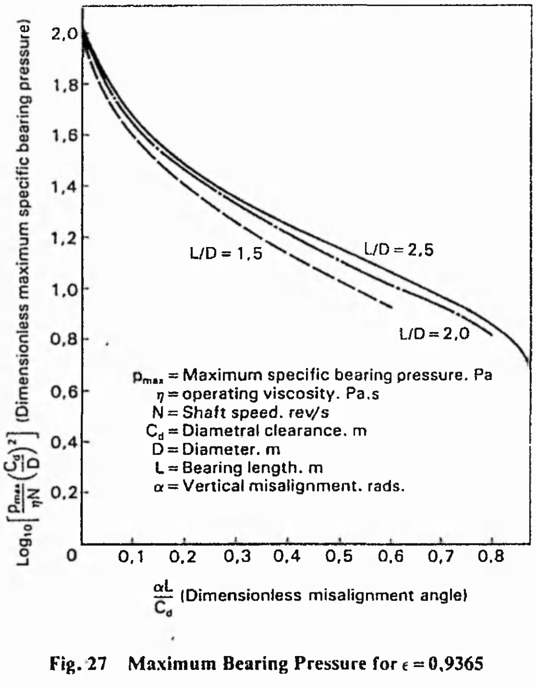

Fig. 27 Maximum Bearing Pressure for $\epsilon = 0.9365$

6. OUTLINE OF FUTURE WORK

The current research programme includes an investigation into the significance of various combinations of the 32 oil film dynamic coefficients, which may be computed by the program "STBSDC". This work will make comparisons of the predicted lateral vibration frequencies, when applying different combinations of coefficients to the analysis. The tests will be conducted on various types of propeller shafting system.

It is also desirable to investigate the non-linear response of sterntube bearings to lateral vibration, which is relevant to situations involving large amplitudes. This could be done by extending the journal orbit analysis method developed for aligned crankshaft bearings, to cover sterntube bearings under dynamic misalignment conditions. In the longer term, a substantially simpler approximate solution to this problem will be necessary, in order to reduce the computation time to a level acceptable for practical application.

Two other areas that are worth investigating are bearing elasticity (elastohydrodynamic lubrication) which is particularly relevent to reinforced resin bearings, and consideration of optimum oil groove locations. As indicated in section 2.6., the oil groove locations must be related to the load direction for a given installation and operating condition.

The research on sterntube bearings described in this paper, has, to date, been entirely theoretical. Comparisons of results with other published theoretical and experimental data have been carried out. The availability of clear reliable experimental data on misaligned bearings in general; and sterntube bearings in particular is, however, extremely limited. There is a consequent need for experimental work in this area, in order to improve confidence in the analysis programs that have been developed. Whilst shipboard measurements may give useful insights into the behaviour of sterntube bearings in their operating invironment, they are no substitute for good quality experimental test rig data. A bearing test rig offers the scope for comprehensive instrumentation, and control over the significant variables. It is hoped that such work will form part of the continuing research in this field.

7. CONCLUSIONS

A numerical hydrodynamic analysis method has been developed for journal bearings. This method takes account of flow continuity throughout the oil film, including the cavitation zone. The cavitation model is a particularly important feature, when considering the non-linearity of an oil film response. For the various aspects of the application of journal bearing analysis to practical situations, the above hydrodynamic analysis method has proved to be a valuable foundation.

The significance of various sterntube bearing design and operating parameters has been studied. As a result of this work, programs covering the steady load performance and oil film dynamic coefficients of misaligned sterntube bearings have been developed. These programs have been designed for practical applications using the Hewlett Packard 9836c desk top computer, and are user friendly. The sterntube bearing performance program is now in regular use to assess the acceptability of bearing operating conditions, particularly where high misalignment angles are involved. This program is also used in conjunction with shaft alignment analyses, in order to predict accurately the location of the effective support point in oil lubricated sterntube bearings.

Generalised guidance on the acceptability of angular misalignment as a function of specific bearing pressure has been given.

An outline of future work in this field has also been presented.

8. ACKNOWLEDGEMENTS

The author is indebted to Mr. S. G. Pratt for the provision of statistical data on sterntube bearing and aft seal defects, to Mr. G. Pumphrey for the preparation of the figures and to Mrs. T. Williams for typing the manuscript.

9 REFERENCES

1. C. Archer and D. K. Martyn: "Static and Dynamic Alignment" Trans.I.Mar.E. Vol.91, Conf. No. 4. Paper C31, (1979).
2. W. S. Vorus and R. L. Gray: "Calculation of Sterntube Bearing Eccentricity Distribution: Applications in States Lines Ro/Ro Bearing Failure Analysis". Trans. I.Mar.E. Vol.91, Conf. No. 4. paper C37, (1979).
3. M. Leemens and F. Roode: "Vibration Analysis of a Rotating Propeller Shaft in a Rubber Stern Tube Bearing". Conf. International Co-operation on Marine Eng. Systems. Trieste. (1984).
4. B. Fantino., J. Frene and M. Godet: "Dynamic Behaviour of an Elastic Connecting Rod Bearing—Theoretical Study". SAE/SP-539—Studies in Engine Bearings and Lubrication. Paper No. 83037. February 1983.
5. G. A. La Bouff and J. F. Booker: "Dynamically loaded journal bearings: A Finite Element treatment for rigid and elastic surfaces". ASME/ASLE Joint Tribology Conference. October 1984. Paper 84-TRIB-II.
6. R. W. Jakeman: "A numerical analysis method based on flow continuity for hydrodynamic journal bearings". Tribology International Vol.17. No. 6. December 1984.
7. I. Etsion and L. P. Ludwig: "Observation of Pressure Variation in the Cavitation Region of Submerged Journal Bearings." ASME Journal of Lubrication Technology. April 1982. Vol.104.
8. C. H. T. Pan: "Dynamic Analysis of Rupture in Thin Fluid Films. I.—A Noninertial Theory". Trans. ASME. Vol.105. January 1983.
9. H. Heshmat and O. Pinkus: "Mixing Inlet Temperatures in Hydrodynamic Bearings". ASLE/ASME Tribology Conference. October 1985. ASME Preprint No. 85-TRIB-26.
10. T. Lloyd., R. Horsenell and H. McCallion: "An investigation into the Performance of Dynamically Loaded Journal Bearings: Theory". Proc.I.Mech.E. Vol.181. Part 33.
11. R. W. Jakeman: "Journal Orbit Analysis taking account of Oil Film History and Journal Mass". 4th International Conference on Numerical Methods in Laminar and Turbulent Flow. Swansea. July 1985.
12. G. J. Jones: "Crankshaft Bearings: Oil Film History" 9th Leeds-Lyon Tribology Symposium. September 1982.
13. R. Holmes and A. H. Craven: "The Influence of Crankshaft and Flywheel Mass on the Performance of Engine Main Bearings". I.Mech.E. Tribology Conf. 1971. Paper C63/71.
14. J. F. Booker: "Dynamically Loaded Journal Bearings: Numerical Application of the Mobility-Method". ASME J.Lub.Tech. January 1971.
15. R. W. Jakeman: "The Influence of Cavitation on the Non-Linearity of Velocity Coefficients in a Hydrodynamic Journal Bearing". To be published in the Proceeding of the 13th Leeds-Lyon Symposium on Tribology. Leeds. September 1986.
16. R. W. Jakeman and D. W. Parkins: "Theoretical and Experimental Orbits of a Dynamically Loaded Hydrodynamic Journal Bearing". To be published in the proceeding of the 13th Leeds-Lyon Symposium on Tribology. Leeds. September 1986.
17. R. H. Bannister: "A Theoretical and Experimental Investigation Illustrating the Influence of the Non-Linearity and Misalignment on the Eight Oil Film Coefficients". Proc.I.Mech.E. 1976. paper C219/76.
18. R. W. Jakeman: "Misaligned Sterntube Bearings: Steady Load Performance Data and Stiffness and Damping Coefficients". L. R. Internal Report—Project 5.1.10. July 1984.
19. Engineering Science Data Unit. Item No. 66023. Steadily Loaded Hydrodynamic Journal Bearings. September 1966.
20. R. W. Jakeman: "Performance Analysis and Stiffness and Damping Coefficients for Misaligned Sterntube Bearings: User Guidance for Programmes STBPER and STBSDC". L. R. Internal Report. Project 5.1.10. June 1985.

APPENDIX 1

NOMENCLATURE

A_{xx} etc.	Oil film stiffness coefficients	See equations [1] [2] in section 3.5.
B_{xx} etc.	Oil film damping coefficients	
B_{tt} etc.	Oil film velocity coefficients	See equations [3] [4]
B_{ow}	Displacement of journal axis at axial centre from straight line joining axis locations at bearing ends.	
C_d	Diametral clearance.	
D	Journal diameter.	
e	Journal eccentricity†	
F	Total oil film force*	
F_r	Oil film radial force†	
F_t	Oil film tangential force†	
F_x	Oil film horizontal force*	
F_y	Oil film vertical force*	
H	Power loss.	
h_{min}	Minimum oil film thickness	
L	Bearing length	
M	Total oil film moment*	
M_x	Oil film moment in horizontal plane*	
M_y	Oil film moment in vertical plane*	
N	Angular velocity of journal about its axis. rev/s.	
p_h	Oil head pressure.	
Q	Oil flow rate from bearing ends.	
$\dot{R}$	Radial velocity of journal†	
u	Journal surface velocity.	
V_n	Normal velocity of journal surface at any given oil film element.	
W	Bearing load (external)	
x,y	Journal horizontal, vertical lateral displacement*	
$\dot{x}$,$\dot{y}$	Journal horizontal, vertical lateral velocity*	
α	Misalignment angle.	
α_x, α_y	Misalignment angle components in horizontal, vertical planes*	
β	Angle of misalignment plane*	
λ, γ	Journal angular displacement in horizontal, vertical plane*	
$\dot{\lambda}$, $\dot{\gamma}$	Journal angular velocity in horizontal, vertical plane*	
$\dot{\theta}$	Angular velocity of journal axis about bearing axis†	
$\dot{\theta}_o$	Equivalent angular velocity of journal†	
θ_f	Angle of total oil film force*	
θ_m	Angle of plane of total oil film moment*	
Δa, Δc	Axial, circumferential oil film element dimensions.	
ϵ	Eccentricity Ratio. ($=2e/C_d$).	
ψ	Attitude Angle*	
ω	Angular velocity of journal about its axis rad/s.†	
η	Effective viscosity.	

*see Fig. 2 †see Fig. 5.

Dimensionless parameters are denoted by a "bar" above them, and are defined as follows:

$$\overline{W} = \frac{W}{\eta NLD}\left(\frac{C_d}{D}\right)^2$$

$$\overline{M} = \frac{M}{\eta NL^2D}\left(\frac{C_d}{D}\right)^2$$

$$\overline{H} = \frac{HC_d}{\eta N^2LD^3}$$

$$\overline{Q} = \frac{Q\eta L^2}{WC_d^3}$$

$$\overline{p}_h = \frac{p_hLD}{W}$$

$$\overline{\alpha} = \frac{\alpha L}{C_d}$$

$$\overline{B}_{ow} = \frac{2.B_{ow}}{C_d}$$

$$\overline{A}_{xx} = \frac{A_{xx}C_d}{W}, \text{ etc.} \qquad \overline{B}_{xx} = \frac{B_{xx}\omega C_d}{WD}, \text{ etc.}$$

$$\overline{A}_{x\lambda} = \frac{A_{x\lambda}C_d}{WL}, \text{ etc.} \qquad \overline{B}_{x\lambda} = \frac{B_{x\lambda}\omega C_d}{WLD}, \text{ etc.}$$

$$\overline{A}_{\lambda x} = \frac{A_{\lambda x}C_d}{WL}, \text{ etc.} \qquad \overline{B}_{\lambda x} = \frac{B_{\lambda x}\omega C_d}{WLD}, \text{ etc.}$$

$$\overline{A}_{\lambda\lambda} = \frac{A_{\lambda\lambda}C_d}{WL^2}, \text{ etc.} \qquad \overline{B}_{\lambda\lambda} = \frac{B_{\lambda\lambda}\omega C_d}{WL^2D}, \text{ etc.}$$

APPENDIX 2

GLOSSARY

Adhered cavitation model Cavitation model in which oil is assumed to be transported through the cavitation zone in a layer adhered to the moving (usually journal) surface. (*See* Fig. 3.)

Boundary lubrication Lubrication regime in which load is carried partly by surface contact and partly by hydrodynamic action.

Cavitation pressure Minimum film pressure, i.e. that pressure at which gas or vapour bubbles start to form thus preventing any further fall in pressure.

Cross axis coupling Refers to hydrodynamic bearing characteristic that journal displacement or velocity in one direction induces oil film force components in direction at right angles.

Damping coefficient Linearised rate of change of oil film force per unit change in journal velocity. Also referred to as velocity coefficient.

Dynamic coefficient Collective term for stiffness and damping coefficients.

Dynamic misalignment Angular misalignment of journal relative to bearing subject to cyclic variation resulting from dynamic load.

Elastohydrodynamic lubrication Hydrodynamic lubrication in which elastic deformation of journal and/or bearing surfaces due to oil film pressure is significant.

Element grading Variation of oil film element dimensions to give better modelling and thus improved accuracy of numerical oil film pressure solution.

Gaseous cavitation Cavitation due to dissolved gas in oil coming out of solution.

Gauss Seidel relaxation method Numerical solution method used to determine oil film pressure distribution. Oil film element pressures are successively computed in terms of current element pressures for adjacent elements until convergence is achieved.

Hydrodynamic lubrication Lubrication in which journal and bearing surfaces are completely separated by lubricant film. Load is carried by hydrodynamic pressure generated in the lubricant film.

Journal That part of the shaft within the bearing.

Journal orbit Displacement path traced by journal centre in a dynamically loaded bearing.

Minimum film thickness Minimum separation of journal and bearing surfaces. Used as a criterion to assess the acceptability of bearing operating conditions.

Misalignment Angle between journal and bearing axes. May be expressed as total value or vertical and horizontal components. Where the journal axis is bowed, the mean angle over the length of the bearing is taken.

Mobility Method Method devised by J. F. Booker for carrying out a fast journal orbit analysis. (*See* reference 14.)

Oil film element Small section of oil film of rectangular planform. Oil film is divided into such elements for numerical solution of the pressure distribution.

Oil film history Concept in the modelling of the oil film in a dynamically loaded bearing. This takes account of the fact that cavitation zones take a finite time to disappear after the journal displacement and velocity conditions causing them are changed.

Over relaxation Technique for obtaining fast convergence in the Gauss-Seidel relaxation process.

Perturbation Small displacement or velocity increment applied to the journal for the purpose of computing linearised stiffness and damping coefficients.

Reaction Method Fast journal orbit analysis method devised by the author. (*See* references 15 and 16.)

Reformation boundary Downstream boundary of cavitation zone at which full oil film reforms.

Rupture boundary Upstream boundary of cavitation zone at which full oil film ruptures.

Short bearing approximation Approximate analytical solution of Reynold's equation which assumes that circumferential film pressure gradients are negligible relative to axial pressure gradients.

Specific bearing pressure Mean bearing pressure based on load divided by projected area, i.e. W/LD.

Sterntube bearing Bearing located within sterntube supporting propeller shaft. In relation to loading conditions and the work covered by this paper, it refers to the bearing adjacent to the propeller and may therefore include "A" bracket bearings, etc.

Stiffness coefficient Linearised rate of change of oil film force per unit change in journal displacement. Also referred to as displacement coefficient.

Striated cavitation model Cavitation model which assumes that oil is transported through the cavitation zone in rectangular section streams extending from the journal to bearing surface. (*See* Fig. 3.)

Squeeze action Generation of hydrodynamic film pressure by the component of lateral journal velocity in the direction of the line connecting the bearing and journal centres.

Vapourous cavitation Cavitation resulting from the formation of vapour bubbles.

Ventilation Form of gaseous cavitation where gas (usually air) is drawn from outside the bearing oil film. This clearly cannot occur in a fully submerged bearing.

Viscosity In the context of this paper this refers to dynamic viscosity, which may be defined as the lubricant shear stress per unit velocity gradient. This is assumed to be constant at a given temperature and pressure, i.e. Newtonian lubricant. This is an approximation since in reality viscosity varies with the magnitude of the velocity gradient, an effect referred to as shear thinning. In normal journal bearing conditions the effects of shear thinning and pressure upon viscosity are negligible.

Wake field Distribution of water velocity around the aft end of a hull. This interacts with the propeller to produce thrust and torque eccentricity.

Wedge action Generation of hydrodynamic film pressure, due to journal surface velocity inducing lubricant into the convergent space between the journal and bearing surfaces.

Discussion on the Paper

STERNTUBE BEARINGS: PERFORMANCE CHARACTERISTICS AND INFLUENCE UPON SHAFTING BEHAVIOUR

by

R. W. Jakeman

DISCUSSION

From Mr. P. F. C. Horne:

At the meeting I said that the original Rule of L/D=4 was determined by service experience nearly 100 years ago. We should not lose sight of service experience today. Some figures extracted by TRO for a submission to IACS by Mr. Siggers are worth considering. These have been graphed as Figs. D1–D4. It will be seen that there is no evidence to support going to very short bearings, even if the Reinforced Resin bearing materials are excluded.

The Author showed the effects of varying each of several parameters independently and showed the advantage of short bearings. This should, however, be considered in the light of the limits of screwshaft diameter. Except where TVC's dictate, it seems unlikely that a screwshaft significantly in excess of Rule diameter would be acceptable to an owner. Thus reduction in L/D implies an increase in bearing pressure in almost all practical applications. It would be interesting to see what Fig. 12 in the paper would look like for a constant shaft diameter.

It seems possible that an increase in bearing loading might well have greater adverse effect under boundary lubrication conditions and could also defer the onset of a hydrodynamic lubrication regime. I wonder whether any consideration has recently been given to the use of hydrostatic lubrication for conditions where a hydrodynamic film has not been established. I believe some work was done on such systems a few years ago and wonder whether any advances have been made.

Large diameter shafts such as have been fitted to some modern high powered low speed systems must be much more rigid in comparison with the stiffness of the bearing supports than with smaller diameter shafts. The alignment calculations as in Ref. 1 must be of doubtful value in such cases. Has the author any information on alternative calculation methods?

From Dr. M. A. Kavanagh:

Answer to the question by Mr. Kunz concerning the likely ill conditioning problems when introducing the stiffness and damping terms, obtained from Mr. Jakeman's oil film program, into a vibration analysis of a complete shafting system:

Preliminary work has been carried out to investigate the effects of introducing the additional stiffness coefficients, as derived from the oil film program, into a NASTRAN finite element model of a complete shafting system. The effect of these terms on the resultant value of the critical vibration frequencies was recorded for a lateral vibration analysis.

At the moment when carrying out a lateral vibration analysis a lateral spring stiffness is introduced at the stern bearing. In this investigation two additional spring coefficients were applied, a rotational spring and a cross coupling spring, that is a spring that produces a force due to rotation and a couple due to a displacement.

The gyroscopic effects have been switched off as these additional terms will only affect the overall location of the criticals.

Fig. D.1

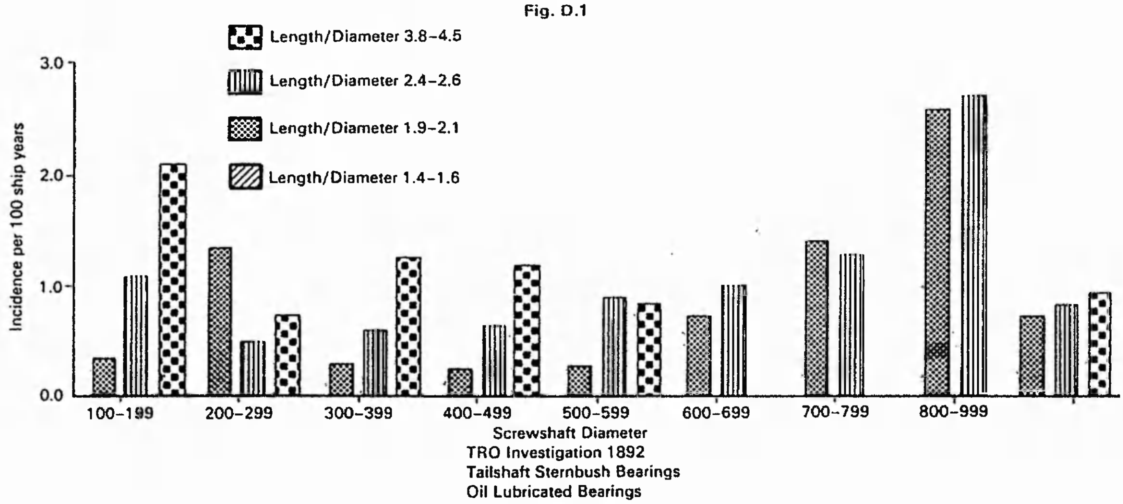

TRO Investigation 1892
Tailshaft Sternbush Bearings
Oil Lubricated Bearings
Other than Synthetic Resin

A.4. -71.

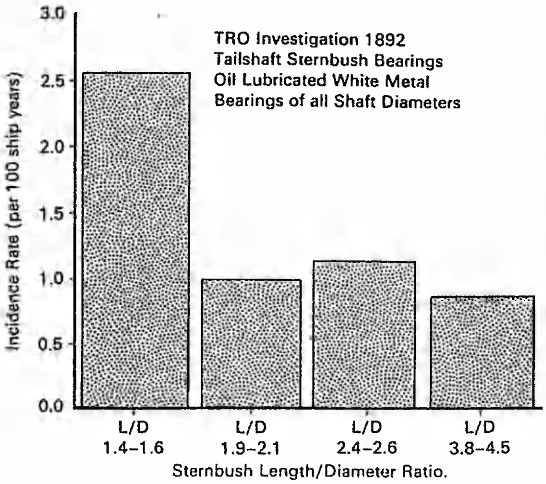

Fig. D.2

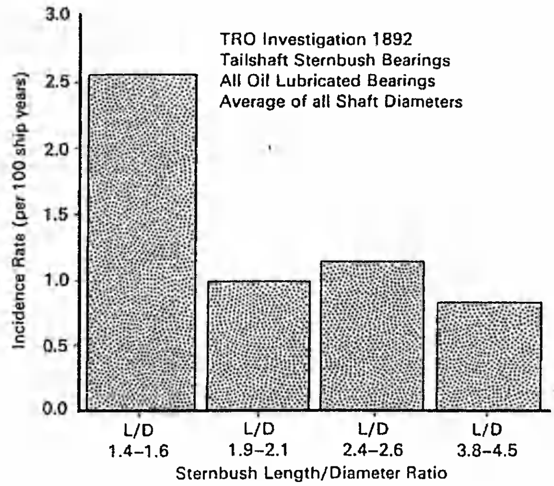

Fig. D.4

Below are listed a summary of the effects of these stiffness terms on the first critical frequency on a typical shaft system:

1. Rigid stern bearing $W_1 = 362$ CPM
2. Lateral spring at the stern bearing $W_1 = 320$ CPM
3. Lateral spring and rotational spring at the stern bearing $W_1 = 353$ CPM
4. Lateral spring and rotational spring and coupling spring $W_1 = 325$ CPM

The results of cases 1 to 3 produce a predictable change, with the first critical increasing as the effective stiffness increases. When the cross coupling term is included however, Case 4, the effective stiffness of the system has been decreased. The sign of the cross coupling term, which will determine its contribution to the effective stiffness, is dependent upon the overall configuration of the sterntube bearing. Consequently the overall effect of all these additional stiffness terms is uncertain and can only be fully assessed in this manner for each specific shafting system.

With regards to ill conditioning of the solutions matrices, no problems were envisaged or experienced with the introduction of these stiffness terms. The next stage in this work however is to introduce damping terms which are also provided by the oil film program. As these damping terms are of a complex form some problems may be experienced. In addition these terms may also cause problems when the gyroscopic effects are switched on since they are also of a complex form.

From Mr. F. Kunz:

Mr. Jakeman is to be thanked for an interesting paper on an important topic and for the considerable effort which must have gone into the preparation of it. It is noted that another area where the Society has expended a sizeable theoretical effort over a number of years has yielded results which are in a form ready for assessment in practical applications.

The 32 coefficients in equation 2 are somewhat overwhelming and I note that more work is proposed to assign numerical values to some of them. Solutions of matrix equations always raise questions of sensitivity and maybe Mr. Jakeman could put my mind at rest by commenting on the likely effects of small changes in input values on the solution. It is noted that the application of the coefficients to shaft lateral vibrations remains to be explored. This would be a worthwhile task because current natural frequency calculations which ignore excitation, damping and the effect of load distribution within the bearings give no

Fig. D.3

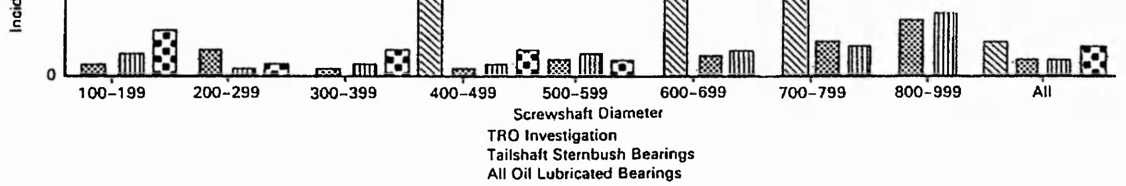

TRO Investigation
Tailshaft Sternbush Bearings
All Oil Lubricated Bearings

help in assessing the significance of any calculated criticals. Experimental evidence of the importance of the sterntube bearing geometry or material on the vibration levels at the sterntube outboard seal has been produced by the Technical Investigations Department. For example, a simple change of bearing material from a resin type bearing to a conventional white metal bearing of the same dimensions but reduced clearance reduced vibrations at the outboard seal by a factor of about two while the sterntube oil leakage which promoted the investigation was reduced from about two hundred litres of oil per day to negligible amounts. This solution to a very significant problem had to be arrived at on a mainly intuitive basis and the use of a rational basis would have saved much concern and help in future cases.

Experience of this type makes me share Mr. Jakeman's views on resin impregnated bearings but it remains a fact that a large number of such bearings perform satisfactorily particularly on larger vessels. It would have been useful to include ship's size in the variables explored for correlation with failure incidence but maybe Mr. Jakeman has already done this. I find the statement that sterntube seal defects invariably result in damage to the bearing rather sweeping as many seals receive attention because of leakage which in the nature of things can be of sea water into the bearing or loss of oil to the sea.

Figure 27, to my mind, is one of the most significant results of Mr. Jakeman's work as it models the effects of internal bearing misalignment, clearance and bearing length. I take it to indicate that length is a somewhat secondary factor, a conclusion which probably should be tempered with the concept that longer bearings may reduce lateral vibration response if well aligned. The great merit of FIGURE 27 is, however, that it shows relationships which can be put to the test and could be modified in the light of experience.

In section 5.2 the statement that misalignment is generally insignificant is at first sight rather challenging and at variance with experience. Maybe it is intended to apply to angular deviations of the centre lines of bearings and shafts rather than the deviations of bearings from their intended relative lateral positions normally associated with misalignment. While it is true that short bearings are less sensitive angular errors between bearing and shaft axes quite a number of problems are known to have arisen from this cause and bedding checks remain valid.

From Mr. R. V. Pomeroy:

The author has shown in this paper how a collection of useful characteristic parameters can be derived theoretically. There is a clear implication that the results of the analysis can be used to optimise the design of sterntube bearings. This presumably will lead to a reduced level of tolerance to deviation from the specified design conditions. In this respect it is observed that there is a great deal of successful service experience based on the use of empirical design methods, crude though some of these may be. Has the author attempted to demonstrate that his theoretical approach does satisfactorily represent the real physical situation? It may, in fact, be useful to conduct a detailed examination of some cases where bearing damage has occurred and see if these would have been avoided if the approach described in the paper had been used. Is the author's contention that the presently used methods are too conservative in general or that the predictions are imprecise and in some cases maybe non- conservative? At what stage will the theoretical analysis method be considered to be sufficiently proven so that it can be adopted as a "production tool"?

The failure statistics presented give a general idea of the frequency of defects but further analysis would seem to be worthwhile to identify areas where most problems arise and the causes thereof. Firstly it is not clear why shaft diameters less than 400mm have been excluded. Does the failure rate continue to decrease as shaft diameter reduces for oil-lubricated bearings? Secondly, what is meant by defect? It would be very useful to know how many of the reported defects were minor and repairable and how many required renewal of the bearing. Perhaps even more interesting would be the number of cases where bearing failure directly results in further damage, to the tailshaft for instance. Although the author appears concerned by the defect rate it is noted that sterntube bearing failures did not feature in Mr. Munro's paper to the LRTA and only one recent case, a resin bearing, is reported in N.D.L. Without an analysis of cause and effect it is not reasonable to draw any conclusions from the information in the paper. Analysis of the data could serve to indicate which are the most useful areas to concentrate on in the continuing research in this subject.

In the paper there is no indication as to the affect of the machinery installation type on the performance of sterntube bearings. Is there any evidence to suggest that the service history is significantly different for:

i) steam turbine ships as opposed to diesel ships,
ii) geared installations as opposed to direct drive,
iii) controllable pitch as opposed to fixed pitch propellers,
iv) multiple as opposed to single screw.

The author has clearly devoted considerable effort in this subject area. It would appear that a reasonably robust calculation method has been developed. If the dynamic results provide a better understanding of shafting vibration then a clear advance will have been made. If however the only end result is that the old-fashioned empirical basis for design is about right all will not be in vain – industry expects that simple design rules can be substantiated! In fairness, with a mature product it would be surprising if any radical design changes are the result of this type of analysis. What undoubtedly improves is the fundamental understanding of the problem and this has been amply demonstrated by the author in this parametric study.

From Mr. W. Y. Ng:

I would like to offer my congratulations to Mr. Jakeman on the presentation of this very informative and comprehensive paper which will be a valuable addition to the study of oil lubricated sterntube bearings.

It is now the time to apply these data to lateral vibration analysis which due to the complexity of the shafting support and also for economical reasons, is possibly one of the least researched areas.

As a matter of interest to find out the influence of constraints on the natural frequency other than the single simple support treatment, Jasper's method (1) was used for a two-support shaft, the calculated natural frequency with linear stiffness (Ayy) together with angular stiffnes (Arr) was over 4% higher than the one with linear stiffness only.

An analysis carried out and claimed by R. Ville (2) including Axx, Ayy, Axy and Ayx, bearing and ship structure stiffness gave a good accuracy.

Could Mr. Jakeman comment (Fig. 17) on the significance of the change in Axy from $-$ve to $+$ve at $\varepsilon = 0.7$. Does it indicate the threshold of the bearing stability? One reference (3) stated that a circular bearing will be stable at eccentricity ratio (ε) greater than 0.75. Were there similar kinks (Figs. 15 & 21) for below or above 0.7? It appears that the kinks occurred at about $\theta_f = 27°$, not 37° as stated in the text paragraph 4.3.

Damping coefficients (B) shown in APPENDIX I are not dimensionless unless ω is changed to linear velocity or D is deleted.

To complete the whole picture, a curve with $\bar{\alpha} = 0$ added in Fig. 9 would be appreciated.

It would be useful if Mr. Jakeman could provide coefficient data or reference for the thrust bearings for axial vibration analysis.

The Society has accepted L/D = 2 for some water lubricated synthetic bearings based on the hydrodynamic lubrication principle, it would be interesting to know if a bearing having this ratio has been installed in any ship. Presently all the latest Canadian Icebreakers have bearings with L/D $\geqslant$ 4. It is quite possible that water lubricated bearings which have the advantage of simplicity and no risk of pollution on failures, will become popular once more.

Oil film stiffness data given in this paper are in good agreement with those in R. Ville's paper.

Reference

1) Norman H. Jasper L.S.p Vol 3 No.20-1956
2) R. Ville ICMES '84 Conference in Trieste
3) Handbook of Turbo Machinery (?) A21

AUTHOR'S REPLY

To Mr. Horne:

I agree that service experience should never be ignored since theoretical analyses are always an approximation to reality. The main value of theoretical work lies in the provision of a rational basis for assessing the relative influence of all the significant variables. It is essential to remember that theoretical predictions are by no means exact, and that the parameters predicted do not in themselves tell us precisely where failure will occur.

It is gratifying to note that Mr. Horne's records support my general conclusion that there is no incentive, with respect to safe operation, in going to shorter bearings. The data for all shaft diameters in Figs. D2 and D4 do, however, appear to disagree with the corresponding results in Figs. D1 and D3.

Mr. Horne's statement that I have shown the advantage of shorter bearings is only true for the very restricted situation of misalignment angles substantially in excess of the levels normally considered to be acceptable (see Fig. 25). Regarding the reference to Fig. 12, since this figure is entirely in dimensionless terms it is valid for any shaft diameter, constant or otherwise.

I have no knowledge of any recent developments with respect to the application of hydrostatic bearings to the sterntube bearing situation. I agree that higher bearing pressures are likely to have an adverse effect on low speed operation under boundary lubrication conditions, and to raise the speed at which hydrodynamic lubrication is attained. Although hydrostatic bearings enable full oil film lubrication to be achieved at low shaft speeds, the required pressurised oil supply poses certain problems in this application. If any sterntube bearing installation becomes dependent upon hydrostatic action, rather than simply improved by it, then a "fail safe" pressurised oil supply would be required.

Shaft alignment calculations taking account of bearing support flexibility can be carried out with the LR291 shaft alignment program. The flexible support facility has been little used due to the dearth of flexibility data. It should be noted that bearing oil films contribute towards bearing support flexibility, and this contribution can be estimated as shown in the paper. In addition, a steady state analysis version has been developed from my forced damped lateral vibration program, to which more detailed reference is made in the reply to Mr. Kunz. This enables a simultaneous vertical and horizontal alignment analysis to be carried out, taking account of all the bearing oil film stiffness terms shown in equation [2] of the paper. In comparison with previous shaft alignment analyses, this new program facilitates the inclusion of angular stiffness terms and vertical– horizontal cross coupling terms. Bearing support structural stiffness values can be combined with the corresponding oil film terms.

To Dr. Kavanagh:

I must thank Dr. Kavanagh for his interesting comments on the application of the oil film stiffness terms to lateral vibration analysis. My only addition to this is the cautionary note that oil films are inherently non-linear. When applying linearised oil film stiffness and damping coefficients there will be some degree of approximation depending upon the vibration amplitudes.

In addition, it should be noted that the various oil film stiffness and damping coefficients are determined by applying appropriate journal displacement or velocity perturbations one at a time, and computing the corresponding changes in the oil film force and moment components. The application of these coefficients to lateral vibration problems implicitly assumes that the principle of superposition applies to any combination of displacement and velocity components occurring simultaneously. The work reported in reference (15) indicated that the influence of cavitation in hydrodynamic bearings in fact negated the principle of superposition in this context. This results in a further source of error when using linearised dynamic coefficients.

To Mr. Kunz:

Mr. Kunz's question regarding the significance of the 32 oil film stiffness and damping coefficients has been partly answered by Dr. Kavanagh's comments, and there is nothing that I can add to these at present. Regarding the long standing need for a lateral vibration response prediction facility, I have in fact developed such a program since completion of the paper. This program models the shaft as a multi-mass-elastic system, incorporates alternative linear and non-linear bearing oil film models and is based on the time-stepping approach. Other features of this program are:

a) The complete propeller damping and entrained mass/inertia matrices are used.
b) Any form of propeller excitation may be specified, i.e. non-sinusoidal components of force and moment.
c) Elastic deflections of each shaft element include both bending and shear components.
d) Gyroscopic effects are considered on all elements.
e) Weight and buoyancy forces are also included.

Satisfactory operation of this program has been achieved. In its present form the program has been tailored to a particular test case corresponding to additional reference (D1). Further development work would be required to refine it to a form suitable for general application, and to improve computing time. There is no immediate prospect of the above development work being carried out since the research project, of which this work formed a part, has been terminated.

The TID case of the effect of changing from a resin to white metal sterntube bearing of reduced clearance was noted with interest.

Ship size was not specifically considered in the failure statistics, but is indirectly covered, albeit rather crudely, by the correlation with shaft diameter.

My statement that seal defects invariably result in bearing damage was, perhaps, just a little sweeping, as noted by Mr. Kunz. Where seal defects are relatively small and a positive oil head pressure is maintained, the bearing may escape damage. The lumping together of seal and bearing defects in much of the statistical data did, however, reflect the fact that these defects do frequently occur together.

Mr. Kunz's remarks on Fig. 27 are much appreciated. The use of a log function for dimensionless maximum specific bearing pressure does in fact make the influence of L/D ratio appear to be rather less than it really is. I agree with Mr. Kunz's view that Fig. 27 should be related to service experience. As noted in the paper, the maximum eccentricity ratio of .9365, used as the basis for computing the curves of Fig. 27, was somewhat arbitrary. The essential value of Fig. 27, lies in its format, in providing a clear guide to the relative significance of all the parameters, rather than the absolute magnitude of safe specific bearing pressures that may be derived from it.

I regret the confusion experienced by Mr. Kunz over the use of the term misalignment in section 5.2. Since hydrodynamic bearings will not support load without some lateral misalignment of the journal and bearing axes, it is reasonable to assume that this type of misalignment will generally be present. In view of the fact that lateral misalignment may therefore be taken for granted, only angular misalignment has any particular significance, and is the only type of misalignment worthy of any specific reference. My usage of the term misalignment in this way is defined in the glossary in Appendix 2.

With regard to shorter bearings, although these are less sensitive to misalignment, they will still be subject to some limit for maximum acceptable misalignment. I would therefore endorse Mr. Kunz's view that alignment checks should be carried out for such bearings. Section 5.2 was, however, written more from the viewpoint of one performing an alignment analysis, where it is reasonable to assume that misalignment will be negligible in shorter bearings. This assumption is based not only on the reduced sensitivity to misalignment, but also on the fact that correction of misalignment in these bearings is generally fairly simple to carry out.

To Mr. Pomeroy:

Mr. Pomeroy mentions the possibility of reduced tolerance to deviation from specified design conditions, if a sterntube bearing design is optimised. Such a reduction would undoubtedly occur if one chose to exploit the optimisation by increasing the permitted load rather than accepting an increased safety margin. This problem also depends on the sensitivity of the bearing load capacity to the various parameters subject to optimisation. For example, the results given in Fig. 15 could be used to optimise the angular location of the oil supply grooves relative to the load vector. This figure shows a high degree of sensitivity around the optimum condition, with a particularly sharp fall in load capacity to the right of the optimum point as θ_f approaches 27°. It is generally assumed that the sterntube bearing load acts vertically downward ($\theta_f = 0°$), which corresponds to operation substantially to the left of the optimum point in Fig. 15. In view of the generally uncertain influence of the propeller–wake interaction on the load vector angle, the above non-optimum condition is preferable in maintaining a reasonable safety margin from the load capacity fall at $\theta_f = 27°$. The influence of the propeller–wake interaction in particular, renders the concept of specified design conditions in a sterntube bearing potentially dangerous (see reference (2)). When assessing the performance of any sterntube bearing, one must therefore make allowance for a fair degree of uncertainty in the actual operating conditions.

Regarding the question of whether the theoretical model satisfactorily represents the real physical situation, as noted in section 6 of the paper, useful measured data for sterntube bearings is somewhat sparse in the published literature. As mentioned in the reply to Mr. Kunz, measured data presented in reference (D1) has been used for correlation with the predictions of my forced-damped lateral vibration response program.

This data is unsuitable for correlation with steady load performance predictions due to the extent of dynamic load present and limited instrumentation. As a result of the above situation, my sterntube bearing performance predictions have only been correlated with those of other theoretical methods. These correlations have been reported in references (6) and (D2). Satisfactory correlation of predicted and measured data for crankshaft type bearings was reported in reference (16). This verified the validity of the hydrodynamic analysis method, the only significant parameter not covered being misalignment.

I would agree with Mr. Pomeroy's suggestion that it would be potentially instructive to carry out analyses of cases where bearing damage has occurred. The results would, however, be masked by the probability that in many such cases the bearing load and misaligment will not be known with any precision. In view of this problem a statistical approach would be appropriate. This would need to involve a large number of cases, both successes and failures, using the best available estimates for bearing load and misalignment in each case.

It would be fair to say that the present methods are a trifle imprecise in that they take account of but three parameters: specific bearing pressure, L/D ratio and (unofficially) misalignment angle. These are considered in isolation from each other by the simple specification of maximum or minimum permitted values. Fig. 27 of the paper shows how the seven relevant parameters may be applied in a rational manner.

The stage at which my theoretical method was adopted as a production tool was passed over two and a half years ago (see Section 7). To put this work into the correct perspective, it would be inappropriate to think in terms of the "Jakeman Theory" which needs to be proved. My work is essentially a refinement of well established theoretical concepts in this field, with specific adaption to the sterntube bearing situation. Within the limitations of the approximations made, this theory undoubtedly provides an adequate description of the way in which the various design and operating parameters interact to determine the bearing performance. The need to correlate performance predictions with service experience has already been covered in the reply to Mr. Horne.

In answer to Mr. Pomeroy's queries on the failure statistics, the 400mm shaft diameter cut off was arbitrary and determined by the availability of previously analysed data. It is noted that Mr. Horne's contribution provided data down to shaft diameters of 100mm. A "defect" is defined as any case reported by a surveyor as requiring remedial action. The extent of details reported is generally inadequate for the purposes of providing a severity breakdown of the statistics. It should be added, however, that defect severity is not necessarily related to importance, since today's minor defect may be tomorrow's total failure if not rectified. Of the possible factors influencing the failure statistics, as queried by Mr. Pomeroy, only the difference for controllable and fixed pitch propellers was investigated. As noted at the foot of Table 1, the type of propeller showed no significant correlation with defect rate. A general problem in this area was that breakdown of the data into groups, such as ship type, frequently reduced the numbers to a level that was statistically insignificant.

Mr. Pomeroy's concluding remarks were much appreciated. I would only add that the old fashioned empirical approach is alright provided one does not extrapolate beyond the range of service experience on which it is based. With the theoretical approach, although the backing of service experience is still desirable for practical applications, we can extrapolate beyond available service experience with greater confidence.

To Mr. Ng:

Mr. Ng's comments on the application of bearing dynamic coefficients to lateral vibration analysis were noted with interest. The only item that I would add to the comments on lateral vibration already made is that Lund and Thomsen (D3) used the following expression to combine the eight stiffness and damping coefficients for an aligned bearing into a single equivalent stiffness:

$$\frac{Ayy.Bxx + Axx.Byy. - Ayx.Bxy - Axy.Byx}{Byy + Bxx}$$

The transition between positive and negative Axy at $\varepsilon = 0.7$ in Fig.17 is not believed to be associated with the onset of instability. The correlation of instability with dynamic coefficients is, however, an area which needs further investigation. Fig. D5 has been added to illustrate the reason for the transition from positive to negative Axy. Each of the four sub figures represents the bearing clearance circle, i.e. the envelope within which the journal centre-line may move. Within the clearance circles, the solid crescent shaped curve represents the path traced out by the journal centre line when subject to a steady downward vertical applied load varying in magnitude from zero to infinity. This is referred to as the static journal locus. The forces shown are the corresponding equal and opposite oil film forces. When the

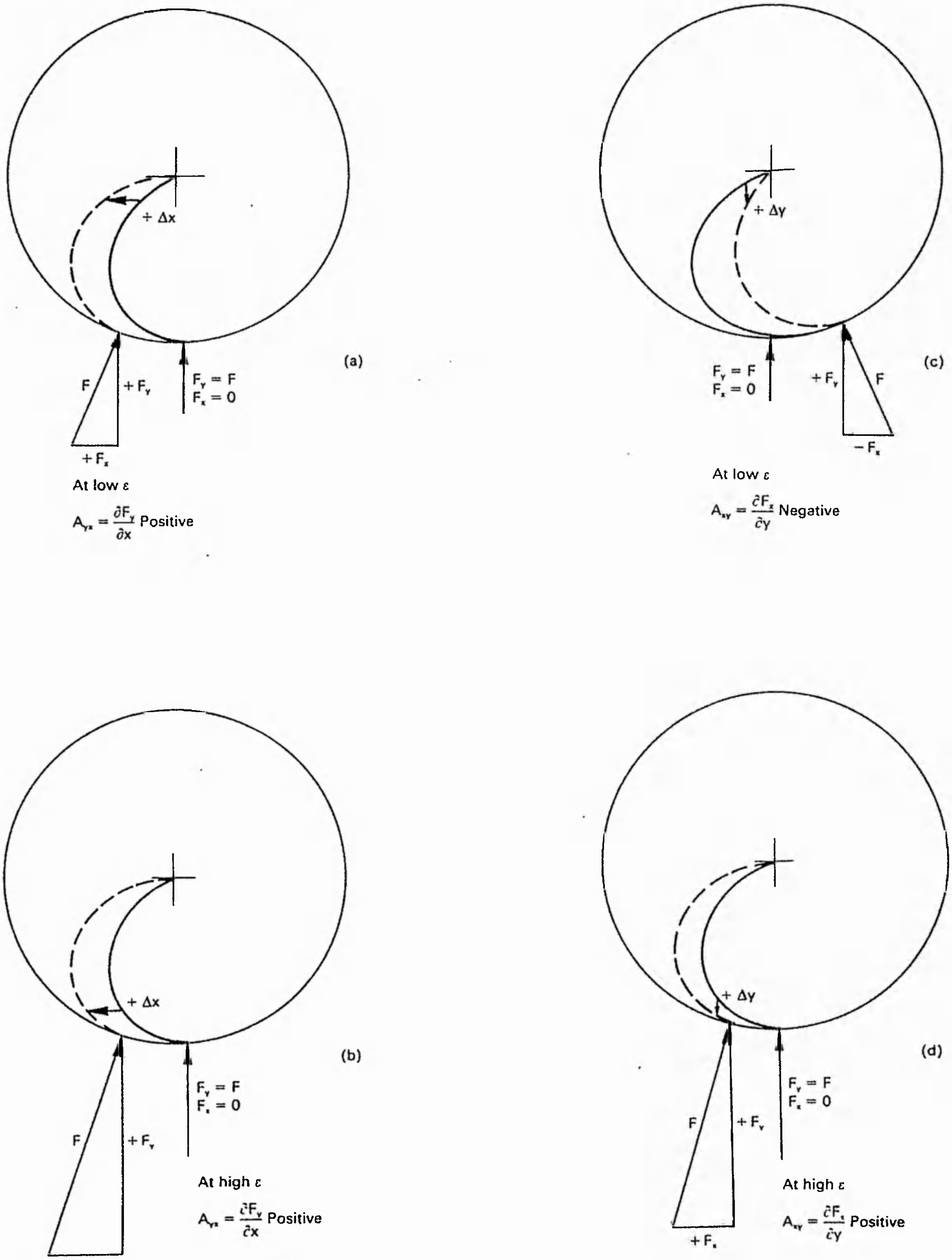

+ Δx
(a)
F
+ F_y
F_y = F
F_x = 0
+ F_x
At low ε
A_yx = ∂F_y/∂x Positive
+ Δy
(c)
F_y = F
F_x = 0
+ F_y
F
− F_x
At low ε
A_xy = ∂F_x/∂y Negative
+ Δx
(b)
F_y = F
F_x = 0
F
+ F_y
+ F_x
At high ε
A_yx = ∂F_y/∂x Positive
+ Δy
(d)
F_y = F
F_x = 0
F
+ F_y
+ F_x
At high ε
A_xy = ∂F_x/∂y Positive

Fig. D.5

force contains a horizontal component (F_x), the static journal locus is rotated through an angle equal to the total force vector angle, to the positions indicated by the dotted crescent curves. The dotted and solid static journal locus on each sub-figure enables the force component changes resulting from positive horizontal displacement perturbations, (a) and (b), and positive vertical displacement perturbations, (c) and (d), to be determined. In a. and b. the horizontal displacements at both high and low ε result in an increase in ε and thus a corresponding increase in F_y. The coefficient Ayx is therefore positive at all ε. Figs. D.5 (c) and (d), however, show that the vertical displacement perturbations correspond to a clockwise shift of the static journal locus at high ε and thus to a positive F_x, but the reverse response is seen to occur at low ε. These figures therefore illustrate the reason why Axy is positive at high ε but negative at low ε.

With regard to Mr. Ng's reference to the kinks seen in Figs. 15 and 21 due to load vector angle (θ_f) variation, this section of the parameter variation study has only been done for $\varepsilon = .7$. Since the kinks result from the interference of an oil groove with the hydrodynamic action, these kinks are expected to occur at other values of ε. The severity of the kinks should diminish with decreasing ε due to the corresponding reduction in the effectiveness of the hydrodynamic action.

Mr. Ng was quite correct in noting that the kinks in Figs. 15 and 21 occurred at $\theta_f = 27°$ and not 37° as stated in the paper.

I must also express my appreciation to Mr. Ng for spotting the errors in the expressions for dimensionless damping coefficient in APPENDIX 1. Originally I used expressions based on journal surface velocity u and later changed to the use of angular velocity ω. The error occurred during this transformation, and the expressions for $\overline{B}$ should be corrected by deleting the D from the denominator. The data given in Figs. 19 and 20 is valid for the correct dimensionless damping coefficients.

Mr. Ng asked for a curve of $\overline{\alpha} = 0$ in Fig. 9. This would be a straight line coincident with the horizontal axis, since zero misalignment results in zero oil film moment!

I have not carried out any work on thrust bearings, and suggest reference (D4) as a possible source of data for dynamic coefficients.

Referring to the Society's acceptance of L/D = 2 for water lubricated sterntube bearings designed for hydrodynamic operation, I am not aware of any related service experience. Water lubricated bearings undoubtedly have the advantage of simplicity, but I do not share Mr. Ng's optimism for any future expansion of their utilisation. The fundamental disadvantage is the much lower viscosity of water in relation to oil. This will continue to prevent the attainment of hydrodynamic lubrication in all but lightly loaded and higher shaft speed applications. The elimination of axial grooves from the bottom half of the bearing would help to promote hydrodynamic lubrication, but the problem of a low viscosity lubricant remains. This situation may be quantified approximately by use of Fig. 27 assuming a viscosity of about 5.10^{-4}Pa.s. for water.

ADDITIONAL REFERENCES

(D1) S. HYAKUTAKE, R. ASAI, M. INOUE, K. FUKAHORI, N. WATANABE and M. NONAKE. "Measurement of Relative Displacement between Sterntube Bearing and Shaft on a 210,000 d.w.t. Tanker". Japan Shipbuilding and Marine Eng. Vol. 7, No. 1, 1973 – pp. 32–40.

(D2) R. W. JAKEMAN. "Performance and Oil Film Dynamic Coefficients of a Misaligned Sterntube Bearing". ASLE Transactions, Vol. 29, No. 4, Oct 1986 – pp. 441–450.

(D3) J. W. LUND and K. K. THOMSEN. "A Calculation Method and Data for the Dynamic Coefficients of Oil Lubricated Journal Bearings". Publication unknown.

(D4) L. VASSILOPOULOS. "Methods for Computing Stiffness and Damping Properties of Main Propulsion Thrust Bearings". International Shipbuilding Progress, Vol. 29, No. 329, Jan 1982 – pp. 13–31.

REFERENCE . 90.

Numerical analysis of hydrodynamic bearings with significant journal lateral velocities

R.W. Jakeman*

The previously reported[1] numerical analysis method for hydrodynamic journal bearings has been extended to take account of significant lateral velocities of the journal. Conditions encountered in bearings with substantial dynamic loading have therefore been covered. This paper is intended to be used in conjunction with reference 1, and it is essentially a refinement of the method described therein. Results obtained by means of the numerical analysis method presented here are given in reference 2. The application of these results to journal orbit prediction, and comparison with experimental orbits is covered by reference 5, and an example is presented herein.

Keywords: *hydrodynamic journal bearings, lateral velocities, numerical analysis method*

The numerical analysis method described in reference 1 has been found to work satisfactorily for steadily loaded bearings, and with the small journal displacement and velocity perturbations required to derive linearized oil-film dynamic coefficients. Recent work[2], involving a study of the non-linearity of velocity coefficients, initially indicated certain anomalies in the results when the journal lateral velocities were large. The essential objective of this paper is to present a further development of the numerical analysis method for hydrodynamic journal bearings[1], in which the above anomalies were eliminated. Situations involving substantial lateral velocities of the journal are dealt with more accurately by this development. The method is thus applicable to bearings subject to significant dynamic loading such as crankshaft bearings and sterntube bearings.

This work is directed towards practical application for bearing performance prediction. The qualities of simplicity (relative!) and robustness are therefore of paramount importance. Limitations in the way the physical realities of the bearing oil-film situation are modelled, particularly those pertaining to cavitation, are acknowledged. In view of the above intended application of this analysis method, such limitations are considered to be acceptable.

It should be noted that the simple consideration of journal lateral velocities at a given journal location within the bearing clearance introduces some degree of approximation in relation to the real dynamic situation. This arises from the fact that no account is taken of previous conditions in the oil film. An oil-film history model based on the numerical analysis method[1] is described in reference 3.

The quasi-steady approach used in this work may involve substantial inaccuracy in situations where oil-film history effects are significant. This has been well illustrated by Jones[4] with respect to oil-feed arrangements. A test case computed by the author for a crankshaft bearing of a 1600 cc four-stroke petrol engine is shown in Fig 1. The bearing concerned was of the half-circumferential groove type, and

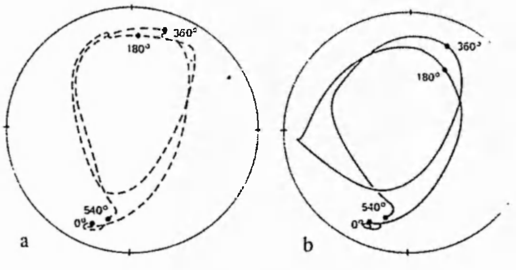

Fig 1 Effect of oil-film history on journal orbits (journal mass = 6.7 kg); half-circumferential groove bearing: (a) without oil-film history; (b) with oil-film history

the figure shows significant differences in the predicted journal orbit when computed both with and without an oil-film history model. Full details are given in reference 3.

The quasi-steady assumption was nevertheless found to be valuable in forming the basis of the oil-film force equations which utilized precomputed velocity coefficients, described in reference 2. The prediction of oil-film forces by means of these equations facilitated the development of a fast journal orbit analysis program, some results from which are presented in reference 5. A particular test case is shown in Fig 2, the bearing concerned being of the full circumferential groove type, and situated in an experimental test rig. In method A, the derivation of the oil-film force components was by numerical solution of the film pressure distribution at each time step. Method B refers to the above fast journal orbit analysis using oil-film force equations. The method A orbit was computed both with and without an oil-film history model, and in this case showed no discernable difference when plotted. Oil-film history was therefore considered to be insignificant in this case due to the combination of an efficient oil feed and a small orbit in relation to the clearance circle. At present, no means of accounting for oil-film history in a fast journal orbit analysis is known to exist.

*Advanced Engineering Services, Lloyds Register of Shipping, 71 Fenchurch Street, London EC3M 4BS.

 0301–679X/87/040170–09 $03.00 © Butterworth & Co (Publishers) Ltd

A.4. - 78.

Equivalent journal velocity

Before presenting the details of the refinements to the numerical hydrodynamic analysis method, the equivalent journal velocity concept will be discussed. The use of equivalent journal velocity was found to be of considerable value in this work.

When considering large amplitudes of journal lateral velocity, it is convenient to work in polar coordinates, since this enables oil-film squeeze and wedge actions to be segregated. For simplicity of presentation, this paper is confined to the rotating-journal and stationary-bearing case. Extension of this work to cover bearing rotation would be quite straightforward. Bearing rotation is considered for clarification purposes only in the following remarks.

Pure wedge action is a function of the velocity of entrainment of oil into the converging space formed between the journal and bearing. Referring to Fig 3, in case (a), the mean angular velocity of the oil due to journal rotation is $\omega/2$. Since the journal axis is rotating about the bearing axis, the converging space itself has an angular velocity of $\dot\psi$. The velocity of entrainment upon which the wedge action depends in thus $\omega/2 - \dot\psi$.

In case (b) of Fig 3, an anti-clockwise velocity of $\dot\psi$ is applied to the complete system, thus resulting in a stationary journal axis and a rotating bearing. The oil film will be unaware of the change and the mean velocity of entrainment will remain $\omega/2 - \dot\psi$.

Finally in case (c) of Fig 3, an equivalent system is postu-

Notation

C_d	diametral clearance (m)
D	journal diameter (m)
e	journal eccentricity (general) (m)
$\dot e$	journal lateral velocity in the direction of the line connecting the journal and bearing axes (m/s); corresponding notation $\dot R$ used in references 2 and 5
e_{cy}, e_{cx}	vertical and horizontal components of journal eccentricity at bearing axial centre (m)
e_{sy}, e_{sx}	as above, but at distance s from the bearing axial centre (positive to the left) (m)
$\dot e_s$, $e_s \cdot \dot\psi_s$	radial and circumferential components of journal lateral velocity corresponding to V_{ys}, V_{xs} (m/s)
h	oil-film thickness (general) (m)
h_a, h_b, h_c, h_d	oil-film thickness at each corner of the element. For element J, I these thicknesses correspond respectively to $h(J, I)$, $h(J, I+1)$, $h(J+1, I)$, $h(J+1, I+1)$ (m)
H_{ci}, H_{co}	element inlet and outlet circumferential pressure flow functions (m^5/Ns)
H_{ai}, H_{ao}	as above but for axial flow (m^5/Ns)
I	axial element position reference
J	circumferential element position reference
K_i, K_o	element inlet and outlet surface velocity induced flow rates (m^3/s)
K_{sc}	factor applied to squeeze-film term $V_n\,\Delta a\,\Delta c$ in the continuity equation for cavitating elements (dimensionless)
L	bearing length (m)
M_c	no. of element rows (circumferential positions)
N_a	no. of element columns (axial positions)
P	film pressure at element centre (Pa)
P_c	cavitation pressure (Pa)
P_p	value of P for a given element during the previous iteration (Pa)
P_{sc}	sub-cavitation pressure initially computed for a cavitating element during the relaxation procedure (Pa)
P_{spec}	specific bearing pressure (load/projected area) (Pa)
$P_{ci}, P_{ai}, P_{co}, P_{ao}$	film pressures at the centres of the elements adjacent to the element under consideration; for element J, I these correspond respectively to $P(J-1, I)$, $P(J, I-1)$, $P(J+1, I)$, $P(J, I+1)$ (Pa)
Q_{vi}, Q_{vo}	inlet and outlet element gas/vapour flow rates (m^3/s)
s	axial distance from the bearing axial centre
U	journal surface velocity corresponding to the equivalent journal velocity ω_o (m/s)
V_n, V_t	components of journal axis velocity normal and tangential to the element (m/s)
V_o	volume of oil in element (m^3)
V_e	total volume of element (m^3)
V_{ys}, V_{xs}	vertical and horizontal components of journal lateral velocity at the axial position s corresponding to the centre of the element column I (m/s)
V_{yrs}, V_{xrs}	that part of V_{ys} and V_{xs} due to $\dot e_s$ only (m/s)
$\dot y$, $\dot x$	vertical and horizontal components of journal lateral velocity at bearing axial centre (m/s)
α_y, α_x	vertical and horizontal components of journal angular misalignment (rad)
$\dot\gamma$, $\dot\chi$	components of journal axis angular velocity in the vertical and horizontal planes (rad/s)
Δa, Δc	element lengths in the axial and circumferential directions (m)
ϵ	eccentricity ratio $2e/C_d$
η	dynamic viscosity (Pa.s)
θ	angular position from bearing top to required circumferential position (degrees)
ψ	attitude angle (degrees)
$\dot\psi$	angular velocity of journal axis about bearing axis (rad/s); corresponding notation $\dot\theta$ used in references 2 and 5
ω	journal rotational velocity (rad/s)
ω_o	equivalent angular velocity of journal (rad/s) (= $\omega - 2\dot\psi$); corresponding notation $\dot\theta_o$ used in references 2 and 5

Suffix s is used to denote axial position s for parameters that are functions of axial position due to steady or dynamic misalignment. For simplicity, this suffix is used only in the section in which the equations for general use are presented.

A.4. - 79.

lated on the basis of the same mean velocity of entrainment, but with both the journal axis and the bearing stationary. The equivalent journal velocity is thus $\omega - 2\dot{\psi}$, and is denoted by ω_o. This concept of equivalent journal velocity has been previously advanced by Cole and Hughes[6] and Marsh[7].

Marsh, however, in reviewing the experimental evidence by Cole and Hughes[6] and additional experimental evidence by White[8], also highlighted possible limitations to the use of equivalent journal velocity. Differences were noted in the appearance of cavitation associated with oil-film conditions in which negative squeeze action became dominant rather than circumferential flow in a divergent passage. In such conditions, the cavitation featured fern-like patterns in contrast to the normal journal-bearing cavitation appearance of parallel streamers passing between large stationary bubbles. The work by White[8] covered the situation of a stationary journal and bearing and rotating load vector. This indicated a substantial loss of load capacity relative to that predicted by the equivalent journal velocity, which

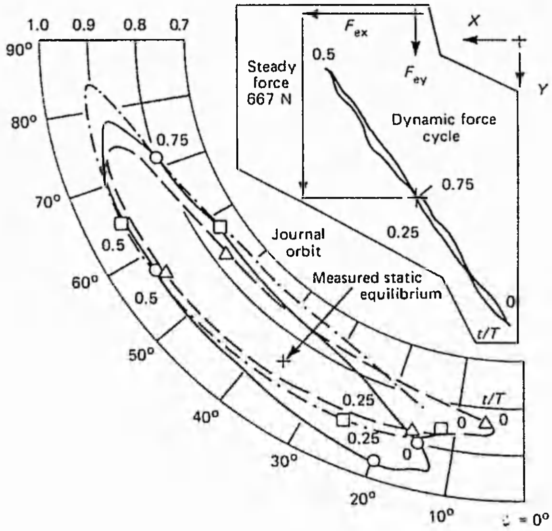

Fig 2 Test condition 1 external force data and journal orbit (full-circumferential groove bearing): —— o —— experimental; — · — □ — · — theoretical method A; — — △ — — theoretical method B

appeared to be associated with the persistance of cavities in the high-pressure region. Similar observations have been reported by Etsion and Ludwig[9]. It is assumed that the above observations indicate that the cavitation was mainly gaseous and that the persistance of cavities in the high-pressure region resulted from the finite time required for gas reabsorption and a tendency for bubbles to cling to the bearing surface. This effectively results in a variable degree of compressibility of the oil film and consequent loss of load-carrying capacity. A finite time is also required for gas release from solution, and this may also account for the frequently reported negative pressure spike preceding the rupture boundary. No acceptable model for the effects of finite gas release and reabsorption times is known to exist at present.

Despite the above apparent limitations to the load prediction accuracy associated with equivalent journal velocity, the work by Cole and Hughes[6], although qualitative, did confirm the general validity of this concept.

Basis of the numerical method

The numerical method previously described[1] is based on the division of the oil film into rectangular elements. Solution of the film pressure distribution is achieved by means of an element continuity equation. This is written in terms of the pressure at the centre of each element, and the corresponding pressures for the circumferentially and axially adjacent elements or oil-film boundaries. Within the full film region, this is equivalent to a numerical solution of Reynold's equation. The cavitation region is not covered by Reynold's equation. However, the numerical method described does satisfy continuity within this region by the introduction of gas/vapour flow terms while imposing a specified constant cavitation pressure. The Swift–Steiber boundary condition of zero pressure gradient at the rupture boundary is automatically met, since this is based on continuity considerations. No such boundary condition is applicable to the reformation boundary, for which the numerical method predicts a non-zero pressure gradient.

It should be noted that considerations of continuity refer only to the lubricant (for simplicity referred to as oil) in a liquid state. The continuity equation is written in terms of volume flow, but since the oil is assumed to be incompressible, mass flow is also covered. In handling cavitation, it is assumed that the volume of liquid oil required for the formation of gas/vapour cavities is negligible in relation to the volume flow of oil remaining in the liquid phase. Since

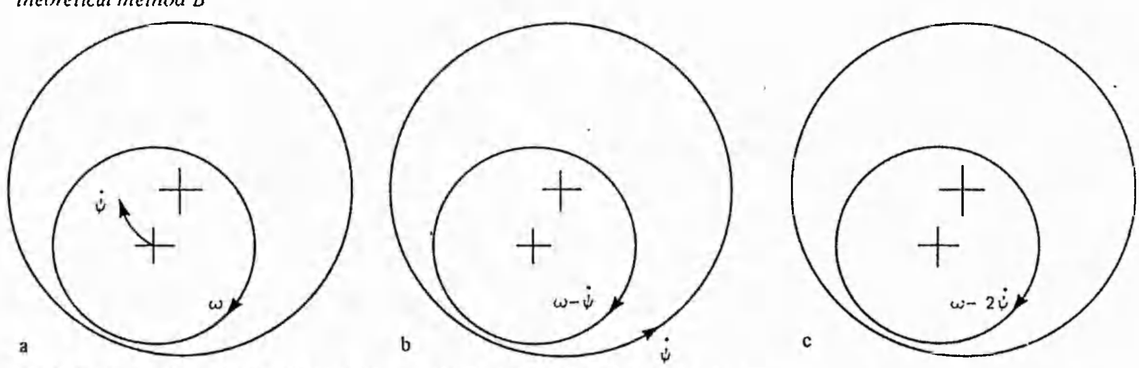

Fig 3 Equivalent journal velocity: case (a) rotating journal axis stationary bearing; case (b) stationary journal axis rotating bearing; case (c) stationary journal axis stationary bearing

the consideration of continuity is in respect of the volume flow of liquid oil only, the gas/vapour flow terms introduced are simply a means of reducing the volume flow of liquid across an element downstream boundary. This flow reduction is necessary in order to restore the balance of the continuity equation for the element concerned, after an initially computed subcavitation pressure has been reset to the specified cavitation pressure.

As previously indicated, this cavitation model takes no account of the finite time required for gas release and reabsorption. Furthermore, no consideration is given to surface-tension effects. At present, the inclusion of the above factors is regarded as impractical in bearing analysis methods intended for service application.

Using the element continuity equation, the oil-film pressure distribution is solved by means of a Gauss–Seidel relaxation procedure with successive over-relaxation. Whenever subcavitation pressures are encountered during relaxation, the pressure is reset to the specified cavitation pressure. A gas/vapour flow term (Q_{vo}) for the downstream boundary of the element concerned is then calculated to restore continuity. In the relaxation procedure, Q_{vo} subsequently appears as an upstream boundary gas/vapour flow term Q_{vi} in the continuity equation for the downstream adjacent element.

This method does not require any prior assumptions regarding the location of cavitation boundaries or boundary pressure gradients. It is therefore a robust, easily used method, suitable for practical applications.

In addition to the assumptions already indicated, an isoviscous Newtonian lubricant operating with laminar flow and negligible inertial effects is assumed, and the bearing and journal are assumed to be rigid and circular.

Equations for the solution of the film pressure matrix

The following is a summary of the equations required for the solution of the film pressure matrix. Some of these equations are identical to those given in reference 1, and the remainder are modified in accordance with the discussions in the following sections. The equations for mean element pressure, flow rate and power loss given in reference 1 remain valid and are not repeated here.

The film geometry equations given in reference 1 are repeated below for completeness of this presentation with respect to the film pressure solution (see Fig 4).

For any axial position in a journal bearing, the film thickness at angle θ from the bearing top may be calculated from

$$h = C_d/2 + e\cos(\theta - \psi) \tag{1}$$

Where the bearing is subject to misalignment, e and ψ are functions of axial position and may be determined via the components of eccentricity in the vertical and horizontal planes thus

$$e_s = [e^2_{sy} + e^2_{sx}]^{1/2} \tag{2}$$

$$\psi_s = \tan^{-1}[e_{sx}/e_{sy}] \tag{3}$$

where

$$e_{sy} = e_{cy} + s\,\alpha_y \tag{4}$$

$$e_{sx} = e_{cx} + s\,\alpha_x \tag{5}$$

For a specified journal eccentricity and misalignment, film thickness h may thus be determined at any circumferential and axial position.

Referring to the oil-film element shown in Fig 5, the oil flow continuity equation may be written as

$$Q_{ci} - Q_{vi} + Q_{ai} + K_{sc}V_n\Delta a\,\Delta c = Q_{co} - Q_{vo} + Q_{ao} \tag{6}$$

where

$$Q_{ci} = K_i - H_{ci}(P - P_{ci}) \tag{7}$$

$$Q_{ai} = -H_{ai}(P - P_{ai}) \tag{8}$$

$$Q_{co} = K_o - H_{co}(P_{co} - P) \tag{9}$$

$$Q_{ao} = -H_{ao}(P_{ao} - P) \tag{10}$$

the pressure flow functions being given by

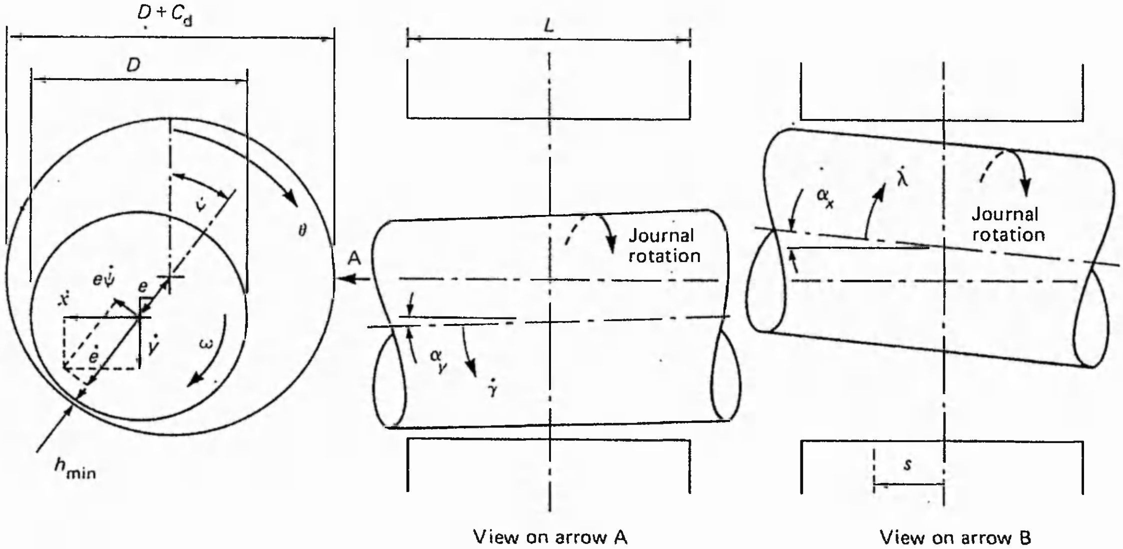

Fig 4 Sign convention for bearing

A.4. - 81.

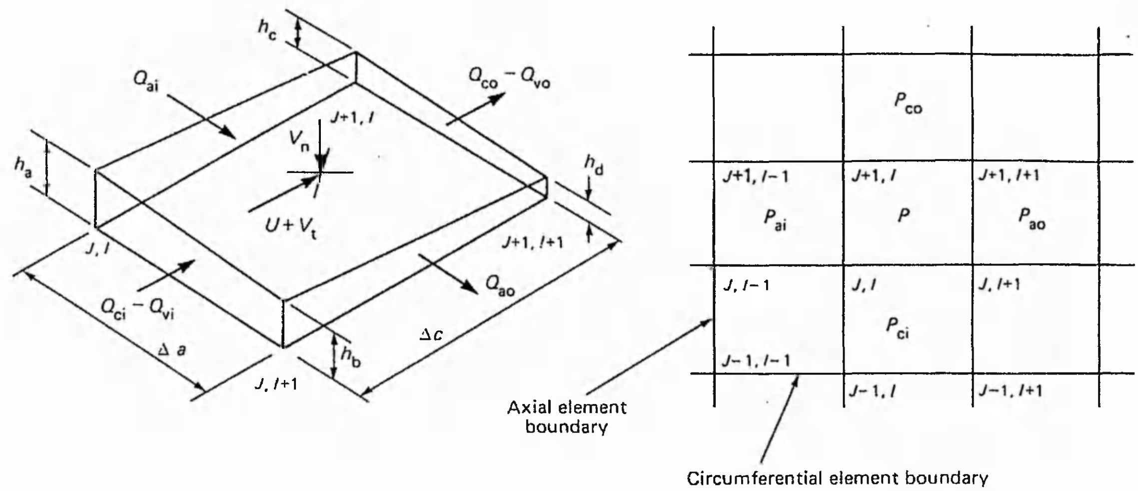

Fig 5 Oil-film element details

$$H_{ci} = \frac{(h_a + h_b)^3}{96\,\eta}\,\frac{\Delta a}{\Delta c} \tag{11}$$

$$H_{ai} = \frac{(h_a + h_c)^3}{96\,\eta}\,\frac{\Delta c}{\Delta a} \tag{12}$$

$$H_{co} = \frac{(h_c + h_d)^3}{96\,\eta}\,\frac{\Delta a}{\Delta c} \tag{13}$$

$$H_{ao} = \frac{(h_b + h_d)^3}{96\,\eta}\,\frac{\Delta c}{\Delta a} \tag{14}$$

and the surface velocity induced flow rates are given by

$$K_i = (h_a + h_b)(U_s + V_{ts})\,\Delta a/4 \tag{15}$$

$$K_o = (h_c + h_d)(U_s + V_{ts})\,\Delta a/4 \tag{16}$$

Note that P is the film pressure at the centre of the oil-film element under consideration, and P_{ci}, P_{ai}, P_{co} and P_{ao} the pressures at the centres of the adjacent oil-film elements. The pressure-flow terms are based on the assumption of linear pressure gradients between the element centres. These gradients are assumed to be the mean values for the element boundaries that they cross for the purpose of computing pressure-induced flow rates. Using the J, I circumferential, axial position reference system, for element J, I we may write: $P(J, I) = P$, $P(J-1, I) = P_{ci}$, $P(J, I-1) = P_{ai}$, $P(J+1, I) = P_{co}$, $P(J, I+1) = P_{ao}$.

For the calculation of P, at each iteration in the relaxation process it is initially assumed that the element is not cavitating, i.e. $P > P_c$ and consequently $Q_{vo} = 0$ and $K_{sc} = 1$. Equation (6) may therefore be transposed for the calculation for P thus

$$P = \frac{H_{ai}P_{ai} + H_{ci}P_{ci} + H_{ao}P_{ao} + H_{co}P_{co} + K_i - K_o - Q_{vi} + V_{ns}\,\Delta a\,\Delta c}{H_{ai} + H_{ci} + H_{ao} + H_{co}} \tag{17}$$

In order to accommodate flow reversal, it should be noted that for $U_s > 0$

$$Q_{vi} = Q_v\,(J, I)$$

and for $U_s < 0$

$$Q_{vi} = Q_v\,(J+1, I)$$

It may be noted that in relation to reference 1, in which the term K was used for the net velocity-induced flow rate out of the element, three terms, K_i, K_o and $V_{ns}\,\Delta a\,\Delta c$, are now used.

In order to compute the normal and tangential components of journal surface velocity, V_{ns}, V_{ts}, in way of the element J, I due to lateral and angular velocity of the journal axis, it is necessary first to compute the vertical and horizontal components of journal axis velocity at the centre of element column I

$$V_{ys} = \dot{\gamma}\,s + \dot{y} \tag{18}$$

$$V_{xs} = \dot{\lambda}\,s + \dot{x} \tag{19}$$

where

$$s = \frac{L}{2}\left[1 - \frac{2}{N_a}\,(I - 0.5)\right] \tag{20}$$

assuming all axial element dimensions Δa are identical. Where axial element grading is used (variation of Δa with axial position), equation (20) will require replacement or modification according to the grading system used.

The corresponding radial and circumferential components of the journal axis velocity are given by

$$\dot{e}_s = V_{ys}\cos\psi_s + V_{xs}\sin\psi_s \tag{21}$$

$$\dot{\psi}_s = (V_{xs}\cos\psi_s - V_{ys}\sin\psi_s)/e_s \tag{22}$$

In order to retransform the above radial and circumferential velocity components into vertical and horizontal components, the following equations apply

$$V_{ys} = \dot{e}_s\cos\psi_s - e_s\,\dot{\psi}_s\sin\psi_s \tag{23}$$

$$V_{xs} = \dot{e}_s\sin\psi_s + e_s\,\dot{\psi}_s\cos\psi_s \tag{24}$$

However, hydrodynamic squeeze and wedge actions are now segregated in the calculation. Where angular misalignment is present, this segregation is a function of axial position and must therefore be applied to each element column. The equivalent journal surface velocity therefore becomes a function of axial position thus

$$U_s = (\omega - 2\,\dot{\psi}_s)\,D/2 \tag{25}$$

A.4. -82.

In addition, since $\dot{\psi}_s$ has been taken into account in equation (25) for U_s, the journal surface velocity components V_{ns} and V_{ts} are made functions of $\dot{e}_s$ only. In order to calculate V_{ns}, V_{ts}, it is first necessary to define vertical and horizontal components of the journal axis velocity as functions of $\dot{e}_s$ only by deleting the $\dot{\psi}_s$ terms from equations (23) and (24) and substituting for $\dot{e}_s$ using equation (21)

$$V_{yrs} = (V_{ys} \cos \psi_s + V_{xs} \sin \psi_s) \cos \psi_s \qquad (26)$$

$$V_{xrs} = (V_{ys} \cos \psi_s + V_{xs} \sin \psi_s) \sin \psi_s \qquad (27)$$

V_{ns} and V_{ts} can then be calculated from

$$V_{ns} = -(V_{yrs} \cos \theta + V_{xrs} \sin \theta) \qquad (28)$$

$$V_{ts} = V_{yrs} \sin \theta + V_{xrs} \cos \theta \qquad (29)$$

As indicated in the previous section and in reference 1, during the film pressure relaxation process, whenever $P < P_c$ is computed by equation (17), the value of P is reset to P_c and a non-zero value of Q_{vo} is computed by rearranging the flow continuity equation (6) into the following form

$$Q_{vo} = K_o - H_{co} (P_{co} - P_c) - H_{ao} (P_{ao} - P_c) - K_i + H_{ci} (P_c - P_{ci}) + H_{ai} (P_c - P_{ai}) + Q_{vi} - K_{sc} V_{ns} \Delta a \Delta c \qquad (30)$$

Again to accommodate flow reversal

$$Q_{vo} = Q_v (J + 1, I); Q_{vi} = Q_v (J, I) \text{ where } U_s > 0$$

and

$$Q_{vo} = Q_v (J, I); Q_{vi} = Q_v (J + 1, I) \text{ where } U_s < 0$$

The factor K_{sc} applied to the squeeze film term facilitates the deletion of this term for cavitating elements. Where the rupture or reformation boundaries are located within the element, K_{sc} enables only part of the squeeze film term to be deleted to give an approximate allowance for the proportion of the element subject to cavitation. Fig 6 shows how the subcavitation pressure P_{sc}, initially computed by equation (17) for a cavitating element during the film pressure relaxation process, is used as the basis for calculating K_{sc}.

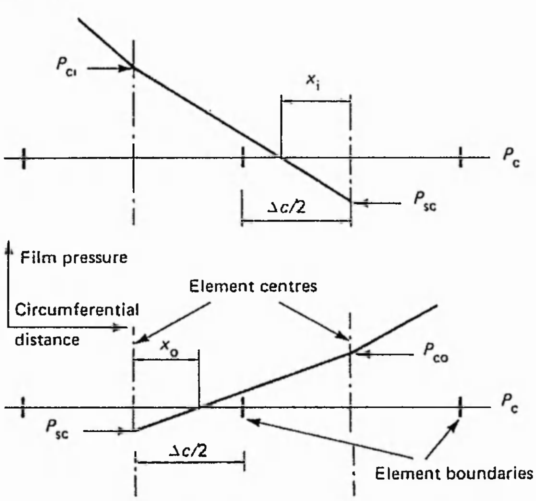

Fig 6 Approximate estimation method for proportion of elements subject to cavitation at boundaries: (a) rupture boundary; (b) reformation boundary

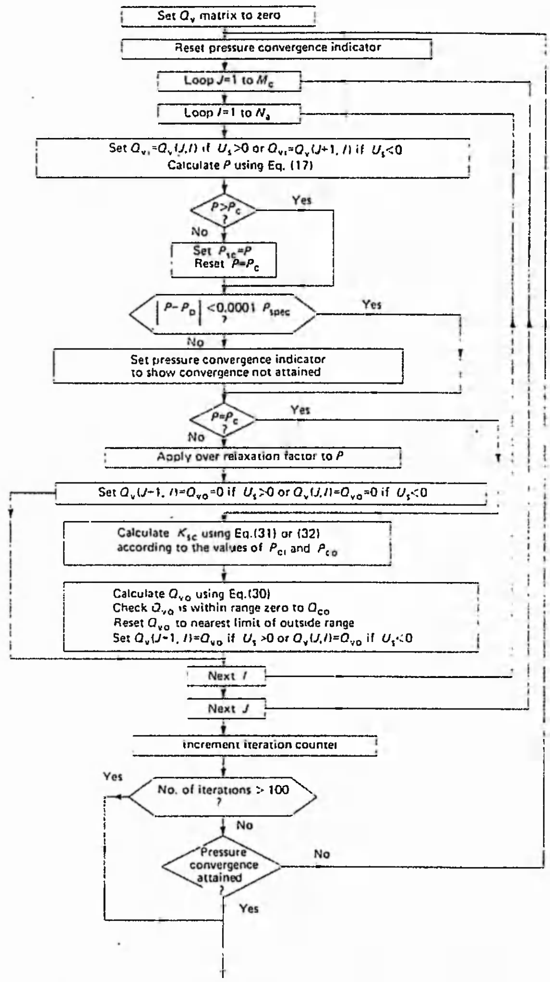

Fig 7 Computer flow diagram for film pressure solution

Referring to Fig 6, elements containing the rupture and reformation boundaries are shown. The approximate proportion of these elements subject to cavitation is $0.5 + x_i/\Delta c$ and $0.5 + X_o/\Delta c$, respectively.

where

$$x_i = \Delta c \left[\frac{P_c - P_{sc}}{P_{ci} - P_{sc}} \right] \quad \text{and } x_o = \Delta c \left[\frac{P_c - P_{sc}}{P_{co} - P_{sc}} \right]$$

Note that a non-zero pressure gradient is shown at the rupture boundary for diagrammatic purposes only. In test solutions, it has been shown that at the rupture boundary $\dfrac{\partial P}{\partial \theta} \to 0$ as $\Delta c \to 0$.

Thus, for the rupture boundary, i.e. where $P_{ci} > P_c$

$$K_{sc} = 0.5 - \left[\frac{P_c - P_{sc}}{P_{ci} - P_{sc}} \right] \qquad (31)$$

and for the reformation boundary, i.e. where $P_{co} > P_c$

$$K_{sc} = 0.5 - \left[\frac{P_c - P_{sc}}{P_{co} - P_{sc}} \right] \qquad (32)$$

A.4. - 83.

The following conditions are also applied

$K_{sc} = 1$ where both $P_{ci} > P_c$ and $P_{co} > P_c$

$K_{sc} = 0$ where both $P_{ci} = P_c$ and $P_{co} = P_c$

$K_{sc} \nless 0$

It must be stressed that the factor K_{sc} is only an approximate means of dealing with the problem of elements containing cavitation boundaries. As indicated in the following discussion, it is, however, quite adequate for the purpose of bearing performance prediction.

A simplified computer flow diagram for the film pressure solution is given in Fig 7.

Reversal of the equivalent journal angular velocity

The first situation in which anomalies were observed in the load capacity predictions of the original analysis method, was that in which the equivalent journal velocity became reversed, i.e. $\dot{\psi} > \omega/2$ thus $\omega_o < 0$. Investigation of the program operation revealed the cause of the anomaly and the means by which the problem could be rectified as detailed below.

In the cavitation model used, the gas/vapour flow term Q_{vo}, computed to satisfy continuity in a cavitating element, must be applied to the element downstream boundary. The logic of this situation is that resetting an initially computed subcavitation pressure to the specified cavitation pressure reduces the element's circumferential inlet flow and increases the circumferential outlet flow. The application of Q_{vo} thus reduces the outlet (i.e. downstream boundary) flow to restore balance.

In the operation of the relaxation process, it is necessary to refer to Q_{vo} by means of the J, I circumferential-axial element reference system; thus for element J, I, Q_{vo} was denoted by Q_v $(J + 1, I)$. This implicitly assumed that the direction of the equivalent journal velocity was the same as the direction of increasing J. In steadily-loaded situations, or where dynamic loading was relatively small, the above assumption was simply met by making the direction of increasing J the same as the direction of journal rotation. Where dynamic loading is large, the resulting amplitude and sense of journal lateral velocities may be such that the equivalent angular velocity becomes reversed. The associated anomaly in the load capacity prediction was found to be due to a failure to take account of such reversals. This resulted in Q_{vo} being computed for what was in fact the element upstream boundary. Convergence of the oil-film pressure relaxation process was still attained, but flow continuity within the cavitation zone was not satisfied under these conditions. The problem was simply solved by introducing a test for reversal of the equivalent journal velocity and identifying Q_{vo} as Q_v (J, I) rather than Q_v $(J + 1, I)$ when reversal was indicated. Q_{vi} thus became Q_v $(J + 1, I)$ in these circumstances.

Squeeze action in cavitating elements

The squeeze-film term V_n Δa Δc was originally used in the continuity equation for cavitating elements from which the equation for Q_{vo} (equation (17) in reference 1) was derived. When applying small velocity perturbations to the journal, for the purpose of computing oil-film damping coefficients, the squeeze-film term was relatively small and therefore had little influence on the extent of cavitation. For bearings subject to significant dynamic loading, the squeeze-film term becomes important. Further consideration of the situation in cavitating elements resulted in the deletion of the squeeze-film term from the equation for Q_{vo} (equation (30)) for the following reasons.

Where squeeze action occurs, oil-film elements within the full film region clearly require the squeeze-film term in their continuity equations, since oil displaced by the normal velocity V_n of the journal surface must be balanced by a corresponding flow across the element boundaries. Within the cavitation zone, however, it is postulated that V_n Δa Δc will result in an axial velocity of the oil streamer boundaries. Any tendency to produce additional circumferential velocities by the squeeze action would largely cancel out between adjacent oil-film elements. Within the cavitation zone, oil displaced by V_n does not therefore result in any additional flow across the element boundaries. consequently the term V_n Δa Δc should be deleted from the continuity equation for cavitating elements.

It should be noted that this analysis method uses the striated cavitation model; i.e. the oil is assumed to divide into rectangular section streamers of full film thickness. In the case of the adhered film cavitation model, as used by Pan[10], the need to delete the V_n Δa Δc term in the cavitation zone is even more apparent. Heshmat *et al*[11] have indicated that in reality the disposition of oil and gas/vapour within a cavitation zone lies somewhere between these two models. The adhered film cavitation model yields a circumferential velocity of the oil within the cavitation zone of ω $D/2$ i.e. twice that for the striated cavitation model. Provided continuity is satisfied throughout the cavitation zone, the choice of model does not result in any difference in the predicted extent of cavitation and hence load-carrying capacity. Tests have been carried out by the author to confirm this. The only material effect of assuming the adhered film cavitation model is the virtual elimination of power loss in the cavitation zone.

As indicated earlier, this work was directed towards modelling the quasi-steady situation in which instantaneous large-amplitude lateral velocities of the journal are considered. In the more realistic dynamic solution using the oil-film history model, cavitating elements are not required to satisfy continuity. The model described in reference 3 computed Q_{vo} in accordance with the assumption that the downstream boundary oil flow in cavitating elements was proportional to their 'degree of filling', i.e. $(Q_{co} - Q_{vo})/Q_{co} = (V_e - V_o)/V_e$. The quasi-steady approach does not provide any such basis for the determination of Q_{vo}; consequently, the computation of Q_{vo} was based on the satisfaction of flow continuity as far as practicable.

Under certain circumstances, the flow continuity criterion yields a result that is physically impossible. For example, when the journal is subject to a large negative radial velocity, cavitation may occur in the converging part of the oil film. In this region, an element may have a downstream boundary oil-flow rate that is less than the inlet flow rate, even when full film conditions are assumed at the downstream boundary. In order to satisfy the flow continuity criterion, a negative Q_{vo} would thus be computed. Since Q_{vo} is simply a means of reducing the downstream oil flow in cavitating elements from the value computed for full film conditions (Q_{co}), then Q_{vo} must clearly lie between Q_{co} and zero. The limits $Q_{co} \geqslant Q_{vo} \geqslant 0$ must therefore be applied, or $Q_{co} \leqslant Q_{vo} \leqslant 0$ where flow reversal occurs and

A.4. - 84.

Q_{co} is consequently negative. Where the value of Q_{vo} computed to satisfy flow continuity lies outside the above limits, it should be reset to the nearest limit. The flow continuity criterion will not be satisfied in the above situation, the net inflow of oil to the element being consistent with the rate of growth of the total element volume. In contrast to the oil-film history model, oil flow continuity in the cavitation zone is therefore satisfied provided this does not lead to an unrealistic result with respect to the magnitude of Q_{vo} relative to Q_{co}. This procedure is considered to be the most appropriate way of dealing with the somewhat artificial quasi-steady situation.

During the computer program development associated with this work, two problems were discovered, both of which resulted from the deletion of the squeeze-film term $V_n\ \Delta a\ \Delta c$ from the continuity equation for cavitating elements. First, a small discrepancy was found between the results for cases having a non-zero value of ω and those with $\omega = 0$ but having an equal equivalent angular velocity of the journal ω_o. Investigations revealed that this discrepancy disappeared if only that part of $V_n\ \Delta a\ \Delta c$ due to the radial component of journal velocity $\dot{e}$ was deleted from the continuity equation for cavitating elements. The most computationally efficient method of resolving this problem was to define the journal surface velocity U_s in terms of ω_o rather than ω (equation (25)) and to delete the $\dot{\psi}$ terms from the derivation of the equations for V_{ns} and V_{ts} (equations (28) and (29)). It should be noted that for the expression $U_s + V_{ts}$, that part of V_{ts} due to $\dot{\psi}$ is then incorporated in U_s. This system effectively segregated hydrodynamic squeeze and wedge action for computational purposes by resolving the actual bearing operating condition into the equivalent condition with $\dot{\psi} = 0$.

Although the above changes eliminated the observed discrepancy related to the deletion of the $V_n\ \Delta a\ \Delta c$ term, some physical interpretation of the situation was sought.

Referring to Fig 8, in case (a), a particle of oil in the cavitation zone 'sees' an apparent negative normal velocity of the journal surface V_n. This is clearly an illusion resulting from the circumferential velocity of the oil relative to the journal axis. In the flow continuity equation for a cavitating element in case (a), deletion of the squeeze film term $V_n\ \Delta a\ \Delta c$ is of no consequence since $V_n = 0$.

Case (b) differs in that a particle of oil in the cavitation zone again sees the same negative V_n. In this case, however, the oil is stationary and V_n is real. The oil particle is nevertheless unaware of the different operating conditions since in both cases it sees the same V_n as a result of its circumferential velocity relative to the journal axis. In order to obtain the same predicted performance for case (b), $V_n\ \Delta a\ \Delta c$ should not be deleted from the flow continuity equation for cavitating elements. The essential explanation of the foregoing situation is that in both of the above examples, one is considering an apparent squeeze film term $V_n\ \Delta a\ \Delta c$ in that since it arises from circumferential motion of the oil relative to the journal axis, it should, therefore, more properly be regarded as wedge rather than squeeze action. The fact that in absolute terms V_n is zero in case (a) and non-zero in case (b) does not affect this argument since it is only the apparent V_n observed by the oil particle that is of significance. In other words, the hydrodynamic action depends only on the relative motion of the oil and journal axis, which is the same for both case (a) and case (b), and not on the absolute motion.

In reality, there is a difference in the character of the cavitation in the case (a) and case (b) situations, as indicated by the experimental work to which reference was made in the section on equivalent journal velocity. However, as noted in the above section, no acceptable theoretical model for the related phenomena is known to exist at present.

In view of the conclusions of the above discussion, only that part of the squeeze film term $V_n\ \Delta a\ \Delta c$ due to $\dot{e}$ is deleted from the flow continuity equation for cavitating elements. Where V_n is a function of $\dot{e}$ only, it is completely

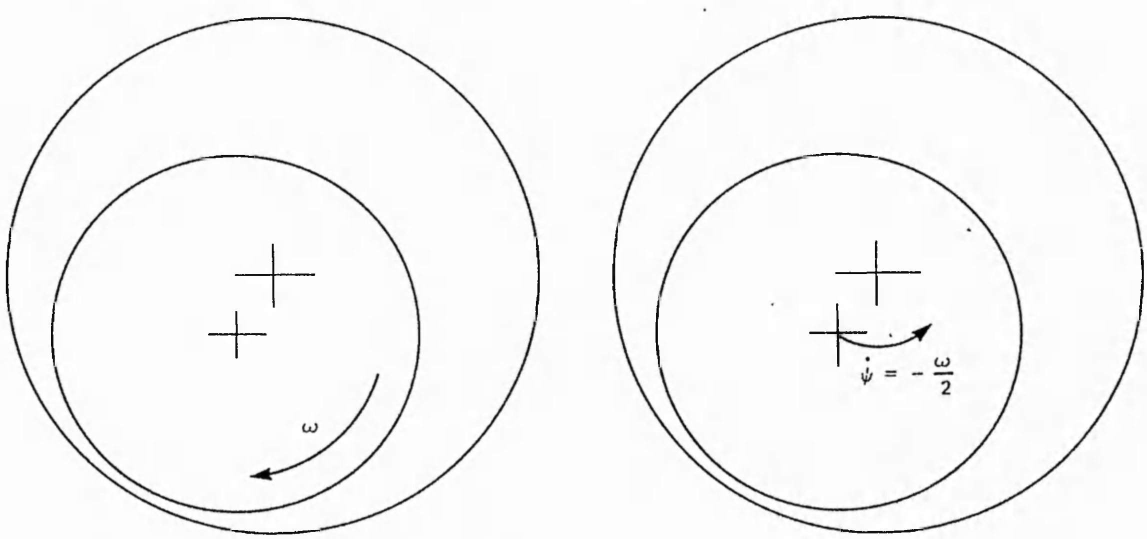

Fig 8 Examples of equal theoretical wedge action: case (A) journal rotating about its stationary axis; case (B) journal axis rotating about bearing axis; journal rotation about its axis is zero

A.4. - 85.

independent of the circumferential velocity of the oil relative to the journal axis. For this method of analysis, only that part of V_n arising from $\dot{e}$ is therefore regarded as pure squeeze action.

The other problem resulting from the elimination of the $V_n \, \Delta a \, \Delta c$ term from the flow continuity equation for cavitating elements, was a slight degree of instability in the film pressure relaxation process involving a few elements adjacent to cavitation boundaries. This problem was caused by the sudden step from $V_n \, \Delta a \, \Delta c$ included to $V_n \, \Delta a \, \Delta c$ excluded at the cavitation boundary. The resulting instability therefore took the form of a few elements fluctuating between being full film and cavitating during the relaxation process. This fluctuation had a negligible effect on the total oil-film force components, but could be of sufficient magnitude to cause a film pressure convergence failure.

Some improvement in the incidence of the above convergence failure was obtained by effectively recognizing that cavitating elements adjacent to the cavitation boundary are generally part full film and part cavitating, i.e. the cavitation boundary in fact lies within the element. In these elements, only a corresponding part of $V_n \, \Delta a \, \Delta c$ should therefore be deleted from the flow continuity equation. This was achieved by making an estimate of the location of the cavitation boundary within the relevant cavitating elements, and then eliminating only a proportion of the $V_n \, \Delta a \, \Delta c$ term in accordance with the proportion of the element subject to cavitation. The location of the cavitation boundaries was estimated by the method indicated in Fig 6, using the subcavitation pressure P_{sc} initially computed in the relaxation procedure. This is undoubtedly a very approximate method of estimating the location of the cavitation boundary. It is nevertheless adequate in that it is simply required to smooth the transition between the application and non-application of $V_n \, \Delta a \, \Delta c$ at the cavitation boundaries.

While the above measure resulted in a worthwhile reduction in the number of analysis cases failing to attain film pressure convergence, it did not completely eliminate the problem. Since this instability had very little effect upon the total film force accuracy, as it involved only a few elements at the cavitation boundary, the problem was solved by simply placing a limit on the maximum number of iterations during the film pressure relaxation process. The number of iterations required when the film pressure matrix converged successfully was generally within the range 30 to 40. A maximum limit of 100 iterations was therefore applied to allow a generous margin.

Conclusions

This paper has presented an extension of the numerical analysis method given in reference 1, to provide more realistic modelling in situations where significant journal lateral velocities occur. The changes to the original method are concerned only with the way in which cavitation is treated. Since a quasi-steady approach has been used, direct experimental verification of data predicted by this method is not feasible. However, in reference 5, velocity coefficients derived from data produced by the extended method were used to predict journal orbits in a full circumferential groove bearing. Corresponding experimental orbits measured on a test rig were presented in reference 5, and showed generally good correlation. Examples of the oil-film force–journal velocity relationship predicted by the above method are given in reference 2. This work provided a clearer understanding of the role of cavitation with respect to the non-linearity of the force–velocity relationship. As a basis for the above study of non-linearity, the extended method reported in this paper was essential.

Acknowledgements

The author wishes to express his gratitude to the Committee of Lloyd's Register of Shipping for permission to publish this paper. In addition, the author is indebted to F.A. Martin of the Glacier Metal Co. Ltd, I. Montgomery of Trent Polytechnic and D. Rennie of Lloyd's Register of Shipping for their helpful discussions and comments on this paper. The cooperation of D.W. Parkins of Cranfield Institute of Technology in providing the experimental data shown in Fig 2 is also gratefully acknowledged.

References

1. Jakeman R.W. 'A numerical analysis method based on flow continuity for hydrodynamic journal bearings'. *Tribology Int.* 17, *6, 1984, 325–333*
2. Jakeman R.W. 'The influence of cavitation on the non-linearity of velocity coefficients in a hydrodynamic journal bearing'. *Proc. 13th Leeds–Lyon Symp. Tribology. September 1986 (to be published)*
3. Jakeman R.W. 'Journal orbit analysis taking account of oil film history and journal mass'. *Proc. 4th Int. Conf. Numerical Methods in Laminar and Turbulent Flow, Swansea, UK, July 1985, 199–210*
4. Jones G.J. 'Crankshaft bearings: oil film history'. *Proc. 9th Leeds–Lyon Symp. Tribology. September 1982, 83–88*
5. Jakeman R.W. and Parkins D.W. 'Theoretical and experimental orbits of a dynamically loaded hydrodynamic journal bearing'. *Proc. 13th Leeds–Lyon Symp. Tribology, September 1986 (to be published)*
6. Cole S.A. and Hughes C.J. 'Visual study of film extent in dynamically loaded complete journal bearings' *Proc. I. Mech.E. Lub. Wear Conf. 1957, 147–150*
7. Marsh H. 'Cavitation in dynamically loaded journal bearings'. *Proc. 1st Leeds–Lyon Symp. Tribology, September 1974, 91–95*
8. White D.C. *Squeeze film journal bearings. PhD dissertation, Cambridge University, UK, 1970*
9. Etsion I. and Ludwig L.P. 'Observation of pressure variation in the cavitation region of submerged journal bearings' *ASME J. Lub. Tech.* 104, *1982, 157–163*
10. Pan C.H.T. 'Dynamic analysis of rupture in thin films' *Trans ASME, 1983,* 105, *96–104*
11. Heshmat H. and Pinkus O. 'Mixing inlet temperatures in hydrodynanic bearings'. *Proc. ASLE/ASME Tribology Conf., Atlanta, USA, October 1985, ASME Preprint No. 85-TRIB-26*

A.4. - 86.

REFERENCE. 91.

A NON-LINEAR OIL FILM RESPONSE MODEL FOR THE DYNAMICALLY MISALIGNED STERNTUBE BEARING.

R.W. Jakeman

Abstract

This paper presents a non-linear oil film response model which has been developed from that previously described by Jakeman (1) for the aligned full circumferential groove bearing.

The model was specificaly intended to represent the dynamically misaligned sterntube bearing, for the purpose of conducting lateral vibration analyses of marine propeller shafting. Some predicted data for the oil film response to lateral and angular motion of the journal axis, upon which the non-linear model was based, are presented. A comparison of lateral vibration predictions using the non-linear and linear oil film models, and measurements by Hyakutake et al (2), will be given in a separate paper.

NOTATION

A	Bearing oil film stiffness coefficient
B	Damping coefficient (general use)
C_d	Bearing diametral clearance
D	Journal diameter
e	Journal eccentricity at bearing axial centre
F	Force
L	Bearing length
M	Moment
P_H	Oil head pressure on bearing
x	Lateral displacement in horizontal direction
y	Lateral displacement in vertical direction
z	Axial direction
λ	Angular displacement in horizontal plane
γ	Angular displacement in vertical plane
ψ	Journal attitude angle relative to Y axis at bearing axial centre
ξ	Angular displacement in plane defined by ψ and z axis
φ	Angular displacement in plane defined by $\psi + 90^{o}$ and z axis
ϵ	Journal eccentricity ratio $(2e/C_d)$
ω	Angular velocity of shaft rotation about z axis
ω_o	Equivalent angular velocity of journal $(= \omega - 2\dot{\psi})$
η	Dynamic viscosity.

Suffixes:

B Bearing

D Datum condition for oil film force and moment

E Non-linear stiffness or damping coefficient for e or $\dot{e}$.

FR Non-linear stiffness or damping coefficient for F_R.

FT Non-linear stiffness or damping coefficient for F_T.

MR Non-linear stiffness or damping coefficient for M_R.

MT Non-linear stiffness or damping coefficient for M_T.

NL Non-linear correction factor for oil film force or moment

R Radial direction defined by ψ at bearing axial centre

T Tangential direction (90^o to above radial direction)

X Horizontal direction } Refers to lateral displacement or

Y Vertical direction } velocity in linear oil film coefficient

λ Horizontal plane } Refers to angular displacement or

γ Vertical plane } velocity in linear oil film coefficient

ξ Non-linear stiffness or damping coefficient for ξ or $\dot{\xi}$.

φ Non-linear stiffness or damping coefficient for φ or $\dot{\varphi}$.

ψ Non-linear stiffness coefficient for ψ.

ω Non-linear damping coefficient for ω_o.

Sign Convention:

Fig. 1 shows the general sign convention.

Fig. 2 shows the bearing polar sign convention used for the non-linear oil film response studies. Note that $X\,o\,Y$ defines the bearing axial centre plane.

M_R (oil film moment) and ξ act in plane $o\,z\,a\,c$.

M_T (oil film moment) and φ act in plane $a\,b\,c\,d$

which is at 90^{o} to plane $ozac$. F_R and F_T are the oil film force components which act in the opposite direction to e and ψ respectively

Introduction

Linearised oil film stiffness and damping coefficients for a dynamically misaligned sterntube bearing have been previously presented by Jakeman (3). In service measurements by Hyakutake et al (2) indicated significant shafting lateral vibration amplitudes in way of the sterntube bearing. These measurements were made on board the 210,000 d.w.t. tanker "KEIYO MARU". This has raised the question of whether satisfactory lateral vibration prediction accuracy can be achieved with the use of linerised coefficients. The objective of this work was therefore to develop a non-linear oil film response model for the above situation. This was based on the model for aligned full circumferential oil groove bearings described by Jakeman (1). Some predicted oil film response characteristics, upon which the non-linear model was based, are presented. The application of this non-linear model, to the prediction of lateral vibration amplitudes in marine propeller shafting, will be dealt with in a separate paper. This will include a comparison with predictions based on the use of linearised oil film coefficients, and measurements by Hyakutake et al (2).

Literature Review

The journal orbit type of analysis is used for dynamically loaded bearings, in which the displacement amplitude of the journal is significant in relation to the clearance circle. It requires the derivation of oil film forces (and moments where misalignment is present) at each of the time steps which constitute the orbit "marching out" process. This form of analysis can therefore be heavy on computing time unless a fast method of obtaining the oil film forces and momemts is adopted. Two such fast methods have been used:

1) The analytical method, in which an approximate solution of Reynolds' equation is obtained by assuming the bearing to be either very short or very long.

2) The use of stored bearing oil film response data, which may be obtained by either numerical solution or by measurement.

The second option is generally considered to be more accurate, and when used in conjunction with the digital computer, is also quite practicable. This approach, with a numerical hydrodynamic solution, was the basis of the non-linear model described in this paper. The literature review will also be confined to such methods.

Probably the most popular form of stored oil film response data is that incorporated in the mobility method. This method was developed by Booker (4). It is restricted, however, to circumferentially symmetrical bearings, and its formulation precludes the inclusion of inertial forces due to journal lateral motion.

Moes et al (5) presented a development of the mobility method referred to as mobility matricies. The mobility matrices used a non-rotating Cartesion reference system which results in improved computational efficiency. The above restrictions to the mobility (vector) method, however, remained applicable to mobility matricies.

Bearing impedance vectors were introduced by Childs et al (6), these being equivalent to the reciprocal of mobility vectors. The formulation of impedance vectors facilitated the inclusion of inertial forces in a journal orbit analysis.

In order to overcome the restriction to circumferentially symmetrical bearings, of the above mobility and impedance methods, Moes et al (7) introduced mobility and impedance tensor methods.

It should be noted that the above mobility and impedance methods (vector and tensor) incur some inaccuracy due to their implicit assumption that the principle of superposition is applicable to squeeze and wedge action. As shown by Jakeman (1), the presence of cavitation introduces a degree of non-linearity which introduces inaccuracy if the principle of superposition is applied to this situation. The amount of inaccuracy would depend on the relative strengths of the squeeze and wedge actions and upon the extent of cavitation, and may be acceptable for some practical applications. A further restriction to the above methods is their inability to handle misaligned bearings. Inaccuracies resulting from their use under misaligned conditions are likely to be particularly significant in sterntube bearings.

The hydrodynamic analysis method used to derive coefficients for the linear bearing oil film model has been described by Jakeman (8). This analysis method was later refined to take account of cavitation effects associated with relatively large lateral velocities of the journal (9). A theoretical study of the influence of cavitation was carried out by Jakeman (1) using the refined analysis method. From the cavitation study, a new form of oil film model was devised for aligned journal bearings. This took account of the influence of cavitation on non-linearity in the relationship between oil film force and journal lateral velocity.

The non-linear model presented in this paper, is a development of the above model for use with circumferentially asymmetric bearings subject to dynamic misalignment conditions.

In relation to the mobility and impedance methods, this non-linear oil film model would only be valid for a restricted orbit size in relation to that of the clearance circle. This restriction was considered to be acceptable for the displacement amplitude ranges indicated by service measurements on sterntube bearings. The main advantages of this new non-linear oil film model were:

1. It's ability to handle steady and dynamic misalignment conditions.
2. Recognition of the non-applicability of the principle of superposition to bearing oil films.

Bearing Oil Film Response

The development of the hydrodynamic analysis method used in this work, and the non-linear oil film model for aligned bearings, has been referred to in the literature review.
In this section, some characteristics of the predicted oil film response under steady and dynamic misalignment conditions will be examined.

The previous work (1) on the oil film response to lateral journal velocities in an aligned bearing showed the following main characteristics:

1. F_R is primarily a function of $\dot{e}$.
2. The relationship between F_R and $\dot{e}$ experiences a marked change in slope between positive and negative $\dot{e}$, the latter being disinctly non-linear.
3. The influence of wedge action ($\omega_o \neq 0$) smooths the above transition between positive and negative $\dot{e}$ and extends the non-linearity into the positive $\dot{e}$ region.
4. Cavitation due to wedge action may be suppressed by high positive $\dot{e}$. Beyond this threshold, that part of F_R due to wedge action falls to zero, and the principle of superposition between squeeze and wedge action becomes applicable.
5. F_T is primarily a function of ω_o.
6. The magnitude of F_T is the same for equal values of positive and negative ω_o, and the sign is the same as that for ω_o.

7. The relationship between F_T and ω_0 is slightly non-linear, but becomes perfectly linear when the magnitude of positive $\dot{e}$ is above the threshold required to suppress cavitation.

Reference (1) presents a more detailed discussion of the influence of cavitation on the above characteristics.

The situation with respect to journal velocities in the misaligned sterntube bearing is considerably more complex for the following reasons:

1. In addition to $\dot{e}$ and ω_0 we have angular velocity components for the journal axis $\dot{\xi}$ and $\dot{\varphi}$.
2. For the aligned bearing, the polar co-ordinate system was clearly defined with reference to the line connecting the journal and bearing centres, which also defines the attitude angle ψ. In the misaligned bearing, ψ generally varies from one end of the bearing to the other. The polar co-ordinate system in this work is defined by ψ at the axial centre plane of the bearing. Variation of ψ along the length of the bearing does, however, prevent the clear distinction between squeeze and wedge action that was possible in the aligned bearing.
3. Due to the two axial oil grooves, the sterntube bearing is not circumferentially symmetrical.
4. In addition to the oil film forces F_R and F_T, the moments M_R and M_T are also important.

The following discussion outlines the main characteristics of the oil film response to journal velocity in a misaligned sterntube bearing. It must be appreciated that as a result of the above complexity, the characteristics are less clearly definable than for the circumferentially symmetrical aligned bearing. The results presented in figs. 3 to 7 illustrate some aspects of the oil film response. These are for the after sterntube bearing of the "KEIYO MARU" at a journal location (ϵ, ψ, ξ, φ) approximately representative of the mean location at the service speed. In view of the number of variables involved, a vast amount of data would be required to explore the behaviour thoroughly. The data presented has been limited to the minimum required to illustrate the main features. The journal velocity ranges used are approximately representative of those estimated from the measured displacement data obtained from the "KEIYO MARU" (2). A complete set of data for this bearing is given in Table 1.

1. The relationship between F_R and $\dot{e}$ remained similar to that previously shown (1) for an aligned bearing. $\dot{\xi}$ has a similar influence to $\dot{e}$ provided the variation of ψ over the bearing length is not large. Subject to this condition with respect to ψ, $\dot{\xi}$ effectively adds to $\dot{e}$ at the aft end, and subtracts from it at the forward end. Since ϵ is higher at the aft end, the additive effect will be dominant. The influence of $\dot{\xi}$ was small, and the associated data is not presented.

2. Fig. 3 shows the influence of $\dot{\psi}$ on F_R . In the aligned bearing (1), curves for $F_R - \dot{e}$ were valid for equal magnitudes for either positive or negative ω_o. This is clearly not the case for a sterntube bearing due to circumferential asymmetry; i.e. the circumferential distance over which wedge action occurs is substantially different for positive and negative ω_o . It is also interesting to note that at negative ω_o, F_R becomes negative. This is due to the partial suppression of cavitation due to the oil head pressure, resulting in a negative wedge action in the longer divergent section, which is more powerful than the positive wedge action in the shorter convergent section. $\dot{\varphi}$ may be considered to combine with ω_o in a similar way to the combination of $\dot{\xi}$ and $\dot{e}$ and subject to the same limitation with respect to ψ variation. The effect of $\dot{\varphi}$ is seen to be generally small, being most significant at $\omega_o = 0$ since at this condition $\dot{\varphi}$ is responsible for generating all the hydrodynamic action.

3. Fig. 4 shows the relationship between F_T and $\dot{\psi}$ to be similar to that for the aligned bearing (1), except for the change in slope at $\omega_o = 0$, and the small influence of $\dot{\varphi}$. These changes are due to the same causes outlined for the $F_R - \dot{\psi}$ data above.

4. The variation of M_R with $\dot{e}$ given in Fig. 5 can be seen to be similar to that for F_R , as shown in reference (1). Angular motion of the journal axis would be

expected to have a stronger influence on oil film moment rather than force, and this is shown by the curves for $\dot{\xi} = \pm 2.10^{-3}$ rad/s. The substantially reduced effectiveness of $\dot{\xi}$ at negative $\dot{e}$ would be due to cavitation in the minimum film thickness region at this condition.

5. Fig. 6 shows the $M_R - \dot{\psi}$ relationship to be similar to that of $F_R - \dot{\psi}$ (Fig. 3). $\dot{\varphi}$ is seen to have a substantially increased influence on M_R compared to that for F_R, and is thus similar, in terms of effectiveness, to $\dot{\xi}$. It should be noted, however, that $\dot{\varphi}$ is mainly associated with wedge action and $\dot{\xi}$ with squeeze action. The different slope of the $M_R - \dot{\psi}$ curves between positive and negative ω_o is due to circumferential asymmetry, as outlined in the discussion of the $F_R - \dot{\psi}$ relationship. At $\dot{\varphi} = 0$, M_R is seen to remain positive at negative ω_o, whereas F_R became negative at this condition. This is probably due to the negative wedge action, previously mentioned in the discussion of oil film response at negative ω_o, being weaker at the aft end due to the more extensive cavitation that would be associated with the higher local ϵ. M_R would be influence by the conditions at the aft end to a much greater extent than F_R. This may explain the different behaviour of M_R and F_R at negative ω_o.

6. The $M_T - \dot{\psi}$ data presented in Fig. 7 relate to the $F_T - \dot{\psi}$ data of Fig. 4 in much the same way as the $M_R - \dot{\psi}$ data in Fig. 6 related to the $F_R - \dot{\psi}$ data of Fig. 3.

OIL FILM RESPONSE MODEL

Linear Oil Film Model

The derivation of 32 linearised oil film coefficients for a bearing subject to dynamic misalignment conditions has been previously outlined (8), and example results presented (3). These coefficients are defined by the equations for oil film force and moment components:

$$
\begin{bmatrix} F_{BX} \\ F_{BY} \\ M_{BX} \\ M_{BY} \end{bmatrix} =
\begin{bmatrix} A_{XX} & A_{XY} & A_{X\lambda} & A_{X\gamma} \\ A_{YX} & A_{YY} & A_{Y\lambda} & A_{Y\gamma} \\ A_{\lambda X} & A_{\lambda Y} & A_{\lambda\lambda} & A_{\lambda\gamma} \\ A_{\gamma X} & A_{\gamma Y} & A_{\gamma\lambda} & A_{\gamma\gamma} \end{bmatrix}
\begin{bmatrix} x - x_D \\ y - y_D \\ \lambda - \lambda_D \\ \gamma - \gamma_D \end{bmatrix} +
$$

$$
\begin{bmatrix} B_{XX} & B_{XY} & B_{X\lambda} & B_{X\gamma} \\ B_{YX} & B_{YY} & B_{Y\lambda} & B_{Y\gamma} \\ B_{\lambda X} & B_{\lambda Y} & B_{\lambda\lambda} & B_{\lambda\gamma} \\ B_{\gamma X} & B_{\gamma Y} & B_{\gamma\lambda} & B_{\gamma\gamma} \end{bmatrix} \cdot
\begin{bmatrix} \dot{x} - \dot{x}_D \\ \dot{y} - \dot{y}_D \\ \dot{\lambda} - \dot{\lambda}_D \\ \dot{\gamma} - \dot{\gamma}_D \end{bmatrix} +
\begin{bmatrix} F_{DX} \\ F_{DY} \\ M_{DX} \\ M_{DY} \end{bmatrix} +
\begin{bmatrix} F_{NLX} \\ F_{NLY} \\ M_{NLX} \\ M_{NLY} \end{bmatrix} \quad \ldots[1]
$$

Note that equation [1] has been written in a form that gives the absolute oil film force and moment components for displacement and velocity changes from a prescribed datum condition. The extreme right hand vector in equation [1] contains non-linear correction terms which are zero for the linear oil film model. In the next section, the derivation of these correction terms will be described.

Non-Linear Oil Film Model

From the predicted oil film rsponse characteristics previously given, the following main observations may be made:

1. The principle of superposition, with respect to various combinations of lateral and angular velocity components, is not applicable when cavitation is present.
2. The slope of force or moment components plotted against velocity may differ substantially for positive and negative velocities.
3. The change in the force or moment-velocity slope, as zero velocity is passed, may be fairly abrupt if either wedge or squeeze action is dominant.
4. For some combinations of simultaneously occuring velocity component magnitudes, the form of force or moment variation with one of the velocity components may be complex. This renders the fitting of equations, to describe the variation accurately, a difficult task.

In view of the above characteristics, it was decided to use a non-linear model based on that developed for aligned full circumferential groove bearings in reference (1). The first essential feature of this model was that it took account of the changes in force or moment slope between positive and negative velocity. Secondly, it recognised that superposition of velocity components cannot be applied without incurring error. The first feature was achieved by selecting different coefficient values according to the sense of the related velocity components. This is an alternative to the use of second order terms of the Taylor's series, as adopted by Bannister (10). The Taylor's series method gives a better fit to a smooth curve, whereas the method chosen is designed to fit two straight lines of differing slope which intersect at zero velocity. Since both forms of force/moment variation with velocity have been predicted, it is unlikely that there will be a significant difference in the overall accuracy of either method. The method adopted for this work, which is referred to as "piecewise linearisation", is considered to be computationally simpler. In order to fulfill the second feature, with respect to superposition, second, third and fourth order terms were used which effectively apply a correction for various combinations of velocity component applied simultaneously. The coefficient values for these higher order terms were also selected according to the sense of each of the relevant velocity components. From the above considerations, the following equation was derived:

$$
\begin{aligned}
F_R = {} & B_{FR} + B_{FRE}\,.\,\dot{e} + B_{FR\xi}\,.\,\dot{\xi} + B_{FR\omega}\,.\,\omega_o + B_{FR\varphi}\,.\,\dot{\varphi} \\
& + B_{FRE\xi}\,.\,\dot{e}\,.\,\dot{\xi} + B_{FRE\omega}\,.\,\dot{e}\,.\,\omega_o + B_{FRE\varphi}\,.\,\dot{e}\,.\,\dot{\varphi} \\
& + B_{FR\xi\omega}\,.\,\dot{\xi}\,.\,\omega_o + B_{FR\xi\varphi}\,.\,\dot{\xi}\,.\,\dot{\varphi} + B_{FR\omega\varphi}\,.\,\omega_o\,.\,\dot{\varphi} \\
& + B_{FRE\xi\omega}\,.\,\dot{e}\,.\,\dot{\xi}\,.\,\omega_o + B_{FRE\xi\varphi}\,.\,\dot{e}\,.\,\dot{\xi}\,.\,\dot{\varphi} \\
& + B_{FRE\omega\varphi}\,.\,\dot{e}\,.\,\omega_o\,.\,\dot{\varphi} + B_{FR\xi\omega\varphi}\,.\,\dot{\xi}\,.\,\omega_o\,.\,\dot{\varphi} \\
& + B_{FRE\xi\omega\varphi}\,.\,\dot{e}\,.\,\dot{\xi}\,.\,\omega_o\,.\,\dot{\varphi}
\end{aligned} \qquad [2.]
$$

Similar equations may be written for F_T, M_R, M_T.
It may be noted that as in reference (1), the effective velocity for wedge action ω_o is used rather than $\dot{\psi}$.
The numbers of coefficents used in equation [2] is given in Table 2. The number of types refers to the number of possible combinations of positive or negative velocity component e.g. $\beta_{FRe\varphi}$ is second order coefficient having four coefficient types covering: $-\dot{e}\ -\dot{\varphi}$; $-\dot{e}\ +\dot{\varphi}$; $+\dot{e}\ -\dot{\varphi}$; $+\dot{e}\ +\dot{\varphi}$.
Derivation of the non-linear damping coefficients β_{FR}, etc. was achieved by computing the force and moment components for all possible combinations of negative, zero and positive velocity component perturbations. 81 hydrodynamic solutions were thus required, from which the 81 coefficients for each of F_R, F_T, M_R and M_T could be computed. It may be noted that the non-linear force and moment equations [2] give an exact fit to the data of all 81 hydrodynamic solutions used to derive the coefficients.

In the previous work (1) on aligned full circumferential bearings, displacement was handled by computing the coefficients for a range of eccentricity ratios ϵ covering the required operating conditions. For any given journal displacement, coefficient interpolation was applied to the adjacent ϵ conditions in the coefficient data bank.
Since for aligned circumferentially symetrical bearings, only 3 first order and 2 second order coefficients were required for both F_R and F_T, and these coefficients were functions of ϵ only, the interpolation system was quite practicable.

In the work covered by this paper, not only was there a considerable increase in the number of coefficients, but the coefficients were functions of ϵ, ψ, ξ and φ. It was therefore evident that the interpolation system would be impracticable in view of the vast coefficient data bank that would be needed.

Some form of simplifying approximation was clearly necessary, and as a first step, an examination of the measured data (2) was made. Numerical differentiation of the measured displacement data indicated that in general, velocity components tended to peak at approximately zero displacement from the mean journal location and vice-versa. In view of the existence of four components of both displacement and velocity, the above observations were inevitably somewhat crude, but could nevertheless be considered to represent a reasonable generalisation of the behaviour. In addition, it was noted that the journal orbits were much smaller in relation to the clearance circle than those commonly encountered in crankshaft main bearings.

As a result of these observations, it was concluded that a single set of non-linear damping coefficients, based on the mean journal location, could be used. In order to cover journal displacements, similar equations to [2] were adopted:

$$
\begin{aligned}
F_R = \; & A_{FR} + A_{FRe}\cdot\Delta e + A_{FR\xi}\cdot\Delta\xi + A_{FR\psi}\cdot\Delta\psi + A_{FR\varphi}\cdot\Delta\varphi \\
& + A_{FRe\xi}\cdot\Delta e\cdot\Delta\xi + A_{FRe\psi}\cdot\Delta e\cdot\Delta\psi + A_{FRe\varphi}\cdot\Delta e\cdot\Delta\varphi \\
& + A_{FR\xi\psi}\cdot\Delta\xi\cdot\Delta\psi + A_{FR\xi\varphi}\cdot\Delta\xi\cdot\Delta\varphi + A_{FR\psi\varphi}\cdot\Delta\psi\cdot\Delta\varphi \\
& + A_{FRe\xi\psi}\cdot\Delta e\cdot\Delta\xi\cdot\Delta\psi + A_{FRe\xi\varphi}\cdot\Delta e\cdot\Delta\xi\cdot\Delta\varphi \\
& + A_{FRe\psi\varphi}\cdot\Delta e\cdot\Delta\psi\cdot\Delta\varphi + A_{FR\xi\psi\varphi}\cdot\Delta\xi\cdot\Delta\psi\cdot\Delta\varphi \\
& + A_{FRe\xi\psi\varphi}\cdot\Delta e\cdot\Delta\xi\cdot\Delta\psi\cdot\Delta\varphi . \qquad [3.]
\end{aligned}
$$

Again, similar equations were written for F_T, M_R, M_T. It should be noted that equation [2] was based on the effective velocity for wedge action ω_o rather than $\dot{\psi}$. When $\omega_o, \dot{\varphi}, \dot{e}, \dot{\xi} = 0$ there is no squeeze or wedge action, and consequently F_R, F_T, M_R and M_T are all zero.

Equation [3] is based on the mean journal location, hence the prefix Δ on all the displacement terms to denote the change from the datum condition. In addition, the datum condition is assumed to correspond to $\dot{\psi}, \dot{\varphi}, \dot{e}, \dot{\xi} = 0$, therefore equation [3] is also based on $\omega_o = \omega$. It can thus be seen that A_{FR} is equal to F_R at the datum condition, and similarly A_{FT}, A_{MR}, A_{MT} are respectively equal to F_T, M_R, M_T at the datum condition. Equation [3] eliminates the errors that would occur when applying the principle of superposition to the displacement components, in the same way that equation [2] fulfilled this function with repsect to velocity components. The use of "piecewise linearisation" may be less accurate for displacements, than adoption of the second order terms of Taylor's series. This is due to the non-linearity related to displacements being primarily a result of the associated oil film geometry changes, since pressure induced flow is proportional to the cube of film thickness. A smoother curvature therefore occurs in the force/moment variation with displacement, compared with the distinctly linked relationship that may be found with velocity changes. The non-linearity associated with journal velocity has been shown (1) to be mainly due to cavitation. Due to a deadline for the completion of this work, detailed examination of the force/moment displacement relationship was not carried out. From the above comments, these relationships are less likely to be as interesting as those for velocity. Despite the possible loss of accuracy, the "piecewise linerisation" method was retained for displacements in view of its relative simplicity.

In order to predict the oil film force and moment components at any combination of journal displacement and velocity components, equations [2] and [3] may be simply combined thus:

$$
\begin{aligned}
F_R = {} & A_{FRE} . \Delta e + A_{FR\xi} . \Delta \xi + A_{FR\psi} . \Delta \psi + A_{FR\varphi} . \Delta \varphi \\
& + A_{FRE\xi} . \Delta e . \Delta \xi + A_{FRE\psi} . \Delta e . \Delta \psi + A_{FRE\varphi} . \Delta e . \Delta \varphi \\
& + A_{FR\xi\psi} . \Delta \xi . \Delta \psi + A_{FR\xi\varphi} . \Delta \xi . \Delta \varphi + A_{FR\psi\varphi} . \Delta \psi . \Delta \varphi \\
& + A_{FRE\xi\psi} . \Delta e . \Delta \xi . \Delta \psi + A_{FRE\xi\varphi} . \Delta e . \Delta \xi . \Delta \varphi \\
& + A_{FRE\psi\varphi} . \Delta e . \Delta \psi . \Delta \varphi + A_{FR\xi\psi\varphi} . \Delta \xi . \Delta \psi . \Delta \varphi \\
& + A_{FRE\xi\psi\varphi} . \Delta e . \Delta \xi . \Delta \psi . \Delta \varphi + B_{FRE} . \dot{e} + B_{FR\xi} . \dot{\xi} \\
& + B_{FR\omega} . \omega_o + B_{FR\varphi} . \dot{\varphi} + B_{FRE\xi} . \dot{e} . \dot{\xi} + B_{FRE\omega} . \dot{e} . \omega_o \\
& + B_{FRE\varphi} . \dot{e} . \dot{\varphi} + B_{FR\xi\omega} . \dot{\xi} . \omega_o + B_{FR\xi\varphi} . \dot{\xi} . \dot{\varphi} \\
& + B_{FR\omega\varphi} . \omega_o . \dot{\varphi} + B_{FRE\xi\omega} . \dot{e} . \dot{\xi} . \omega_o + B_{FRE\xi\varphi} . \dot{e} . \dot{\xi} . \dot{\varphi} \\
& + B_{FRE\omega\varphi} . \dot{e} . \omega_o . \dot{\varphi} + B_{FR\xi\omega\varphi} . \dot{\xi} . \omega_o . \dot{\varphi} \\
& + B_{FRE\xi\omega\varphi} . \dot{e} . \dot{\xi} . \omega_o . \dot{\varphi} \qquad [4.]
\end{aligned}
$$

Once again the equations for F_T , M_R , M_T will follow the above form.

Equation [4] implicitly assumes that the principle of superposition is valid for combinations of displacement and velocity components. This is not so, but the probable level of errors incurred was considered to be acceptable, in view of the observation that displacement peaks tend to coincide with zero velocity, and vice-versa. It may be noted that the A_{FR} term has been dropped since at $\dot{\psi}, \dot{\varphi}, \dot{e}, \dot{\xi} = 0$ we have $\omega_o = \omega$ and both A_{FR} and $B_{FR\omega} . \omega_o$ are equal to the datum F_R .
In combining equations [2] and [3] to form [4] it is clearly necessary to drop one of these terms. Since $B_{FR\omega} . \omega_o$ was required to cover ω_o variation, A_{FR} was omitted

from equation [4]. This will generally cause a small error, since in most cases the positive ω_o perturbation used to compute $\beta_{FR\omega}$ will not be equal to ω . The error is due to the non-linearity of the F_R — ω_o relationship, and was found to cause a small difference in the location of the mean positions for orbits predicted with the linear and non-linear models. The coefficient β_{FR} has also been omitted in equation [4], since it has been shown to be zero. These comments are equally applicable to the coefficients for F_T , M_R and M_T .

The magnitude of the displacement and velocity perturbations, used to derive the non-linear coefficients, should correspond roughly to the anticipated level of displacement and velocity variation in the case to be analysed. This matching operation will determine the accuracy of the non-linear model. No sensitivity tests with respect to the above accuracy dependence have been carried out in this work, but previous tests (1) indicated the sensitivity level to be acceptable.

No attempt has been made to generalise the non-linear coefficients in this situation. In view of the complexity, and number of variables, the practicability of generalisation is considered to be questionable.

For utilisation of the non-linear model in the equations of motion for lateral vibration analysis, it was necessary to convert to the Cartesian form of equation [1]. The procedure for calculating the required Cartesian stiffness and damping coefficents followed that outlined in reference (8), where displacement and velocity perturbations were individually applied. In this analysis, the non-linear model was used to derive F_x, F_y, M_x, M_y instead of applying the film pressure relaxation solution, for each perturbation. This results in a substantial saving in computing time. The perturbations are set to the corresponding estimated displacement and velocity component changes during the current time step, and the datum conditions F_{Dx}, x_D, etc, are defined as those at the start time for that step. Note that these datum conditions change at each time step, and therefore differ from the fixed datum conditions upon which the non-linear coefficients are based. Appropriate Cartesian - Polar transformations are used when calling the subroutine for the non-linear model.

The non-linear terms F_{NLx}, etc. in equation [1] were introduced to correct for the non-applicability of the principle of superposition when using the 32 Cartesian oil film coefficients. During each time step, the displacement and velocity changes which defined the perturbations used to compute the 32 coefficients, do in fact occur simultaneously. The oil film forces and moments corresponding to the time step end conditions, i.e. with the above pertubations applied simultaneously, may be derived directly using the non-linear model. The non-linear correction terms F_{NLx}, etc. may then be calculated to make the forces and moments produced by equation [1] equal to those calculated directly for the time step end. Development tests indicated that these non-linear correction terms varied smoothly, and by reasonably small amounts, in relation to the rate of change of displacement and velocity components during the time stepping procedure.

Apart from the non-linear correction terms the main difference between the linear and non-linear versions of equation [1] is that the former uses fixed coefficients and datum conditions. The non-linear version, however, uses variable Cartesian coefficients and datum conditions corresponding to each time step start point.

CONCLUSIONS

A new form of non-linear oil film response model has been presented. This has been developed for use in the lateral vibration analysis of marine propeller shafting. It is applicable to circumferentially asymmetric bearings subject to dynamic misalignment conditions. The model was based on the results of a range of hydrodynamic analysis cases for the above bearing situation, some examples of which have been shown and discussed.

ACKNOWLEDGEMENTS

The author wishes to express his gratitude to the Committee of Lloyd's Register of Shipping for permission to publish this paper. In addition, the author is indebted to F.A. Martin of the Glacier Metal Co. Ltd., and J. Montgomery of Trent Polytechnic for their helpful discussions and comments.

REFERENCES

1. JAKEMAN R.W. "The Influence of Cavitation on the Non-Linearity of Velocity Coefficients in a Hydrodynamic Journal Bearing". Proc. 13th. Leeds - Lyon Tibol. Symp. Sept. 1986 pp 473-480.

2. HYAKUTAKE J., ASAI. R., INOUE. M, FUKAHORI K., WATANABE N. and NONAKE M. "Measurement of Relative Displacement between Sterntube Bearing and Shaft of 210,000 d.w.t. Tanker". Japan Shipbuilding and Marine Engineering Vol. 7 No. 1. 1973 pp 32-40.

3. JAKEMAN R.W. "Performance and Oil Film Dynamic Coefficients of a Misaligned Sterntube Bearing". A.S.L.E. Trans. Vol. 29 No. 4 Oct. 1986 pp 441-450.

4. BOOKER J.F. "Dynamically Loaded Journal Bearings: Numerical Application of the Mobility Method". Trans. A.S.M.E. Series F. Vol. 93 Jan. 1971 pp 168-176.

5. MOES H., SIKKES E.G. and BOSMA R. "Dynamic Analysis of Diesel Engine Main Bearings". Proc. 10th Leeds - Lyon. Tribol. Symp. Sept. 1983 pp 239-246.

6. CHILDS D., MOES H. and VAN LEEUWEN H. "Journal Bearing Impedance Descriptions for Rotordynamic Applications". A.S.M.E. Jnl. Lub. Tech. April 1977 pp 198-214.

7. MOES H., SIKKES E.G. and BOSMA R. "Mobility and Impedance Tensor Methods for Full and Partial - Arc Journal Bearings". A.S.L.E./A.S.M.E. Tribol. Conf. A.S.M.E. Paper No. 85 - Trib - 25 Oct. 1985.

8. JAKEMAN R.W. "A Numerical Analysis Method Based on Flow Continuity for Hydrodynamic Journal Bearings". Tribol. Int. Vol. 17. No.6 Dec. 1984. pp 325-333.

9. JAKEMAN R.W. "Numerical Analysis of Hydrodynamic Bearings with Significant Journal Lateral Velocities". Tribol. Int. Vol. 20. No. 4. Aug. 1987 pp 170-178.

10. BANNISTER R.H. "A Theoretical and Experimental Investigation Illustrating the Influence of Non-linearity and Misalignment on the Eight Oil Film Force Coefficients". Proc. I.Mech.E. Conf.. on Vibrations in Rotating Machinery, Paper C219/76. 1976 pp 271-278.

Table 1 "KEIYO MARU" After Sterntube Bearing Data

Dimensions:

D = 875 mm L = 2390 mm C_d = 1.6 mm

Conditions for Figs. 3 to 7.

ω = 9.1106 rads/s (87 R.P.M.) P_H = 0.12245 MPa.

η = 0.07201 Pa.s.

ϵ = 0.5363 ψ = 43.45°

$$\underbrace{\gamma = 3.6138.\ 10^{-5}\ \text{rad} \qquad \lambda = 3.0895.10^{-6}\ \text{rad}}$$

$$\equiv \left(\xi = 2.836.10^{-5}\ \text{rad}, \qquad \varphi = -2.261.10^{-5}\ \text{rad} \right)$$

At bearing ends:

Aft	ϵ = 0.57965	ψ = 40.110°
Forward	ϵ = 0.49509	ψ = 47.362°

Table 2 Non-Linear Coefficients

Order	No. of Coefficients	No. of Types	Total
0	1	1	1
1	4	2	8
2	6	4	24
3	4	8	32
4	1	16	16
	16		81

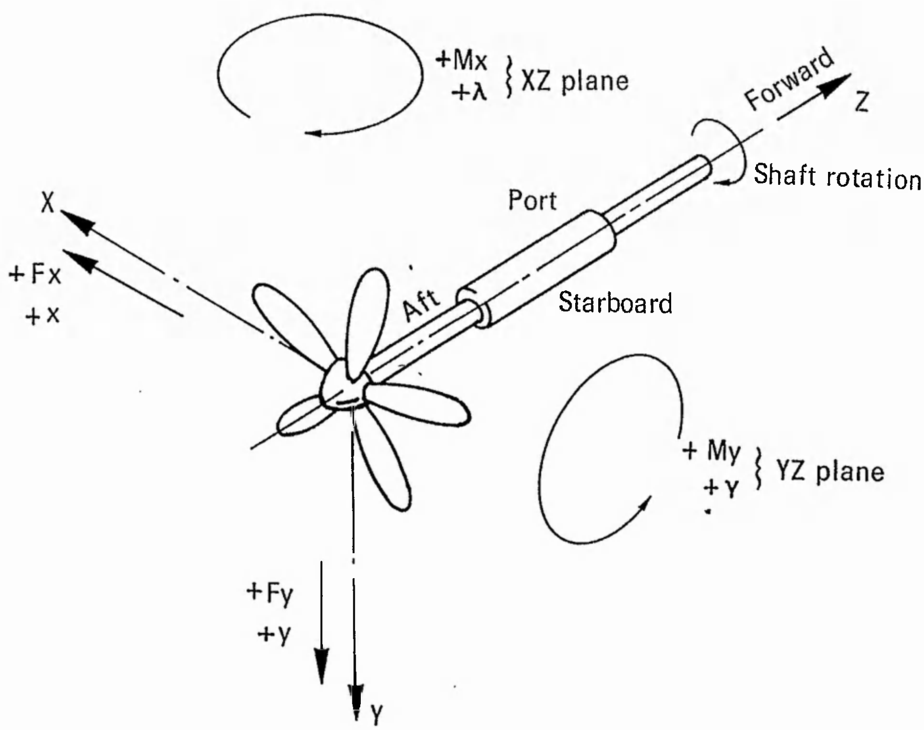

Fig 1 GENERAL SIGN CONVENTION.

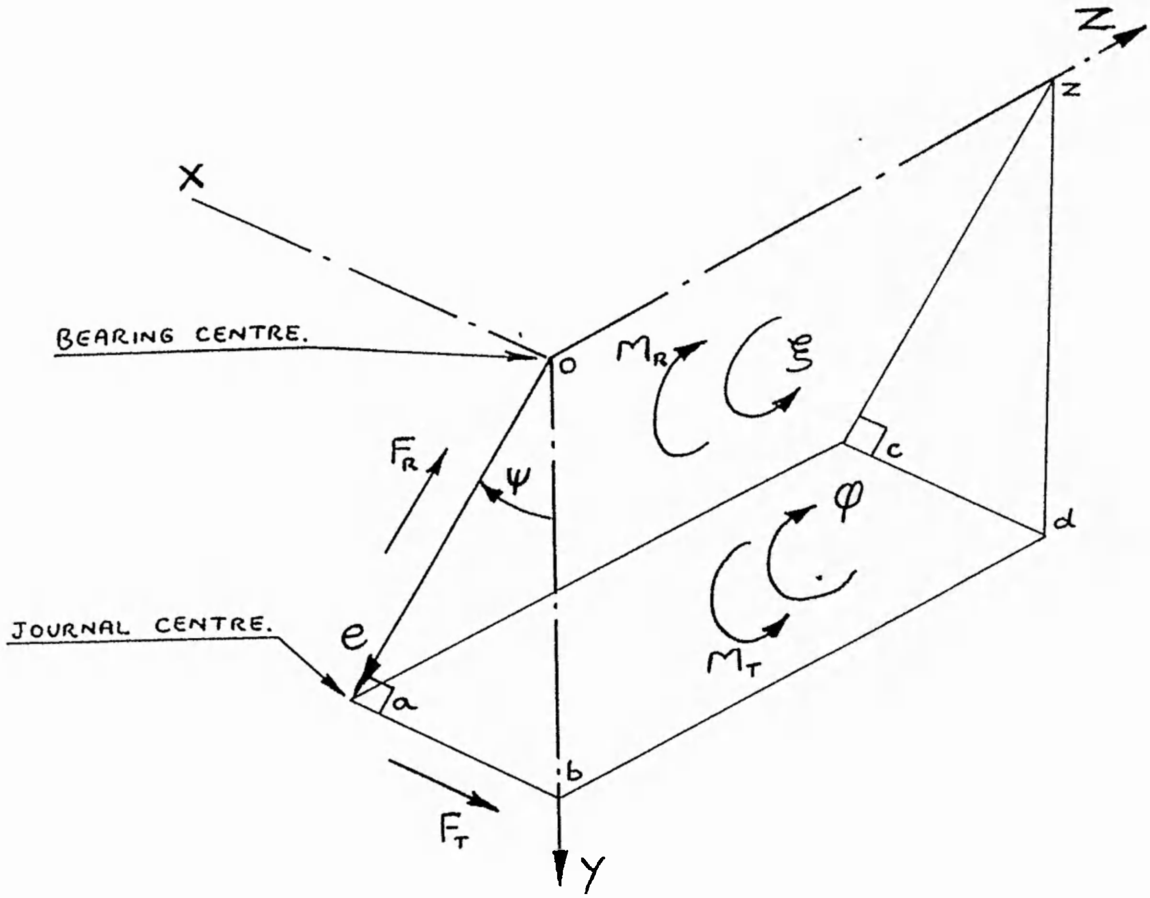

FIG. 2. BEARING POLAR SIGN CONVENTION.

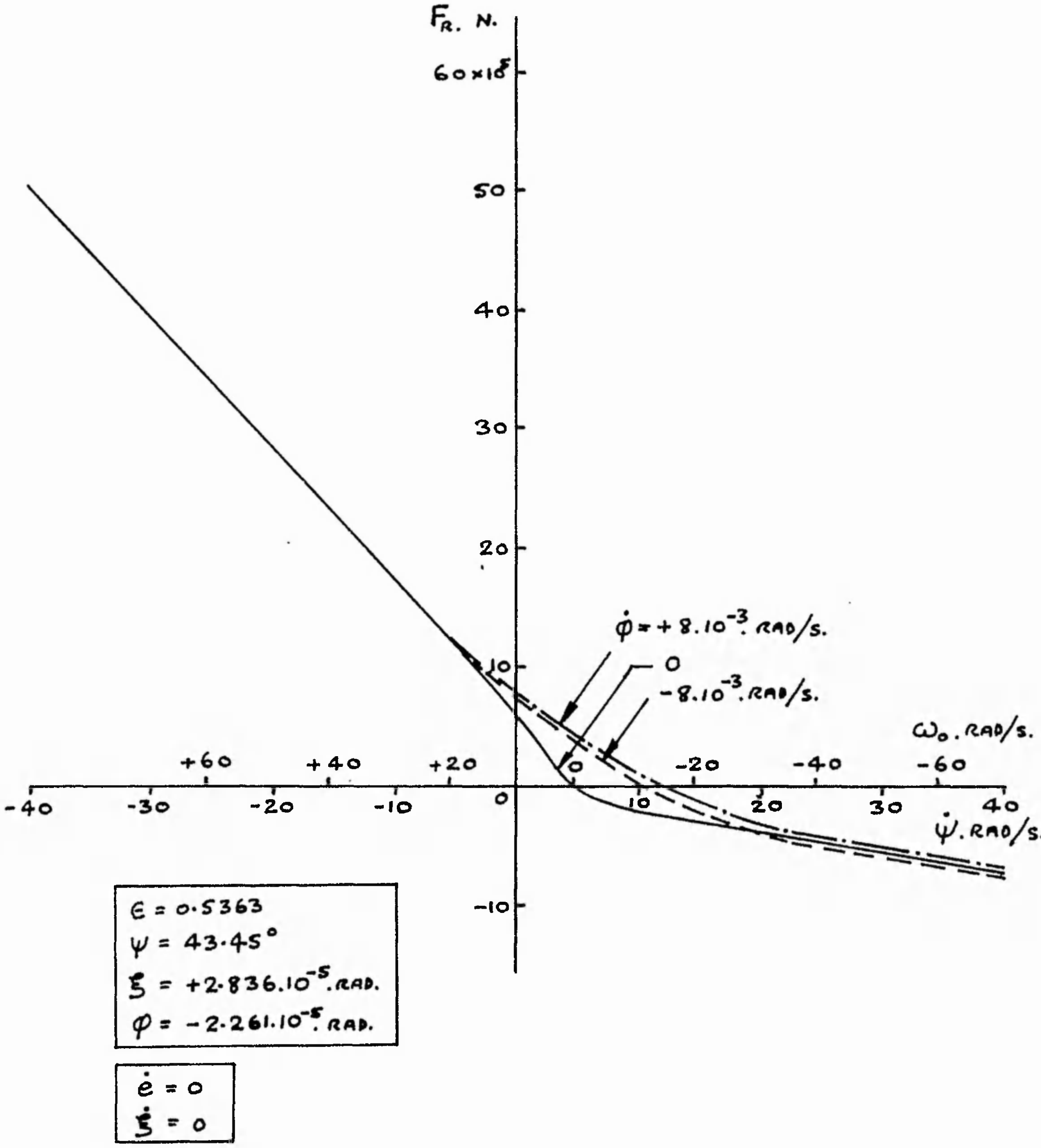

FIG. 3. F_R VARIATION WITH $\dot{\psi}$ (ω_o) (AND $\dot{\varphi}$).

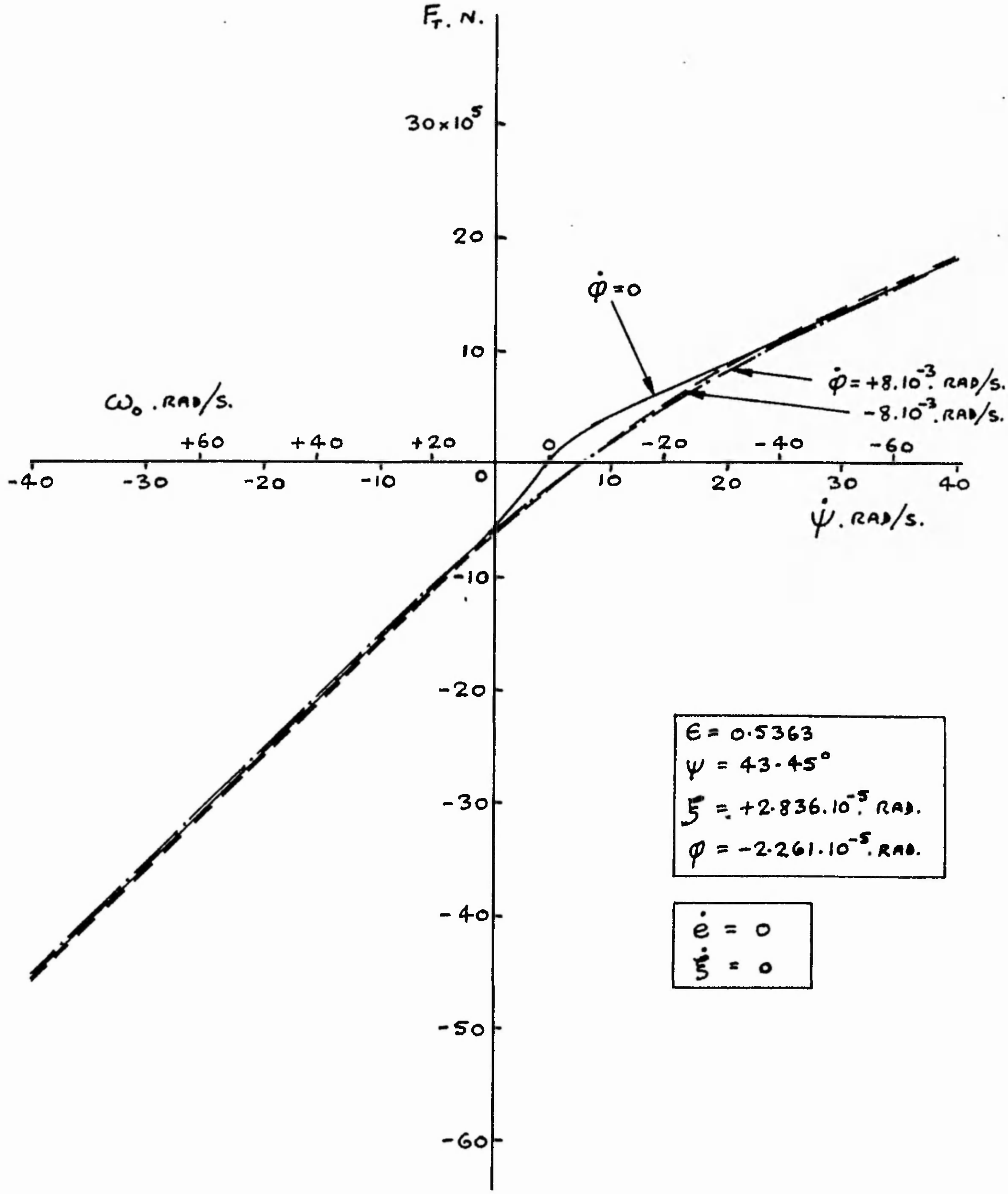

FIG. 4. F_T VARIATION WITH $\dot{\psi}$ (ω_o) (AND $\dot{\varphi}$).

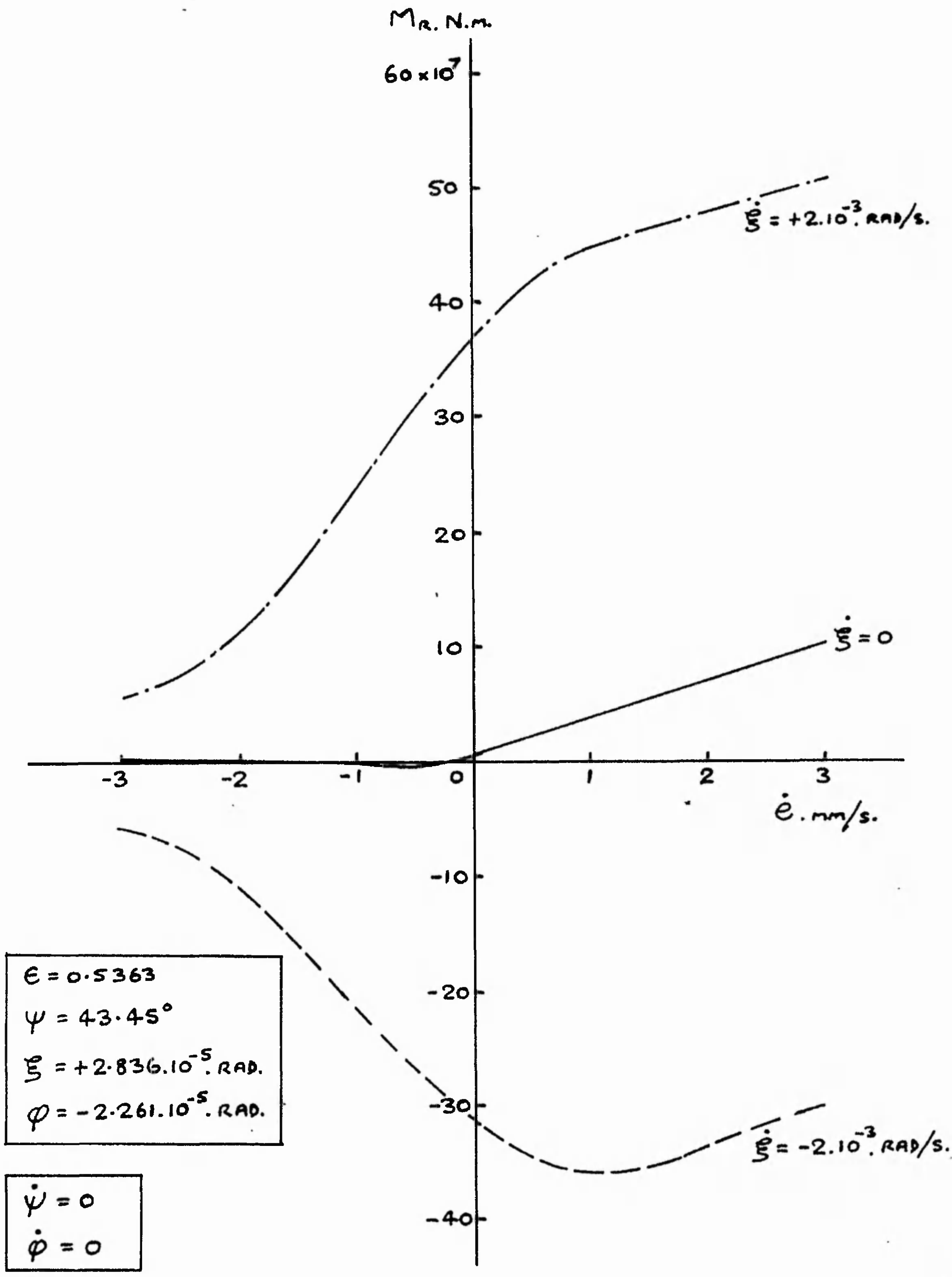

FIG. 5. M_R VARIATION WITH $\dot{e}$ (AND $\dot{\xi}$)

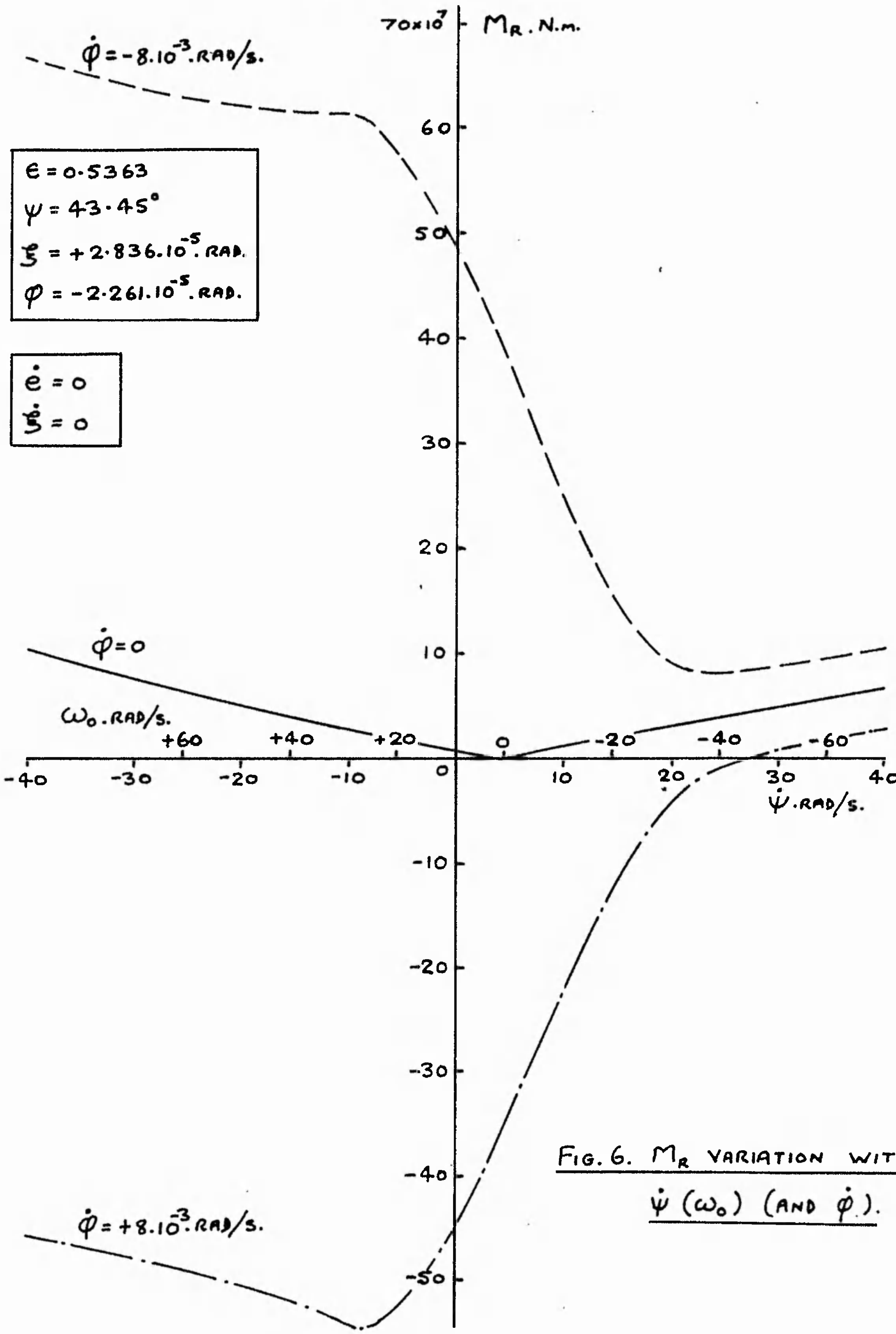

FIG. 6. M_R VARIATION WITH $\dot{\psi}$ (ω_o) (AND $\dot{\varphi}$).

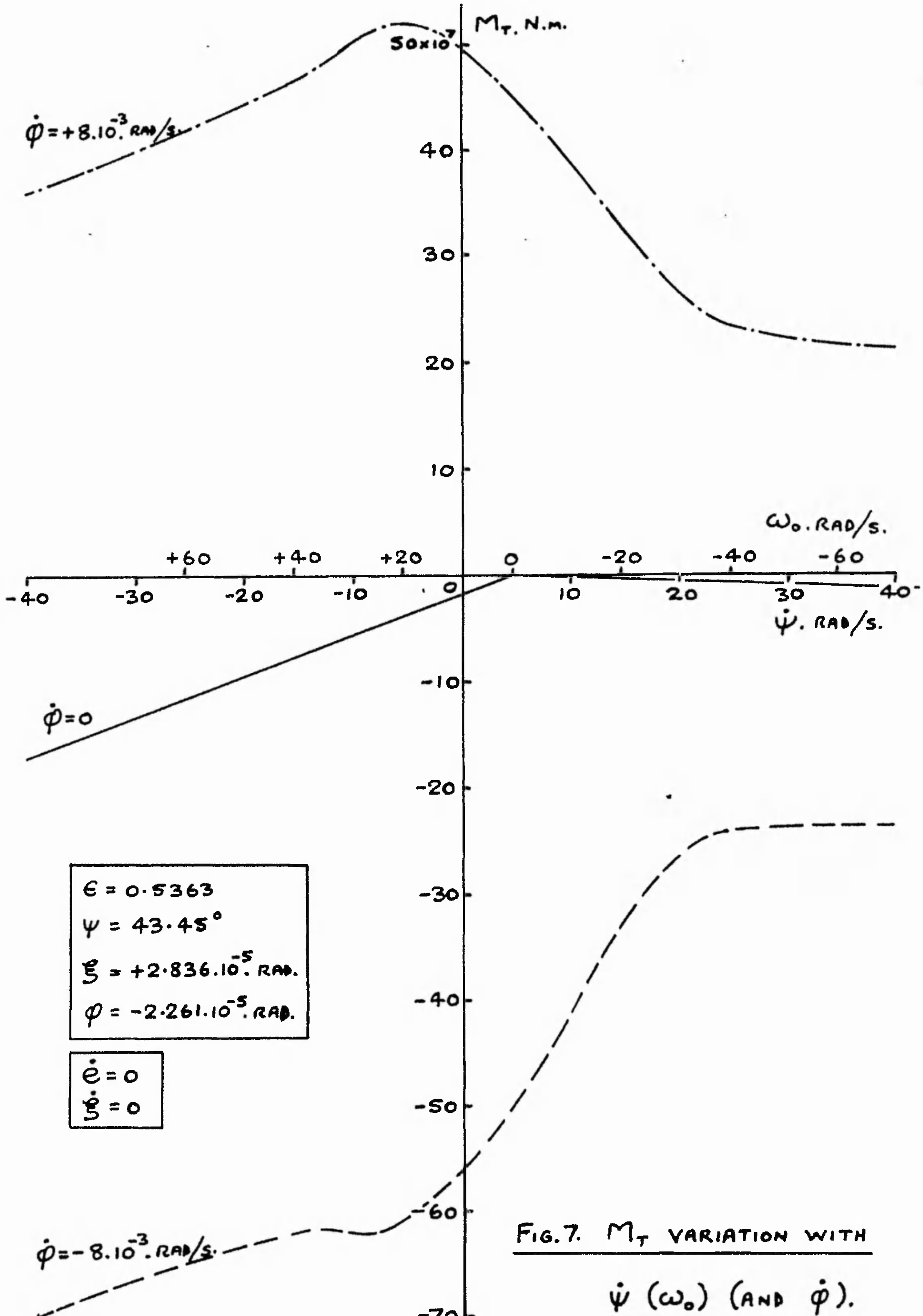

FIG. 7. M_T VARIATION WITH $\dot{\psi}$ (ω_0) (AND $\dot{\varphi}$).

REFERENCE. 92.

THE INFLUENCE OF STERNTUBE BEARINGS ON LATERAL VIBRATION AMPLITUDES IN MARINE PROPELLER SHAFTING

R.W. Jakeman

Abstract

In a previous paper (1) the steady load performance characteristics and oil film dynamic coefficients of a misaligned sterntube bearing were investigated. This paper reports further development in which the interaction of a sterntube bearing with the propeller shafting was considered in terms of the shafts lateral vibration.

Vibration amplitudes predicted with linear and non-linear after sterntube bearing oil film models, did not differ signifcantly. For the example case, the results indicated the effective damping to be in excess of critical. The predicted lateral vibration amplitude distribution along the shafting, with the after sterntube bearing length reduced to 54% of the original, showed the effectiveness of oil film angular stiffness and damping. A comparison with measured lateral vibrations by Hyakutake et al (2) gave good qualitative agreement with computed results, but a discrepancy in amplitude indicated substantial elastic deformation of the after sterntube bearing.

NOTATION

a	Shaft section area
A	Bearing oil film stiffness coefficient
B	Damping coefficient (general use)
C_d	Bearing diametral clearance
D	Journal diameter
e	Journal eccentricity at bearing axial centre
E	Young's Modulus for shaft material
F	Force
g	Gravitational acceleration
G	Shear Modulus for shaft material
I	Diametral second moment of area of shaft section
J	Diametral mass moment of inertia
J_p	Polar mass moment of inertia
K	Damping parameter
$K_1 - K_4$	Shaft elastic parameters. See equations [7] to [10]
ℓ	Shaft element length for stiffness
L	Bearing length
m	Mass
M	Moment
s	Displacement amplitude
S	Shaft element stiffness coefficient
t	Current time
T	Dynamic cycle time
W	Propeller entrained water (mass, inertia or coupled term)
x	Lateral displacement in horizontal direction
y	Lateral displacement in vertical direction

z Axial direction

λ Angular displacement in horizontal plane

γ Angular displacement in vertical plane

Δt Time step increment

ψ Journal attitude angle relative to y axis at bearing axial centre.

ϵ Journal eccentricity ratio $(2e/C_d)$.

ω Angular velocity of shaft rotation about z axis

ρ_s Density of shaft mass element material (steel)

ρ_F Density of fluid in which the mass element is immersed (sea water, oil or air)

Suffixes:

A Shaft element stiffness coefficient for angular displacement

B Bearing

c Critical frequency

D Datum condition for oil film force and moment

F Shaft element stiffness coefficient for force

I Inertial

L Shaft element stiffness coefficient for lateral displacement

m Shaft element stiffness coefficient for moment

N Mass station number

NL Non-linear correction factor for oil film force or moment

P Propeller

S Shaft element

W Propeller-wake.

x	Horizontal direction	Refers to lateral displacement or velocity in linear oil film coefficient
y	Vertical direction	
Δ	Value at $t + \Delta t$	
λ	Horizontal plane	Refers to angular displacement or velocity in linear oil film coefficient
γ	Vertical plane	

Sign Convention:

Fig. 2 shows the general sign convention

Introduction

Sterntube bearings are quite unique with respect to the nature and complexity of their operating environment, and their relatively large length to diameter ratios. This situation has been previously described, and some predicted sterntube bearing performance characteristics presented (1). Particularly interesting operational features are the steady and dynamic components of angular misalignment, which are rendered significant by unusually large bearing lengths. This misalignment is the result of cantilever loading comprising the propeller weight, and hydrodynamic forces and moments due to the operation of the propeller in a non-uniform wake field generated by the hull.

The previous work (1) was essentially concerned with the performance of the sterntube bearing itself, with the object of ensuring that operating conditions were satisfactory. This work also included the prediction of linearised oil film stiffness and damping coefficients covering dynamically misaligned operating conditions. The application of these coefficients to the shafting dynamics was not inlcuded.

In this paper, the influence of the sterntube bearing on lateral vibration amplitudes in marine propeller shafting is examined. A description is given of the time stepping analysis method used, which inlcudes alternative linear and non-linear bearing oil film models. The development of the non-linear oil film model will be reported in a separate paper.

Measurements made by Hyakutake et al (2) on the 210,000 deadweight ton tanker "KEIYO MARU", are used for correlation with the results of the analysis method. Details of the propeller shafting system of this vessel are given in Fig. 1. The predicted lateral vibration amplitudes are dependent on the propeller performance characteristics and wake field data. Detailed consideration of the methods of estimating propeller related data are outside the scope of this paper.

A clear need for a realistic lateral vibration amplitude prediction facility, for marine propeller shafting, has been highlighted by the inadequacy of commonly used lateral vibration analysis programs. The problem is that these programs are restricted to lateral vibration resonant frequency prediction only. Their use has resulted in an over-conservative approach in many cases. This has been demonstrated by several examples in which lateral vibration resonance has been predicted within the operating speed range. Subsequent measurements during trials have shown little or no discernable resonant response. The propeller shafting of the "KEIYO MARU", in which Hyakutake et al (2) made their measurements, had a predicted fundamental mode lateral vibration resonance in the region of the service speed. This made it a particularly interesting analysis test case.

The main objective of this work, was to develop an analysis method for the prediction of lateral vibration amplitudes in marine propeller shafting. An additional objective was the investigation of the influence of sterntube bearings on lateral vibration amplitudes. This incorporated a comparison of results obtained with alternative linear and non-linear oil film models for the after sterntube bearing.

LITERATURE REVIEW

Previous Publications

With regard to lateral vibration amplitude prediction in marine propeller shafting, relatively few papers have been published. The following is an outline of the main developments in the last nine years:

Hylarides and Gent (3) predicted torsional, axial and lateral vibrations excited by the propeller - wake field interaction. The model used, however, was rather simple in that the only mass considered was that of the propeller. Linear stiffness terms were used to cover, collectively, elastic deflections of the shafting and surrounding hull structure, and the bearing oil film response. The excitation was apparently assumed to be sinusoidal, thus permitting a direct solution (i.e. non-time stepping) of the dynamic response. This paper was mainly concerned with the effects of propeller damping and entrained water. Bearing oil film damping was not included, which is a significant omission.

The later paper by Hayama and Anoda (4) was similar to that of Hylarides and Gent (3) in the use of a single mass (propeller) model. Other points of similarity were the approximation of the propeller-wake field excitation to sinusoidal form, and the use of combined structural and oil film linear stiffness terms. In this case, however, the vertical and horizontal stiffness terms were assumed to be equal, and cross coupling terms were not considered. Hayama and Anoda dealt more explicitly with the estimation of propeller excitation using the quasi-steady theory for simplicity. No specific reference to bearing damping was made, and it is assumed that again this was neglected.

A much more realistic propeller shafting lateral vibration model was presented in the recent paper by Karni et al (5). Non-sinusoidal propeller-wake field excitation could be handled by this analysis method, although sinusoidal excitation, in the vertical direction only, was used in the example case given. The other advances over the previous analyses in this field were the use of a multi mass-elastic system, and a finite element analysis of the after sterntube bearing oil film, the other bearings being simply represented by linear stiffness terms. Oil film cavitation was modelled by the rather approximate procedure of simply truncating negative pressures after solution of the pressure distribution. In view of the non-linearity of the oil film model, and the acceptance of non-sinusoidal excitation, a time stepping type of solution was necessary. The three dimensional finite element analysis of the shafting included bending, shear, axial and elastic foundation effects. Unlike the previously cited propeller shafting analyses, the analysis by Karni et al did not appear to consider gyroscopic effects. The example case used in the paper was a fairly simple test rig, for which only steady load results were available.

<u>Relationship of the paper with previous work</u>

The paper by Karni et al (5) is the most recent known to have been published in the area of marine propeller shafting analysis. It is consequently the most comparable to the work described in this paper. In terms of analysis advancement, the most significant contribution of this work is the use of pre-computed coefficients for the estimation of bearing oil film forces and moments. This yields a substantial reduction in computing time, as indicated by Jakemen (6) in the earlier work on aligned bearings. Comparative results have been produced with both linear and non-linear oil film models. For an example case, the choice of the real propeller shafting system, from which measurements were taken by Hyakutake et al (2), is considered to enhance the value of this work.

The close proximity of the predicted fundamental mode lateral vibration resonance to the service speed, made the inclusion of shaft mass in the model essential. It was noted that Karni et al (5) took account of propeller thrust, using the mean value only. In the example case, fundamental mode lateral resonant speeds predicted with and without propeller thrust were separated by only 0.5 r.p.m. The simplification of omitting consideration of propeller thrust from this analysis was therefore regarded as justifiable.

It is acknowledged that propeller thrust may have a significant influence in more slender shafting systems.

MASS-ELASTIC MODEL

In this section, all the features of the mass-elastic model will be outlined. This model is used for the lateral vibration analysis, and the numerical data refers specifically to the "KEIYO MARU" test case. Most of the data were kindly provided by Mitsubishi Heavy Industries, but that which related to propeller entrained water and wake excitation had to be estimated.

Mass-Elastic Element Distribution

The mass-elastic model adopted is shown in Fig. 3, and is seen to comprise a three bearing system with six concentrated mass elements joined by six massless elastic shaft elements.

Mass element 1 (m_1) includes the propeller and entrained water plus half the mass of shaft element 1 (S_1). The remaining mass elements comprise half the mass of each of the adjacent shaft elements except for m_6 which inlcudes half the mass of S_5 and an equal mass from S_6 . For stiffness computation, a built in forward end condition at the location of the forward plummer bearing was specified for S_6 This was a somewhat coarse approximation to the real situation, but it was considered to be adequate since all the excitation was applied to the aft end of the shafting. The lateral vibration amplitudes at the forward end of the shafting were therefore assumed to be small.

Each element had four degrees of freedom : x, y, λ, γ.
In the above outline only the term mass was used for simplicity, but since angular element motion was considered, diametral mass moment of inertia was also covered by this term. Gyroscopic effects were accounted for in each element, therefore the above reference to mass also included polar mass moment of inertia.

Propeller Wake Excitation

The estimated force and moment components acting on the propeller, due to its interaction with the wake field, are given in Fig. 4. This is the only form of excitation considered, since out of balance forces should be relatively small, and excitation from the geared steam turbine drive would be of low amplitude and high frequency, and therefore insignificant.

A quasi-steady analysis was used to estimate the propeller-wake excitation. This is a simple approximate method, and for greater accuracy the unsteady lifting surface theory should be used. Since no wake field data was available for the "KEIYO MARU", use was made of a typical tanker wake field with a consequently uncertain accuracy. The employment of a quasi-steady method was therefore consistent with the limited accuracy attainable. Only the wake field for axial components of water flow were considered, and this was taken to be symmetrical about the y axis.

Propeller Entrained Water

Vibrating marine propellers tend to entrain a certain quantity of adjacent water. This adds to their effective mass and mass moments of inertia by amounts that are significant with respect to the lateral vibration of the shafting. Various coupling effects exist which render the situation fairly complex as shown by the following equation:

$$\begin{bmatrix} F_{IY} \\ F_{IX} \\ M_{IY} \\ M_{IX} \end{bmatrix} = \begin{bmatrix} m + W_{YY} & W_{YX} & W_{Y\gamma} & W_{Y\lambda} \\ W_{XY} & m + W_{XX} & W_{X\gamma} & W_{X\lambda} \\ W_{\gamma Y} & W_{\gamma X} & J + W_{\gamma\gamma} & W_{\gamma\lambda} \\ W_{\lambda Y} & W_{\lambda X} & W_{\lambda\gamma} & J + W_{\lambda\lambda} \end{bmatrix} \cdot \begin{bmatrix} \ddot{y} \\ \ddot{x} \\ \ddot{\gamma} \\ \ddot{\lambda} \end{bmatrix} \quad \text{...[1]}$$

The novel notation W has been chosen since the entrained water terms represent not only mass and diametral mass moment of inertia, but also cross mass-inertia terms; e.g. $W_{Y\gamma}$. All the entrained water terms have been given a unique designation for clarity, but due to the symmetry of a propeller many are in fact identical, e.g. $W_{YY} = W_{XX}$; $W_{Y\gamma} = W_{X\lambda}$; $W_{\lambda\gamma} = W_{\gamma\lambda}$; etc.

Entrained water associated with propeller vibration along and about the z axis is not coupled to that covered by equation [1]. The polar mass moment of inertia required for the gyroscopic terms therefore requires only one entrained water term. For simplicity the J_p value relating to the propeller includes entrained water.

The entrained water data was obtained from a computer program based on the work by Parsons and Vorus (7).

Propeller Damping Forces and Moments

A vibrating propeller clearly experiences damping due to the surrounding water. The format for the presentation of propeller damping terms is similar to that for entrained water:

$$\begin{bmatrix} F_{px} \\ F_{py} \\ M_{px} \\ M_{py} \end{bmatrix} = \begin{bmatrix} B_{xx} & B_{xy} & B_{x\lambda} & B_{x\gamma} \\ B_{yx} & B_{yy} & B_{y\lambda} & B_{y\gamma} \\ B_{\lambda x} & B_{\lambda y} & B_{\lambda\lambda} & B_{\lambda\gamma} \\ B_{\gamma x} & B_{\gamma y} & B_{\gamma\lambda} & B_{\gamma\gamma} \end{bmatrix} \cdot \begin{bmatrix} \dot{x} \\ \dot{y} \\ \dot{\lambda} \\ \dot{\gamma} \end{bmatrix} \qquad \text{.......} [2.]$$

Equality of some damping coefficients due to propeller symmetry is also similar to that for entrained water, and the source of data (7) was the same.

Polar damping (for rotation about the z axis) was not required in this work.

Bearing Oil Film Forces and Moments

The bearing oil film forces and moments are given by the following equation:

$$\begin{bmatrix} F_{BXN} \\ F_{BYN} \\ M_{BXN} \\ M_{BYN} \end{bmatrix} = \begin{bmatrix} A_{XXN} & A_{XYN} & A_{X\lambda N} & A_{X\gamma N} \\ A_{YXN} & A_{YYN} & A_{Y\lambda N} & A_{Y\gamma N} \\ A_{\lambda XN} & A_{\lambda YN} & A_{\lambda\lambda N} & A_{\lambda\gamma N} \\ A_{\gamma XN} & A_{\gamma YN} & A_{\gamma\lambda N} & A_{\gamma\gamma N} \end{bmatrix} \cdot \begin{bmatrix} x_N - x_{DN} \\ y_N - y_{DN} \\ \lambda_N - \lambda_{DN} \\ \gamma_N - \gamma_{DN} \end{bmatrix} +$$

$$\begin{bmatrix} B_{XXN} & B_{XYN} & B_{X\lambda N} & B_{X\gamma N} \\ B_{YXN} & B_{YYN} & B_{Y\lambda N} & B_{Y\gamma N} \\ B_{\lambda XN} & B_{\lambda YN} & B_{\lambda\lambda N} & B_{\lambda\gamma N} \\ B_{\gamma XN} & B_{\gamma YN} & B_{\gamma\lambda N} & B_{\gamma\gamma N} \end{bmatrix} \cdot \begin{bmatrix} \dot{x}_N - \dot{x}_{DN} \\ \dot{y}_N - \dot{y}_{DN} \\ \dot{\lambda}_N - \dot{\lambda}_{DN} \\ \dot{\gamma}_N - \dot{\gamma}_{DN} \end{bmatrix} + \begin{bmatrix} F_{DXN} \\ F_{DYN} \\ M_{DXN} \\ M_{DYN} \end{bmatrix} + \begin{bmatrix} F_{NLXN} \\ F_{NLYN} \\ M_{NLXN} \\ M_{NLYN} \end{bmatrix}$$

...... [3]

The above equation may be used for both linear and non-linear oil film models. Full details are given in a separate paper describing the development of the non-linear model.

Datum conditions used for the computation of the linearised bearing oil film coefficients are given in Table 1. The corresponding displacement and velocity perturbations used are given in Table 2. In Table 3 the linearised coefficients are presented together with the entrained water and damping coefficients for the propeller. The computation of coefficients for the aft sterntube bearing non-linear model was based on the corresponding datum conditions of Table 1. Polar displacement and velocity pertubations of the same order of magnitude as the corresponding Cartesian pertubations in Table 2 were also used.

Shaft Elastic Forces and Moments

Relative lateral and angular displacements of adjacent mass stations results in the induction of elastic forces and moments in the shaft elements that join them. The elastic forces and moments acting on mass station N are given by:

$$F_{SYN-1} = S_{FLN-1}.(y_N - y_{N-1}) + S_{FAN-1}.(\gamma_N + \gamma_{N-1}) \quad \text{....[4]}$$

$$M_{SYN-1} = S_{MLN-1}.(y_N - y_{N-1}) + S_{MAON-1}.\gamma_N - S_{MAEN-1}.\gamma_{N-1} \quad \text{...[5]}$$

$$F_{SYN} = S_{FLN}.(y_N - y_{N+1}) - S_{FA}.(\gamma_N + \gamma_{N+1}) \quad \text{....[6]}$$

$$M_{SYN} = -S_{MLN}.(y_N - y_{N+1}) + S_{MAO}.\gamma_N - S_{MAEN}.\gamma_{N+1} \quad \text{---[7]}$$

where:

$$S_{FLN-1} = S_{FLN} = -1/K_1$$

$$S_{FAN-1} = S_{FAN} = -1/K_2$$

$$S_{MLN-1} = S_{MLN} = -K_3 . K_4 / K_1$$

$$S_{MAON-1} = S_{MAON} = -K_3 \left(1 + K_4 / K_2\right)$$

$$S_{MAEN-1} = S_{MAEN} = -K_3 \left(1 - K_4 / K_2\right)$$

and:

$$K_1 = \frac{\ell^3}{12EI} + \frac{2\ell}{3Ga} \quad ; \quad K_2 = \frac{\ell^2}{6EI} + \frac{4}{3Ga} \quad ;$$

$$K_3 = \frac{EI}{\ell} \quad ; \quad K_4 = \frac{\ell^2}{2EI} + \frac{4}{3Ga}$$

Note that ℓ, a and I must correspond to the shaft element for which the stiffness coefficient is being calculated.

The above equations relate to the y direction and yz plane, but their format is equally valid for the x direction and xz plane, and the corresponding stiffness coefficients are identical. There is no cross coupling between the y and x axes. The equations were derived from simple bending and shear theory, taking a shear factor of 0.75 for the circular section shaft.

Equations of Motion

The general equations of motion for any mass element in the shafting system are as follows:

$$(m_N + W_{xx}).\ddot{x}_N + W_{xy}.\ddot{y}_N + W_{x\lambda}.\ddot{\lambda}_N + W_{x\gamma}.\ddot{\gamma}_N$$
$$= F_{wx} + F_{sxN-1} + F_{sxN} + F_{pxN} + F_{BxN} \text{ --------- } [8]$$

$$W_{yx}.\ddot{x}_N + (m_N + W_{yy}).\ddot{y}_N + W_{y\lambda}.\ddot{\lambda}_N + W_{y\gamma}.\ddot{\gamma}_N$$
$$= F_{wy} + F_{syN-1} + F_{syN} + F_{pyN} + F_{ByN} + m_N.g.\left(\frac{\rho_s - \rho_F}{\rho_s}\right)$$
$$\text{-------} [9]$$

$$W_{\lambda x}.\ddot{x}_N + W_{\lambda y}.\ddot{y}_N + (J_N + W_{\lambda\lambda}).\ddot{\lambda}_N + W_{\lambda\gamma}.\ddot{\gamma}_N - J_{pN}.\omega.\dot{\gamma}_N$$
$$= M_{wx} + M_{sxN-1} + M_{sxN} + M_{pxN} + M_{BxN} \text{ ------- } [10]$$

$$W_{\gamma x}.\ddot{x}_N + W_{\gamma y}.\ddot{y}_N + W_{\gamma\lambda}.\ddot{\lambda}_N + (J_N + W_{\gamma\gamma}).\ddot{\gamma}_N + J_{pN}.\omega.\dot{\lambda}_N$$
$$= M_{wy} + M_{syN-1} + M_{syN} + M_{pyN} + M_{ByN} \text{ ------ } [11]$$

In view of the general format of the above equations, the following points related to specific mass elements should be noted:

1. The entrained water terms W_{xx}, etc. and propeller-wake excitation terms F_{wx}, etc. are applicable to the propeller (m_1) only, and are zero for the remaining mass elements.

2. The aft shaft elastic forces and moments F_{SXN-1}, etc. are zero for m_1 since there is no shafting aft of the propeller.

3. The full matrix of damping terms covered by F_{PXN}, etc. is applicable to the propeller (m_1) only. It was, however, found to be necessary to apply small amounts of direct damping B_{XXN}, B_{YYN}, $B_{\lambda\lambda N}$, $B_{\gamma\gamma N}$ to mass elements that would otherwise be undamped, in order to maintain stability in the time stepping process. The terms F_{PXN}, etc with the above direct damping coefficients only, were therefore applied to m_3 and m_5.

4. The bearing force and moment terms F_{BXN}, etc. are zero for mass elements other than those in way of bearings. Note that for the aft sterntube bearing (m_2), either the linear or non-linear oil film model could be selected. Only linear models were used for the other two bearings.

Time Step Solution

The time step solution was based on that described by Jakeman (8) for a single mass system. This involves writing the equations of motion [8] to [11] in terms of the mean conditions during a time step from t to $t + \Delta t$. The following features are incorporated in this approach:

1. The acceleration terms may be expressed as:

$$\overline{\ddot{x}_N} = (\dot{x}_{N\Delta} - \dot{x}_N) / \Delta t \qquad \ldots\ldots\ldots [12]$$

and similarly for $\overline{\ddot{y}_N}$, $\overline{\ddot{\lambda}_N}$, $\overline{\ddot{\gamma}_N}$.

2. Acceleration is assumed to vary linearly with time during the step, therefore it can be shown that:

$$\dot{x}_{N\Delta} = \frac{3}{\Delta t}(x_{N\Delta} - x_N) - 2\dot{x}_N - \frac{\Delta t}{2} . \ddot{x}_N \qquad \ldots\ldots [13]$$

and similarly for $\dot{y}_{N\Delta}$, $\dot{\lambda}_{N\Delta}$ and $\dot{\gamma}_{N\Delta}$.

Note that in equation [13], $\ddot{x}_N$ refers to the start of the time step at t. $\overline{\ddot{x}_N}$ in equation [12] represents the mean acceleration during the time step as substituted for the $\ddot{x}_N$ terms in the equations of motion [8] to [11].

3. All force and moment terms on the right hand side of equations [8] to [11] are assumed to vary linearly with time during the step therefore:

$$\overline{F_{BYN}} = (F_{BYN\Delta} + F_{BYN}) / 2 \quad ; \quad \text{etc.} \quad \ldots. [14].$$

4. The mean angular velocities of the shaft rotational axis z , for the gyroscopic terms, were taken as

$(\dot{\lambda}_{N\Delta} + \dot{\lambda}_N) / 2$ and $(\dot{\gamma}_{N\Delta} + \dot{\gamma}_N) / 2$.

This is not consistent with the assumption of linear variation of acceleration, but having regard to the significance of the gyroscopic terms, the likely errors were considered to be acceptable.

The conditions at the time step start point t will be known, and the conditions at the end point $t + \Delta t$ may be solved by means of equations [8] to [11] in the following manner:

1. The acceleration terms on the left hand sides are replaced by $(\dot{x}_{N\Delta} - \dot{x}_N)/\Delta t$; etc.
2. Propeller-wake excitation forces and moments are replaced by $(F_{wx\Delta} + F_{wx})/2$; etc. These forces and moments may be obtained for both t and $t + \Delta t$ from Fig.4.
3. Shaft element elastic forces and moments are replaced by $(F_{sxN-1\Delta} + F_{sxN-1})/2$; etc. and the appropriate coefficient expressions in accordance with equations [4] to [7] are then substituted.
4. Propeller and general damping forces and moments are replaced by $(F_{pxN\Delta} + F_{pxN})/2$; etc. and coefficient expressions in accordance with equation [2] are then substituted.
5. Bearing forces and moments are replaced by $(F_{BxN\Delta} + F_{BxN})/2$ etc. and coefficient expressions in accordance with equation [3] substituted.
6. In the resulting equations of motion for the mean conditions during the time step, all velocity components at $t + \Delta t$ were then subject to substitutions of the form given in equation [13]. This reduced the unknown quantitites, at $t + \Delta t$ in the equations of motion for the mean time step conditions, to displacement terms only.
7. For each of the six mass elements there are four equations of motion corresponding to [8] to [11]. Since these equations had been reduced to a form in which they contained the twenty four unknown displacements

($x_{N\Delta}$, $y_{N\Delta}$, $\lambda_{N\Delta}$, $\gamma_{N\Delta}$ for N = 1 to 6), they could be solved by separating the known terms and performing a matrix inversion solution.

8. A steady equilibrium solution for any given constant propeller-wake force and moment components could also be obtained by means of equations [8] to [11]. This was achieved by reverting to the instantaneous parameter form in place of the time step mean parameter form. The accelerations and velocities were then set to zero, and the equations solved for the equilibrium displacements (x_N, y_N, λ_N, γ_N for N = 1 to 6) by matrix inversion as above.

Time Stepping Procedure

The time stepping procedure may be started from an arbitary set of displacement, velocity and acceleration components for all of the mass elements. It is then continued until the cyclic variation of the above parameters converges to an acceptable degree. The time required for convergance will clearly depend upon the starting conditions chosen, and upon the degree of damping in the system being modelled. In this work the procedure was started from the time corresponding to a rotation angle of 30°, with the displacements determined by an equilibrium solution using F_{WX}, F_{WY}, M_{WX}, M_{WY} for that angle taken from Fig. 4. The selection of a rotation angle of 30° was due to there being no substantial variation of F_{WX}, F_{WY}, M_{WX}, M_{WY} for a reasonable time after that point. This facilitated a smooth start to the time stepping procedure.

The time stepping type of analysis is prone to numerical instability problems. In order to deal with instability, the simplest method is to use very small time step durations. This can lead to excessive computing times, and several methods for containing instability, whilst permitting reasonable time step durations, have been used. The method used in this work was based on that outlined by Jakeman (8), and is shown in simplified form by Fig. 5. Although this method was found to work satisfactorily, the program is in an early stage of development, and substantial refinement is undoubtedly feasible.

RESULTS

Comparison of Predicted and Measured Journal Orbits

Predicted journal orbits and those measured by Hyakutake et al (2) at the aft and forward ends of the aft sterntube bearing and at the forward sterntube bearing, are shown in Figs. 6, 7 and 8 respectively. The aft sterntube bearing ends are a significant distance from its axial centre, at which the predicted data were computed, i.e. at m_2 . In order to refer the predicted data to the bearing ends for Figs. 6 and 7, interpolation of the data for m_1 and m_2 and for m_2 and m_3 respectively, was carried out assuming a linear variation of slope (λ, γ).

The following observations may be made with respect to these results:

1. Journal orbits predicted with the linear and non-linear

aft sterntube bearing oil film models did not differ in any significant way. The small difference in the mean position of the orbits was due to the formulation of the non-linear model. This is explained in a separate paper covering the development of the non-linear model.

2. The measured orbits are seen to be significantly larger than those predicted, particularly in the vertical direction.

3. For the aft sterntube bearing the measured orbits indicate a substantial negative misaligment in the horizontal plane (mean λ). The predicted orbits have a positive horizontal misalignment of smaller magnitude.

4. All orbits, measured and predicted, are clockwise.

5. Both measured and predicted orbits at the forward and aft ends of the aft sterntube bearing are in antiphase. The journal is therefore tending to pivot about a point within the bearing, and the angular motion of the journal axis is significant.

6. Agreement between measured and predicted orbits is better at the forward sterntube bearing.

7. The location of the journal orbits within the clearance circle of the forward sterntube bearing is consistent with the indication of Mitsubishi Heavy Industries, that this bearing was unloaded. The diamteral clearance of the forward sterntube bearing was 2.12 mm compared with 1.60 mm for the aft sterntube bearing. This larger

clearance clearly promoted the unloading of the forward sterntube bearing.

Reasonant Response

As previously indicated, a lateral vibration resonant frequency prediction was carried out for the "KEIYO MARU" shafting system. A program of the type described by Toms and Martyn (9) was used to perform the above analysis. This indicated the fundamental resonance to occur at about the test condition speed of 87 rpm. Due to gyroscopic effects, two resonant speeds are given by the above program, these corresponding to the forward and backward whirl modes. Exact resonant speeds cannot be given due to a degree of uncertainty regarding the precise effective bearing support stiffness.

In view of the above situation, it was considered to be particularly desirable to investigate the predicted lateral vibration amplitudes over a range of speeds covering the predicted resonance. This included the hypothetical response at zero shaft speed using the steady equilibrium solution at regular angles of rotation in conjunction with the Fig. 4 excitation data. Constant excitation and stiffness and damping values, corresponding to 87 r.p.m., were maintained throught these tests. The predictions at speeds other than 87 r.p.m. are somewhat academic, since the excitation and oil film stiffness and damping will all vary significantly with shaft speed. However, the essential purpose of this exercise was to explore the amplitude response in the region of the predicted resonance. In particular this part of the investigation was intended to determine the effective level of damping, since the "KEYO MARU" appeared to be operating virtually on the fundamental lateral vibration resonance. For the above objectives, the assumption of constant excitation, stiffness and damping was acceptable, and in relation to the investigation method used, it was appropriate.

The results for these tests are shown by the plotted points in Fig. 9 as the vertical and horizontal components of displacement amplitude at the propeller. In order to assess the predicted response, curves were fitted to the data points at 0, 77 and 97 r.p.m. using the classical single mass forced-damped response form of equation:

$$\frac{S}{S_o} = \left[\left\{1-\left(\frac{\omega}{\omega_c}\right)^2\right\}^2 + \left(\frac{K}{\omega_c}\right)^2 \cdot \left(\frac{\omega}{\omega_c}\right)^2\right]^{-\frac{1}{2}} \qquad \ldots\ldots [15]$$

where: S_o = propeller amplitude at zero speed

ω = excitation frequency ($= 5 \times \frac{2\pi}{60} \times$ r.p.m.)

ω_c = critical frequency

Predicted response data and fitted curves are also given for a shorter (1300 mm) aft sterntube bearing as discussed in the next section.

The predicted data presented in Fig. 9 were obtained with the linear aft sterntube bearing model. A similar exercise was carried out using the non-linear model, and the main results for both are given in Table 4. The critical frequency prediction program indicated the fundamental lateral vibration resonance to occur at about 106 r.p.m. with the shorter (1300 mm) aft sterntube bearing. Correlation of the critical speed produced by this analysis with that of the above program was therefore better for the actual (2390 mm) aft sterntube bearing. However, sensitivity tests for this analysis were carried out on the linear model data for the short aft sterntube bearing, and the results are shown in Table 5. This indicates the results of the analysis to be fairly sensitive to the accuracy of the displacement amplitude data. The analysis was, however, regarded as a relatively simple means of assessing the resonant response characteristics of the propeller shaft system, and in particular, the significance of damping. With such a method, the results cannot be considered as anything other than a fairly approximate indication of the characteristics, particularly since it applied the theory of a single mass with simple harmonic excitation, to a multi-mass system with complex non-sinusoidal excitation and significant cross axis coupling. Cross coupling effects were probably the main reason for the poorer fit of the predicted horizontal displacement data to the equation [15] curves, in relation to that for the vertical displacements. Despite these limitations, the analysis nevertheless clearly indicated that the effective damping was at a level that prevented any peaking of the displacement amplitude at resonance. The reason why the "KEIYO MARU" could operate at the fundamental lateral resonant speed without any consequent harmful effects was therefore evident. This conclusion is consistent with several cases of vessels in which fundamental lateral vibration resonance has been predicted in the upper part of the operating speed range, and no related problems have been experienced.

Effect of Reducing Aft Sterntube Bearing Length

For some time now the length of aft sterntube bearings has been the subject of some controversy. Given any fixed shaft diameter, provided the bearing is well aligned, increasing the bearing length clearly increases the load capacity. Aft sterntube bearings are, however, frequently subject to substantial misalignment and in these circumstances it has been argued that the greater sensitivity to misalignment of the longer bearing offsets the above advantage. Jakeman (1) quantified these conflicting factors, and showed that for a steadily loaded bearing the misalignment angle would have to be well in excess of generally accepted limits before there was any advantage in reducing the L/D ratio below 2. In this work the investigation of the effect of reducing bearing length has been extended to the more realistic dynamically loaded situation.

The aft sterntube bearing of the "KEIYO MARU" was 2390 mm long giving a relatively large (by oil lubricated sterntube bearing standards) L/D ratio of 2.7314. A 45.6% reduction in the aft sterntube bearing length to 1300 mm (L/D = 1.4857) was applied for this investigation. In order that this work should be relevant in practical terms, the length reduction was from the forward end of the aft sterntube bearing. The propeller overhang from the aft edge of the bearing was therefore unchanged. No other changes to the propeller shaft system were made.

Mass m_2 was located at the axial centre of the aft sterntube bearing, and the above alteration resulted in a 545 mm shift of this point in the aft direction. Minor modifications to the mass-elastic model were therefore introduced to accommodate this change.

As previously indicated, the forced damped response charactertistics with the shorter aft sterntube bearing are given in Fig. 9 and Table 4. These results indicated an increase in the effective damping in the horizontal direction, and a reduction in the vertical direction. With the number of damping coefficients involved, the situation is complex, and the significance of individual damping coefficients has not been examined to date. Without sensitivity test results for each coefficient, it is dangerous to make sweeping comments about a situation of this complexity. However, a few simple observations can be made:

1. Reducing the aft sterntube bearing length increases the specific bearing pressure, which in turn increases ϵ. This produces a general tendency to increase the magnitude of the force-lateral motion stiffness and damping coefficients.
2. The above length reduction results in a decrease in the magnitude of the moment-angular motion stiffness and damping coefficients.

The mode shape of the complete shafting model was examined for both the 2390 mm and 1300 mm long aft sterntube bearing cases, and the results are shown in Fig. 10. These results show the lateral vibration amplitudes in the vertical direction. It was not practicable to represent the absolute displacement relative to the straight line datum for the shafting, since the bearing offsets from this datum were large in relation to the vibration amplitudes (see Table 1). Fig. 10 was therefore based on the mean displacement for each mass being set to zero. Both positive and negative amplitudes have been plotted, as they are not exactly equal due to the non-sinusoidal excitation and to the asymmetric oil film response when using the non-linear model. The mass and bearing positions covering the 2390 mm and 1300 mm long aft sterntube bearings, are indicated on the hoizontal axis.

Results obtained with both the linear and non-linear oil film models for the 2390 mm long aft sterntube bearing are presented in Fig. 10. These confirmed the insignificant differences indicated by the orbital plots (Figs. 6 to 8). Only the linear model results are shown for the 1300 mm long aft sterntube bearing. These show a substantial increase in amplitude in the shaft span between the aft sterntube and aft plummer bearings. The virtually unloaded forward sterntube bearing was clearly offering little restraint to lateral vibration.

DISCUSSION OF RESULTS

Accuracy

The differences between the predicted and measured journal orbits, at the ends of the aft sterntube bearing, are believed to be partly due to bearing and support structure elastic deformation. Such deformations were not accounted for in the theory. This view is supported by the differences being larger in the vertical direction, where the bearing loading (steady and dynamic) was greater. The above hypothesis is consistent with the better correlation of predicted and measured orbits in way of the forward sterntube bearing, since this bearing carried very little load. It may be noted that similar differences between predicted and measured journal orbits were reported by Myrick and Rylander (10). In reference (6) small but nevertheless significant differences between theoretical and experimental journal orbits were found. These could only be attributed to bearing elasticity, despite the use of a substantial bearing housing in the test rig.

In addition to the contribution of bearing elasticity, to the discrepancy between predicted and measured journal orbits, there are two other possible factors. The first is the possibility of substantial error in the estimated propeller excitation. This was due to the necessity of assuming a typical wake field and the use of a quasi-steady analysis method. Furthemore, the "KEIYO MARU" measurements were taken in the ballast condition, which could have resulted in even greater differences between the actual and assumed wake fields.

Lastly, whilst not wishing in any way to denigrate the valuable work by Hyakutake et al (2), allowance must be made for the difficulties of measurements taken under service conditions, which can lead to a substantial loss of accuracy. This is particularly true of measurements on ships, since the sea state can cause dynamic distortion of the hull structure supporting the shafting, and variation of the wake field. The published measurements (2) indicated that the above phenomena were experienced. There is also likely to be some degree of uncertainty regarding the accuracy of the bearing and journal geometry under service conditions.

A cavitation pressure of zero gauge was assumed for the bearing hydrodynamic analysis. The actual cavitation pressure may be lower than this, but since the extent of cavitation in the bottom half of the aft sterntube bearing was less than 3% at the datum condition, the effect of reducing the cavitation pressure would be negligible.

This work showed insignificant differences between the results produced using linear and non-linear oil film models for the aft sterntube bearing. The use of the linear model for practical application of this type of analysis is considered, therefore, to be justifiable. If the excitation is approximated to sinusoidal form and combined with the use of linear oil film models, then a direct (i.e. non time-stepping) solution can be achieved. This would yield a dramatic reduction in computing time. Some caution should, however, be exercised when applying linear oil film models. In situations where the dynamic loading is larger, the accuracy of the linear model may be expected to deteriorate relative to that of the non-linear model.

Significance of Damping

It has been shown that the shafting system of the "KEIYO MARU" test case could operate satisfactorily at the fundamental lateral vibration resonance, due to the amount of damping in the system. General experience indicates that occurrance of this situation is common.

Reference to Table 3 shows the aft sterntube bearing damping to be greater than that of the propeller, particularly with respect to the force-lateral velocity terms, where the difference is 2 to 3 orders of magnitude. However, in the absence of appropriate sensitivity tests, no conclusions are drawn at present regarding the relative importance of propeller and bearing damping. The differences in vibration velocity, between the propeller and aft sterntube bearing, would offset the relative significance of the bearing damping as indicated by the coefficients.

Aft Sterntube Bearing Length

The reduction in aft sterntube bearing length resulted in a significant increase in the predicted lateral vibration amplitude between the aft sterntube and aft plummer bearings. This amplitude increase was clearly related to the reduction in oil film moment-angular motion coefficients for the aft sterntube bearing. The lateral displacement amplitude at the propeller was only slightly increased by the reduction in aft sterntube bearing length. Fig. 10 showed this to be due to the increased angular displacement amplitude, in way of the bearing, being offset by the shift in the aft direction of the effective support point. This situation also resulted in a negligible change in the lateral vibration amplitude in way of the aft seal. The angular vibration amplitude was increased by the above bearing length reduction, but the corresponding axial movement of the shaft surface relative to the aft seal did not appear to be significant. Both lateral and angular motion of the shaft in way of the forward seal were increased by the substitution of a 1300 mm long aft sterntube bearing. The forward seal was located close to the forward side of the forward sterntube bearing as shown in Fig. 1. Had the shaft alignment been such that the forward sterntube bearing was carrying a reasonable load, the vibration amplitude in way of the forward seal would have been substantially reduced for either length of aft sterntube bearing.

Considering the aft sterntube bearing itself, the length reduction has been shown to increase significantly the level of dynamic misalignment. When this is translated to lateral displacement at the bearing ends, the increased angular motion was shown to be of lesser influence than the length reduction itself. However, the ϵ_p values shown in Table 4 reinforced the previously indicated (1) deleterious effect on steady load performance of bearing length reduction.

Fig. 10 underlined the importance of ensuring an adequate minimum load on the forward sterntube bearing, in order to limit the vibration amplitude in way of the forward seal. Provided this condition is met, the results indicated that the change in dynamic response due to an aft sterntube bearing length reduction, would not seriously affect the safe operation of the shafting.

CONCLUSIONS

A time stepping type of lateral vibration program, specially developed for the marine propeller shafting situation, has been presented. This incorporated alternative linear and non-linear oil film models for the aft sterntube bearing.

A good qualitative correlation of preicted and measured lateral vibration characteristics was achieved at the service speed. Quantitative differences indicated significant bearing and support structure elastic deformation. Other possible sources for this discrepancy were outlined.

The results showed the shafting system of the test case to be highly damped, to the extent that it could operate satisfactorily at the fundamental lateral vibration resonance.

Differences in the results predicted with the linear and non-linear aft sterntube bearing oil film models were found to be small. The combination of linear oil film models, with propeller excitation approximated to sinusoidal form, provides the possibility of a direct solution of the lateral vibration problem. This would enable a consiserable saving in computing time to be achieved.

Significant changes in the lateral vibration response were found to result from a reduction in the aft sterntube bearing length. The practical implications of this change were discussed. In particular, the importance of ensuring an adequate minimum mean load on bearings, especailly those close to seals, was shown.

ACKNOWLEDGEMENTS

The author wishes to express his gratitude to the Committee of Lloyd's Register of Shipping for permission to publish this paper. In addition, the author is indebted to F.A. Martin of the Glacier Metal Co. Ltd., and J. Montgomery of Trent Polytechnic, for their helpful discussions and comments.
The assistance of Mitsubishi Heavy Industries, in providing unpublished data for the shafting system of the "KEIYO MARU", is also gratefully acknowledged.

References

1. JAKEMAN R.W. "Performance and Oil Film Dynamic Coefficients of a Misaligned Sterntube Bearing". A.S.L.E. Trans. Vol. 29. No. 4. Oct. 1986 pp 441-450

2. HYAKUTAKE J., ASAI. R., INOUE M., FUKAHORI K., WATANABE N. and NONAKE M. "Measurement of Relative Displacement between Sterntube Bearing and Shaft of 210,000 dwt Tanker". Japan Shipbuilding & Marine Engineering Vol. 7 No. 1 1973 pp 32-40.

3. HYLARIDES S. and VAN GENT W. "Hydrodynamic Reactions to Propeller Vibrations". Trans. I.Mar.E. (C) Vol. 91 Conf. No. 4 Paper C36 1979 pp 78-91.

4. HAYMA S. and ANODA Y. "Dynamic Responses of Lateral Vibration of Marine Shafting due to Propeller-Induced Forces and Moments". 3rd Int. Symp. on Marine Engineering I.S.M.E. Tokyo 1983 pp 691-698.

5. KARNI Z.H., PARSONS M.G. and MOURELATOS Z.P. "Time-varying Behaviour of a Statically Indeterminate Shafting System in a Hydrodynamic Journal Bearing". A.S.M.E. Paper No.86 - Trib - 33 1986.

6. JAKEMAN R.W. and PARKINS D.W. "Theoretical and Experimental Orbits of a Dynamically Loaded Journal Bearing".
Proc. 13th Leeds-Lyon Tribol. Symp. Sept. 1986 pp 355-362

7. PARSONS M.G. and VORUS W.S. "Added Mass and Damping Estimates for Vibrating Propellers".
S.N.A.M.E. Propellers '81 Symp. May 1981 pp 273-302

8. JAKEMAN R.W. "Journal Orbit Analysis taking account of Oil Film History and Journal Mass".
Proc. 4th Int. Conf. Numerical Methods in Laminar and Turbulent Flow Jul. 1985 pp 199-210.

9. TOMS A.E. and MARTYN D.K. "Whirling of Line Shafting"
Trans. I.Mar.E. Vol. 84 1972 pp 176-191.

10. MYRICK S.T. and RYLANDER H.G. "Analysis of flexible rotor whirl and whip using a realistic hydrodynamic journal bearing model".
A.S.M.E. Jnl. of Eng. for Ind. Nov. 1976 pp 1136-1144.

Table 1 Bearing Datum Conditions for Linearised Coefficients

	AFT STERNTUBE BEARING		FORWARD STERNTUBE BEARING	AFT PLUMMER BEARING
	2390 mm LONG	1300 mm LONG		
ϵ_D	0.5000	0.7196	0.3307	0.6165
ψ'_D deg	47.12	40.15	37.81	41.05
x_D mm	0.2931	0.3712	0.2149	0.1619
y_D mm	0.2722	0.4400	0.2769+0.76*	0.1860+2.39*
λ_D rad	0	0	0	0
γ_D rad	$3.287.10^{-5}$	$-5.262.10^{-5}$	$-3.6087.10^{-4}$	0
F_{Dx} N	$1.814.10^{2}$	$3.709.10^{3}$	$6.843.10^{3}$	$-9.652.10^{1}$
F_{Dy} N	$-7.805.10^{5}$	$-7.352.10^{5}$	$-1.667.10^{4}$	$-1.289.10^{5}$
M_{Dx} Nm	$5.543.10^{3}$	$1.256.10^{2}$	$-9.396.10^{1}$	0
M_{Dy} Nm	$-1.388.10^{4}$	$1.452.10^{4}$	$7.116.10^{1}$	0
η Pa.s	0.07123	0.08174	0.1077	0.08237

* Bearing offset from datum line

Note: all datum velocities were zero

Table 2 Journal Displacement and Velocity Perturbations used to derive Linearised Coefficients

	DISPLACEMENT	VELOCITY
Lateral	0.1 mm	4.6 mm/s
Angular	$1.8.10^{-4}$ rad	$8.2.10^{-3}$ rad/s

These perturbations were estimated to be of the same order as the deviations from the mean in the actual shafting lateral vibration, and thus made some allowance for non-linearity.

Table 3 Linerarized Propeller and Bearing Coefficients

W_{xx},etc. = Propeller entrained water coefficients in kg. m. units.
A_{xx},etc. = Bearing stiffness coefficients in N.m. units
B_{xx},etc. = Propeller & bearing damping coefficients in N.m.s. units

	PROPELLER	AFT STERNTUBE BEARING		FORWARD STERNTUBE BEARING	AFT PLUMMER BEARING
		2390 mm LONG	1300 mm LONG		
W_{xx}/A_{xx}	$3.459.10^{3}$	$-1.175.10^{9}$	$-1.657.10^{9}$	$-9.455.10^{6}$	$-8.891.10^{8}$
W_{xy}/A_{xy}	$-3.785.10^{2}$	$5.250.10^{8}$	$-3.539.10^{6}$	$3.551.10^{7}$	$2.306.10^{7}$
$W_{x\lambda}/A_{x\lambda}$	$-1.543.10^{3}$	$-3.651.10^{7}$	$4.469.10^{7}$	$8.164.10^{4}$	$9.362.10^{3}$
$W_{x\gamma}/A_{x\gamma}$	$-1.735.10^{4}$	$3.155.10^{7}$	$3.451.10^{7}$	$-4.717.10^{5}$	$1.995.10^{3}$
W_{yx}/A_{yx}	$3.785.10^{2}$	$-2.792.10^{9}$	$-3.438.10^{9}$	$-8.669.10^{7}$	$-1.610.10^{9}$
W_{yy}/A_{yy}	$3.459.10^{3}$	$-1.282.10^{9}$	$-3.430.10^{9}$	$-1.686.10^{7}$	$-1.988.10^{9}$
$W_{y\lambda}/A_{y\lambda}$	$1.735.10^{4}$	$-9.428.10^{7}$	$1.035.10^{8}$	$3.357.10^{5}$	$-1.729.10^{4}$
$W_{y\gamma}/A_{y\gamma}$	$-1.543.10^{3}$	$-8.866.10^{7}$	$1.741.10^{8}$	$1.449.10^{5}$	$-7.109.10^{3}$
$W_{\lambda x}/A_{\lambda x}$	$1.543.10^{3}$	$-3.018.10^{7}$	$4.929.10^{7}$	$1.585.10^{5}$	0
$W_{\lambda y}/A_{\lambda y}$	$1.735.10^{4}$	$4.176.10^{7}$	$3.317.10^{7}$	$-4.259.10^{5}$	0
$W_{\lambda\lambda}/A_{\lambda\lambda}$	$1.348.10^{5}$	$-3.967.10^{8}$	$-1.316.10^{8}$	$-5.292.10^{4}$	$-3.583.10^{6}$
$W_{\lambda\gamma}/A_{\lambda\gamma}$	$-1.503.10^{4}$	$1.958.10^{8}$	$-7.066.10^{6}$	$2.688.10^{5}$	$1.959.10^{5}$
$W_{\gamma x}/A_{\gamma x}$	$-1.735.10^{4}$	$-8.558.10^{7}$	$1.101.10^{8}$	$4.075.10^{5}$	0
$W_{\gamma y}/A_{\gamma y}$	$1.543.10^{3}$	$-6.026.10^{7}$	$1.885.10^{8}$	$3.506.10^{5}$	0
$W_{\gamma\lambda}/A_{\gamma\lambda}$	$-1.503.10^{4}$	$-9.121.10^{8}$	$-2.742.10^{8}$	$-4.499.10^{5}$	$-6.331.10^{6}$
$W_{\gamma\gamma}/A_{\gamma\gamma}$	$1.348.10^{5}$	$-4.869.10^{8}$	$-3.191.10^{8}$	$-1.996.10^{5}$	$-1.006.10^{7}$
B_{xx}	$-5.668.10^{5}$	$-1.131.10^{8}$	$-1.606.10^{8}$	$-6.608.10^{6}$	$-6.458.10^{7}$
B_{xy}	$-3.924.10^{5}$	$-7.807.10^{7}$	$-1.644.10^{8}$	$-1.062.10^{6}$	$-5.465.10^{7}$
$B_{x\lambda}$	$-2.229.10^{6}$	$-9.470.10^{6}$	$5.524.10^{6}$	$8.349.10^{4}$	$-1.836.10^{2}$
$B_{x\gamma}$	$3.489.10^{6}$	$-2.348.10^{6}$	$4.767.10^{6}$	$7.469.10^{3}$	$1.625.10^{2}$
B_{yx}	$3.924.10^{5}$	$-8.928.10^{7}$	$-1.780.10^{8}$	$-1.359.10^{6}$	$-5.486.10^{7}$
B_{yy}	$-5.668.10^{5}$	$-4.600.10^{8}$	$-4.861.10^{8}$	$-1.724.10^{7}$	$-1.681.10^{8}$
$B_{y\lambda}$	$-3.489.10^{6}$	$-9.457.10^{6}$	$8.835.10^{6}$	$1.559.10^{5}$	0
$B_{y\gamma}$	$-2.229.10^{6}$	$-8.679.10^{6}$	$1.297.10^{7}$	$6.132.10^{4}$	$-2.286.10^{2}$
$B_{\lambda x}$	$2.229.10^{6}$	$-5.005.10^{6}$	$5.331.10^{6}$	$4.676.10^{4}$	0
$B_{\lambda y}$	$-3.489.10^{6}$	$-2.251.10^{6}$	$5.069.10^{6}$	$9.507.10^{3}$	0
$B_{\lambda\lambda}$	$-2.730.10^{7}$	$-3.867.10^{7}$	$-1.451.10^{7}$	$-5.207.10^{4}$	$-3.992.10^{5}$
$B_{\lambda\gamma}$	$-2.063.10^{7}$	$-1.287.10^{8}$	$-1.404.10^{7}$	$-1.380.10^{4}$	$-1.067.10^{6}$
$B_{\gamma x}$	$3.489.10^{6}$	$-8.708.10^{6}$	$7.972.10^{6}$	$7.140.10^{4}$	0
$B_{\gamma y}$	$-2.229.10^{6}$	$-9.442.10^{6}$	$1.242.10^{7}$	$7.377.10^{4}$	0
$B_{\gamma\lambda}$	$2.063.10^{7}$	$-2.553.10^{7}$	$-1.554.10^{7}$	$-1.407.10^{4}$	$-3.762.10^{5}$
$B_{\gamma\gamma}$	$-2.730.10^{7}$	$-1.287.10^{8}$	$-3.904.10^{7}$	$-1.083.10^{5}$	$-1.067.10^{6}$

Table 4 Results of Resonant Response Analysis for Propeller Lateral Vibration

AFT STERNTUBE BEARING	2390 mm LONG				1300 mm LONG			
A.S.B. OIL FILM MODEL	LINEAR		NON-LINEAR		LINEAR		NON-LINEAR	
DISPLACEMENT DIRECTION	X	Y	X	Y	X	Y	X	Y
CRITICAL SPEED R.P.M.	87	90	89	82	90	66	98	72
$\frac{\text{DAMPING}}{\text{CRITICAL}} \left(\frac{K}{\omega_c}\right)$	0.65	6.32	0.88	5.33	0.92	3.06	1.37	3.62

Table 5 Sensitivity Tests on Resonant Response Analysis for Propeller Lateral Vibration

These tests were applied to the vertical response analysis for the 1300m long aft sterntube bearing case with the linear oil film model. Displacement amplitudes at 0 and 97 r.p.m. were as predicted.

CHANGE IN DISPLACEMENT AMPLITUDE AT 77 R.P.M. FROM PREDICTED VALUE	+2.2%	-3.4%
RESULTING CHANGE IN CRITICAL SPEED	-9.9%	+61.8%
RESULTING CHANGE IN EFFECTIVE DAMPING	-21.6%	+171.0%

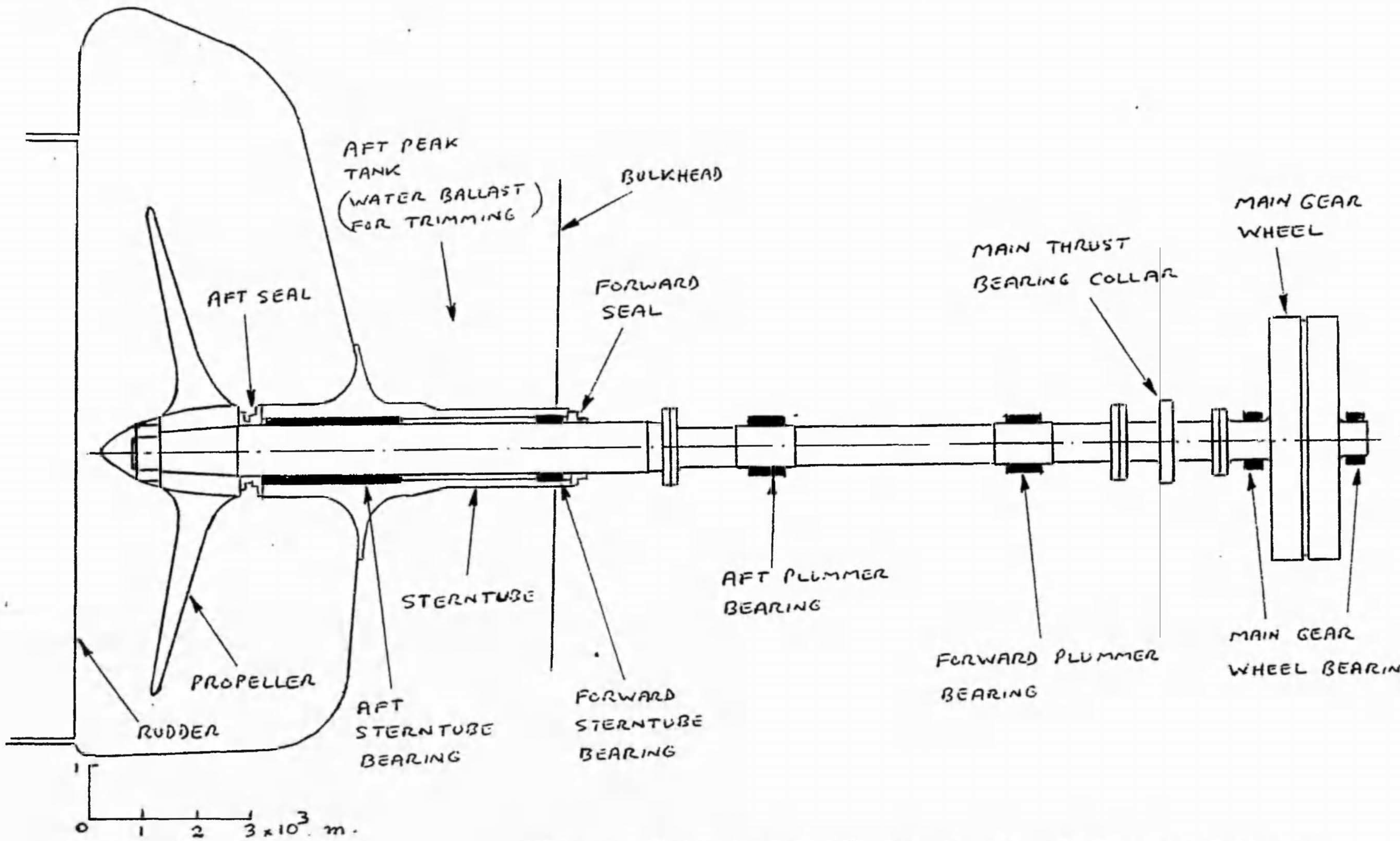

FIG 1. "KEIYO MARU" PROPELLER SHAFTING SYSTEM.

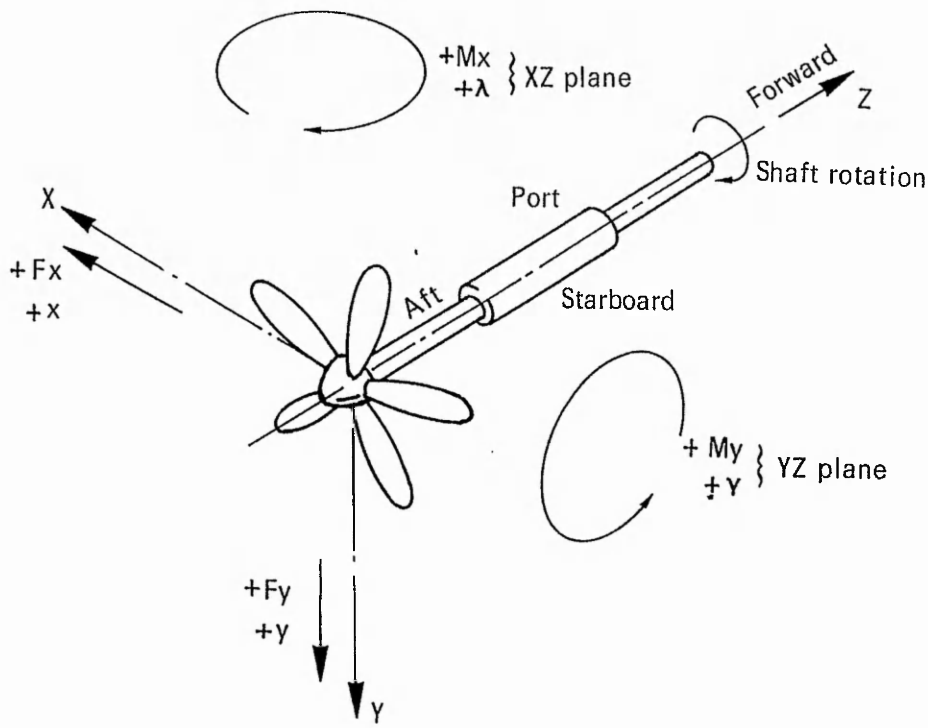

FIG. 2. GENERAL SIGN CONVENTION.

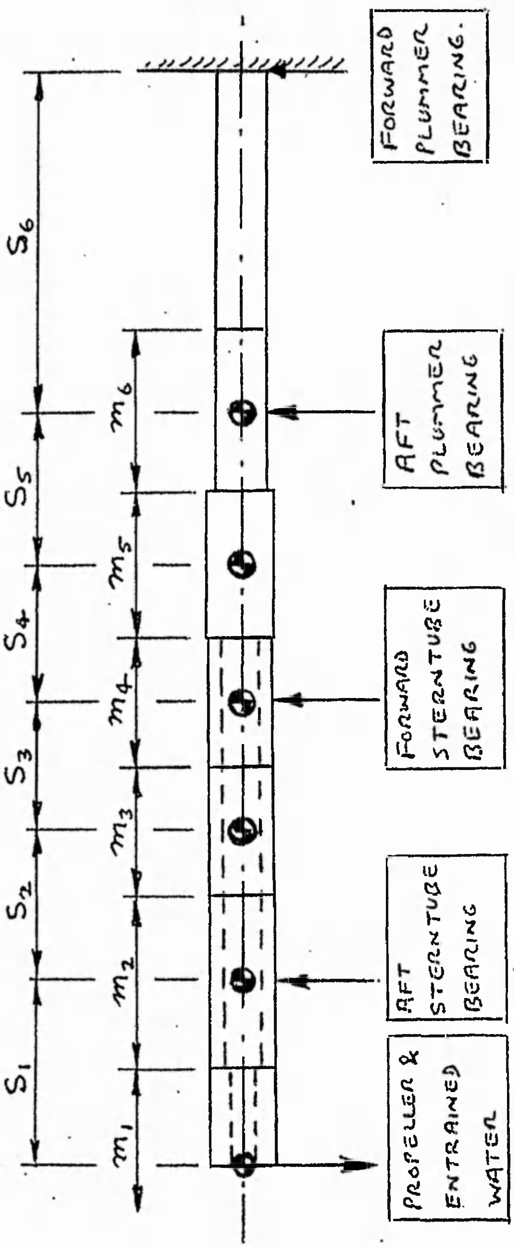

FIG. 3. MASS-ELASTIC MODEL.

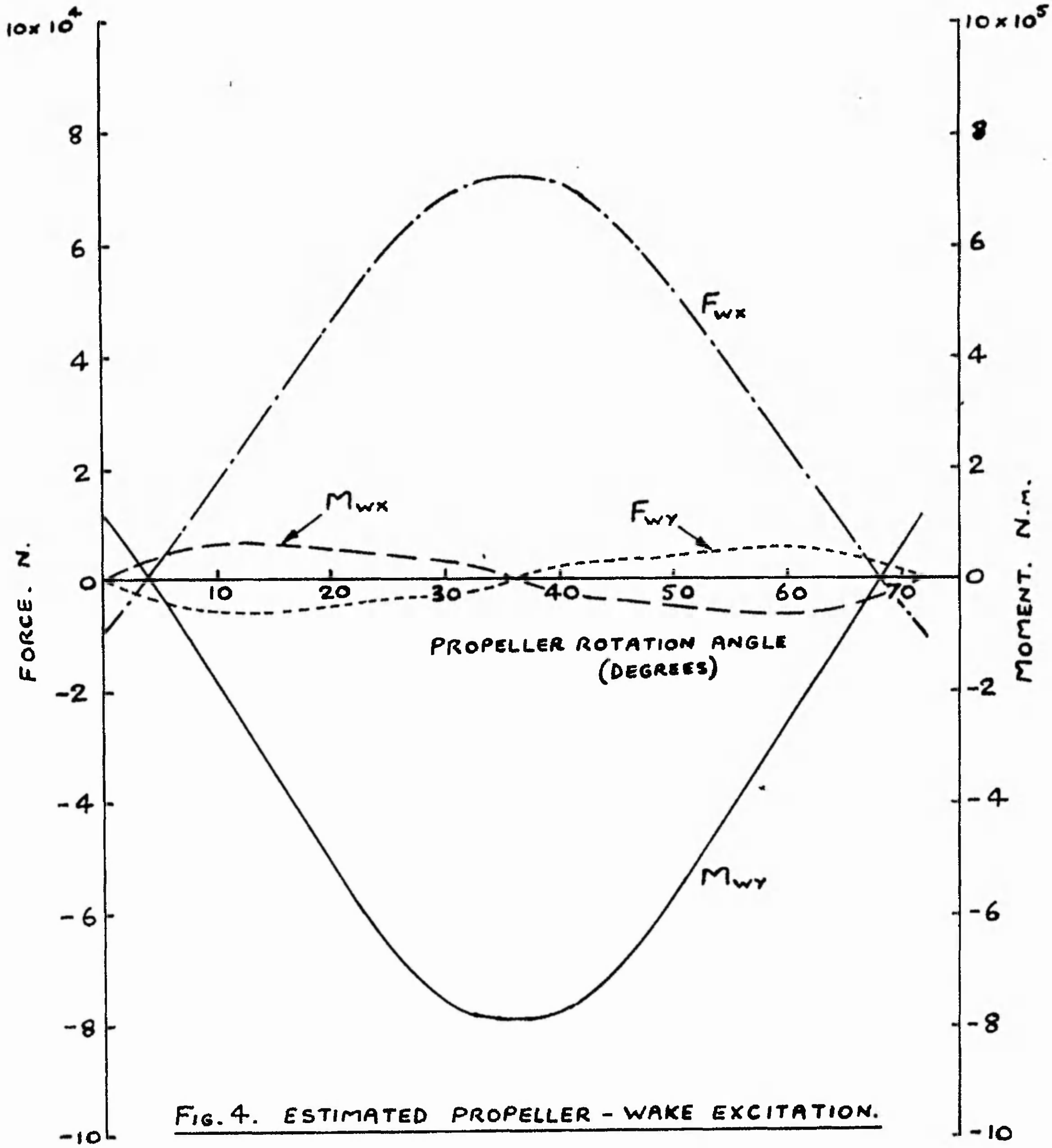

Fig. 4. ESTIMATED PROPELLER - WAKE EXCITATION.

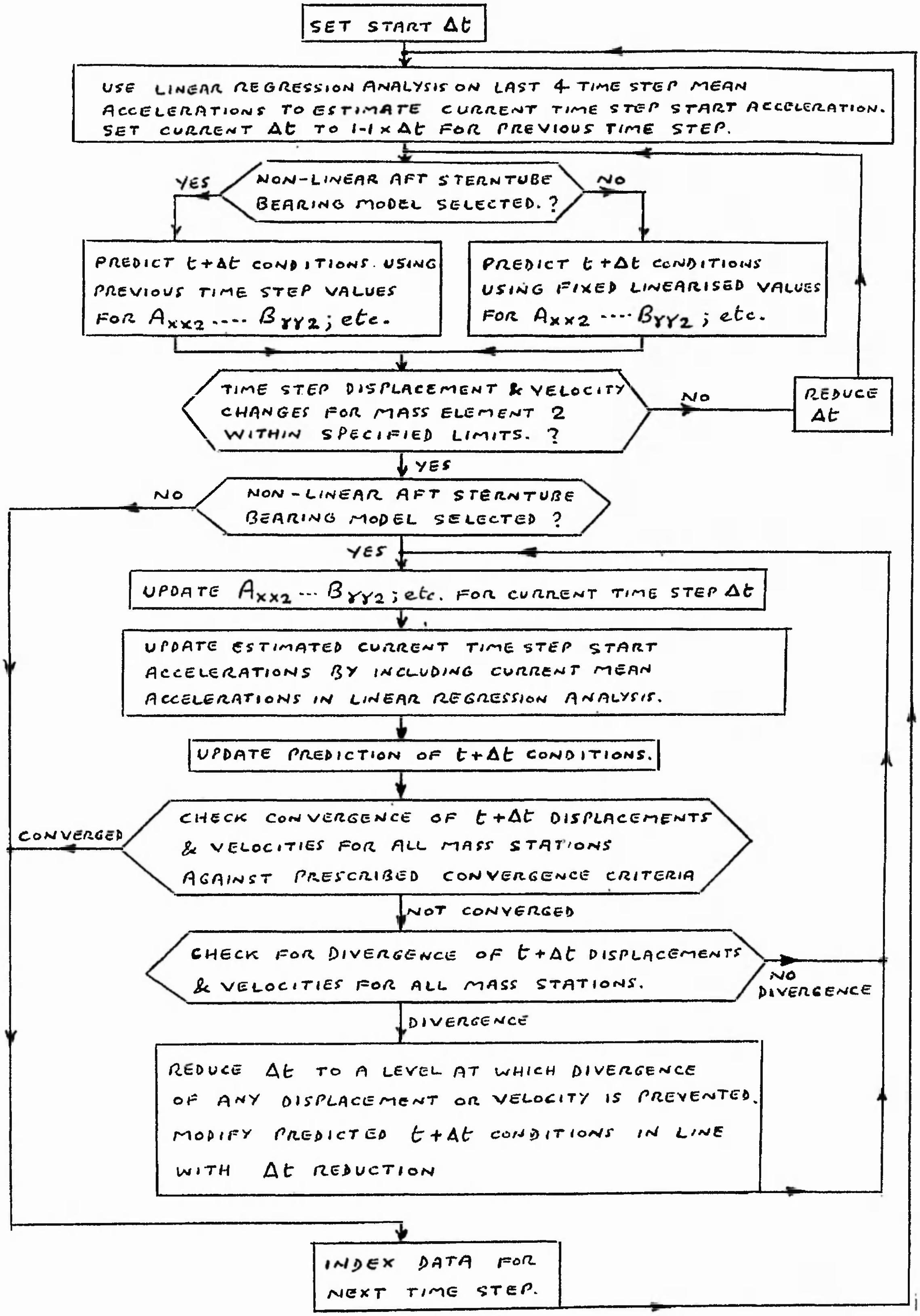

FIG. 5. TIME STEPPING PROCEDURE.

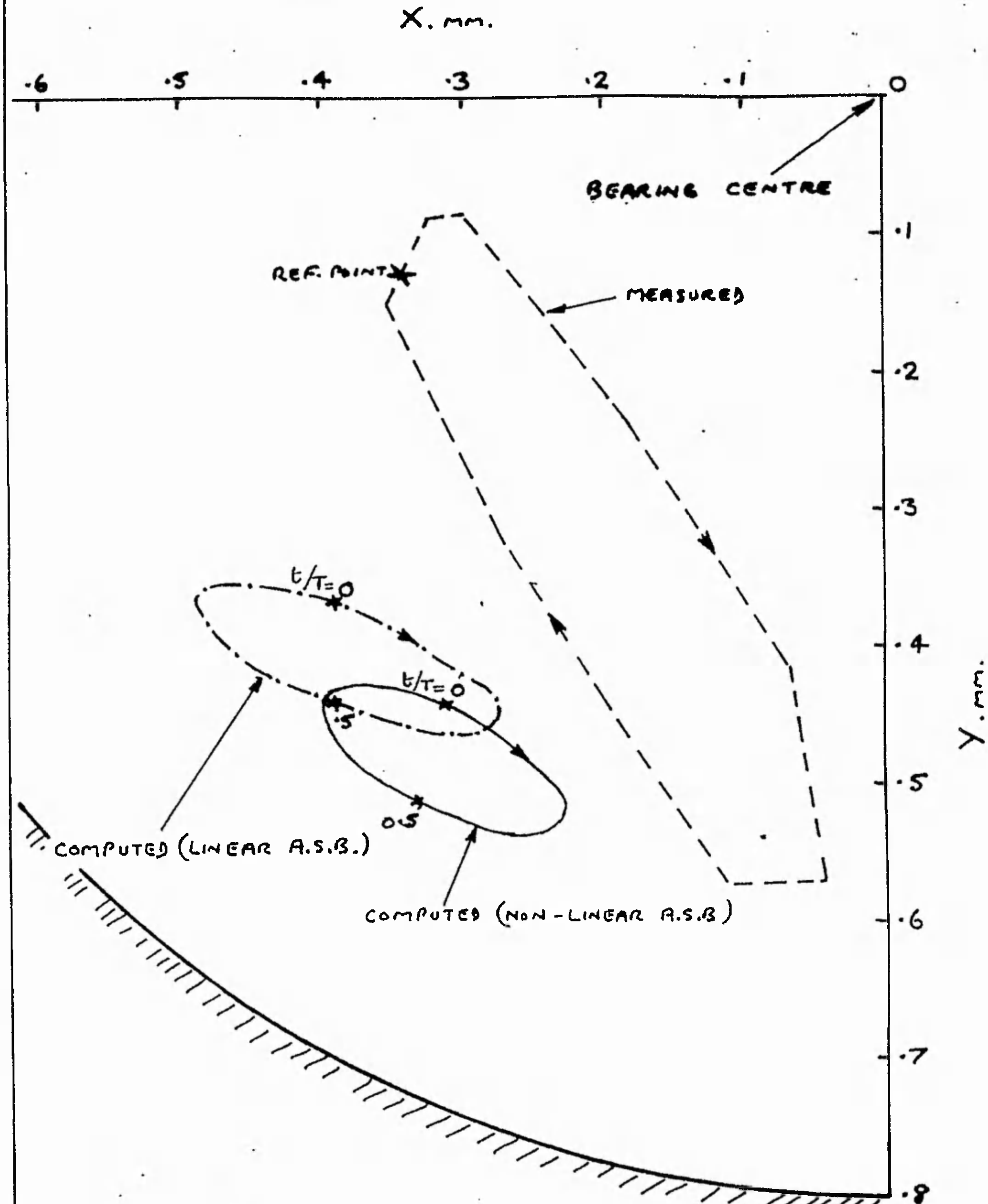

FIG. 6. "KEIYO MARU" – JOURNAL ORBITS AT AFT END OF AFT STERNTUBE-BEARING AT 87. R.P.M.

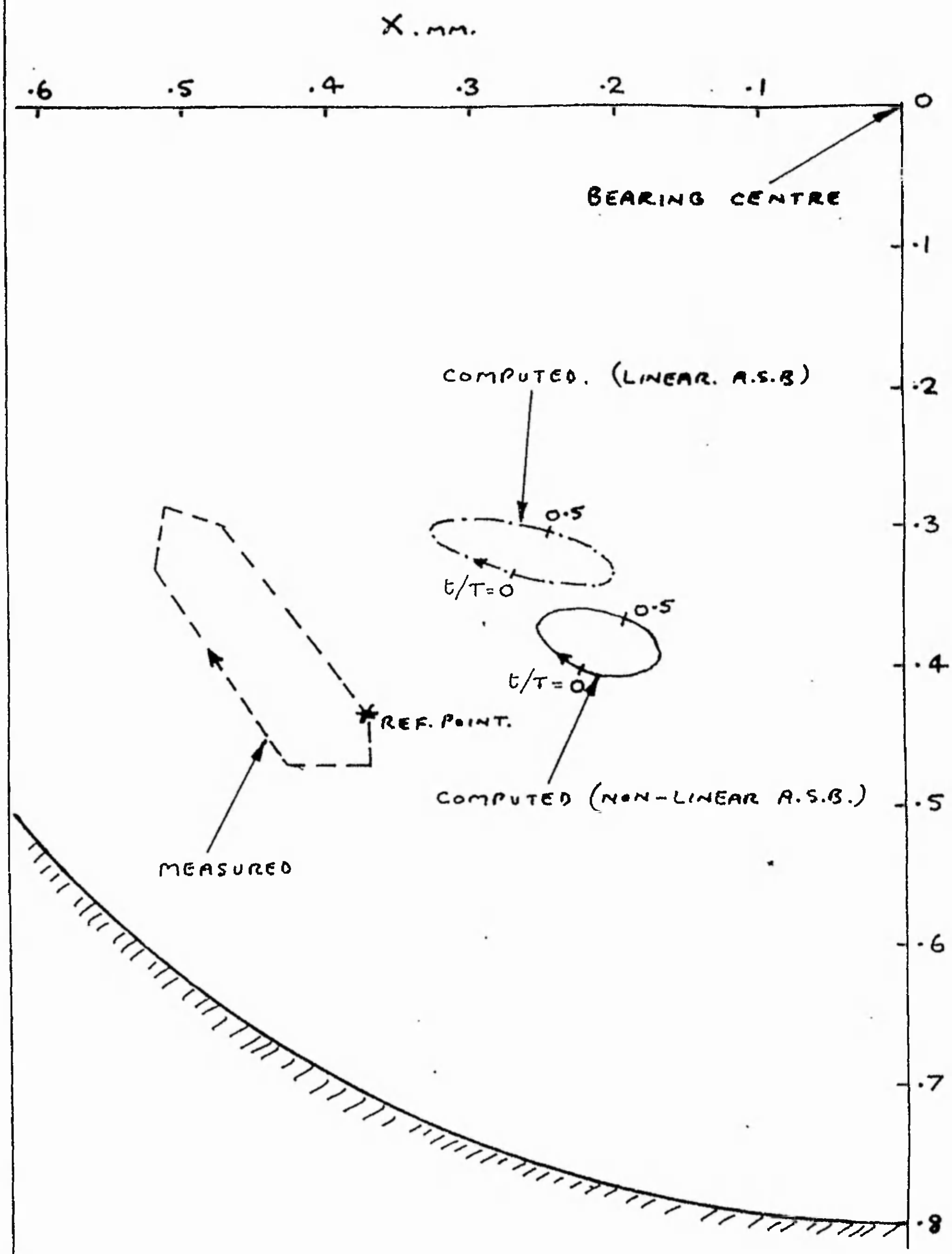

FIG. 7. "KEIYO MARU" - JOURNAL ORBITS AT FORWARD END OF AFT STERNTUBE BEARING AT 87. R.P.M.

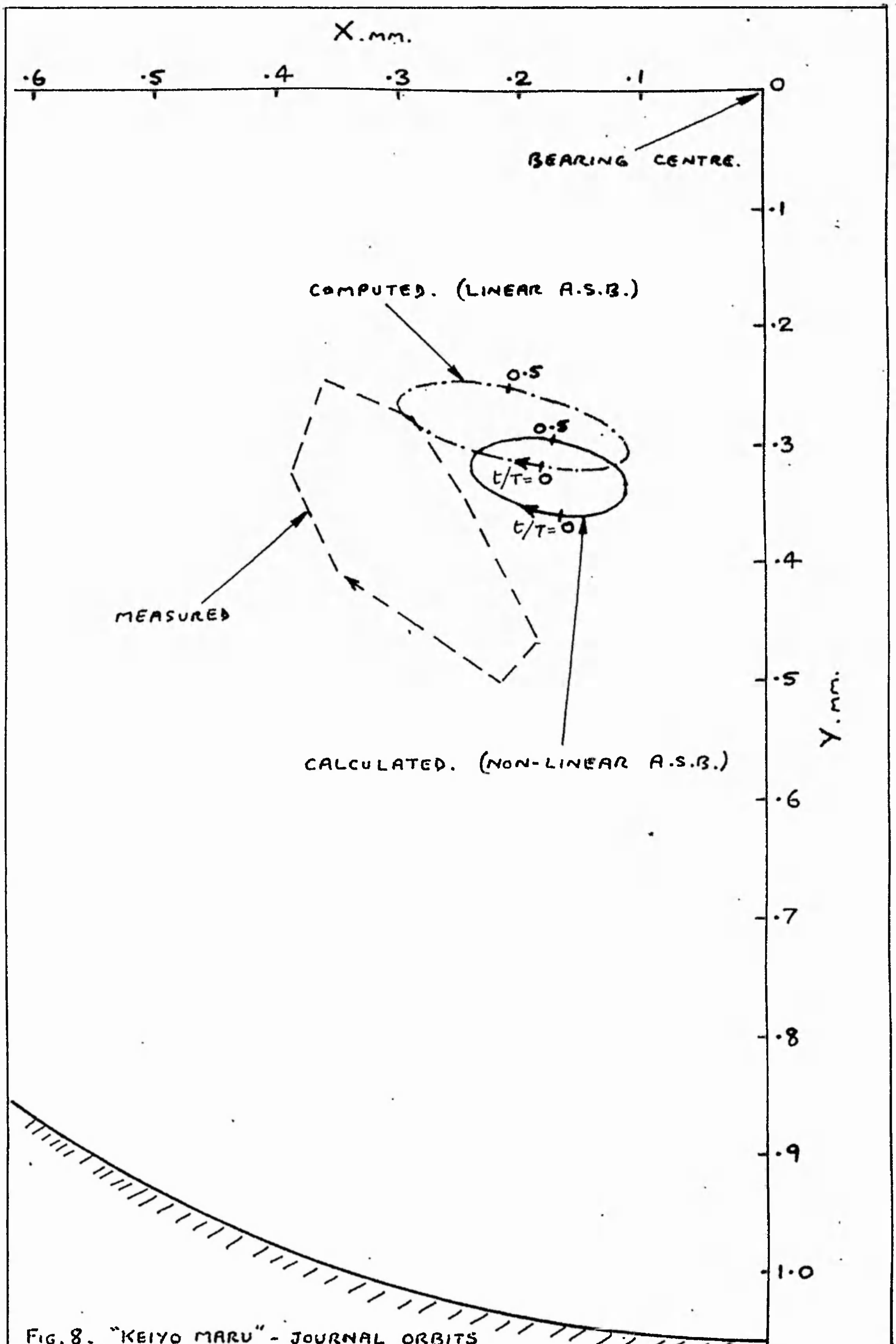

FIG. 8. "KEIYO MARU" - JOURNAL ORBITS AT FORWARD STERNTUBE BEARING AT 87. R.P.M.

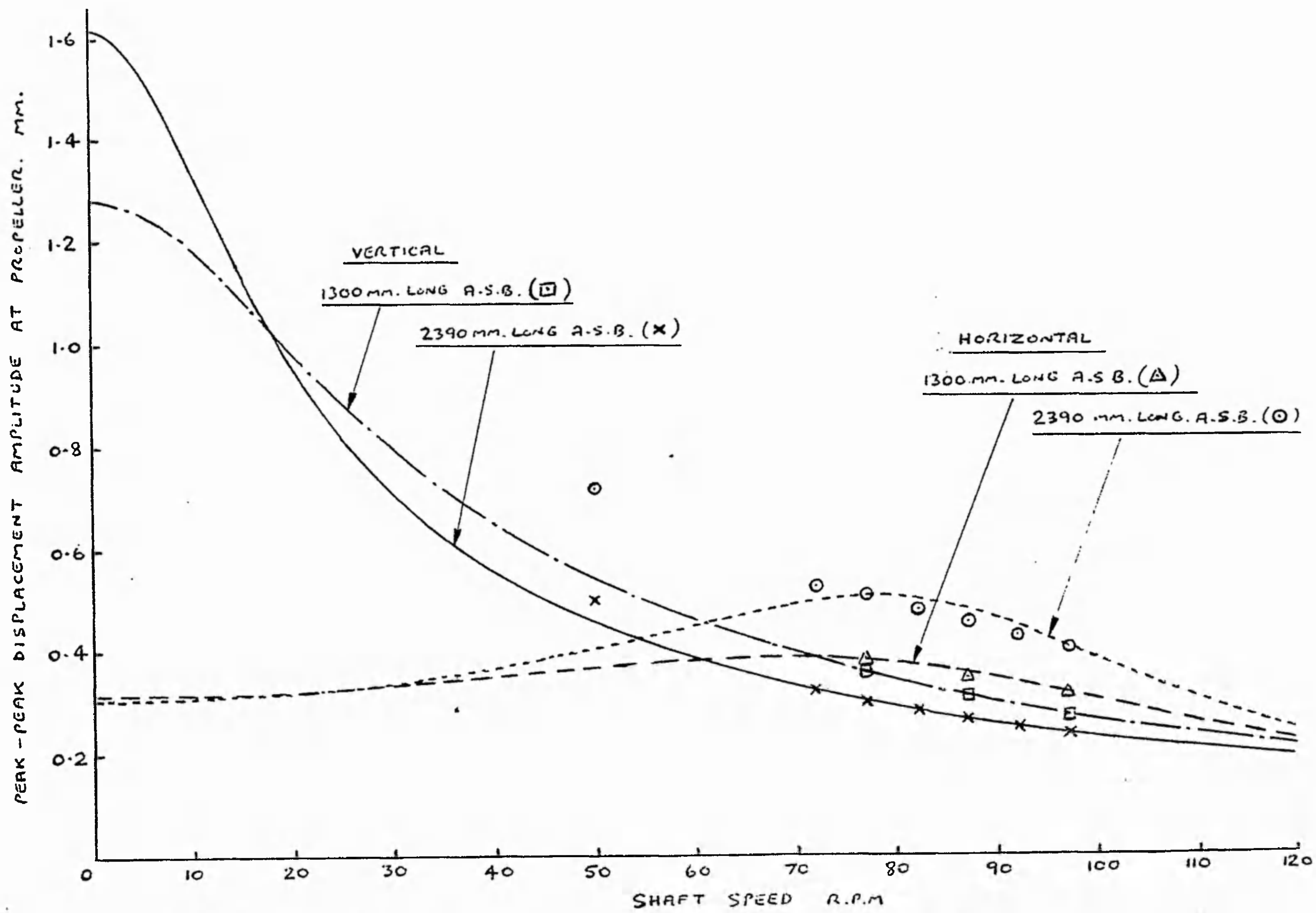

FIG. 9. "KEIYO MARU" FORCED - DAMPED RESONANT RESPONSE ANALYSIS

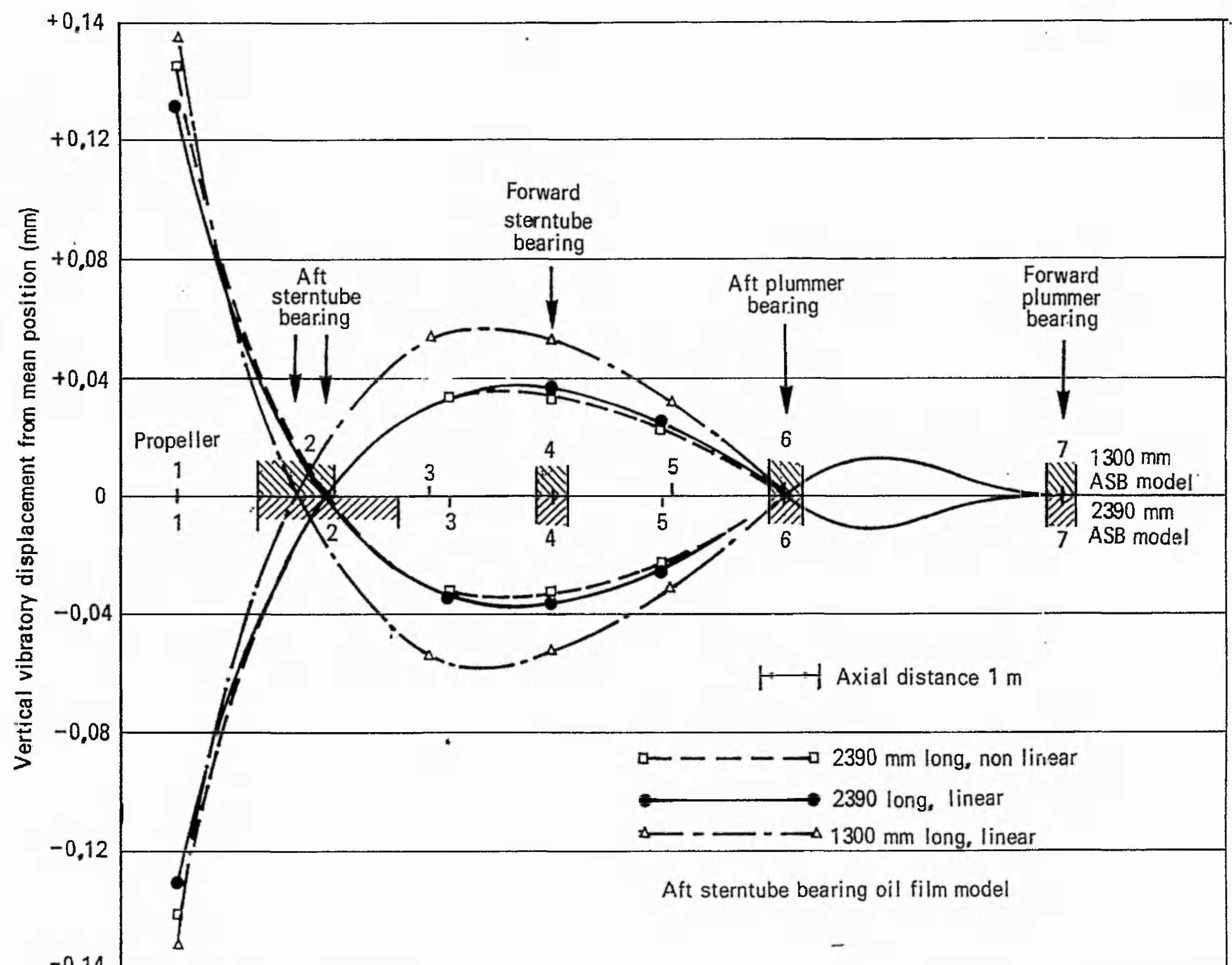

Fig 10 'Keiyo Maru' Vertical Lateral Vibratory Amplitudes at 87 RPM